OPTIMIZED LAND USE AND LAND COVER ALLOCATION FOR
FLOOD MITIGATION WITH GOAL PROGRAMMING, MUEANG
CHAIYAPHUM DISTRICT, CHAIYAPHUM PROVINCE, THAILAND

ATHIWAT PHINYOYANG

A Thesis Submitted in Partial Fulfillment of the Requirements for the
Degree of Doctor of Philosophy in Geoinformatics
Suranaree University of Technology
Academic Year 2021

การจัดสรรการใช้ประโยชน์ที่ดินและสิ่งปกคลุมดินอย่างเหมาะสมที่สุด สำหรับบรรเทาน้ำท่วมด้วยโปรแกรมเชิงเป้าหมาย อำเภอเมืองชัยภูมิ จังหวัดชัยภูมิ ประเทศไทย

นายอธิวัฒน์ ภิญโญยาง

วิทยานิพนธ์นี้เป็นส่วนหนึ่งของการศึกษาตามหลักสูตรปริญญาวิทยาศาสตรดุษฎีบัณฑิต
สาขาวิชาภูมิสารสนเทศ
มหาวิทยาลัยเทคโนโลยีสุรนารี
ปีการศึกษา 2564

OPTIMIZED LAND USE AND LAND COVER ALLOCATION FOR FLOOD MITIGATION WITH GOAL PROGRAMMING, MUEANG CHAIYAPHUM DISTRICT, CHAIYAPHUM PROVINCE, THAILAND

Suranaree University of Technology has approved this thesis submitted in partial fulfillment of the requirements for the Degree of Doctor of Philosophy.

Thesis Examining Committee
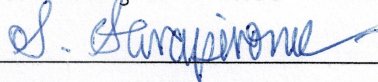
_____
(Asst. Prof. Dr. Sunya Sarapirome)

Chairperson
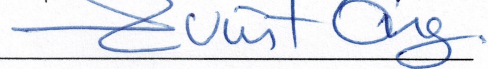
_____
(Assoc. Prof. Dr. Suwit Ongsomwang)

Member (Thesis Advisor)
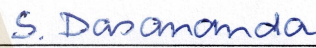
_____
(Assoc. Prof. Dr. Songkot Dasananda)

Member
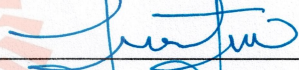
_____
(Asst. Prof. Dr. Pantip Piyatadsananon)

Member
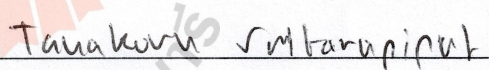
_____
(Dr. Tanakorn Sritarapipat)

Member

_____
(Assoc. Prof. Dr. Chatchai Jothityangkoon)

Vice Rector for Academic Affairs

and Quality Assurance
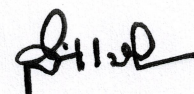
_____
(Prof. Dr. Santi Maensiri)

Dean of Institute of Science

อธิวัฒน์ ภิญโญยาง : การจัดสรรการใช้ประโยชน์ที่ดินและสิ่งปกคลุมดินอย่างเหมาะสมที่สุด สำหรับบรรเทาน้ำท่วมด้วยโปรแกรมเชิงเป้าหมาย อำเภอเมืองชัยภูมิ จังหวัดชัยภูมิ ประเทศ ไทย (OPTIMIZED LAND USE AND LAND COVER ALLOCATION FOR FLOOD MITIGATION WITH GOAL PROGRAMMING, MUEANG CHAIYAPHUM DISTRICT, CHAIYAPHUM PROVINCE, THAILAND) อาจารย์ที่ปรึกษา : รองศาสตราจารย์ ดร.สุวิทย์ อ๋องสมหวัง, 337 หน้า.

คำสำคัญ: การจัดสรรการใช้ประโยชน์ที่ดินและสิ่งปกคลุมดินอย่างเหมาะสมที่สุด/ แบบจำลอง CLUE-S/ วิธีการ SCS-CN/ โปรแกรมเชิงเป้าหมาย/ จังหวัดชัยภูมิ

น้ำท่วมได้ก่อให้เกิดความสูญเสียอย่างมหาศาลต่อสภาพเศรษฐกิจ สังคมและสิ่งแวดล้อมทาง นิเวศวิทยาทั่วโลก ด้วยเหตุผลดังกล่าวจึงได้ทำการศึกษาการจัดสรรการใช้ประโยชน์ที่ดินและสิ่งปก คลุมดินที่เหมาะสมที่สุดสำหรับการบรรเทาน้ำท่วมโดยอาศัยค่าสัมประสิทธิ์น้ำท่าด้วยโปรแกรมเชิง เป้าหมายในพื้นที่อำเภอเมืองชัยภูมิ จังหวัดชัยภูมิ วัตถุประสงค์ของการศึกษา คือ (1) เพื่อจำแนก ข้อมูลการใช้ประโยชน์ที่ดินและสิ่งปกคลุมดินในปี พ.ศ. 2544 2553 และ 2562 (2) เพื่อคาดการณ์ การเปลี่ยนแปลงการใช้ประโยชน์ที่ดินและสิ่งปกคลุมดินใน 2 ช่วงเวลาโดยอาศัยข้อมูลการใช้ ประโยชน์ที่ดินและสิ่งปกคลุมดินที่ได้ทำการจำแนก (3) เพื่อประมาณค่าปริมาณน้ำท่าในระหว่างปี พ.ศ. 2544 ถึง 2562 (4) เพื่อจัดสรรและจัดทำแผนที่การใช้ประโยชน์ที่ดินและสิ่งปกคลุมดินที่ เหมาะสมที่สุดภายใต้เงื่อนไขปริมาณน้ำฝนที่แตกต่างกัน และ (5) เพื่อประเมินมูลค่าทางเศรษฐกิจ และการให้บริการทางระบบนิเวศและการเปลี่ยนแปลงของการจัดสรรการใช้ประโยชน์ที่ดินและสิ่งปก คลุมดินที่เหมาะสมสำหรับการบรรเทาน้ำท่วมในแง่ของมูลค่าที่ได้รับเพิ่มขึ้นหรือสูญเสียลดลง วิธี การศึกษาประกอบไปด้วยการรวบรวมและการจัดเตรียมข้อมูลและ องค์ประกอบการวิจัยที่สำคัญ 6 องค์ประกอบ

จากผลการศึกษาที่ได้รับ พบว่า ค่าความถูกต้องโดยรวมและค่าสัมประสิทธิ์แคปปาแฮทที่ได้ จากการประเมินความถูกต้องของแผนที่การใช้ประโยชน์ที่ดินและสิ่งปกคลุมดินในปี พ.ศ. 2544 2553 และ 2562 มีค่ามากกว่าร้อยละ 85 และพบว่า ประเภทการใช้ประโยชน์ที่ดินและสิ่งปกคลุมดินที่ เพิ่มขึ้นอย่างมีนัยสำคัญในระหว่างปี พ.ศ. 2544 ถึง พ.ศ. 2562 ได้แก่ อ้อย ยางพาราและที่ดินที่ไม่มี การใช้ประโยชน์ ขณะเดียวกัน ประเภทการใช้ประโยชน์ที่ดินและสิ่งปกคลุมดินที่ลดลงอย่างมี นัยสำคัญ ได้แก่ นาข้าว พื้นที่ป่าไม้และมันสำปะหลัง สำหรับแผนที่การคาดการณ์การใช้ประโยชน์ ที่ดินและสิ่งปกคลุมดินใน 2 ช่วงเวลา (พ.ศ. 2545 ถึง พ.ศ. 2552 และ พ.ศ. 2554 ถึง พ.ศ. 2561) ด้วยแบบจำลอง CLUE-S ให้ผลลัพธ์ที่สมเหตุสมผลตามที่คาดหวัง โดยมีค่าเบี่ยงเบนอยู่ระหว่าง -0.05

ถึง 0.05 ตารางกิโลเมตร ในขณะเดียวกัน ปริมาณน้ำท่าแบบอนุกรมเวลาภายใต้สภาพความชื้นใน
อดีตที่เหมาะสม (AMC-II) มีค่าผันแปรอยู่ระหว่าง 1,003.60 ล้านลูกบาศก์เมตร ในปี พ.ศ. 2557 ถึง
6,366.80 ล้านลูกบาศก์เมตร ในปี พ.ศ. 2551 สำหรับการตรวจสอบความถูกต้องของแบบจำลอง
SCS-CN พบว่า มีค่า NSE และ R^2 มากกว่า 0.65 และค่า PBIAS น้อยกว่าร้อยละ ±10 อนึ่ง หลังจาก
การจัดสรรการใช้ประโยชน์ที่ดินและสิ่งปกคลุมดินเพื่อลดปริมาณน้ำท่าให้มีปริมาณน้อยที่สุดสำหรับ
การบรรเทาน้ำท่วมในปี พ.ศ. 2572 2582 และ 2592 โดยอาศัยค่าสัมประสิทธิ์น้ำท่าเฉลี่ยของแต่ละ
ประเภทการใช้ประโยชน์ที่ดินและสิ่งปกคลุมดินภายใต้เงื่อนไขปริมาณน้ำฝนที่แตกต่างกันด้วย
โปรแกรมเชิงเป้าหมาย พบว่า ข้อมูลการใช้ประโยชน์ที่ดินและสิ่งปกคลุมดินที่ได้ถูกจัดสรรอย่าง
เหมาะสมทั้งหมด ไม่ว่าจะเป็นปี พ.ศ. และเงื่อนไขปริมาณน้ำฝนที่แตกต่างกัน สามารถลดปริมาณ
น้ำท่ารายปีได้ระหว่าง 12.95 ถึง 52.31 ล้านลูกบาศก์เมตร การจัดสรรการใช้ประโยชน์ที่ดินและสิ่ง
ปกคลุมดินที่เหมาะสมเพื่อลดปริมาณน้ำท่าสำหรับการบรรเทาน้ำท่วมภายใต้เงื่อนไขปริมาณน้ำฝนที่
แตกต่างกันทั้ง 3 รูปแบบ เกิดขึ้นในปี พ.ศ. 2592 นอกจากนี้ หากพิจารณามูลค่าทางเศรษฐกิจและ
การให้บริการทางระบบนิเวศในอนาคตและการเปลี่ยนแปลงที่เกิดขึ้น พบว่า การจัดสรรการใช้
ประโยชน์ที่ดินและสิ่งปกคลุมดินที่เหมาะสมสำหรับการบรรเทาน้ำท่วมในปี พ.ศ. 2592 ภายใต้สภาพ
น้ำฝนแบบปีปกติ สามารถให้มูลค่าทางเศรษฐกิจในอนาคตและมูลค่าที่ได้รับเพิ่มขึ้นสูงสุด ใน
ขณะเดียวกัน การจัดสรรการใช้ประโยชน์ที่ดินและสิ่งปกคลุมดินที่เหมาะสมสำหรับการบรรเทาน้ำ
ท่วมในปี พ.ศ. 2592 ภายใต้สภาพน้ำฝนแบบปีแล้งสามารถให้มูลค่าการให้บริการทางระบบนิเวศและ
มูลค่าที่ได้รับเพิ่มขึ้นสูงสุด นอกจากนี้ หากพิจารณาการลดลงของปริมาณน้ำท่า พบว่า การจัดสรรการ
ใช้ประโยชน์ที่ดินและสิ่งปกคลุมดินที่เหมาะสมที่สุดสำหรับการบรรเทาน้ำท่วมในปี พ.ศ. 2592 คือ
สภาพน้ำฝนแบบปีปกติ

จากผลการศึกษาที่ได้รับทั้งหมด สามารถสรุปได้ว่า ผลลัพธ์ที่ได้จากการศึกษาครั้งนี้สามารถ
ใช้เป็นสารสนเทศพื้นฐานที่สำคัญสำหรับการดำเนินโครงการการบรรเทาน้ำท่วมได้ นอกจากนี้ กรอบ
แนวคิดและขั้นตอนการวิจัยที่ได้นำเสนอ สามารถนำมาใช้เป็นแนวทางให้หน่วยงานของรัฐในการ
ตรวจสอบรายละเอียดเพิ่มเติมเกี่ยวกับการบรรเทาน้ำท่วมในพื้นที่อำเภอเมืองชัยภูมิ จังหวัดชัยภูมิ ได้

สาขาวิชาภูมิสารสนเทศ   ลายมือชื่อนักศึกษา_____

ปีการศึกษา 2564   ลายมือชื่ออาจารย์ที่ปรึกษา_____

ATHIWAT PHINYOYANG : OPTIMIZED LAND USE AND LAND COVER ALLOCATION FOR FLOOD MITIGATION WITH GOAL PROGRAMMING, MUEANG CHAIYAPHUM DISTRICT, CHAIYAPHUM PROVINCE, THAILAND. THESIS ADVISOR : ASSOC. PROF. SUWIT ONGSOMWANG, Dr. rer. Nat. 337 PP.

The flood has caused enormous losses to economies, societies, and ecological environments worldwide. The optimizing LULC allocation for flood mitigation based on the surface runoff coefficient value of LULC types with Goal programming, Mueang Chaiyaphum District, Chaiyaphum Province, was conducted. The research objectives were (1) to classify LULC data in 2001, 2010, and 2019, (2) to predict LULC change in two periods based on classified LULC data, (3) to estimate surface runoff between 2001 and 2019, (4) to optimize and map LULC allocation for flood mitigation under three rainfall conditions, and (5) to evaluate economic and ecosystem service values and change of suitable LULC allocation for flood mitigation in terms of gain and loss. The research procedures consisted of data collection and preparation and six significant research components.

As a result, the overall accuracy and Kappa hat coefficient of classified LULC maps in 2001, 2010, and 2019 were more than 85%. The significant increase in LULC types between 2001 and 2019 was sugarcane, para rubber, and unused land, while the significant decrease in LULC types was paddy field, forest land, and cassava. The predicted LULC map in two periods (2002-2009 and 2011-2018) by the CLUE-S model provided realistic results as expected, with deviation values from -0.05 to 0.05 km^2. Meanwhile, time-series surface runoff with suitable AMC-II varied from 1,003.60 million m^3 in 2014 to 6,366.80 million m^3 in 2008. For SCS-CN model validation, the derived NSE and R^2 values are more than 0.65, and the PBIAS value is less than $\pm$ 10%. After optimizing LULC allocation to minimize surface runoff for flood mitigation in 2029, 2039, and 2049 based on the average surface runoff coefficient from each LULC type under three rainfall conditions using Goal programming, all allocated LULC data in

different years, and rainfall conditions could reduce annual surface runoff by 12.95 to 52.31 million m³. The suitable LULC allocation for flood mitigation under three rainfall conditions was in 2049. Considering future economic and ecosystem service values and changes, the suitable LULC allocation for flood mitigation in 2049 under a normal year could provide the highest future economic value and gain. In the meantime, the suitable LULC allocation for flood mitigation in 2049 under a drought year could provide the highest ecosystem service value and gain. Besides, the most suitable LULC allocation for flood mitigation in 2049 by considering runoff reduction is a normal year.

In conclusion, the derived results of this study can be used as primary information for flood mitigation project implementation. Additionally, the presented conceptual framework and research workflows can be used as a guideline for government agencies to investigate in more detail flood mitigation at Mueang Chaiyaphum district, Chaiyaphum province.
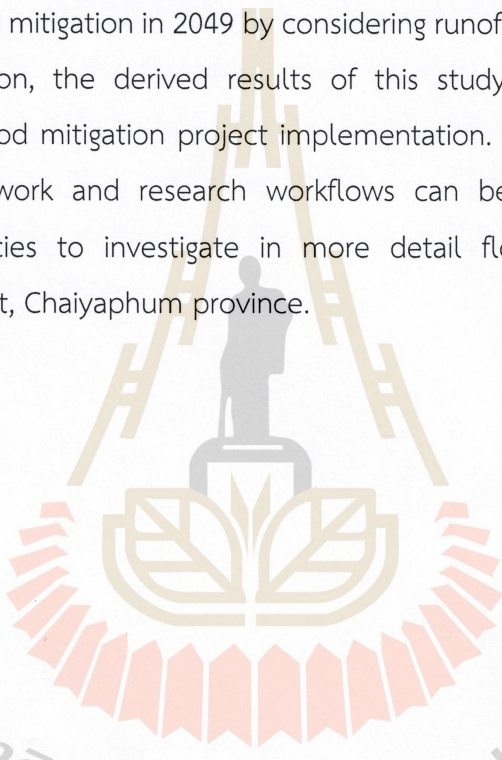
School of Geoinformatics

Academic Year 2021

Student's Signature_____

Advisor's Signature_____

ACKNOWLEDGEMENTS

CONTENTS

CONTENTS (Continued)

CONTENTS (Continued)

CONTENTS (Continued)

CONTENTS (Continued)

LIST OF TABLES

LIST OF TABLES (Continued)

LIST OF TABLES (Continued)

LIST OF TABLES (Continued)

LIST OF TABLES (Continued)

LIST OF FIGURES

LIST OF FIGURES (Continued)

LIST OF FIGURES (Continued)

LIST OF FIGURES (Continued)

LIST OF FIGURES (Continued)

LIST OF FIGURES (Continued)

LIST OF FIGURES (Continued)

LIST OF FIGURES (Continued)

LIST OF ABBREVIATIONS

AMC	=	Antecedent moisture condition
AUC	=	Area under curve
CART	=	Classification and regression trees
CLUE-S	=	Conversion of Land Use and its Effects at Small regional extent
CN	=	Curve number
DEM	=	Digital elevation model
ESV	=	Ecosystem service value
GIS	=	Geographic Information System
GP	=	Goal programming
HSG	=	Hydrologic soil group
LDD	=	Land Development Department
LP	=	Linear programming
LULC	=	Land use and land cover
MNDWI	=	Modified Normalized Difference Wetness Index
MODA	=	Multi-objective Decision Analysis
MSL	=	Mean Sea Level
NDBI	=	Normalized Difference Built-up Index
NDVI	=	Normalized Difference Vegetation Index
NDWI	=	Normalized Difference Wetness Index
NSE	=	Nash and Sutcliffe's coefficient of efficiency
NSO	=	National Statistical Office
OA	=	Overall accuracy
OAE	=	Office of Agricultural Economics
PA	=	Producer's accuracy
PBIAS	=	Percent of bias
PV	=	Present value
R^2	=	Coefficient of determination

LIST OF ABBREVIATIONS (Continued)

RE   =   Relative Error

RF   =   Random Forests

RID   =   Royal Irrigation Department

RMSE   =   Root Mean Square Error

ROC   =   Receiver operating characteristics

RS   =   Remote Sensing

SCS-CN   =   Soil Conservation Service Curve Number

SPI   =   Standardized Precipitation Index

SWAT   =   Soil and Water Assessment Tool

UA   =   User's accuracy

USDA   =   United States Department of Agriculture

VIF   =   Variance inflation factor

WGP   =   Weighted goal programming

CHAPTER I

INTRODUCTION

1.1 Background problems and significance of the study

Flood represents one of the most severe natural disasters threatening the development of human society worldwide, including Thailand. It has caused enormous losses to economies, societies, and ecological environments (Yu et al., 2018). Besides, the flood-related damage to agriculture and other related activities resulted in the country's economy and development (Jothityangkoon, Maskong, Sangthong, and Kosa, 2015).

In general, the primary cause of the flooding is heavy rainfall. However, many other causes are also due to human activities, such as land degradation, deforestation of catchment areas, urban growth and increased population along riverbanks (Mbow, Diop, Diaw, and Niang, 2008), poor land use planning, zoning, and control of flood plain development, poor drainage particularly in cities, and insufficient management of discharges from river reservoirs (Danumah, 2016).

In recent decades, Chaiyaphum province has experienced a problem with flooding almost every year. It has caused a loss of lives and affected economic losses, asset or housing losses, inundated farmlands, and decreased crop productivity to people who live in this area. According to the Department of Disaster Prevention and Mitigation report, Ministry of Interior in 2019, floods in 2010 caused property damage of 495 million Baht. More than 322,000 persons were affected. At least seven persons lost their lives, agricultural productions were affected by about 1,046.4 km^2, and more than 1,000 facilities (school, temple, government place, road, etc.) were affected (Department of Disaster Prevention and Mitigation, 2019). The summary of flood damage in Chaiyaphum province between 2006 and 2018 is presented in Table 1.1. In addition, the spatial distribution of flood of GISTDA (Geo-Informatics and Space Technology Development Agency) between 2005 and 2018 is displayed in Figure 1.1.

Table 1.1 Flood damage in Chaiyaphum province between 2006 and 2018.

	Flood damage in Chaiyaphum province												
Year	People (person)	Household	Evacuate (person)	Deaths (person)	Missing (person)	Livestock	Agricultural area (km²)	Fish/Shrimp Pond	Road	Temples	Schools	Government places	Compensate Budget (Baht)
2006	2,354	710	156	11	-	-	395.60	-	113	-	-	-	288,253,679
2007	21,258	5,898	210	6	-	21	34.36	326	133	-	1	7	34,805,174
2008	296,345	64,621	-	4	-	-	413.85	2,935	874	-	-	-	139,753,922
2009	204,866	82,817	-	-	-	99,276	124.26	-	201	-	-	-	165,127,287
2010	322,341	85,496	60	7	-	123	1,047.23	8,278	938	6	-	1	495,427,300
2011	-	71,335	-	12	-	-	721.33	9,452	871	-	-	-	98,155,417
2012	108,677	30,566	-	-	-	635	179.06	388	282	-	-	-	-
2013	289,471	108,522	1	3	-	1,270	805.75	5,836	1,598	4	1	-	53,296,320
2014*	-	-	-	-	-	-	-	-	-	-	-	-	-
2015*	-	-	-	-	-	-	-	-	-	-	-	-	-
2016	136,494	48,211	-	-	-	-	771.98	1,816	592	3	2	-	56,837,481
2017	10,940	4,795	-	-	1	35	234.49	244	134	-	1	-	4,684,859
2018	54,219	33,745	-	-	-	384	667.38	1,892	300	4	2	-	12,279,214

Source: Department of Disaster Prevention and Mitigation (2019).

* Data is not available.

Due to the risk of large-scale damage to public and private property in Chaiyaphum province, the Royal Thai Government has allocated a significant budget to mitigate flood effects using structural measures, such as channel modification, bank protection, dikes, and reservoir development. However, problems persist and are becoming exacerbated (Sriwongsitanon, 2010). Because it is difficult to fundamentally mitigate flood damage using only flood prevention facilities (Banba, 2016), a comprehensive flood control measure should consider land use and land cover change and optimum land use allocation.

Tajbakhsh, Memarian, and Kheyrkhah (2018) stated that LULC strongly influences flood risk and affects the probability of flood and its consequences in several ways. LULC change can affect the hydrological characteristics of a river basin through the influences of land uses on the runoff generation processes. This study chooses the SCS-CN method, which represents a distributed hydrologic model, to estimate the time-series surface runoff according to LULC changes in the study period

(2001-2019). These changes may alter the quantity of surface/subsurface runoff generation, river flooding regimes, and extent. (Kuntiyawichai, 2012). Therefore, defining optimal strategies for appropriate flood management, especially LULC management, is very important and necessary (Tingsanchali and Karim, 2010) for flood mitigation in Chaiyaphum province.
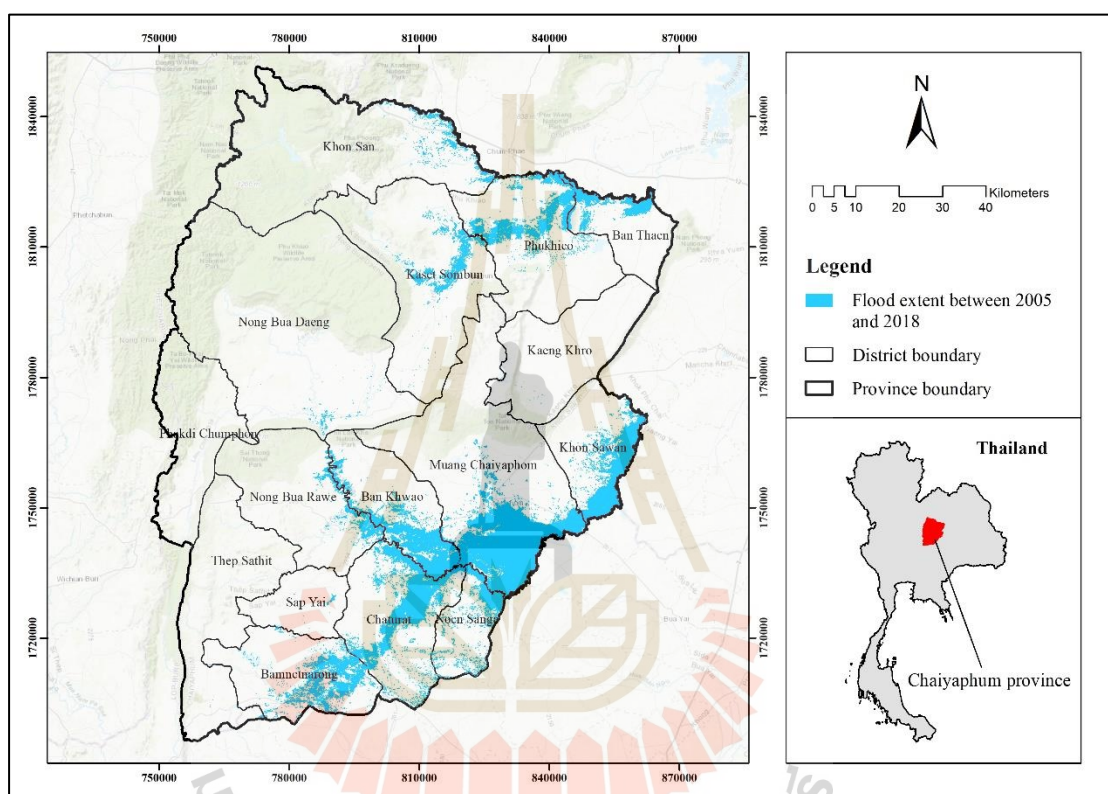
Source: Geo-Informatics and Space Technology Development Agency (2019).

Figure 1.1 Spatial distribution of cumulative flood of Chaiyaphum province between 2005 and 2018.

Land use optimization is one of the proper solutions for soil and water conservation at the watershed level. It can help decision-makers determine the best scenario of various land use alternatives without sacrificing economic values obtained from the available land use (Riedel, 2003; Sadeghi, Jalili, and Nikkami, 2009). Land use arrangement can be optimized using a programming model to increase land use earnings and reduce environmental impacts, especially surface runoff (Riedel, 2003). The essence of management science manifested in the modeling and programming

techniques is considered an essential tool for allocating rare resources optimally to gain the most benefits (Nikkami, Elektorowicz, and Mehuys, 2002).

In recent decades, new programming methods developed can be employed under conflicting conditions of the goals and limited resources for decision-maker. In natural resources management, there are many optimization techniques. Still, some approaches like linear programming (LP), and goal programming (GP), or weighted goal programming (WGP) are widely employed in land use optimization at the watershed level (Tajbakhsh et al., 2018). For instance, Owji, Nikkami, Mahdian, and Mahmoudi (2012) applied linear programming for land use optimization in the Jajrood watershed, Iran, to reduce surface runoff and sediment yield. Yeo, Gordon, and Guldmann (2004) applied the LP to optimize land use to peak discharge minimization at Old Woman Cheek watershed, Ohio State, USA. Likewise, the WGP was applied to optimize LULC allocation for surface runoff and sediment load minimization at the Bayg watershed by Tajbakhsh et al. (2018). Similarly, Gonfa and Kumar (2015) applied the LP and GP for optimum land use to minimize soil erosion and maximize net benefit in Ethiopia's Mojo watershed. Recently, Al-Zahrani, Musa, and Chowdhury (2016) developed the GP for optimizing water resources in Riyadh, Saudi Arabia.

Therefore, the optimizing LULC allocation for flood mitigation based on the surface runoff coefficient value of LULC types with goal programming at Mueang Chaiyaphum district, Chaiyaphum province, Thailand, is here conducted for the Ph.D. thesis. Consequently, the derived results can be used as a guideline to relevant government agencies, particularly the Land Development Department, Royal Irrigation Department, Department of Disaster Prevention and Mitigation, and Department of Public Works and Town & Country Planning to investigate in more detail flood mitigation at the watershed level.

In this study, a novel classification method, Random Forests, was first applied to classify LULC maps. Then, they are used to predict a time-series LULC between 2001 and 2019 by the CLUE-S model for time-series surface runoff estimation using the SCS-CN model with suitable antecedent moisture condition (AMC). After that, LULC allocation for flood mitigation based on the average runoff coefficient of LULC type between 2001 and 2019 under three different rainfall conditions according to the

Standardized Precipitation Index (SPI) was optimized using goal programming for the years 2029, 2039, and 2049. Finally, economic and ecosystem service value change between the existing LULC data in 2019 and the optimizing LULC allocation in three different years were examined using the present value (PV) model and the simple benefit transfer method for gain and loss evaluation.

1.2   Research objectives

The Ph.D. research aims to optimize LULC allocation for flood mitigation at Mueang Chaiyaphum district, Chaiyaphum province, Thailand, by the integration of advanced LULC classification method (RF), land use change modeling (CLUE-S), distributed hydrological model (SCS-CN), and goal programming (What's Best!). Specific research objectives are set as follows:

(1)   To classify LULC data in 2001, 2010, and 2019 using Random Forests classifier;

(2)   To predict LULC change in two periods (2002-2009 and 2011-2018) based on historical LULC in 2001, 2010, and 2019 using CLUE-S model;

(3)   To estimate surface runoff from 2001 to 2019 using SCS-CN method;

(4)   To optimize LULC allocation for flood mitigation based on average runoff coefficient of LULC type between 2001 and 2019 under three different rainfall conditions using goal programming;

(5)   To map an optimizing LULC allocation under three different rainfall conditions for flood mitigation of Mueang Chaiyaphum district, Chaiyaphum province using CLUE-S model; and

(6)   To examine economic and ecosystem service evaluation and change of optimizing LULC allocation under three different rainfall conditions using the PV model and simple benefit transfer method in terms of gain and loss for project implementation

1.3   Scope and limitations of the study

1.3.1   Scope of the study

The scope of the study can be summarized as follows:

(1) LULC data in 2001, 2010, and 2019 were classified from Landsat 5-TM and Landsat 8-OLI data using the RF classifier under EnMAP-Box software. Here, the LULC classification system consists of (1) urban and built-up area, (2) paddy field, (3) sugarcane, (4) cassava, (5) other field crops, (6) para rubber, (7) perennial trees and orchards, (8) forest land, (9) water body, (10) rangeland, (11) marsh and swamp, and (12) unused land.

(2) Driving forces for LULC prediction were identified by multicollinearity test and binary logistic regression analysis based on driving forces for LULC change, including physical, proximity, and socio-economic factors. In this study, an optimum local parameter of the CLUE-S model was validated by comparing the predicted LULC map in 2019 and the classified LULC map in 2019 using overall accuracy and Kappa hat coefficient of agreement. Herein, the accepted values of overall accuracy and Kappa hat coefficient of the agreement should be equal or more than 80 percent.

(3) LULC prediction data of two periods (2002-2009 and 2011-2018) were conducted to create time-series LULC data between 2001 and 2019 using the CLUE-S model based on the optimum local parameter, elasticity value, LULC conversion matrix, and land requirement of each LULC type based on historical LULC development from three classified LULC data (2001, 2010, and 2019) using Markov Chain model.

(4) The SCS-CN method was used to estimate time-series surface runoff between 2001 and 2019 based on LULC, soil, and annual rainfall data in each respective year. Herein, observed runoff data between 2001 and 2010 of E.21, E.23, and E.6C hydrological stations of the RID were used to identify suitable AMC for surface runoff estimation while observed runoff data between 2011 and 2019 from those stations were applied to validate the result of the SCS-CN method for surface runoff estimation.

(5) The SPI was used to identify three different rainfall conditions: drought, normal, and wet years between 2001 and 2019. Then the average annual surface runoff volume of each LULC type under three different rainfall conditions was calculated to represent the surface runoff coefficient of each LULC type for surface runoff minimization.

(6) The goal programming of multi-objective decision analysis (MODA) was applied to allocate LULC to minimize surface runoff for flood mitigation based on the surface runoff coefficient of each land use type between 2001 and 2019 under three different rainfall conditions with the "What's Best!" extension of MS-Excel software. The constraints for optimizing LULC allocation under three different rainfall conditions were assigned for LULC in 2029, 2039, and 2049 based on the historical LULC development between 2010 and 2019 using the Markov Chain model. This study will examine for LULC change every ten years according to historical LULC development and cover 30 years of long terms reforestation program.

(7) Economic and ecosystem service value and change were separately evaluated using the present value (PV) model and simple benefit transfer method based on LULC data in 2019 and the optimizing LULC allocation data for flood mitigation under three different rainfall conditions and in terms of gain and loss.

1.3.2 Limitation of the study

The limitation of the study can be summarized as follows:

(1) Due to the limitation of the existing ground reference information on LULC type in 2001 and 2010, color orthophotograph in 2000-2001 was used as reference ground information to perform a thematic accuracy assessment of the LULC map 2001. Meanwhile, very high spatial resolution imageries from Google Earth in 2010 were applied as reference ground information for the thematic accuracy assessment of LULC classification in 2010.

1.4 Study area

The study area is the Second Part of the Lam Nam Chi watershed, covering approximately 3,794 km^2. It is a part of the Chi River Basin. The selected study area

covers the flood-prone area at Mueang Chaiyaphum district, Chaiyaphum province, as mentioned earlier in the background problems and significance of the study.

The topography of the area is generally characterized by hilly-rolling terrain and flat areas. Elevation ranges from 162 meters above mean sea level (MSL) in the lower part of the watershed to about 1,034 meters above MSL in the upper part of the watershed (Figure 1.2). Based on the reconnaissance soil survey at a scale of 100,000, the study area consists of 32 soil series types that can be grouped by soil texture property into nine soil groups: clay, clay loam, loam, loamy sand, sandy loam, sandy clay loam, silty clay, silty loam, and silty clay loam (Figure 1.3). In the year 2015, the top three dominant agriculture types are paddy field (43.47%), cassava (12.69%), and sugarcane (9.18%), while forest land includes dense and disturbing evergreen and deciduous forests, and forest plantation account for 12.48%. Meanwhile, other land use types include urban and built-up area, perennial trees and orchards, waterbody, and miscellaneous land cover area of 4.62%, 5.70%, 4.11%, and 7.67%, respectively (Figure 1.4).
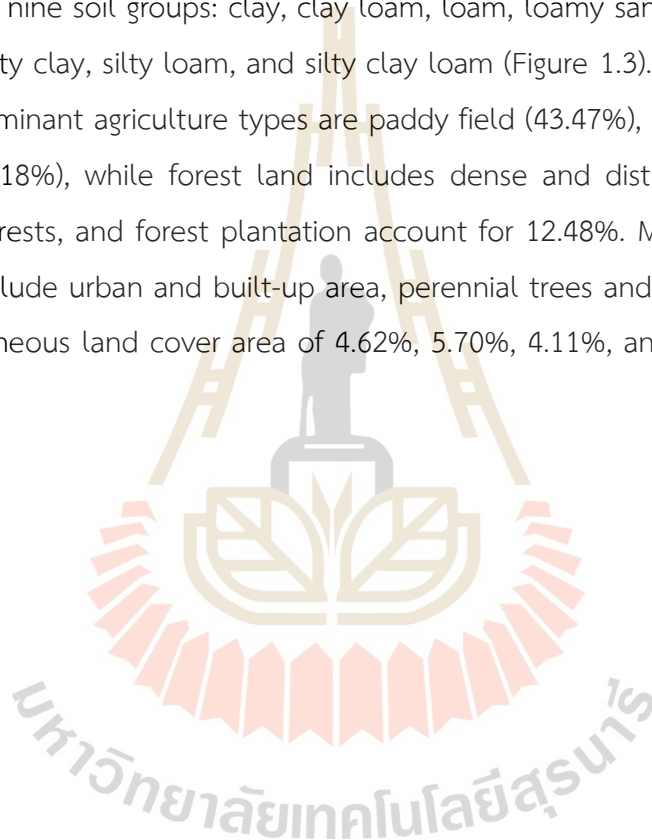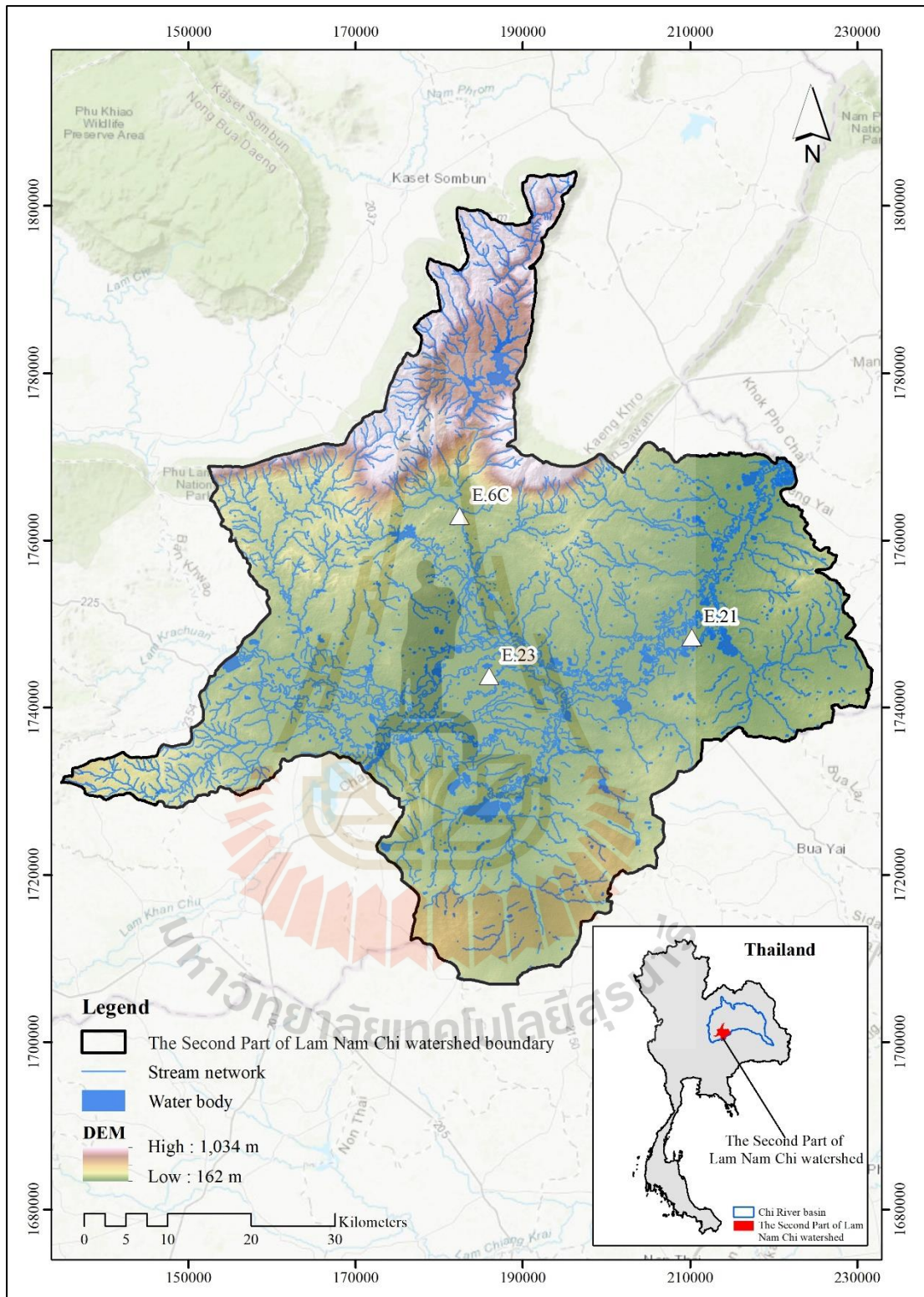
Figure 1.2 Terrain characteristics of the study area and location of RID hydrologic stations.
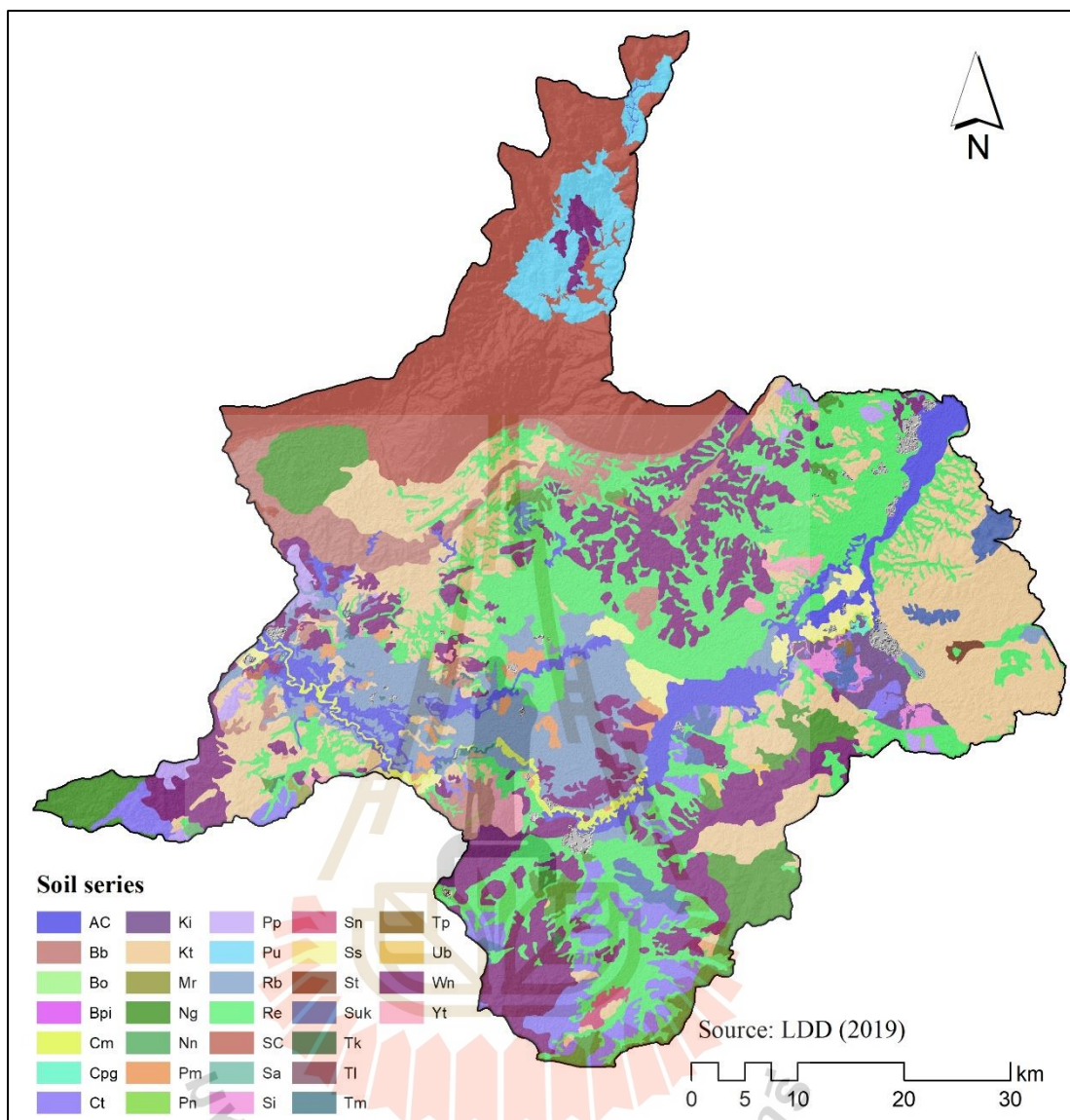
Figure 1.3 Spatial distribution of soil series in the study area.
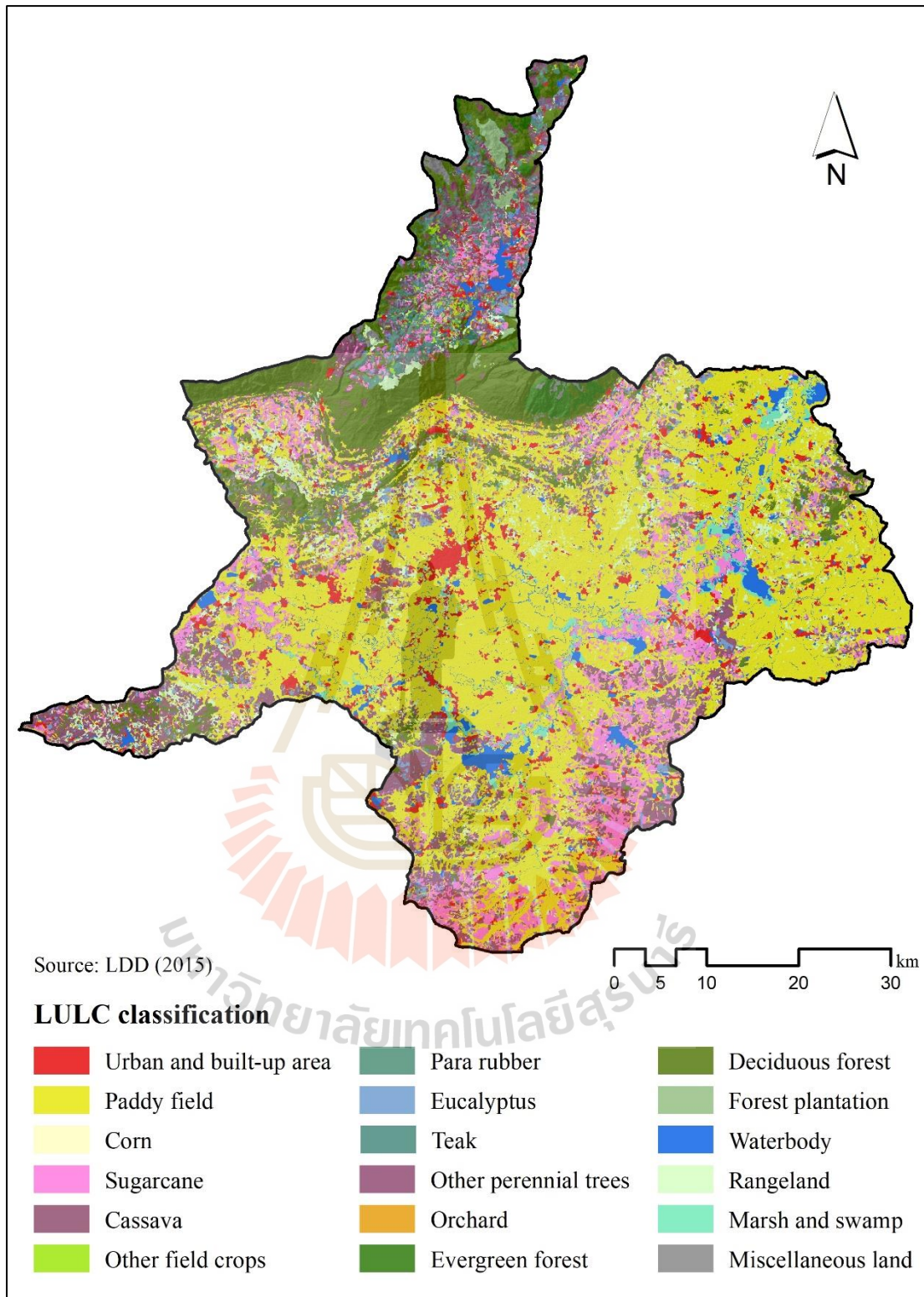
Figure 1.4 Spatial distribution of LULC in 2015 in the study area.

1.5   Benefits of the study

The benefits of the study, which are covered all research objectives, are as follow:

(1) LULC data in 2001, 2010, and 2019 by using Random Forests classifier,

(2) An optimum local parameter for LULC prediction by using the CLUE-S model,

(3) Time-series classified and predicted LULC data between 2001 and 2019,

(4) Time-series estimated surface runoff data between 2001 and 2019,

(5) Rainfall conditions (drought, normal and wet year) in the study area according to SPI calculation from historical records of rainfall data between 1987 and 2019,

(6) Optimizing LULC allocation for flood mitigation based on the average surface runoff coefficient of each LULC type between 2001 and 2019 under three different rainfall conditions in 2029, 2039, and 2049 using goal programming,

(7) Optimizing LULC allocation map in 2029, 2039, and 2049 for flood mitigation in the future,

(8) Basic information on economic and ecosystem service value change in terms of gain and loss for flood mitigation project implementation, and

(9) The research methodology framework can guide relevant government agencies for a detailed study on flood mitigation at the watershed level.

CHAPTER II

RELATED CONCEPTS AND LITERATURE REVIEWS

Related concepts and literature reviews of this study, including (1) Random Forests classifier, (2) CLUE-S model, (3) SCS-CN method, (4) Linear and goal programming, and (5) Standardized Precipitation Index, are summarized and synthesized in this chapter.

2.1   Random Forests classifier

A relatively new algorithm that uses a binary decision tree classification is called Random Forests (RF). The RF algorithm firstly creates several decision trees, and the collection of trees container is then used to classify an image. Classification accuracy using RF is higher than using a single tree approach such as classification and regression trees (CART) (Gislason, Benediktsson, and Sveinsson, 2006), and there is no need to edit the trees, so it is much easier to use when compared to other binary decision tree approaches.

The RF, which Breiman firstly developed in 2001, is an ensemble and multiple-decision-tree classifier for supervised classification. It confides in the assumption that different independent predictors predict incorrectly in changed areas. Combining the prediction results makes it possible to improve the overall prediction accuracy (Polikar, 2006). The RF offers several advantages for classification include:

(1) Data can be binary, categorical, or continuous;

(2) The classifier performs internal cross-validation through "bootstrapping," which provides a robust estimate of classification accuracy using out of bag estimates;

(3) It is a non-parametric classifier and is relatively insensitive to outliers in the training data;

(4) It requires little user input (the number of decision trees and the number of variables for each decision tree);

(5) It produces a classification map, but more importantly, probability maps (strength of membership in each lithological class); and

(6) It ranks the input variables with respect for their importance in the predictions (Breiman, 2001; Breiman, Friedman, Olshen, and Stone, 1984).

Breiman (2001) stated that training data is required for the RF approach, similar to other supervised classifiers. In each tree, the number of decision trees is first determined by the operator, a random selection of the input variables (i.e., remotely sensed image bands are then made. The number of variables selected for each tree is a fraction of the total number of variables; the square root of the number of variables is often used. Each tree employs a "bagging" process (i.e., "bootstrap" sample) whereby approximately two-thirds of the training areas (pixels) are used to create a prediction (referred to as in-bag) and one-third to validate the accuracy of the prediction (referred to as out of the bag, or OOB). This random sampling with the replacement of the training dataset is undertaken for every tree. In-bag data are used to create multiple decision trees that are applied to produce independent classifications. The best split is chosen from a random sample of variables at each node of the individual decision tree. Each tree is grown to the maximum extent with no pruning. In practice, the Gini index is applied to determine the impurity at each node (Harris and Grunsky, 2015) as:

$$\text{Gini Index} = \sum_{c=1}^{K} g_c(1\text{-}g_c) \tag{2.1}$$

where K is the number of classes and g_c is the probability or the relative frequency of class c at the considered node and is given by

$$g_c = \frac{n_c}{n} \tag{2.2}$$

where n_c is the number of samples belonging to class c and n is the total number of samples within a particular node.

The stop criterion for splitting each node is based on the minimum of samples in a node (used 1) and the minimum impurity in a node (used 0), allowing the full growth of the decision trees (no pruning). Thus, an ensemble of trees (predictions) is

created, and a voting procedure is employed to assign the majority class to each pixel in the final prediction map (Breiman, 2001).

According to Breiman (2001) and Gislason et al. (2006), the RF is not sensitive to noise or over-fitting. There is no need for cross-validation as it is estimated internally. However, as with any supervised classification method, an independent check of the training dataset of each litho-type is still required to calculate an unbiased and more robust estimate of classification accuracy. Additionally, the probability of membership in each class is also generated, which can be used to assess the uncertainty of the RF classification.

Harris and Grunsky (2015) summarized the RF classification process, as shown in Figure 2.1.
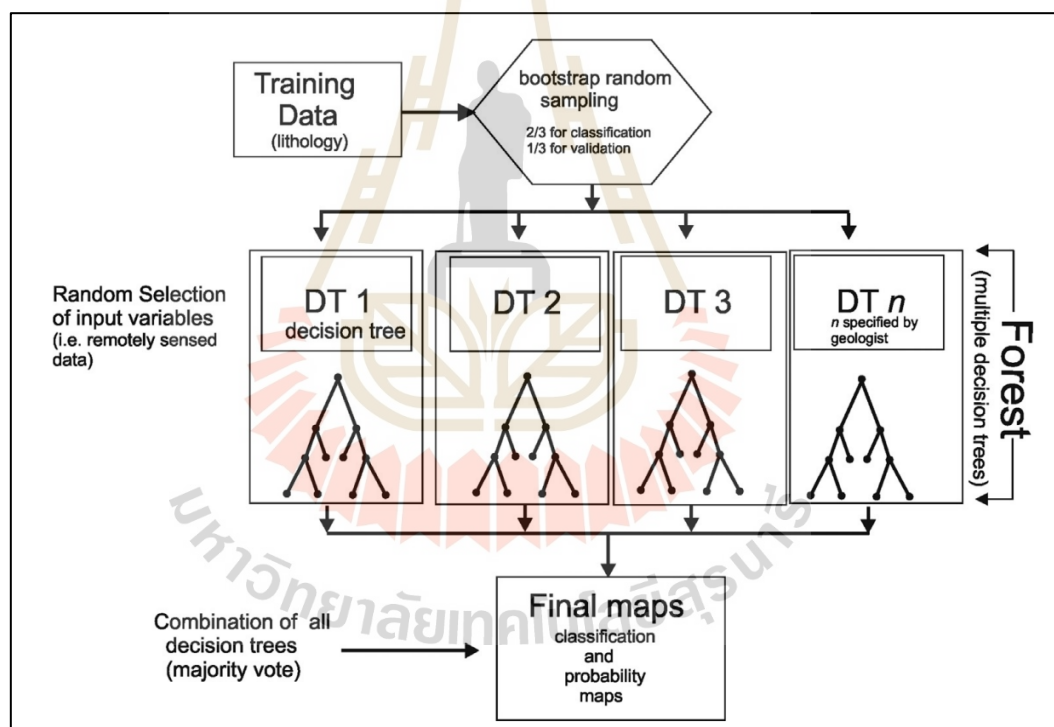
Source: Harris and Grunsky (2015).

Figure 2.1 Summary of the RF classification process.

2.2   CLUE-S model

The Conversion of Land Use and its Effects (CLUE) modeling framework was developed to simulate land use change using empirically quantified relations between land use and its driving factors in combination with dynamic modeling (Veldkamp and

Fresco, 1996; Verburg, De Koning, Kok, Veldkamp, and Bouma, 1999). This model was developed for the national and continental levels. Verburg et al. (2002) claimed that the study areas, to a large extent, the spatial resolution for analysis was coarse or pixel size varying between 7x7 and 32x32 km. For instance, Central America (Kok and Winograd, 2002), Ecuador (de Koning, Verburg, Veldkamp, and Fresco, 1999), China (Verburg, Chen, and Veldkamp, 2000), and Indonesia (Verburg, Veldkamp, and Bouma, 1999) are available. Each land use is represented by assigning the relative cover of each land use type to the pixels. However, the CLUE model cannot directly be applied at the regional scale.

Therefore, the modeling approach has been modified and is now called CLUE-S (Conversion of Land Use and its Effects at Small regional extent). Verburg (2010) stated that the CLUE-S is developed explicitly for the spatially explicit simulation of land use change based on an empirical analysis of location suitability combined with the dynamic simulation of competition and interactions between the spatial and temporal dynamics of land use systems. Figure 2.2 shows an overview of the information needed to run the CLUE-S model. The required information of CLUE-S can categorize into four groups: (1) spatial policies and restrictions, (2) specific land use type conversion settings, (3) land requirements, and (4) location characteristics (Verburg, 2010; Verburg and Lesschen, 2014).
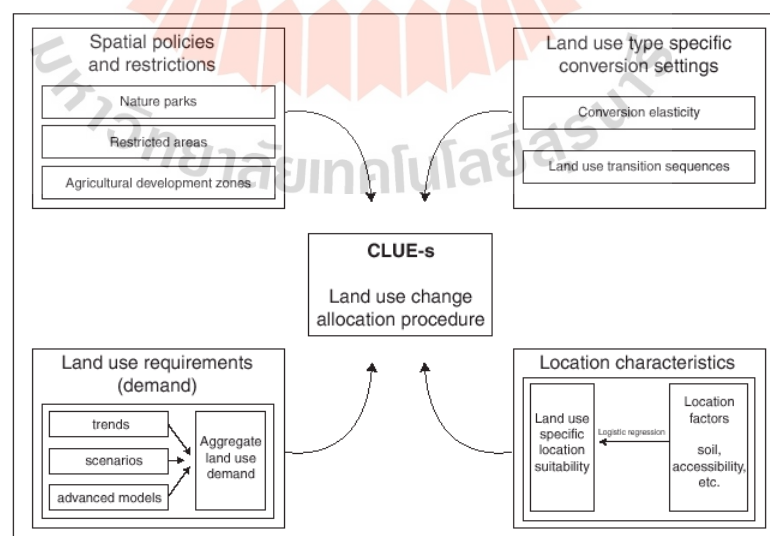
Source: Verburg (2010).

Figure 2.2 Overview of the information flow in the CLUE-S model.

(1) Spatial policies and restrictions

Spatial policies and restrictions mainly indicate areas where land use changes are restricted through policies or tenure status. Some spatial policies restrict all land use change in a particular area, e.g., a log-ban within a forest reserve. Other land use policies restrict a set of specific land use conversions, e.g., residential construction in designated agricultural areas or permanent agriculture in the buffer zone of a nature reserve. The conversions restricted by a specific spatial policy can be indicated in a land use conversion matrix: for all possible land use conversions, it is indicated if the spatial policy applies (Verburg, 2010; Verburg and Lesschen, 2014).

(2) Specific land use type conversion settings

Specific land use type conversion settings determine the temporal dynamics of the simulations. Therefore, two sets of parameters are needed to characterize the individual land use types: conversion elasticities and land use transition sequences.

The first parameter set, the conversion elasticities, is related to the reversibility of land use change. Land use types with the high capital investment will not easily be converted to other uses as long as there is sufficient demand. Examples are residential locations but also plantations with permanent crops (e.g., fruit trees). Other land use types easily shift location when the location becomes more suitable for other land use types. Therefore, the land use type must specify the relative elasticity to change from 0 (easy conversion) to 1 (not allow).

The second set of land use type characteristics that need to be specified include land use type conversion settings and their temporal characteristics. These settings are specified in a conversion matrix. Verburg (2010) suggested that the conversion matrix definition should be answered the following questions:

- What other land use types the present land use type can be converted or not.

- Which regions a specific conversion is allowed to occur and in which regions it is not allowed.

- How many years (or time steps) the land use type at a location should remain the same before changing into another land use type.

(3) Land use requirements (demand)

Land use requirements (demand) are calculated at the aggregate level as part of a specific scenario. Land use requirements constrain the simulation by defining the total required change in land use. All changes in individual pixels should add up to these requirements. The extrapolation of trends in land use change of the recent past into the near future is a common technique to calculate land use requirements (Verburg, 2010; Verburg and Lesschen, 2014).

(4) Location characteristics

Land use conversions are expected to occur at locations with the highest preference for the specific type of land use at that moment in time. The preference of a location is empirically estimated from a set of factors based on the different disciplinary understandings of the determinants of land-use change. The preference is calculated using the following equation:

$$R_{ki} = a_k X_{1i} + b_k X_{2i} + ...$$ (2.3)

where R is the preference to devote location, i to land use type, k, $X_{1,2,...,}$ are biophysical or socio-economical characteristics of the location, i and a_k and b_k the relative impact of these characteristics on the preference for land use type k.

A statistical model can be developed as a binomial logit model of two choices: convert location i into land use type k or not. The preference R_{ki} is assumed to be the underlying response of this choice. However, the preference R_{ki} cannot be observed or measured directly and must be calculated as a probability. The function that relates these probabilities with the biophysical and socio-economic location characteristics is defined as a logit model using the following equation:

$$\text{Log}\left(\frac{P_i}{1-P_i}\right) = \beta_0 + \beta_1 X_{1,i} + \beta_2 X_{2,i} ..... + \beta_n X_{n,i}$$ (2.4)

where P_i is the probability of a grid cell for the occurrence of the considered land use type on location i, and the X is the location factors. The coefficients (β) are estimated through logistic regression using the actual land use pattern as the dependent variable (Verburg, Koning, Koning, Veldkamp, and Bouma, 1999).

In summary, the allocation procedure is displayed in Figure 2.3. The following steps are taken to allocate the changes in land use:

(1) The first step includes the determination of all grid cells that are allowed to change. Grid cells that are either part of a protected area or presently under a land use type that is not allowed to change are excluded from the further calculation. Also, the locations where specific conversions are not allowed due to the specification of the conversion matrix are identified.

(2) For each grid cell i, the total probability ($TPROP_{i,u}$) is calculated for each of the land use types u according to:

$$TPROP_{i,u} = P_{i,u} + ELAS_u + ITER_u \tag{2.5}$$

where $P_{i,u}$ are the suitability of location i for land use type u (based upon the logit model), $ELAS_u$ is the conversion elasticity for land use u, and $ITER_u$ is an iteration variable that is specific to the land use type and indicative for the relative competitive strength of the land use type. $ELAS_u$, the specific land use type elasticity to change the value, is only added if grid-cell i is already under land use type u in the year considered. $P_{i,u}$ consists of a part based on the biophysical and socio-economic factors and a neighborhood interaction part.

(3) A preliminary allocation is made with an equal value of the iteration variable ($ITER_u$) for all land use types by allocating the land use type with the highest total probability for the considered grid cell. Conversions that are not allowed according to the conversion matrix are not allocated. This allocation process will cause a certain number of grid cells to change land use.

(4) The total allocated area of each land use is now compared to the land use requirements (demand). For land use types where the allocated area is smaller than the demanded area, the value of the iteration variable is increased. For land use types for which too much is allocated, the value is decreased. Through this procedure, the local suitability based on the location factors may be overruled by the iteration variable due to the differences in regional demand. The procedure followed balances the bottom-up allocation based on location suitability and the top-down allocation based on regional demand.

Steps 2 to 4 are repeated as long as the demands are not correctly allocated. When allocation equals demand, the final map is saved, and the calculations can continue for the next time step. Some of the allocated changes are irreversible, while

others depend on the changes in earlier steps. Therefore, the simulations tend to result in complex, non-linear changes in land use patterns, characteristics for complex systems (Verburg, 2010; Verburg and Lesschen, 2014).
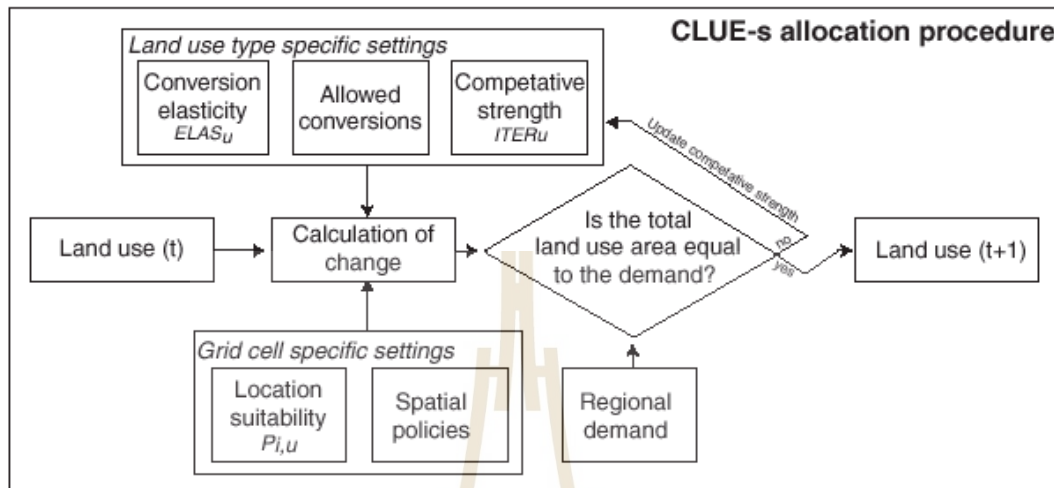
Source: Verburg (2010).

Figure 2.3 Flow chart of the allocation module of the CLUE-S model.

2.3   SCS-CN method

The Soil Conservation Service Curve Number (SCS-CN) method (now called Natural Resources Conservation Service Curve Number, NRCS-CN method) was developed by the United States Department of Agriculture (USDA) for estimating total storm runoff from total storm rainfall. This method estimates direct runoff, consisting of channel runoff, surface runoff, and an unknown proportion of subsurface runoff (National Resources Conservation Service, 2004). Developing the runoff curve number from field experiments of runoff in small catchments is presented in Technical Release 55 (TR-55) (United States Department of Agriculture, 1986). The curve number (CN) determination depends on the watershed's soil and covers conditions representing a hydrologic soil group, cover type, treatment, and hydrologic condition.

In principle, the SCS-CN method is based on the water balance equation and two fundamental hypotheses. The first hypothesis equates the ratio of the actual amount of direct surface runoff (Q) to the total rainfall (P), the amount of actual infiltration (F), and the initial abstraction (I_a). The second hypothesis shows relationships

among I_a, the amount of the potential maximum retention (S). Thus, the CN method consists of the following equations (Mishra and Singh, 2003):

(a) Water balance equation

$$P = I_a + F + Q \qquad (2.6)$$

(b) Proportional equality hypothesis

$$\frac{Q}{P - I_a} = \frac{F}{S} \qquad (2.7)$$

(c) I_a-S hypothesis

$$I_a = \lambda S \qquad (2.8)$$

where P is total rainfall; I_a is an initial abstraction; F is cumulative infiltration excluding I_a; Q is direct surface runoff; S is potential maximum retention; λ is regional parameter dependent on geologic and climate factors ($0.1 \leq \lambda \leq 0.3$). The I_a consists mainly of interception, infiltration, antecedent soil moisture, and depression storage, all of which occur before surface runoff begins (Grunwald and Norton, 2000). The relation between I_a and S was developed by analyzing the rainfall-runoff data from experiments in small watersheds and expressed as $I_a = 0.2S$. Combining the water balance equation and proportional equality hypothesis, the CN equation is presented as:

$$Q = \frac{(P - I_a)^2}{P - I_a + S} \qquad (2.9)$$

Eq. (9) is valid for $P > I_a$; otherwise, $Q=0$. For $\lambda = 0.2$, Eq. (10) can be written as:

$$Q = \frac{(P - 0.2S)^2}{P + 0.8S} \qquad (2.10)$$

The parameter S in Eq. (11) is defined as:

$$S = \frac{1000}{CN} - 10 \qquad (2.11)$$

where S is measured in inch, and CN is curve number values, which vary based on land use, land treatment, hydrologic soil group, and antecedent moisture condition (AMC) of the watershed. Mohammed, Yohannes, and Zeleke (2004) suggested that the CN values are the most sensitive parameter, should be carefully determined through field assessment based on local conditions such as cultural practices, land use, and topography. Figure 2.4 and Table 2.1 solve equations 2.10 and 2.11 for a range of CNs and rainfall.
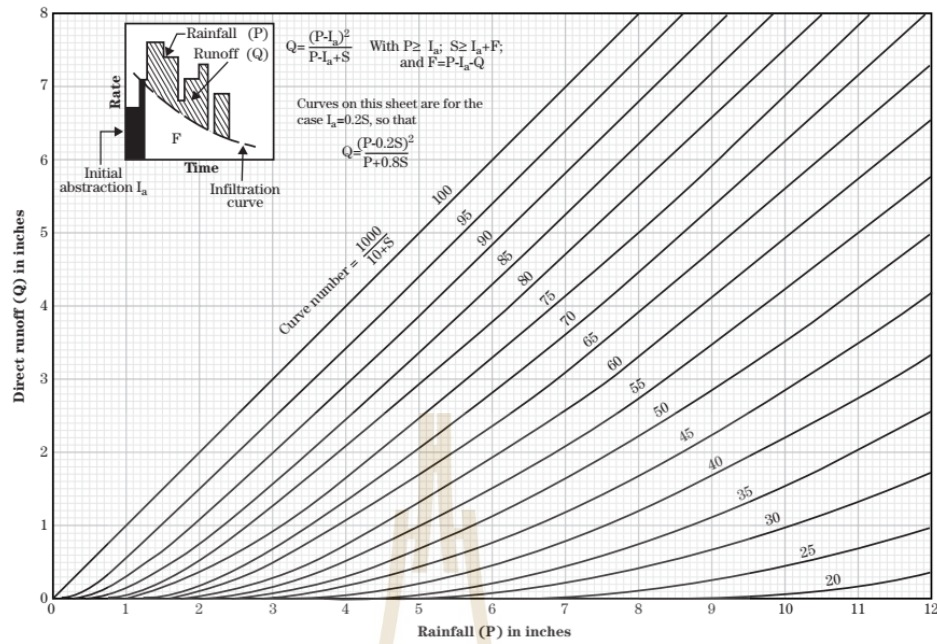
Source: National Resources Conservation Service (2004).

Figure 2.4 Solution of runoff equation.

Table 2.1 Runoff depth for selected CNs and rainfall amounts[1].

Rainfall	Runoff depth for curve number of -												
	40	45	50	55	60	65	70	75	80	85	90	95	98
1.0	0.00	0.00	0.00	0.00	0.00	0.00	0.00	0.03	0.08	0.17	0.32	0.56	0.79
1.2	0.00	0.00	0.00	0.00	0.00	0.00	0.03	0.07	0.15	0.27	0.46	0.74	0.99
1.4	0.00	0.00	0.00	0.00	0.00	0.02	0.06	0.13	0.24	0.39	0.61	0.92	1.18
1.6	0.00	0.00	0.00	0.00	0.01	0.05	0.11	0.20	0.34	0.52	0.76	1.11	1.38
1.8	0.00	0.00	0.00	0.00	0.03	0.09	0.17	0.29	0.44	0.65	0.93	1.29	1.58
2.0	0.00	0.00	0.00	0.02	0.06	0.14	0.24	0.38	0.56	0.80	1.09	1.48	1.77
2.5	0.00	0.00	0.02	0.08	0.17	0.30	0.46	0.65	0.89	1.18	1.53	1.96	2.27
3.0	0.00	0.02	0.09	0.19	0.33	0.51	0.71	0.96	1.25	1.59	1.98	2.45	2.77
3.5	0.02	0.08	0.20	0.35	0.53	0.75	1.01	1.30	1.64	2.02	2.45	2.94	3.27
4.0	0.06	0.18	0.33	0.53	0.76	1.03	1.33	1.67	2.04	2.46	2.92	3.43	3.77
4.5	0.14	0.30	0.50	0.74	1.02	1.33	1.67	2.05	2.46	2.91	3.40	3.92	4.26
5.0	0.24	0.44	0.69	0.98	1.30	1.65	2.04	2.45	2.89	3.37	3.88	4.42	4.76
6.0	0.50	0.80	1.14	1.52	1.92	2.35	2.81	3.28	3.78	4.30	4.85	5.41	5.76
7.0	0.84	1.24	1.68	2.12	2.60	3.10	3.62	4.15	4.69	5.25	5.82	6.41	6.76
8.0	1.25	1.74	2.25	2.78	3.33	3.89	4.46	5.04	5.63	6.21	6.81	7.40	7.76
9.0	1.71	2.29	2.88	3.49	4.10	4.72	5.33	5.95	6.57	7.18	7.79	8.40	8.76
10.0	2.23	2.89	3.56	4.23	4.90	5.56	6.22	6.88	7.52	8.16	8.78	9.40	9.76
11.0	2.78	3.52	4.26	5.00	5.72	6.43	7.13	7.81	8.48	9.13	9.77	10.39	10.76
12.0	3.38	4.19	5.00	5.79	6.56	7.32	8.05	8.76	9.45	10.11	10.76	11.39	11.76

Table 2.1 (Continued).

Rainfall	Runoff depth for curve number of -												
	40	45	50	55	60	65	70	75	80	85	90	95	98
13.0	4.00	4.89	5.76	6.61	7.42	8.21	8.98	9.71	10.42	11.10	11.76	12.39	12.76
14.0	4.65	5.62	6.55	7.44	8.30	9.12	9.91	10.67	11.39	12.08	12.75	13.39	13.76
15.0	5.33	6.36	7.35	8.29	9.19	10.04	10.85	11.63	12.37	13.07	13.74	14.39	14.76

[1] Interpolating the values shown to obtain runoff depths for CN's rainfall amounts is not shown.

Source: United States Department of Agriculture (1986).

The SCS-CN method uses a soil cover curve number for computing excess precipitation. The curve number is related to the hydrologic soil group, cover type and treatment, hydrologic condition, antecedent runoff condition, and impervious areas connected/unconnected to the closed drainage system.

2.3.1 Hydrologic soil groups (HSGs)

Hydrologic soil groups (HSGs) are the infiltration rates of soils. According to their minimum infiltration rates, soils are classified into four HSG's (A, B, C, and D), obtained for bare soil after prolonged wetting. The infiltration rate is the rate at which water enters the soil at the soil surface. This factor is controlled by the soil profile (United States Department of Agriculture, 1986). USDA defines the four groups of HSG as follows (National Resources Conservation Service, 2009):

(1) Group A, soil having low runoff potential when thoroughly wet. Water is transmitted freely through the soil. In this group, soils typically have less than 10 percent clay and more than 90 percent sand or gravel and have gravel or sand textures.

(2) Group B, soil having moderately low runoff potential when thoroughly wet. Water transmission through the soil is unimpeded. In this group, soils typically have between 10 percent and 20 percent clay and 50 percent to 90 percent sand and have loamy sand or sandy loam textures.

(3) Group C, soil having moderately high runoff potential when thoroughly wet. Water transmission through the soil is somewhat restricted. In this group, soils typically have between 20 percent and 40 percent clay and less than 50 percent sand and have loam, silt loam, sandy clay loam, clay loam, and silty clay loam textures.

(4) Group D, soil having high runoff potential when thoroughly wet. In this group, soils typically have greater than 40 percent clay, less than 50 percent sand, and have clayey textures.

2.3.2 Cover type and treatment

Cover type and treatment factors are used to prepare hydrological soil-cover complex, which is used in estimating direct runoff. Land use types are classified on runoff production: fallow bare soil, row crops, small grains, legumes or rotation meadow, pasture, brush, vegetation, woods, and farmsteads, including impervious surfaces. For the first four cropping cover types, combinations of treatments describe the land use. The treatment aspect of the cover complex considers the percentage area covered with crop residue and the type of tillage system or combination (National Resources Conservation Service, 2009).

2.3.3 Hydrologic condition

The hydrologic condition (good, fair, or poor) indicates the effects of cover type and treatment on infiltration and runoff. Some factors to consider in estimating the effect of cover on infiltration and runoff are (a) canopy or density of lawns, crops, or other vegetative areas; (b) amount of year-round cover; (c) amount of grass or close-seeded legumes in rotations; (d) percent of residue cover; and (e) degree of surface roughness. The good hydrologic condition indicates that the soil usually has a low runoff potential for that specific hydrologic soil group, cover type, and treatment (National Resources Conservation Service, 2009).

2.3.4 Antecedent runoff condition (ARC)

Antecedent runoff condition (ARC) is the index of runoff potential before a storm event, which is an attempt to account for the variation in the CN at a site from storm to storm. The CN for the average ARC at a site is the median value taken from sample rainfall and runoff data.

2.3.5 Impervious areas connected/unconnected to drainage system

The Technical Release, number 55 (TR-55) also suggests that consideration is given to whether impervious areas are connected (outlet directly to the drainage system) or disconnected (flow is spread out over a pervious area before entering the drainage system) in curve number selection and includes graphical figures

based on the percent directly connected impervious areas to select the appropriate curve number (National Resources Conservation Service, 2009).

2.3.6 Antecedent Moisture Condition

The antecedent moisture condition (AMC) indicates the moisture content of the soil at the beginning of the rainfall event. The AMC attempts to account for the variation in curve numbers in an area under consideration from time to time. Three levels of AMC were documented by SCS: AMC-I (dry), AMC-II (normal), and AMC-III (wet). The limits of these three different AMC classes are based on the rainfall magnitude of the previous five days and season (dormant season and growing season) (Ahmad, Ahmad, and Verma, 2015). Formulae for CN conversion from AMC- II (CN-II) to AMC-I (CN-I) and AMC-II to AMC-III (CN-III) are displayed in Table 2.2.

Table 2.2 CN conversion formulae of AMC I and III.

Method	AMC-I	AMC-III
Sobhani (1975)	$CN_I = \dfrac{CN_{II}}{2.334-0.01334CN_{II}}$	$CN_{III} = \dfrac{CN_{II}}{0.4036+0.005964CN_{II}}$
Hawkins et al. (1985)	$CN_I = \dfrac{CN_{II}}{2.281-0.01281CN_{II}}$	$CN_{III} = \dfrac{CN_{II}}{0.427+0.00573CN_{II}}$
Chow et al. (1988)	$CN_I = \dfrac{4.2CN_{II}}{10-0.058CN_{II}}$	$CN_{III} = \dfrac{23CN_{II}}{10+0.13CN_{II}}$
Neitsch et al. (2002)	$CN_I = CN_{II} - \dfrac{20(100-CN_{II})}{\left\{100-CN_{II}+\exp\left[2.533-0.0636(100-CN_{II})\right]\right\}}$	$CN_{III} = \dfrac{CN_{II}}{0.430+0.0057CN_{II}}$

Source: Mishra, Jain, Suresh Babu, Venugopal, and Kaliappan (2008).

2.4 Linear and Goal programming

2.4.1 Basic concepts of linear programming

Bazaraa, Jarvis, and Sherali (2009) explained the general concept of the LP, which is concerned with the optimization (minimization or maximization) of a linear function while satisfying a set of linear equality and/or inequality of constraints or restrictions. George B. Dantzig first conceived the linear programming problem in 1947 while working as a mathematical advisor to the United States Air Force

Comptroller to develop a mechanized planning tool for a time-staged deployment, training, and logistical supply program.

The LP is a mathematical technique for finding optimal solutions to problems expressed using linear equations and inequalities. If a real-world problem can be represented accurately by the mathematical equations of a linear program, the method will find the best solution to the problem. Indeed, few complex real-world problems can be perfectly expressed in a set of linear functions. Nevertheless, linear programs can provide reasonably realistic representations of many real-world problems, particularly if a bit of creativity is applied in the mathematical formulation of the problem (McDill, 1999).

The LP is not a programming language like C++, Java, or Visual Basic. The LP can be defined as: *"A mathematical method to allocate scarce resources to competing activities in an optimal manner when the problem can be expressed using a linear objective function and linear inequality constraints."* A linear program consists of a set of variables, a linear objective function indicating the contribution of each variable to the desired outcome, and a set of linear constraints describing the limits on the values of the variables. The "answer" to a linear program is a set of values for the problem variables that result in the best -largest or smallest- value of the objective function and yet is consistent with all the constraints. The formulation is the process of translating a real-world problem into an LP. Once a problem has been formulated as a linear program, a computer program can solve the problem. In this regard, solving a linear program is relatively easy. The hardest part of applying linear programming is formulating the problem and interpreting the solution (McDill, 1999).

The following example case presents minimization as the optimization function of a single objective. Any general LP problem can be expressed in accepted form as (Bazaraa et al., 2009):

Minimize:

$$z = min(c_1x_1+c_2x_2+...+c_3x_3); \hspace{3cm} (2.12)$$

subject to:

$$a_{11}x_1 + a_{12}x_2 + \ldots + a_{1n}x_n \geq b_1;$$
$$a_{21}x_1 + a_{22}x_2 + \ldots + a_{2n}x_n \geq b_2;$$
$$\vdots$$
$$a_{m1}x_1 + a_{m2}x_2 + \ldots + a_{mn}x_n \geq b_m; \tag{2.13}$$

and:

$$x_1, x_2, \ldots, x_n \geq 0 \tag{2.14}$$

where objective function, $c_1x_1 + c_2x_2 + \ldots + c_3x_3$ is the objective function (or criterion function) to be minimized and denoted by z. The coefficients $c_1, c_2, \ldots, c_n$ are the (known) cost coefficients and $x_1, x_2, \ldots, x_n$ are the decision variables (unknown) to be determined.

Constraint set: the inequality $\sum_{j=1}^{n} a_{ij}x_j \geq b_i$ denotes the ith constraint set. In practice, the condition of constraints can be $\geq$ or $=$ or $\leq$ as long as it serves the optimization objective.

The coefficients a_{ij} for $i = 1, 2, \ldots, m$, $j = 1, 2, \ldots, n$ are called the technological coefficients. The coefficients are usually expressed in a matrix form of A.

$$A = \begin{bmatrix} a_{11} & a_{12} & \cdots & a_{1n} \\ a_{21} & a_{22} & \cdots & a_{2n} \\ \vdots & \vdots & & \vdots \\ a_{m1} & a_{m2} & \cdots & a_{mn} \end{bmatrix}$$

The column vector, whose ith component is b_i, which is referred to as the right-hand-side vector, represents the minimal requirement to be satisfied.

Non-negativity constraints: the constraints $x_1, x_2, \ldots, x_n \geq 0$ are the non-negativity constraints. A set of variables $x_1, \ldots, x_n$ satisfying all the constraints is called a feasible point or vector. The set of all such points constitutes the feasible region or space.

2.4.2   Basic concepts of goal programming

Goal programming is a form of linear programming that allows for the consideration of multiple goals. Whereas linear programming identifies, from the set of feasible solutions, the point that optimizes a single objective, goal programming determines the point that best satisfies the setting of goals in the decision problem. Furthermore, it attempts to minimize deviations from the goals (Malczewski, 1999). The

goal programming methods require the decision-maker to specify the most desirable value (goal) for each objective (criterion) as the aspiration level or target value. The objective functions (Eq. 2.15) are then transformed into goals as follows (Malczewski and Rinner, 2015):

$$f_k(x) + d_k^- - d_k^+ = a_k \qquad \text{for } k = 1, 2, ..., q \tag{2.15}$$

$$d_k^-, d_k^+ \geq 0, (d_k^-, d_k^+) = 0 \tag{2.16}$$

where a_k is the aspiration level for the kth objective, d_k^- and d_k^+ are negative and positive goal deviations, respectively; that is, non-negative state variables that measure deviations of the achieved value of the kth objective function from the corresponding aspiration level. Thus, two types of variables are part of any goal programming formulation: the decision variables, x_i, and the deviational variables, d_k.

Many measures of multidimensional deviations (achievement functions) and corresponding goal programming forms have been proposed by Jones and Tamiz (2010). The achievement function, $g(d_k^-, d_k^+)$, can be formulated in terms of the weighted Lp norm as follows:

$$g(d_k^-, d_k^+) = \left[\sum_{k=1}^{n} (w_k^- d_k^- + w_k^+ d_k^+) \right]^{\frac{1}{p}} \tag{2.17}$$

where w_k^- and w_k^+ are weights corresponding to the kth goal deviations. The weights represent additional information reflecting the decision maker's preferences for the deviation variables. One can generate several models by changing the value of p.

2.5 Standardized Precipitation Index

Standardized Precipitation Index (SPI) was developed by McKee et al. in 1993 at Colorado State University to quantify the precipitation deficit for multiple time scales such as 1, 3, 6, 9, 12, 24, and 48 months (Rahmat, Jayasuriya, and Bhuiyan, 2015). Generally, the original precipitation data is not a completely normal distribution essential to transforming precipitation time series into a standardized normal distribution. This index can be calculated by fitting the Gamma probability function to a given frequency of total precipitation (Sayari, Bannayan, Alizadeh, and Farid, 2013).

The computation of the SPI index requires the following steps (Karavitis, Alexandris, Tsesmelis, and Athanasopoulos, 2011; McKee, Doesken, and Kleist, 1993; Rahmat et al., 2015):

(1) Fit a cumulative probability distribution function (PDF) (usually gamma distribution) on aggregated monthly (k) precipitation series (namely, k = 3, 6, and 12 months). The gamma PDF, g(x), is defined as:

$$g(x) = \frac{1}{\beta^{\alpha}\Gamma(\alpha)} x^{\alpha-1} e^{-\frac{x}{\beta}} \tag{2.18}$$

For x ≥ 0, otherwise g(x) = 0,

where β is a scale parameter, α is a shape parameter, which can be estimated using maximum likelihood, x is the precipitation amount, and is the gamma function at α. $\Gamma(\alpha)$ is the gamma distribution function.

$$\Gamma(\alpha) = \int_{0}^{\infty} y^{\alpha-1} e^{-y} dy \tag{2.19}$$

The estimated parameters can find the cumulative PDF of observed precipitation events for the given month and particular time scale. The cumulative distribution function (CDF) is obtained by integrating Equation 2.20.

$$G(x) = \int_{0}^{x} g(x)dx = \int_{0}^{x} \frac{1}{\hat{\beta}^{\hat{\alpha}}\Gamma(\hat{\alpha})} x^{\hat{\alpha}-1} e^{-\frac{x}{\hat{\beta}}} dx \tag{2.20}$$

$$\hat{\alpha} = \frac{1}{4A}\left(1+\sqrt{1+\frac{4A}{3}}\right) \tag{2.21}$$

$$\hat{\beta} = \frac{\hat{x}}{\hat{a}} \tag{2.22}$$

$$A = \ln(\bar{x}) - \frac{\sum \ln(x)}{n} \tag{2.23}$$

$$G(x) = \frac{1}{\Gamma(\hat{\alpha})} \int_{0}^{x} t^{\hat{\alpha}-1} e^{-t} dt, \ t = \frac{x}{\hat{\beta}} \tag{2.24}$$

where n is the number of precipitation observation and refer to the sample mean of the data.

(2) Since the gamma distribution is undefined for x = 0 and q = P(x = 0) > where P(x = 0) is the probability of zero precipitation, CDF becomes as follow:

$$H(x) = q+(1-q)G(x) \tag{2.25}$$

where q is the probability of zero precipitation

The cumulative probability distribution is then transformed into the standard normal distribution to yield the SPI and classified SPI categories (Table 4).

In addition, two critical factors that should be carefully considered when applying SPI include an adequate length of precipitation record and the nature of the probability distribution (Mishra, Singh, and Desai, 2009).

Table 2.3 The SPI drought classification.

SPI values	SPI category
2.00 and above	Extreme wet
1.50 to 1.99	Severe wet
1.00 to 1.49	Moderate wet
0.50 to 0.99	Mild wet
-0.49 to 0.49	Near normal
-0.99 to -0.50	Mild drought
-1.49 to -1.00	Moderate drought
-1.99 to -1.50	Severe drought
-2.0 and less	Extreme drought

Source: Liu et al. (2014).

2.6   Previous studies

The previous studies related to this study are summarized, including the application of Random Forests, the CLUE-S model, the SCS-CN method, Linear and Goal programming, and SPI.

2.6.1   Application of Random forests

Tatsumi, Yamashiki, Canales Torres, and Taipe (2015) applied the RF classifier for cropland classification in the Ica region of Peru. A time series of moderate spatial resolution with enhanced vegetation index (EVI) of Landsat 7 ETM+ and its

summary statistics were used to develop crop type classification. The evaluation was based on several criteria, i.e., sensitivity to training dataset size, number of variables, and mapping accuracy. The results showed that the training dataset size strongly affects the classifier accuracy. The RF classifier provided an overall accuracy of 81% and a Kappa hat coefficient of agreement of 0.70. These values indicated high model performance.

Jhonnerie, Siregar, Nababan, Prasetyo, and Wouthuyzen (2015) used the RF classifier for mangrove land cover mapping in Kembung River, Bengkalis Island, Indonesia. The results were compared with a standard pixel-based classification algorithm (Maximum Likelihood: ML). Their study used seven input data derived from Landsat 5 TM, SAR, and spectral transformations (NDVI, NDWI, NDBI) to examine both classifiers. Overall accuracy (OA), user's accuracy (UA), producer's accuracy (PA), and Kappa statistics were used to compare classification results. The results showed that the more data model used produced higher overall accuracy and kappa statistics for RF classifier. The overall accuracy achieved by the RF classifier was 81.1% and 0.76 for the Kappa statistic. Meanwhile, for the ML classifier, the overall accuracy achieved was 77.7% and 0.71 for the Kappa statistic.

Eisavi, Homayouni, Yazdi, and Alimohammadi (2015) evaluated the potential of multitemporal Landsat 8-OLI spectral and thermal imageries using a random forests classifier. They used a grid search approach based on the out-of-bag (OOB) estimate of the error to optimize the RF parameters. In this study, four different scenarios were considered in this research: (1) multitemporal spectral images, (2) multitemporal LST images, (3) all multitemporal LST and spectral images, and (4) selected important or optimum features to classify land covers mapping in the northwest of Iran. The results indicated that the overall accuracies of the first, second, third, and fourth scenarios were equal to 86.48, 82.26, 90.63, and 91.82 %, respectively. The results also demonstrated that the most essential or optimum features increase class separability. In contrast, the spectral and thermal features produced a more moderate increase in the land cover mapping accuracy.

Midekisa et al. (2017) applied the RF classifier to quantify continental LULC changes over a long period (15 years) in continental Africa. In this study, Landsat

7 ETM+ data and Google Earth Engine cloud computing platform with spectral indices of Landsat data were used to classify 7 LULC classes. A total of 7,084 sample points was used to capture the LULC map by 80% of the sample points (5,664) from each class were randomly selected as training data, while 20% of sample points (1,420) were for the validation dataset. The results showed that the overall accuracy was 88%, while the producer's and user's accuracy ranged from 79% to 96% and 84% to 94%, respectively.

Liu, Gong, Hu, and Gong (2018) applied the RF algorithm for forest types mapping in Wuhan, China. They evaluate the potential of freely available multi-source imagery included Sentinel-2A, Sentinel-1A, SRTM DEM, and multi-temporal Landsat 8-OLI images, with seven different sets of explanatory variables for classifying eight forest types. The results indicated that using only Sentinel-2A and Landsat 8-OLI cannot obtain satisfactory results. The overall accuracy was increased by adding DEM and multi-temporal Landsat-8 imagery. The highest overall accuracy (82.78%) was achieved with fused imagery, the terrain, and multi-temporal data contributing the most to forest type identification.

Pareeth, Karimi, Shafiei, and De Fraiture (2019) developed the RF machine learning algorithm to extract irrigated land use types with the time-series Landsat 8-OLI data (2013-2016) in the Mashhad basin of Iran. This study used the HPF-based data fusion technique to develop the LULC map at the moderate spatial resolution of 15 m with nine classes of land use types. The results indicated that the total irrigated area was estimated at 1,796.16 km^2, 1,581.7 km^2, and 1,578.26 km^2 for the cropping years 2013/2014, 2014/2015, and 2015/2016, respectively. The overall accuracy of the final LULC map was 87.2% and Kappa hat coefficient of 0.85.

Srichaichana, Trisurat, and Ongsomwang (2019) applied the RF method to classify LULC in 2010 and 2017 from Landsat 5 and 8 images at Klong U-Tapao watershed, Songkhla province, Thailand. The classified LULC types include urban and built-up area, paddy field, rubber plantation, oil palm plantation, perennial tree and orchard, aquatic cultural area, evergreen forest, mangrove forest, marsh and swamp, water body, and miscellaneous land. As a result, the overall accuracy and

Kappa hat coefficient of thematic LULC maps of two years were 91.36% and 84.00% for 2010 and 94.32% and 87.00% for 2017.

In summary, it can be observed that many researchers have applied the RF classifier to classify LULC types. Most input data is free-downloaded with moderate spatial resolution, e.g., Landsat images, Sentinel images. The RF classifier provides an overall accuracy and Kappa hat coefficient of agreement of more than 80%. Besides, the finding also indicates that the RF classifier can provide higher accuracy results than other classifier algorithms.

However, the split rules for the LULC classification of the RF are unknown; therefore, it can be considered a black-box type classifier as the Artificial Neuron Network. Besides, users are generally required to observe the preliminary result of LULC classification and add more sample points to increase thematic accuracy (Tatsumi et al., 2015).

2.6.2   Application of CLUE-S model

Ongsomwang and Iamchuen (2015) studied the integration of geospatial models for optimum land use allocation in three different scenarios in the Upper Lam Phra Phloeng watershed, Nakhon Ratchasima province, Thailand. Their study used the CLUE-S model to simulate the LULC map of three different scenarios, i.e., historical land use evolution, energy crop extension, forest conservation, and prevention. Furthermore, the logistic regression model applied the physical and socio-economic factors to indicate the preference for a specific type of land use. The results indicated that population density is the most important driving factor for the location preference of the LULC types. Besides, the simulation of three LULC scenarios in 2023 by the CLUE-S model revealed that urban and built-up land, cassava, sugarcane, water body, and miscellaneous land were increased while maize, perennial trees/orchard, and forest land were decreased under Scenario I. At the same time, the increase in cassava and sugarcane under Scenario II came from maize, forest land, and miscellaneous land, while most of the increasing forest land under Scenario III was converted from maize, sugarcane, and miscellaneous land.

Zhou, Zhang, Ye, Wang, and Su (2016) developed the CLUE-S model to simulate future land use change and urban growth from 2009 to 2027 in Xinzhuang

town of Changshu city, China. In their study, three scenarios were designed to represent a different implementation of the spatial policies and restrictions, i.e., the current trend, urban planning, ecological protection. Also, the logistic regression model with eleven driving factors of land use change is taken into account as independent factors for the current land use pattern to indicate the preference for a specific type of land use. Furthermore, the pixel-based comparison for the simulated land use map of 2009 and the actual land use map of 2009 was performed to evaluate the accuracy of the predicted map. The results showed that the ROC value was more significant for all land use types than 0.7, suggesting the strong explanatory power of the selected driving factors employed to explain the land use spatial patterns. Meanwhile, it was found that the probability of correct classification of the given land-use types ranges between 77.3% and 83.1%, indicating that the CLUE-S model gave excellent simulation accuracy for land use change prediction.

Zare, Nazari Samani, Mohammady, Salmani, and Bazrafshan (2017) applied the CLUE-S model to simulate land use in the Kasilian watershed of Iran. In this study, the predicted LULC map of five scenarios in 2030 was simulated based on the LULC map in 1986, 2000, and 2011. Meanwhile, the logistics regression model used nine driving factors to indicate a specific type of land use preference. The results showed that the AUC value was higher than 0.8 for total land use types, which meant good accuracy in assessing the driving forces for LULC prediction. Therefore, they concluded that the CLUE-s model is suitable for modeling future land use transitions.

Mohammady et al. (2018) studied modeling and assessing the effects of land use changes on runoff generation with the CLUE-S and WetSpa models. Baghsalian watershed in the north of Iran was selected as the study area. In this study, the land use map of the year 2030 was simulated using the CLUE-S model based on land use change in the year 1986 to 2012 period. The results indicated that the primary land use changes in the study area between 1986, 2012, and 2030 were converting forest and rangeland to agriculture and residential land use types. Besides, they concluded that the CLUE-S model could provide future land use conditions for better planning and management.

Kucsicsa et al. (2019) applied the CLUE-S model to simulate future LULC in Romania. The predicted map of two different scenarios in 2007-2050 was simulated based on LULC data in 1990 and 2006. The first scenario LULC was predicted based on the annual rates of change between 1990 and 2000. The second scenario assumes that LULC will change based on the historical LULC dynamics between 2000 and 2006. In this study, biophysical and socio-economic variables associated with the current land use and land cover pattern were used to indicate a specific type of land use preference. In the meantime, the receiver operating characteristic (ROC) method was assessed to evaluate the performance of the predicted data. As a result, they found that biophysical variables make the most significant contribution to explaining the current spatial pattern of LULC. Also, the predicted data reveal that changes in land use and land cover will affect about 7.0% of the total study area under scenario 1 and 15.2% under scenario 2.

Srichaichana et al. (2019) applied the CLUE-S model to predict LULC in Klong U-Tapao watershed, Songkhla province, Thailand. Their study used the LULC map in 2010 and 2017 to predict LULC change from 2018 to 2024 under three different scenarios using the CLUE-S model. Meanwhile, logistic regression analysis was performed to identify LULC type location preference according to the driving force on LULC change. As a result, it was found that the most dominant driving factor for all LULC type allocation was the distance to settlement, and followed by distance to water bodies and road network. Furthermore, the study result showed that the significant increasing of LULC types during 2010-2017 were rubber plantations and urban and built-up areas. The significant decreasing areas of LULC classes were evergreen forest and miscellaneous land. Moreover, they also concluded that the derived LULC prediction of three different scenarios from the CLUE-S model could provide realistic results as expected.

In summary, the CLUE-S model has been studied by many researchers to simulate the spatial allocation of LULC in the future based on different scenarios. Biophysical and socio-economic variables are the most dominant driving factor for LULC type allocation. The logistic regression analysis was performed to identify LULC

type location preference for land allocation. Also, the literature reveals that the CLUE-S model can provide accurate results for better planning and management.

On the contrary, the model's main limitation is its incapability to simulate land use dynamics in areas without a land-use change history, e.g., deforestation in a pristine forest area. Because the model uses an empirically derived relationship based on the existing land-use patterns for land use change allocation. The only possible way around this limitation is using empirical relations derived in an area with very similar characteristics (Verburg et al., 2002).

2.6.3 Application of SCS-CN method

Phetprayoon, Sarapirome, Navanugraha, and Wonprasaid (2012) developed distributed geospatial models to simulate runoff and sediment yield for the Upper Lam Phra Phloeng watershed, Thailand. In this study, the SCS-CN method was used to simulate event-based runoff. Calibration and validation of the model were performed by comparing predicted runoff with corresponding instream measurements from two gauging stations within the watershed in 2008. As a result, it was found that calibration results show a reasonable agreement for both the coefficient of determination (R^2) and coefficient of efficiency (NSE) within ranges of 0.87-0.94 and 0.91-0.95, respectively. Meanwhile, the validation results show R^2 and NSE values ranging from 0.68-0.87 and 0.75-0.89, respectively. They also confirmed that the grid-based modified SCS-CN method is applicable to surface runoff estimation and is helpful for the study area.

Ongsomwang and Pimjai (2014) applied the SCS-CN method to estimate surface runoff in the Mueang Maha Sarakham and Kantharawichai districts of Maha Sarakham province. The regression analysis coefficient of determination (R^2) value explained the spatiotemporal relationship between urbanization and runoff depth from 2001 to 2021. The results indicated that the urban area and total surface runoff depth positively correlated with R^2 at 0.98. Also, they concluded that the urban and built-up area, which consists of an impervious surface, is a significant cause of the increased surface runoff in the study area.

Lal et al. (2017) applied the SCS-CN method to estimate surface runoff of natural storm events from 27 agricultural plots in India. In this study, the CN values

of a plot are designated as CN_{HT} (HT refers to the handbook tables), CN_{LSn} (for natural dataset), and CN_{LSo} (for ordered dataset). Meanwhile, the performance evaluation is primarily based on statistical analysis, i.e., the coefficient of determination (R^2), Nash Sutcliffe efficiency coefficient (NSE), number of times (n_t), and percent bias (PBIAS) for individual plot data. The results indicated that the runoff prediction using former CNs was insufficient for the data of 22 (out of 24) plots. However, the match was slightly better for higher CN values, consistent with the general notion that the existing SCS-CN method performs better for high rainfall-runoff (high CN) events.

Rawat and Singh (2017) applied Earth observation data sets and the SCS-CN method to estimate the surface runoff from Jhagrabaria, an agricultural watershed of Allahabad district, Uttar Pradesh, India. This study used three antecedent moisture conditions (AMC) in the CN method: AMC-I for dry conditions, AMC-II for normal conditions, and AMC-III for wet conditions. In addition, the coefficient of determination (R^2) was used to observe between satellite drive rainfall and runoff to validate the model. The results showed that the CN values of three conditions (AMC-I, II, and III were 79.35, 61.76, and 89.84, respectively. Meanwhile, the validation results show *an* R^2 value of 0.91.

Rizeei, Pradhan, and Saharkhiz (2018) applied the SCS-CN method to simulate the maximum probable surface runoff in 2000, 2010, and 2020. The Semenyih watershed, Selangor State, Malaysia, was selected as the study area. The Root Mean Square Error (RMSE) was used to calibrate the model results in this study. As a result, it was found that the accumulative simulated surface runoff as the basin outlet was successfully calibrated with the RMSE value of 0.75. Besides, the results showed that deforestation and urbanization have occurred at the given time, and they are anticipated to increase. Secondly, the amount of rainfall has non-stationary declined from 2000 till 2015, and this trend is estimated to continue by 2020. Thirdly, due to damaging changes in LULC, the surface runoff has been increased till 2010, and it is forecasted to exceed by 2020 gradually.

Li et al. (2019) studied an assessment of the impact of land use land and cover change and rainfall change on surface runoff in China. In their study, the SCS-CN method was used to estimate surface runoff in 2005, 2010, and 2015. In

addition, the NSE and R^2 were used to calibrate and validate the model. The results showed that the calibration result shows the R^2 and NSE values as 0.95 and 0.94, respectively, while the R^2 and NSE values of 0.96 and 0.93, respectively, for model validation. In the meantime, the average annual runoff depths in 2005, 2010, and 2015 were 78 mm, 83 mm, and 90 mm, respectively.

In summary, the SCS-CN method has been widely applied by many researchers to estimate surface runoff. The SCS-CN method is flexible for use with local or regional scale, especially in the agricultural watershed. Besides, Weng (2010) stated that the development and maturity of GIS technology in the late 1980s have made it possible to combine various data sources to derive model input parameters and have automated the SCS modeling process. Additionally, the main criteria for choosing the model are to be in line with specific problems, data requirements, model accuracy, model capability, and ease of use (Beckers et al., 2009; Calow and Petts, 1994) since the efficiency in developing a new model can be based on several facets such as research budget, study objectives and available time. Therefore, the SCS-CN method is chosen to estimate surface runoff for optimized LULC allocation for flood mitigation with goal programming modeling.

2.6.4 Application of linear and goal programming

Yeo, Gordon, and Guldmann (2004) studied optimizing land use patterns to reduce peak runoff flow and non-point source pollution with an integrated hydrological and land use model in Old Woman Creek watershed, Ohio State, USA. This study used the SCS-CN method to analyze the geographical impacts of land uses with DEM, soil, and LULC data. For land use optimization, an optimization algorithm (LP) is integrated with the simulation model to evaluate different land use patterns and their response to rainfall-runoff events and search for optimal land use patterns to minimize peak surface runoff. The results showed that by utilizing land use optimization, the level of peak runoff was reduced by 15-20%.

Evelyn (2009) applied the LP to maximize forest cover, minimize soil loss, runoff, groundwater loss, and agricultural production loss based on varying constraints, i.e., land availability, land capacity, urban and industrial, slope, soil type/depth, and ecological. In this study, the Rio Minho watershed of Jamaica was

selected as the study area. The results indicated that after optimization, spatial patterns in the upper parts of the watershed, which increased the forest cover from 16.76% to 37.47%, could significantly reduce runoff where the forest cover was optimized and simulated in a hydrological model.

Owji, Nikkami, Mahdian, and Mahmoudi (2012) studied LULC allocation to minimize surface runoff and sediment yield in the Jajrood watershed of Iran. The SCS-CN method was used to compute the amount of surface runoff with three different land use scenarios. At the same time, the LP-based on simplex method was used to allocate optimum LULC. As a result, irrigated farming and pasture were reduced by using optimization, while the orchard area was increased. Furthermore, after optimization, the watershed surface runoff and sediment yield will be reduced by 73.03% and 36.93%, respectively.

Huang, Kuo, and Tsou (2013) developed a multi-objective spatial optimization for land use allocation in high flood risk areas. The main objective of this study was to assess future land use patterns based on a multi-objective programming model in mountain land use, Tai Po Township, Chiayi County, Taiwan. This study used the LP of multi-objective programming to maximize economic benefit, environmental benefit (biological oxygen demanding load), and soil erosion based on varying constraints. The results showed that after optimization, the economic benefit output value was increased (from 198,929,030 to 422,672,234 NT/year), soil erosion was reduced (from 129,771 to 72,086 tons/year), and biological oxygen demanding load was the same (from 2,026 to 2,404 kg/year). Therefore, they concluded that multi-objective programming is helpful for high flood risk areas.

Sunandar, Suhendang, Hendrayanto, Jaya, and Marimin (2014) integrated the LP and SWAT model for land use optimization in the Asahan watershed. Their study used LP to minimize erosion with several constraints and consider the land's economic value. Meanwhile, spatial optimization uses the query method based on land capability category to obtain a combination of optimal land use area to be simulated using the SWAT model. After optimization, the results indicate a significant change in forest area, increased plantation and rice field areas, reduced dry farmland areas, and barren land soil and shrubs converted into other vegetated areas. These

changes can reduce erosion without reducing water yield in the SWAT model simulation.

Gonfa and Kumar (2015) studied optimal land use planning in mojo watersheds with multi-objective linear programming. This study used the SWAT model to predict annual sediment yield and net income per unit area in each land use as the coefficient of decision variables in the optimization process. In the meantime, the LP was used to minimize soil erosion and maximize net benefit. The results showed that on solving the problem using a goal programming, net income from the watershed is increased by 29.91%, and soil erosion decreased by 16.14% with the reduction of dryland farming by 18.45% and increasing the current rangeland 946.36 ha to 15,419.74 ha and 45.96 ha under irrigated agriculture to 25,526.69 ha.

Sokouti and Nikkami (2017) applied the LP to determine the optimal use of land to reduce erosion and increase the resident's income of the Qushchi watershed in West Azerbaijan province, Iran. In this study, three different options, including the current status of land use without and with land management and the standard status of land use, multi-objective LP model was established by LINGO software. The results showed that in the case of the optimization of land use, soil erosion and the profitability of the whole area would decrease by 0.75% and increase by 3.68%, respectively. For land management practices, soil erosion will reduce by 42.27%, and the profitability will increase by 21.39%. In contrast, soil erosion will decrease by 60.95%, and profitability will increase by 24.20% in standard conditions.

Al-Zahrani, Musa, and Chowdhury (2016) developed a multi-objective model for optimal water distribution from multiple resources to multiple users in Riyadh, Saudi Arabia. In this study, weighted GP based on specific objectives were used to (1) satisfy water quality, (2) maximize treated wastewater (TWW) reuse and groundwater (GW) conservation, and (3) minimize overproduction of desalinated water (DW) and overall cost. The results showed that in 2015, the required allocations of GW, DW, and TWW are 3,286, 662, and 609 MCM, respectively, which are projected to be 4,345, 1,554, and 1,305 MCM in 2050, respectively. In addition, the GW source is likely to satisfy the predicted withdrawal of GW till 2035, while probabilities of non-

satisfaction of total demands of GW in 2040, 2045, and 2050 were 0.04, 0.23, and 0.51, respectively.

Tajbakhsh, Memarian, and Kheyrkhah (2018) applied the GP to optimize land allocation in the Bayg watershed, Iran. The GP of multi-objective was used to allocate five categories of land uses, i.e., irrigated orchard, rangeland, irrigated farming, rain-fed farming, and almond orchard, to minimize surface runoff and sediment yield and to increase net income. The results indicated that combining the techniques weighted GP, AHP, and multi-objective land allocation can optimize land use and land covers based on the conflicting objectives (runoff and sediment load minimization and net income maximization).

In summary, linear programming (LP) has been applied by many researchers to optimize LULC allocation based on different objective function problems, e.g., to minimize surface runoff, sediment yield, soil erosion. The simplex method is a popular method that can be used to solve the problem in the LP model. Meanwhile, the LP model can be integrated with any hydrological model, including the Soil Conservation Service Curve Number (SCS-CN) method and the Soil and Water Assessment Tool (SWAT) model.

Likewise, goal programming (GP) is a subdivision of multi-objective optimization, which can support linear programming to deal with multiple and usually conflicting objectives. The GP has been used to solve the objective function problem based on the target or goal. The finding indicates that most researchers have applied the GP to allocate LULC based on different objective problems. Therefore, if any problem with multi-objective optimization (minimization or maximization) exists, the GP might be helpful to solve such a problem.

2.6.5 Application of SPI

In recent decades, the standardized precipitation index has been widely used to characterize dry and wet conditions in many countries and regions due to its simplicity and variable timescales, which requires only the precipitation as input data to quantify water deficit and surplus for long-term normal conditions for multiple time scales (Zhang, Xu, and Zhang, 2009; Du, Fang, Xu, and Shi, 2013; Liu and Liu, 2019). However, the SPI calculation requires at least 20-30 years of monthly

precipitation data, and 50-60 years or more is ideal (Tan, Yang, and Li, 2015). For instance, Seiler, Hayes, and Bressan (2002) analyzed the potential of using SPI to monitor flood risk in the Southern Cordoba province in Argentina during the last 25 years. The SPI index was calculated on time scales of 1, 3, 12, and 24 months. They found that SPI satisfactorily explains the development of conditions leading up to the three main flood events in the region. Karavitis et al. (2011) used time-series data from 46 precipitation stations covering 1947-2004 (57 years) with time scales of 1, 3, 6, 12, and 24 months to calculated SPI values in Greece.

Likewise, the daily precipitation data, covering 1951 to 2007 (56 years), was used to calculate the annual SPI value in China's Hunan province. The time series of SPI at multiple time scales of 2, 6, 12, and 24 months were calculated to determine their potential usefulness for detecting dry/wet periods and monitoring drought/flood risk by Du et al. (2013). Zhang and Jia (2013) used the long-term monthly precipitation data from 1960 to 2010 (51 years) to construct SPI series at 1, 3, 6, 9, and 12-month time scales for each weather station. Similarly, Tan et al. (2015) used monthly precipitation data from 1971 to 2011 (41 years) to calculate the monthly SPI value for Ningxia, China.

CHAPTER III

RESEARCH PROCEDURES

The ultimate goal of this study focuses on optimizing LULC allocation for flood mitigation in the Second Part of Lam Nam Chi watershed, Mueang Chaiyaphum district, Chaiyaphum province. The research procedures involve data collection and preparation and six major components: (1) LULC classification, (2) LULC prediction, (3) surface runoff estimation, (4) optimization of LULC allocation for flood mitigation, (5) mapping of LULC allocation for flood mitigation, and (6) economic and ecosystem service value evaluation and change. The overview framework of the research procedures is schematically illustrated in Figure 3.1. The detailed information about data collection and preparation and main research components are separately summarized in the following sections.

3.1   Data collection and preparation

The required input data for the study include GIS data, remote sensing data, and primary and secondary data, which were collected and prepared in advance as a summary in Table 3.1.

Table 3.1 List of data collection and preparation for data analysis in the study.

Data	Data collection	Data Preparation	Source	Component
Primary	- Ground reference	-	-	1
Secondary	- Runoff	-	RID	3
	- Annual rainfall	Interpolation	TMD	3 and 4
	- Socio-economic data	Population density	DOPA	2
		Income per capita	NESDC	2
Remote Sensing	- Landsat 5 TM: Path 128 Row 49, Date 6 January 2001 and Path 129 Row 49, Date 14 February 2001	1. Radiometric correction 2. Geometric correction	USGS	1

Table 3.1 (Continued).

Data	Data collection	Data Preparation	Source	Component
Remote Sensing	- Landsat 5 TM: Path 128 Row 49, Date 16 February 2010 and Path 129 Row 49, Date 23 February 2010	-		1
	- Landsat 8 OLI: Path 128 Row 49, Date 24 January 2019 and Path 129 Row 49, Date 31 January 2019			1
	- Satellite image from Google Earth in 2010		Google	1
	- Color orthophotograph	-	RTSD	1
GIS	- Administrative boundary	-	DEQP	1 and 3
	- Soil (soil series)	Recode	LDD	3
	- Watershed boundary	-	RID	1, 2, and 3
	- Elevation	Extract from DEM	SRTM	2
	- Slope	Extract from DEM	SRTM	2
	- Road network	Buffering	MOT, DEQP	2
	- Stream	Buffering	RTSD	2
	- Urban area	Buffering	LULC data	2

Note: USGS: United States Geological Survey; RTSD: Royal Thai Survey Department; DEQP: Department of Environmental Quality Promotion; TMD: Thai Meteorological Department; RID: Royal Irrigation Department; LDD: Land Development Department; NESDC: Office of the National Economic and Social Development Council; SRTM: Shuttle Radar Topography Mission: MOT: Ministry of Transport, DOPA: Department of Provincial Administration.
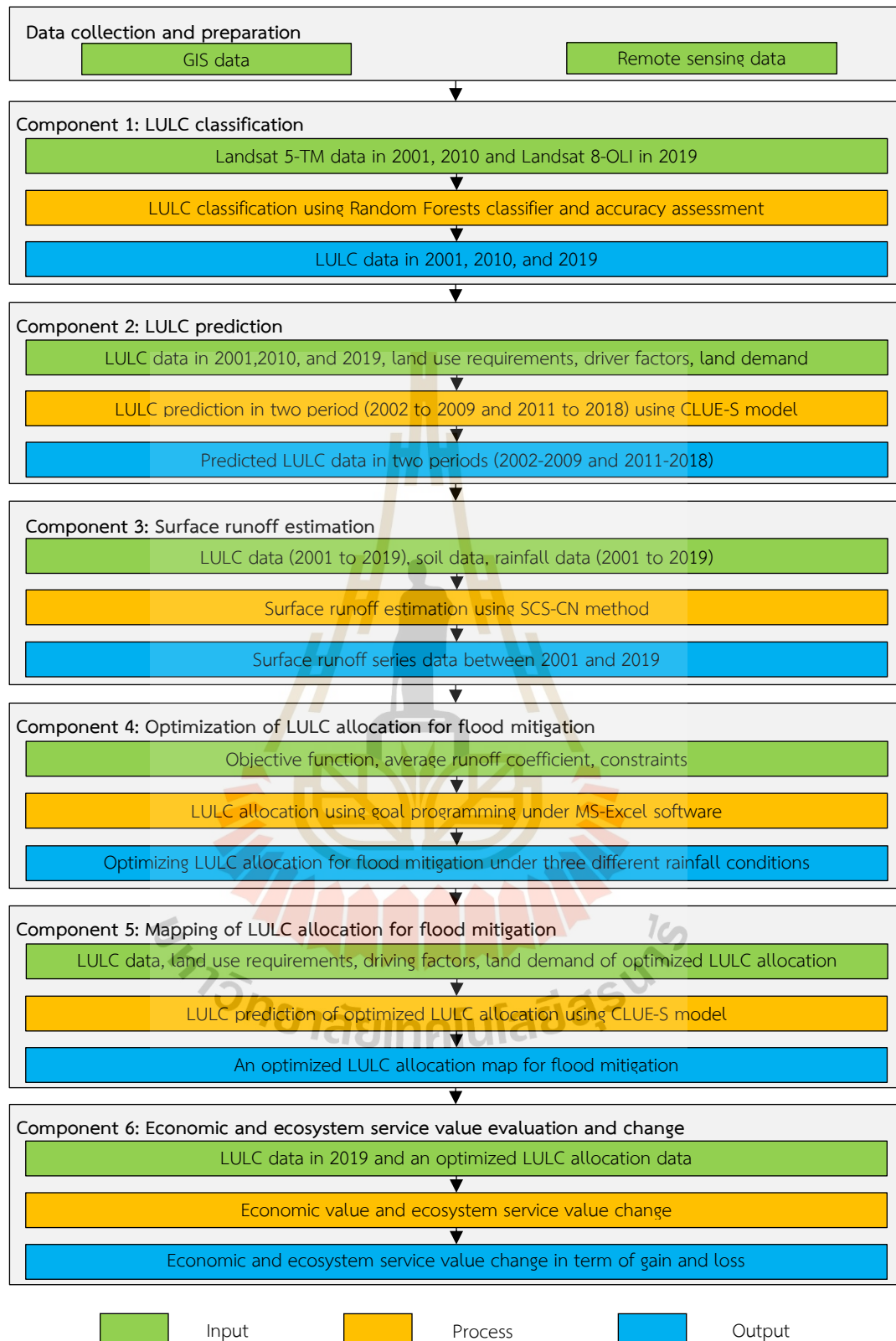
Figure 3.1 Overview framework of research procedures.

3.2   Component 1: LULC classification

Under this component, three Landsat imageries in 2001, 2010, and 2019 are firstly downloaded from the USGS website (www.earthexplore.usgs.gov) for LULC classification using the RF classifier. Then, the preliminary LULC maps in 2001, 2010, and 2019 were assessed accuracy based on the reference data from the aerial photograph in 2001, Google satellite image in 2010, and field survey in 2020, respectively. This study estimated the number of sample points for accuracy assessment based on multinomial distribution with stratified random sampling. The derived results of this component will be further applied for LULC prediction between 2002 and 2018 in the next component. The schematic workflow of the LULC classification, including input, process, and output, is displayed in Figure 3.2.

Brief information on significant tasks under this component includes (1) LULC classification using the RF classifier and (2) accuracy assessment summarized in the following sections.

3.2.1   LULC classification using RF classifier

Training areas of LULC type from three Landsat images in 2001, 2010, and 2019 were separately prepared to extract multiple decision trees for LULC classification using the RF classifier of EnMap-Box software. Herein, spectral reflectance data product (Level 2) of Landsat 5-TM (band 1, 2, 3, 4, 5, and 7) in 2001 and 2010 or Landsat 8-OLI (band 2, 3, 4, 5, 6, and 7) in 2019 with spectral indices (NDVI, MNDWI, and NDBI) and elevation were applied to classify LULC in the corresponding years. The additional bands represent a particular characteristic for enhancing LULC classification under non-parametric statistics of the RF. Generally, NDVI (Normalized Difference Vegetation Index) represents vegetation characteristics (Rouse et al., 1974), while MNDWI (Modified Normalized Difference Wetness Index) signifies moisture regime (Xu, 2008), and NDBI (Normalized Difference Built-up Index) indicates a built-up area (Zha, Gao, and Ni, 2003). Meanwhile, the distribution of LULC types is directly related to elevation, e.g., paddy fields are generally situated in floodplains while forests are primarily located in mountainous areas.

In this study, 200 random decision trees with a Gini coefficient index of the impurity were applied to classify LULC with majority voting using RFs classifiers.
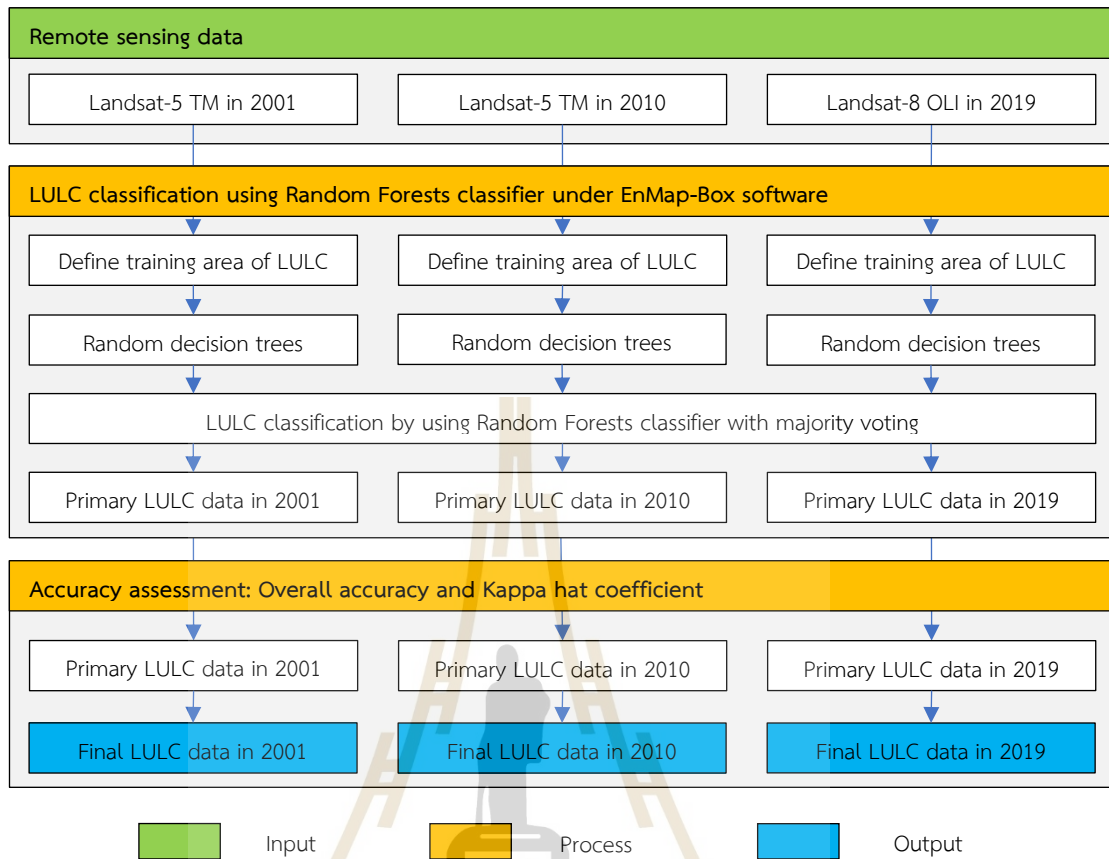
Figure 3.2 Schematic workflow of LULC classification.

In this study, the LULC classification system, which was modified from the standard land use classification system of the LDD, consists of (1) urban and built-up area, (2) paddy field, (3) sugarcane, (4) cassava, (5) other field crops, (6) para rubber, (7) perennial trees and orchards, (8) forest land, (9) water body, (10) rangeland, (11) marsh and swamp, and (12) unused land. The description of the LULC types is summarized in Table 3.2.

Table 3.2 Description of LULC classification system.

LULC type	Description
Urban and built-up area	All land uses to construct human structures, including villages, urban areas, industrial areas, and road networks.
Paddy field	Rice agriculture cultivation area is determined by the inundating of fields.
Sugarcane	The area consists of a multi-growth stage of sugarcane.
Cassava	The area consists of a multi-growth stage of cassava.
Other field crops	The area consists of a multi-growth stage of field crops, which excludes sugarcane and cassava.
Para rubber	The area consists of a multi-growth stage of para rubber.
Perennial trees and orchard	Area covered by tree and orchard, which excludes para rubber.
Forest land	Area covered by trees, dense forest, opened forest, and forest plantation.
Water body	Area covered by lake, river, and drainages, and artificial water areas.
Rangeland	Area covered by grass, shrubs, uncultivated land, lands with herbaceous types of cover. Tree and shrub cover are less than 10%.
Marsh and swamp	Marsh exists along river banks, characterized by poor drainage moisture. Swamp is situated on the shallow margins of bays, lakes, ponds, streams, and artificial impoundments such as reservoirs.
Unused land	Area covered by uncultivated areas including abandoned land, bare land, pit, landfill, and outcrop.

3.2.2 Accuracy assessment

The preliminary LULC maps in 2001, 2010, and 2019 were assessed accuracy (overall accuracy, producer's accuracy, user's accuracy, and Kapa hat coefficient of agreement) based on the reference data from color orthophotograph in 2000-2001, very high spatial resolution imageries from Google Earth in 2010, and field survey in 2020, respectively. This study estimated the number of sample sizes for thematic accuracy assessment based on multinomial distribution with a stratified random sampling scheme, as suggested by (Congalton and Green, 2019).

3.3 Component 2: LULC prediction

Two significant tasks implemented under this component include (1) optimum local parameter for LULC prediction using CLUE-S model and (2) LULC prediction of two periods: 2002-2009 and 2011-2018 using CLUE-S model.

3.3.1 Optimum local parameter identification for LULC prediction using CLUE-S model

In this study, optimum local parameters for LULC prediction using the CLUE-S model were justified by comparing the predicted LULC map in 2019 and the classified LULC map in 2019 using thematic accuracy assessment.

In practice, basic parameters of the CLUE-S model, which include (1) elasticity value, (2) LULC conversion matrix, and (3) land requirement of each LULC type in 2019 were extracted based on the final LULC map in 2001 and 2010 using the Markov Chain model. At the same time, three selected driving factor categories on LULC change include physical, socio-economic, and proximity, which was reviewed from the previous studies of many researchers (Table 3.3), were examined multicollinearity and identified LULC type location preference using binomial logistic regression analysis for allocating LULC type during LULC prediction in 2019 by CLUE-S model.

Then, the predicted LULC map in 2019 was compared with the classified map in 2019 using a wall-to-wall accuracy assessment with overall accuracy and Kappa hat coefficient of agreement. If the overall accuracy and Kappa hat coefficient are equal to or more than 80%, then the selected driving factor on LULC

change is chosen as the optimum local parameter of the CLUE-S model for LULC prediction.

    3.3.2   LULC prediction of two periods: 2002-2009 and 2011-2018

        The optimum local parameter, elasticity value, LULC conversion matrix, and land requirement of each LULC type in two periods (2002-2009 and 2011-2018), which were extracted using the Markov Chain model based on the corresponding LULC data in 2001, 2010, and 2019, were applied to predict LULC data in two periods. The derived time-series of LULC data between 2001 and 2019 from classification and prediction will be further applied to estimate the time-series surface runoff data using the SCS-CN method in the next component.

        The workflow of optimum local parameters for LULC prediction and LULC prediction of two periods using CLUE-S is displayed in Figure 3.3.

Table 3.3 Driving factors on LULC change for LULC type location preference.

Categories	Driving factors	References
Physical factor	Elevation	Trisurat et al. (2010) ; Han et al. (2015); Ongsomwang and Iamchuen (2015); Zheng et al. (2015) ; Xu et al. (2016) ; (Gao et al., 2016); Ongsomwang and Boonchoo (2016); Phompila et al. (2017); Arowolo and Deng (2018); Palchowdhuri and Roy (2018); Ongsomwang, Pattanakiat, and Srisuwan (2019).
	Slope	Trisurat et al. (2010); Han et al. (2015); Ongsomwang and Iamchuen (2015); Zheng et al. (2015); Xu et al. (2016); Gao et al. (2016); Ongsomwang and Boonchoo (2016); Phompila et al. (2017); Arowolo and Deng (2018); Palchowdhuri and Roy (2018); Ongsomwang et al. (2019).
	Annual rainfall	Ongsomwang and Iamchuen (2015); Xu et al. (2016); Gao et al. (2016); Li et al. (2016) ; Arowolo and Deng (2018); Palchowdhuri and Roy (2018).
Socio-economic factor	Average income per capita at sub-district level	Gao et al. (2016); Ongsomwang and Boonchoo (2016); Li et al. (2016); Arowolo and Deng (2018); Ongsomwang et al. (2019).
	Population density at sub-district level	Trisurat et al. (2010); Han et al. (2015); Ongsomwang and Iamchuen (2015); Zheng et al. (2015); Gao et al. (2016); Ongsomwang and Boonchoo (2016); Arowolo and Deng (2018); Palchowdhuri and Roy (2018); Ongsomwang et al. (2019).
Proximity	Distance to road network	Trisurat et al. (2010); Han et al. (2015); Ongsomwang and Iamchuen (2015); Zheng et al. (2015); Ongsomwang and Boonchoo (2016); Phompila et al. (2017); Arowolo and Deng (2018); Ongsomwang et al. (2019).
	Distance to stream	Trisurat et al. (2010); Han et al. (2015); Ongsomwang and Iamchuen (2015); Gao et al. (2016); Phompila et al. (2017); Ongsomwang et al. (2019).
	Distance to the existing urban area	Han et al. (2015); Xu et al. (2016); Ongsomwang and Boonchoo (2016); Ongsomwang et al. (2019).
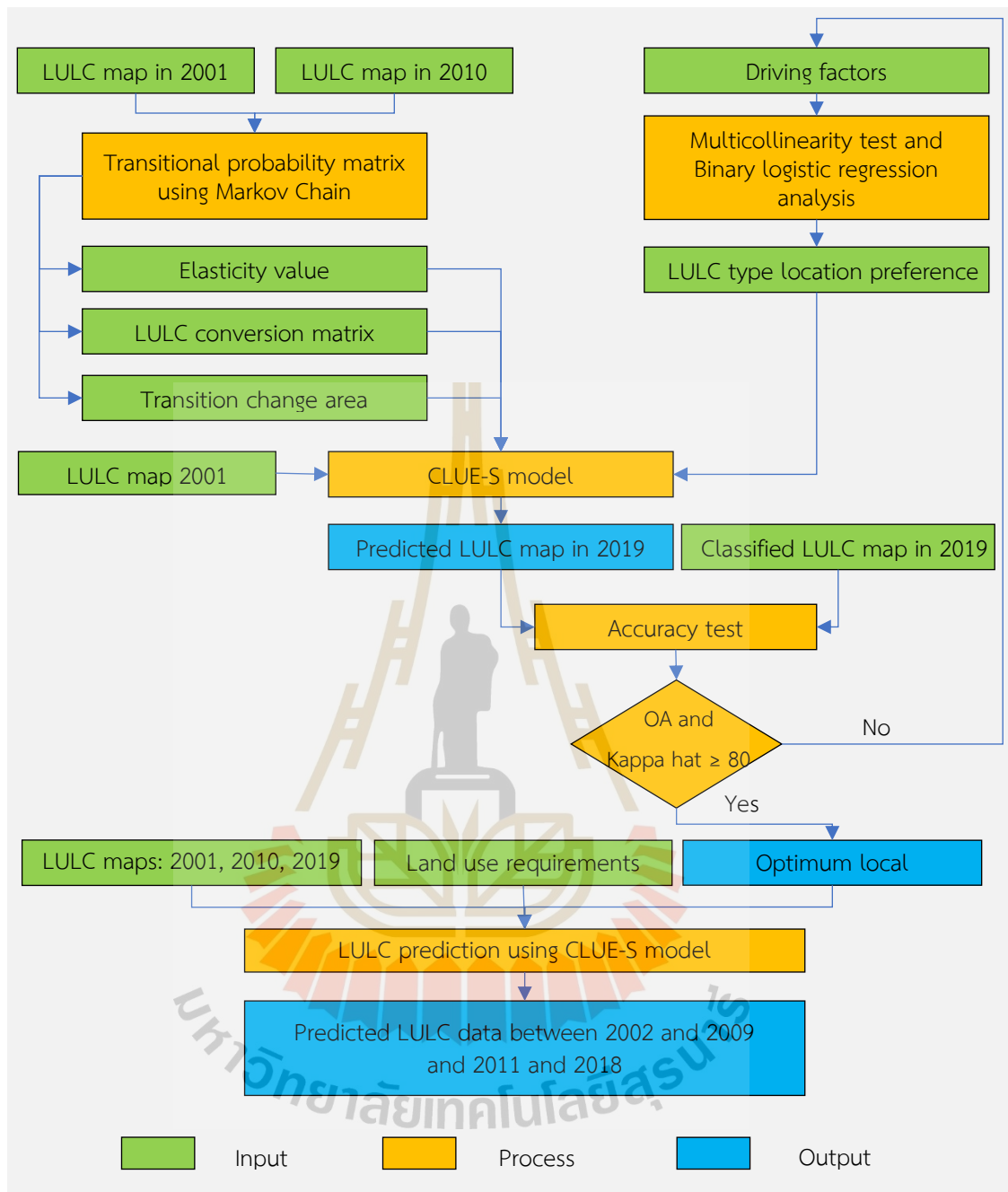
Figure 3.3 Schematic workflow of optimum local parameter for LULC prediction and LULC prediction of two periods using CLUE-S model.

3.4   Component 3: Surface runoff estimation

This study estimates time-series surface runoff between 2001 and 2019 based on the classified and predicted LULC data, soil series, and rainfall data using the SCS-CN method with suitable AMC under ESRI ArcGIS software. Two significant tasks implemented under this component include (1) suitable AMC for surface runoff estimation using the SCS-CN method and (2) time-series surface runoff estimation between 2001 and 2019.

3.4.1   Suitable AMC for surface runoff estimation using SCS-CN method

Suitable AMC for surface runoff estimation using the SCS-CN method was examined based on the classified and predicted LULC data from 2001 and 2010 with three different CN values of three different AMCs, as suggested by Chow, Maidment, and Mays (1988) using the following equations.

$$CN_I = \frac{4.2CN_{II}}{10-0.058CN_{II}} \qquad (3.1)$$

$$CN_{III} = \frac{23CN_{II}}{10+0.13CN_{II}} \qquad (3.2)$$

where CN_I is the runoff curve number value of each LULC type of AMC-I, CN_{II} is the runoff curve number value of each LULC type of AMC-II, and CN_{III} is the runoff curve number value of each LULC type of AMC-III.

The runoff curve number value of each LULC type in three antecedent moisture conditions (AMC-I, AMC-II, and AMC-III) is summarized in Tables 3.4 to 3.6.

Table 3.4 Runoff curve number under AMC-I with the dry condition.

Land cover	Treatment	Hydrologic condition[1]	The appropriate assumption to land use in the study area	Curve numbers for hydrologic soil group			
				A	B	C	D
Urban districts		85% of the average impervious area	Urban and built-up area	77.26	82.85	86.81	88.86
Row crop	Straight row	Poor	Cassava and other field crops	51.92	64.16	75.49	80.94
	Straight row	Partial cover[2]	Sugarcane	28.75	48.32	61.24	68.80
Small grain	Straight row	Poor	Paddy field	43.82	57.08	68.80	75.49
Pasture, grassland, or range continuous forage for grazing[3]		Fair	Rangeland	28.75	48.32	61.24	68.80
Woods-grass combination (orchard or tree farm)		Fair	Para rubber, and perennial trees and orchard	24.06	43.82	57.08	65.68
Woods[4]		Good	Forest land	15.25	33.92	49.49	58.44
Impervious and water surface			Water body, and marsh and swamp	95.37	95.37	95.37	95.37
Fallow		-	Unused land	58.44	72.07	80.94	86.81

Sources: Modified from (National Resources Conservation Service, 2004; Phetprayoon, 2010).

[1] Hydrologic condition is based on combinations of factors that affect infiltration and runoff, including (a) density and canopy of vegetative areas, (b) amount of year-round cover, (c) amount of grass or close-seeded legumes, (d) percent of residue cover on the land surface, and (e) degree of surface roughness.

　Poor: Factors impair infiltration and tend to increase runoff.

　Good: Factors encourage average and better than average infiltration and tend to decrease runoff.

[2] Sugarcane degrees of cover.

　Partial cover-Cane in a transition period between limited and completed cover; canopy over half to nearly the entire field area.

[3] Pasture, grassland, or range continuous forage for grazing.

　Fair: 50 to 70%ground cover and not heavily grazed.

[4] Woods

　Good: Woods are protected from grazing, and litter and brush adequately cover the soil.

Table 3.5 Runoff curve number under AMC-II with normal condition.

Land cover	Treatment	Hydrologic condition[1]	The appropriate assumption to land use in the study area	Curve numbers for hydrologic soil group			
				A	B	C	D
Urban districts		85% of the average impervious area	Urban and built-up area	89	92	94	95
Row crop	Straight row	Poor	Cassava and other field crops	72	81	88	91
	Straight row	Partial cover[2]	Sugarcane	49	69	79	84
Small grain	Straight row	Poor	Paddy field	65	76	84	88
Pasture, grassland, or range continuous forage for grazing[3]		Fair	Rangeland	49	69	79	84
Woods-grass combination (orchard or tree farm)		Fair	Para rubber, and perennial trees and orchard	43	65	76	82
Woods[4]		Good	Forest land	30	55	70	77
Impervious and water surface			Water body, and marsh and swamp	98	98	98	98
Fallow		-	Unused land	77	86	91	94

Sources: (National Resources Conservation Service, 2004; Phetprayoon, 2010).

[1] Hydrologic condition is based on combinations of factors that affect infiltration and runoff, including (a) density and canopy of vegetative areas, (b) amount of year-round cover, (c) amount of grass or close-seeded legumes, (d) percent of residue cover on the land surface, and (e) degree of surface roughness.

    Poor: Factors impair infiltration and tend to increase runoff.

    Good: Factors encourage average and better than average infiltration and tend to decrease runoff.

[2] Sugarcane degrees of cover.

    Partial cover-Cane in a transition period between limited and completed cover; canopy over half to nearly the entire field area.

[3] Pasture, grassland, or range continuous forage for grazing.

    Fair: 50 to 70%ground cover and not heavily grazed.

[4] Woods

    Good: Woods are protected from grazing, and litter and brush adequately cover the soil.

Table 3.6 Runoff curve number under AMC-III with wet condition.

Land cover	Treatment	Hydrologic condition[1]	The appropriate assumption to land use in the study area	Curve numbers for hydrologic soil group			
				A	B	C	D
Urban districts		85% of the average impervious area	Urban and built-up area	94.90	96.36	97.30	97.76
Row crop	Straight row	Poor	Cassava and other field crops	85.54	90.75	94.40	95.88
	Straight row	Partial cover[2]	Sugarcane	68.85	83.66	89.64	92.35
Small grain	Straight row	Poor	Paddy field	81.03	87.93	92.35	94.40
Pasture, grassland, or range continuous forage for grazing[3]		Fair	Rangeland	68.85	83.66	89.64	92.35
Woods-grass combination (orchard or tree farm)		Fair	Para rubber, and perennial trees and orchard	63.44	81.03	87.93	91.29
Woods[4]		Good	Forest land	49.64	73.76	84.29	88.51
Impervious and water surface			Water body, and marsh and swamp	99.12	99.12	99.12	99.12
Fallow		-	Unused land	88.51	93.39	95.88	97.30

Sources: Modified from (National Resources Conservation Service, 2004; Phetprayoon, 2010).

[1] Hydrologic condition is based on combinations of factors that affect infiltration and runoff, including (a) density and canopy of vegetative areas, (b) amount of year-round cover, (c) amount of grass or close-seeded legumes, (d) percent of residue cover on the land surface, and (e) degree of surface roughness.

    Poor: Factors impair infiltration and tend to increase runoff.

    Good: Factors encourage average and better than average infiltration and tend to decrease runoff.

[2] Sugarcane degrees of cover.

    Partial cover-Cane in a transition period between limited and completed cover; canopy over half to nearly the entire field area.

[3] Pasture, grassland, or range continuous forage for grazing.

    Fair: 50 to 70%ground cover and not heavily grazed.

[4] Woods

    Good: Woods are protected from grazing, and litter and brush adequately cover the soil.

In practice, three runoff curve numbers of hydrologic soil group of each LULC type were separately applied to estimate potential maximum storage under three different AMCs using the following equation.

$$S=25.4\times\frac{1000}{CN}-10 \tag{3.3}$$

where CN is the runoff curve number of the hydrologic soil group (HSG)-land cover complex.

The calculated potential maximum storage was further applied to estimate the surface runoff depth of three different AMCs using Eq. 3.4, as suggested by the United States Department of Agriculture (1986); Weng (2010).

$$Q=\frac{(P-0.2S)^2}{(P+0.8S)} \tag{3.4}$$

where Q is surface runoff depth (mm), P is annual rainfall (mm), S is potential maximum storage.

Then, the estimated surface runoff depth of three different AMCs from 2001 to 2010 was converted into surface runoff volume using Equation 3.5. These surface runoff volumes were further used to identify the suitable AMC of the watershed for surface runoff estimation according to model performance (Table 3.7) using Nash and Sutcliffe's coefficient of efficiency (NSE), coefficient of determination (R^2), and percent of bias (PBIAS) (Equations 3.6-3.8). In this study, the observed runoff data between 2001 and 2010 from the hydrological station gauge at E.21, E.23, and E.6C of the RID were used to calculate an average NSE, R^2, and PBIAS for suitable AMC identification. The schematic workflow of suitable AMC identification for surface runoff estimation using the SCS-CN method is displayed in Figure 3.4.

$$\text{Surface runoff volume}=\frac{\text{Surface runoff depth}}{1000}\times\text{cell size} \tag{3.5}$$

$$NSE=1-\left[\frac{\sum_i^n (Q_{simi}-Q_{obsi})^2}{\sum_i^n (Q_{obsi}-Q_{avg})^2}\right] \tag{3.6}$$

where n is the number of years, Q_{simi} is the simulated surface runoff, Q_{obsi} is the observed surface runoff, and Q_{avg} is the average observed surface runoff over the

simulation period. The values for E can be varied from -∞ to 1, with 1 indicating a perfect fit.

$$R^2 = \left\{ \frac{\sum_{i=1}^{n} (Q_{obsi}-Q_{obsavg})(Q_{simi}-Q_{simavg})}{\left[\sum_{i=1}^{n} (Q_{obsi}-Q_{obsavg})^2 \sum_{i=1}^{n} (Q_{simi}-Q_{simavg})^2\right]^{0.5}} \right\}^2 \qquad (3.7)$$

where, Q_{obsi} is observed surface runoff at year i, Q_{simi} is the simulated surface runoff at year i, Q_{obsavg} is the average of observed surface runoff over the calibration or validation period, Q_{obsavg} is the average of simulated surface runoff over the validation period, i is the year, and n is the total counting of data pairs.

$$PBIAS = \left[\frac{\sum_{i=1}^{n} (Y_i^{obs}-Y_i^{sim})*(100)}{\sum_{i=1}^{n} (Y_i^{obs})}\right] \qquad (3.8)$$

where, Y_i^{obs} is observed surface runoff at time step i, and Y_i^{sim} simulated surface runoff at time step i.

Table 3.7 Criteria for model performance.

Statistics measurement	Performance ratings			
	Unsatisfactory	Satisfactory	Good	Very good
NSE	< 0.5	0.5-0.65	0.65-0.75	0.75-1
R^2	< 0.5	0.5-0.6	0.6-0.7	0.7-1
PBAIS	> 25	15-25	10-15	< 10

Source: Me, Abell, and Hamilton (2015).
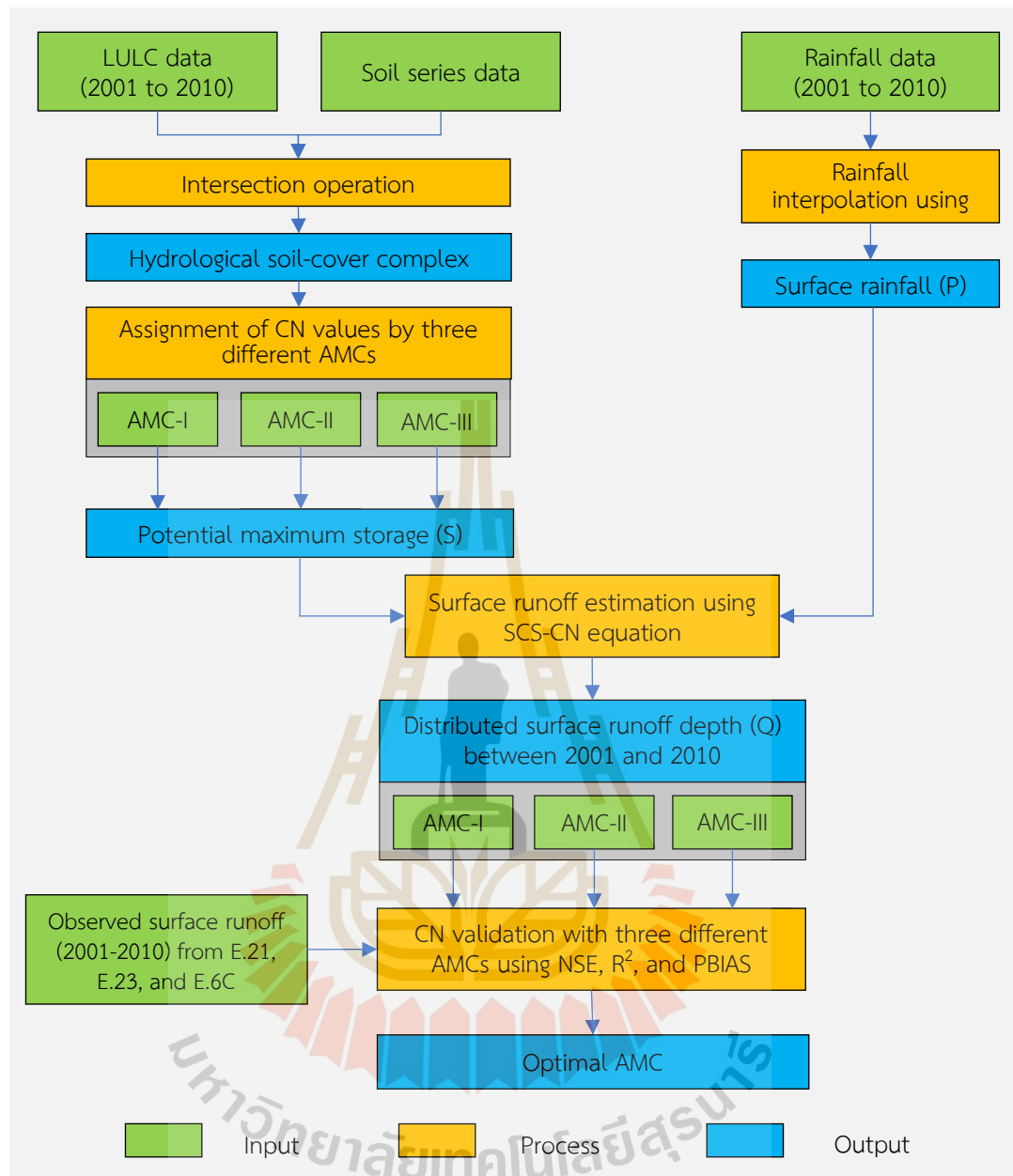
Figure 3.4 Workflow of suitable AMC identification for surface runoff estimation using SCS-CN method.

3.4.2 Time-series surface runoff estimation between 2011 and 2019

The runoff curve number of suitable AMC was applied to estimate time-series surface runoff between 2011 and 2019. The estimated surface runoff was validated based on observed runoff data between 2011 and 2019 from the hydrological station gauge of RID at E.21, E.23, and E.6C using NSE, R^2, and PBIAS according to model performance (See Table 3.7). If three performance ratings are satisfied, the derived results are accepted under the validation phase. The schematic workflow of time-series surface runoff estimation between 2001 and 2019 is displayed in Figure 3.5. Additionally, an overview of the GIS raster-based approach for time-series surface runoff estimation is shown in Figure 3.6. It is a GIS raster-based spatial analysis applying all the mathematic equations present in the SCS-CN method algorithm.

The derived results of this component will be further applied to calculate the average surface runoff coefficient of each LULC type between 2001 and 2019 under three different rainfall conditions according to SPI calculation based on annual rainfall data between 1987 and 2019.
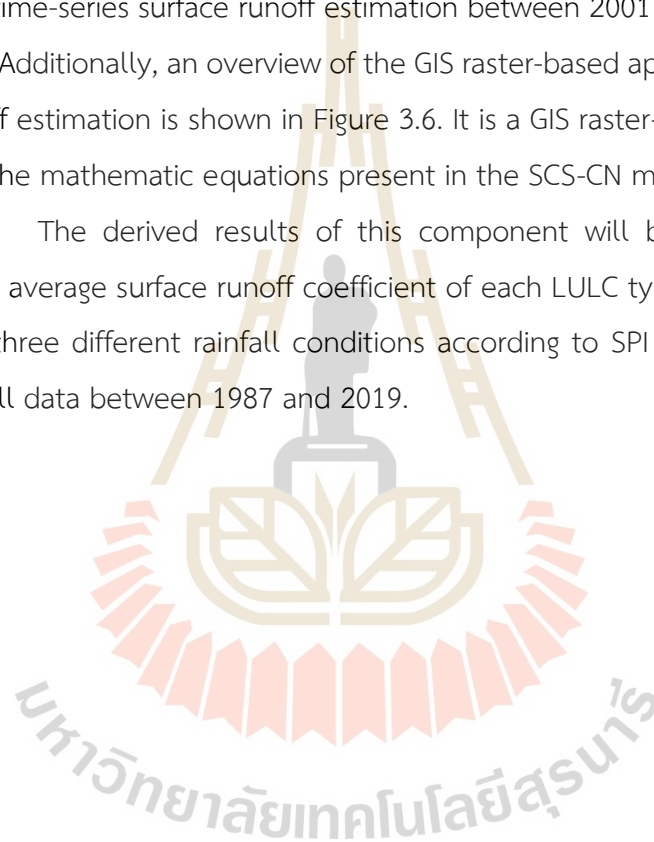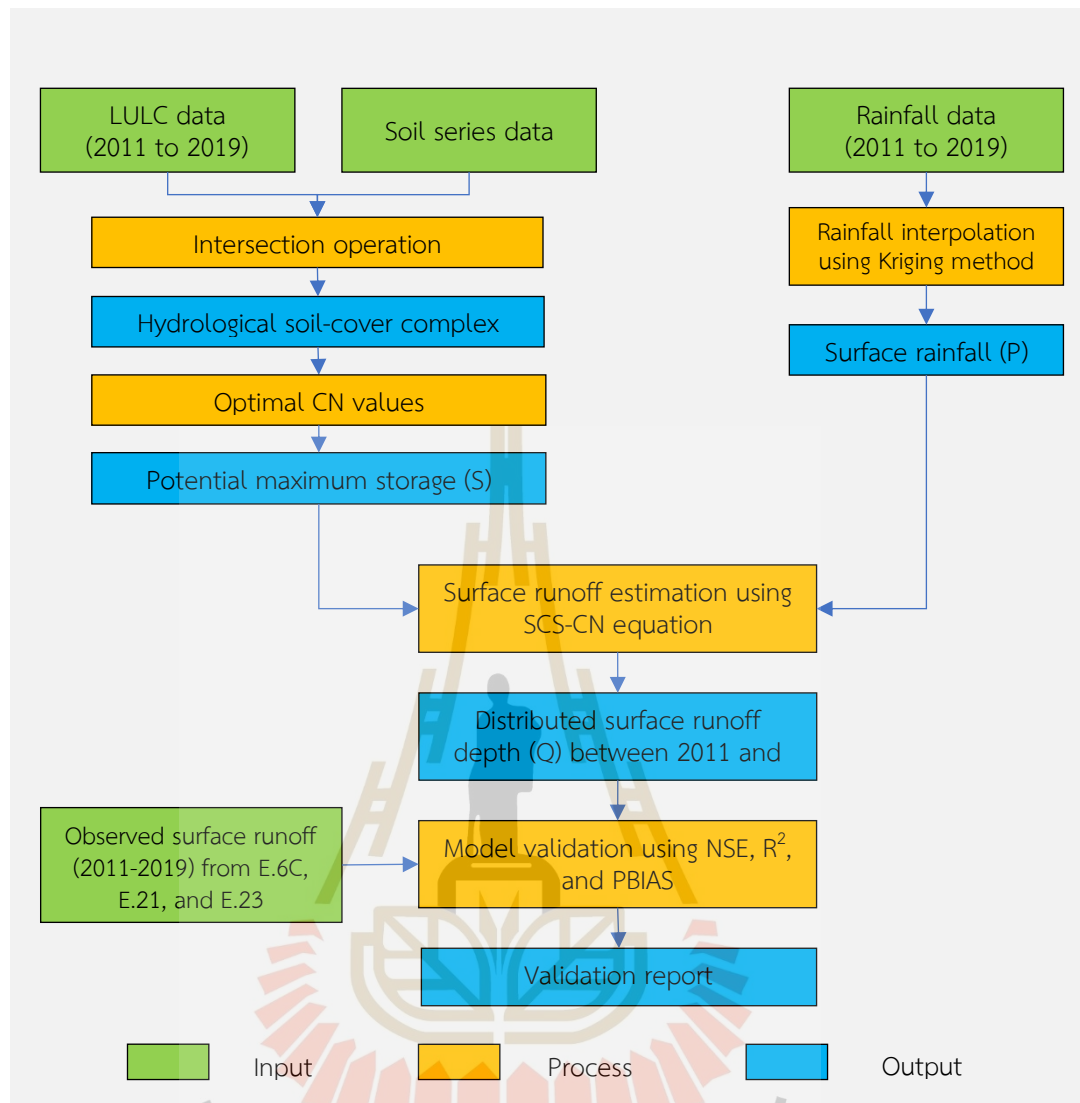
Figure 3.5 Workflow of time-series surface runoff estimation between 2001 and 2019.
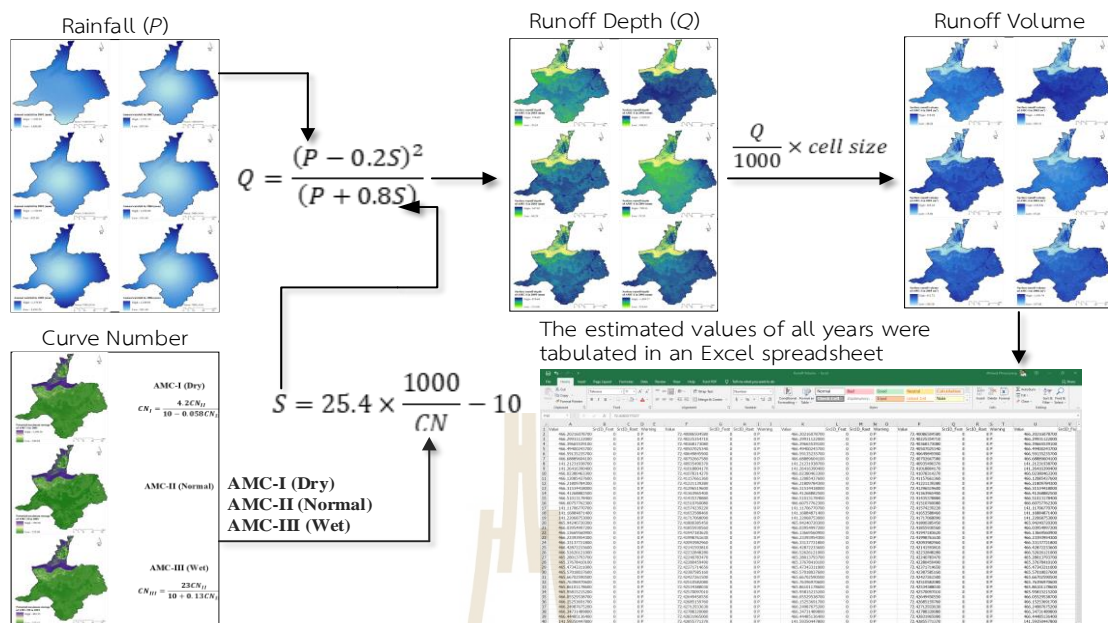
Figure 3.6 Overview of estimated surface runoff from GIS raster-based SCS-CN method.

3.5 Component 4: Optimization of LULC allocation for flood mitigation

The optimization of LULC allocation for flood mitigation based on the surface runoff coefficient value of LULC types under three different rainfall conditions (drought, normal, and wet years) are implemented using goal programming with the "What's Best!" extension under MS-Excel software. Under this component, two significant tasks include (1) SPI calculation for rainfall condition identification and (2) optimization of LULC allocation to minimize surface runoff for flood mitigation.

3.5.1 SPI calculation for rainfall condition identification

Annual rainfall data between 1987 and 2019 were used to calculate the 12-month SPI value and classified according to the SPI drought classification of Liu et al. (2014) for rainfall conditions identification (See Table 2.3). The derived cumulative probability of SPI values was then reclassified into three rainfall conditions as follows:

1. If any year has an SPI value less than or equal to -0.50, then it is categorized as a drought year condition,

2. If any year has an SPI value between -0.49 and 0.49, it is categorized as a normal year condition. and

3. If any year has an SPI value more than or equal to 0.50, it is categorized as a wet year condition.

Then, the average surface runoff coefficient for each LULC type of each rainfall condition was extracted from the time-series surface runoff data and LULC data using zonal statistical analysis.

3.5.2 Optimization of LULC allocation to minimize surface runoff for flood mitigation

Optimization of LULC allocation for flood mitigation was implemented using goal programming. The objective of the analysis was the minimization of surface runoff under certain constraints of three different rainfall conditions (drought, normal and wet years). In practice, the constraints set for optimizing LULC allocation in 2029, 2039, and 2049 were assigned based on the historical LULC development between 2010 and 2019 using the Markov Chain model. The changing area of each LULC type was considered according to the derived transitional area from the Markov Chain model. Then, the derived average runoff coefficient and constraints of the objective function were applied to optimize LULC allocation for flood mitigation under drought, normal, and wet year conditions using goal programming with "What's Best!" as an extension program under the MS-Excel environment. Moreover, the average surface runoff between 2001 and 2019 under drought, normal, and wet year conditions were used to set up the goal to minimize runoff based on the LULC type in 2019 under goal programming.

The goal programming model working as surface runoff minimization function can be expressed as the following equations:

Minimize surface runoff:

$$\text{Min} (Z) = \sum_{i=1}^{n} C_i X_i \tag{3.9}$$

Subject to constraints:

$$\sum_{i=1}^{n} X_i = A \tag{3.10}$$

$$\sum_{i=1}^{n} X_i \geq A \tag{3.11}$$

$$\sum_{i=1}^{n} X_i \leq A \tag{3.12}$$

$$X_i \geq 0 \tag{3.13}$$

where Z is the total annual surface runoff of the study area (m³/yr), C_i is the average surface runoff coefficient in each land use type (m³/km²/yr), X_i is the area of land use class i (km²), n is the number of land use classes, and A is the total area of land use classes (km²).

The schematic workflow of optimization of LULC allocation for flood mitigation under three different rainfall conditions is displayed in Figure 3.7. The derived results will be further applied to map optimizing LULC allocation for flood mitigation under three different rainfall conditions in the future (2029, 2039, and 2049).
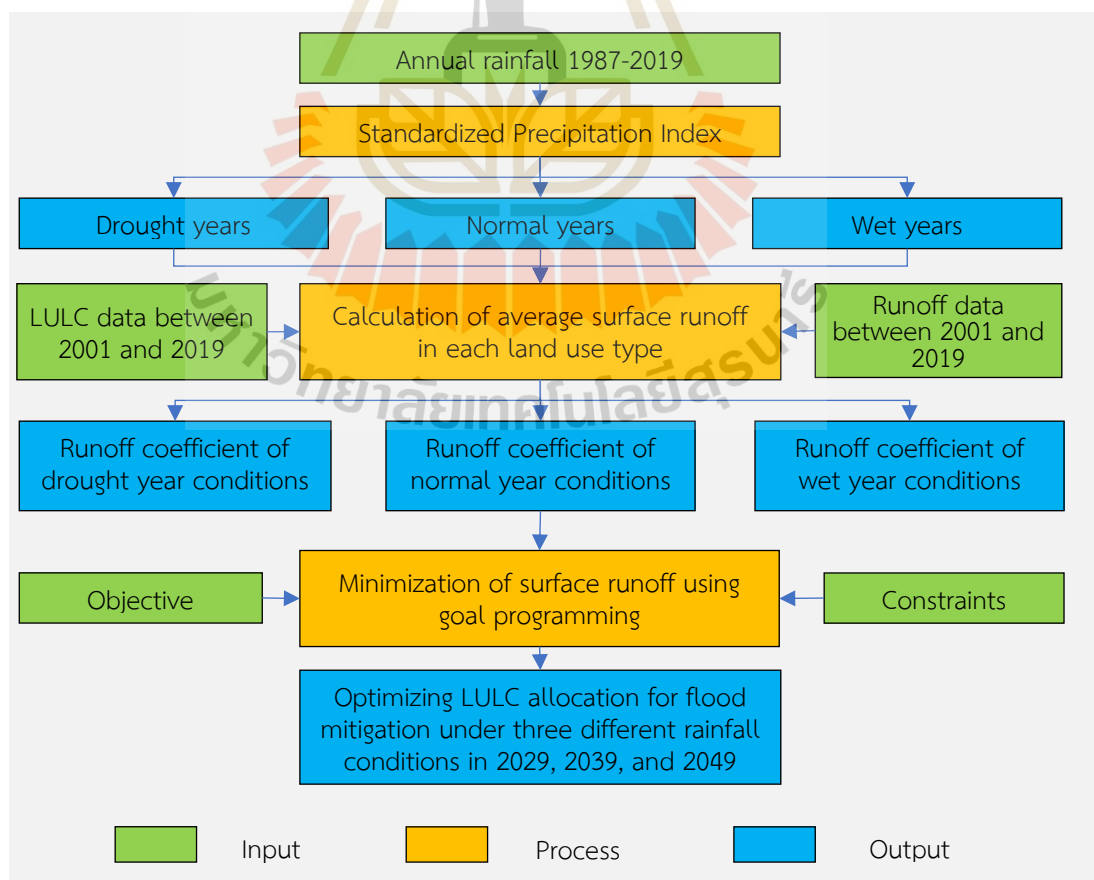
Figure 3.7 Workflow of optimization of LULC allocation for flood mitigation.

3.6   Component 5: Mapping of LULC allocation for flood mitigation

Under this component, an optimizing LULC allocation for flood mitigation in 2029, 2039, 2049 under three different rainfall conditions was mapped using the CLUE-S model. In practice, input data, which includes LULC data in 2019, an optimum local parameter (driving factors for each LULC type location preference, elasticity value, LULC conversion matrix), and optimizing LULC allocation data of three different rainfall conditions, as the land demand, were applied to map LULC maps using CLUE-S model.

The schematic workflow of mapping LULC allocation for flood mitigation under three different rainfall conditions is presented in Figure 3.8. The derived optimum LULC data for flood mitigation will be further applied to evaluate economic and ecosystem service value change in the next component.
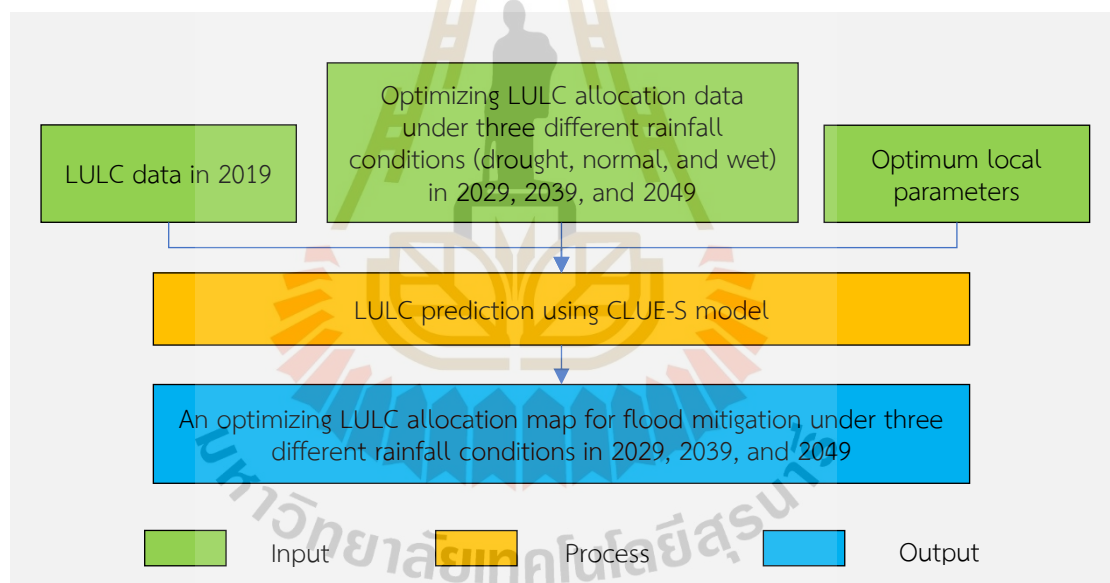
Figure 3.8 Workflow of mapping of LULC allocation for flood mitigation.

3.7   Component 6: Economic and ecosystem service values evaluation and change

Economic and ecosystem service values evaluation and change were separately evaluated using the present value (PV) model and simple benefit transfer method based on LULC data in 2019 and optimizing LULC allocation data for flood

mitigation under three different rainfall conditions in terms of gain and loss for project implementation.

3.7.1 Economic values evaluation and change

For economic value evaluation, LULC data in 2019 and optimizing LULC allocation data in a specific year (2029, 2039, or 2049) for flood mitigation under three different rainfall conditions were first calculated economic values using the PV model (Eq. 3.14) as suggested by Rossiter (1994).

$$PV = FV \cdot \left[\frac{100}{100+IR} \right]^Y \quad (3.14)$$

where PV is the present value, FV is the future value, IR is the interest rate in percent, and Y is the number of years from the present, counting from zero.

Then the economic value change in terms of gain and loss for flood mitigation between the current LULC data in 2019 and optimized LULC data in a specific year under three different rainfall conditions were compared using image algebra change detection algorithm.

3.7.2 Ecosystem service value evaluation and change

In brief, ecosystem services are categorized into four groups: regulating, supporting, provisioning, and cultural service (Millennium Ecosystem Assessment, 2005), as a summary in Table 3.8. Ecosystem services represent a dynamic field in current scientific research, linking ecological, economic, and social aspects, demanding practical applications and methodologies at different spatial scales, and maintaining environmental management and decision making processes (Costanza et al., 1997; Millennium Ecosystem Assessment, 2005; TEEB, 2010).

For ecosystem service value evaluation, the ecosystem service value (ESV) were first calculated based on LULC in 2019 and optimizing LULC allocation data in a specific year (2029, 2039, or 2049) for flood mitigation under drought, normal, and wet year conditions were calculated using a simple benefit transfer method (Costanza et al., 1997) (Eq. 3.15).

$$ESV = \sum (A_k \times VC_k) \quad (3.15)$$

where ESV denotes the total value of ecosystem service while A_k and VC_k represent the area and value coefficient for proxy LULC type 'k', respectively. The coefficient value for different LULC types for ESV calculation is shown in Table 3.9.

Then, ecosystem service value change in terms of gain and loss for flood mitigation between the current LULC data in 2019 and optimize LULC data in a specific year under three different rainfall conditions were compared using an image algebra change detection algorithm.

Finally, economic and ecosystem service value changes of optimal LULC allocation in terms of gain and loss for flood mitigation by each rainfall condition (drought, normal, and wet year) were reported.

The schematic workflow of economic and ecosystem service values evaluation and change is presented in Figure 3.9. The derived information on economic and ecosystem service value evaluation and change in terms of gain and loss can be informed to policy-makers for flood mitigation at Mueang Chaiyaphum district, Chaiyaphum province in the future.
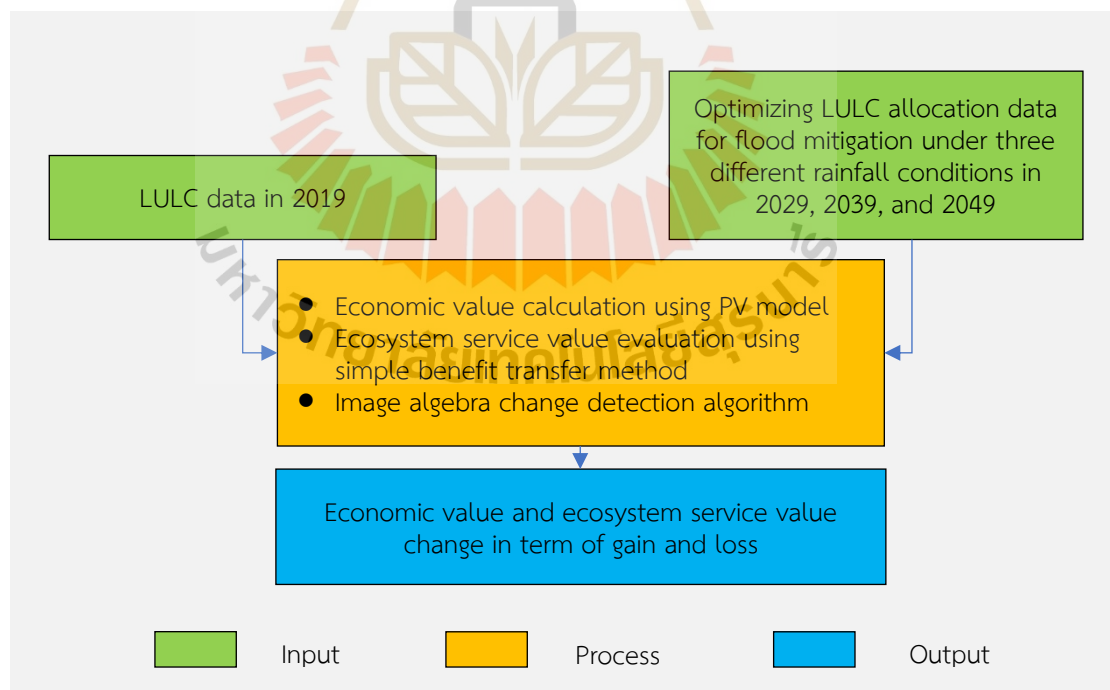
Figure 3.9 Workflow of economic and ecosystem service value evaluation and change.

Table 3.8 Classification of ecosystem services.

Ecosystem services

Provisioning services

- Food (crops, livestock, wild foods, etc.)
- Fiber (timber, cotton, wood fuel)
- Genetic resources
- Biochemical, natural medicines, pharmaceutical
- Freshwater

Regulating services

- Air quality regulation
- Climate regulation
- Water regulation
- Erosion regulation
- Natural hazard regulation
- Pollination
- Disease regulation
- Pest regulation

Cultural services

- Aesthetic values
- Spiritual and religious values
- Recreation and ecotourism

Supporting services

- Nutrient cycling
- Soil formation
- Primary production

Source: Millennium Ecosystem Assessment (2005).

Table 3.9 Coefficient value for different LULC types for ESV estimation.

Ecosystem services category	Ecosystem services function	LULC types							
		Urban and built-up area	Paddy field	Field crop	Forest land	Water body	Rangeland	Marsh and swamp	Unused land
1. Regulating services	1.1 Gas regulation	0	74.7	74.7	299.4	0	104	268.9	4.2
	1.2 Climate regulation	0	133.0	133.0	282.1	68.7	108	2,554.7	9.0
	1.3 Waste treatment	0	245.0	245.0	119.2	2,719.0	91.5	2,716.0	18.0
2. Supporting services	2.1 Soil formation	0	218.1	218.1	278.6	1.5	155	255.5	11.8
	2.2 Biodiversity protection	0	106.1	106.1	312.6	372	130	373.5	27.7
3. Provision services	3.1 Water supply	0	89.6	89.6	283.5	3,047.7	105	2,315.6	4.8
	3.2 Food production	0	149.4	149.4	22.9	14.9	29.8	44.8	1.4
	3.3 Raw materials	0	14.9	14.9	206.5	1.5	25	10.5	2.8
4. Cultural services	4.1 Recreation and culture	12.7	1.5	1.5	144.2	648.4	60.3	829.2	16.6
Total		12.7	1,032.3	1,032.3	1,949.0	6,873.7	808.6	9,368.7	96.3

Source: Modified from Mamat, Halik, and Rouzi (2018).

CHAPTER IV
LAND USE AND LAND COVER CLASSIFICATION AND CHANGE
DETECTION

This chapter presents the first objective results focusing on the classification of LULC in 2001, 2010, and 2019 based on Landsat 5-TM, Landsat 5-TM, and Landsat 8-OLI with supplementary data, including NDVI, MNDWI, NDBI, and DEM using the RF classifier. Spatial distribution of Landsat and supplemental data for LULC classification using the RF classifier are displayed in Figures 4.1 to 4.6. In the study, the LULC classification system, which was modified from the standard land use classification system of LDD, consists of (1) urban and built-up area, (2) paddy field, (3) sugarcane, (4) cassava, (5) other field crops, (6) para rubber, (7) perennial trees and orchard, (8) forest land, (9) water body, (10) rangeland, (11) marsh and swamp, and (12) unused land (See detail in Table 3.2 of Chapter III). Furthermore, the change detection between 2001 and 2019 using a post-classification comparison change detection algorithm is also presented. The significant results in this chapter consist of (1) LULC classification in 2001, (2) LULC classification in 2010, (3) LULC classification in 2019, (4) LULC change between 2001 and 2010, and (5) LULC change between 2010 and 2019 are described and discussed in details.
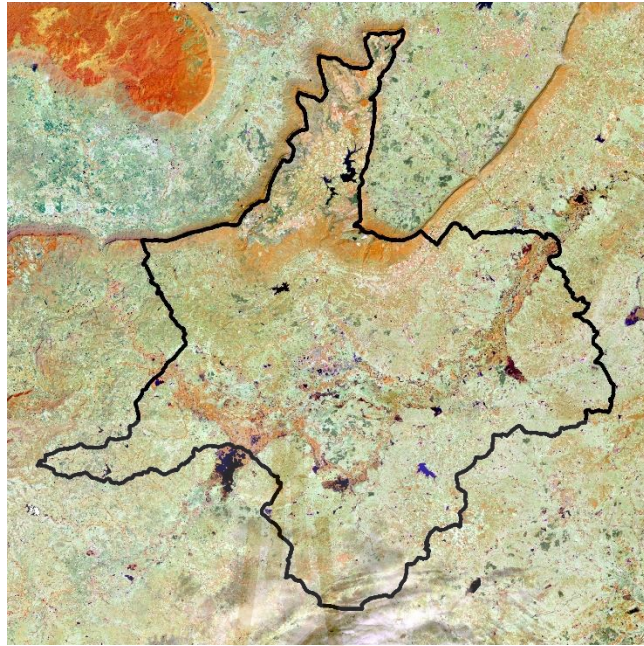
Figure 4.1 False-color composite image of Landsat 5-TM in 2001 (RGB: 453).

(a) NDVI

(b) MNDWI
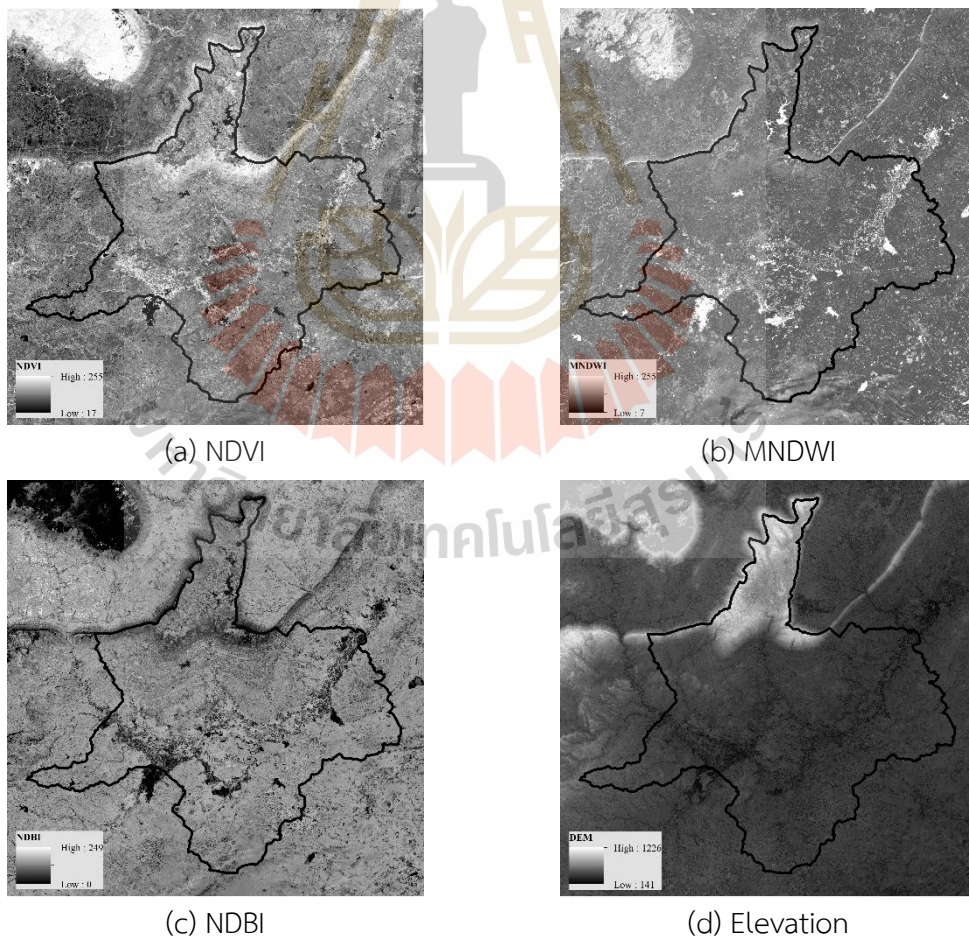
(c) NDBI

(d) Elevation

Figure 4.2 Supplementary data for LULC classification in 2001 (a) NDVI, (b) MNDWI, (c) NDBI, and (d) elevation.
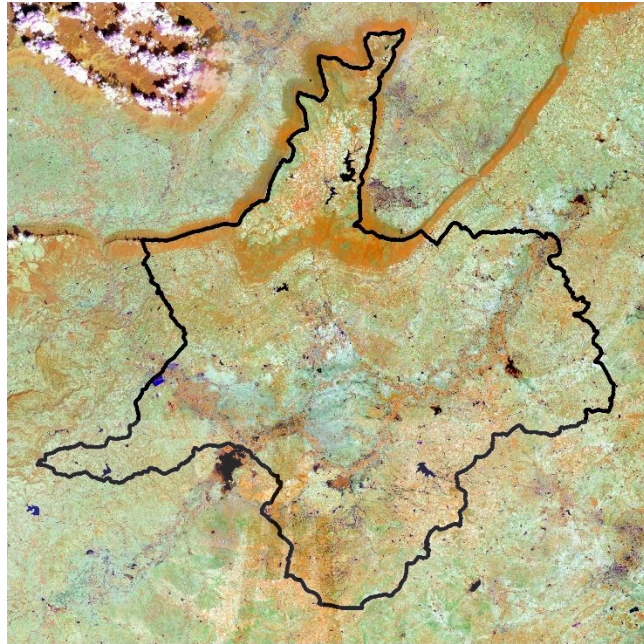
Figure 4.3 False-color composite image of Landsat 5-TM in 2010 (RGB: 453).

(a) NDVI

(b) MNDWI
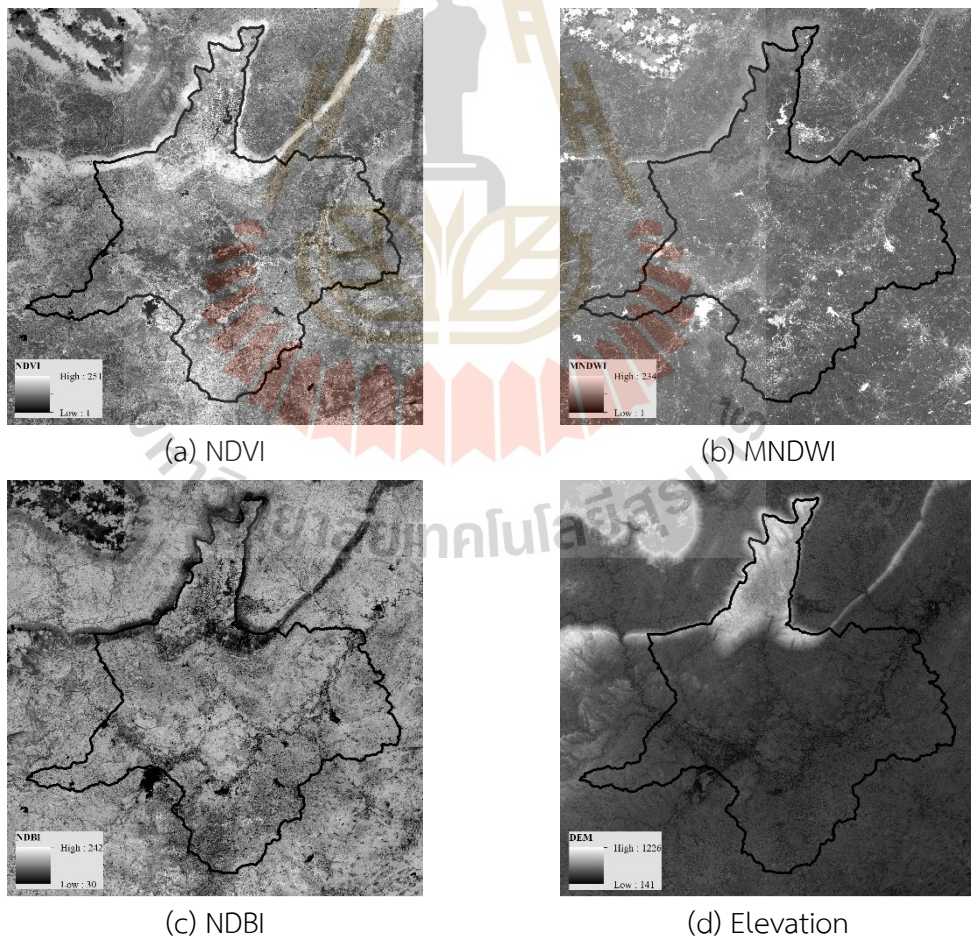
(c) NDBI

(d) Elevation

Figure 4.4 Supplementary data for LULC classification in 2010 (a) NDVI, (b) MNDWI, (c) NDBI, and (d) elevation.
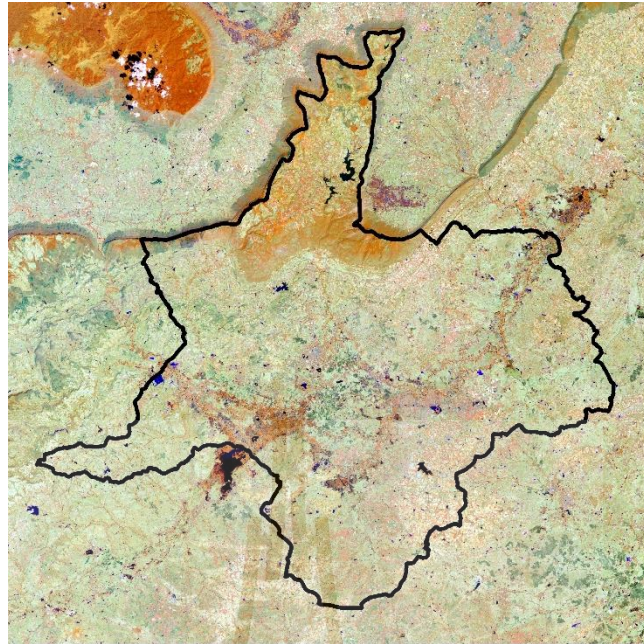
Figure 4.5 False-color composite image of Landsat 8-OLI in 2019 (RGB: 453).

(a) NDVI

(b) MNDWI
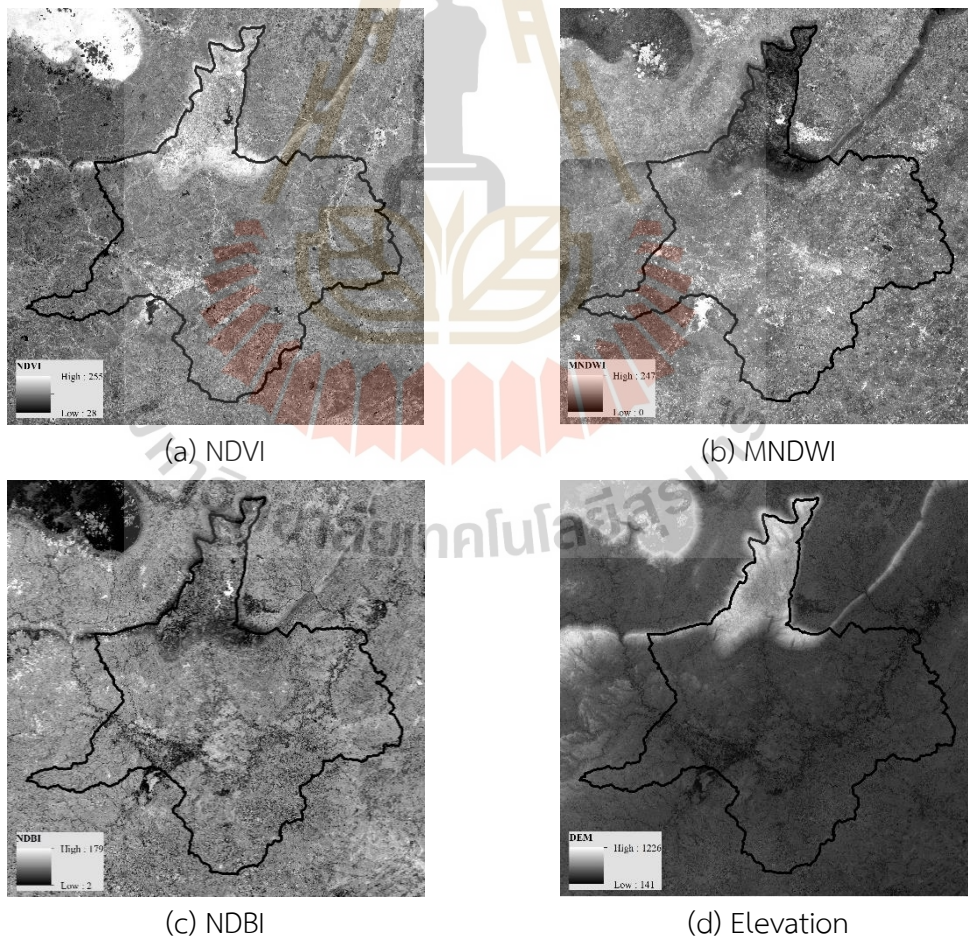
(c) NDBI

(d) Elevation

Figure 4.6 Supplementary data for LULC classification in 2019 (a) NDVI, (b) MNDWI, (c) NDBI, and (d) elevation.

4.1   LULC classification in 2001

The spatial distribution of training points identified from the input dataset for LULC classification in 2001 by the RF classifier is displayed in Figure 4.7. Meanwhile, LULC classification in 2001 as a historical record in this study is spatially shown in Figure 4.8. In the meantime, the area and percentage of LULC data in 2001 are summarized in Table 4.1.

The results reveal that the top three most dominant LULC types in 2001 are paddy field, forest land, and cassava, covering 2,344.39 km^2 (61.79%), 632.00 km^2 (16.66%), and 532.95 km^2 (14.05%), respectively. Additionally, it can be observed that most of the paddy fields are situated on the central plain of the study. Simultaneously, forest lands are primarily located in the mountainous in the northern part of the study area. In the meantime, cassava fields are situated in undulated areas in the southern part of the study area. On the contrary, the top three least dominant LULC types in 2001 are other field crops, marsh and swamp, and para rubber, which are randomly situated in the study area, covering an area of 2.09 km^2 (0.06%), 11.64 km^2 (0.30%), and 16.56 km^2 (0.44%), respectively.
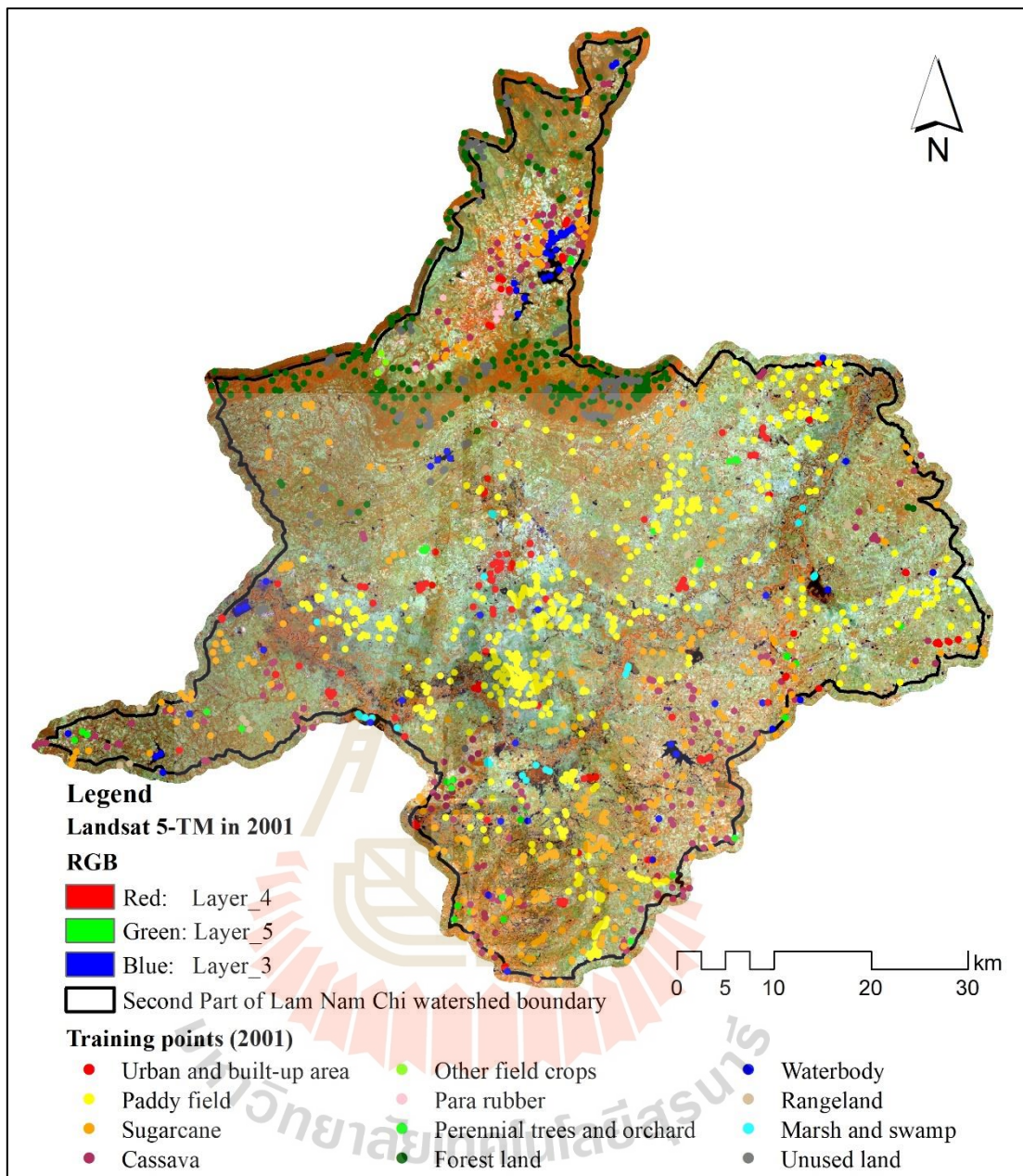
Figure 4.7 Spatial distribution of training points for LULC classification in 2001.
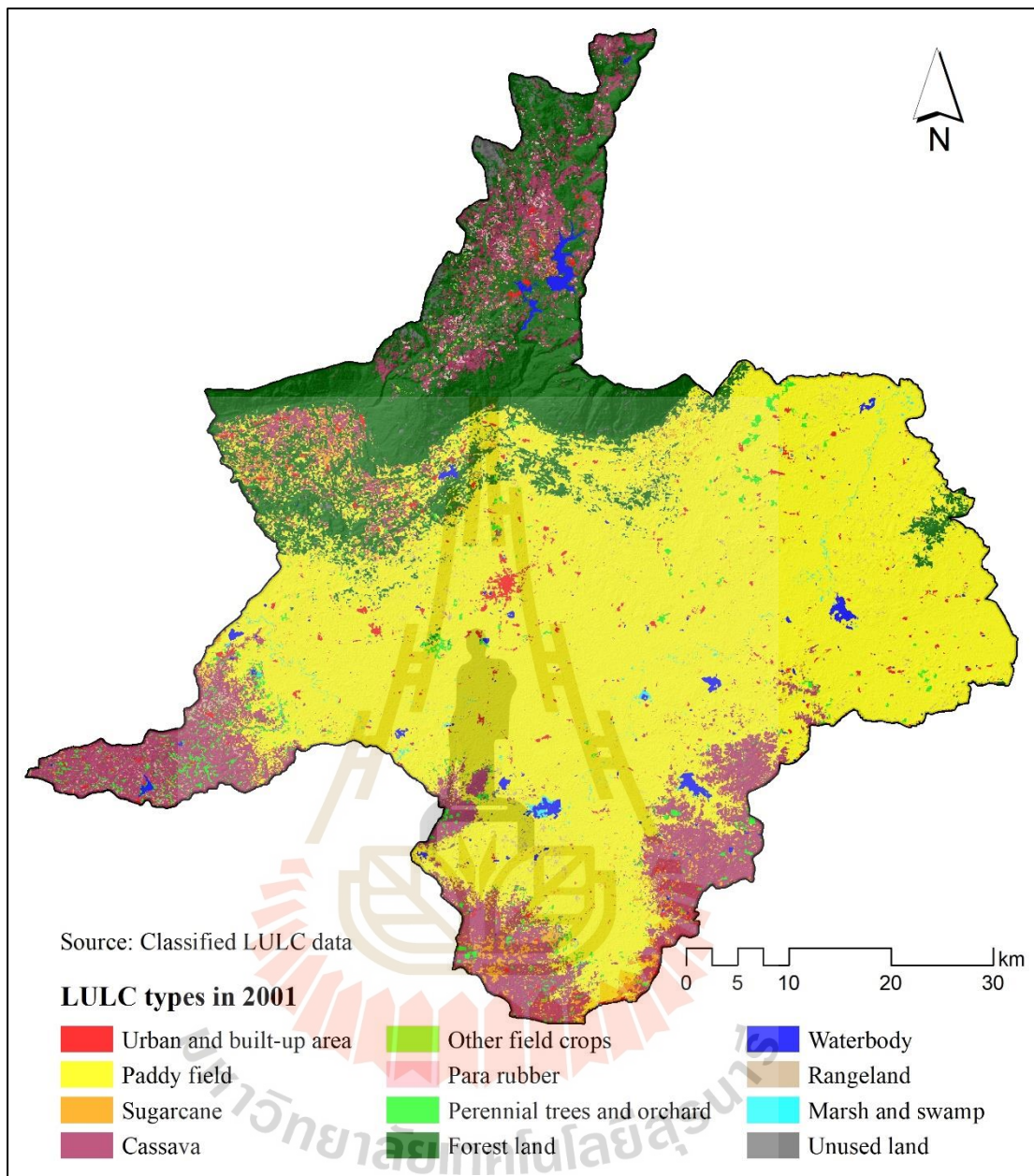
Figure 4.8 Spatial distribution of LULC classification in 2001.

Table 4.1 Area and percentage of LULC data in 2001.

No.	LULC type	Area in km^2	Area percentage
1	Urban and built-up area	46.17	1.22
2	Paddy field	2,344.39	61.79
3	Sugarcane	61.25	1.61
4	Cassava	532.95	14.05
5	Other field crops	2.09	0.06
6	Para rubber	16.56	0.44
7	Perennial trees and orchard	55.76	1.47
8	Forest land	632.00	16.66
9	Water body	36.81	0.97
10	Rangeland	26.03	0.69
11	Marsh and swamp	11.64	0.31
12	Unused land	28.57	0.75
	Total	3,794.22	100.00

The classified LULC map in 2001 was compared with ground reference information from color orthophotograph in 2000-2001 for a thematic accuracy assessment using overall accuracy (OA), producer's accuracy (PA), user's accuracy (UA), and the Kappa hat coefficient. For the LULC map in 2001, the required 800 stratified random sampling points based on multinomial distribution theory with the desired confidence level of 95 percent and a precision of 5 percent were used for a thematic accuracy assessment (Figure 4.9). The error matrix and accuracy assessment of the LULC map in 2001 between the classified LULC in 2001 and the ground reference information from color orthophotograph in 2000-2001 is shown in Table 4.2.

For thematic accuracy assessment, overall accuracy is 89.88%, and the Kappa hat coefficient is 84.88%. Meanwhile, the producer's accuracy (PA), which represents omission error, varies between 73.91% for sugarcane and 95.72% for the paddy field. The user's accuracy (UA), which describes commission error, varies between 71.43% for rangeland and 100.00% for the water body.
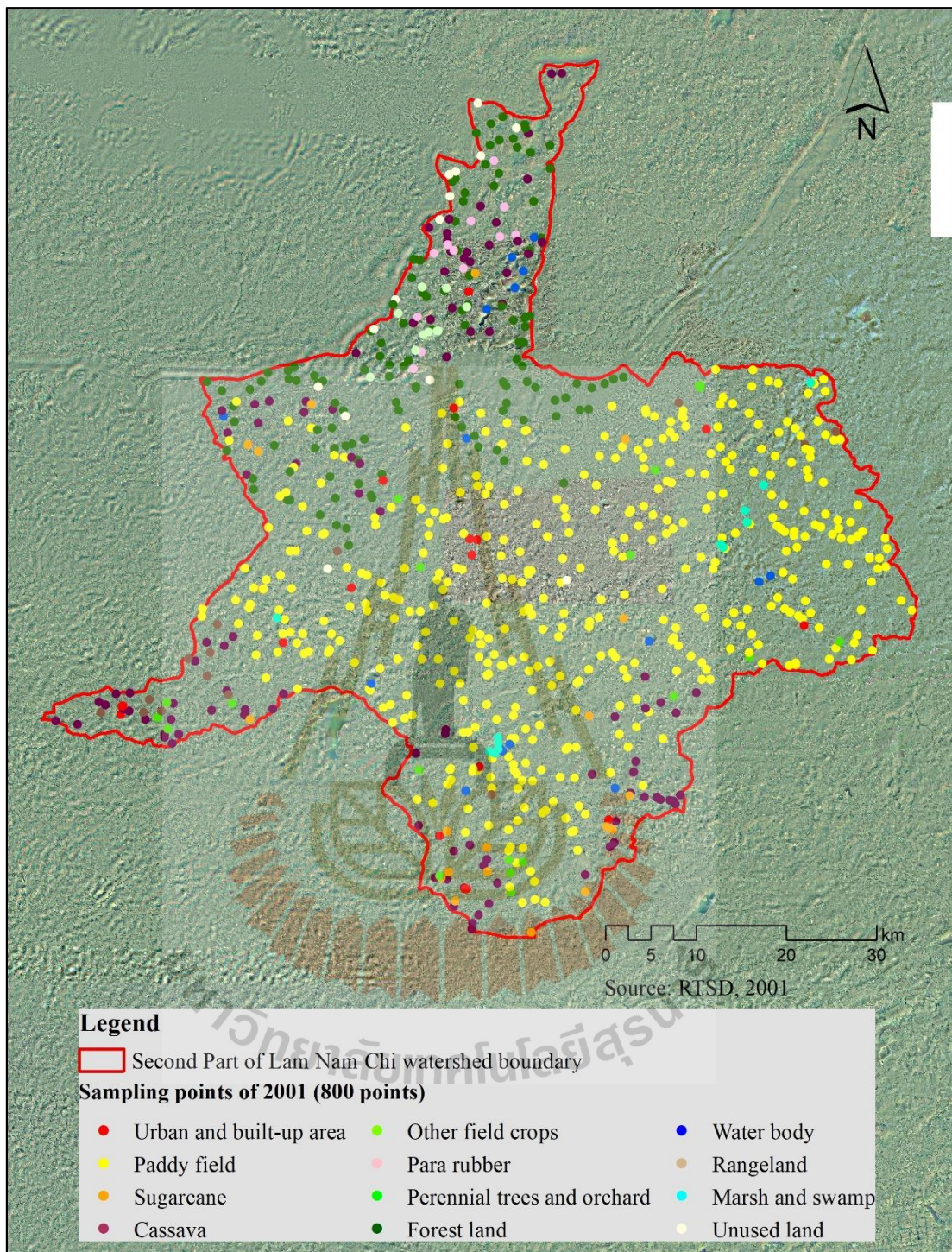
Figure 4.9 Spatial distribution of sampling points overlaid on aerial photograph for accuracy assessment of thematic LULC map in 2001.

As a result, the overall accuracy of more than 85% of the LULC map can provide acceptable results, as suggested by Anderson, Hardy, Roach, and Witmer (1976). Likewise, the Kappa hat coefficient of the agreement is more than 80% representing strong agreement or accuracy between the classified map and the ground reference information (Fitzpatrick-Lins, 1981). Besides, the derived overall accuracy and Kappa hat coefficient in the current study is similar to the previous research of Jhonnerie, Siregar, Nababan, Prasetyo, and Wouthuyzen (2015), who applied Landsat 5-TM to classify land cover by the RF classifier in Kembung River, Bengkalis Island, Indonesia, their study provides an overall accuracy of 81.10% and 76.00% for the Kappa hat coefficient. Furthermore, Srichaichana, Trisurat, and Ongsomwang (2019) applied the RF classifier to classify the LULC map from Landsat 5-TM at Klong U-Tapao watershed, Songkhla province, Thailand, and their study shows an overall accuracy of 91.36% and Kappa hat coefficient of 84.00%. Similarly, Na, Zhang, Li, Yu, and Liu (2010) Classified LULC mapping using the RF classifier from Landsat 5-TM at Sanjiang Plain, China. Their study provides an overall accuracy of 91.30% and the Kappa hat coefficient of 89.43%.

Table 4.2 Error matrix and accuracy assessment of LULC in 2001.

LULC types	Ground reference data from color orthophotograph in 2000-2001												
	UR	PA	SU	CA	FC	PR	PO	FO	WA	RA	MA	UL	Total
Urban and built-up area (UR)	16	2											18
Paddy field (PA)	3	403	1	20					2		3		432
Sugarcane (SU)		1	17	2	1								21
Cassava (CA)		12	4	87	1		1			1			106
Other field crops (FC)			1	1	8								10
Para rubber (PR)						9		2		1			12
Perennial trees and orchard (PO)				1			16	3					20
Forest land (FO)				1		1	4	115				3	124
Waterbody (WA)									16				16
Rangeland (RA)		1		2						10		1	14
Marsh and swamp (MA)		1							1		10		12
Unused land (UL)		1						2				12	15
Total	19	421	23	114	10	10	21	122	19	12	13	16	800
Producer's accuracy (%)	84.21	95.72	73.91	76.32	80.00	90.00	76.19	94.26	84.21	83.33	76.92	75.00	
User's accuracy (%)	88.89	93.29	80.95	82.08	80.00	75.00	80.00	92.74	100.00	71.43	83.33	80.00	
Overall accuracy (%)	89.88												
Kappa hat coefficient (%)	84.88												

Also, it can be observed that the significant omission error of sugarcane comes from cassava because the brightness value of sugarcane in the tillering phase is similar to cassava in the canopy development phase (Figure 4.10). In the meantime, most of the significant commissions of rangeland come from the cassava because the cassava fields without weeding are frequently mixed with grass, giving them a similar appearance to the rangeland (Figure 4.11).
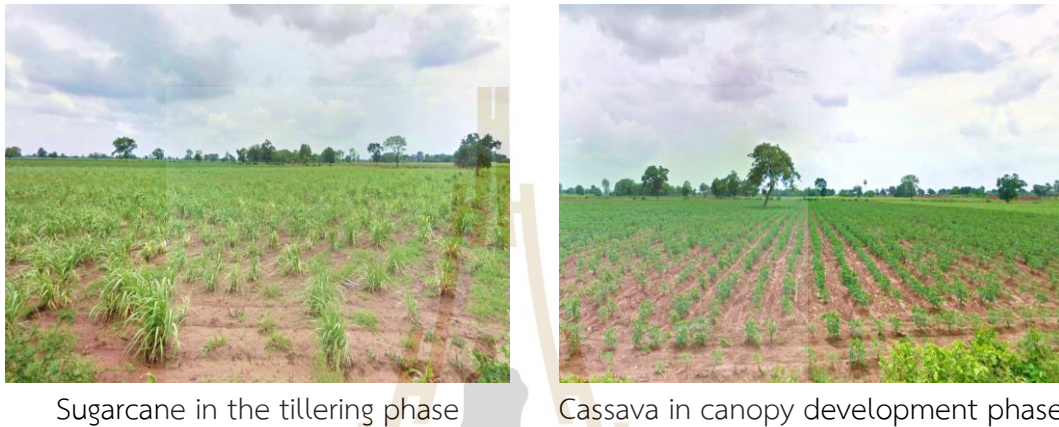
Sugarcane in the tillering phase   Cassava in canopy development phase

Figure 4.10 Comparison of growth stage between sugarcane and cassava from a field survey in 2020.

Cassava fields without weeding

Figure 4.11 Cassava fields and mixed-grass from a field survey in 2020.

4.2   LULC classification in 2010

The spatial distribution of training points identified from the input dataset for LULC classification in 2010 by the RF classifier is presented in Figure 4.12. Meanwhile, the result of the LULC classification in 2010, as a historical record in this study, is

spatially shown in Figure 4.13. In the meantime, the area and percentage of LULC data in 2001 are summarized in Table 4.3.

As a result, it was found that the top three most dominant LULC types in 2010 are paddy field, cassava, and forest land, covering 2,070.71 km^2 (54.58%), 629.33 km^2 (16.59%), and 604.70 km^2 (15.94%), respectively. Conversely, the top three least dominant LULC types in 2001 are other field crops, marsh and swamp, and para rubber, covering 5.19 km^2 (0.14%), 30.05 km^2 (0.79%), and 33.40 km^2 (0.88%), respectively.
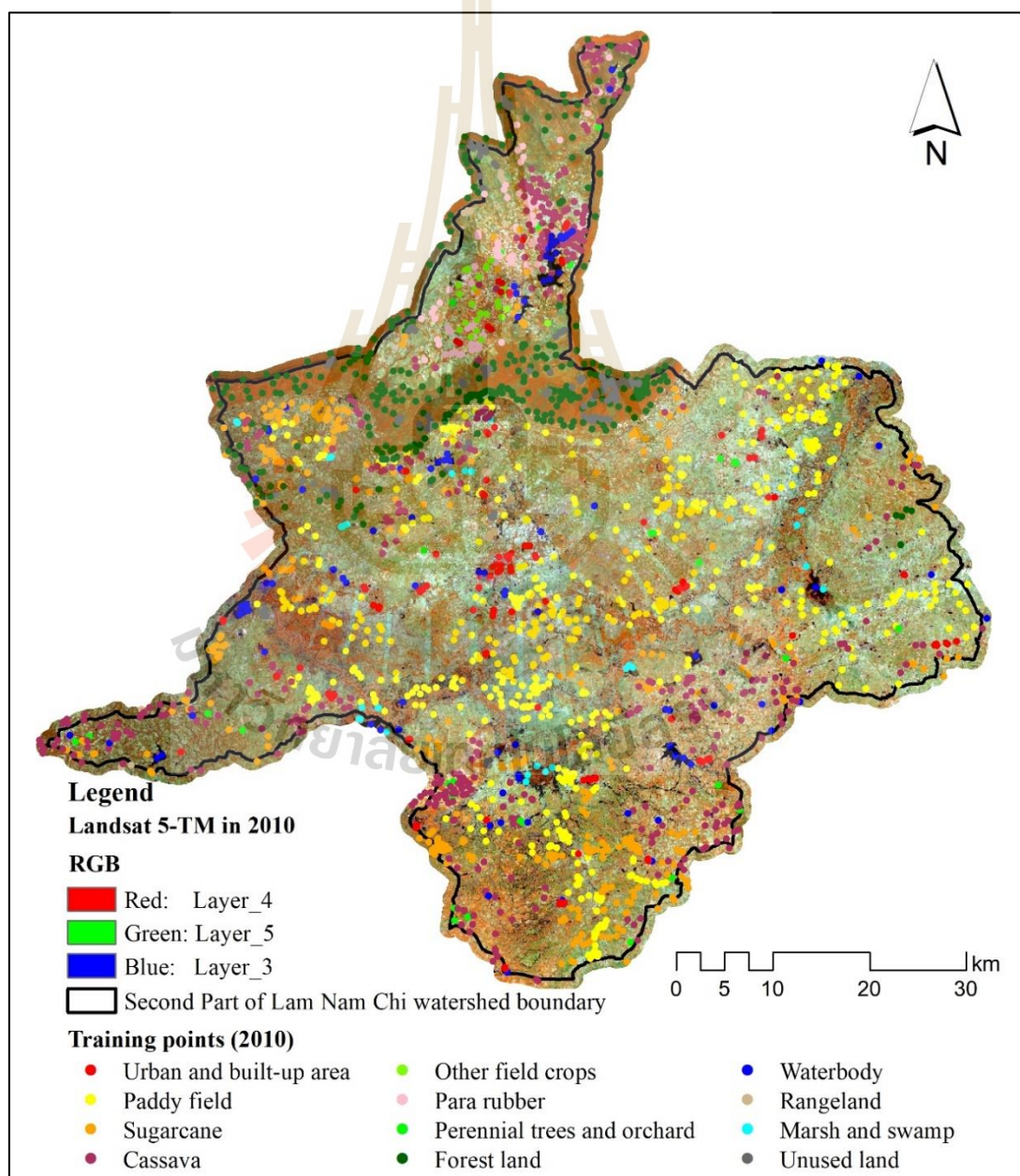
Figure 4.12 Spatial distribution of training points for LULC classification in 2010.
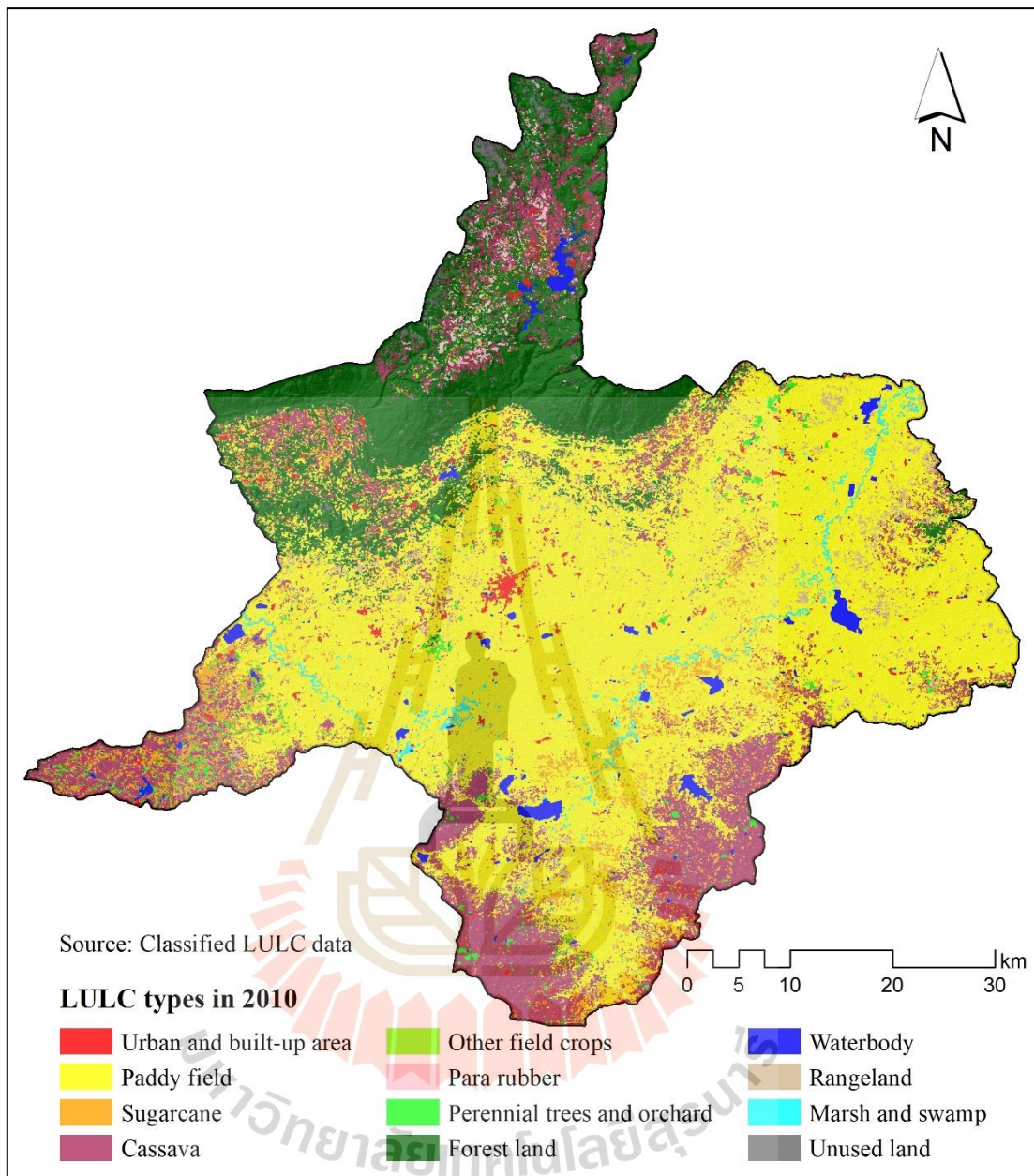
Figure 4.13 Spatial distribution of LULC classification in 2010.

Table 4.3 Area and percentage of LULC data in 2010.

No.	LULC type	Area in km²	Area percentage
1	Urban and built-up area	53.21	1.40
2	Paddy field	2,070.71	54.58
3	Sugarcane	153.52	4.05
4	Cassava	629.33	16.59
5	Other field crops	5.19	0.14
6	Para rubber	30.05	0.79
7	Perennial trees and orchard	50.21	1.32
8	Forest land	604.70	15.94
9	Waterbody	57.46	1.51
10	Rangeland	72.11	1.90
11	Marsh and swamp	33.40	0.88
12	Unused land	34.33	0.90
	Total	3,794.22	100.00

In addition, the classified LULC map in 2010 was compared with ground reference data from very high spatial resolution imageries from Google Earth in 2010 for thematic accuracy assessment using OA, PA, UA, and Kappa hat coefficient. For the LULC map in 2010, the required 840 stratified random sampling points based on multinomial distribution theory with the desired confidence level of 95 percent and a precision of 5 percent were used for accuracy assessment (Figure 4.14). The error matrix and accuracy assessment between the classified LULC in 2010 and the ground reference information from very high spatial resolution imageries from Google Earth in 2010 is shown in Table 4.4.

The overall accuracy is 90.71%, and the Kappa hat coefficient is 87.03%. Meanwhile, the PA varies from 65.22% for perennial trees and orchards to 100.00% for water bodies, while the UA varies from 78.95% for perennial trees and orchards to 95.00% for water bodies.
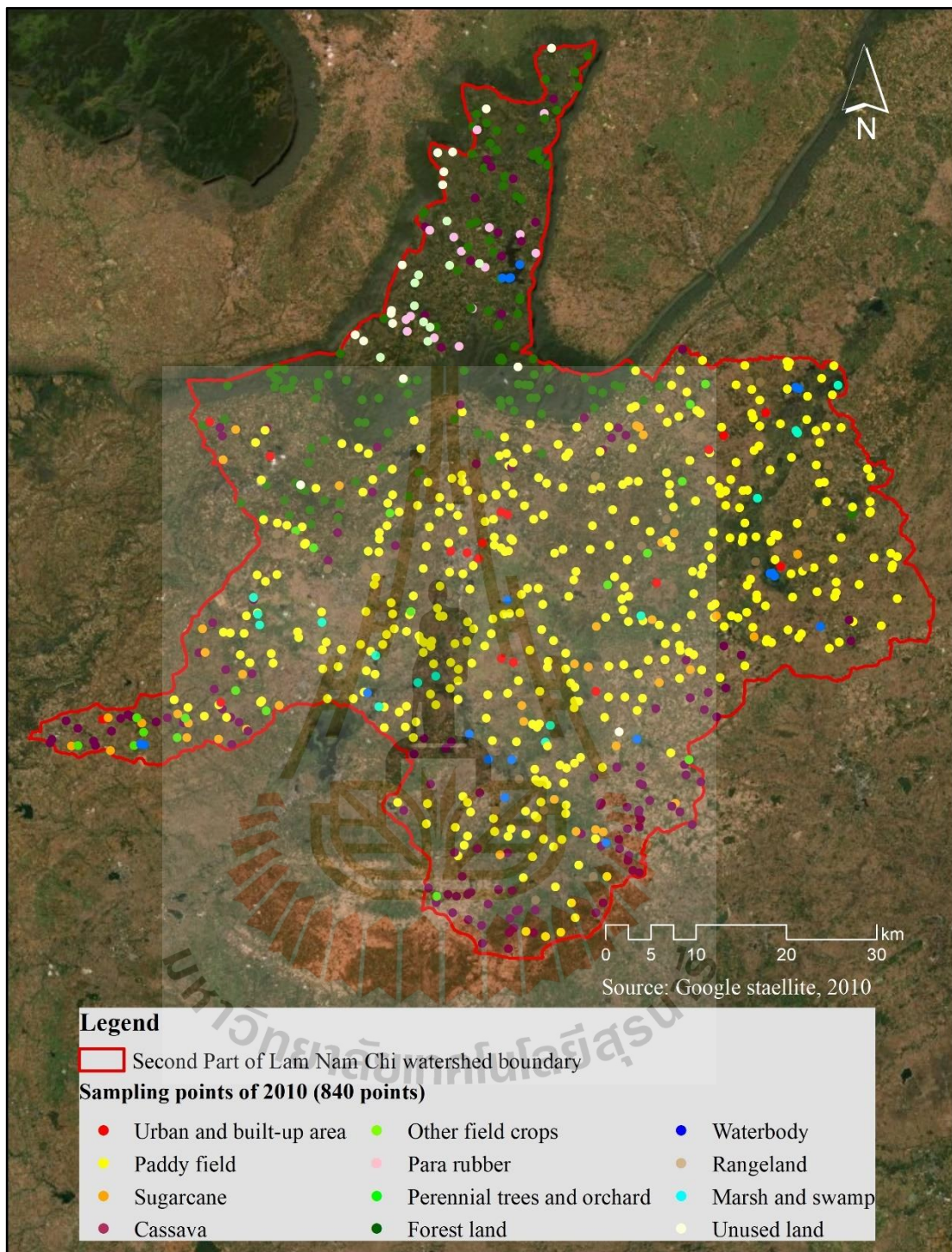
Figure 4.14 Spatial distribution of sampling points overlaid on a very high spatial resolution from Google Earth for accuracy assessment of thematic LULC map in 2010.

As a result, the overall accuracy of more than 85% of the LULC map can provide acceptable results, as suggested by Anderson et al. (1976). Likewise, the Kappa hat coefficient of more than 80% represents strong agreement or accuracy between the classified map and the ground reference information (Fitzpatrick-Lins, 1981). Besides, the derived overall accuracy and Kappa hat coefficient in the current study are similar to the previous research of Rodriguez-Galiano, Ghimire, Rogan, Chica-Olmo, and Rigol-Sanchez (2012). They applied the RF classifier to classify land cover from Landsat 5-TM at Granada province, South of Spain. Their study shows overall accuracy of 92.00% and a Kappa hat coefficient of 92.00%. Similarly, Kulkarni and Lowe (2016) applied the RF to classify LULC with Landsat 5-TM at the Yellowstone and Mississippi. Their study provides an overall accuracy of 96.00% and a Kappa hat coefficient of 94.00%. Likewise, Gartzia, Alados, Pe´rez-Cabello, and Bueno (2013) applied Landsat 5-TM to classify vegetation categories using the RF at Ordesa and Monte Perdido National Park, Spain. Their study shows the Kappa hat coefficient of 94.00%.

Table 4.4 Error matrix and accuracy assessment of LULC in 2010.

LULC types	Ground reference data from Google Earth in 2010												
	UR	PA	SU	CA	FC	PR	PO	FO	WA	RA	MA	UL	Total
Urban and built-up area (UR)	17	2											19
Paddy field (PA)	5	386	6	4			1			3	3		408
Sugarcane (SU)		1	36	1	1								39
Cassava (CA)	1	13	3	108	2		3						130
Other field crops (FC)			1	1	8								10
Para rubber (PR)						14		1					15
Perennial trees and orchard (PO)				1			15	3					19
Forest land (FO)						2	4	114		2		4	126
Waterbody (WA)									19		1		20
Rangeland (RA)		2	2							19			23
Marsh and swamp (MA)		3									12		15
Unused land (UL)			1	1								14	16
Total	23	407	49	116	11	16	23	118	19	24	16	18	840
Producer's accuracy (%)	73.91	94.84	73.47	93.10	72.73	87.50	65.22	96.61	100.00	79.17	75.00	77.78	
User's accuracy (%)	89.47	94.61	92.31	83.08	80.00	93.33	78.95	90.48	95.00	82.61	80.00	87.50	
Overall accuracy (%)	90.71												
Kappa hat coefficient (%)	87.03												

Classified LULC data in 2010

Besides, it can be observed that the significant omission and commission errors of perennial trees and orchard comes from forest land because the appearance and brightness value of perennial trees and orchards are similar to the dominant dipterocarps forest type in forest land (Figure 4.15).

Figure 4.15 Perennial trees and orchard nearby dipterocarps forest type in forest land.

4.3   LULC classification in 2019

The spatial distribution of training points identified from the input dataset for LULC classification in 2019 by the RF classifier is displayed in Figure 4.16. Additionally, characteristic of training points, including LULC type, composite Landsat image, spectral plot, and ground photographs, is presented in Table 4.5. In practice, average spectral reflectance, spectral indices, and elevation values from each LULC type training point were plotted against the number of bands to characterize its signature as a spectral plot. As a result, it can be observed that spectral plot patterns (with spectral reflectance from Bands 2 to 7) from other field crops (pineapple), para rubber, and forest land are similar, but the reflectance values are different. In the meantime, unique patterns of the spectral plot are exhibited from other LULC types.

Meanwhile, LULC classification in 2019, as a recent record in this study, is spatially displayed in Figure 4.17. In the meantime, the area and percentage of LULC data in 2019 are summarized in Table 4.6.

As a result, the top three most dominant LULC types in 2019 are paddy field, cassava, and forest land, covering 2,012.16 km^2 (53.03%), 489.91 km^2 (12.91%), and 481.30 km^2 (12.68%), respectively. On the other hand, the top three least dominant LULC types in 2019 are other field crops, marsh and swamp, and water bodies, covering an area of 6.19 km^2 (0.16%), 27.73 km^2 (0.73%), and 53.30 km^2 (1.40%), respectively.
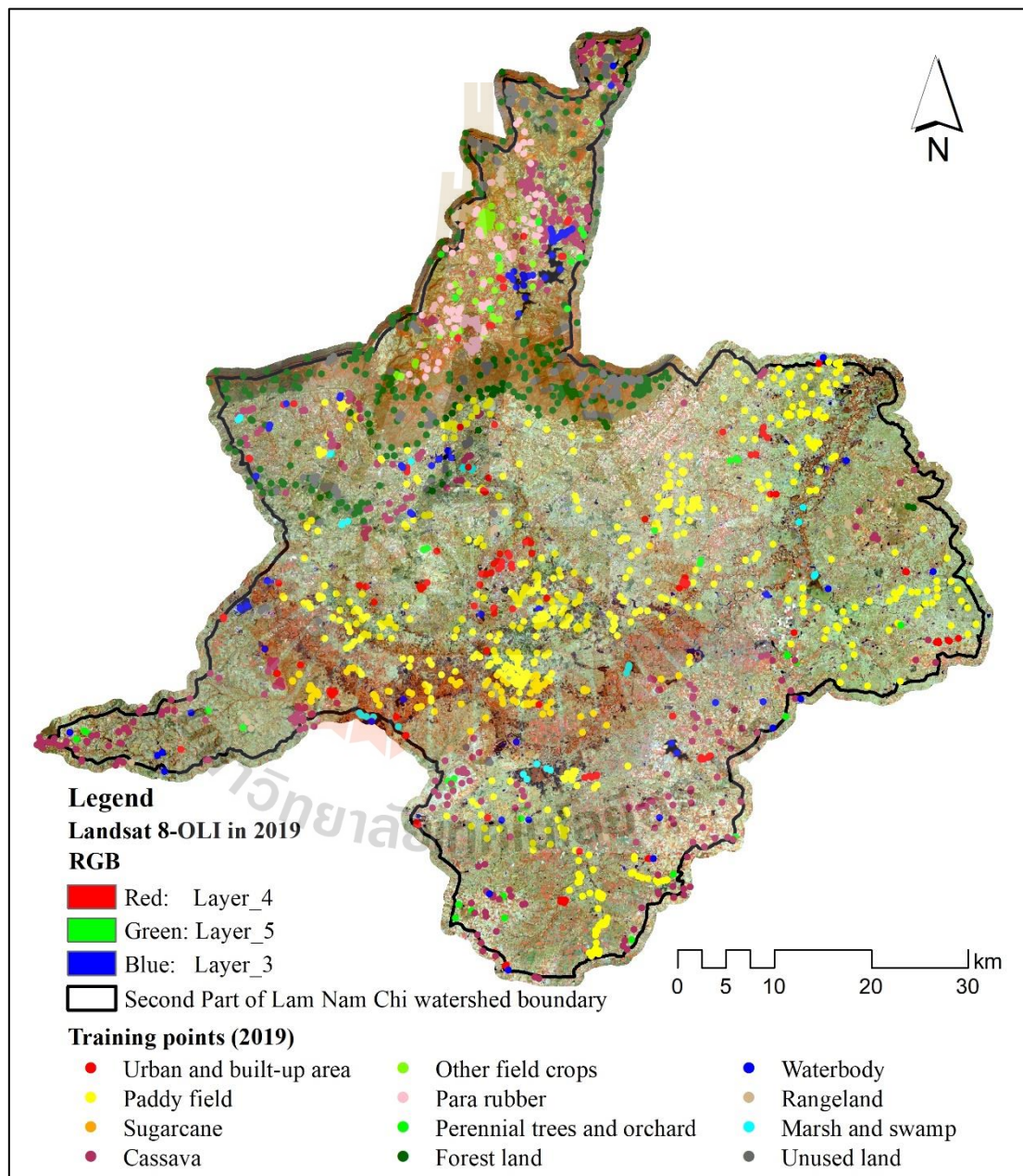
Figure 4.16 Spatial distribution of training points for LULC classification in 2019.

Table 4.5 Characteristic of training points for LULC classification with the RF classifier.

LULC type	Composite Landsat image (RGB: 453)	Spectral plot	Ground photographs
1. Urban and built-up area			
2. Paddy field			
3. Sugarcane			
4. Cassava			
5. Other field crops			
6. Para rubber			
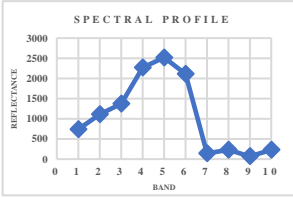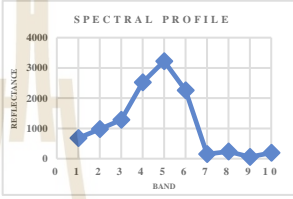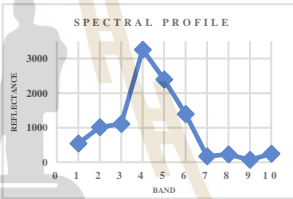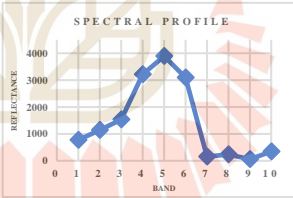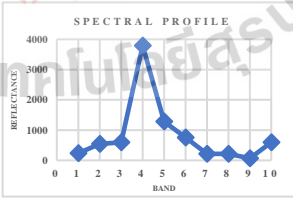
Table 4.5 (Continued).

LULC type	Composite Landsat image (RGB: 453)	Spectral plot	Ground photographs
7. Perennial trees and orchard			
8. Forest land			
9. Water body			
10. Rangeland			
11. Marsh and swamp			
12. Unused land			
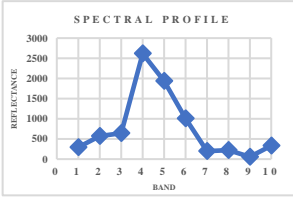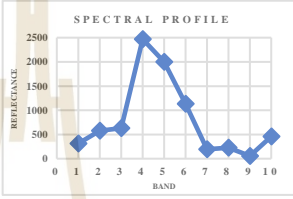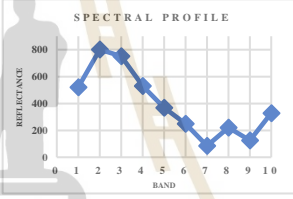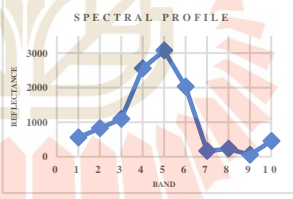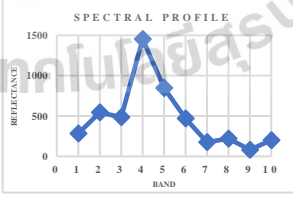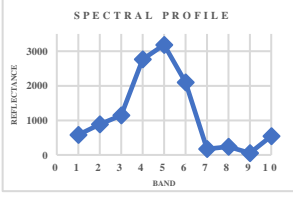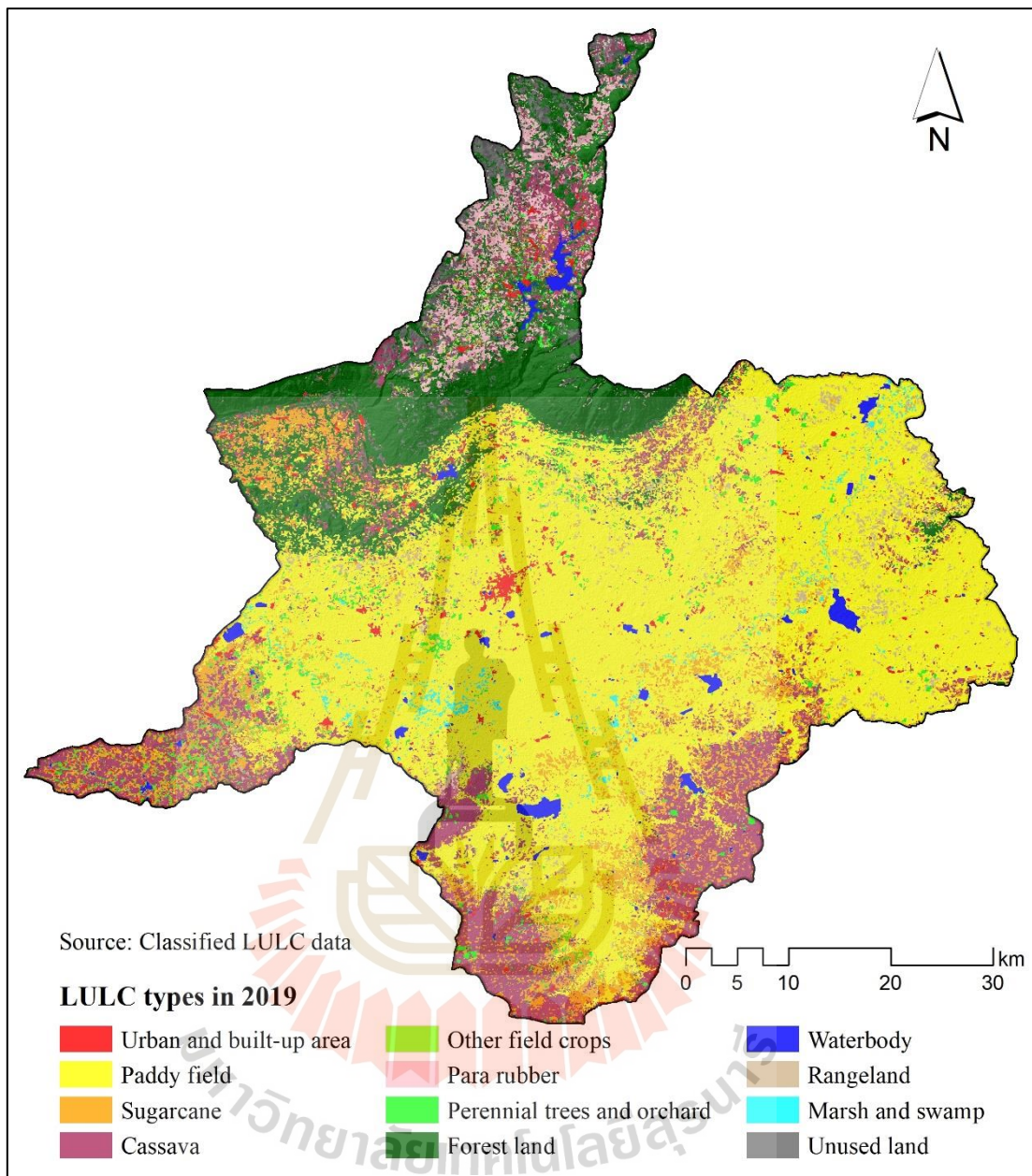
Figure 4.17 Spatial distribution of LULC classification in 2019.

Table 4.6 Area and percentage of LULC data in 2019.

No.	LULC type	Area in km^2	Area percentage
1	Urban and built-up area	65.84	1.74
2	Paddy field	2,012.16	53.03
3	Sugarcane	306.85	8.09
4	Cassava	489.91	12.91
5	Other field crops	6.19	0.16
6	Para rubber	97.03	2.56
7	Perennial trees and orchard	88.95	2.34
8	Forest land	481.30	12.68
9	Water body	53.30	1.40
10	Rangeland	71.65	1.89
11	Marsh and swamp	27.73	0.73
12	Unused land	93.32	2.46
	Total	3794.22	100.00

Furthermore, the classified LULC map in 2019 was compared with ground reference data from ground information by field survey in 2020 for a thematic accuracy assessment using overall accuracy and kappa hat coefficient of agreement. For the LULC map in 2019, the required 846 stratified random sampling points based on multinomial distribution theory with the desired confidence level of 95 percent and a precision of 5 percent were used for accuracy assessment (Figure 4.18). The error matrix and accuracy assessment between the classified LULC in 2019 and the ground reference information from ground information by field survey in 2020 is shown in Table 4.7.

As a result, the overall accuracy is 91.37%, and the Kappa hat coefficient is 88.26%. In the meantime, the PA varies between 71.43% for rangeland and 100.00% for a water body. Meanwhile, the UA varies between 71.43% for marsh and swamp and 96.43% for para rubber.
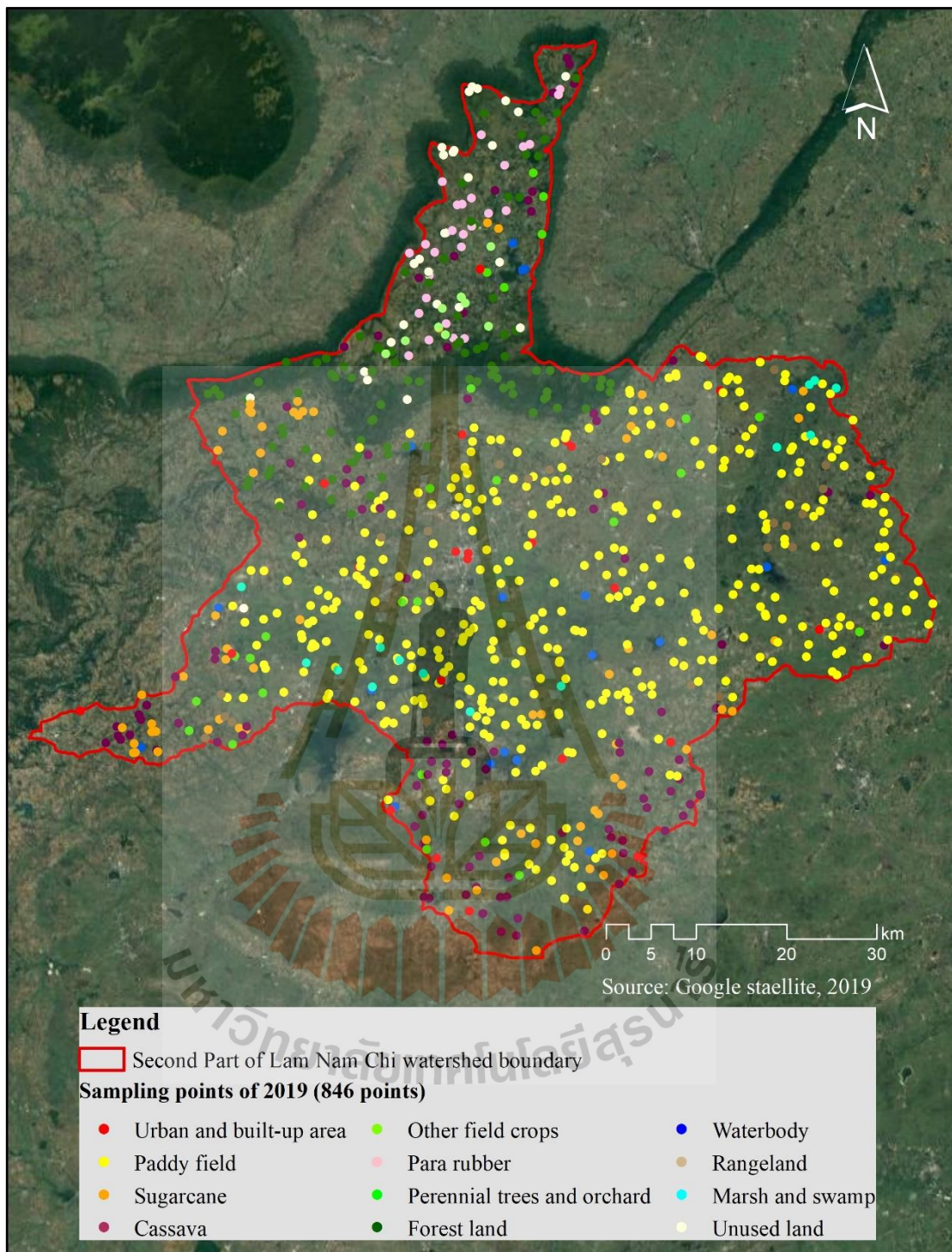
Figure 4.18 Spatial distribution of sampling points overlaid on Google satellite for accuracy assessment of thematic LULC map in 2019.

As a result, the overall accuracy of more than 85% of the LULC map can provide acceptable results, as suggested by Anderson et al. (1976). Likewise, the Kappa hat coefficient of more than 80% represents strong agreement or accuracy between the classified map and the ground reference information(Fitzpatrick-Lins, 1981). Besides, the derived overall accuracy and Kappa hat coefficient in the current study are similar to the previous research of Eisavi, Homayouni, Yazdi, and Alimohammadi (2015), who applied the RF to classify land cover data from Landsat 8-OLI at Naghadeh city, West Azerbaijan province, Iran. Their study provides an overall accuracy of 91.82% and 90.00% for the Kappa hat coefficient. Likewise, Pareeth, Karimi, Shafiei, and De Fraiture (2019) applied the RF classifier to extract land use types with Landsat 8-OLI data at the Mashhad basin, Iran. Their study shows an overall accuracy of 87.20% and Kappa hat coefficient of 85.00%. Similarly, Srichaichana et al. (2019) applied the RF classifier to classify the LULC map from Landsat 8-OLI at Klong U-Tapao watershed, Songkhla province, Thailand, and their study provide an overall accuracy of 91.36% and Kappa hat coefficient of 84%. Hence, the classified LULC in 2010 in this current study can be accepted and applied for LULC change detection and prediction in this study.

Besides, it can be observed that the significant commission error of marsh and swamp comes from paddy fields because the appearance of marsh and swamp in the dry season is similar to abandoned paddy fields (Figure 4.19). Meanwhile, rangeland is a significant omission error mostly from forest land because the brightness value of the rangeland with bush and shrub is similar to the dominant dry dipterocarps forest of forest land (Figure 4.20).

Table 4.7 Error matrix and accuracy assessment of LULC in 2019.

LULC types	Ground reference data from a field survey in 2020												
	UR	PA	SU	CA	FC	PR	PO	FO	WA	RA	MA	UL	Total
Urban and built-up area (UR)	19	2										1	22
Paddy field (PA)	5	383	5	4							2	2	401
Sugarcane (SU)		3	65		1								69
Cassava (CA)	1	6	3	89		3	1			1			104
Other field crops (FC)			2		8								10
Para rubber (PR)						27	1						28
Perennial trees and orchard (PO)						2	19	4		1			26
Forest land (FO)						2	3	93		4		1	103
Waterbody (WA)									18		1		19
Rangeland (RA)		2		1						20			23
Marsh and swamp (MA)		4									10		14
Unused land (UL)				1		1		1		2		22	27
Total	25	400	75	95	9	35	24	98	18	28	13	26	846
Producer's accuracy (%)	76.00	95.75	86.67	93.68	88.89	77.14	79.17	94.90	100.00	71.43	76.92	84.62	
User's accuracy (%)	86.36	95.51	94.20	85.58	80.00	96.43	73.08	90.29	94.74	86.96	71.43	81.48	
Overall accuracy (%)	91.37												
Kappa hat coefficient (%)	88.26												

(Classified LULC data in 2019)

Abandoned paddy field

Figure 4.19 Field photograph of abandoned paddy field.

Rangeland with bush and shrub

Figure 4.20 Field photograph of rangeland with bush and shrub.

In summary, it can be here concluded that the RF classifier under the EnMap BOX software can be used as an efficient tool to classify the LULC from remotely sensed data since it can provide high classification accuracy. In this study, overall accuracy varies from 89.88% to 91.37%, and the Kappa hat coefficient ranges from 84.88% to 88.26%. However, selecting appropriate training points of each LULC type, particularly the number of points and their locations, requires much more time to classify the final LULC maps in three different years. A phenological cycle of agricultural LULC type and natural vegetation plays a significant role in training point selection because the appearance of some LULC types is similar when they display on the screen with specific color composition (Band 4, 5, and 3: RGB), for example, rangeland and unused land (abandoned land).

4.4 LULC change between 2001 and 2010

A simple comparison of LULC change between 2001 and 2010, with the annual change rate, is presented in Table 4.8 and Figure 4.21.

Table 4.8 Comparison of LULC change between 2001 and 2010.

LULC	LULC type (Area in km^2)											
	UR	PA	SU	CA	PC	PR	PO	FO	WA	RA	MA	UL
In 2001	46.17	2344.39	61.25	532.95	2.09	16.56	55.76	632.00	36.81	26.03	11.64	28.57
In 2010	53.21	2070.71	153.52	629.33	5.19	30.05	50.21	604.70	57.46	72.11	33.40	34.33
Change area	7.04	-273.68	92.27	96.38	3.11	13.49	-5.54	-27.30	20.65	46.08	21.76	5.76
Annual change rate	0.78	-30.41	10.25	10.71	0.35	1.50	-0.62	-3.03	2.29	5.12	2.42	0.64
Percentage of change	0.19	-7.21	2.43	2.54	0.08	0.36	-0.15	-0.72	0.54	1.21	0.57	0.15
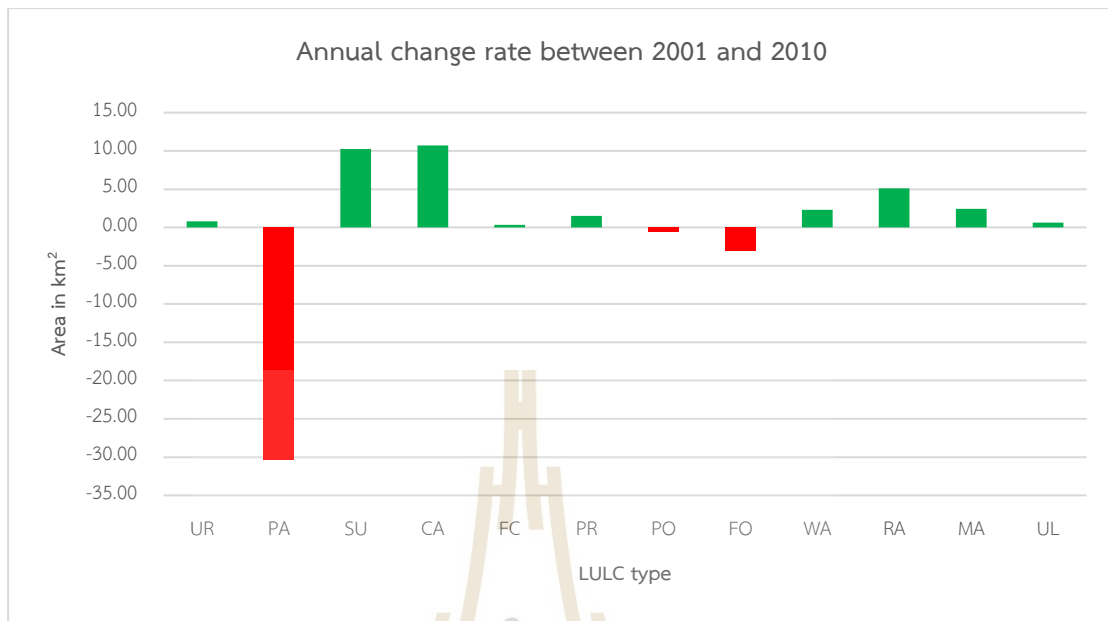
Figure 4.21 Comparison of the annual change rate of LULC type between 2001 and 2010.

As a result, the significant increase of LULC types between 2001 and 2010 are cassava, sugarcane, and rangeland, with an annual change rate of 10.71, 10.25, and 5.12 km^2 per year, respectively. In the meantime, the minor increase of LULC types in this period are marsh and swamp, waterbody, para rubber, urban and built-up area, unused land, and other field crops, with an annual change rate of 2.42, 2.29, 1.50, 0.78, and 0.35 km^2 per year, respectively. In contrast, the significant decrease of LULC type between 2001 and 2010 is paddy field, with an annual change rate of 30.41 km^2 per year, while the minor decrease of LULC types in this period are forest land and perennial trees and orchard, with an annual change rate of 3.03 and 0.62 km^2 per year, respectively.

Meanwhile, a transitional change matrix of LULC between 2001 and 2010, which provides "from-to" change class information, is summarized in Table 4.9, and the LULC change map in this period is displayed in Figure 4.22.

Table 4.9 Transitional matrix of LULC change between 2001 and 2010.

LULC types	LULC in 2010 (km^2)												
	UR	PA	SU	CA	FC	PR	PO	FO	WA	RA	MA	UL	Total
Urban and built-up area (UR)	46.17	-	-	-	-	-	-	-	-	-	-	-	**46.17**
Paddy field (PA)	6.54	2,007.89	69.31	169.46	-	-	-	-	16.82	48.79	25.19	0.40	**2,344.39**
Sugarcane (SU)	0.01	4.65	31.19	24.57	-	0.13	-	-	0.29	0.09	0.09	0.23	**61.25**
Cassava (CA)	0.05	39.56	51.34	415.26	3.01	12.12	-	-	1.84	5.17	-	4.61	**532.95**
Other field crops (FC)	-	-	-	-	2.09	-	-	-	-	-	-	-	**2.09**
Para rubber (PR)	-	-	-	0.07	-	16.48	-	-	-	-	-	-	**16.56**
Perennial trees and orchard (PO)	0.03	1.23	0.41	3.57	-	-	49.94	-	0.48	0.09	-	-	**55.76**
Forest land (FO)	0.34	15.83	0.29	6.23	0.10	1.13	-	604.70	0.01	1.07	-	2.30	**632.00**
Waterbody (WA)	-	0.14	0.10	0.45	-	0.19	-	-	35.91	-	-	0.01	**36.81**
Rangeland (RA)	0.05	0.04	0.56	8.33	-	-	0.27	-	0.01	16.77	-	0.02	**26.03**
Marsh and swamp (MA)	0.01	0.54	0.28	0.57	-	-	-	-	2.10	0.02	8.12	-	**11.64**
Unused land (UL)	0.02	0.82	0.05	0.81	-	-	-	-	0.01	0.10	-	26.77	**28.57**
Total	53.21	2,070.70	153.52	629.33	5.19	30.05	50.21	604.70	57.46	72.11	33.40	34.33	3,794.22

LULC in 2001 (km^2)
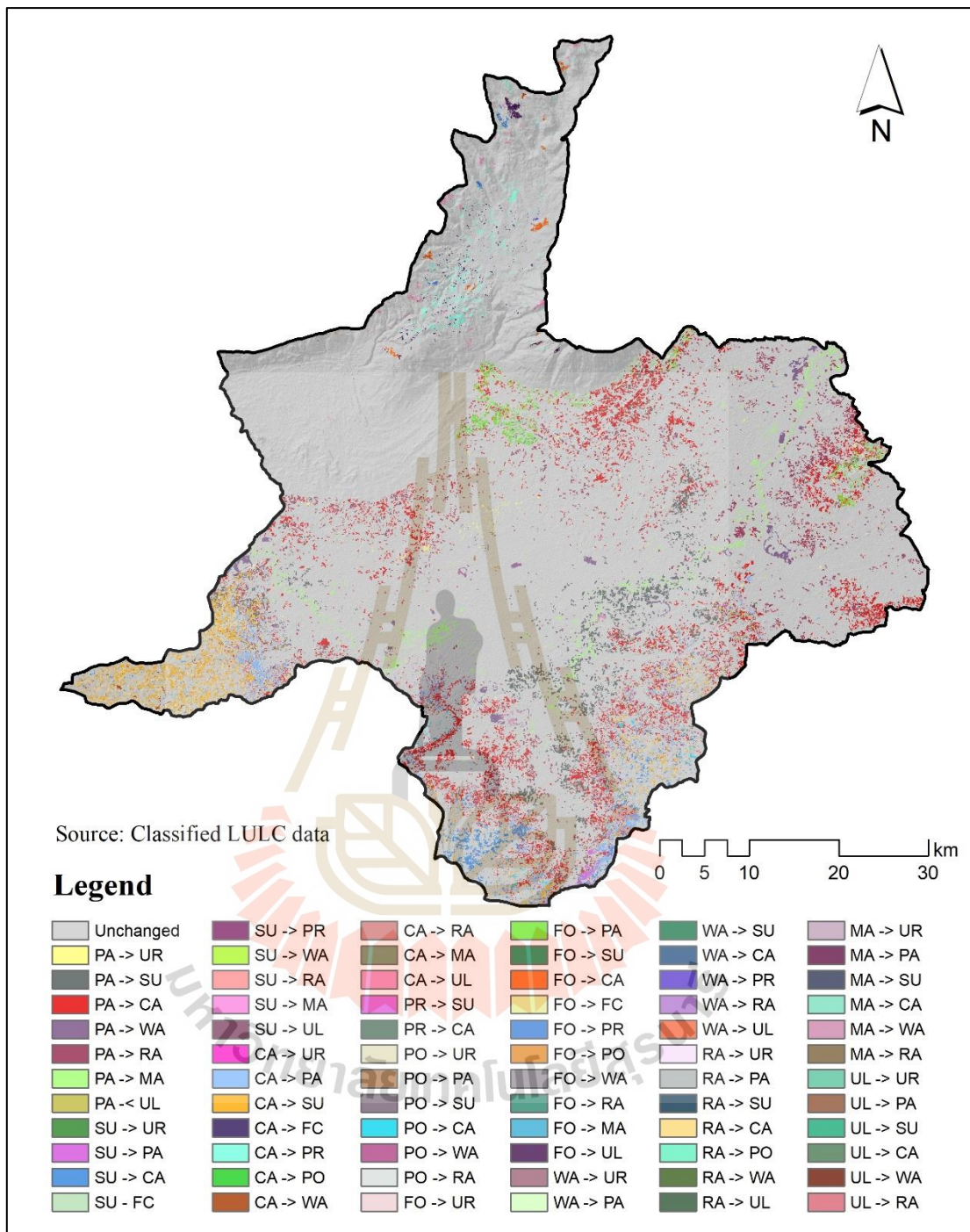
Figure 4.22 Spatial distribution of LULC change between 2001 and 2010.

As a result, urban and built-up areas in 2001 were not converted into other LULC classes in 2010, and the increased area of urban and built-up areas in 2010 mainly comes from the paddy field, with an area of 6.54 km^2 in 2001. Likewise, other field crops in 2001 were not converted into other LULC classes in 2010.

For the significant increasing area of LULC types between 2001 and 2010, areas of cassava, which increased by about 96.38 km^2 in 2010, mainly came from the paddy field (169.46 km^2) sugarcane (24.57 km^2) in 2001. Meanwhile, areas of sugarcane, which increased by about 92.27 km^2 in 2010, mainly came from paddy field (69.31 km^2) and cassava (51.34 km^2) in 2001. These phenomena indicate changeable agriculture practices among economic crops by farmers. Generally, the market price of economic crops dictates agricultural practice to farmers. Table 4.10 shows the market price of economic crops, including paddy field, cassava, sugarcane, and para rubber in Thailand between 2001 and 2019, while Figure 4.23 compares the fluctuation of the market price of three main dominant crops: paddy field, cassava, and sugarcane in the study period. As a result, it can be observed that the market price of sugarcane is relatively stable while the market price of the paddy field is unstable. Generally, the agriculture practice by the farmers is considered the market prices in previous years (2-3 years).

In the meantime, areas of rangeland, which increased by about 46.08 km^2 in 2010, mainly came from paddy fields (48.79 km^2) in 2001. This finding indicates the existing abandoned paddy field in rangeland, which is defined as an area covered by grass, shrubs, uncultivated land, lands with herbaceous types of cover. This phenomenon is unpredictable, and it depends on economic and weather conditions.

Details for the irrelevant increasing area of LULC types between 2001 and 2010 are presented in Table 4.9. The spatial distribution of significant increasing cassava, sugarcane, and rangeland areas between 2001 and 2010 is displayed in Figures 4.24 to 4.26, respectively.

Table 4.10 Market price of economic crops in Thailand between 2001 and 2019.

Year	Paddy field [1] (Baht/ton)	Cassava [1] (Baht/ton)	Sugarcane [2] (Baht/ton)	Para rubber [3] (Baht/kg)
2001	6,116.00	690.00	513.00	20.52
2002	5,139.00	1,050.00	434.00	227.69
2003	6,562.00	930.00	469.00	37.76
2004	8,437.00	800.00	367.00	44.13
2005	7,711.00	1,330.00	521.00	53.57
2006	7,887.00	1,290.00	691.00	66.24
2007	8,326.00	1,180.00	684.00	68.90
2008	9,650.00	1,930.00	574.00	73.00
2009	12,726.00	1,190.00	698.00	66.00
2010	13,770.00	1,860.00	860.00	58.47
2011	13,127.00	1,800.00	920.00	102.76
2012	15,196.00	1,870.00	947.00	124.16
2013	15,379.00	1,830.00	906.00	87.15
2014	14,672.00	1,870.00	854.00	74.75
2015	12,781.00	1,870.00	844.00	53.93
2016	11,632.00	1,810.00	745.00	44.31
2017	8,896.00	1,430.00	949.00	48.81
2018	11,879.00	1,520.00	968.00	55.81
2019	15,367.00	1,430.00	900.00	40.96

Source: [1] Office of Agricultural Economics: OAE (2019), [2] Office of the Cane and Sugar Board: OCSB (2019), and [3] Rubber Authority of Thailand: RAOT (2019).
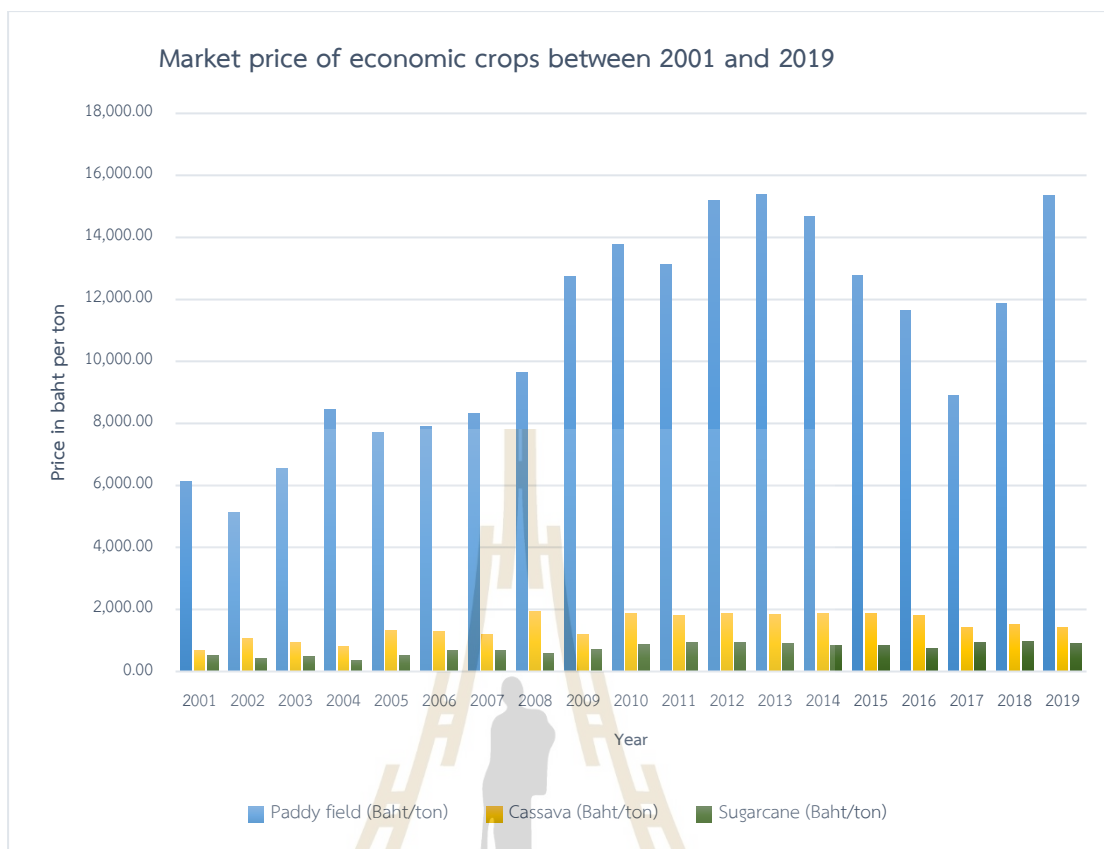
Figure 4.23 Market price of economic crops (paddy field, cassava, and sugarcane between 2001 and 2019.

On the contrary, for the extensive decreasing area of LULC types between 2001 and 2010, areas of paddy field in 2001, which are decreased by about 273.68 km^2 in 2010, are mostly converted into cassava (169.46 km^2), sugarcane (69.31 km^2) and rangeland (48.79 km^2). These phenomena indicate changeable practice among economic crops by farmers, and active paddy fields become abandoned fields in rangeland, as mentioned earlier. Meanwhile, areas of forest land in 2001, which decreased by about 27.30 km^2 in 2010, are mostly converted into paddy fields (15.83 km^2). The finding indicates forest encroachment activity for agricultural area expansion in the study area.

Details for the irrelevant decreasing area of LULC types between 2001 and 2010 are reported in Table 4.9. The spatial distribution of significant decreasing paddy field and forest land areas between 2001 and 2010 is displayed in Figures 4.27 and 4.28, respectively.
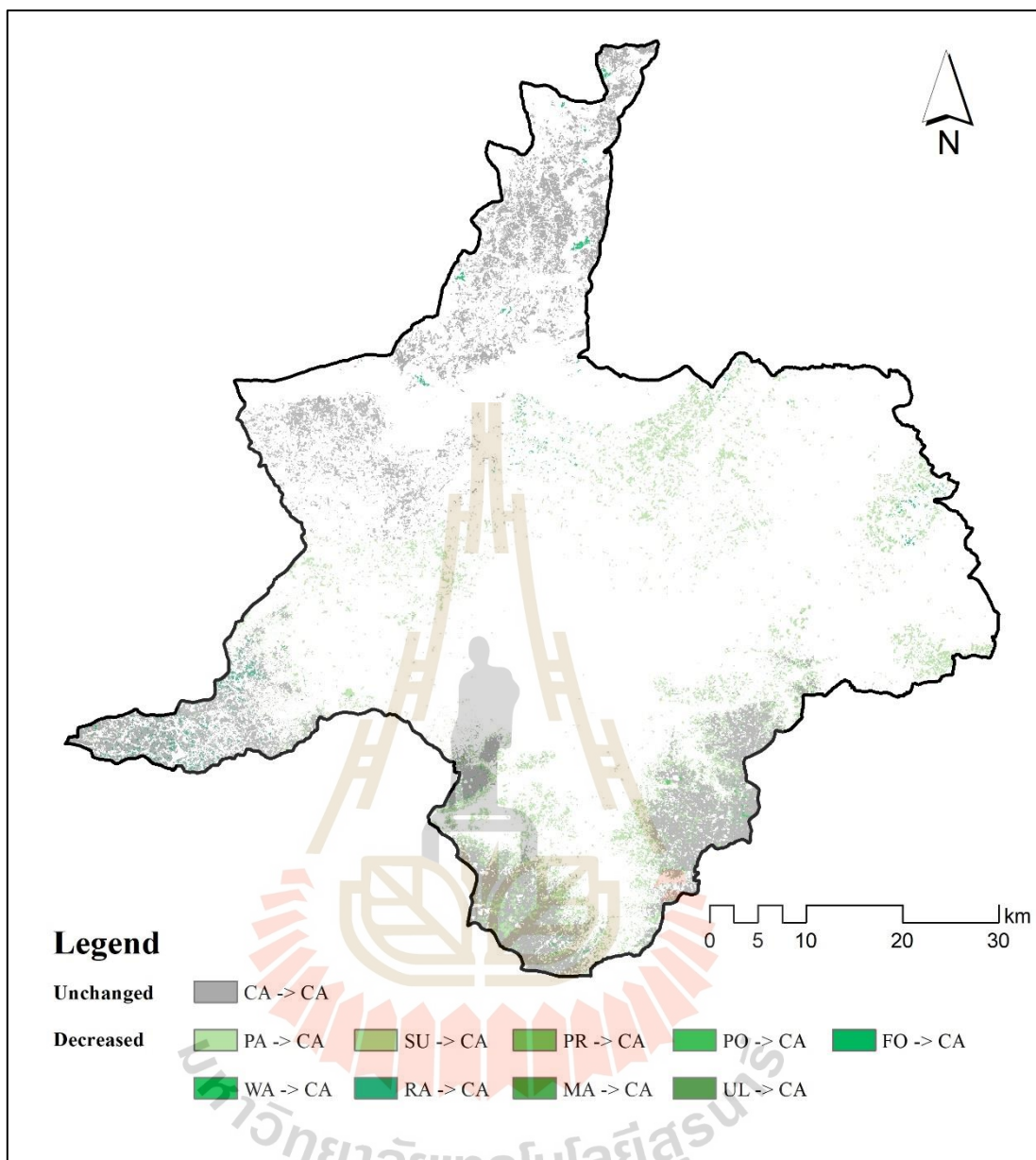
Figure 4.24 Spatial distribution of increased and unchanged areas of cassava between 2001 and 2010.
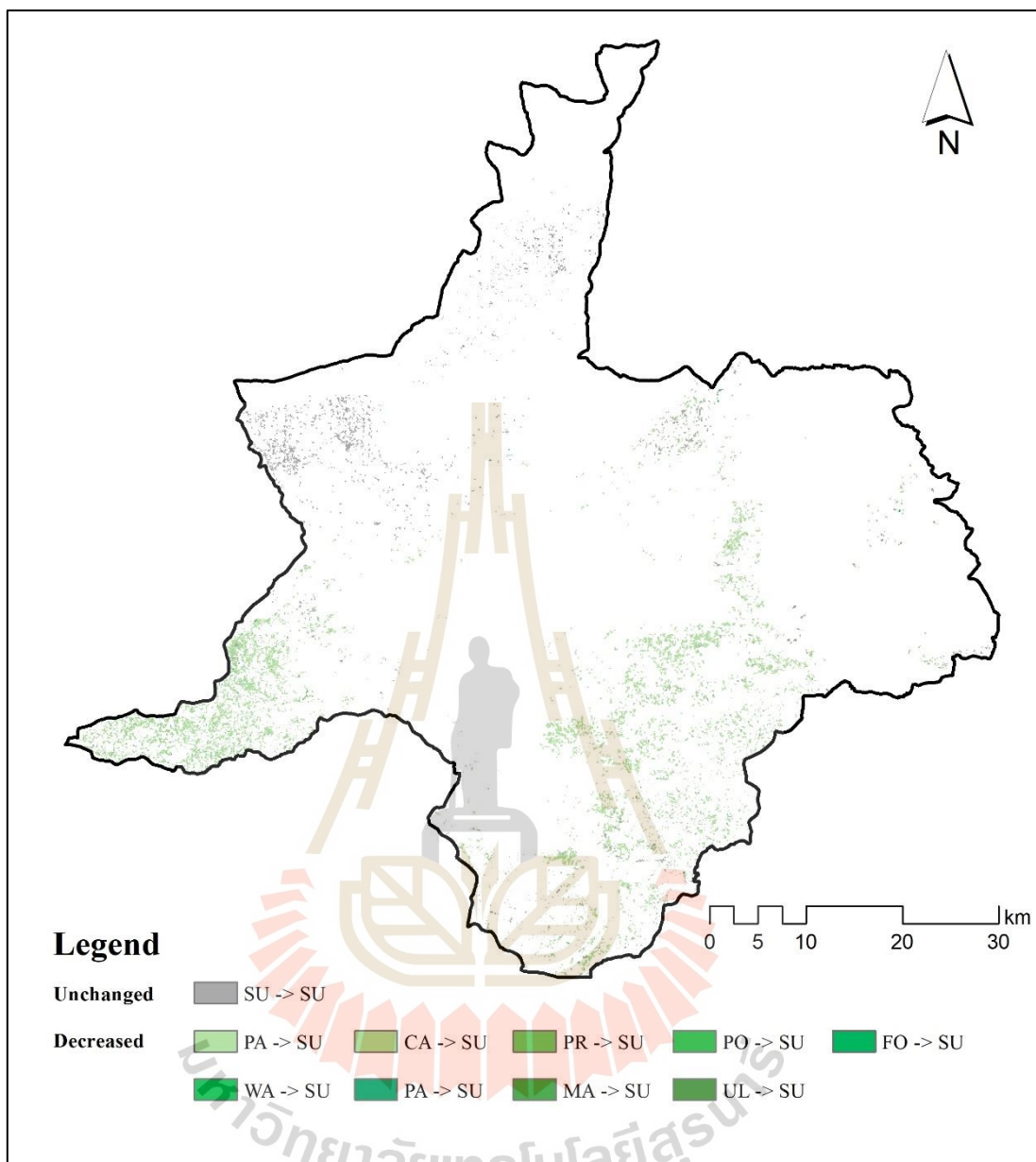
Figure 4.25 Spatial distribution of increased and unchanged areas of sugarcane between 2001 and 2010.
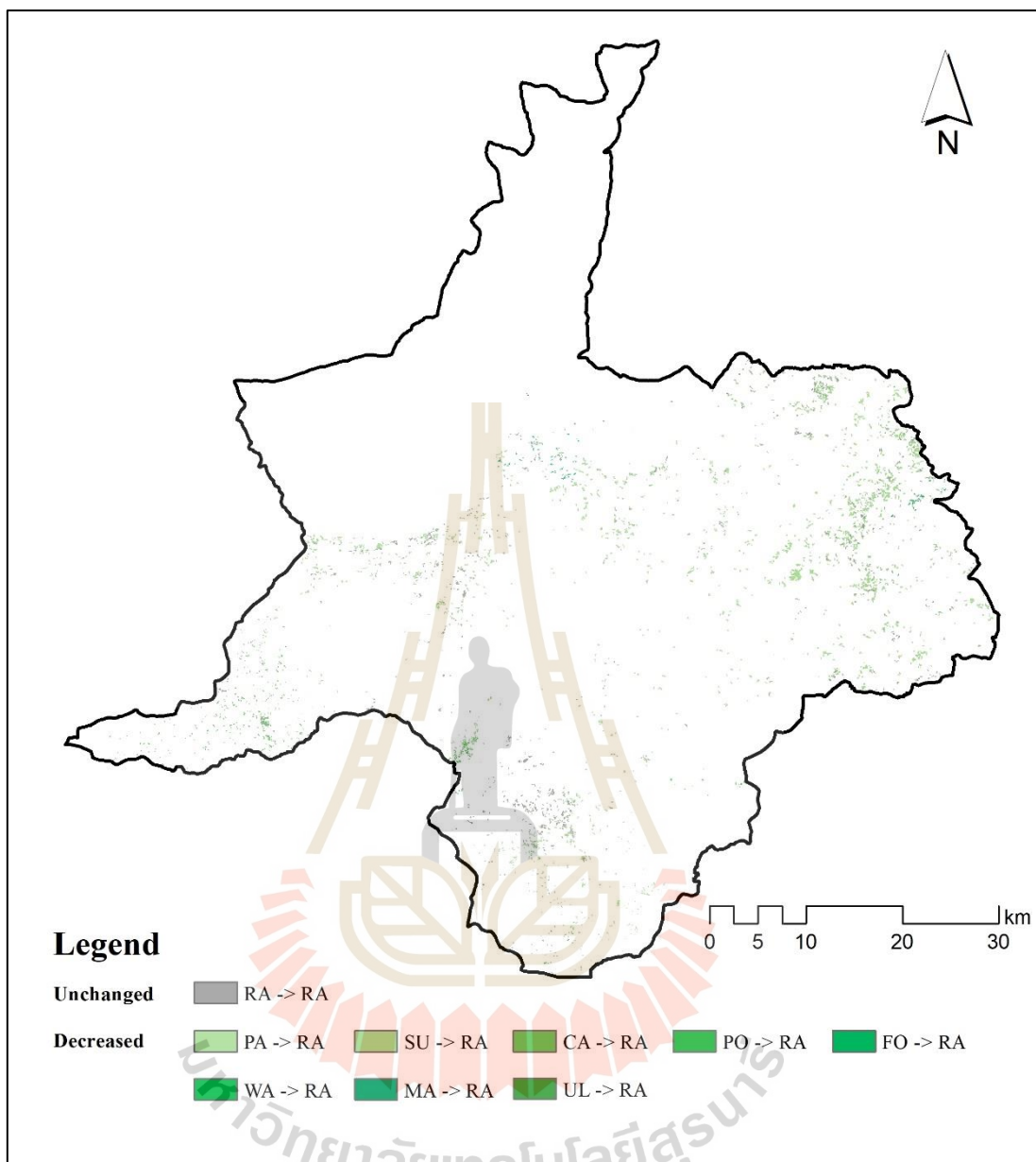
Figure 4.26 Spatial distribution of increased and unchanged areas of rangeland between 2001 and 2010.
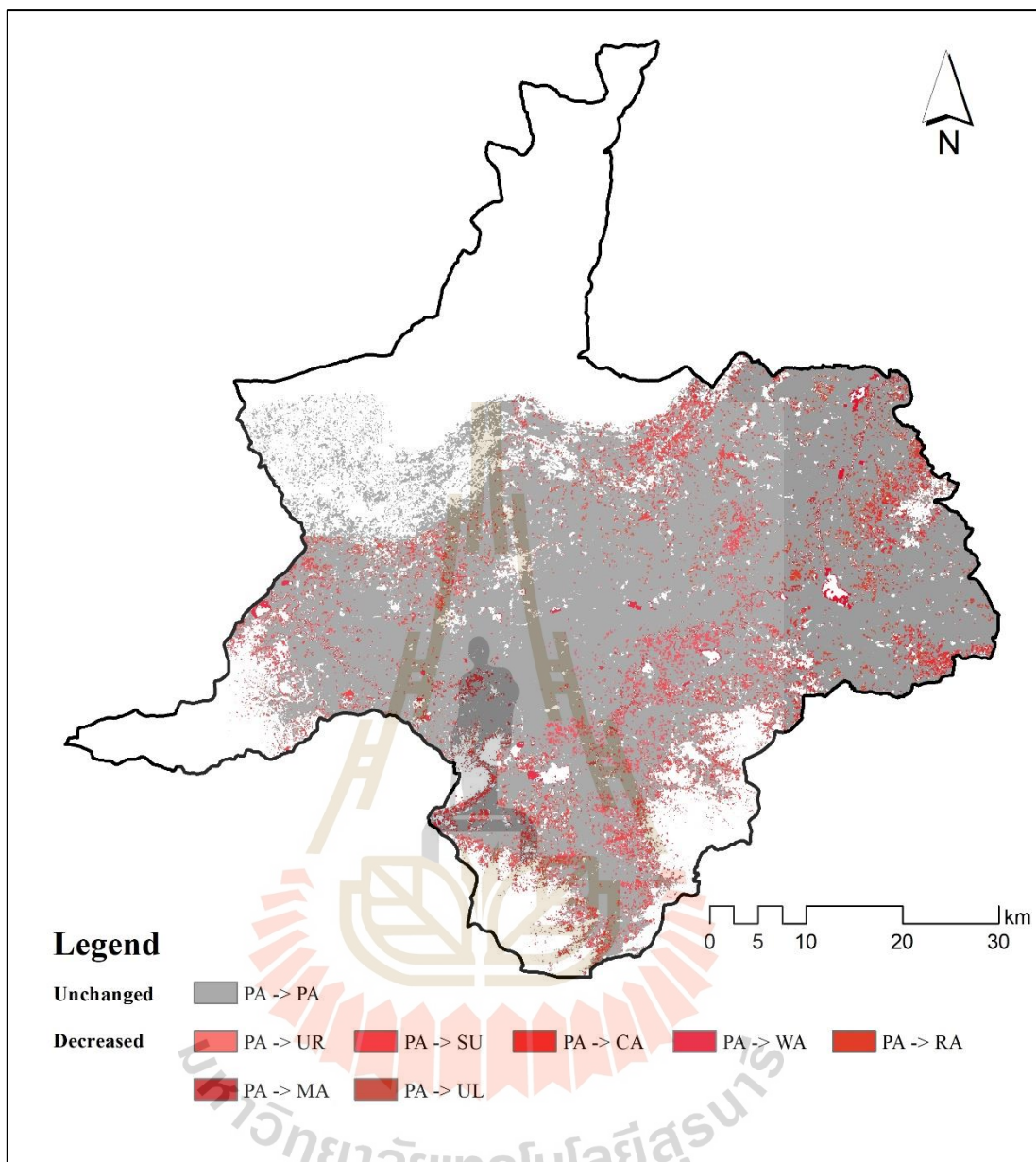
Figure 4.27 Spatial distribution of decreased and unchanged areas of paddy fields between 2001 and 2010.
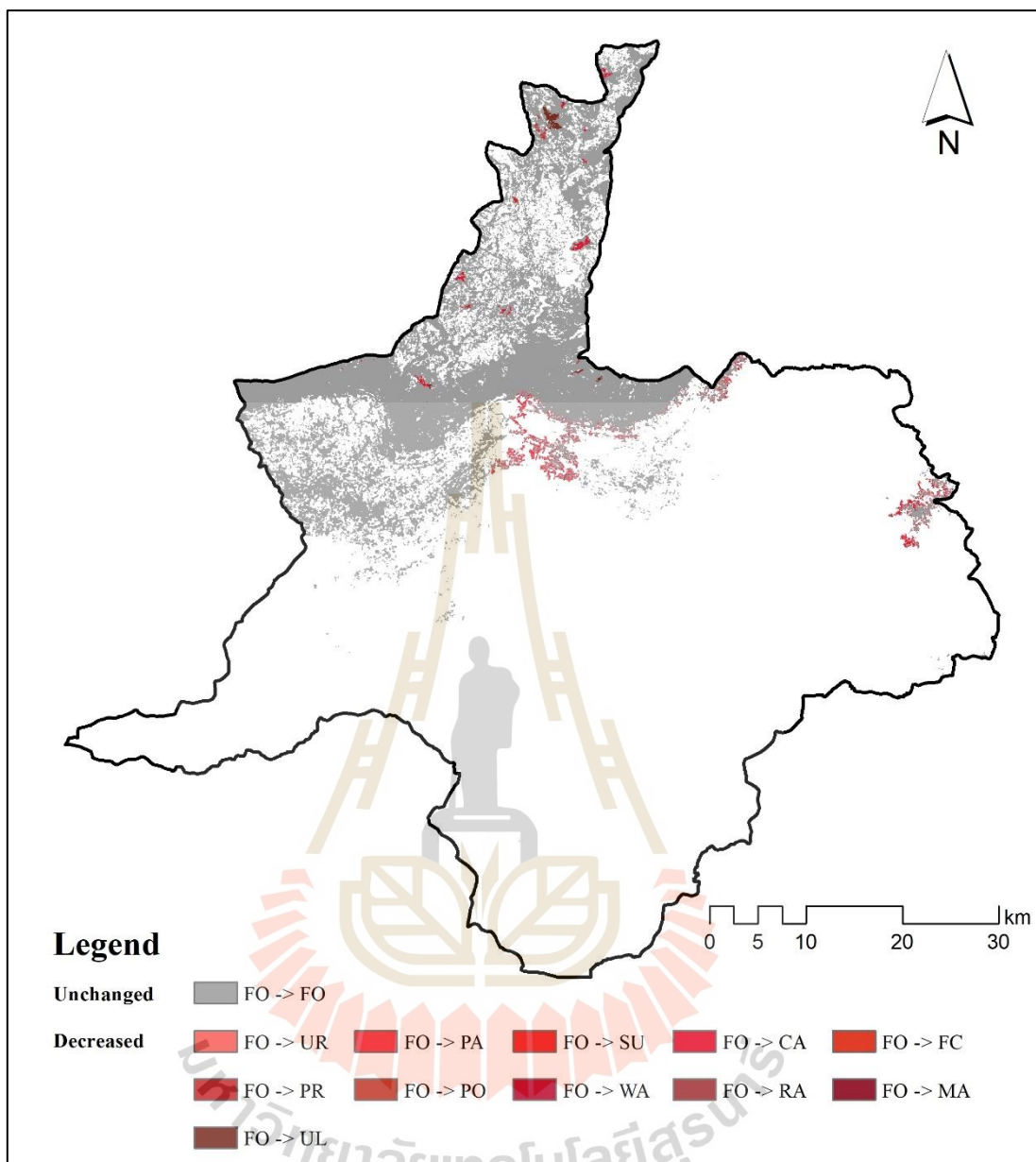
Figure 4.28 Spatial distribution of decreased and unchanged areas of forest land between 2001 and 2010.

4.5 LULC change between 2010 and 2019

A simple comparison of LULC change between 2010 and 2019, with the annual change rate, is presented in Table 4.11 and Figure 4.29.

Table 4.11 Comparison of LULC change between 2010 and 2019.

LULC	LULC type (Area in km^2)											
	UR	PA	SU	CA	PC	PR	PO	FO	WA	RA	MA	UL
In 2010	53.21	2,070.71	153.52	629.33	5.19	30.05	50.21	604.70	57.46	72.11	33.40	34.33
In 2019	65.84	2,012.16	306.85	489.91	6.19	97.03	88.95	481.30	53.30	71.65	27.73	93.32
Change area	12.63	-58.55	153.33	-139.41	1.00	66.99	38.73	-123.41	-4.16	-0.47	-5.67	58.99
Annual change rate	1.40	-6.51	17.04	-15.49	0.11	7.44	4.30	-13.71	-0.46	-0.05	-0.63	6.55
Percentage of change	0.33	-1.54	4.04	-3.67	0.03	1.77	1.02	-3.25	-0.11	-0.01	-0.15	1.55
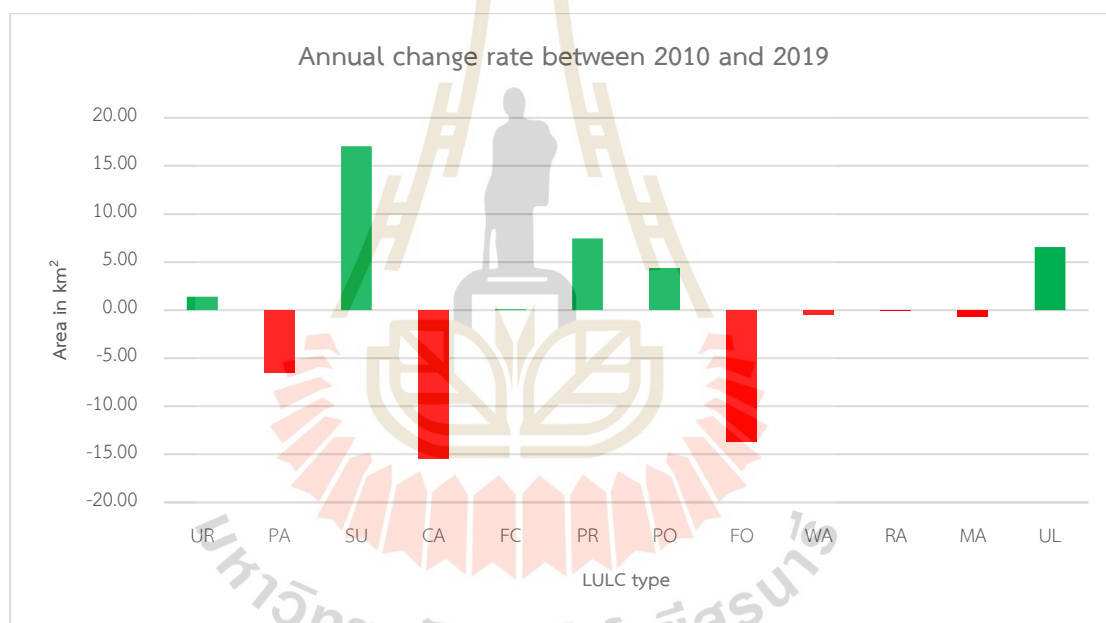
Figure 4.29 Comparison of the annual change rate of LULC type between 2010 and 2019.

As a result, the significant increase of LULC types between 2010 and 2019 are sugarcane, para rubber, perennial trees and orchard, and unused land, with an annual change rate of 17.04, 7.44, 6.55, and 4.30 km^2 per year, respectively. Meanwhile, the minor increase of LULC types in this period are urban and built-up areas and other field crops with an annual change rate of 1.40 and 0.11 km^2 per year. On the opposite, the significant decrease of LULC type between 2010 and 2019 are cassava, forest land, and paddy field, with an annual change rate of 15.49, 13.71, and 6.51 km^2 per year,

while the minor decrease of LULC types in this period are marsh and swamp, waterbody, and rangeland, with an annual change rate of 0.63, 0.46, and 0.05 km^2 per year, respectively.

Meanwhile, a transitional change matrix of LULC between 2010 and 2019, which provides "from-to" change class information, is summarized in Table 4.12, and the LULC change map in this period is displayed in Figure 4.30.
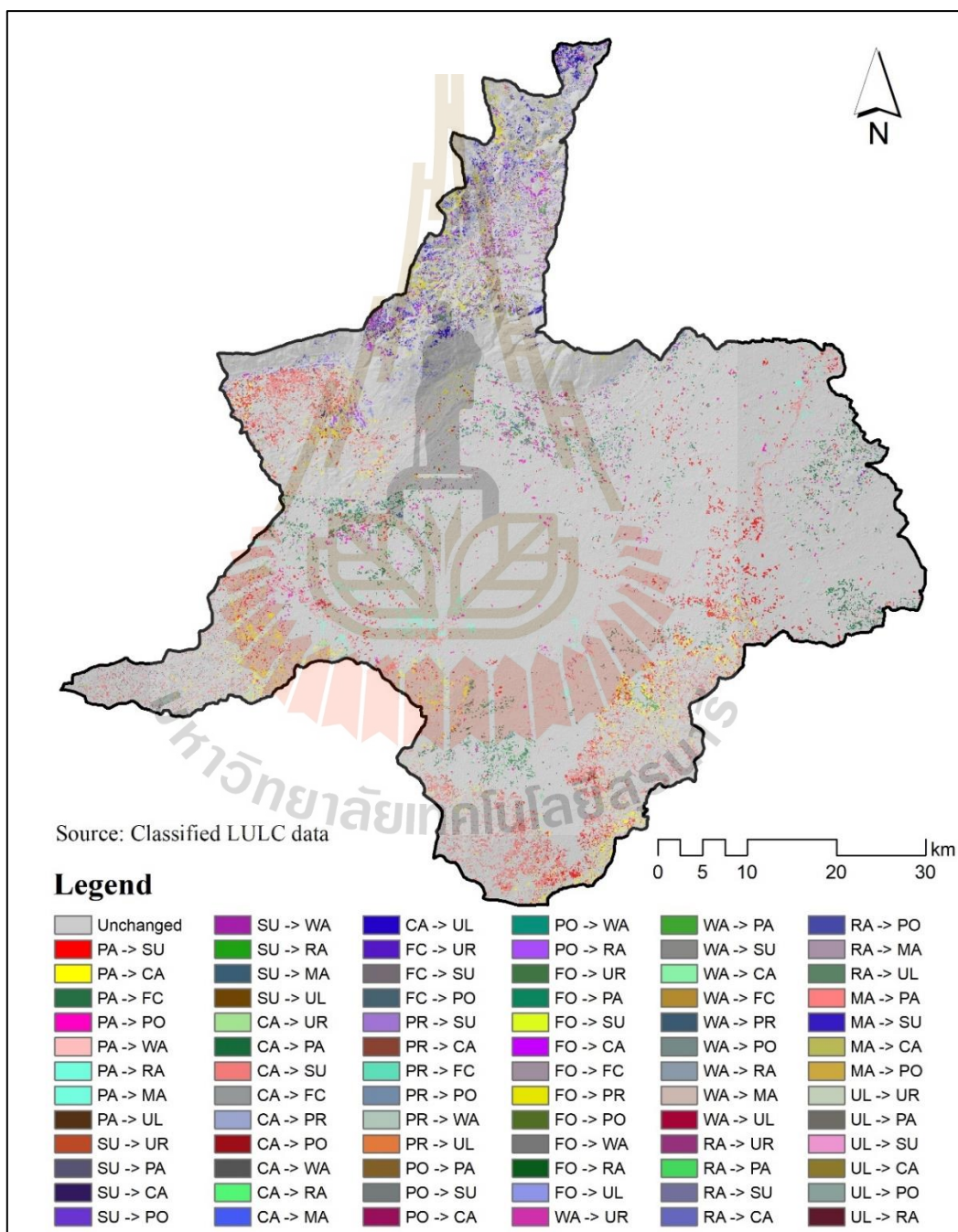
Figure 4.30 Spatial distribution of LULC change between 2010 and 2019.

Table 4.12 Transitional matrix of LULC change between 2010 and 2019.

LULC types	LULC in 2019 (km²)												
	UR	PA	SU	CA	FC	PR	PO	FO	WA	RA	MA	UL	Total
Urban and built-up area (UR)	53.21	-	-	-	-	-	-	-	-	-	-	-	**53.21**
Paddy field (PA)	-	1,932.32	58.92	40.78	0.01	-	19.64	-	0.39	3.42	14.38	0.86	**2,070.71**
Sugarcane (SU)	0.86	1.06	143.01	7.45	-	-	0.96	-	0.05	0.10	0.02	0.01	**153.52**
Cassava (CA)	8.94	37.71	100.15	407.10	-	41.97	7.68	-	0.05	2.12	0.04	23.57	**629.33**
Other field crops (FC)	0.01	-	-	-	5.14	-	0.04	-	-	-	-	-	**5.19**
Para rubber (PR)	-	-	0.12	3.32	0.29	23.92	0.78	-	0.01	-	-	1.61	**30.05**
Perennial trees and orchard (PO)	-	0.07	0.30	0.28	-	-	49.55	-	-	0.01	-	-	**50.21**
Forest land (FO)	2.19	13.42	1.81	28.88	0.75	31.12	8.89	481.30	0.26	1.64	-	34.44	**604.70**
Waterbody (WA)	0.22	2.10	1.35	0.74	-	0.02	0.12	-	52.54	-	0.33	0.03	**57.46**
Rangeland (RA)	0.01	5.91	0.16	1.17	-	-	0.51	-	-	64.35	-	-	**72.11**
Marsh and swamp (MA)	0.17	18.50	0.97	0.07	-	-	0.74	-	-	-	12.96	-	**33.40**
Unused land (UL)	0.23	1.08	0.04	0.13	-	-	0.05	-	-	-	-	32.80	**34.33**
Total	65.84	2,012.16	306.85	489.91	6.19	97.03	88.95	481.30	53.30	71.65	27.73	93.32	3,794.22

LULC in 2010 (km²)

As a result, urban and built-up areas in 2010 were not converted into other LULC classes in 2019, and the increased area of urban and built-up areas in 2019 mainly comes from the cassava, with an area of 8.94 km^2 in 2010.

For the significantly increasing LULC types between 2010 and 2019, areas of sugarcane, which are increased by about 153.33 km^2 in 2019, mostly come from cassava (100.15 km^2) paddy field (58.92 km^2) in 2010. Meanwhile, para rubber areas, which increased by about 66.99 km^2 in 2019, mainly came from cassava (41.97 km^2) and forest land (31.12 km^2) in 2010. These findings indicate changeable practice among economic crops by farmers and the forest encroachment activities for agricultural area expansion, especially para rubber. Figure 4.31 shows the distribution of para rubber plots allocated in natural forests in the study area based on a very high spatial resolution from Google Earth. In the meantime, areas of unused land, which increased by about 58.99 km^2 in 2019, mainly came from forest land (34.44 km^2) and cassava (23.57 km^2) in 2010. These findings indicate uncultivated cassava fields in unused land, which is covered by uncultivated areas including abandoned land, bare land, pit, landfill, and outcrop. Additionally, forest fires frequently occur in the dry dipterocarps forest during the dry season become unused land. Figure 4.32 shows forest fire that occurred in the study during the field survey in 2020.

Details for the irrelevant increasing area of LULC types between 2001 and 2010 are reported in Table 4.12. The spatial distribution of significant increasing areas of sugarcane, para rubber, and unused land between 2010 and 2019 is displayed in Figures 4.33 to 4.35, respectively.

Figure 4.31 Distribution of para rubber plots allocated in the natural forest from a very high spatial resolution from Google Earth.

Figure 4.32 Forest fire in the study during a field survey in 2020.
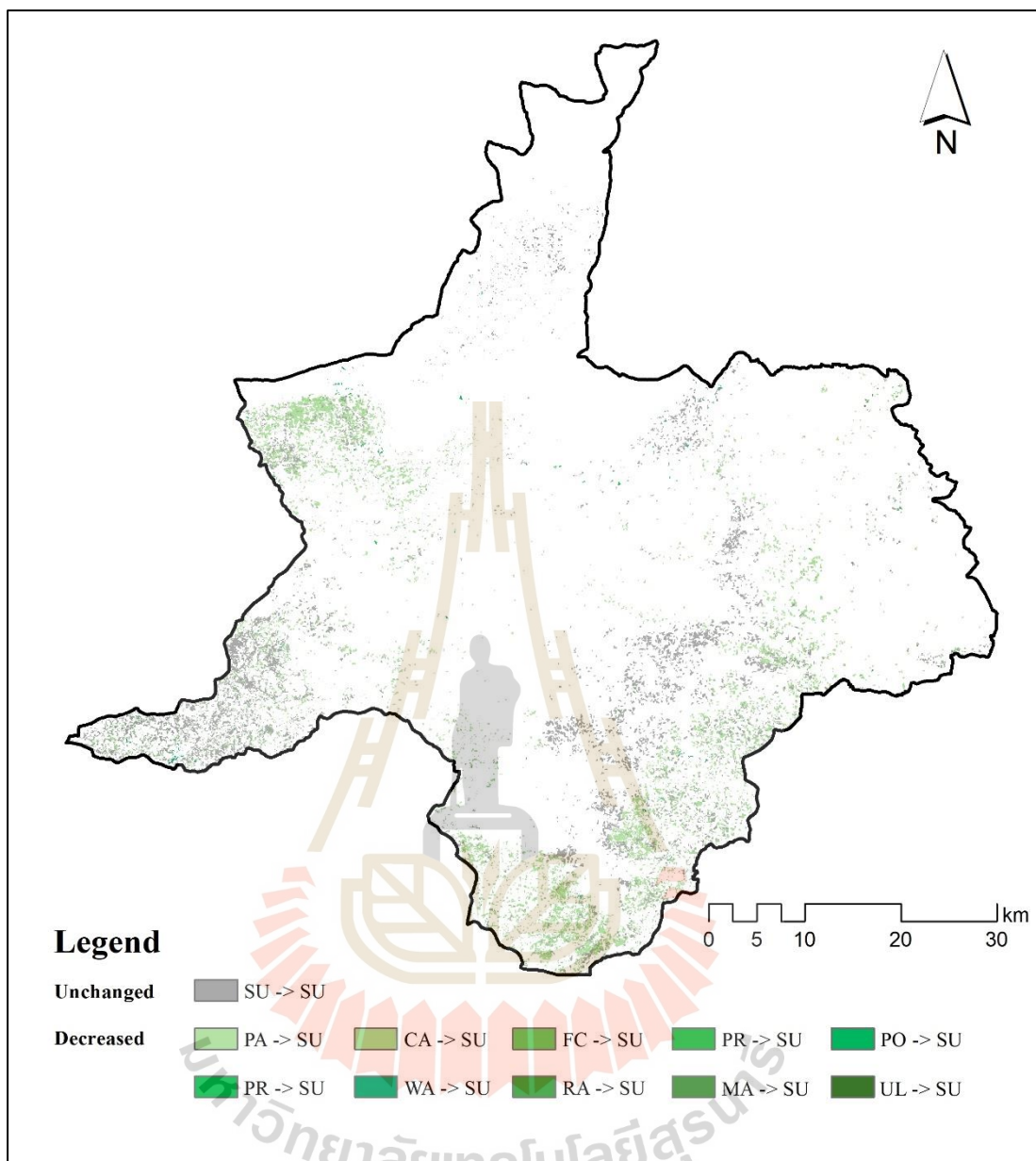
Figure 4.33 Spatial distribution of increased and unchanged areas of sugarcane between 2010 and 2019.
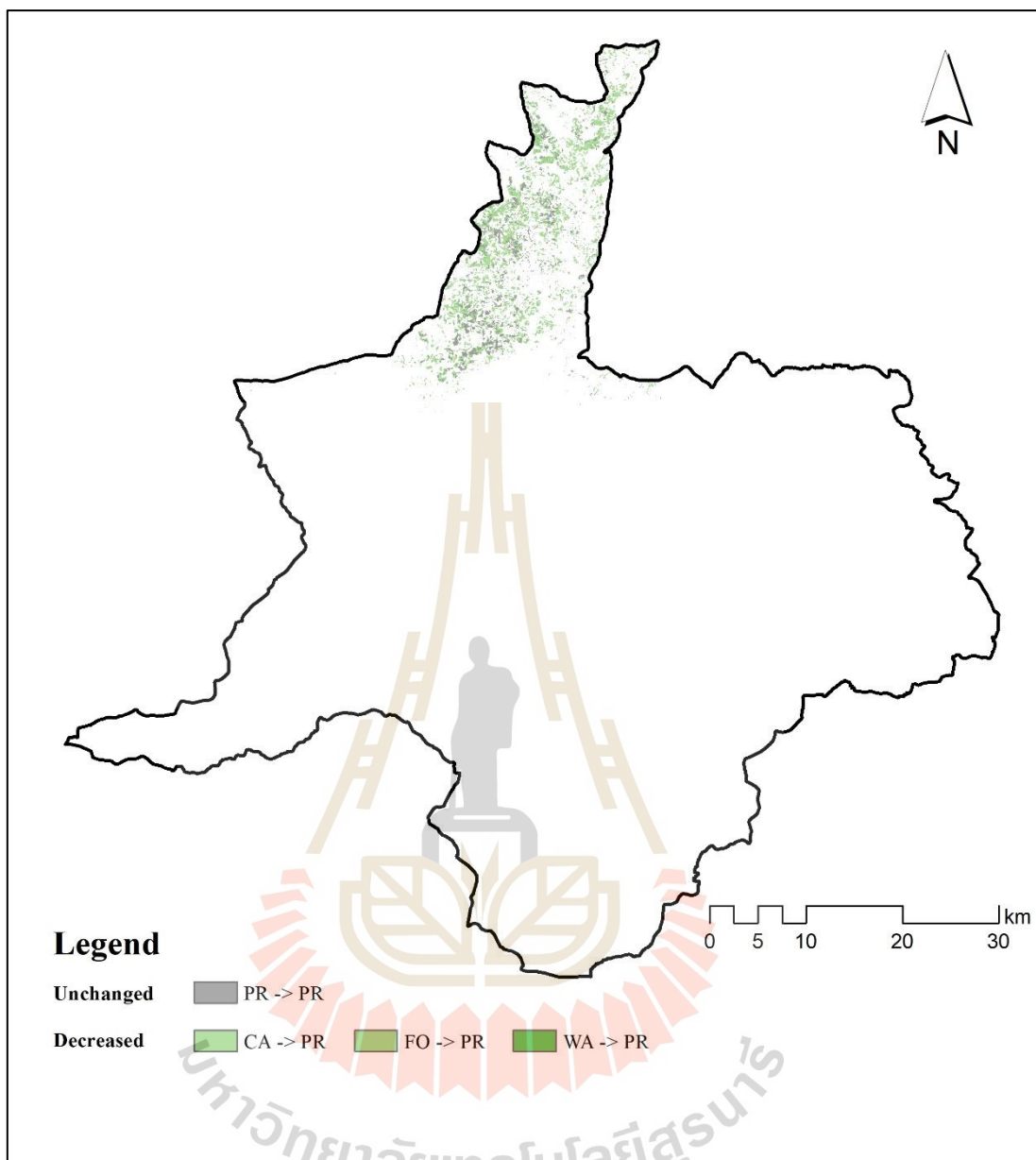
Figure 4.34 Spatial distribution of increased and unchanged areas of para rubber between 2010 and 2019.
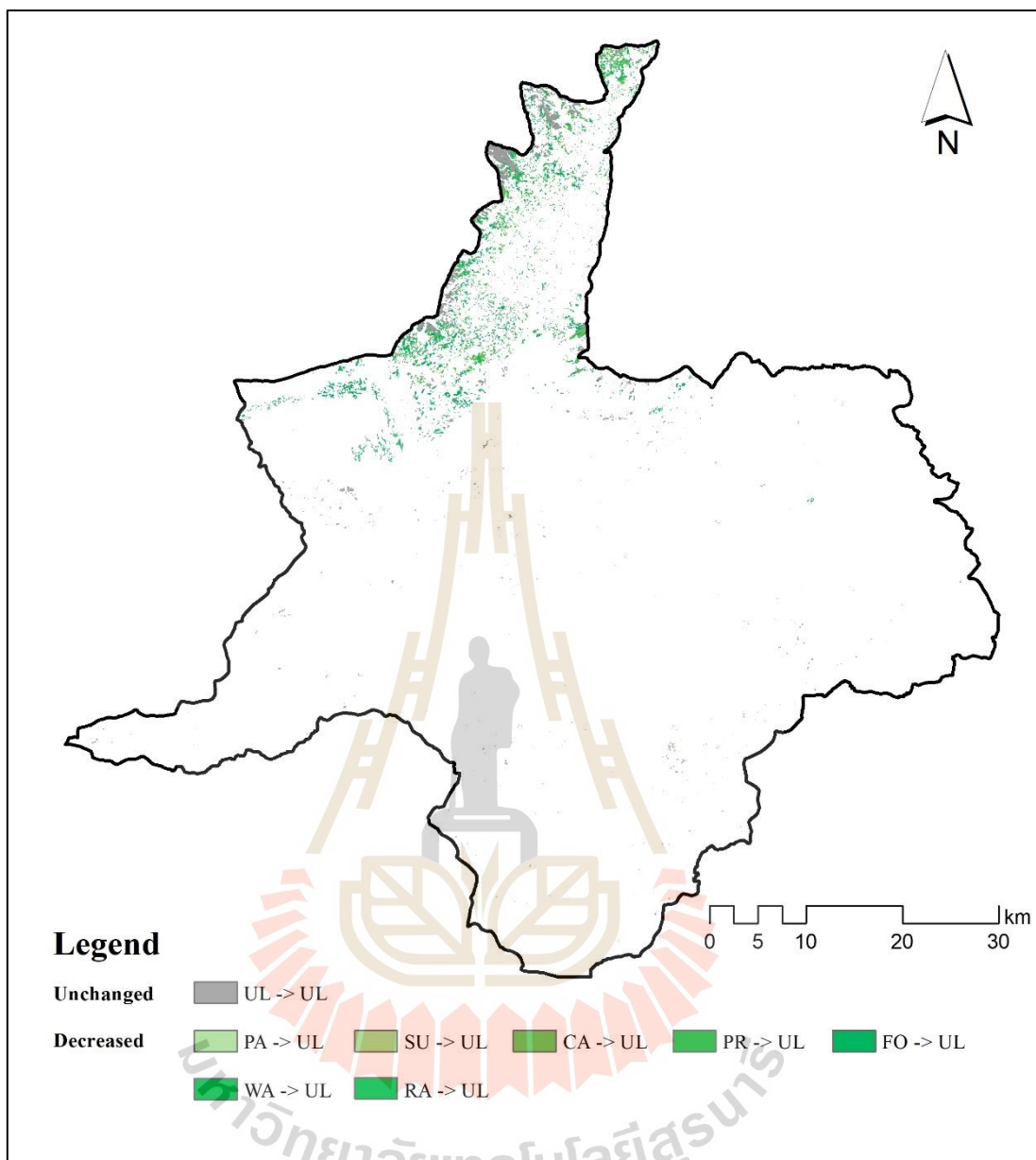
Figure 4.35 Spatial distribution of increased and unchanged areas of unused land between 2010 and 2019.

On the contrary, for the extensive decreasing area of LULC types between 2010 and 2019, areas of cassava in 2010, which are decreased about 139.41 km^2 in 2019, are mainly converted into sugarcane (100.15 km^2), para rubber (41.97 km^2), paddy field (37.71 km^2), and unused land (23.57 km^2). These phenomena indicate changeable agriculture practice among economic crops by farmers, and active cassava fields become uncultivated areas in unused land. Meanwhile, areas of forest land in 2010, which decreased by about 123.41 km^2 in 2019, are mostly converted into unused land (34.44 km^2), para rubber (31.12 km^2), and cassava (28.88 km^2). These phenomena imply forest fire and encroachment activities for non-timber products collection and agricultural area expansion in natural forest in the study area. Figure 4.36 displays encroachment activities that occurred in the forest land areas of the study area. In the meantime, areas of paddy field in 2010, which decreased by about 58.55 km^2 in 2019, are mostly converted into sugarcane (58.92 km^2) and cassava (40.78 km^2). These phenomena imply changeable agriculture practice among economic crops by farmers.

Details for the irrelevant decreasing area of LULC types between 2001 and 2010 are presented in Table 4.12. The spatial distribution of significant decreasing areas of cassava, forest land, and paddy field between 2010 and 2019 is displayed in Figures 4.37 to 4.39, respectively.

Figure 4.36 Encroachment activities in the forest land areas from a field survey in 2020.
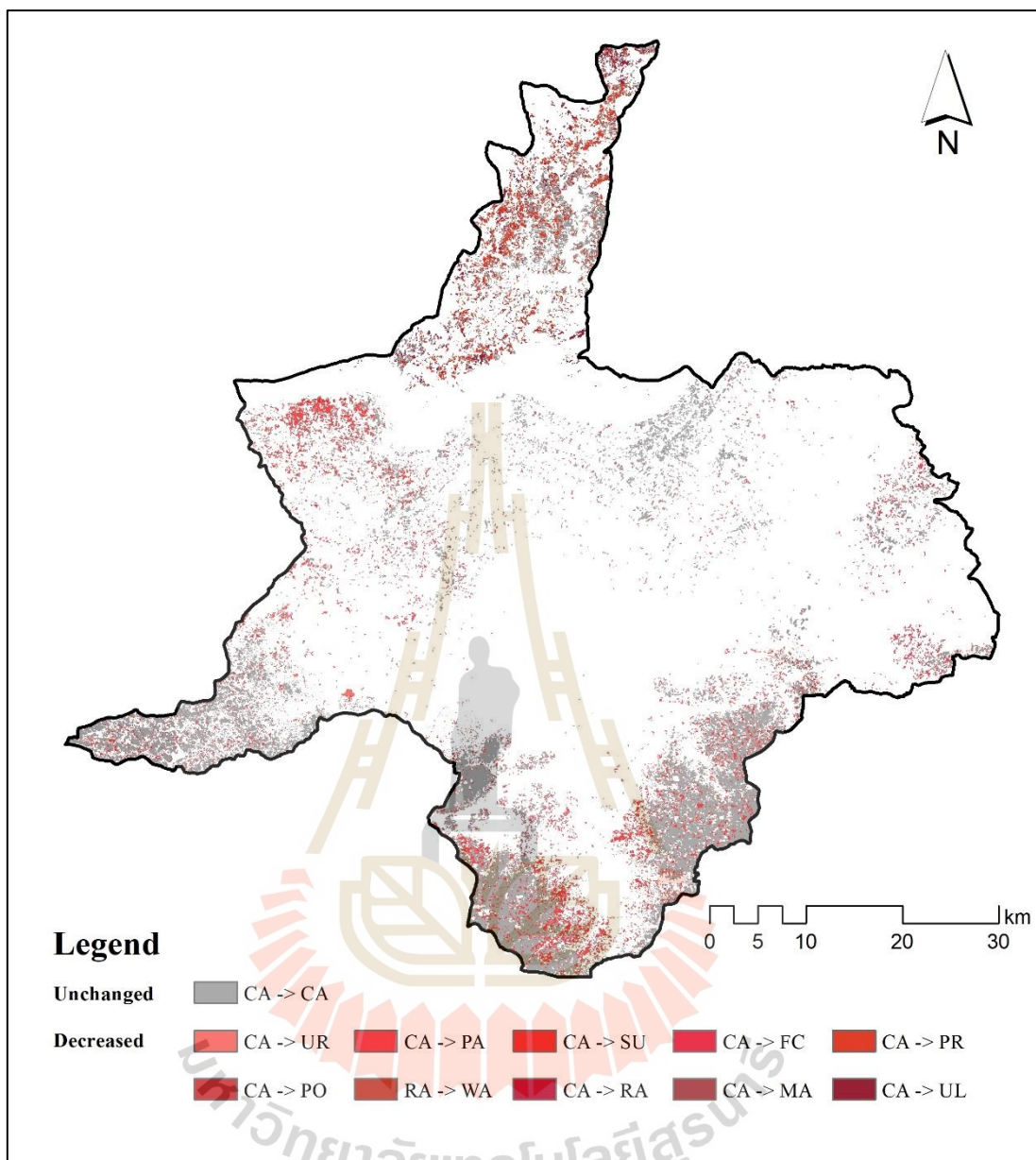
Figure 4.37 Spatial distribution of decreased and unchanged areas of cassava between 2010 and 2019.
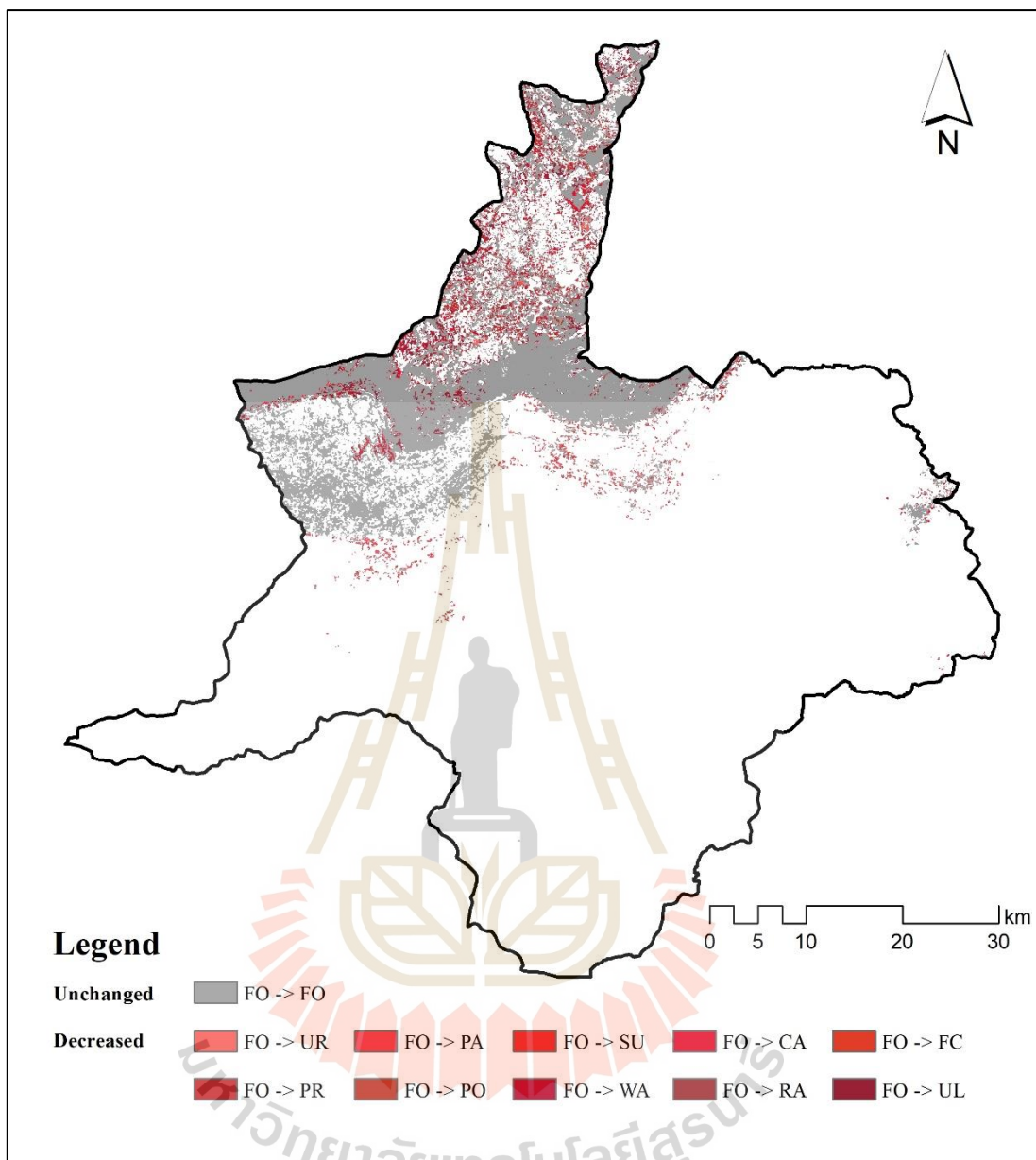
Figure 4.38 Spatial distribution of decreased and unchanged areas of forest land between 2010 and 2019.
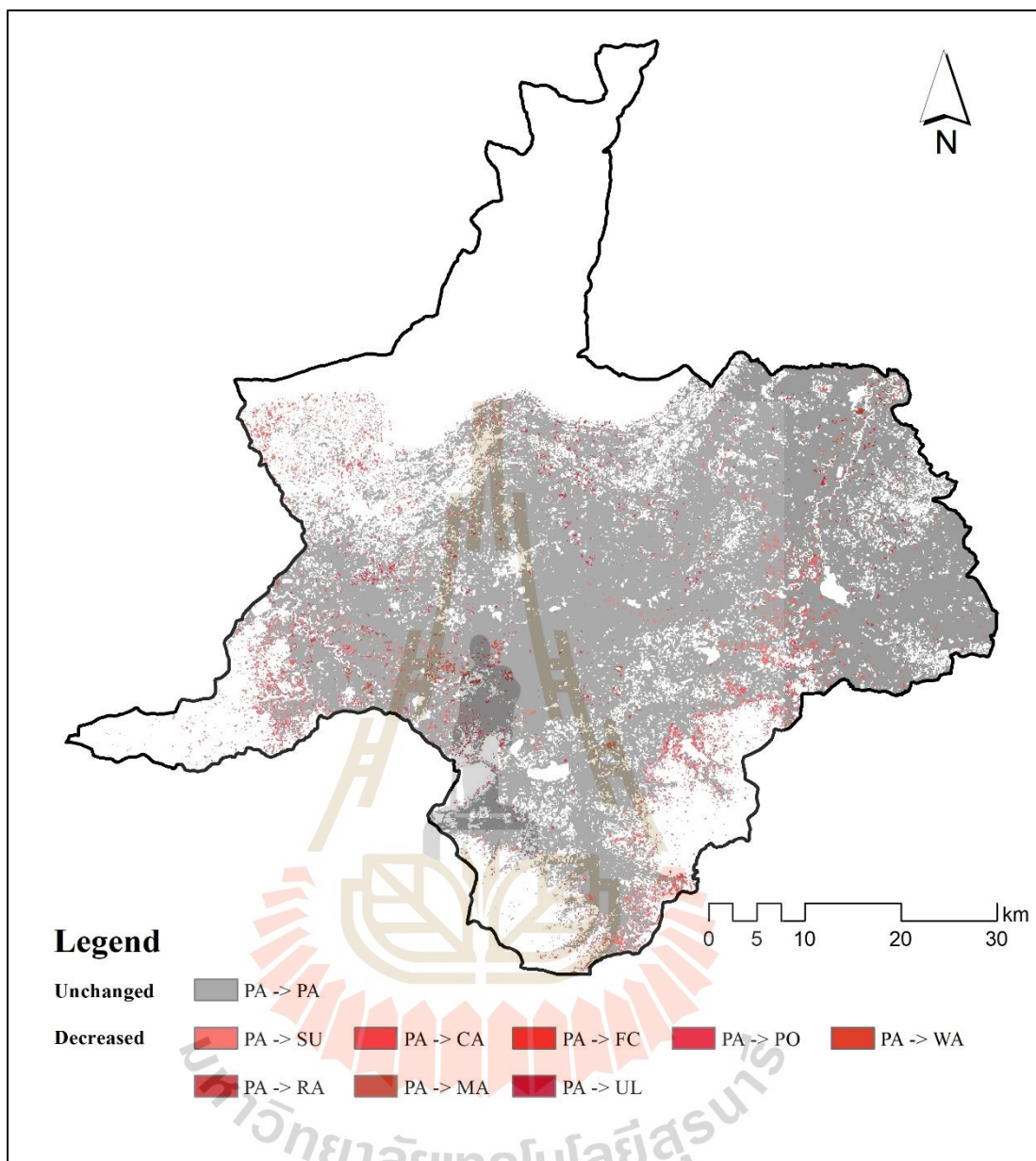
Figure 4.39 Spatial distribution of decreased and unchanged areas of paddy field between 2010 and 2019.

In summary, LULC change's tendency can be observed based on the derived area of each LULC type in 2001, 2010, and 2019, as a summary in Table 4.13 and Figure 4.40. As a result, areas of significant LULC types include urban and built-up areas, sugarcane, para rubber, other field crops, and unused land, tend to increase in the future. On the contrary, areas of substantial LULC types include paddy fields and forest land, tend to decrease in the future. Meanwhile, cassava, perennial trees and orchards, waterbody, and marsh and swamps tend to be unstable and unpredictable in the future.

Additionally, the post-classification comparison change detection algorithm can provide detailed from-to-change class information in two different periods (2001-2010 and 2010-2019). However, reliable information depends on the accuracy of LULC maps, as mentioned by Jensen (2005).

Table 4.13 Area of each LULC type in 2001, 2010, and 2019.

No.	LULC type	Area of LULC type in km^2		
		2001	2010	2019
1	Urban and built-up area	46.17	53.21	65.84
2	Paddy field	2,344.39	2,070.71	2012.16
3	Sugarcane	61.25	153.52	306.85
4	Cassava	532.95	629.33	489.91
5	Other field crops	2.09	5.19	6.19
6	Para rubber	16.56	30.05	97.03
7	Perennial trees and orchard	55.76	50.21	88.95
8	Forest land	632	604.7	481.3
9	Waterbody	36.81	57.46	53.3
10	Rangeland	26.03	72.11	71.65
11	Marsh and swamp	11.64	33.4	27.73
12	Unused land	28.57	34.33	93.32
	Total	3794.22	3794.22	3794.22
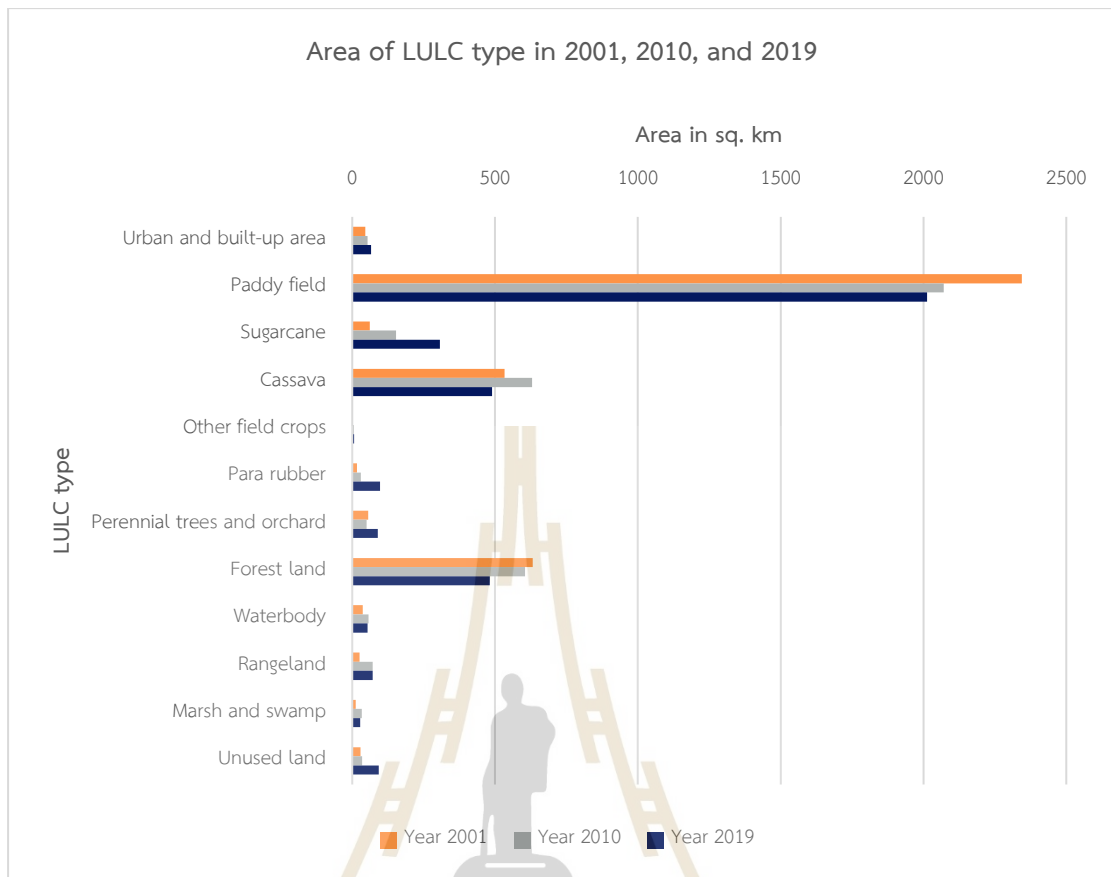
Figure 4.40 Area of each LULC type in 2001, 2010, and 2019.

CHAPTER V

PREDICTION OF TIME-SERIES OF LAND USE AND LAND COVER BY CLUE-S MODEL

This chapter presents the second objective results focusing on predicting time-series of LULC between 2002 and 2009 and 2011 and 2018, which were predicted based on the classified LULC data in 2001, 2010, and 2019 using the CLUE-S model. The significant results in this chapter consist of (1) driving force identification for LULC change, (2) optimum local parameter of the CLUE-S model, (3) LULC prediction between 2002 and 2009, and (4) LULC prediction between 2011 and 2018 are here described and discussed in detail.

5.1 Driving force identification for LULC change

Driving factors are the factors that influence the allocation of land use changes. According to Table 3.3 of Chapter III, the selected driving force for LULC change included (1) elevation, (2) slope, (3) annual rainfall, (4) average income per capita at the sub-district level, (5) population density at the sub-district level, (6) distance to the road network, (7) distance to stream, and (8) distance to the existing urban area (Figure 5.1) are firstly prepared in raster format with a cell size of 100 m. They were then used to identify the significant driving factors for each LULC type using a multicollinearity test and logistic regression analysis. Brief information on the driving factor on LULC changes is summarized below:

Elevation. Elevation was computed from the digital elevation model (DEM), which was downloaded from the SRTM. The domain value of elevation varies between 160 and 1,034 meters above mean sea level.

Slope. The percentage slope was calculated from DEM, and its domain value varies between 0 and 47 percent.

Annual rainfall. Annual rainfall was interpolated as a continuous annual rainfall surface using the IDW method from Chaiyaphum meteorological station and

surrounding TMD stations. The domain value of annual rainfall in 2019 varies between 743.44 and 823.35 millimeters.

The average income per capita at the sub-district level. The average income per capita at the sub-district level was computed from Basic Minimum Need data (BMN) by average income per capita at the sub-district level. The average income per capita at the sub-district level in 2019 varies between 27,888 and 133,728 Baht per year.

Population density at the sub-district level. The population density of each sub-district was calculated based on population data from the Department of Provincial Administration in 2019. The population density of each district diverges between 34.31 and 1,128.92 persons per km^2.

Distance to the road network. Distance to the road network was computed from the exiting road network using the Euclidean distance method. The domain value of distance to road network varies between 0 and 4,080.44 m.

Distance to stream. Distance to the stream was calculated from the stream network using the Euclidean distance method. The domain value of distance to the stream network varies between 0 and 4,000 m.

Distance to the existing urban area. Distance to the existing urban area was computed from the existing urban area of interpreted LULC using the Euclidean distance method. The domain value of distance to the existing urban area varies between 0 and 9,780.08 m.

(a) Elevation   (b) Slope
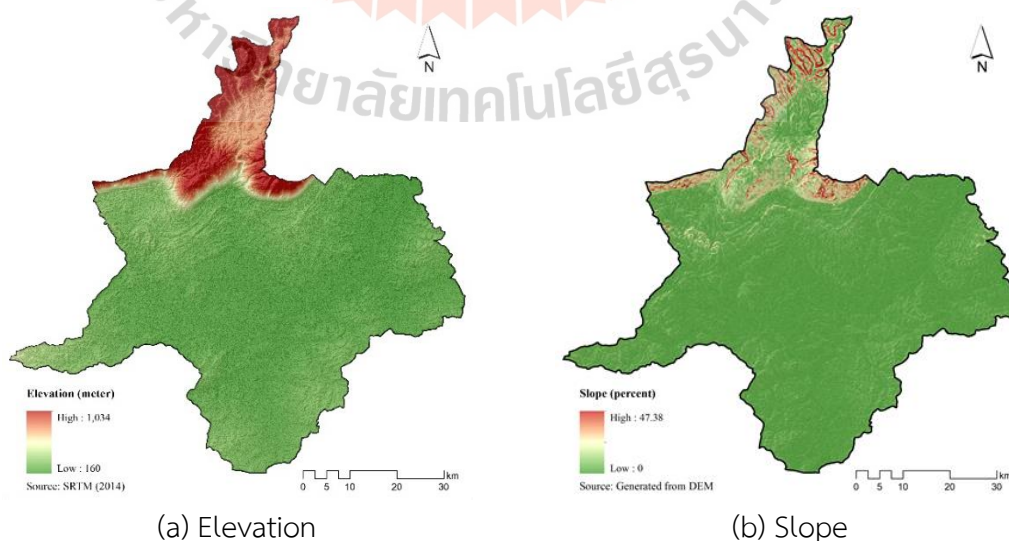
Figure 5.1 Driving factors on LULC change.

(c) Annual rainfall

(d) Average income per capita

(e) Population density

(f) Distance to road network

(g) Distance to stream

(h) Distance to the existing urban area
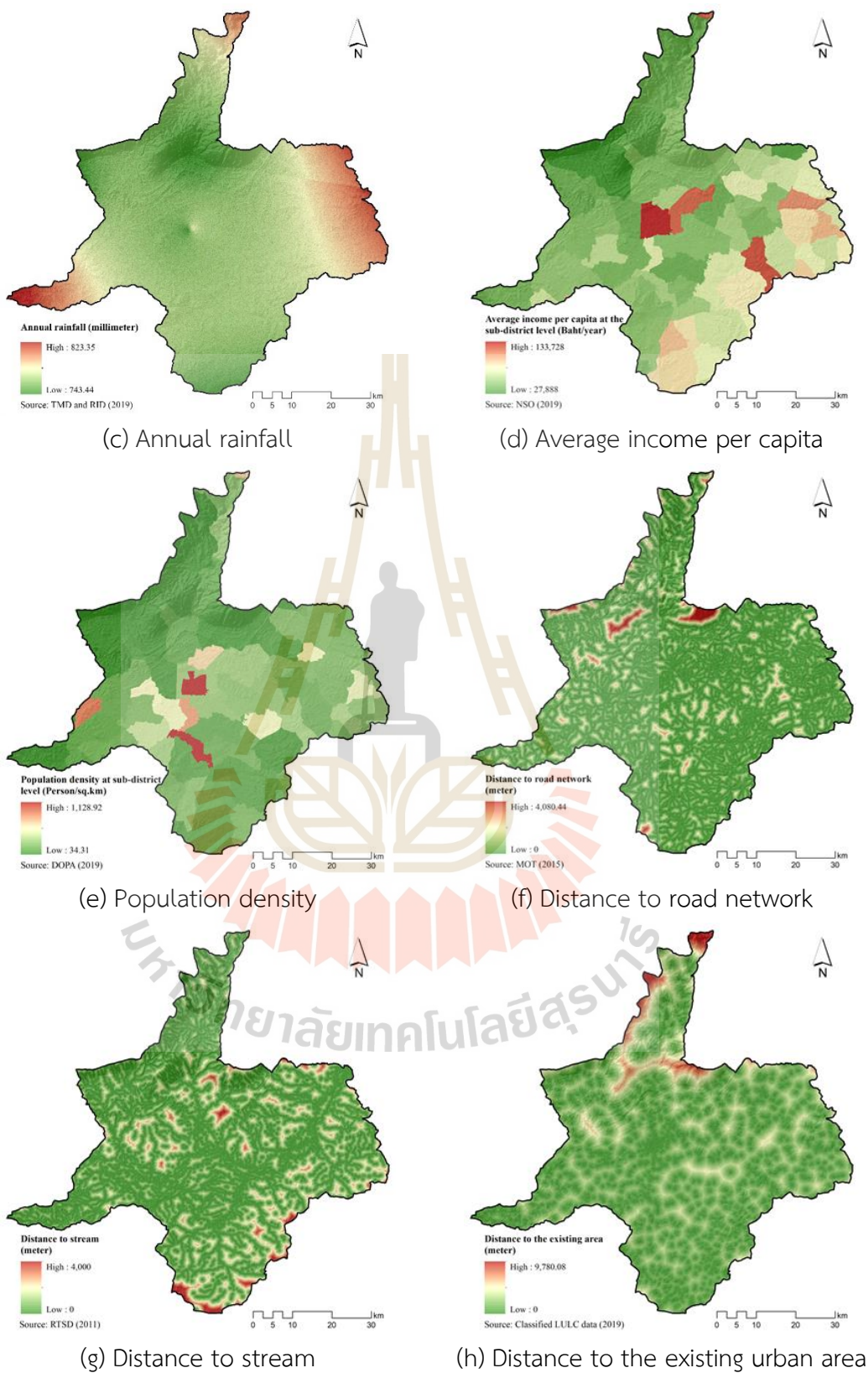
Figure 5.1 (Continued).

The multicollinearity test result among independent variables with correlation coefficient and VIF values is summarized in Tables 5.1 and 5.2, respectively. It was found that the correlation between a pair of covariates is very low, while the variance inflation factor (VIF) values that are calculated to examine the correlation among driving factors are lower than 10. These values imply that they are uncorrelated among driving factors, and it is reasonable to use them for logistic regression analysis for a specific LULC type allocation (Liang et al., 2020; Shrestha and Shrestha, 2017). Meanwhile, the multiple linear regression equation by logistic regression analysis of each LULC type for its location preference with the area under curve (AUC) value is summarized in Table 5.3.

Table 5.1 The correlation coefficient among driving factors on LULC change.

Driving factor	Correlation coefficient							
	X_1	X_2	X_3	X_4	X_5	X_6	X_7	X_8
Elevation (X_1)	**1.000**	0.521	0.022	0.088	0.045	0.065	0.001	0.285
Slope (X_2)	0.521	**1.000**	0.023	0.061	0.031	0.097	0.000	0.185
Annual rainfall (X_3)	0.022	0.023	**1.000**	0.021	0.003	0.011	0.003	0.002
Average income per capita at the sub-district level (X_4)	0.088	0.061	0.021	**1.000**	0.388	0.027	0.008	0.032
Population density at the sub-district level (X_5)	0.045	0.031	0.003	0.388	**1.000**	0.011	0.004	0.025
Distance to road network (X_6)	0.065	0.097	0.011	0.027	0.011	**1.000**	0.000	0.135
Distance to stream (X_7)	0.001	0.000	0.003	0.008	0.004	0.000	**1.000**	0.004
Distance to the existing urban area (X_8)	0.285	0.185	0.002	0.032	0.025	0.135	0.004	**1.000**

Table 5.2 Multicollinearity statistics test of driving factors and VIF value.

Driving factor	Unstandardized Coefficients		Standardized Coefficient	t-test	Sig.	VIF
	Beta	Std. error				
Elevation (X_1)	0.008	0.000	0.429	72.315	0.000	2.578
Slope (X_2)	0.092	0.003	0.167	30.129	0.000	2.255
Annual rainfall (X_3)	-0.031	0.001	-0.085	-22.311	0.000	1.067
Average income per capita at the sub-district level (X_4)	-0.005	0.000	-0.070	-14.149	0.000	1.815
Population density at the sub-district level (X_5)	-0.001	0.000	-0.062	-12.870	0.000	1.688
Distance to road network (X_6)	0.001	0.000	0.073	17.966	0.000	1.203
Distance to stream (X_7)	0.006	0.000	0.001	0.387	0.000	1.052
Distance to the existing urban area (X_8)	-0.005	0.000	-0.007	-1.472	0.001	1.574

Table 5.3 Identified driving force for each LULC type allocation as equation form with AUC using binary logistic regression analysis.

LULC	Driving Factors									AUC
	Constant	X_1	X_2	X_3	X_4	X_5	X_6	X_7	X_8	
1. Urban and Built-Up area (UR)	0.09295	n. s.	n. s.	n. s.	n. s.	0.00084	-0.00640	n. s.	-0.01816	0.98239
2. Paddy field (PD)	10.88306	-0.09471	n. s.	0.01299	n. s.	-0.00179	n. s.	n. s.	n. s.	0.97633
3. Sugarcane (SU)	94.65603	-0.00009	-0.19427	-0.12635	n. s.	-0.01166	n. s.	n. s.	n. s.	0.76771
4. Cassava (CA)	-38.47663	0.00422	-0.10302	0.04774	n. s.	-0.01475	n. s.	0.00095	n. s.	0.79419
5. Other field crops (FC)	207.97836	0.01012	-0.21443	-0.28499	n. s.	n. s.	n. s.	n. s.	n. s.	0.93547
6. Para rubber (PR)	24.18697	0.00834	-0.07301	-0.03984	n. s.	-0.01857	n. s.	-0.00138	n. s.	0.94398
7. Perennial trees and orchard (OP)	-38.48305	n. s.	-0.13142	0.04540	n. s.	-0.00426	n. s.	n. s.	n. s.	0.61857
8. Forest land (FO)	87.34838	0.00321	0.18855	-0.11672	n. s.	-0.01130	n. s.	n. s.	n. s.	0.92888
9. Waterbody (WA)	-4.68618	0.00683	-0.67145	n. s.	n. s.	n. s.	0.00143	-0.00369	n. s.	0.83181
0. Rangeland (RA)	-80.01175	-0.00429	n. s.	0.09908	n. s.	-0.00595	n. s.	n. s.	n. s.	0.74452
11. Marsh and swamp (MA)	5.04358	-0.04668	n. s.	n. s.	n. s.	-0.00589	n. s.	-0.00526	n. s.	0.86275
12. Unused land (UL)	-8.63439	0.00932	-0.02903	n. s.	n. s.	n. s.	n. s.	n. s.	n. s.	0.86930

Remark: All explanatory variables are significant at $p < 0.05$ error level; n. s. is not significant at 0.05 level.

5.1.1 Driving factor for urban and built-up area allocation

The multiple linear equation of the binomial logit regression model for urban and built-up area allocation after multicollinearity test is as follows:

$$\text{Log} \left(\frac{P_i}{1-P_i} \right) = 0.09295 + 0.00084X_5 - 0.00640X_6 - 0.01816X_8 \qquad (5.1)$$

where X_5 is Population density at the sub-district level (person per km^2),

X_6 is Distance to road network (m), and

X_8 is Distance to the existing urban area (m).

According to Equation 5.1, it was found that two driving factors include distance to the road network and distance to the existing urban area, have a negative relationship with the probability of urban and built-up area allocation. Meanwhile, only one driving factor, population density at the sub-district level, positively correlates with the probability of urban and built-up area allocation. All significant driving factors genuinely play an essential role in urban and built-up area allocation. These results imply that when the distance to the road and the existing urban area decreases, the probability of urban and built-up areas increases. Meanwhile, when the population density at the sub-district level increases, the probability of urban and built-up areas increases.

The AUC value for urban and built-up area allocation with a value of 0.98 suggests an excellent fit between the predicted and real LULC transition (Liang et al., 2020; Pontius and Schneider, 2001; Vilar del Hoyo, Martín Isabel, and Martínez Vega, 2011).

5.1.2 Driving factor for paddy field allocation

The multiple linear equation of the binomial logit regression model for paddy field allocation after multicollinearity test is as follows:

$$\text{Log} \left(\frac{P_i}{1-P_i} \right) = 10.88306 - 0.09471X_1 + 0.01299X_3 - 0.00179X_5 \qquad (5.2)$$

where X_1 is Elevation (m),

X_3 is Annual rainfall (mm), and

X_5 is Population density at the sub-district level (person per km^2).

Equation 5.2 reveals that two driving factors include elevation and population density at the sub-district level, negatively affecting the probability of

paddy field allocation. In the meantime, only one driving factor, annual rainfall, has a positive relationship with the probability of paddy field allocation. All significant driving factors truly play an important role in paddy field allocation. These results indicate that the paddy field prefers to situate at low elevation or flat area, low population density, and high annual rainfall.

The AUC value for paddy field allocation with a value of 0.97 suggests an excellent fit between the predicted and real LULC transition (Liang et al., 2020; Pontius and Schneider, 2001; Vilar del Hoyo et al., 2011).

5.1.3 Driving factor for sugarcane allocation

The multiple linear equation of the binomial logit regression model for sugarcane allocation after multicollinearity test is as follows:

$$\text{Log} \left(\frac{P_i}{1-P_i} \right) = 94.65603 - 0.00009X_1 - 0.19427X_2 - 0.12635X_3 - 0.01166X_5 \quad (5.3)$$

where X_1 is Elevation (m),

        X_2 is Slope (percent),

        X_3 is Annual rainfall (mm), and

        X_5 is Population density at the sub-district level (person per km^2).

According to Equation 5.3, it was found that four driving factors include elevation, slope, annual rainfall, and population density at the sub-district level, having a negative relationship with the probability of sugarcane allocation. The most crucial sugarcane factors are slope, annual rainfall, and population density at the sub-district level. These imply that sugarcane prefers to situate at an undulating terrain with low annual rainfall and population density.

The AUC value for sugarcane allocation with a value of 0.76 suggests a fair fit between the predicted and real LULC transition (Liang et al., 2020; Pontius and Schneider, 2001; Vilar del Hoyo et al., 2011).

5.1.4 Driving factor for cassava allocation

The multiple linear equation of the binomial logit regression model for cassava allocation after multicollinearity test is as follows:

$$\text{Log} \left(\frac{P_i}{1-P_i} \right) = -38.47660 + 0.00422X_1 - 0.10302X_2 + 0.04774X_3 - 0.01475X_5$$
$$+ 0.00095X_7 \quad (5.4)$$

where X_1 is Elevation (m),

      X_2 is Slope (percent),

      X_3 is Annual rainfall (mm),

      X_5 is Population density at the sub-district level (person per km^2), and

      X_7 is Distance to stream (m).

According to Equation 5.4, it was found that three driving factors include elevation, annual rainfall, and distance to stream, having a positive relationship with the probability of cassava allocation. Meanwhile, two driving factors include slope and population density at the sub-district level, negatively affecting cassava allocation. The most crucial cassava factors were slope, annual rainfall, and population density at the sub-district level. These imply that sugarcane prefers to situate at an undulating terrain, has low population density, and has high annual rainfall.

The AUC value for cassava allocation with a value of 0.79 suggests a fair fit between the predicted and real LULC transition (Liang et al., 2020; Pontius and Schneider, 2001; Vilar del Hoyo et al., 2011).

5.1.5 Driving factor for other field crops allocation

The multiple linear equation of the binomial logit regression model for other field crops allocation after multicollinearity test is as follows:

$$\text{Log}\left(\frac{P_i}{1-P_i}\right) = 207.97840+0.01012X_1-0.21443X_2-0.28499X_3 \tag{5.5}$$

where X_1 is Elevation (m),

   X_2 is Slope (percent), and

   X_3 is Annual rainfall (mm).

Equation 5.5 reveals that two driving factors include slope and annual rainfall, negatively affecting other field crop allocation probability. Meanwhile, only one driving factor, elevation, positively relates with other field crop allocation probability. The most critical factors for other field crops occurrence are slope and annual rainfall. These results show that when these factors decreased, the probability for other field crops occurrence increased. Other field crops frequently occurred in the low terrace area in the study area.

The AUC value for other field crops allocation with a value of 0.93 suggests an excellent fit between the predicted and real LULC transition (Liang et al., 2020; Pontius and Schneider, 2001; Vilar del Hoyo et al., 2011).

5.1.6 Driving factor for para rubber allocation

The multiple linear equation of the binomial logit regression model for para rubber allocation after multicollinearity test is as follows:

$$\text{Log}\left(\frac{P_i}{1-P_i}\right) = 24.18697 + 0.00834X_1 - 0.07301X_2 - 0.04774X_3 - 0.01857X_5$$

$$-0.00138X_7 \tag{5.6}$$

where X_1 is Elevation (m),

                X_2 is Slope (percent),

                X_3 is Annual rainfall (mm),

                X_5 is Population density at the sub-district level (person per km^2), and

                X_7 is Distance to stream (m).

According to Equation 5.6, it was found that four driving factors include slope, annual rainfall, population density at the sub-district level, and distance to stream, having a negative relationship with the probability of para rubber allocation. But, only one driving factor, elevation, has a positive relationship with para rubber allocation. All significant driving factors play an essential role in para rubber allocation. These results show that para rubber prefers to situate at high elevation and hilly slope, close to the stream, low population density, and low annual rainfall.

The AUC value for para rubber allocation with a value of 0.94 suggests an excellent fit between the predicted and real LULC transition (Liang et al., 2020; Pontius and Schneider, 2001; Vilar del Hoyo et al., 2011).

5.1.7 Driving factor for perennial trees and orchard allocation

The multiple linear equation of the binomial logit regression model for perennial trees and orchard allocation after multicollinearity test is as follows:

$$\text{Log}\left(\frac{P_i}{1-P_i}\right) = -38.48310 - 0.13142X_2 + 0.04540X_3 - 0.00426X_5 \tag{5.7}$$

where X_2 is Slope (percent),

                X_3 is Annual rainfall (mm), and

                X_5 is Population density at the sub-district level (person per km^2).

According to Equation 5.7, it was found that two driving factors include slope and population density at the sub-district level, having a negative relationship with the probability of perennial trees and orchard allocation. In the meantime, only one driving factor, annual rainfall, has a positive relationship with the probability of perennial trees and orchard allocation. All significant driving factors play an essential role in perennial trees and orchard allocation. These results indicate that the perennial trees and orchards prefer to be located in a flat area with low population density and high annual rainfall.

The AUC value for paddy field allocation with a value of 0.61 suggests a poor fit between the predicted and real LULC transition (Liang et al., 2020; Pontius and Schneider, 2001; Vilar del Hoyo et al., 2011).

5.1.8 Driving factor for forest land allocation

The multiple linear equation of the binomial logit regression model for forest land allocation after multicollinearity test is as follows:

$$\text{Log}\left(\frac{P_i}{1-P_i}\right) = 87.34838 + 0.00321X_1 + 0.18855X_2 - 0.11672X_3 - 0.01130X_5 \qquad (5.8)$$

where
X_1 is Elevation (m),

X_2 is Slope (percent),

X_3 is Annual rainfall (mm), and

X_5 is Population density at the sub-district level (person per km^2).

According to Equation 5.8, it was found that two driving factors include elevation and slope, have a positive relationship with the probability of forest land. Meanwhile, two driving factors, namely annual rainfall and population density at the sub-district level, negatively affect forest land allocation probability. All significant driving factors play an essential role in forest land allocation. These results show that forest land prefers to be located at a high area and steep slope, with low population density and annual rainfall.

The AUC value for forest land allocation with a value of 0.92 suggests an excellent fit between the predicted and real LULC transition (Liang et al., 2020; Pontius and Schneider, 2001; Vilar del Hoyo et al., 2011).

5.1.9 Driving factor for waterbody area allocation

The multiple linear equation of the binomial logit regression model for waterbody allocation after multicollinearity test is as follows:

$$\text{Log}\left(\frac{P_i}{1-P_i}\right) = -4.68618+0.00683X_1-0.67145X_2+0.00143X_6-0.00369X_7 \qquad (5.9)$$

where X_1 is Elevation (m),

X_2 is Slope (percent),

X_6 is Distance to road (m), and

X_7 is Distance to stream (m).

Equation 5.9 reveals that two driving factors, elevation, and distance to road, positively affect waterbody's probability. On the other hand, two driving factors, namely slope and distance to stream, negatively affect waterbody allocation probability. All significant driving factors play an essential role in waterbody allocation. These results indicate that waterbody prefers to situate in a flat area, far from the road network and close to the stream.

The AUC value for waterbody allocation with a value of 0.83 suggests a good fit between the predicted and real LULC transition (Liang et al., 2020; Pontius and Schneider, 2001; Vilar del Hoyo et al., 2011).

5.1.10 Driving factor for rangeland allocation

The multiple linear equation of the binomial logit regression model for rangeland allocation after multicollinearity test is as follows:

$$\text{Log}\left(\frac{P_i}{1-P_i}\right) = -80.01180-0.00429X_1+0.09908X_3-0.00595X_5 \qquad (5.10)$$

where X_1 is Elevation (m),

X_3 is Annual rainfall (mm), and

X_5 is Population density at the sub-district level (person per km^2).

According to Equation 5.10, it was found that two driving factors include elevation and population density at the sub-district level, have a negative relationship with the probability of rangeland allocation. But, only one driving factor, annual rainfall, negatively affects rangeland allocation probability. All significant driving factors play an important role in rangeland allocation. These results indicate that

rangeland prefers to situate at low elevation and population density with high annual rainfall.

The AUC value for rangeland allocation with a value of 0.74 suggests a fair fit between the predicted and real LULC transition (Liang et al., 2020; Pontius and Schneider, 2001; Vilar del Hoyo et al., 2011).

5.1.11 Driving factor for marsh and swamp allocation

The multiple linear equation of the binomial logit regression model for marsh and swamp allocation after multicollinearity test is as follows:

$$\text{Log}\left(\frac{P_i}{1-P_i}\right) = 5.04358-0.04668X_1-0.00589X_5-0.00526X_7 \tag{5.11}$$

where
X_1 is Elevation (m),

X_5 is Population density at the sub-district level (person per km^2), and

X_7 is Distance to stream (m).

Equation 5.11 reveals that three driving factors include elevation, population density at the sub-district level, and distance to stream, negatively affect marsh and swamp allocation probability. All significant driving factors play an essential role in marsh and swamp allocation. These results indicate that marsh and swamp prefer to locate at low elevation and population density, with an area close to the stream.

The AUC value for marsh and swamp allocation with a value of 0.86 suggests a good fit between the predicted and real LULC transition (Liang et al., 2020; Pontius and Schneider, 2001; Vilar del Hoyo et al., 2011).

5.1.12 Driving factor for unused land allocation

The multiple linear equation of the binomial logit regression model for unused land allocation after multicollinearity test is as follows:

$$\text{Log}\left(\frac{P_i}{1-P_i}\right) = -8.63439+0.00932X_1-0.02903X_2 \tag{5.12}$$

where
X_1 is Elevation (m), and

X_2 is Slope (percent)

Equation 5.12 reveals that elevation has a positive relationship with the probability of unused land allocation. Meanwhile, slope negatively affect unused land allocation probability. Thus, all significant driving factors play an essential role in

marsh and swamp allocation. These results show that unused land prefers to situate at high elevations and steep slopes in the study area.

The AUC value for unused land allocation with a value of 0.86 suggests a good fit between the predicted and real LULC transition (Liang et al., 2020; Pontius and Schneider, 2001; Vilar del Hoyo et al., 2011).

In summary, as mentioned in Section 5.1.1-5.1.12, it was found that the most common vital driving force for all LULC type change was the elevation. Meanwhile, the most important driving force for field crops (sugarcane, cassava, and other field crops) include elevation, slope, and annual rainfall. The specific driving factors for each LULC type preference from binary logistics regression are further applied to allocate LULC type for predicting LULC change under the CLUE-S model.

5.2   Optimum local parameter of the CLUE-S model

Two required parameters for the optimum local parameter examination, including land use type conversion matrix and land use type resistance (elasticity), were first defined based on the transitional probability change matrix between 2010 and 2019 by the Markov Chain model. At the same time, the land requirement in the same period was estimated based on the transitional area change matrix using the Markov Chain model. After that, LULC in 2019 was predicted with the preference LULC type allocation under the CLUE-S model. The predicted LULC in 2019 was further compared with the classified LULC in 2019 using the wall-to-wall accuracy assessment for validating an optimum local parameter of the CLUE-S model. In this study, if overall accuracy and the Kappa hat coefficient of the predicted LULC map are equal to or more than 80 percent, the assigned parameter values of elasticity and conversion matrix are accepted as an optimum local parameter of the CLUE-S model. The brief information of two predefine parameter are summarized below:

(1) Land use type conversion matrix

Land use type-specific conversion settings represents the behavior of one specific land use type. A value must be specified for each land use type representing the relative conversion resistance, ranging from 0 (not allowed to change) to 1 (allowed to change). In general, the modeler decides on this factor based on expert knowledge

or observed behavior in the recent past (Verburg, 2010). In this study, the conversion matrix for each LULC type possibly changes between 2010 and 2019 was assigned based on transitional LULC change between 2001 and 2010 as the summary in Table 5.4. It can be observed that urban and built-up areas in 2010 did not change to any LULC types in 2019.

Table 5.4 Conversion matrix of possible change between 2010 and 2019.

LULC types	LULC type possible change in 2019											
	UR	PA	SU	CA	FC	PR	PO	FO	WA	RA	MA	UL
Urban and built-up area (UR)	1	0	0	0	0	0	0	0	0	0	0	0
Paddy field (PA)	0	1	1	1	0	0	1	0	0	1	1	0
Sugarcane (SU)	1	1	1	1	0	0	1	0	0	0	0	0
Cassava (CA)	1	1	1	1	0	1	1	0	0	1	0	1
Other field crops (FC)	0	0	1	1	1	0	0	0	0	0	0	0
Para rubber (PR)	0	0	0	1	1	1	0	0	0	0	0	1
Perennial trees and orchard (PO)	0	0	1	0	0	0	1	0	0	0	0	0
Forest land (FO)	1	0	0	0	0	1	1	1	0	1	0	1
Waterbody (WA)	1	0	1	0	0	0	0	0	1	0	1	0
Rangeland (RA)	0	1	0	0	0	0	1	0	0	1	0	0
Marsh and swamp (MA)	1	1	1	1	0	0	1	0	0	0	1	0
Unused land (UL)	1	1	0	0	0	0	0	0	0	0	0	1

(Row label group: LULC in 2010)

Remark: 0 is not allowed and 1 is allowed.

(2) Land use type resistance (elasticity)

The conversion resistance is one of the land use type-specific settings that determine the temporal dynamic of prediction. The conversion resistance or elasticity relates to the reversibility of land use changes. In principle, land use type resistance represents the relative elasticity to conversion, ranging from 0 (easy conversion) to 1 (irreversible change) (Verburg, 2010). In this study, the transition probability matrix of LULC change between 2010 and 2019 from the Markov Chain model is displayed in Table 5.5. Here, the elasticity value of the urban and built-up area, paddy field, sugarcane, cassava, other field crops, para rubber, perennial trees and orchard, forest land, waterbody, rangeland, marsh and swamp, and unused land are 1.00, 0.93, 0.93, 0.65, 0.99, 0.80, 0.99, 0.80, 0.91, 0.89, 0.39 and 0.96, respectively. The assigned elasticity value is suggested by Ongsomwang and Iamchuen (2015). They found that an optimum

local parameter for LULC prediction under the CLUE-S model should be probability values of the transition probability matrix of LULC change between two periods.

Table 5.5 Elasticity of LULC change for LULC prediction between 2010 and 2019.

LULC types	LULC type possible change in 2019											
	UR	PA	SU	CA	FC	PR	PO	FO	WA	RA	MA	UL
Urban and built-up area (UR)	1.00	-	-	-	-	-	-	-	-	-	-	-
Paddy field (PA)	-	0.93	0.03	0.02	-	-	0.01	-	-	-	0.01	-
Sugarcane (SU)	0.01	0.01	0.93	0.05	-	-	0.01	-	-	-	-	-
Cassava (CA)	0.01	0.06	0.16	0.65	-	0.07	0.01	-	-	-	-	0.04
Other field crops (FC)	-	-	-	-	0.99	-	0.01	-	-	-	-	-
Para rubber (PR)	-	-	-	0.11	0.01	0.80	0.03	-	-	-	-	0.05
Perennial trees and orchard (PO)	-	-	0.01	0.01	-	-	0.99	-	-	-	-	-
Forest land (FO)	-	0.02	-	0.05	-	0.05	0.01	0.80	-	-	-	0.06
Waterbody (WA)	-	0.04	0.02	0.01	-	-	-	-	0.91	-	0.01	-
Rangeland (RA)	-	0.08	-	0.02	-	-	0.01	-	-	0.89	-	-
Marsh and swamp (MA)	0.01	0.55	0.03	-	-	-	0.02	-	-	-	0.39	-
Unused land (UL)	0.01	0.03	-	-	-	-	-	-	-	-	-	0.96

(Row label group on left side: LULC in 2010)

The error matrix and accuracy assessment between the classified LULC in 2019 by the RF and the predicted LULC in 2019 by the CLUE-S model is presented in Table 5.6. Simultaneously, the spatial distribution of predicted LULC by the CLUE-S model and classified LULC by RF classifier is compared as shown in Figure 5.2. As a result, it was found that the overall accuracy and Kappa hat coefficient were 86.95% and 80.72%, respectively. Both accuracy values were more than 80 percent as a requirement. Therefore, predefined parameters (land use type conversion matrix and land use type resistance) can be accepted for LULC prediction in 2002-2009 and 2011-2018, respectively.
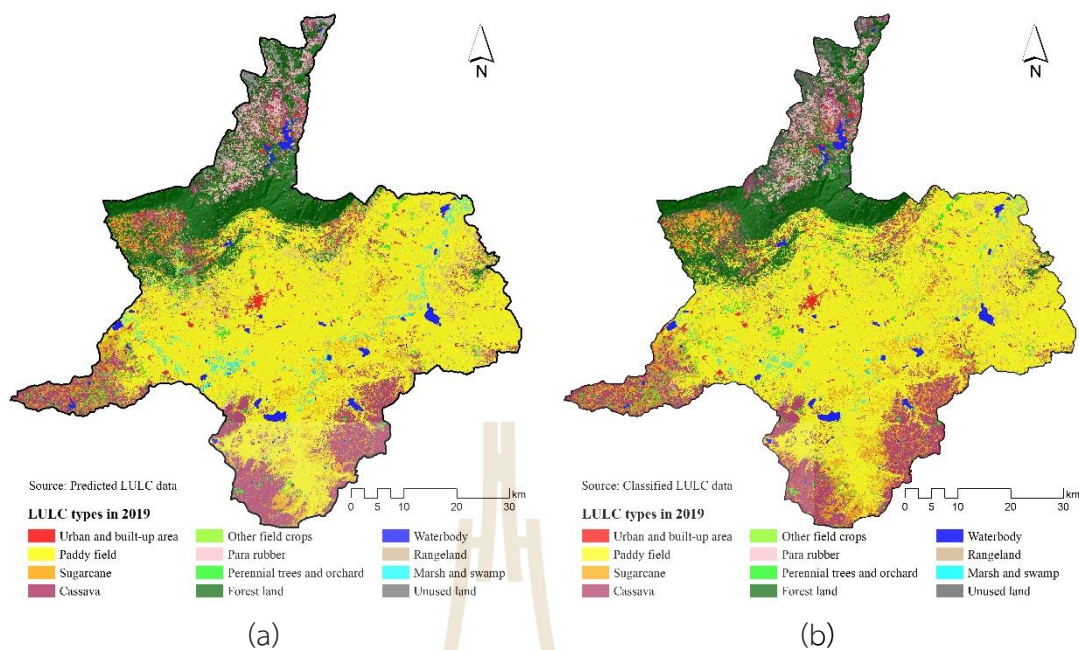
Figure 5.2 Comparison of spatial LULC distribution in 2019: (a) predicted LULC by the CLUE-S model and (b) classified LULC by RF classifier.

Table 5.6 Error matrix and accuracy assessment between classified LULC in 2019 and predicted LULC in 2019.

LULC types	Predicted LULC in 2019 (pixel)												
	UR	PA	SU	CA	FC	PR	PO	FO	WA	RA	MA	UL	Total
Urban and built-up area (UR)	6,414	13	51	86	0	0	3	12	0	0	3	1	6,583
Paddy field (PA)	3	189,634	3,581	4,459	2	37	1,856	176	440	361	564	103	201,216
Sugarcane (SU)	48	4,309	20,298	5,208	0	384	301	0	6	76	45	11	30,686
Cassava (CA)	34	3,095	5,553	36,672	0	1,050	535	3	5	138	4	1,902	48,991
Other field crops (FC)	2	0	0	116	497	0	4	0	0	0	0	0	619
Para rubber (PR)	20	680	133	480	31	6,986	1,043	0	0	88	0	242	9,703
Perennial trees and orchard (PO)	5	1,504	96	180	0	795	4,859	755	2	695	1	3	8,895
Forest land (FO)	14	0	107	1,002	88	31	6	46,175	23	51	0	633	48,130
Waterbody (WA)	25	593	139	82	0	0	16	0	4,440	0	32	3	5,330
Rangeland (RA)	1	870	16	114	0	0	27	386	0	5,751	0	0	7,165
Marsh and swamp (MA)	10	131	98	7	0	0	72	300	405	0	1,750	0	2,773
Unused land (UL)	13	388	611	587	0	420	181	323	8	0	370	6,430	9,331
Total	6,589	201,217	30,683	48,993	618	9,703	8,903	48,130	5,329	7,160	2,769	9,328	379,422
Producer's accuracy (%)	97.34	94.24	66.15	74.85	80.42	72.00	54.58	95.94	83.32	80.32	63.20	68.93	
User's accuracy (%)	97.43	94.24	66.15	74.85	80.29	72.00	54.63	95.94	83.30	80.27	63.11	68.91	
Overall accuracy (%)	86.95												
Kappa hat coefficient (%)	80.72												

Classified LULC in 2019 (pixel)

5.3 LULC prediction between 2002 and 2009

Under this section, the derived optimum local parameter of the CLUE-S model from the previous section was applied to predict LULC data between 2002 and 2009. Simultaneously, specific land demand was calculated based on the LULC change rate between 2001 and 2010 using the Markov Chain model, summarized in Tables 5.7 and 5.8.

Table 5.7 The matrix of transition area of LULC change between 2001 and 2010.

LULC type	LULC in 2010 (Area in km^2)											
	UR	PD	SU	CA	FC	PR	PO	FO	WA	RA	MA	UL
Urban and built-up area (UR)	46.17	-	-	-	-	-	-	-	-	-	-	-
Paddy field (PD)	6.54	2,007.89	69.31	169.46	-	-	-	-	16.82	48.79	25.19	0.40
Sugarcane (SU)	0.01	4.65	31.19	24.57	-	0.13	-	-	0.29	0.09	0.09	0.23
Cassava (CA)	0.05	39.56	51.34	415.26	3.01	12.12	-	-	1.84	5.17	-	4.61
Other field crops (FC)	-	-	-	-	2.09	-	-	-	-	-	-	-
Para rubber (PR)	-	-	-	0.07	-	16.48	-	-	-	-	-	-
Perennial trees and orchard (PO)	0.03	1.23	0.41	3.57	-	-	49.94	-	0.48	0.09	-	-
Forest land (FO)	0.34	15.83	0.29	6.23	0.10	1.13	-	604.70	0.01	1.07	-	2.30
Waterbody (WA)	-	0.14	0.10	0.45	-	0.19	-	-	35.91	-	-	0.01
Rangeland (RA)	0.05	0.04	0.56	8.33	-	-	0.27	-	0.01	16.77	-	0.02
Marsh and swamp (MA)	0.01	0.54	0.28	0.57	-	-	-	-	2.10	0.02	8.12	-
Unused land (UL)	0.02	0.82	0.05	0.81	-	-	-	-	0.01	0.10	-	26.77

Table 5.8 Annual land requirement of LULC prediction between 2001 and 2010 for each LULC type.

Year	LULC type (Area in km^2)												Total
	UR	PA	SU	CA	FC	PR	PO	FO	WA	RA	MA	UL	
2001	46.17	2,344.39	61.25	532.95	2.09	16.56	55.76	632.00	36.81	26.03	11.64	28.57	3,794.22
2002	46.95	2,314.01	71.53	543.60	2.45	18.03	55.15	628.98	39.12	31.16	14.03	29.19	3,794.22
2003	47.71	2,283.59	81.77	554.34	2.79	19.54	54.54	625.95	41.40	36.28	16.46	29.84	3,794.22
2004	48.50	2,253.18	91.96	565.05	3.13	21.09	53.90	622.90	43.70	41.38	18.94	30.47	3,794.22
2005	49.30	2,222.70	102.27	575.78	3.50	22.54	53.27	619.88	46.00	46.51	21.30	31.16	3,794.22
2006	50.05	2,192.30	112.51	586.50	3.83	24.10	52.66	616.83	48.28	51.63	23.78	31.74	3,794.22
2007	50.82	2,161.94	122.76	597.16	4.17	25.57	52.07	613.81	50.57	56.77	26.17	32.40	3,794.22
2008	51.61	2,131.48	133.03	607.87	4.51	27.08	51.47	610.77	52.86	61.90	28.60	33.03	3,794.22
2009	52.41	2,101.12	143.27	618.63	4.87	28.53	50.84	607.74	55.16	66.99	30.97	33.69	3,794.22
2010	53.21	2,070.70	153.51	629.33	5.19	30.05	50.21	604.70	57.46	72.11	33.40	34.33	3,794.22
Annual rate	0.79	-30.42	10.24	10.71	0.33	1.52	-0.63	-3.03	2.29	5.12	2.44	0.64	

According to Table 5.8, the increasing LULC types are urban and built-up area, sugarcane, cassava, other field crops, para rubber, waterbody, rangeland, marsh and swamp, and unused land, with an increasing annual change rate of 0.79, 10.24, 10.71,

0.33, 1.52, 2.29, 5.12, 2.44, and 0.64 km^2 per year, respectively. On the other hand, decreasing LULC types are paddy fields, perennial trees and orchards, and forest land, with a decreasing annual change rate of 30.42, 0.63, and 3.03 km^2 per year, respectively. In principle, land requirement dictates the final allocated area of each LULC type in different years under the CLUE-S model. The spatial distribution of the predicted LULC data between 2002 and 2009 is presented in Figure 5.3. Meanwhile, the area and percentage of predictive LULC types between 2002 and 2009 are summarized in Tables 5.9 to 5.10, respectively.

Predicted LULC in 2002 · Predicted LULC in 2003 · Predicted LULC in 2004 · Predicted LULC in 2005
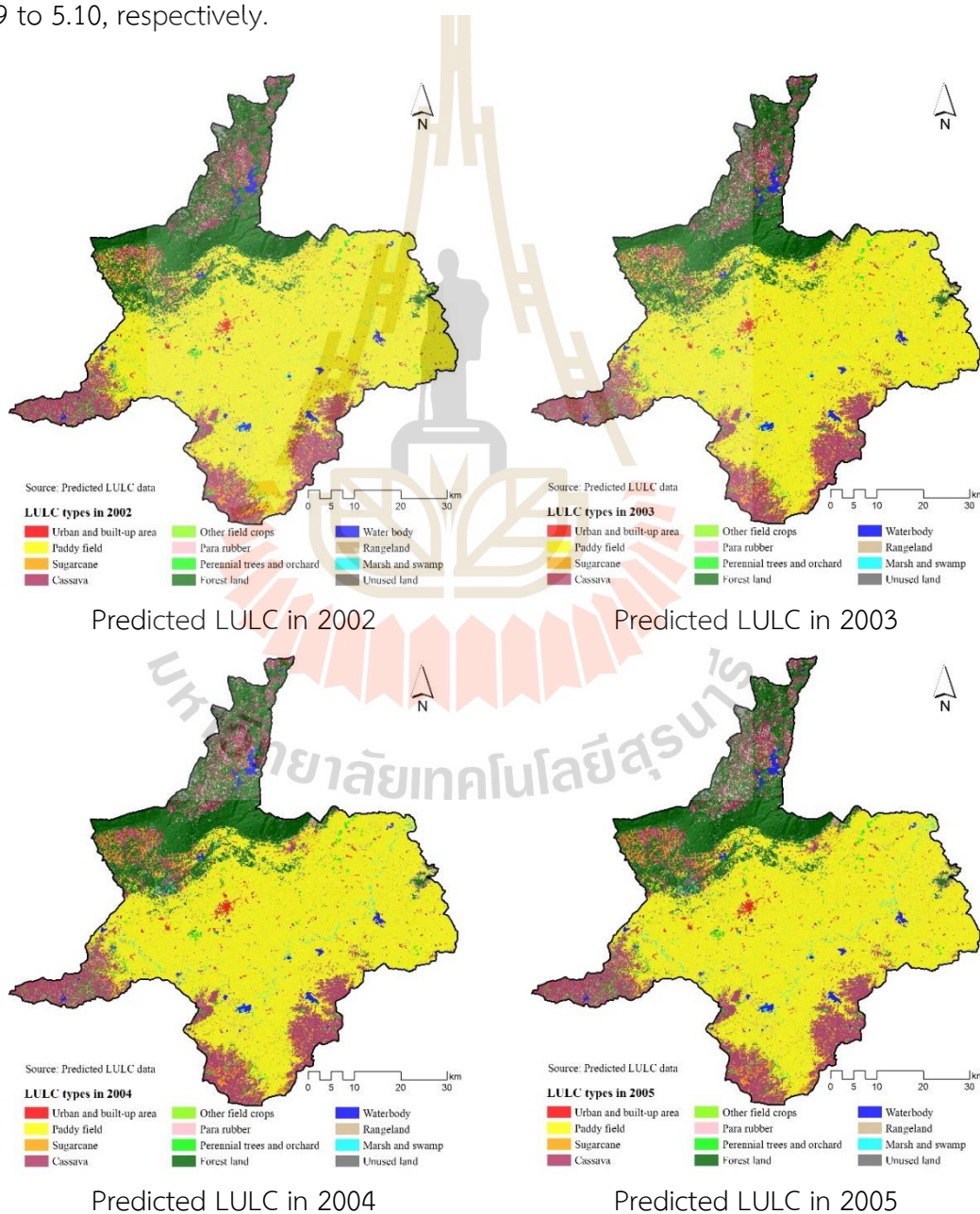
Figure 5.3 Spatial distribution of predicted LULC data between 2002 and 2009.

Source: Predicted LULC data

LULC types in 2006

■ Urban and built-up area	■ Other field crops	■ Waterbody
■ Paddy field	■ Para rubber	■ Rangeland
■ Sugarcane	■ Perennial trees and orchard	■ Marsh and swamp
■ Cassava	■ Forest land	■ Unused land

Predicted LULC in 2006

Source: Predicted LULC data

LULC types in 2007

■ Urban and built-up area	■ Other field crops	■ Waterbody
■ Paddy field	■ Para rubber	■ Rangeland
■ Sugarcane	■ Perennial trees and orchard	■ Marsh and swamp
■ Cassava	■ Forest land	■ Unused land

Predicted LULC in 2007

Source: Predicted LULC data

LULC types in 2008

■ Urban and built-up area	■ Other field crops	■ Waterbody
■ Paddy field	■ Para rubber	■ Rangeland
■ Sugarcane	■ Perennial trees and orchard	■ Marsh and swamp
■ Cassava	■ Forest land	■ Unused land

Predicted LULC in 2008

Source: Predicted LULC data

LULC types in 2009

■ Urban and built-up area	■ Other field crops	■ Waterbody
■ Paddy field	■ Para rubber	■ Rangeland
■ Sugarcane	■ Perennial trees and orchard	■ Marsh and swamp
■ Cassava	■ Forest land	■ Unused land

Predicted LULC in 2009

Figure 5.3 (Continued).

Table 5.9 Area of predicted LULC type between 2002 and 2009.

LULC types	Area of predicted LULC type in km^2							
	2002	2003	2004	2005	2006	2007	2008	2009
Urban and built-up area (UR)	46.95	47.71	48.50	49.30	50.05	50.82	51.61	52.41
Paddy field (PD)	2,314.01	2,283.59	2,253.18	2,222.70	2,192.30	2,161.94	2,131.48	2,101.12
Sugarcane (SU)	71.53	81.77	91.96	102.27	112.51	122.76	133.03	143.27
Cassava (CA)	543.60	554.34	565.05	575.78	586.50	597.16	607.87	618.63
Other field crops (FC)	2.45	2.79	3.13	3.50	3.83	4.17	4.51	4.87
Para rubber (PR)	18.03	19.54	21.09	22.54	24.10	25.57	27.08	28.53
Perennial trees and orchard (PO)	55.15	54.54	53.90	53.27	52.66	52.07	51.47	50.84
Forest land (FO)	628.98	625.95	622.90	619.88	616.83	613.81	610.77	607.74
Waterbody (WA)	39.12	41.40	43.70	46.00	48.28	50.57	52.86	55.16
Rangeland (RA)	31.16	36.28	41.38	46.51	51.63	56.77	61.90	66.99
Marsh and swamp (MA)	14.03	16.46	18.94	21.30	23.78	26.17	28.60	30.97
Unused land (UL)	29.19	29.84	30.47	31.16	31.74	32.40	33.03	33.69
Total	3,794.22	3,794.22	3,794.22	3,794.22	3,794.22	3,794.22	3,794.22	3,794.22

Table 5.10 Percentage of predicted LULC type between 2002 and 2009.

LULC types	Area of predicted LULC type in the percentage							
	2002	2003	2004	2005	2006	2007	2008	2009
Urban and built-up area (UR)	1.24	1.26	1.28	1.30	1.32	1.34	1.36	1.38
Paddy field (PD)	60.99	60.19	59.38	58.58	57.78	56.98	56.18	55.38
Sugarcane (SU)	1.89	2.16	2.42	2.70	2.97	3.24	3.51	3.78
Cassava (CA)	14.33	14.61	14.89	15.18	15.46	15.74	16.02	16.30
Other field crops (FC)	0.06	0.07	0.08	0.09	0.10	0.11	0.12	0.13
Para rubber (PR)	0.48	0.51	0.56	0.59	0.64	0.67	0.71	0.75
Perennial trees and orchard (PO)	1.45	1.44	1.42	1.40	1.39	1.37	1.36	1.34
Forest land (FO)	16.58	16.50	16.42	16.34	16.26	16.18	16.10	16.02
Waterbody (WA)	1.03	1.09	1.15	1.21	1.27	1.33	1.39	1.45
Rangeland (RA)	0.82	0.96	1.09	1.23	1.36	1.50	1.63	1.77
Marsh and swamp (MA)	0.37	0.43	0.50	0.56	0.63	0.69	0.75	0.82
Unused land (UL)	0.77	0.79	0.80	0.82	0.84	0.85	0.87	0.89
Total	100.00	100.00	100.00	100.00	100.00	100.00	100.00	100.00

5.4   LULC prediction between 2011 and 2018

The derived optimum local parameter of the CLUE-S model from section 5.2 was applied to predict LULC data between 2011 and 2018. Simultaneously, specific land demand was calculated based on the LULC change rate between 2010 and 2019 using the Markov Chain model were summarized in Tables 5.11 and 5.12.

Table 5.11 Transition area matrix of LULC change between 2010 and 2019 from Markov Chain model.

LULC type	LULC in 2019 (Area in km^2)											
	UR	PD	SU	CA	FC	PR	PO	FO	WA	RA	MA	UL
Urban and built-up area (UR)	53.21	0.00	0.00	0.00	0.00	0.00	0.00	0.00	0.00	0.00	0.00	0.00
Paddy field (PD)	0.00	1,932.32	58.92	40.78	0.01	0.00	19.64	0.00	0.39	3.42	14.38	0.86
Sugarcane (SU)	0.86	1.06	143.01	7.45	0.00	0.00	0.96	0.00	0.05	0.10	0.02	0.01
Cassava (CA)	8.94	37.71	100.15	407.10	0.00	41.97	7.68	0.00	0.05	2.12	0.04	23.57
Other field crops (FC)	0.01	0.00	0.00	0.00	5.14	0.00	0.04	0.00	0.00	0.00	0.00	0.00
Para rubber (PR)	0.00	0.00	0.12	3.32	0.29	23.92	0.78	0.00	0.01	0.00	0.00	1.61
Perennial trees and orchard (PO)	0.00	0.07	0.30	0.28	0.00	0.00	49.55	0.00	0.00	0.01	0.00	0.00
Forest land (FO)	2.19	13.42	1.81	28.88	0.75	31.12	8.89	481.30	0.26	1.64	0.00	34.44
Waterbody (WA)	0.22	2.10	1.35	0.74	0.00	0.02	0.12	0.00	52.54	0.00	0.33	0.03
Rangeland (RA)	0.01	5.91	0.16	1.17	0.00	0.00	0.51	0.00	0.00	64.35	0.00	0.00
Marsh and swamp (MA)	0.17	18.50	0.97	0.07	0.00	0.00	0.74	0.00	0.00	0.00	12.96	0.00
Unused land (UL)	0.23	1.08	0.04	0.13	0.00	0.00	0.05	0.00	0.00	0.00	0.00	32.80

(Row labels grouped under: LULC in 2010 (Area in km^2))

Table 5.12 Annual land requirement of LULC prediction between 2010 and 2019 for each LULC type.

Year	LULC type (Area in km^2)												Total
	UR	PA	SU	CA	FC	PR	PO	FO	WA	RA	MA	UL	
2010	53.21	2,070.71	153.52	629.33	5.19	30.05	50.21	604.70	57.46	72.11	33.40	34.33	3,794.22
2011	54.58	2,064.15	170.56	613.86	5.32	37.51	54.49	591.02	57.00	72.09	32.75	40.88	3,794.22
2012	55.99	2,057.68	187.61	598.35	5.43	44.93	58.80	577.30	56.54	72.03	32.13	47.42	3,794.22
2013	57.46	2,051.17	204.62	582.86	5.53	52.39	63.17	563.53	56.06	71.98	31.48	53.98	3,794.22
2014	58.81	2,044.70	221.65	567.39	5.65	59.83	67.42	549.87	55.61	71.85	30.90	60.55	3,794.22
2015	60.27	2,038.20	238.68	551.89	5.74	67.26	71.78	536.14	55.15	71.81	30.21	67.07	3,794.22
2016	61.65	2,031.64	255.75	536.39	5.87	74.71	76.06	522.43	54.70	71.81	29.59	73.61	3,794.22
2017	63.06	2,025.15	272.80	520.90	5.97	82.14	80.37	508.74	54.25	71.71	28.95	80.18	3,794.22
2018	64.41	2,018.69	289.83	505.42	6.08	89.59	84.63	495.02	53.76	71.71	28.33	86.75	3,794.22
2019	65.84	2,012.16	306.85	489.91	6.19	97.03	88.95	481.30	53.30	71.65	27.73	93.32	3,794.22
Annual rate	1.40	-6.51	17.04	-15.49	0.11	7.44	4.30	-13.71	-0.46	-0.05	-0.63	6.55	

As a result, the increasing LULC types are urban and built-up area, sugarcane, other field crops, para rubber, perennial trees and orchard, and unused land, with an increasing annual change rate of 1.40, 17.04, 0.11, 7.44, 4.30, and 6.55 km^2 per year,

respectively. In contrast, decreasing LULC types are paddy field, cassava, forest land, waterbody, rangeland, and marsh and swamp, decreasing the annual change rate of 6.51, 15.49, 13.71, 0.46, 0.05, and 0.63 km^2 per year, respectively. In principle, land requirement dictates the final area of each LULC type in each predicted year under the CLUE-S model. The spatial distribution of the predicted LULC between 2011 and 2018 is displayed in Figure 5.4. Meanwhile, the area and percentage of LULC type between 2011 and 2018 are summarized in Tables 5.13 and 5.14, respectively.

Predicted LULC 2011

Predicted LULC 2012

Predicted LULC 2013

Predicted LULC 2014
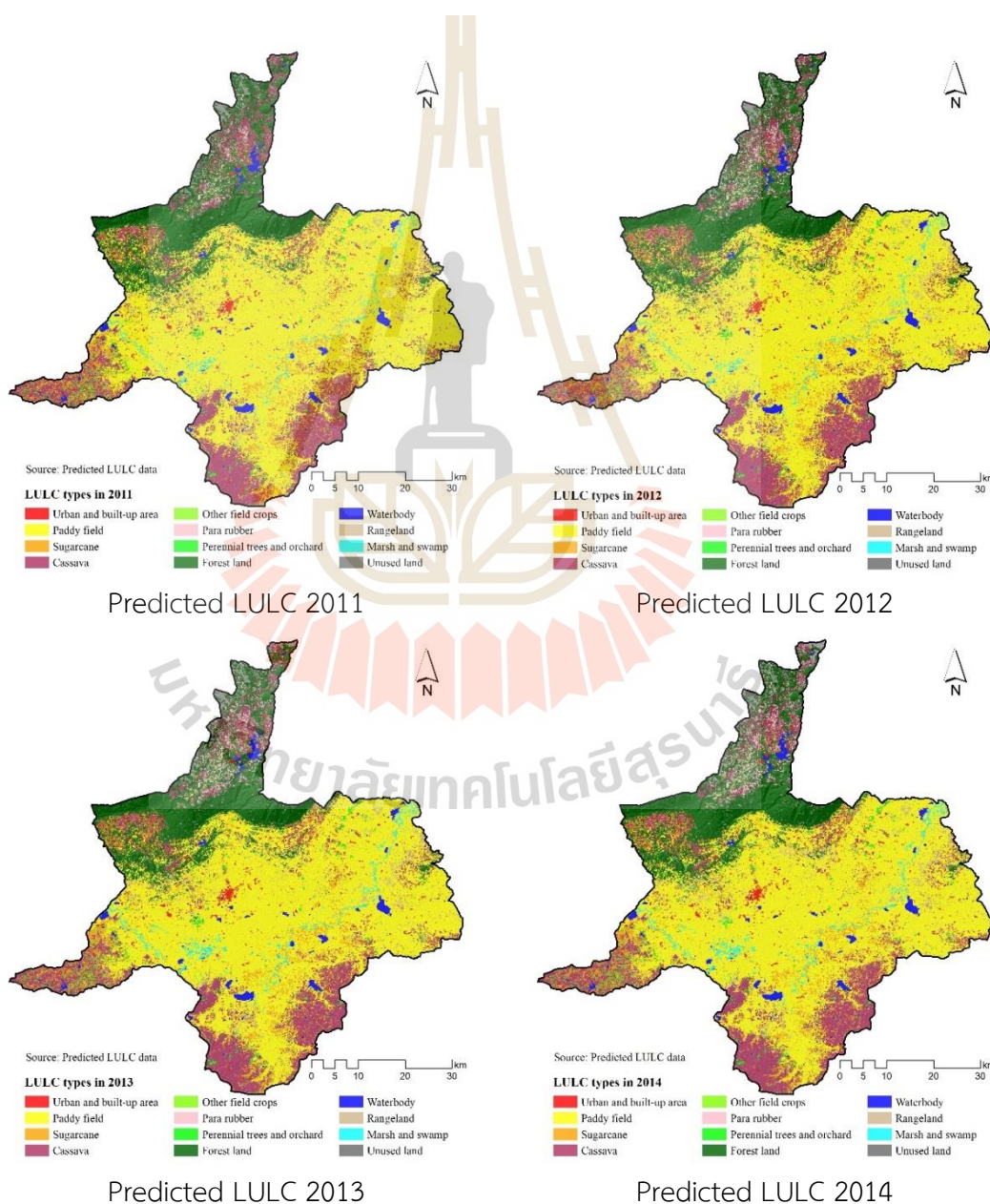
Figure 5.4 Spatial distribution of predicted LULC data between 2011 and 2018.

Source: Predicted LULC data

LULC types in 2015

⬛	Urban and built-up area	⬛	Other field crops	⬛	Waterbody
⬛	Paddy field	⬛	Para rubber	⬛	Rangeland
⬛	Sugarcane	⬛	Perennial trees and orchard	⬛	Marsh and swamp
⬛	Cassava	⬛	Forest land	⬛	Unused land

Predicted LULC 2015

Source: Predicted LULC data

LULC types in 2016

⬛	Urban and built-up area	⬛	Other field crops	⬛	Waterbody
⬛	Paddy field	⬛	Para rubber	⬛	Rangeland
⬛	Sugarcane	⬛	Perennial trees and orchard	⬛	Marsh and swamp
⬛	Cassava	⬛	Forest land	⬛	Unused land

Predicted LULC 2016

Source: Predicted LULC data

LULC types in 2017

⬛	Urban and built-up area	⬛	Other field crops	⬛	Waterbody
⬛	Paddy field	⬛	Para rubber	⬛	Rangeland
⬛	Sugarcane	⬛	Perennial trees and orchard	⬛	Marsh and swamp
⬛	Cassava	⬛	Forest land	⬛	Unused land

Predicted LULC 2017

Source: Predicted LULC data

LULC types in 2018

⬛	Urban and built-up area	⬛	Other field crops	⬛	Waterbody
⬛	Paddy field	⬛	Para rubber	⬛	Rangeland
⬛	Sugarcane	⬛	Perennial trees and orchard	⬛	Marsh and swamp
⬛	Cassava	⬛	Forest land	⬛	Unused land

Predicted LULC 2018

Figure 5.4 (Continued)

Table 5.13 Area of predicted LULC type between 2011 and 2018.

LULC types	Area of predicted LULC type in km²							
	2011	2012	2013	2014	2015	2016	2017	2018
Urban and built-up area (UR)	54.58	55.99	57.46	58.81	60.27	61.65	63.06	64.41
Paddy field (PD)	2,064.15	2,057.68	2,051.17	2,044.70	2,038.20	2,031.64	2,025.15	2,018.69
Sugarcane (SU)	170.56	187.61	204.62	221.65	238.68	255.75	272.80	289.83
Cassava (CA)	613.86	598.35	582.86	567.39	551.89	536.39	520.90	505.42
Other field crops (FC)	5.32	5.43	5.53	5.65	5.74	5.87	5.97	6.08
Para rubber (PR)	37.51	44.93	52.39	59.83	67.26	74.71	82.14	89.59
Perennial trees and orchard (PO)	54.49	58.80	63.17	67.42	71.78	76.06	80.37	84.63
Forest land (FO)	591.02	577.30	563.53	549.87	536.14	522.43	508.74	495.02
Waterbody (WA)	57.00	56.54	56.06	55.61	55.15	54.70	54.25	53.76
Rangeland (RA)	72.09	72.03	71.98	71.85	71.81	71.81	71.71	71.71
Marsh and swamp (MA)	32.75	32.13	31.48	30.90	30.21	29.59	28.95	28.33
Unused land (UL)	40.88	47.42	53.98	60.55	67.07	73.61	80.18	86.75
Total	3,794.22	3,794.22	3,794.22	3,794.22	3,794.22	3,794.22	3,794.22	3,794.22

Table 5.14 Percentage of predicted LULC type between 2011 and 2018.

LULC types	Percentage of predicted LULC type							
	2011	2012	2013	2014	2015	2016	2017	2018
Urban and built-up area (UR)	1.44	1.48	1.51	1.55	1.59	1.62	1.66	1.70
Paddy field (PD)	54.40	54.23	54.06	53.89	53.72	53.55	53.37	53.20
Sugarcane (SU)	4.50	4.94	5.39	5.84	6.29	6.74	7.19	7.64
Cassava (CA)	16.18	15.77	15.36	14.95	14.55	14.14	13.73	13.32
Other field crops (FC)	0.14	0.14	0.15	0.15	0.15	0.15	0.16	0.16
Para rubber (PR)	0.99	1.18	1.38	1.58	1.77	1.97	2.16	2.36
Perennial trees and orchard (PO)	1.44	1.55	1.66	1.78	1.89	2.00	2.12	2.23
Forest land (FO)	15.58	15.22	14.85	14.49	14.13	13.77	13.41	13.05
Waterbody (WA)	1.50	1.49	1.48	1.47	1.45	1.44	1.43	1.42
Rangeland (RA)	1.90	1.90	1.90	1.89	1.89	1.89	1.89	1.89
Marsh and swamp (MA)	0.86	0.85	0.83	0.81	0.80	0.78	0.76	0.75
Unused land (UL)	1.08	1.25	1.42	1.60	1.77	1.94	2.11	2.29
Total	100.00	100.00	100.00	100.00	100.00	100.00	100.00	100.00

In summary, it can be concluded that the predicted LULC map in two periods (2002-2009 and 2011-2018) using the CLUE-S model can provide realistic results as expected. Thus, the CLUE-S model can be used as an efficient tool to predict LULC based on historical development. In practice, the optimum derived multiple linear equations from the binary logit regression analysis for the LULC allocation, land requirement, and model parameters (elasticity and LULC conversion matrix) are very important for predicting the time-series LULC under the CLUE-S model. The suitable eight driving factors on LULC change in the study area include elevation, slope, annual rainfall, average income per capita at the sub-district level, population density at the sub-district level, distance to road network, distance to stream, and distance to the existing urban area. The LULC prediction applies specific multiple linear equations from the binomial logistic regression analysis, which provide AUC values from 0.61857 (poor fit) to 0.98239 (excellent fit) for specific LULC type allocation. The deviation values between the land use requirement and the predicted area of each LULC type varies from -0.0005% to 0.0005% or -0.05 km^2 (underestimation) to 0.05 km^2 (overestimation). The deviation value depends on iteration driving factors of each LULC type, which indicates the different maximum allowance between the required and allocated area of LULC type under the CLUE-S model (Liu, Wang, Li, and Xia, 2013; van Asselen and Verburg, 2013; Xu, Li, Song, and Yin, 2013). Therefore, the predicted LULC map in two periods (2002-2009 and 2011-2018) using the CLUE-S model can be validated and accepted for time-series surface runoff estimation in the next chapter. The area and percentage of each LULC type from time-series LULC data between 2001 and 2019 based on RF classification and CLUE-S prediction are presented in Tables 5.15 and 5.16 and Figure 5.5.

Table 5.15 Area of each LULC type from time-series LULC data between 2001 and 2019 based on RF classification and CLUE-S prediction.

LULC type	2001	2002	2003	2004	2005	2006	2007	2008	2009	2010	2011	2012	2013	2014	2015	2016	2017	2018	2019
Urban and built-up area	46.17	46.95	47.71	48.5	49.3	50.05	50.82	51.61	52.41	53.21	54.58	55.99	57.46	58.81	60.27	61.65	63.06	64.41	65.84
Paddy field	2,344.39	2,314.01	2,283.59	2,253.18	2,222.70	2,192.30	2,161.94	2,131.48	2,101.12	2,070.71	2,064.15	2,057.68	2,051.17	2,044.70	2,038.20	2,031.64	2,025.15	2,018.69	2,012.16
Sugarcane	61.25	71.53	81.77	91.96	102.27	112.51	122.76	133.03	143.27	153.52	170.56	187.61	204.62	221.65	238.68	255.75	272.8	289.83	306.85
Cassava	532.95	543.6	554.34	565.05	575.78	586.5	597.16	607.87	618.63	629.33	613.86	598.35	582.86	567.39	551.89	536.39	520.9	505.42	489.91
Other field crops	2.09	2.45	2.79	3.13	3.5	3.83	4.17	4.51	4.87	5.19	5.32	5.43	5.53	5.65	5.74	5.87	5.97	6.08	6.19
Para rubber	16.56	18.03	19.54	21.09	22.54	24.1	25.57	27.08	28.53	30.05	37.51	44.93	52.39	59.83	67.26	74.71	82.14	89.59	97.03
Perennial trees and orchard	55.76	55.15	54.54	53.9	53.27	52.66	52.07	51.47	50.84	50.21	54.49	58.8	63.17	67.42	71.78	76.06	80.37	84.63	88.95
Forest land	632	628.98	625.95	622.9	619.88	616.83	613.81	610.77	607.74	604.7	591.02	577.3	563.53	549.87	536.14	522.43	508.74	495.02	481.3
Waterbody	36.81	39.12	41.4	43.7	46	48.28	50.57	52.86	55.16	57.46	57	56.54	56.06	55.61	55.15	54.7	54.25	53.76	53.3
Rangeland	26.03	31.16	36.28	41.38	46.51	51.63	56.77	61.9	66.99	72.11	72.09	72.03	71.98	71.85	71.81	71.81	71.71	71.71	71.65
Marsh and swamp	11.64	14.03	16.46	18.94	21.3	23.78	26.17	28.6	30.97	33.4	32.75	32.13	31.48	30.9	30.21	29.59	28.95	28.33	27.73
Unused land	28.57	29.19	29.84	30.47	31.16	31.74	32.4	33.03	33.69	34.33	40.88	47.42	53.98	60.55	67.07	73.61	80.18	86.75	93.32
Total	3,794.22	3,794.22	3,794.22	3,794.22	3,794.22	3,794.22	3,794.22	3,794.22	3,794.22	3,794.22	3,794.22	3,794.22	3,794.22	3,794.22	3,794.22	3,794.22	3,794.22	3,794.22	3794.22

Note: LULC data in 2001, 2010, and 2019 are classified by RF classifier, while LULC data in 2002, 2003, 2004,2005,2006, 2007, 2008, 2009, 2011, 2012, 2013, 2014, 2015, 2016, 2017 and 2018 are predicted by CLUE-S model.

Table 5.16 Percentage of each LULC type from time-series LULC data between 2001 and 2019 based on RF classification and CLUE-S prediction.

LULC type	2001	2002	2003	2004	2005	2006	2007	2008	2009	2010	2011	2012	2013	2014	2015	2016	2017	2018	2019
Urban and built-up area	1.22	1.24	1.26	1.28	1.30	1.32	1.34	1.36	1.38	1.40	1.44	1.48	1.51	1.55	1.59	1.62	1.66	1.70	1.74
Paddy field	61.79	61.00	60.20	59.40	58.60	57.80	57.00	56.20	55.40	54.58	54.40	54.20	54.10	53.90	53.70	53.60	53.40	53.20	53.03
Sugarcane	1.61	1.89	2.16	2.42	2.70	2.97	3.24	3.51	3.78	4.05	4.50	4.94	5.39	5.84	6.29	6.74	7.19	7.64	8.09
Cassava	14.05	14.30	14.60	14.90	15.20	15.50	15.70	16.00	16.30	16.59	16.20	15.80	15.40	15.00	14.60	14.10	13.70	13.30	12.91
Other field crops	0.06	0.06	0.07	0.08	0.09	0.10	0.11	0.12	0.13	0.14	0.14	0.14	0.15	0.15	0.15	0.15	0.16	0.16	0.16
Para rubber	0.44	0.48	0.51	0.56	0.59	0.64	0.67	0.71	0.75	0.79	0.99	1.18	1.38	1.58	1.77	1.97	2.16	2.36	2.56
Perennial trees and orchard	1.47	1.45	1.44	1.42	1.40	1.39	1.37	1.36	1.34	1.32	1.44	1.55	1.66	1.78	1.89	2.00	2.12	2.23	2.34
Forest land	16.66	16.60	16.50	16.40	16.30	16.30	16.20	16.10	16.00	15.94	15.60	15.20	14.90	14.50	14.10	13.80	13.40	13.10	12.68
Waterbody	0.97	1.03	1.09	1.15	1.21	1.27	1.33	1.39	1.45	1.51	1.50	1.49	1.48	1.47	1.45	1.44	1.43	1.42	1.40
Rangeland	0.69	0.82	0.96	1.09	1.23	1.36	1.50	1.63	1.77	1.90	1.90	1.90	1.90	1.89	1.89	1.89	1.89	1.89	1.89
Marsh and swamp	0.31	0.37	0.43	0.50	0.56	0.63	0.69	0.75	0.82	0.88	0.86	0.85	0.83	0.81	0.80	0.78	0.76	0.75	0.73
Unused land	0.75	0.77	0.79	0.80	0.82	0.84	0.85	0.87	0.89	0.90	1.08	1.25	1.42	1.60	1.77	1.94	2.11	2.29	2.46
Total	100	100	100	100	100	100	100	100	100	100	100	100	100	100	100	100	100	100	100

Note: LULC data in 2001, 2010, and 2019 are classified by RF classifier, while LULC data in 2002, 2003, 2004,2005,2006, 2007, 2008, 2009, 2011, 2012, 2013, 2014, 2015, 2016, 2017 and 2018 are predicted by CLUE-S model.
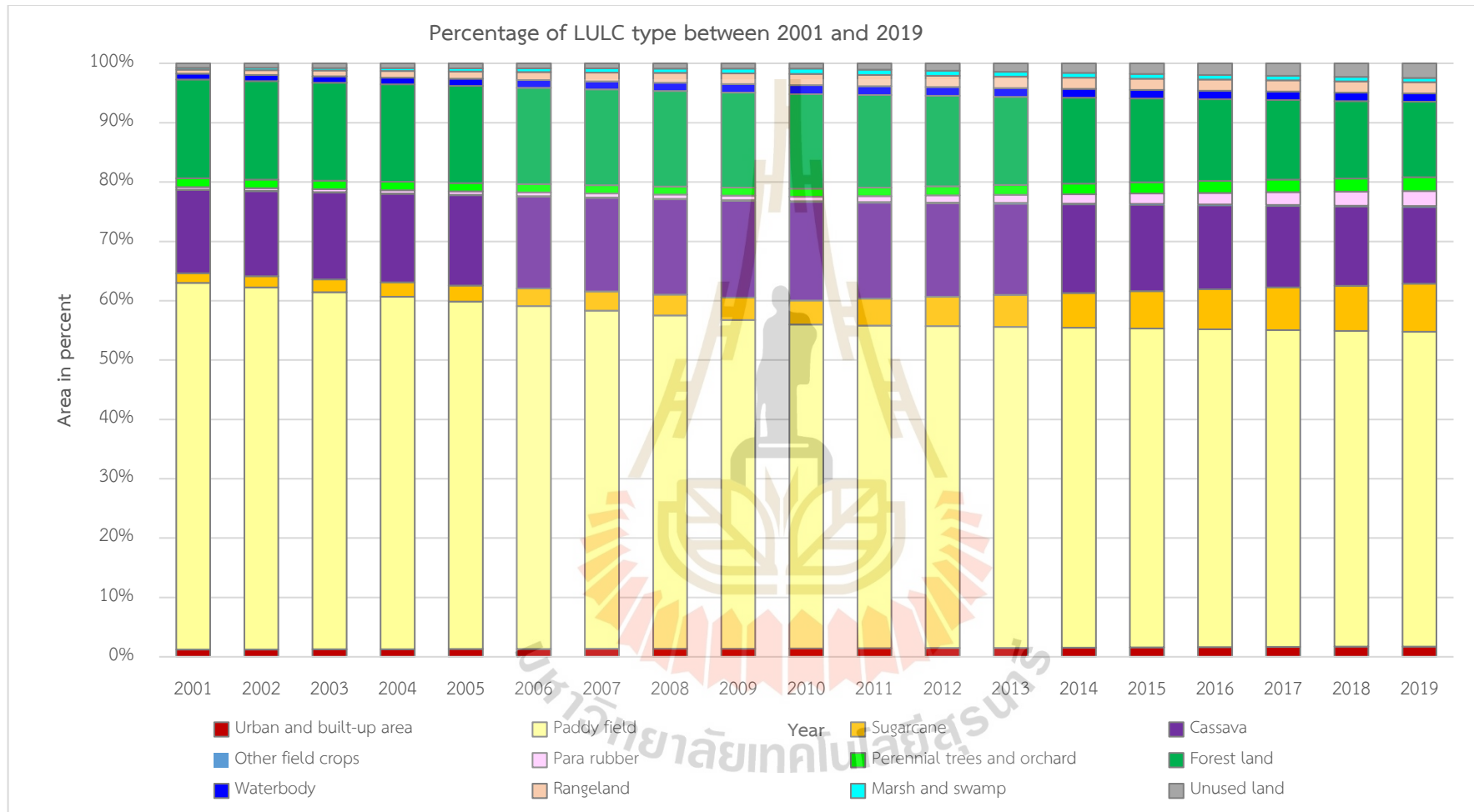
Figure 5.5 Contribution of LULC type of time-series LULC data between 2001 and 2019.

CHAPTER VI

TIME-SERIES SURFACE RUNOFF ESTIMATION USING SCS-CN METHOD

This chapter presents the third objective results focusing on estimating time-series surface runoff between 2001 and 2019 based on the classified and predicted LULC data, annual rainfall data, and soil series data using the SCS-CN method. The significant results in this chapter consist of (1) basic information of input data for surface runoff estimation, (2) surface runoff estimation between 2001 and 2010, (3) surface runoff estimation between 2011 and 2019, and (4) contribution of time-series LULC data on surface runoff are here described and discussed in detail.

6.1   Basic information of input data for surface runoff estimation

The required input data for surface runoff estimation using the SCS-CN method include LULC, soil series, rainfall, and hydrologic soil group (HSG) data prepared in raster format with a cell size of 30 meters under raster-based GIS operation. Basic information and its distribution of input data for surface runoff estimation are separately described in the following sections.

6.1.1   LULC data

For surface runoff estimation, time-series LULC data between 2001 and 2019 were classified and predicted LULC data. The classified LULC data are the LULC data in 2001, 2010, and 2019, which were classified from remotely sensed data using the Random Forest classifier, as reported in the details in Chapter IV: LAND USE AND LAND COVER CLASSIFICATION AND CHANGE DETECTION. Meanwhile, the predicted LULC data are LULC data from 2002 to 2009 and 2011 to 2018, which predicted based on the actual LULC data in 2001, 2010, and 2019 by the CLUE-S model, as described in the details in Chapter V: SIMULATION OF TIME-SERIES OF LAND USE AND LAND COVER DATA BY CLUE-S MODEL. The spatial distribution of LULC data between 2001 and 2019 is displayed in Figure 4.8, Figure 5.3, Figure 4.13, Figure 5.4, and Figure 4.17. Additionally,

areas and percentage of each LULC type from time-series LULC data between 2001 and 2019 based on the RF classification and CLUE-S prediction are summarized in Tables 5.15 and 5.16.

6.1.2   Soil series data

Recent soil series data obtained from LDD consist of thirty-two soil series types with texture attributes, as shown in Figure 6.1. Based on the reconnaissance soil survey at the scale of 100,000, thirty-two soil series types can be grouped by soil texture property into nine soil groups: clay, clay loam, loam, loamy sand, sandy loam, sandy clay loam, silty clay, silty loam, and silty clay loam (Table 6.1).

Table 6.1 Area and percentage of soil groups in the study area.

Soil series	Area in km^2	Area in percent
Alluvial Complex (AC)	184.62	4.87
Ban Phai Series (Bpi)	0.35	0.01
Bo Thai Series (Bo)	0.70	0.02
Borabu series (Bb)	158.42	4.18
Chaiyaphum Series	2.05	0.05
Chatturat Series (Ct)	124.16	3.27
Chiang Mai Series (Cm)	25.21	0.66
Chum Phuang Series (Cpg)	1.77	0.05
Korat series (Kt)	597.21	15.74
Kula Ronghai Series (Ki)	31.41	0.83
Mae Rim Series (Mr)	3.05	0.08
Nakhon Phanom Series (Nn)	2.83	0.07
Nam Phong Series (Ng)	207.24	5.46
Phu Phan (Pu)	103.23	2.72
Phimai Series (Pm)	27.70	0.73
Phon Phisai Series (Pp)	33.52	0.88
Ratdhaburi Series (Rb)	252.91	6.67
Roi-et Series (Re)	791.82	20.87

Table 6.1 (Continued).

Soil series	Area in km^2	Area in percent
Sapphaya Series (Sa)	1.81	0.05
Satuk Series (Suk)	52.67	1.39
Si Khiu Series (Si)	14.39	0.38
Si Song Khram Series (Ss)	42.98	1.13
Si Thon Series (St)	3.67	0.10
Slope Complex (SC)	524.06	13.81
Sung Noen Series (Sn)	6.87	0.18
Takhli Series (Tk)	1.40	0.04
Tha Li Series (Tl)	0.96	0.03
Tha Muang Series (Tm)	4.66	0.12
That Phanom Series (Tp)	1.24	0.03
Ubon Series (Ub)	3.84	0.10
Warin Series (Wn)	531.18	14.00
Waterbody (Wa)	33.68	0.89
Yasothon Series (Yt)	22.61	0.60
SUM	3,794.22	100.00

Figure 6.1 Spatial distribution of soil series type.

6.1.3 Rainfall data

In this study, the Thai Meteorological Department (TMD) provided annual rainfall data between 2001 and 2019 with twelve rain gauge stations located within and nearby the watershed (Table 6.2). The location of meteorological stations is displayed in Figure 6.2. The continuous surface of the annual rainfall surface data was interpolated using the IDW method instead of assuming a constant annual rainfall over the entire watershed. It creates a grid of spatially distributed values extracted from the attribute table of rain gauge points with a cell size of 30 meters.

Table 6.2 Basic information of rainfall station for annual rainfall interpolation.

Station name	Station code	Location	
		Easting	Northing
Loei	353201	790332.52	1931415.21
Loei Agromet	353301	790411.68	1925878.53
Phetchabun	379201	725962.82	1732117.41
Wichian Buri	379402	729594.70	1816243.52
Khon Kaen	381201	263695.74	1821481.81
Tha Phra Agromet	381301	266745.10	1807057.70
Chaiyaphum	403201	182156.06	1749054.65
Lop Buri	426201	673984.44	1636832.43
Bua Chum	426201	735378.87	1688699.21
Nakhon Ratchasima	431201	185546.48	1656281.57
Pak Chong Agromet	431301	749975.08	1620219.57
Chok Chai	431401	195101.71	1629149.48
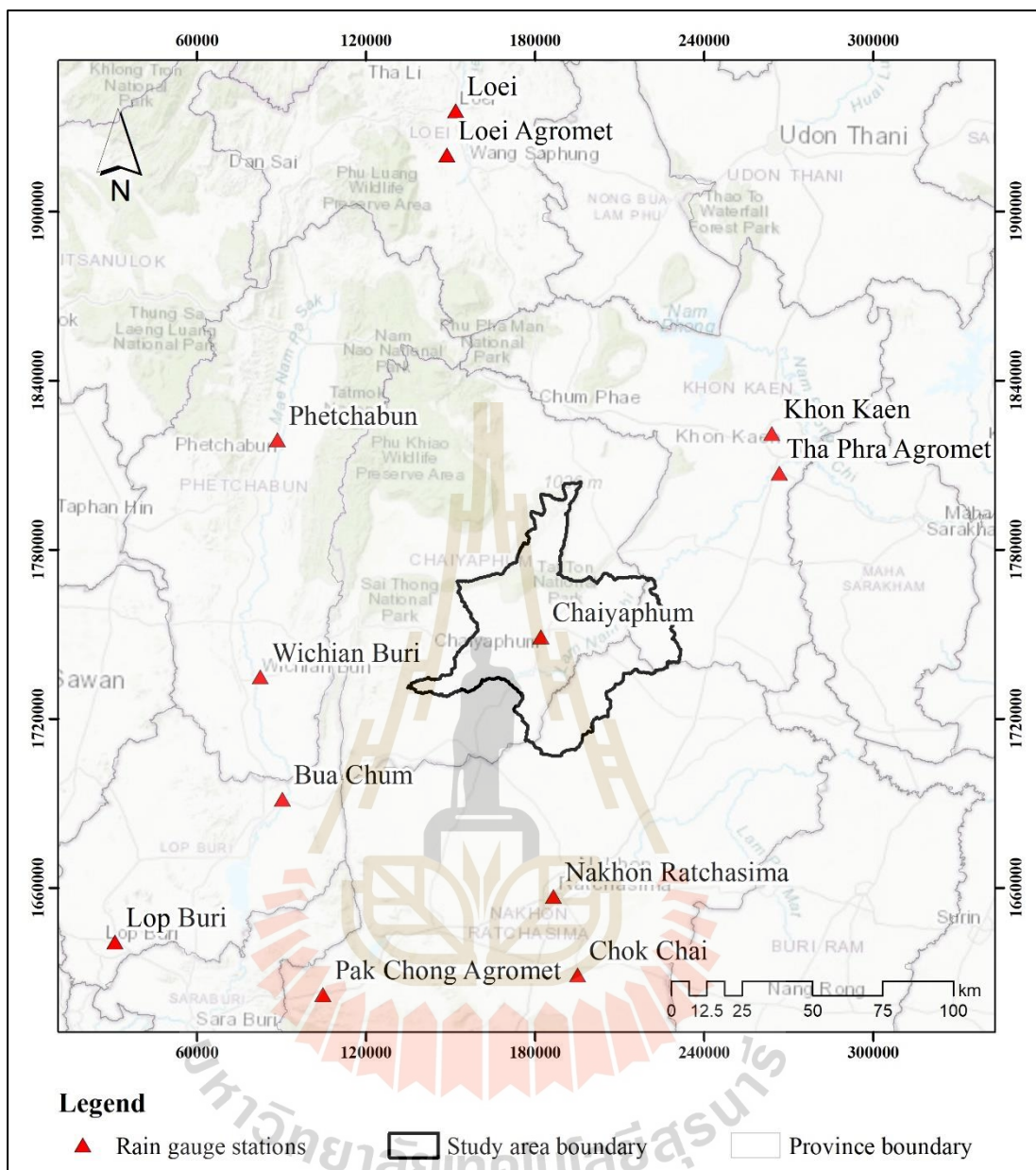
Figure 6.2 Location of meteorological stations for rainfall data interpolation.

The spatial distribution of annual interpolated rainfall data between 2001 and 2010, which were used to examine and validate a suitable AMC condition for surface runoff estimation, is displayed in Figure 6.3. The primary statistical data of the interpolated rainfall data from 2001 to 2010 are presented in Table 6.3.

Meanwhile, annual interpolated rainfall data between 2011 and 2019, which were applied to estimate surface runoff with the suitable AMC, is shown in Figure

6.4. The primary statistical data of the interpolated rainfall data from 2011 to 2019 are presented in Table 6.4.
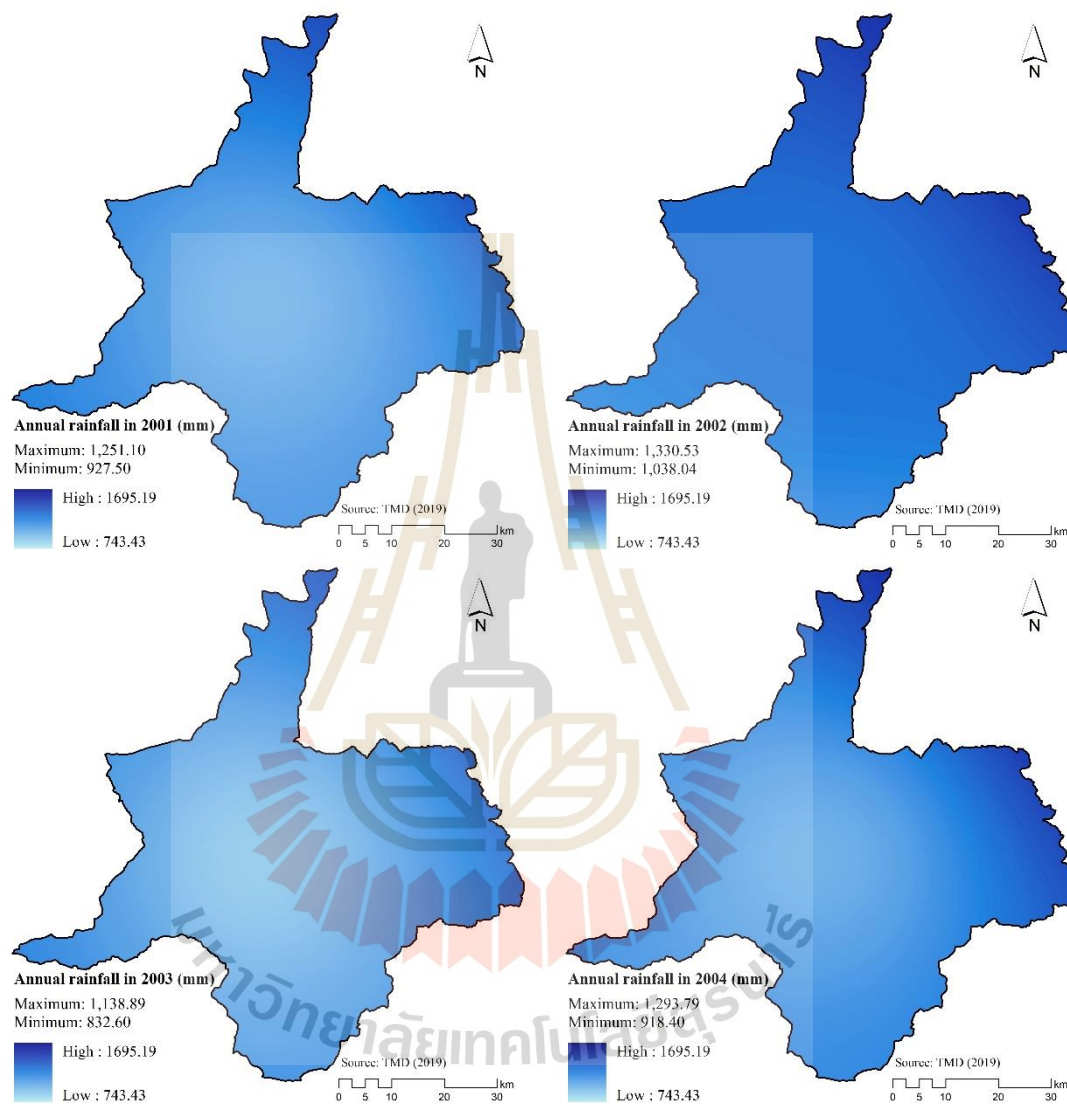
Figure 6.3 Spatial distribution of annual interpolated rainfall data between 2001 and 2010.
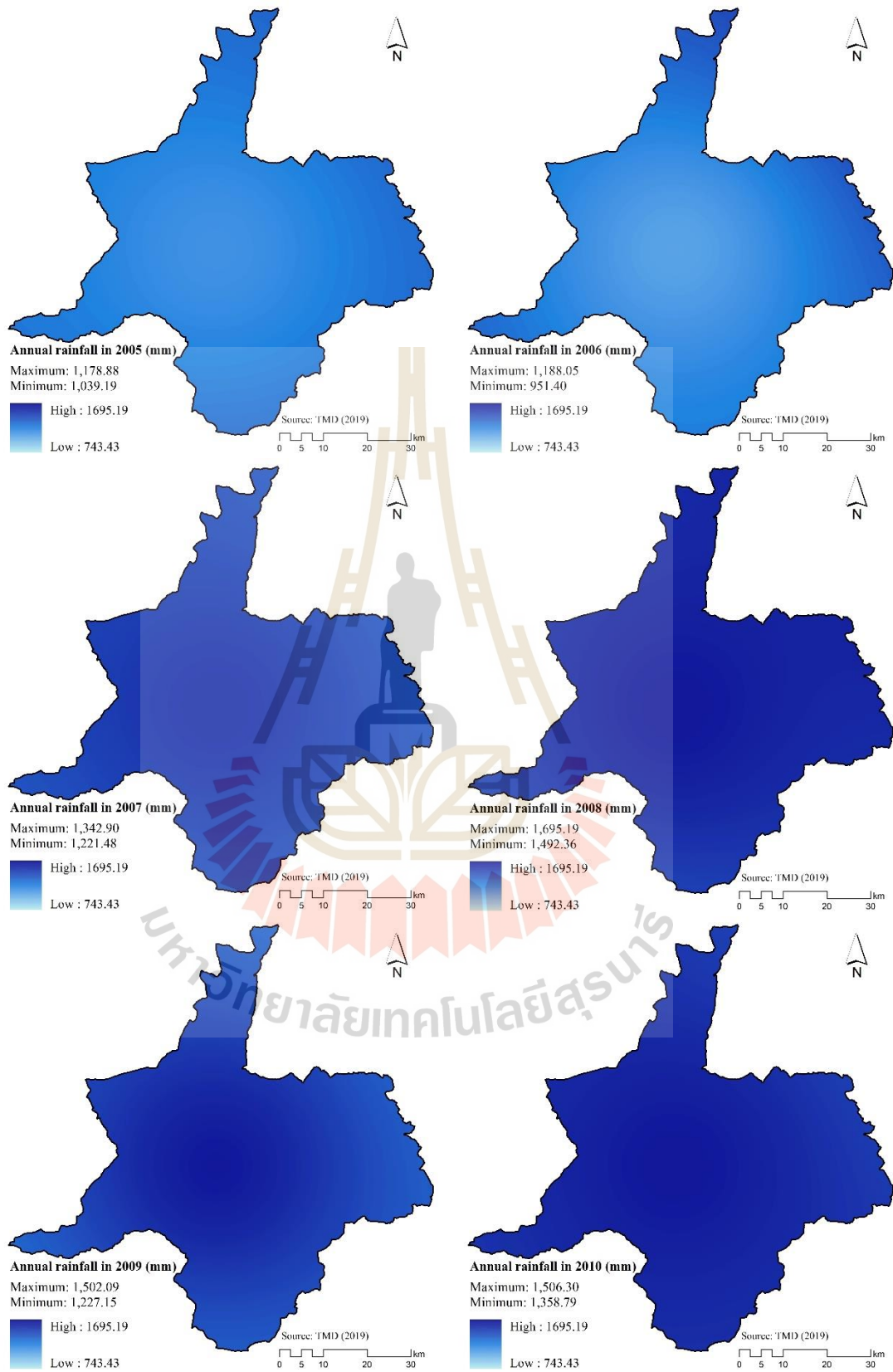
Figure 6.3 (Continued).
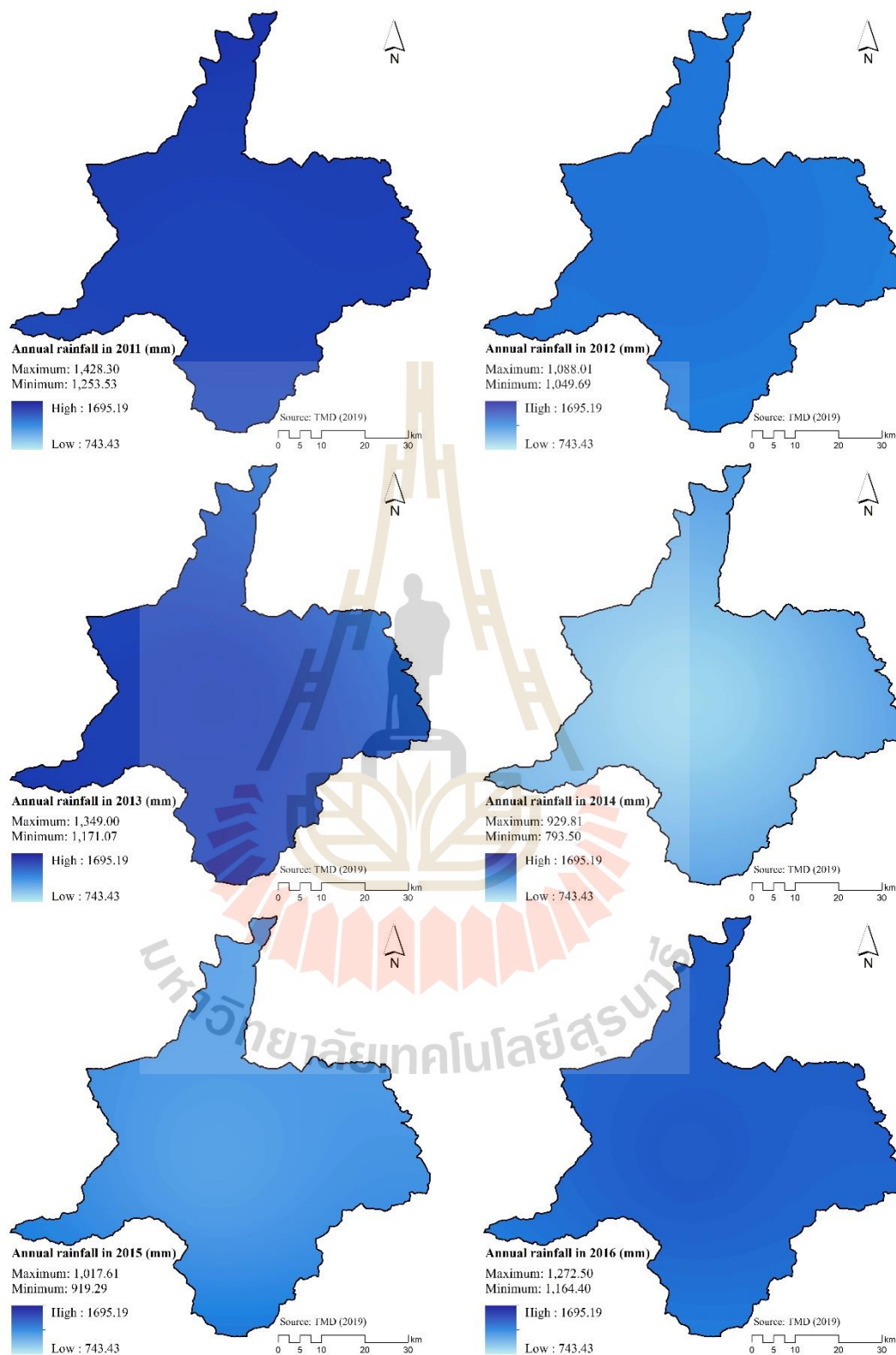
Figure 6.4 Spatial distribution of annual interpolated rainfall data between 2011 and 2019.
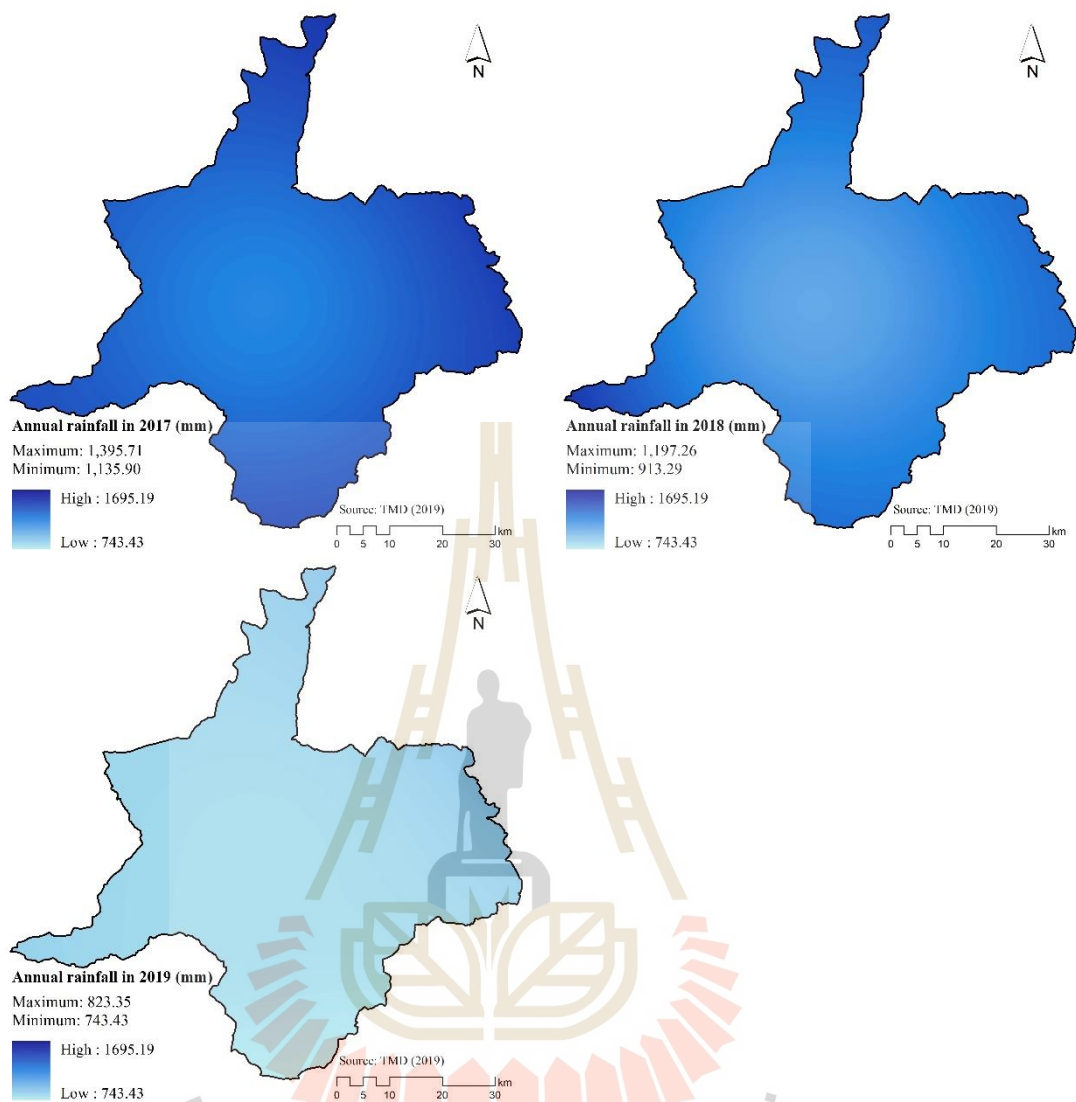
Figure 6.4 (Continued).

Table 6.3 Basic statistical data of annual interpolated rainfall data between 2001 and 2010 for suitable AMC identification and validation.

Year	Minimum	Maximum	Mean	Standard deviation
2001	927.50	1,251.10	1,025.52	65.71
2002	1,038.04	1,330.53	1,155.79	47.19
2003	832.60	1,138.89	928.08	63.17
2004	918.40	1,293.79	1,023.05	77.71
2005	1,039.19	1,178.88	1,093.19	32.56
2006	951.40	1,188.05	1,028.21	48.74
2007	1,221.48	1,342.90	1,291.01	30.63
2008	1,492.36	1,695.19	1,639.37	36.50
2009	1,227.15	1,502.09	1,391.12	64.17
2010	1,358.79	1,506.30	1,456.08	31.85
Average	**1,100.69**	**1,342.77**	**1,203.14**	**49.82**

Table 6.4 Basic statistical data of annual interpolated rainfall data between 2011 and 2019 for surface runoff estimation with suitable AMC.

Year	Minimum	Maximum	Mean	Standard deviation
2011	1,253.53	1,428.30	1,377.00	9.25
2012	1,049.69	1,088.01	1,075.88	8.08
2013	1,171.07	1,349.00	1,296.83	36.01
2014	793.5	929.81	845.45	30.82
2015	619.29	1,017.61	943.52	18.39
2016	1,164.40	1,272.50	1,245.55	21.68
2017	1,135.90	1,395.71	1,234.51	59.75
2018	913.29	1,197.26	995.81	47.45
2019	743.44	823.35	782.12	12.29
Average	**982.68**	**1,166.84**	**1,088.52**	**27.08**

As a result, in Figure 6.3 and Table 6.3, annual interpolated rainfall data patterns from 2001 to 2010 are similar, except in 2007, 2008, 2009, and 2010. The mean annual interpolated rainfall data between 2007 and 2010 are higher than the average mean annual interpolated rainfall data (Figure 6.5). Meanwhile, patterns of annual interpolated rainfall data from 2011 to 2019 are different according to Figure 6.4 and Table 6.4. The mean annual interpolated rainfall data in 2011, 2012, 2013, 2016, and 2017 are higher than the average of mean annual interpolated rainfall data (Figure 6.6). Patterns of annual interpolated rainfall data play an essential role in annual surface runoff estimation using the SCS-CN method since this method is distributed surface runoff model. (See Figure 3.6).
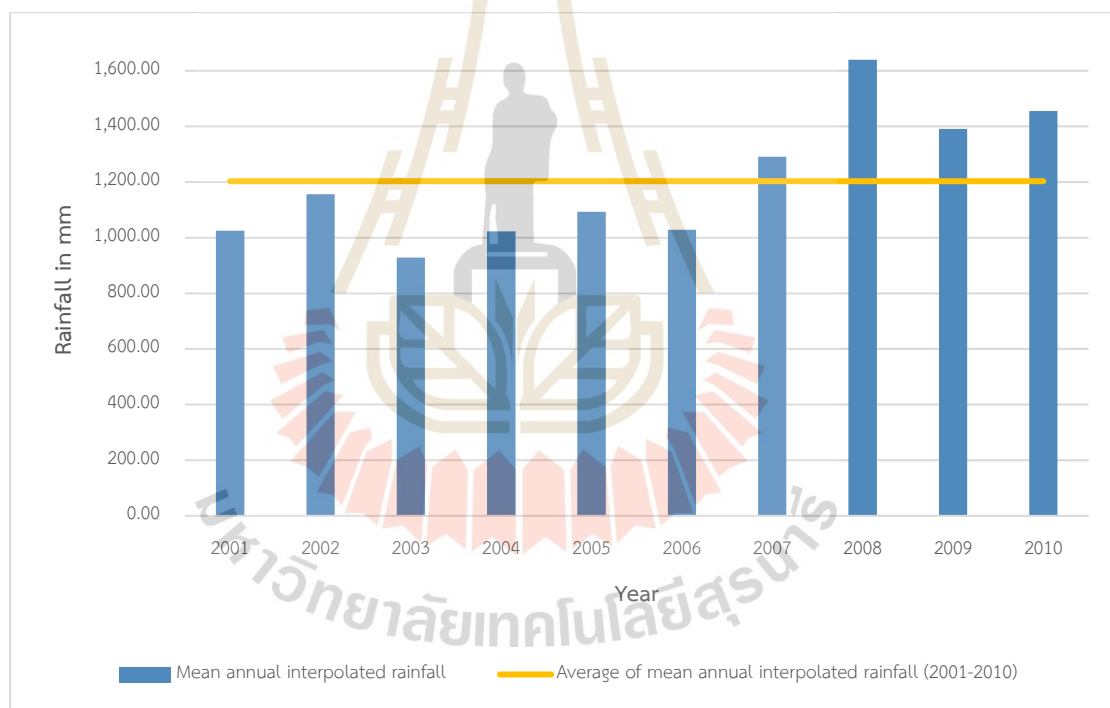
Figure 6.5 Mean annual and average mean annual interpolated rainfall between 2001 and 2010.
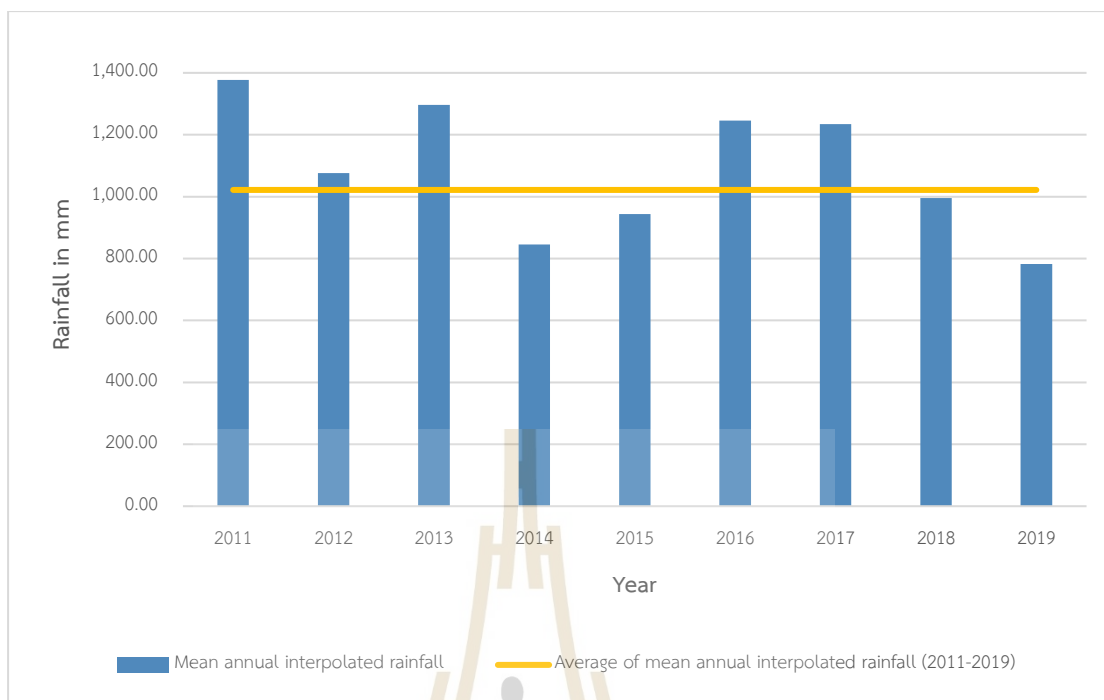
Figure 6.6 Mean annual and average mean annual interpolated rainfall between 2011 and 2019.

6.1.4 Hydrologic soil group (HSG) data

Soil series data were used to classify soil texture classes based on the percentage of sand, silt, and clay, resulting in Table 6.5. The spatial distribution of the soil texture class is presented in Figure 6.7. The soil texture class was further applied to assign potential runoff group as hydrologic soil group (HSG) into four groups (A, B, C, and D) based on the suggested criteria of the National Resources Conservation Service (National Resources Conservation Service, 2009), as a summary in Table 6.6.

In general, the HSG data account for soils' infiltration characteristics. They are further combined with LULC data as hydrologic soil group-land cover complex to indicate a specific runoff potential as the Curve Number (CN) according to the watershed's antecedent moisture condition (AMC). See Tables 3.4 to 3.6 in Chapter III: RESEARCH PROCEDURES.

In this study, a suitable AMC condition is first examined and validated for time-series surface runoff estimation between 2001 and 2010. Then the suitable

AMC condition is further chosen to estimate time-series surface runoff between 2011 and 2019.

Table 6.5 Soil series properties for hydrologic soil group determination.

Soil series	Particle size analysis LDD (2004)			Soil texture class	HSG
	%sand	%silt	%clay		
Alluvial Complex (AC)	5.6	40.6	53.8	Silty clay	C
Ban Phai Series (Bpi)	87.5	8.0	4.5	Loamy sand	B
Bo Thai Series (Bo)	76.8	17.1	6.1	Loamy sand	B
Borabu series (Bb)	86.0	11.5	2.5	Loamy sand	B
Chaiyaphum Series	31.7	46.0	22.3	Clay loam	C
Chatturat Series (Ct)	11.1	34.4	55.5	Silty clay	C
Chiang Mai Series (Cm)	70.1	22.2	9.7	Sandy loam	B
Chum Phuang Series (Cpg)	78.8	14.7	6.5	Loamy sand	B
Korat series (Kt)	68.0	24.0	8.0	Sandy loam	B
Kula Ronghai Series (Ki)	57.5	28.4	14.1	Sandy loam	B
Mae Rim Series (Mr)	69.5	16.0	14.5	Sandy loam	B
Nakhon Phanom Series (Nn)	5.1	58.8	36.1	Silty clay	C
Nam Phong Series (Ng)	87.0	11.0	2.0	Sandy loam	B
Phu Phan Series (Pu)	40.8	43.3	15.9	Loam	C
Phimai Series (Pm)	14.0	38.2	47.9	Clay	D
Phon Phisai Series (Pp)	50.0	25.5	24.5	Sandy clay loam	C
Ratdhaburi Series (Rb)	6.0	17.5	76.5	Clay	D
Roi-et Series (Re)	64.5	5.0	30.5	Sandy loam	B
Sapphaya Series (Sa)	16.0	55.0	29.0	Silty clay loam	C
Satuk Series (Suk)	26.0	51.0	23.0	Sandy clay loam	C
Si Khiu Series (Si)	58.0	33.1	8.9	Sandy loam	B
Si Song Khram Series (Ss)	3.6	47.6	48.9	Clay	D
Si Thon Series (St)	75.1	20.6	4.3	Sandy clay loam	C
Slope Complex (SC)	-	-	-	Slope Complex	A

Table 6.5 (Continued).

Soil series	Particle size analysis LDD (2004)			Soil texture class	HSG
	%sand	%silt	%clay		
Sung Noen Series (Sn)	22.5	57.0	20.5	Silty loam	C
Takhli Series (Tk)	21.5	37.5	41.0	Clay	D
Tha Li Series (Tl)	34.3	3.6	22.1	Loam	C
Tha Muang Series (Tm)	43.0	44.8	12.2	Sandy loam	B
That Phanom Series (TP)	34.6	50.6	14.8	Silty loam	C
Ubon Series (Ub)	87.0	10.5	2.5	Loamy sand	B
Warin Series (Wn)	43.0	30.0	27.0	Clay loam	C
Yasothon Series (Yt)	77.1	3.2	19.7	Sandy loam	B

Table 6.6 Criteria for hydrologic soil group determination.

HSG	Runoff potential	Percent of clay and sand	Soil texture
A	low runoff potential	%clay<10 and %sand>90	gravel or sand textures
B	moderately low runoff potential	%clay10-20 and %sand50-90	loamy sand or sandy loam textures
C	moderately high runoff potential	%clay20-40 and %sand<50	loam, silt loam, sandy clay loam, clay loam, and silty clay loam textures
D	high runoff potential	%clay>40 and %sand<50	clayey textures

Source: National Resources Conservation Service (2009).
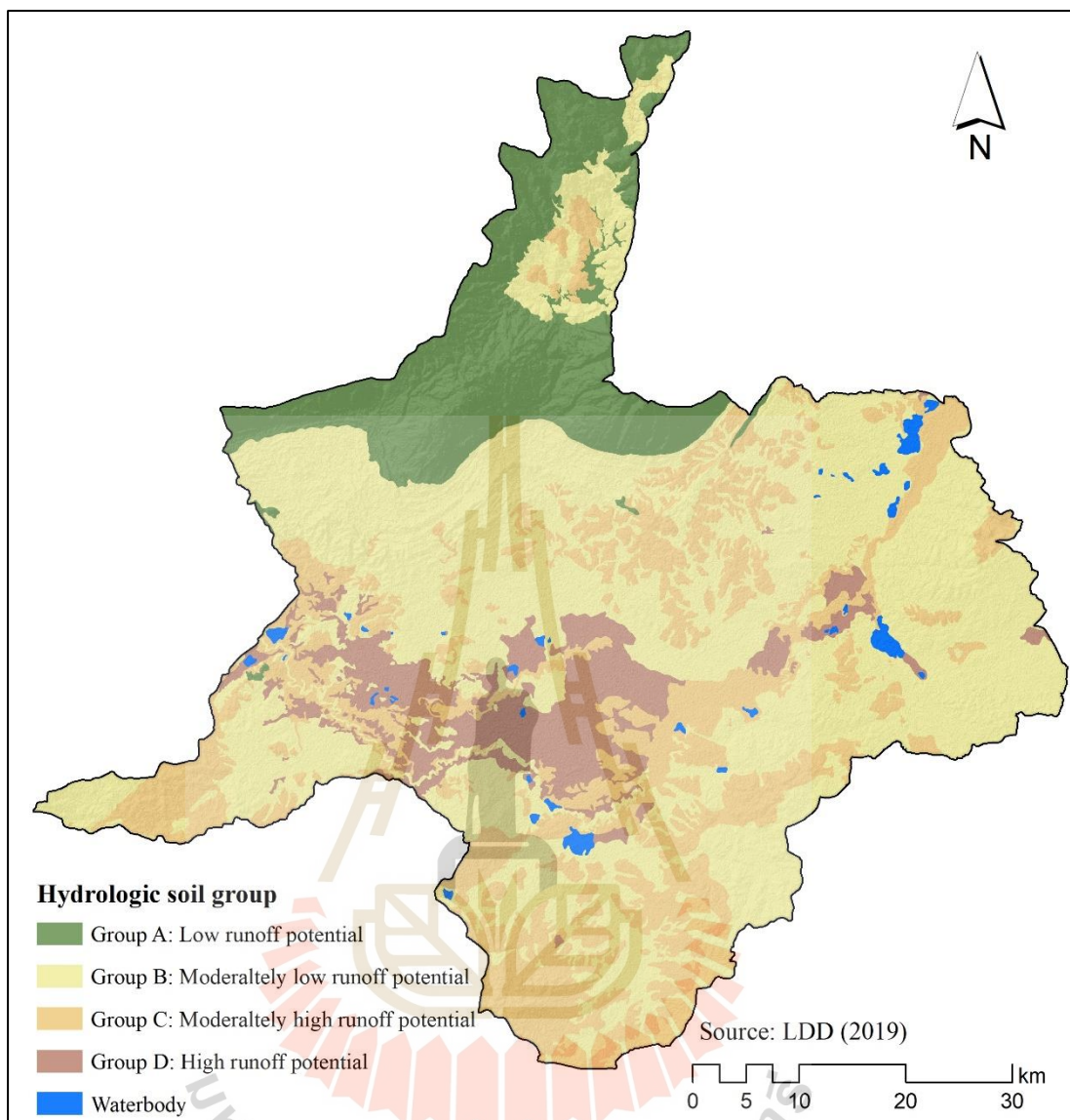
Figure 6.7 Spatial distribution of hydrologic soil group.

6.2 Surface runoff estimation between 2001 and 2010

The digital LULC data between 2001 and 2010, annual rainfall data between 2001 and 2010, and hydrologic soil group were used to estimate surface runoff for suitable AMC identification. In practice, relative surface runoff in each cell was generated based on runoff curve numbers (CN) according to hydrological soil-cover complex using Model Builder of ArcGIS^{TM} as shown in Figure 6.8.

Figure 6.8 Schematic diagram of Model Builder for surface runoff estimation

In this phase, the runoff curve number (CN) values were assigned based on three different AMCs: AMC-I for dry, AMC-II for normal, and AMC-III for wet conditions (Tables 3.4 to 3.6). In principle, the AMC is an indicator of watershed wetness and availability of soil storage. The spatial distribution of CN values between 2001 and 2010 of three different AMC conditions was displayed in Figures 6.9 to 6.11.

Figure 6.9 Spatial distribution of runoff CN values of AMC-I between 2001 and 2010.
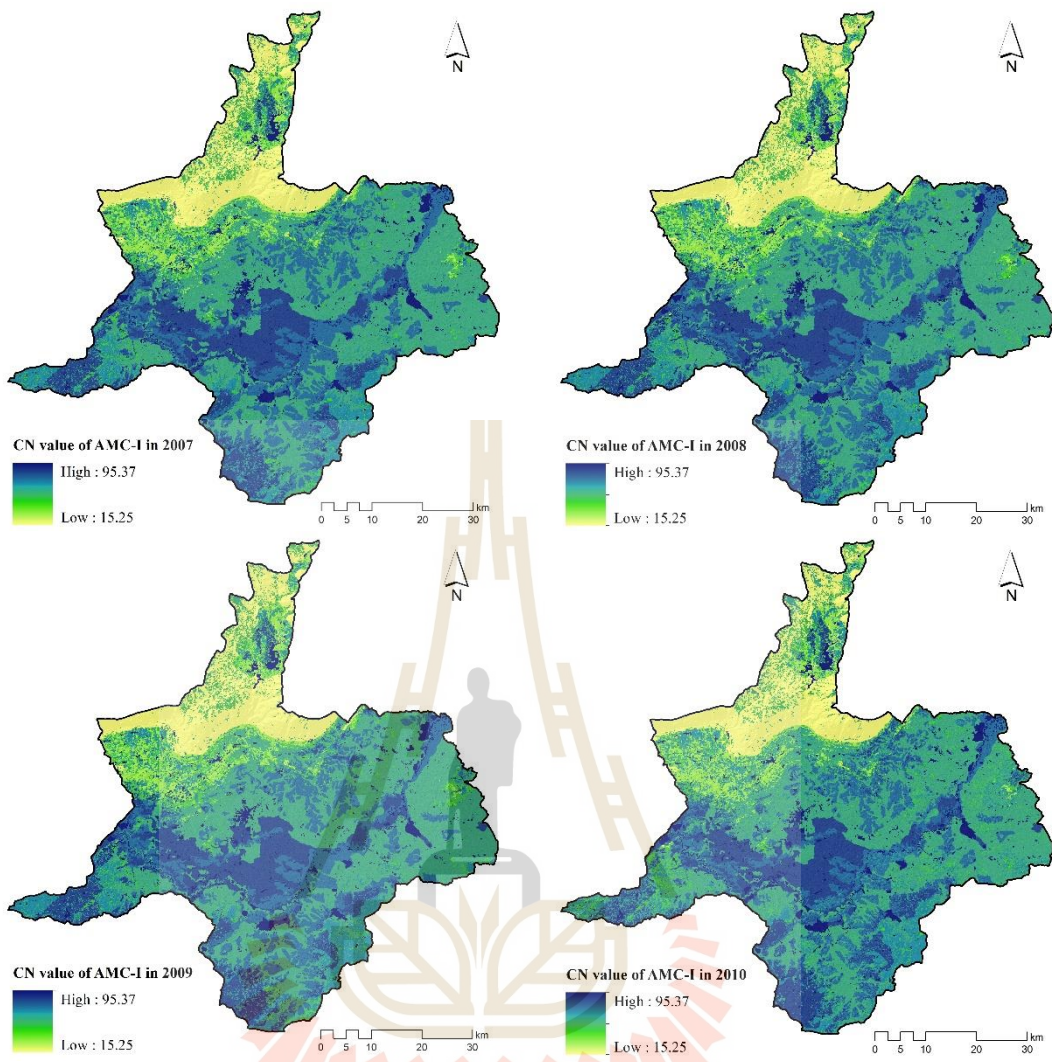
Figure 6.9 Continued.
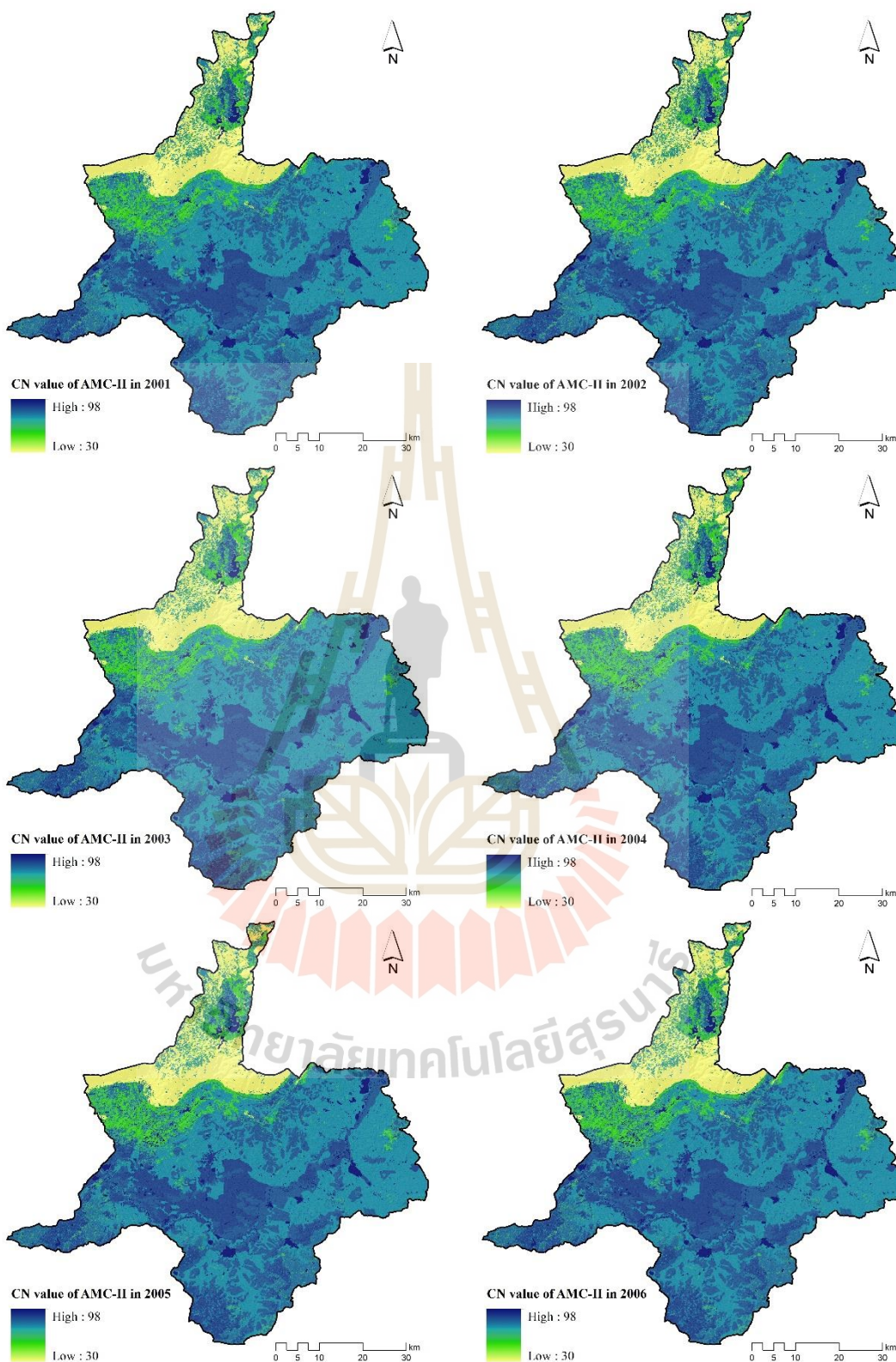
Figure 6.10 Spatial distribution of runoff CN values of AMC-II between 2001 and 2010.
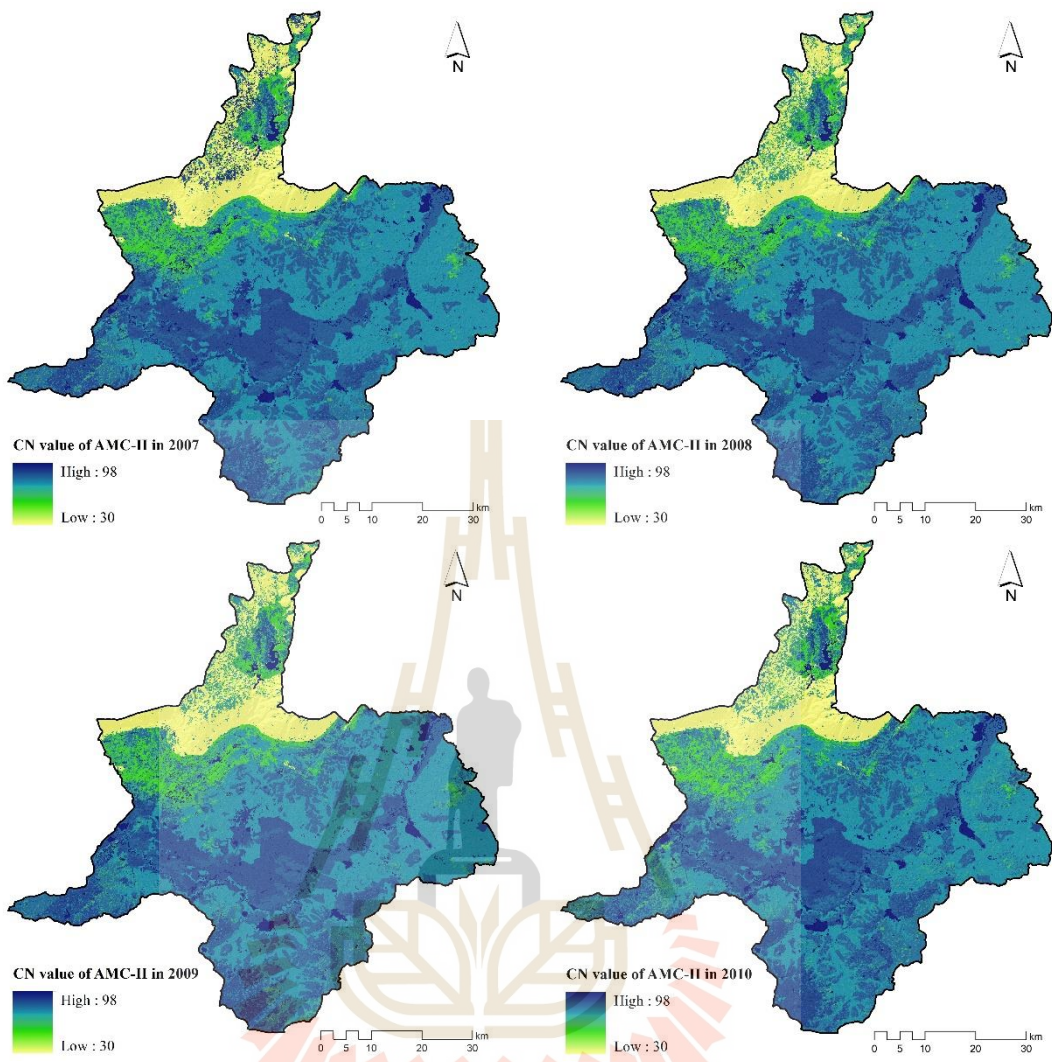
Figure 6.10 (Continued).
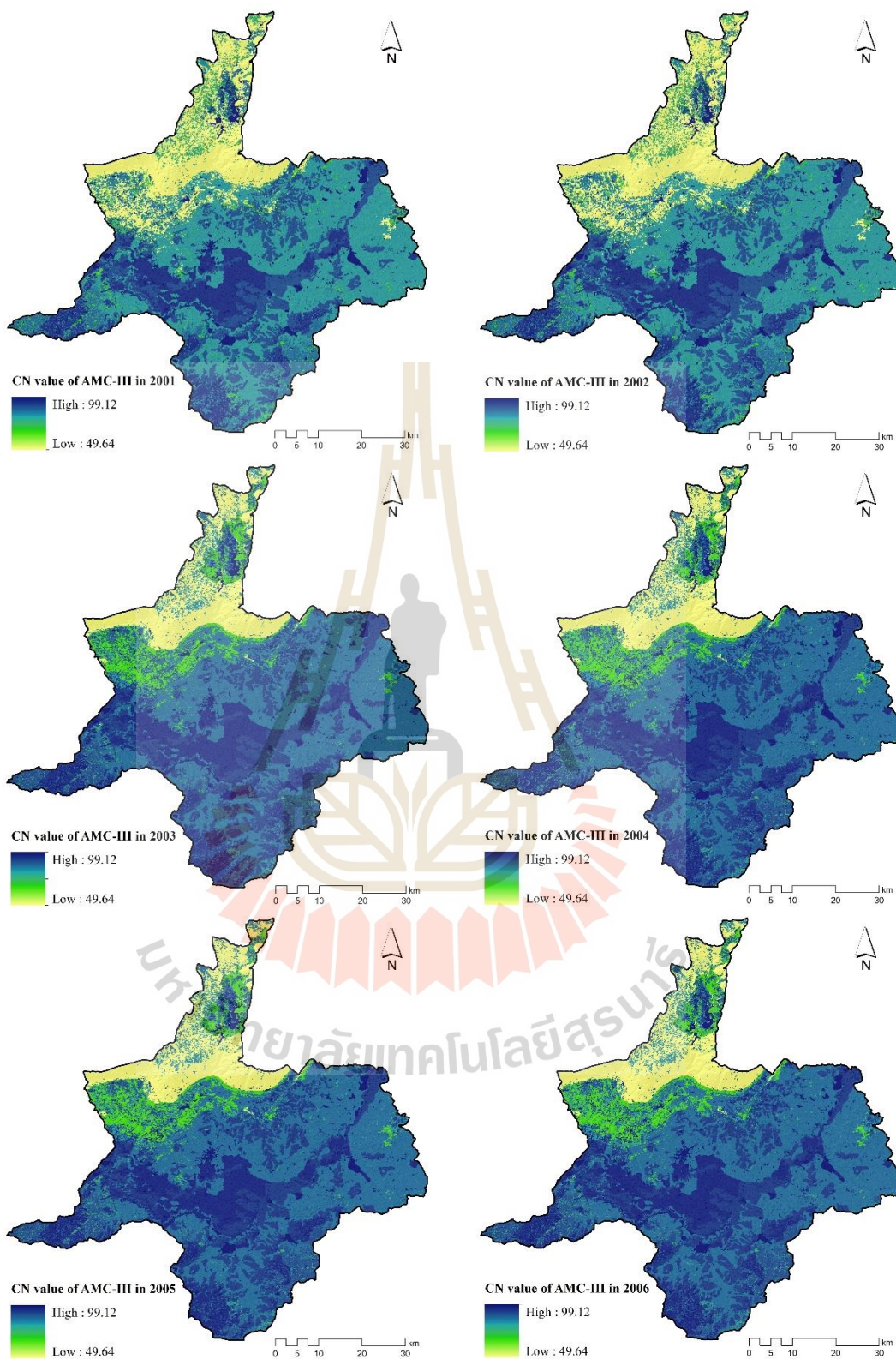
Figure 6.11 Spatial distribution of runoff CN values of AMC-III between 2001 and 2010.
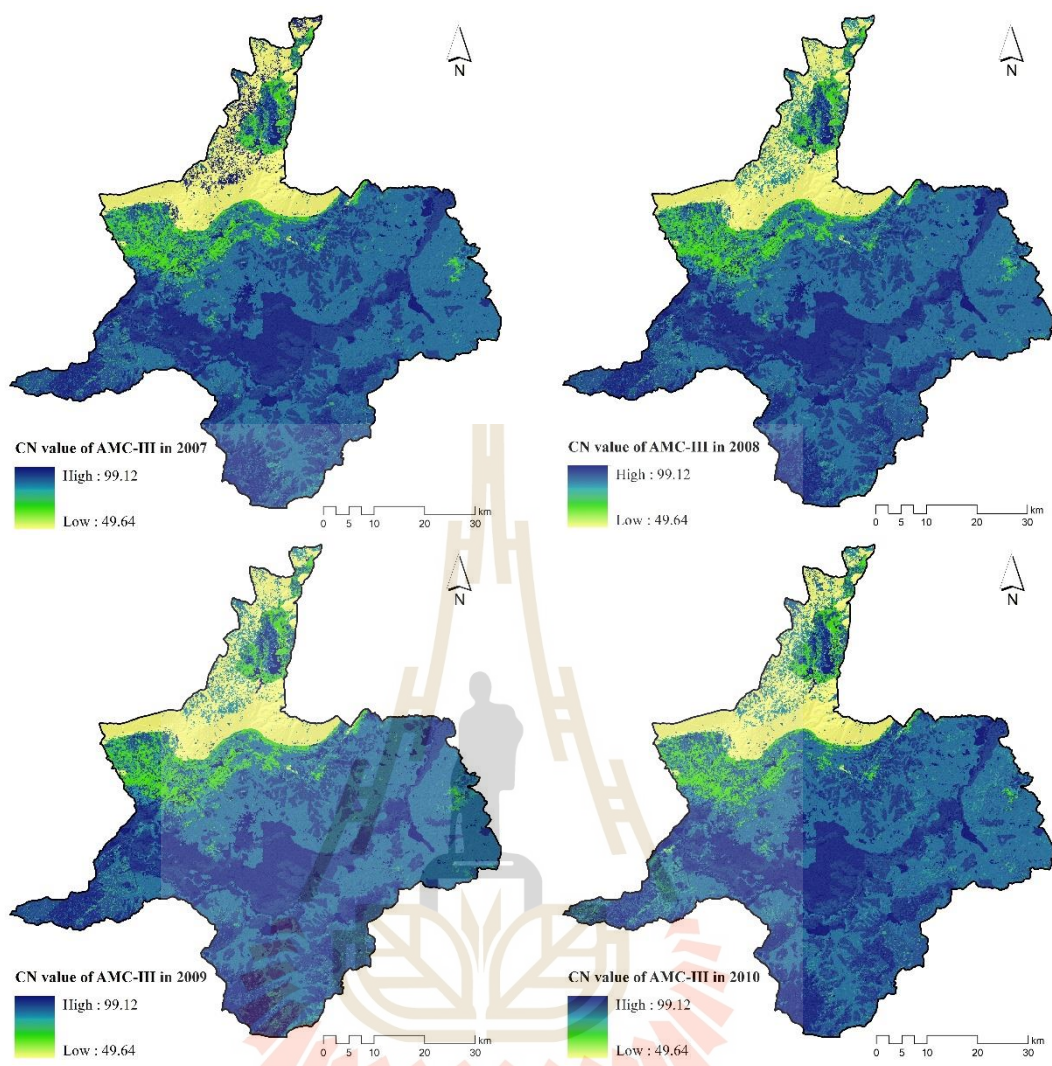
Figure 6.11 (Continued).

Based on the derived CN values of the hydrologic soil group of each LULC type, the potential maximum storage (S) was further calculated under three different AMCs using Equation 3.3 in Chapter III. Figures 6.12 to 6.14 illustrate the spatial distribution of potential maximum storage of three different AMCs between 2001 and 2010.

As a result, the values of potential maximum storage with a depth of AMC-I vary from 246.89 mm to 1,596.56 mm. Meanwhile, the values of potential maximum storage with a depth of AMC-II and AMC-III vary from 235.00 mm to 798.50 mm and 237.17 mm to 483.55 mm, respectively. It can be observed that the potential maximum storage of AMC-I provides the highest values because AMC-I represents the

dry of soil moisture condition; the soil can retain a maximum quantity of water until it reaches saturation.
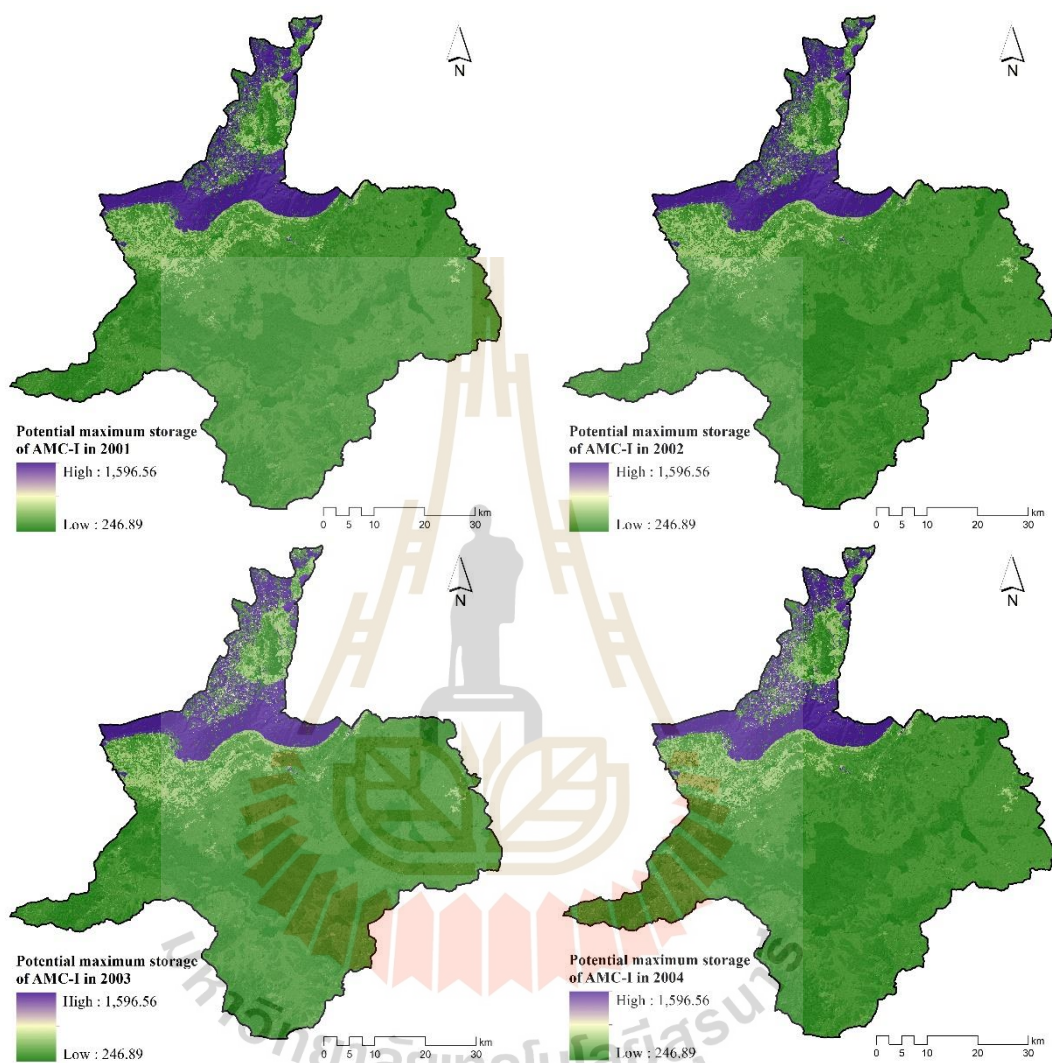
Figure 6.12 Spatial distribution of potential maximum storage (S) of AMC-I between 2001 and 2010.
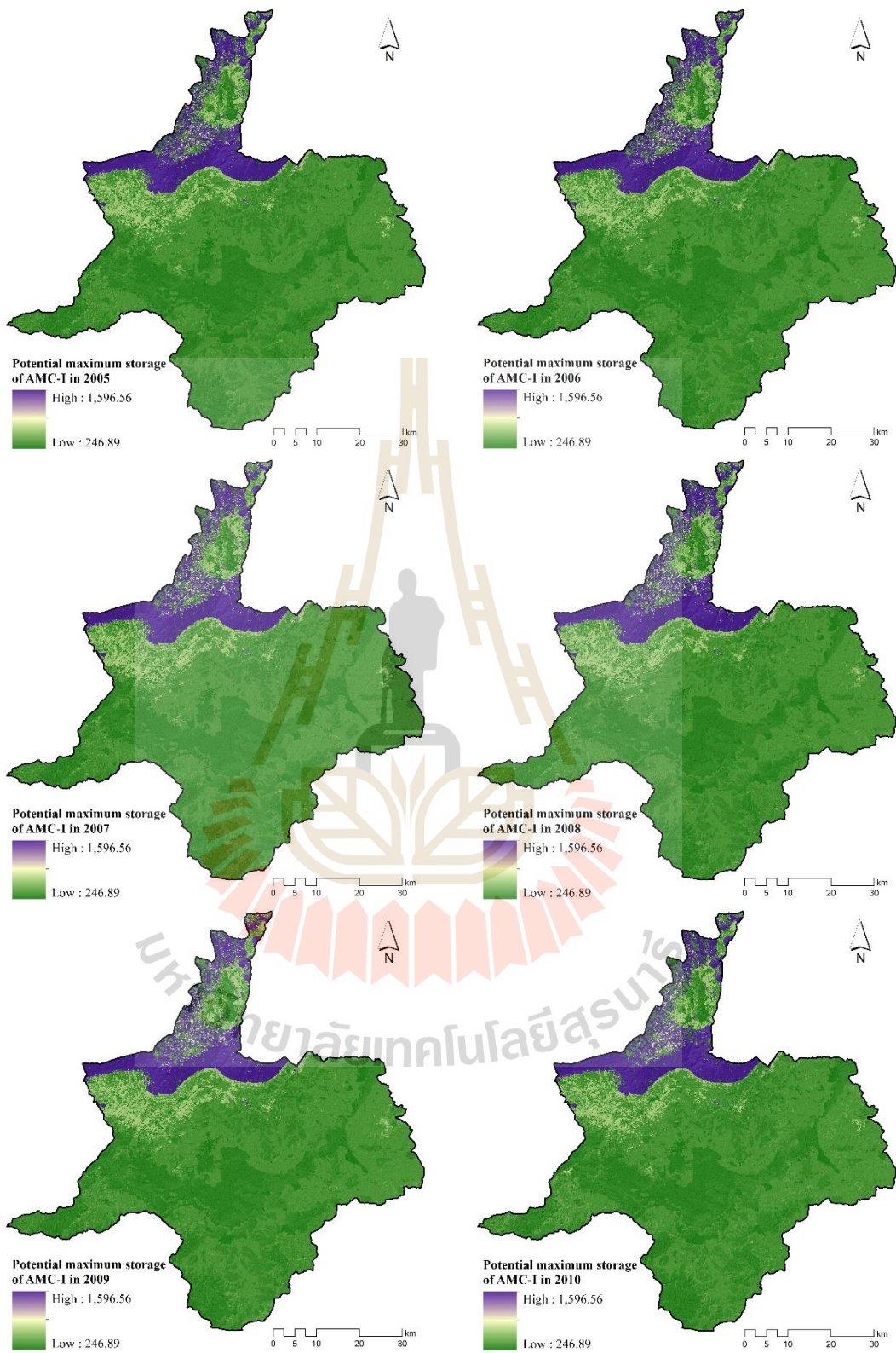
Figure 6.12 (Continued).
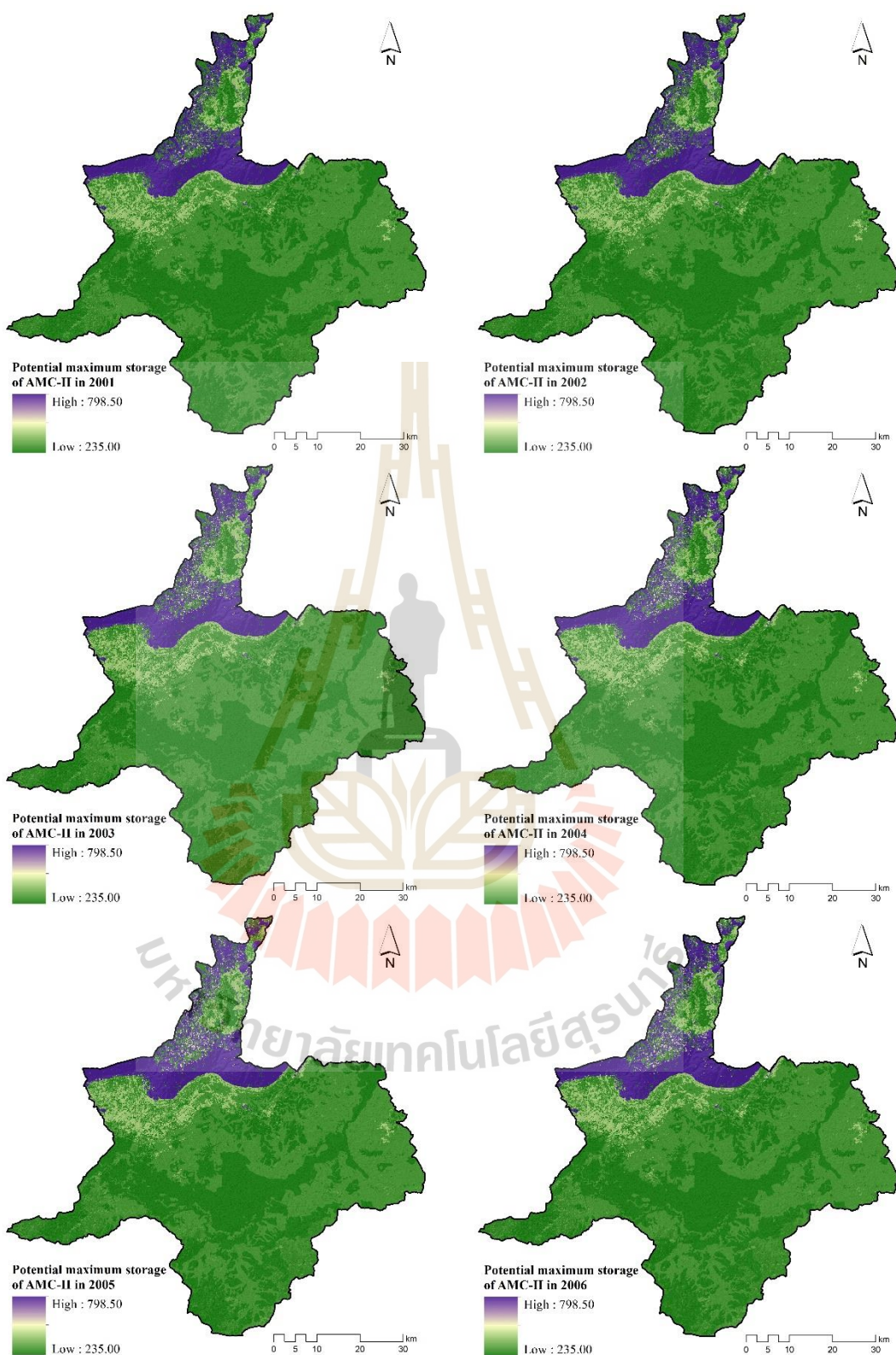
Figure 6.13 Spatial distribution of potential maximum storage (S) of AMC-II between 2001 and 2010.
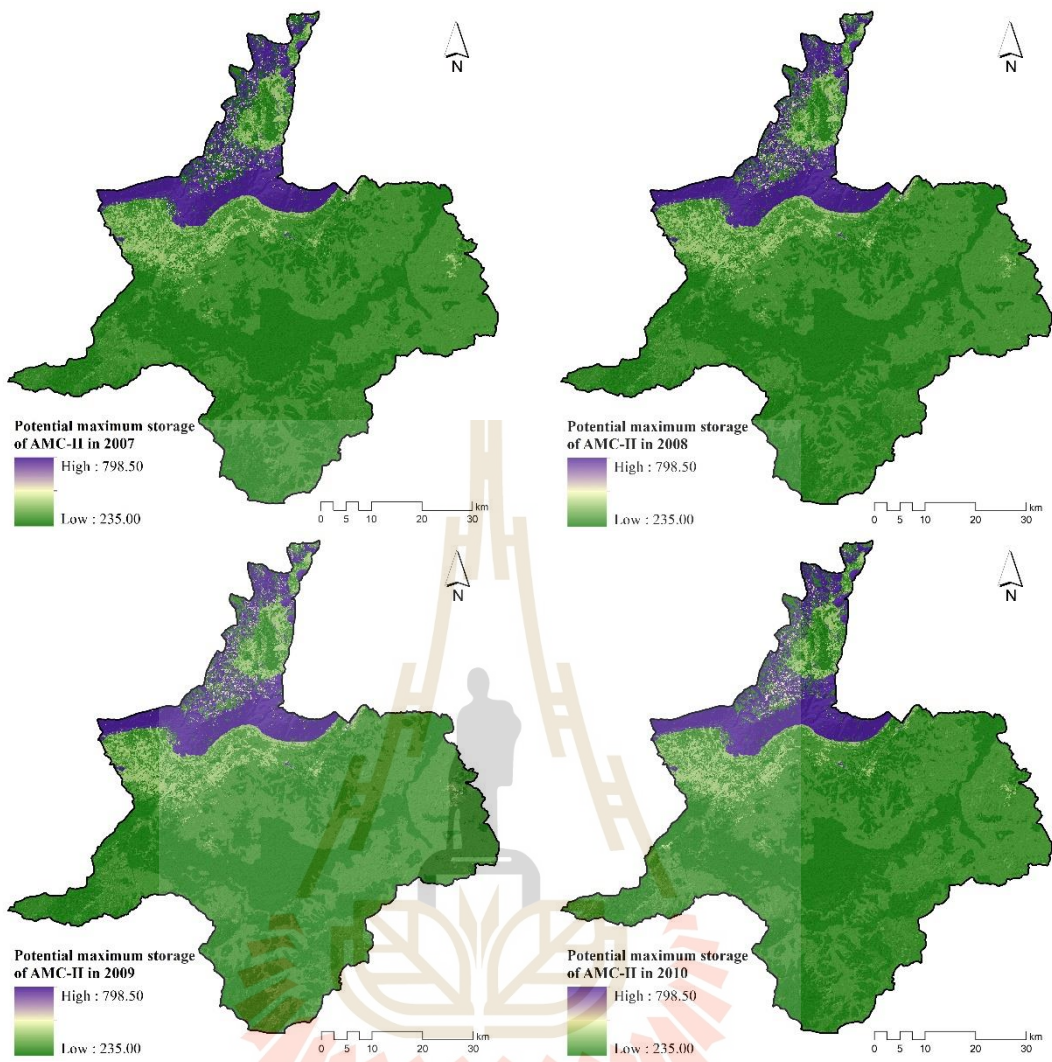
Figure 6.13 (Continued).
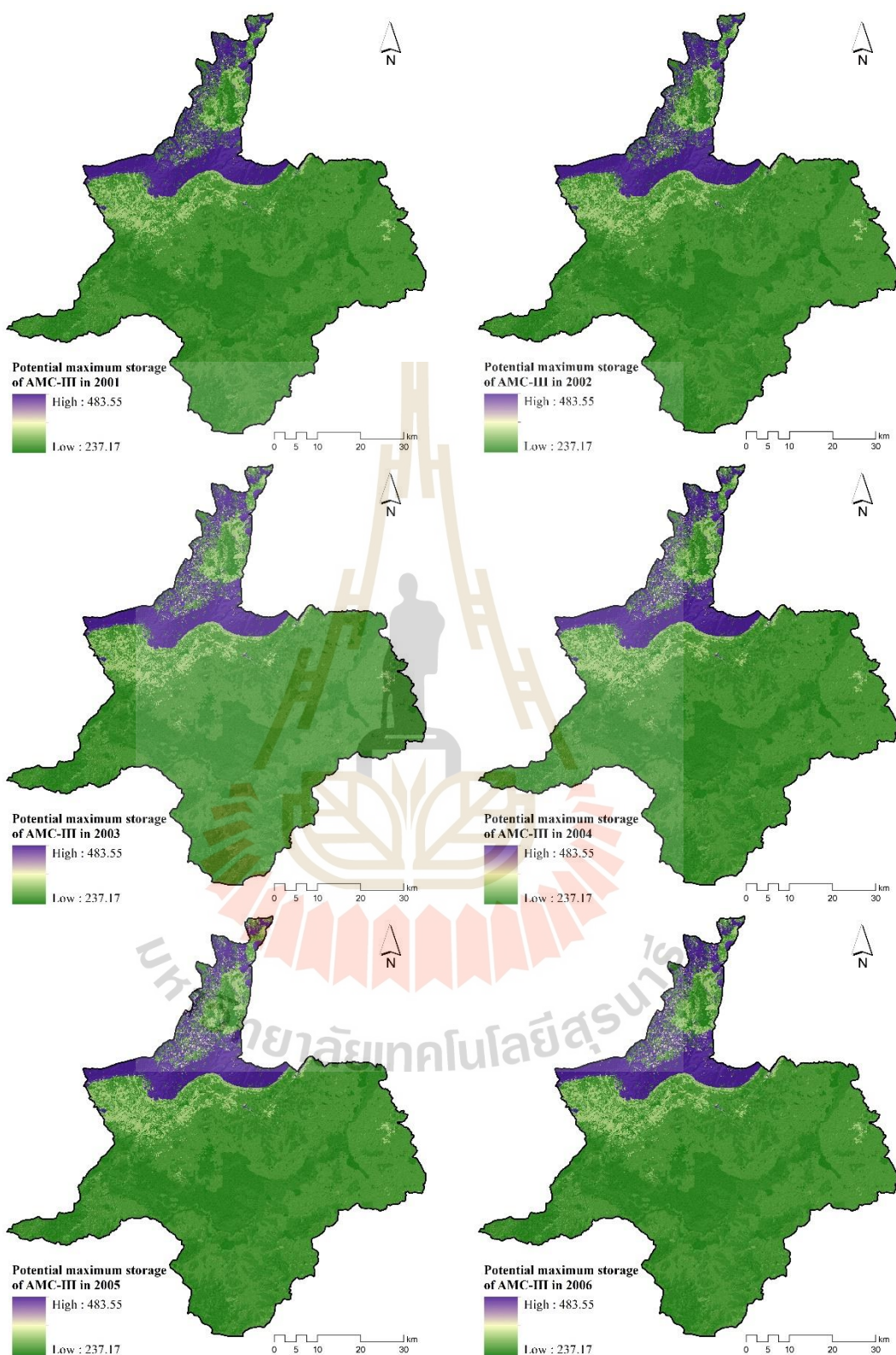
Figure 6.14 Spatial distribution of potential maximum storage (S) of AMC-III between 2001 and 2010.
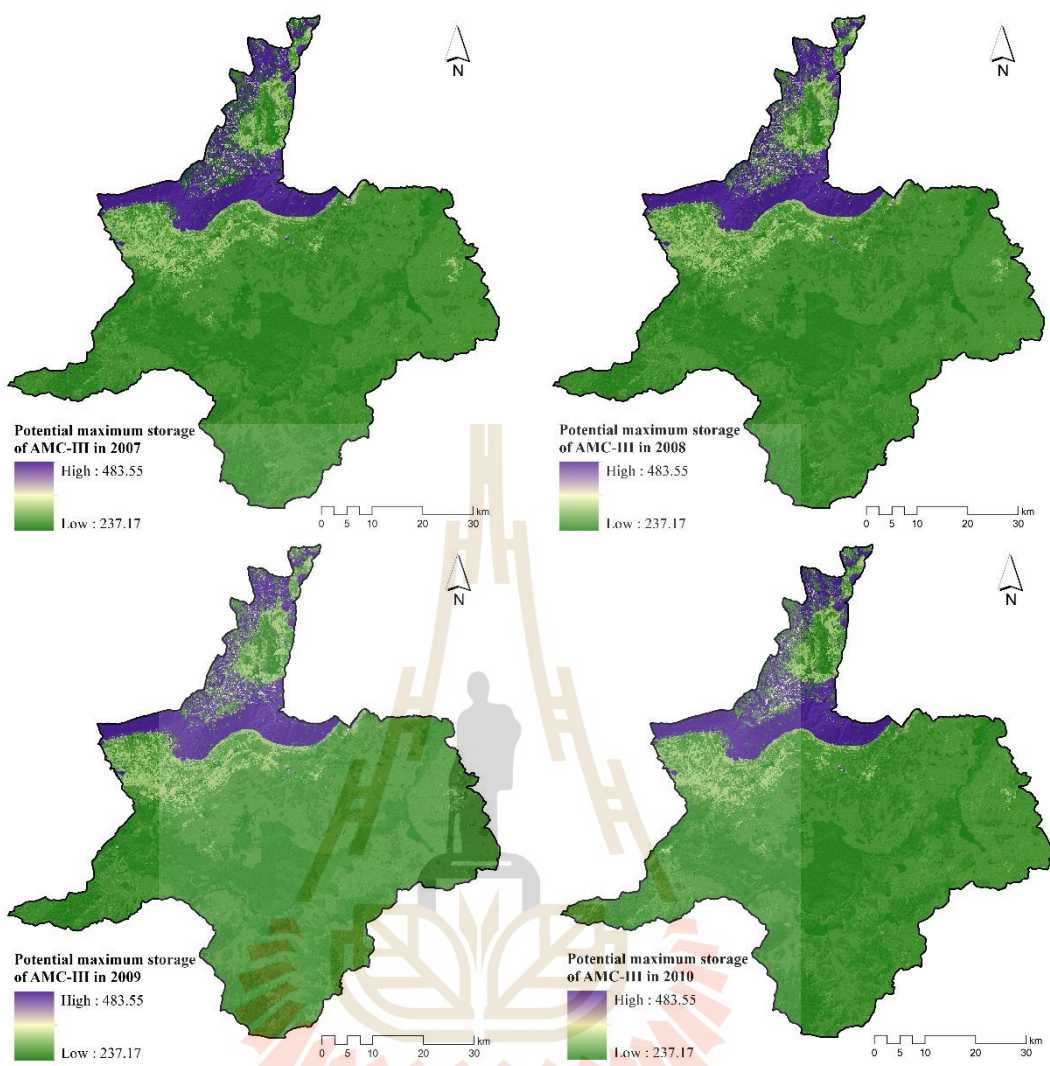
Figure 6.14 (Continued).

Then, surface runoff of three different AMCs was estimated based on annual rainfall and potential maximum storage between 2001 and 2010 using the surface runoff depth equation using Equation 3.4. After that, the estimated surface runoff depth of three different AMCs was separately converted into surface runoff volume using Equation 3.5 for suitable AMC identification.

The spatial distribution of surface runoff of three different AMCs between 2001 and 2010 was displayed in Figures 6.15 to 6.17. Meanwhile, the summary of accumulated surface runoff volume and rainfall in three AMCs between 2001 and 2010 was presented in Table 6.7.
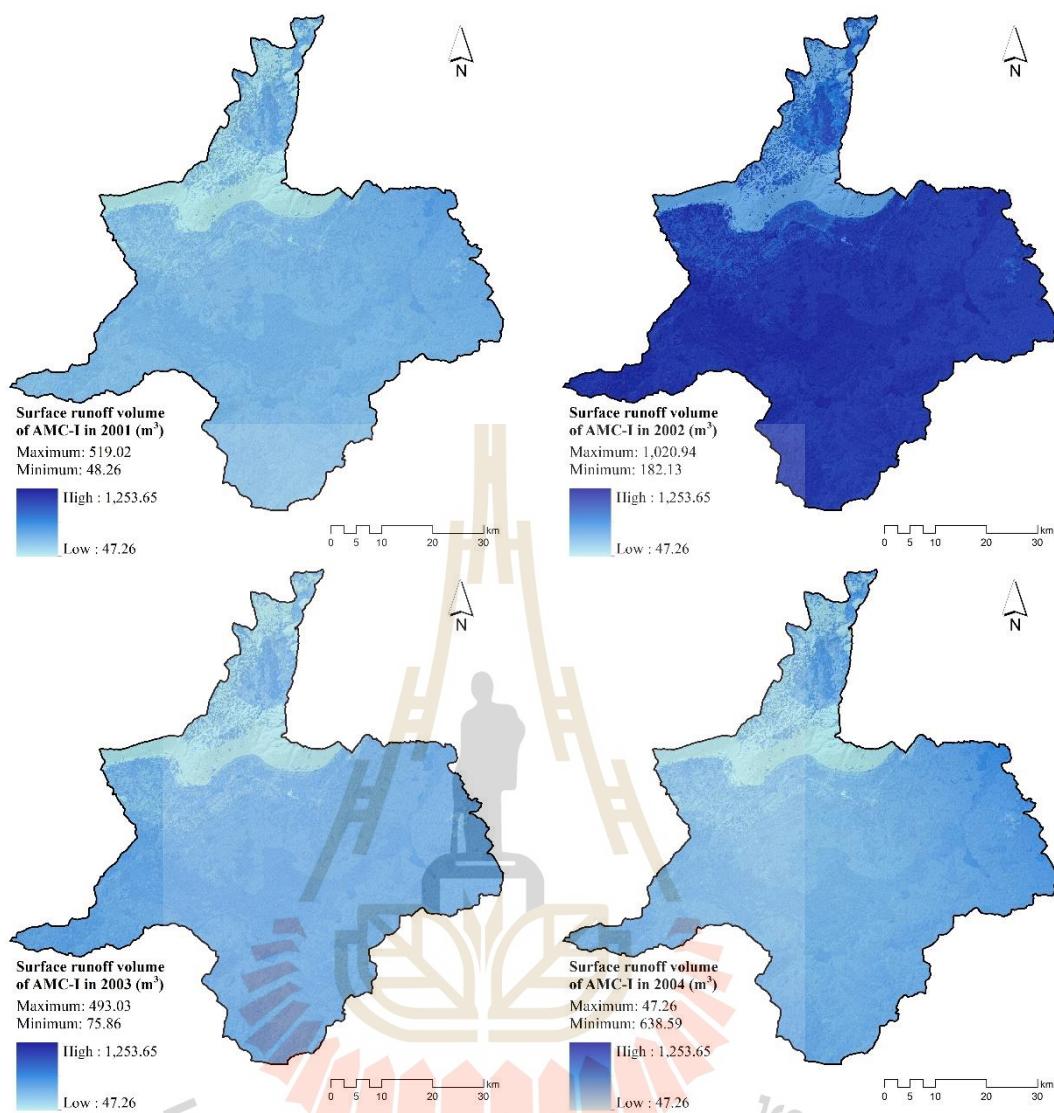
Figure 6.15 Spatial distribution of surface runoff volume of AMC-I between 2001 and 2010.

Surface runoff volume
of AMC-I in 2005 (m³)
Maximum: 493.03
Minimum: 75.86

High : 1,253.65

Low : 47.26

Surface runoff volume
of AMC-I in 2006 (m³)
Maximum: 1,163.79
Minimum: 317.85

High : 1,253.65

Low : 47.26

Surface runoff volume
of AMC-I in 2007 (m³)
Maximum: 977.34
Minimum: 293.18

High : 1,253.65

Low : 47.26

Surface runoff volume
of AMC-I in 2008 (m³)
Maximum: 1,242.67
Minimum: 377.47

High : 1,253.65

Low : 47.26

Surface runoff volume
of AMC-I in 2009 (m³)
Maximum: 1,046.49
Minimum: 174.27

High : 1,253.65

Low : 47.26

Surface runoff volume
of AMC-I in 2010 (m³)
Maximum: 1,208.17
Minimum: 313.72

High : 1,253.65

Low : 47.26

Figure 6.15 (Continued).

Figure 6.16 Spatial distribution of surface runoff volume of AMC-II between 2001 and 2010.

Surface runoff volume of AMC-II in 2007 (m³)
Maximum: 987.27
Minimum: 545.46
High : 1,253.65
Low : 47.26

Surface runoff volume of AMC-II in 2008 (m³)
Maximum: 1,253.65
Minimum: 757.16
High : 1,253.65
Low : 47.26

Surface runoff volume of AMC-II in 2009 (m³)
Maximum: 1,057.24
Minimum: 462.83
High : 1,253.65
Low : 47.26

Surface runoff volume of AMC-II in 2010 (m³)
Maximum: 1,219.02
Minimum: 680.84
High : 1,253.65
Low : 47.26
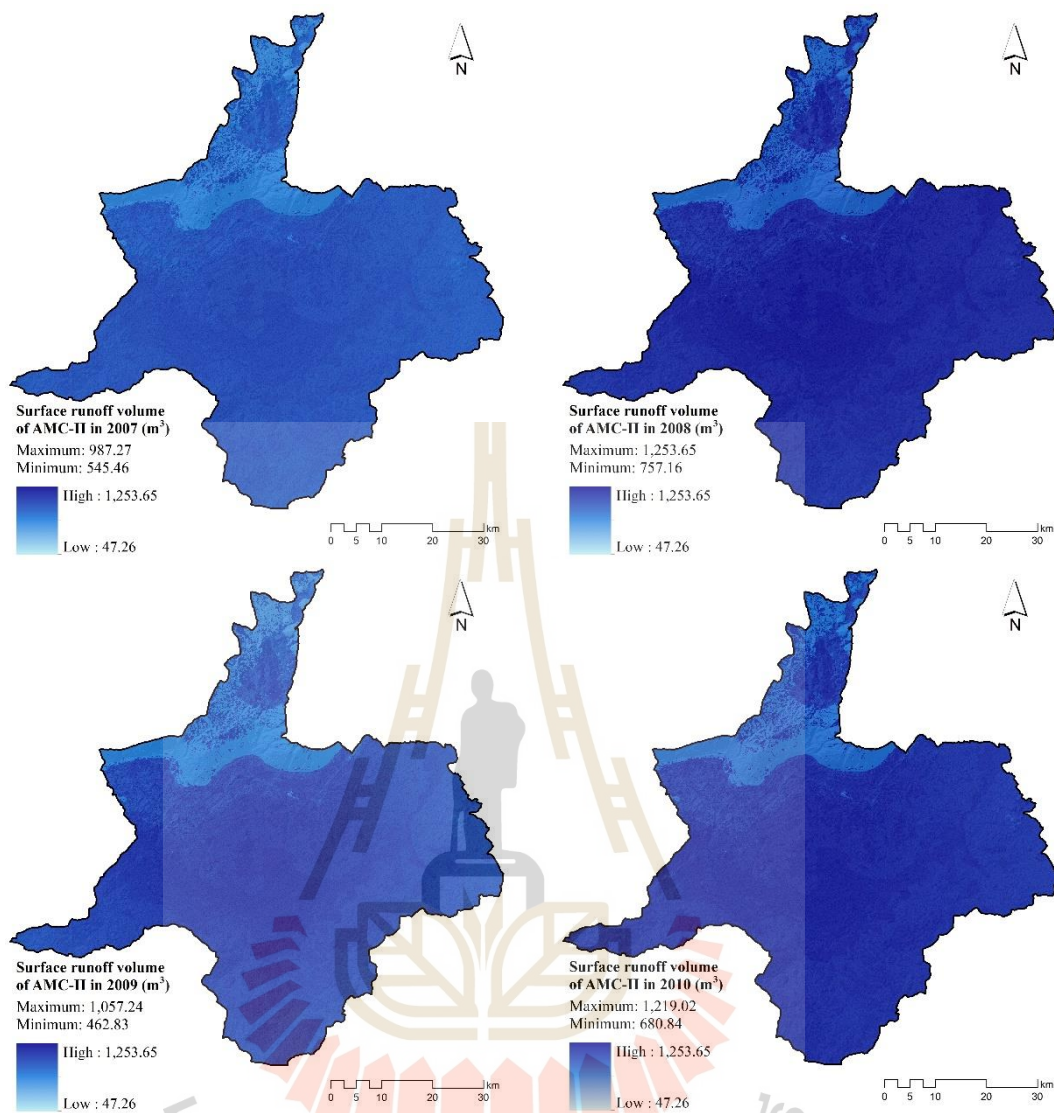
Figure 6.16 (Continued).
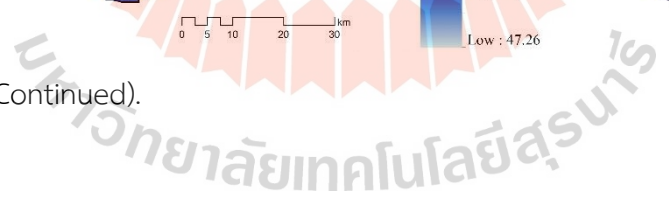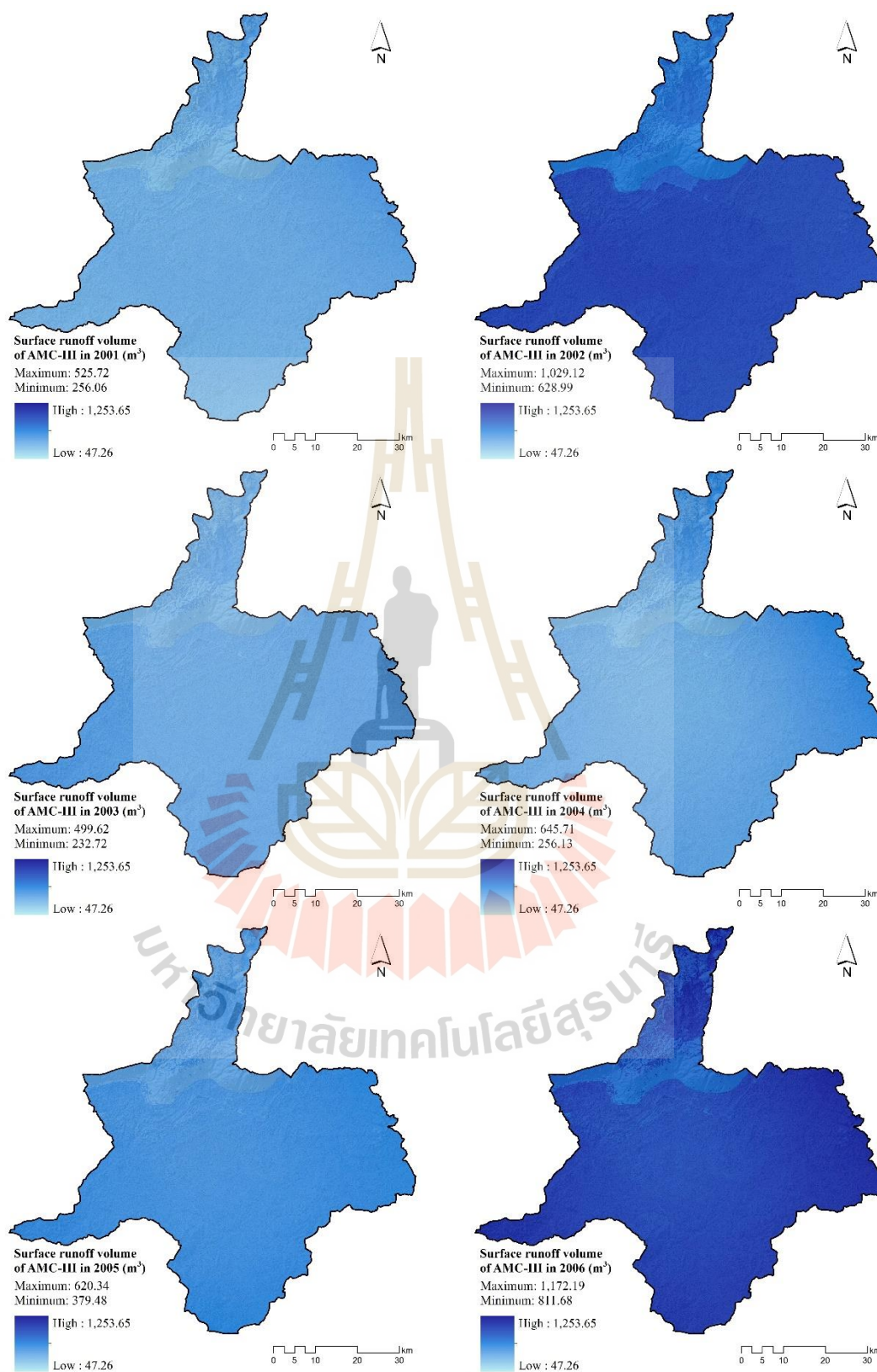
Figure 6.17 Spatial distribution of surface runoff volume of AMC-III between 2001 and 2010.
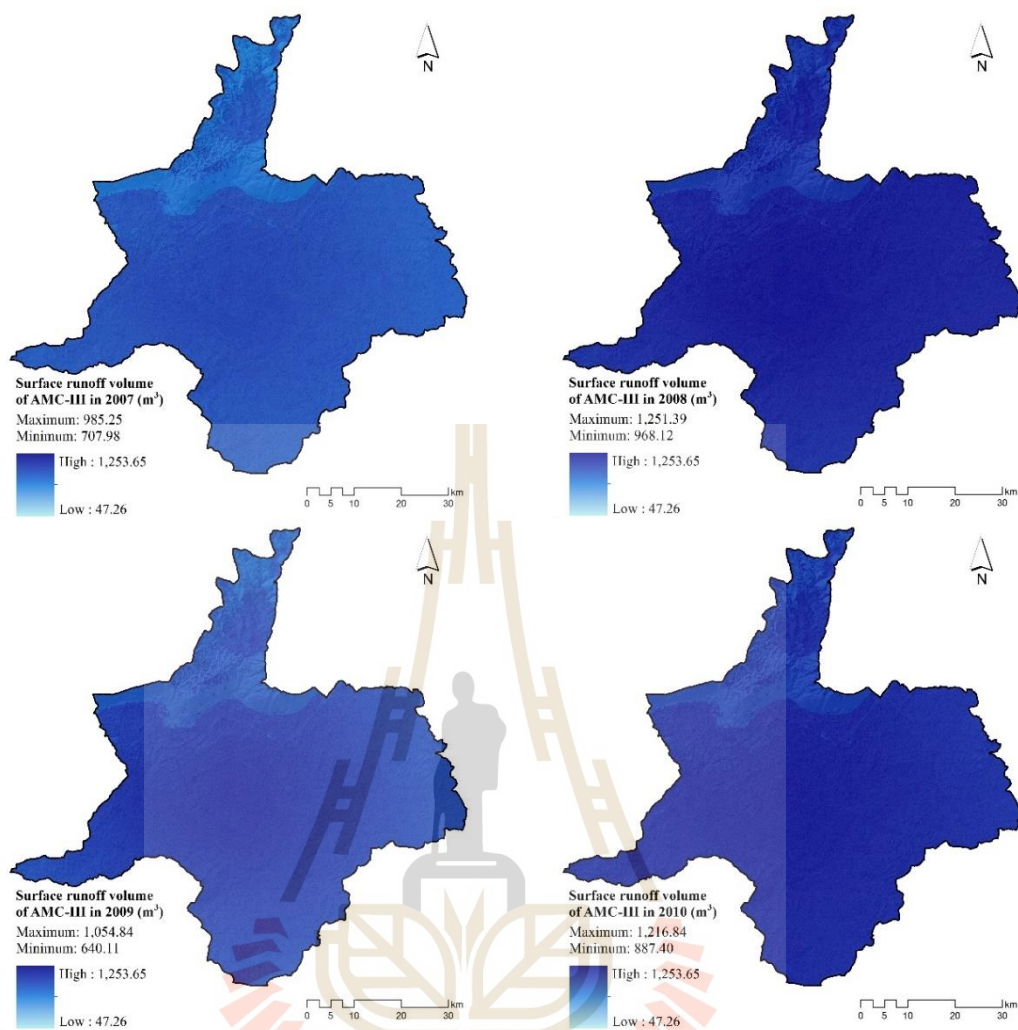
Figure 6.17 (Continued).

Table 6.7 Accumulated surface runoff volume and rainfall in three different AMCs.

Year	Annual rainfall (mm)	Surface runoff volume (million m^3)		
		AMC-I	AMC-II	AMC-III
2001	939.70	1,178.41	1,429.77	1,537.88
2002	1,191.60	4,057.74	4,483.62	4,652.40
2003	900.80	1,444.46	1,719.46	1,836.21
2004	915.40	1,335.34	1,602.36	1,716.51
2005	1,039.00	1,754.45	2,057.88	2,185.22
2006	1,196.00	4,229.13	4,672.73	4,847.85
2007	1,342.90	3,234.72	3,636.14	3,795.55
2008	1,695.20	5,869.54	6,366.80	6,558.70
2009	1,502.10	4,189.38	4,629.86	4,804.03
2010	1,506.30	5,761.81	6,249.33	6,437.31

As a result, the accumulated surface runoff volume in the study area ranges from 1,178.41 million m^3 in 2001 of AMC-I to 6,558.70 million m^3 in 2008 of AMC-III. Figure 6.18 shows the temporal change of the estimated surface runoff volume between 2001 and 2010 and the annual rainfall data of Chaiyaphum Meteorological station, located at the center of the study area. Consequently, it revealed that the pattern of surface runoff volume of three different AMCs and annual rainfall is similar. The higher the annual rainfall, the higher the surface runoff. This finding was confirmed by simple linear regression analysis, as a result in Figures 6.19 to 6.21. The surface runoff correlates with annual rainfall with the coefficient of determination (R^2) of 0.8503, 0.8511, and 0.8513 for AMC-I, AMC-II, and AMC-III, respectively. These coefficient values show a strong relationship between annual rainfall and surface runoff, according to Me, Abell, and Hamilton (2015). The coefficient of determination from each AMC condition indicates that the variation in annual rainfall accounts for 85% of the variation in surface runoff.

Additionally, it can be observed that surface runoff volumes with three different AMC conditions show a positive correlation to rainfall with a strong coefficient of determination of more than 0.85. (See Figures 6.19 to 6.21). This finding was similar to the results of Kasei, Ampadu, and Sapanbil (2013). They applied linear regression analysis to identify the relationship between rainfall and runoff in the White Volta River at Pwalugu of the Volta Basin in Ghana.
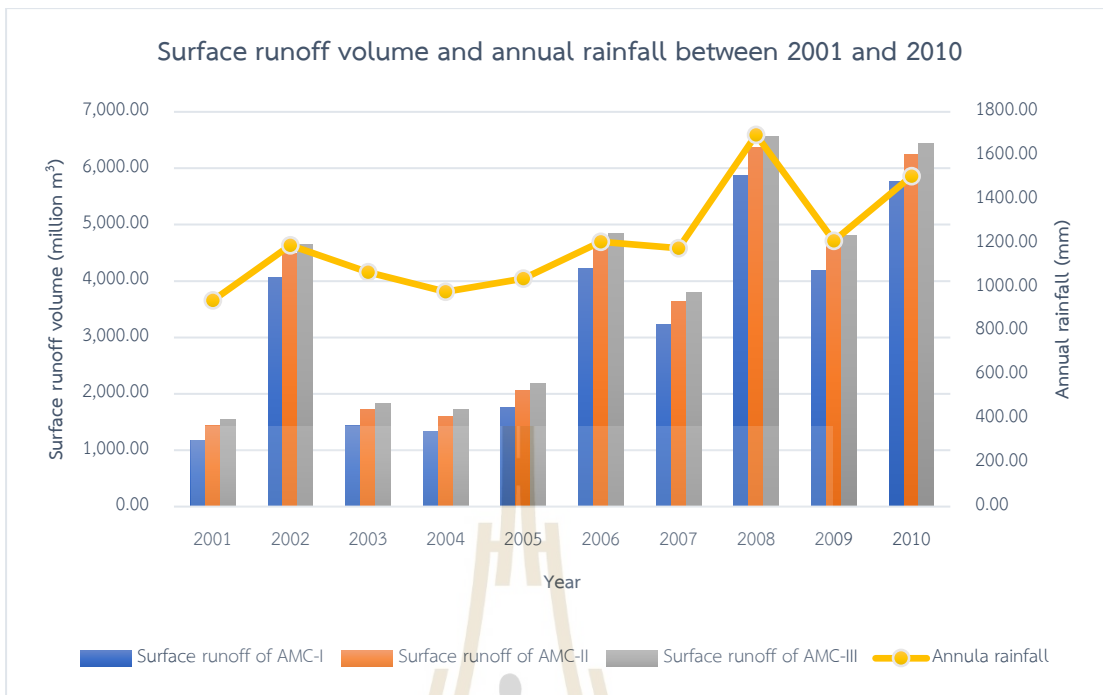
Figure 6.18 Pattern of surface runoff volume and annual rainfall of three different AMCs between 2001 and 2010.
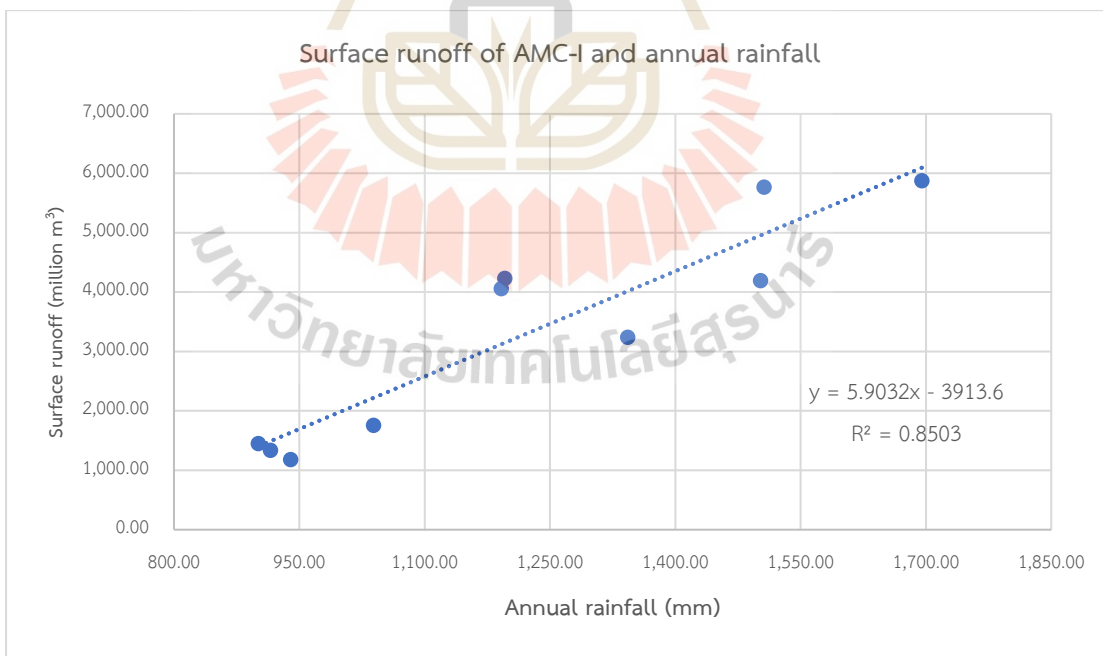
Figure 6.19 Relationship between surface runoff and annual rainfall of AMC-I.
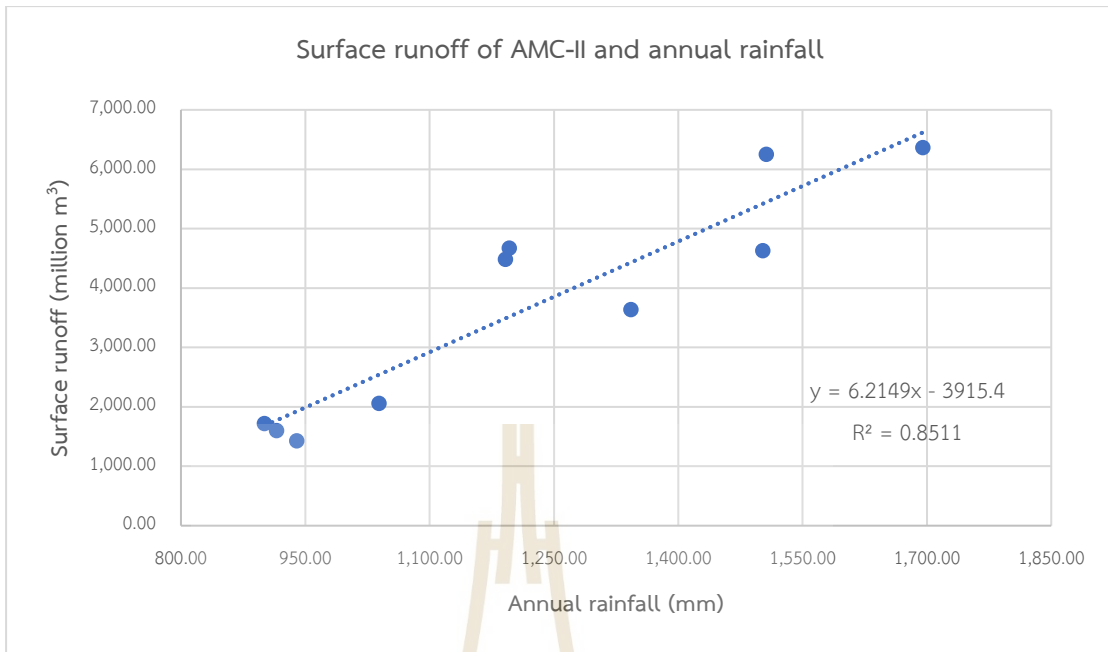
Figure 6.20 Relationship between surface runoff and annual rainfall of AMC-II.
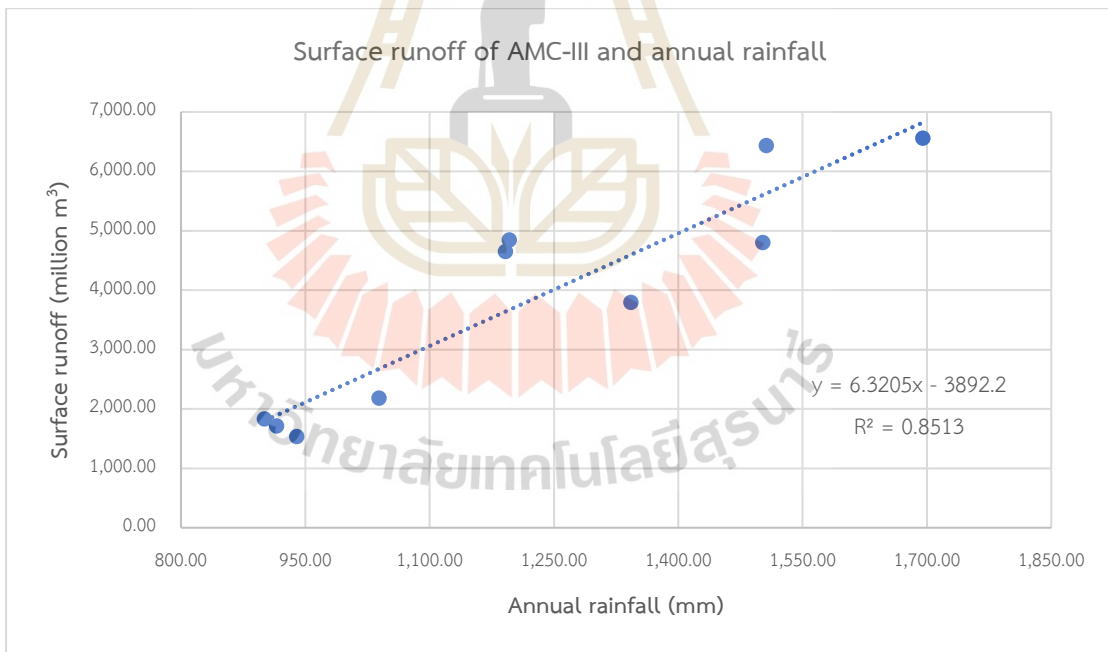
Figure 6.21 Relationship between surface runoff and annual rainfall of AMC-III.

The estimated surface runoff data in three different AMCs between 2001 and 2010 from the SCS-CN method were further used to measure model performance based on the observed runoff from the hydrological station gauge at E.21, E.23, and E6C of the Hydrology and Water Center Management for the Upper Northeastern Region (Figure 6.22) using Nash and Sutcliffe's coefficient of efficiency (NSE), coefficient of determination (R^2), and percent of bias (PBIAS) (Equations 3.6 to 3.8). The best model performance statistics from the estimated surface runoff in three different AMCs were applied to validate and identify suitable AMC identification.

Table 6.8 presented the comparison between observed surface runoff values from three sub-watershed (E.21, E23, and E.6C stations) and estimated surface runoff and their relative error (RE) values in three different AMCs.
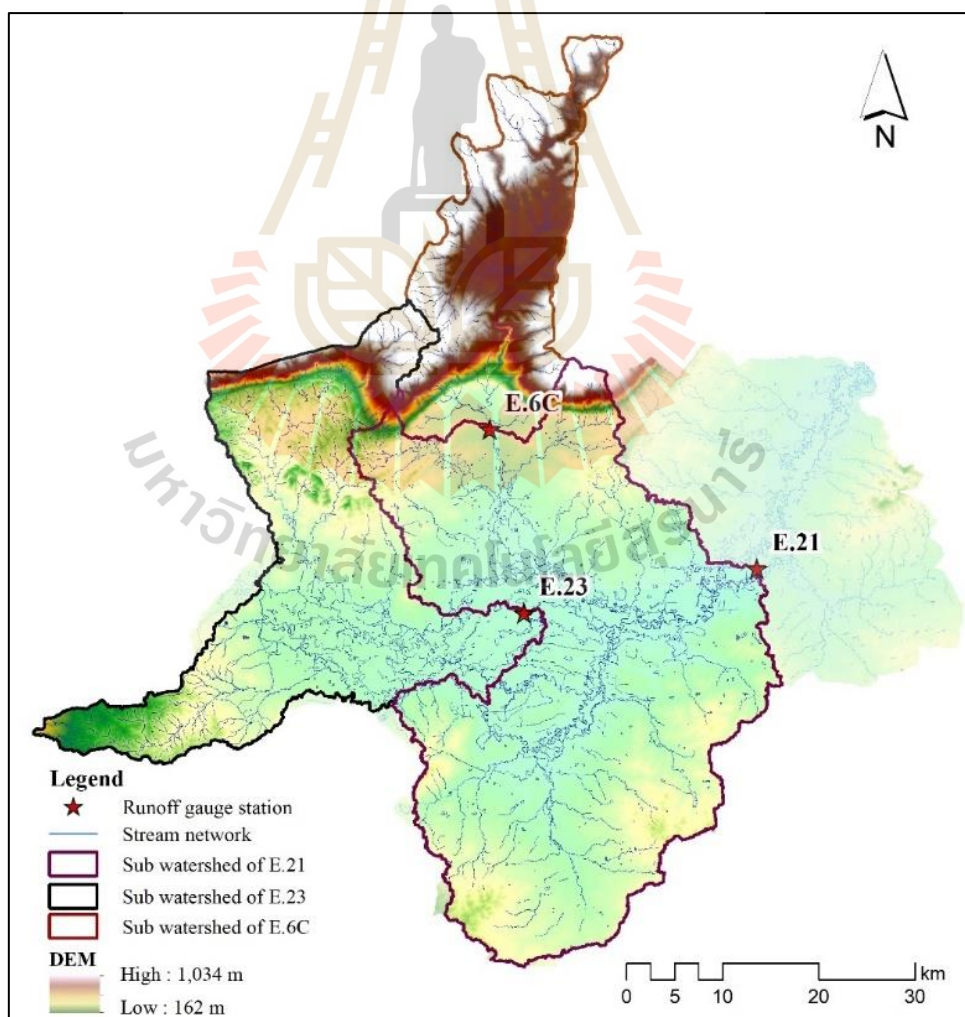
Figure 6.22 Spatial distribution of sub-watershed of the hydrological station

As a result, in Table 6.8, it can be observed that surface runoff in three different sub-watersheds with three soil conditions (AMC-I, AMC-II, and AMC-III) are over and underestimated in a specific year according to rainfall data as mentioned earlier. (See Figures 6.19 to 6.21). Furthermore, according to the RE values based on average observed and estimated values in Table 6.8, the estimated surface runoff in the upstream watershed at E.6C station and downstream watershed at E.21 station is underestimated with AMC-I soil condition and is overestimated with AMC-II and III. However, the estimated surface runoff in the middle stream watershed at E.23 station is underestimated with all AMC conditions. These findings indicate an effect of LULC on surface runoff, particularly in the case of middle-stream and downstream watersheds, where patterns of mean annual rainfall between 2001 and 2010 are almost the same (Figure 6.23).
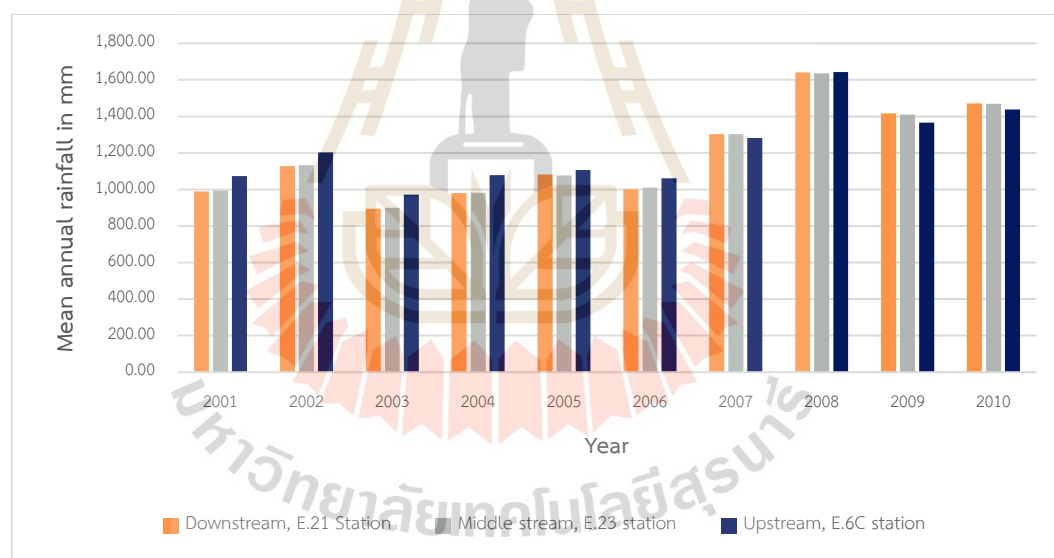
Figure 6.23 Mean annual rainfall of over downstream (E21 station), middle stream (E.23 station), and upstream (E.6C station) between 2001 and 2010.

The result of model performance using NSE, R^2, and PBIAS for identifying suitable AMC for surface runoff estimation is reported in Table 6.9.

Table 6.8 Comparison between observed (Q_{obs}) and simulated (Q_{sim}) surface runoff of three hydrological stations.

Year	E.21 hydrological station							E.23 hydrological station							E.6C hydrological station						
	Q_{obs}	AMC-I		AMC-II		AMC-III		Q_{obs}	AMC-I		AMC-II		AMC-III		Q_{obs}	AMC-I		AMC-II		AMC-III	
		Q_{sim}	RE (%)	Q_{sim}	RE (%)	Q_{sim}	RE (%)		Q_{sim}	RE (%)	Q_{sim}	RE (%)	Q_{sim}	RE (%)		Q_{sim}	RE (%)	Q_{sim}	RE (%)	Q_{sim}	RE (%)
2001	633.4	601.82	4.99	695.90	-9.87	725.99	-14.62	373.10	292.79	21.53	354.69	4.93	382.87	-2.62	36.64	25.82	29.53	45.19	-23.33	61.25	-67.17
2002	1,954.20	1,820.05	6.86	1,959.27	-0.26	2,001.76	-2.43	1,500.70	929.33	38.07	1,032.16	31.22	1,074.94	28.37	166.38	113.11	32.02	169.23	-1.71	204.97	-23.19
2003	656.7	650.03	1.02	746.73	-13.71	777.44	-18.39	575.60	316.30	45.05	379.93	33.99	408.74	28.99	50.63	21.60	57.34	37.64	25.65	51.78	-2.26
2004	549.9	838.14	-52.42	945.00	-71.85	978.53	-77.95	542.40	409.53	24.50	482.10	11.12	514.13	5.21	41.21	31.16	24.40	53.41	-29.60	71.19	-72.74
2005	854.7	1,077.71	-26.09	1,195.42	-39.86	1,232.06	-44.15	653.80	530.00	18.94	612.45	6.33	648.20	0.86	84.33	54.38	35.51	90.48	-7.30	116.27	-37.88
2006	2,230.50	2,439.22	-9.36	2,590.81	-16.15	2,636.54	-18.20	1,630.70	1,246.65	23.55	1,364.56	16.32	1,412.19	13.40	73.37	35.22	51.99	61.22	16.56	81.35	-10.88
2007	1,914.30	1,450.86	24.21	1,581.28	17.40	1,621.40	15.30	845.50	724.36	14.33	819.84	3.04	859.75	-1.69	85.42	47.58	44.30	82.78	3.10	107.02	-25.28
2008	3,494.50	3,173.60	9.18	3,334.97	4.57	3,383.21	3.18	1,932.20	1,625.72	15.86	1,754.19	9.21	1,804.98	6.58	180.45	146.87	18.61	214.70	-18.98	256.12	-41.93
2009	2,180.20	2,181.08	-0.04	2,328.33	-6.79	2,372.98	-8.84	1,560.00	1,121.68	28.10	1,234.52	20.86	1,280.50	17.92	151.03	122.82	18.68	184.17	-21.94	222.61	-47.40
2010	3,188.90	3,033.46	4.87	3,189.97	-0.03	3,237.17	-1.51	2,174.40	1,570.83	27.76	1,698.55	21.88	1,749.15	19.56	206.15	181.51	11.95	255.45	-23.92	299.02	-45.05
Avg	1,765.73	1,726.60	2.22	1,856.77	-5.16	1,896.71	-7.42	1,178.84	876.72	25.63	973.3	17.44	1,013.54	14.02	107.56	78.01	27.47	119.43	-11.04	147.16	-36.82

Note: observed (Q_{obs}) and simulated (Q_{sim}) surface runoff in a million m^3.

Table 6.9 Statistical data of model performance for suitable AMC identification and model validation.

AMC	Year	E.21 station			E.23 station			E.6C station		
		NSE	R^2	PBIAS	NSE	R^2	PBIAS	NSE	R^2	PBIAS
AMC-II	2001	0.95	0.96	0.18	0.67	0.96	0.68	0.71	0.96	1.01
	2002			0.76			4.85			4.95
	2003			0.04			2.20			2.70
	2004			-1.63			1.13			0.93
	2005			-1.26			1.05			2.78
	2006			-1.18			3.26			3.55
	2007			2.62			1.03			3.52
	2008			1.82			2.60			3.12
	2009			-0.01			3.72			2.62
	2010			0.88			5.12			2.29
AMC-II	2001	0.94	0.96	-0.35	0.82	0.96	0.16	0.85	0.97	-0.79
	2002			-0.03			3.97			-0.27
	2003			-0.51			1.66			1.21
	2004			-2.24			0.51			-1.13
	2005			-1.93			0.35			-0.57
	2006			-2.04			2.26			1.13
	2007			1.89			0.22			0.25
	2008			0.90			1.51			-3.18
	2009			-0.84			2.76			-3.08
	2010			-0.01			4.04			-4.58
AMC-III	2001	0.94	0.96	-0.52	0.86	0.96	-0.08	0.32	0.97	-2.29
	2002			-0.27			3.61			-3.59
	2003			-0.68			1.42			-0.11
	2004			-2.43			0.24			-2.79
	2005			-2.14			0.05			-2.97
	2006			-2.30			1.85			-0.74
	2007			1.66			-0.12			-2.01
	2008			0.63			1.08			-7.03
	2009			-1.09			2.37			-6.66
	2010			-0.27			3.61			-8.63

As a result, the model performance results at the E.21 hydrological station shows that the NSE value is 0.95, 0.94, and 0.94, which indicates a perfect fit for surface runoff estimation of AMC-I, AMC-II, and AMC-III, respectively, and a very high correlation between the observed and estimated surface runoff with an R^2 of 0.96 for all AMCs. Meanwhile, the PBIAS value varies from 0.93% in 2004 to 4.95% in 2002 for underestimation.

The scatter plots of the observed and estimated surface runoff between 2001 and 2010 at station E.21 of three different AMCs, along with the 1:1 line (solid line), are shown in Figure 6.24. It is observable that all of the AMC relation lines are almost identical to the 1:1 line. However, the AMC-I relation line is slightly below the 1:1 line, indicating that the model is slightly underestimated. In contrast, the AMC-II and AMC-III relation lines are slightly above the 1:1 line, indicating that the model is slightly overestimated.

(a) AMC-I

(a) AMC-II

(a) AMC-III
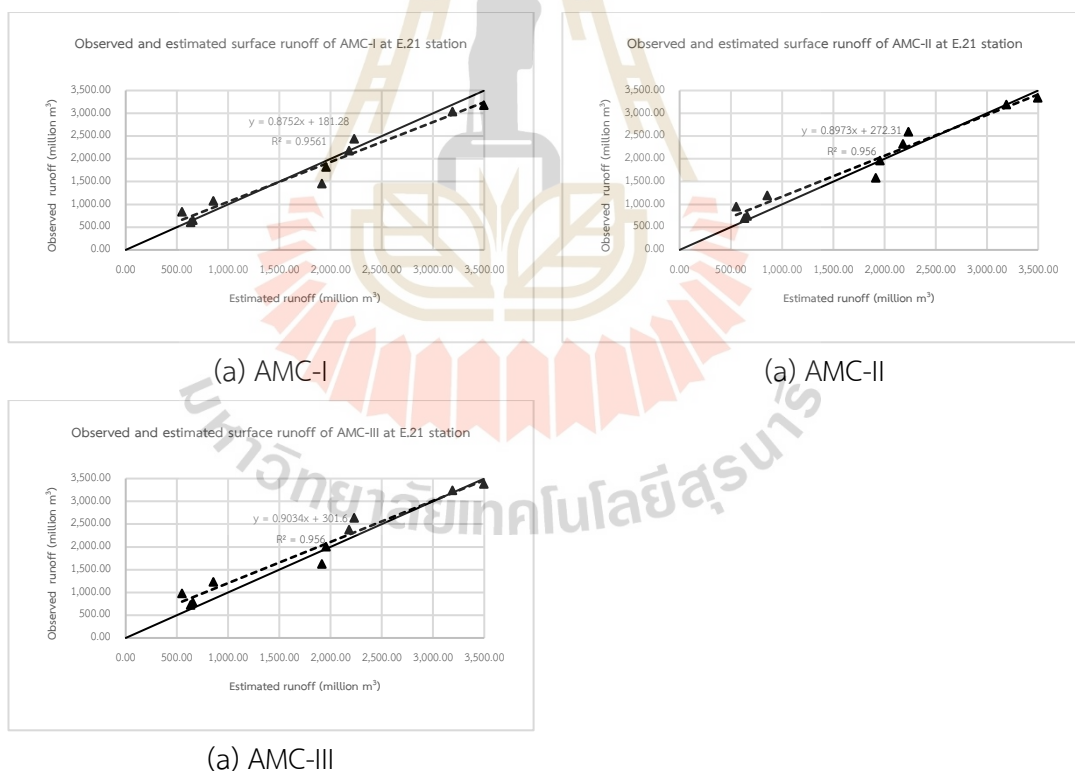
Figure 6.24 Relationship between observed and estimated runoff between 2001 and 2010 at the E.21 stations.

In the meantime, the model performance results at the E.23 hydrological station reveal that the NSE value is 0.67, 0.82, and 0.86, which shows a good and very good fit for surface runoff estimation and a very high correlation between the observed and estimated surface runoff with R^2 of 0.96 for all AMCs. Meanwhile, the PBIAS value varies from -4.58% for overestimation bias in 2010 to 1.21% for underestimation bias in 2003. The scatter plots of the observed and estimated surface runoff between 2001 and 2010 at station E.23 of three different AMCs, along with the 1:1 line, are shown in Figure 6.25. It can be observed that all of the AMC relation lines are slightly below the 1:1 line, indicating that the model is slightly underestimated. However, all AMC's well-distributed scatter plots are entirely satisfactory.

(a) AMC-I   (a) AMC-II

(a) AMC-III
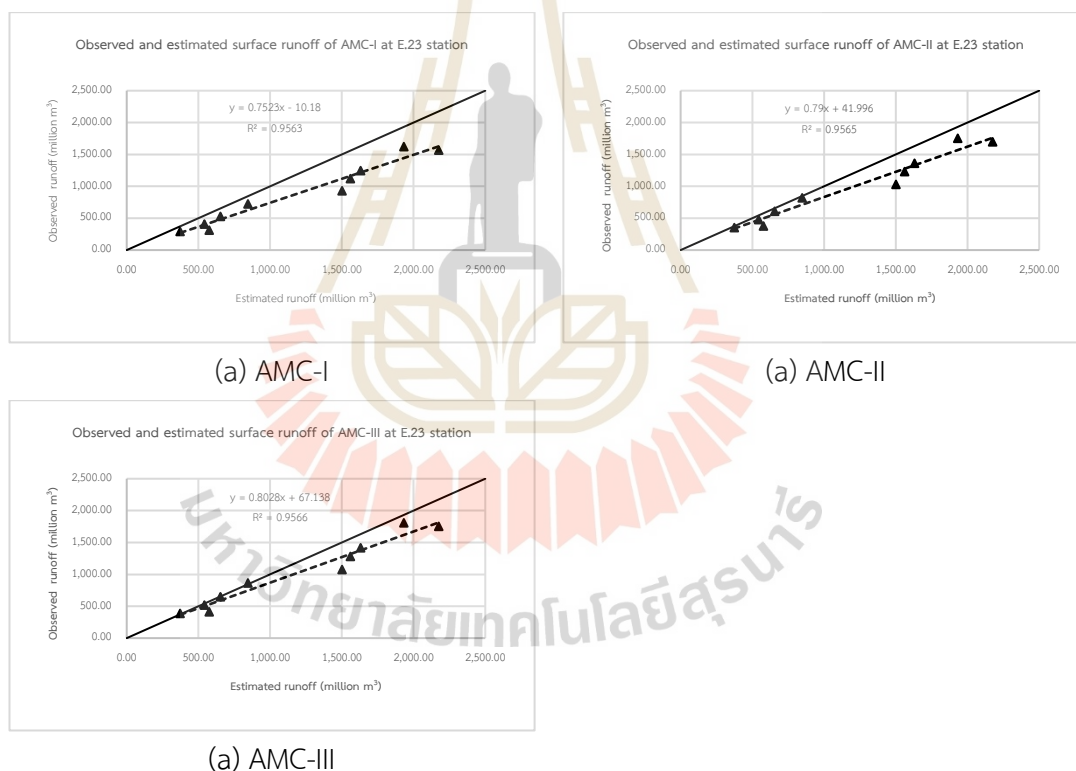
Figure 6.25 Relationship between observed and estimated runoff between 2001 and 2010 at the E.23 stations.

Likewise, the model performance results at the E.6C hydrological station show a good, very good, and unsatisfactory fit for surface runoff estimation of AMC-I, AMC-II, and AMC-III, with NSE values of 0.71, 0.85, and 0.32, respectively. Meanwhile,

the model provides the R^2 values of 0.96, 0.97, and 0.97, which indicates a very high correlation between the observed and estimated surface runoff. At the same time, the PBIAS value varies from -8.63% in 2010 to -0.11 in 2003 for overestimation bias. Figure 6.26 illustrates the scatter plots of the observed and estimated surface runoff between 2001 and 2010 at station E.6C of three different AMCs along with the 1:1 line. It reveals that all AMC's well-distributed scatter plots are quite satisfactory. The AMC-I relation line is slightly below the 1:1 line, indicating that the model is slightly underestimated. In contrast, the AMC-II and AMC-III relation lines are slightly above the 1:1 line, indicating that the model is slightly overestimated.

(a) AMC-I

(b) AMC-II

(c) AMC-III
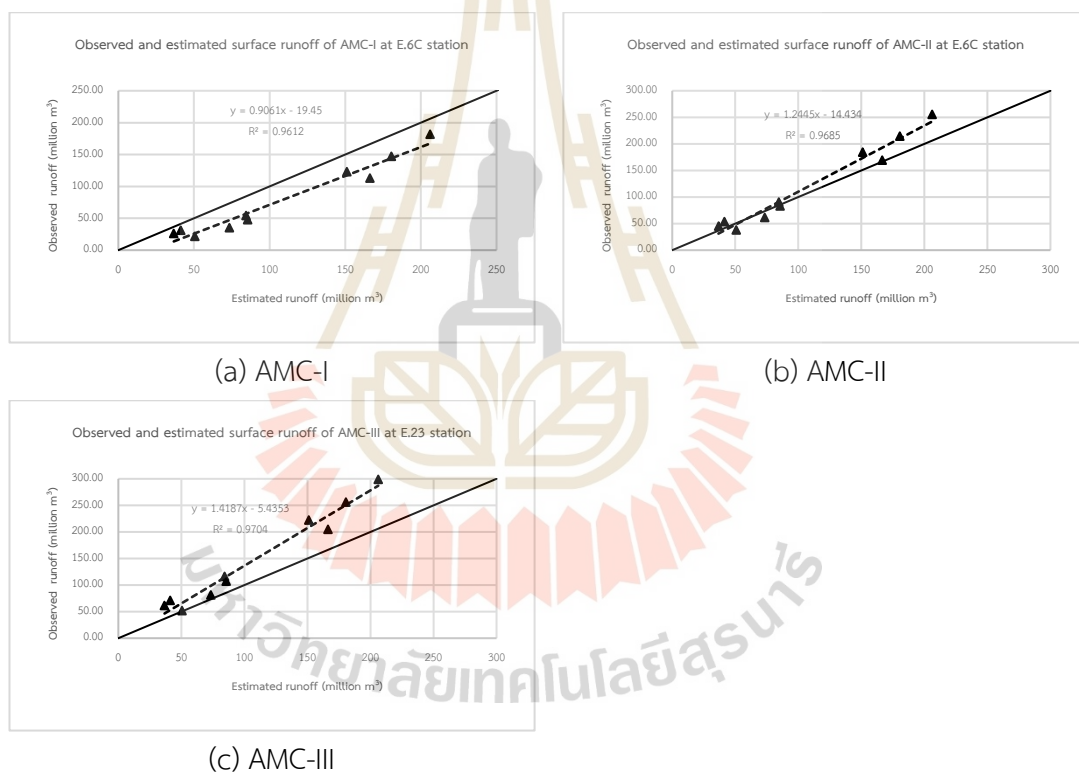
Figure 6.26 Relationship between observed and estimated runoff between 2001 and 2010 at the E.6C stations.

According to the model performance scale suggested by Me, Abell, and Hamilton (2015), the derived NSE and R^2 values are more than 0.65, and the PBIAS value is less than ± 10. Therefore, surface runoff estimation using the SCS-CN method in the current study can be accepted.

Besides, NSE, R^2, and PBIAS of all AMCs were compared to identify the suitable AMC for surface runoff estimation between 2011 and 2019, as shown in Table 6.10. As a result, it was found that AMC-II can provide all average statistics measurements better than other AMCs. Thus, the AMC-II condition was chosen as the suitable AMC for surface runoff estimation in the second period (2011-2019).

Table 6.10 Comparison of average statistics measurement for suitable AMC examination.

AMC	Average statistics measurement		
	NSE	R^2	PBIAS
AMC-I	0.78	0.96	1.84
AMC-II	0.87	0.96	0.04
AMC-III	0.71	0.96	-1.01

6.3   Surface runoff estimation between 2011 and 2019

The digital LULC data between 2011 and 2019, annual rainfall data between 2011 and 2019, and hydrologic soil group were used to estimate surface runoff with suitable AMC conditions. In practice, relative surface runoff in each cell was generated based on runoff curve numbers (CN) according to hydrological soil-cover complex using Model Builder of ArcGIS^{TM}, as mentioned earlier in the previous section (See Figure 6.6). The runoff curve number (CN) values were assigned based on the AMC-II condition, as the suitable AMC in this study. The spatial distribution of CN values between 2011 and 2019 is displayed in Figure 6.27.
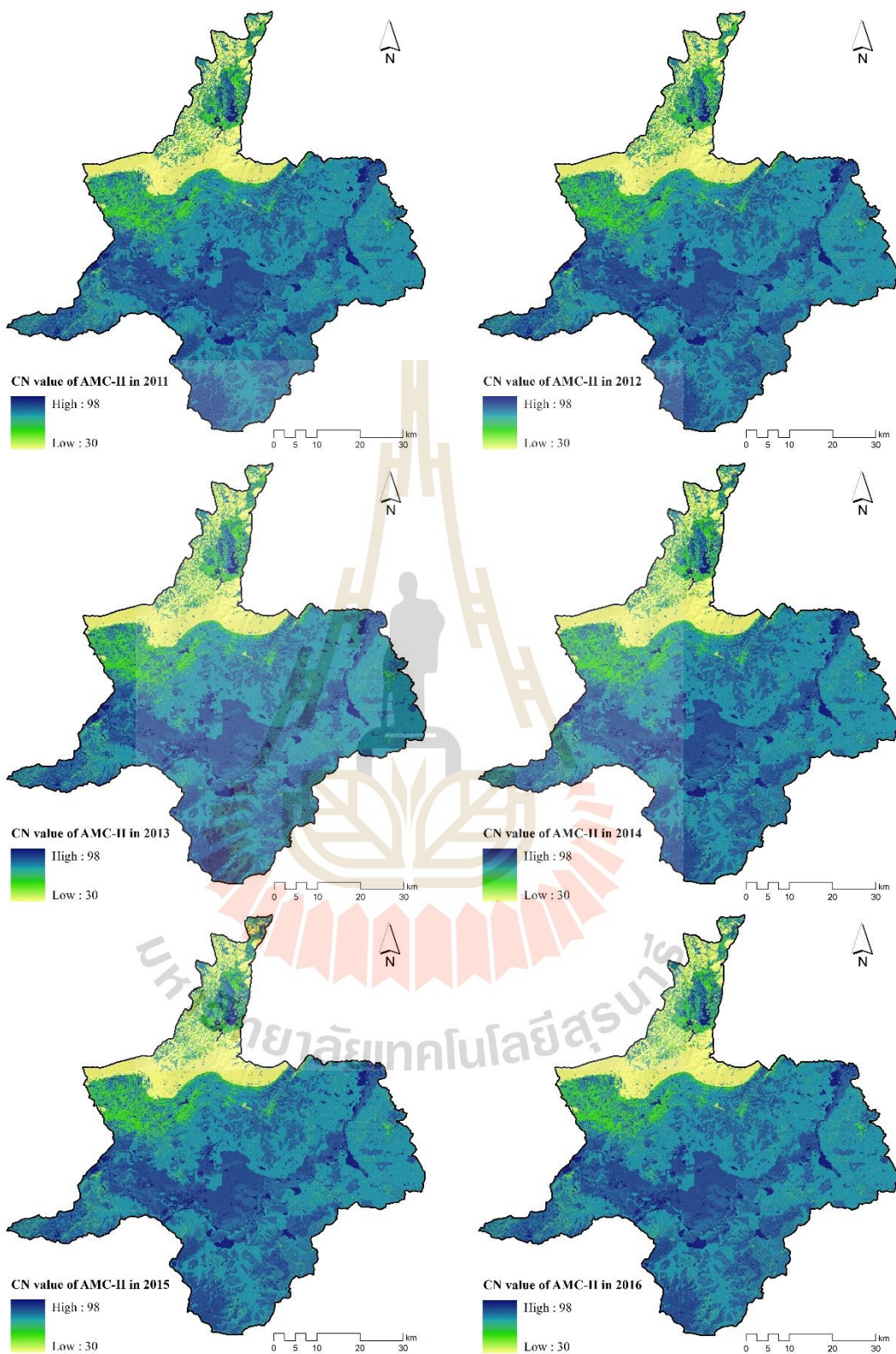
Figure 6.27 Spatial distribution of runoff CN values with AMC-II between 2011 and 2019.
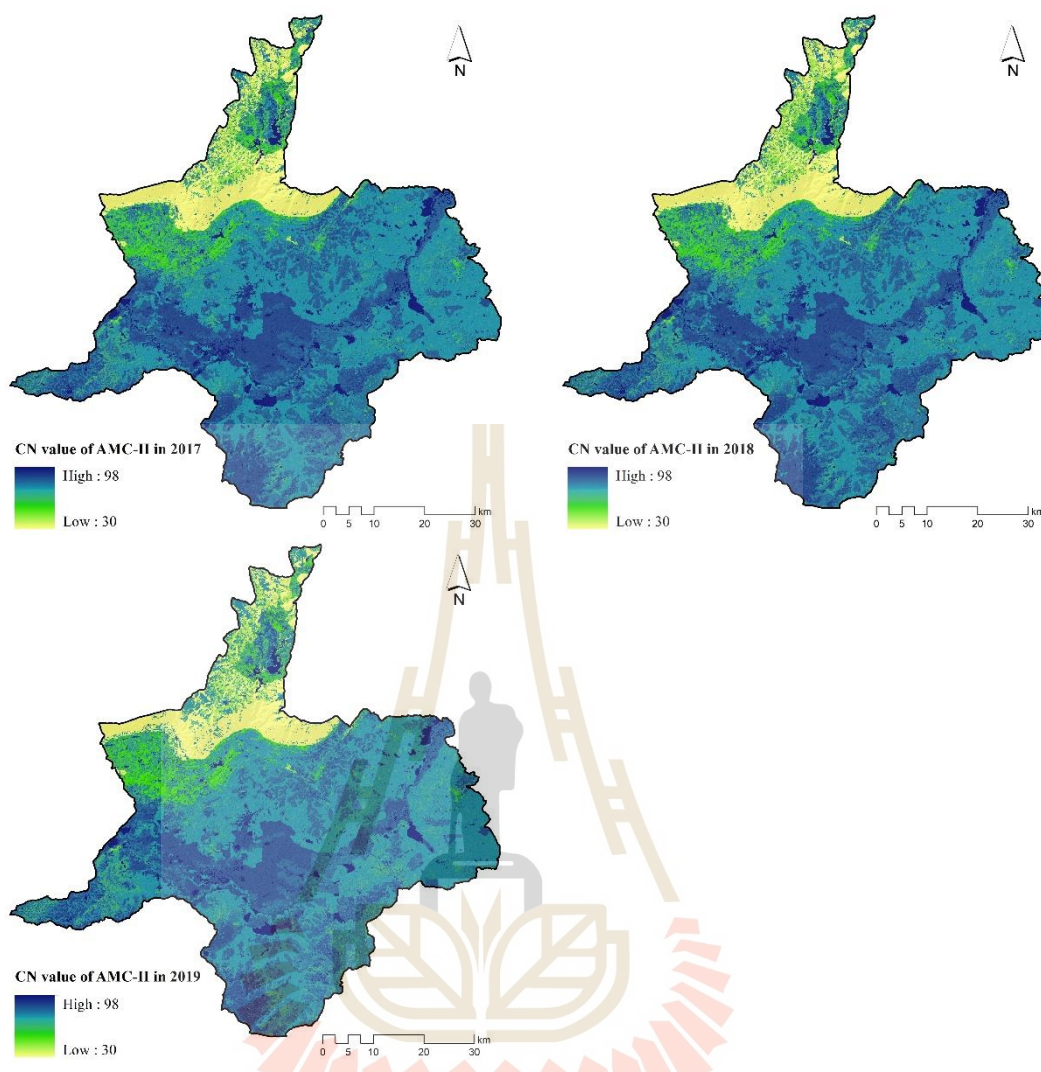
Figure 6.27 (Continued).

Based on the derived CN values of the hydrologic soil group of each LULC type, the potential maximum storage (S) was calculated using Equation 3.3. The spatial distribution of potential maximum storage with AMC-II between 2011 and 2019 was displayed in Figure 6.28. As a result, it was found that the values of potential maximum storage in depth between 2011 and 2019 vary from 235.00 mm to 789.50 mm.
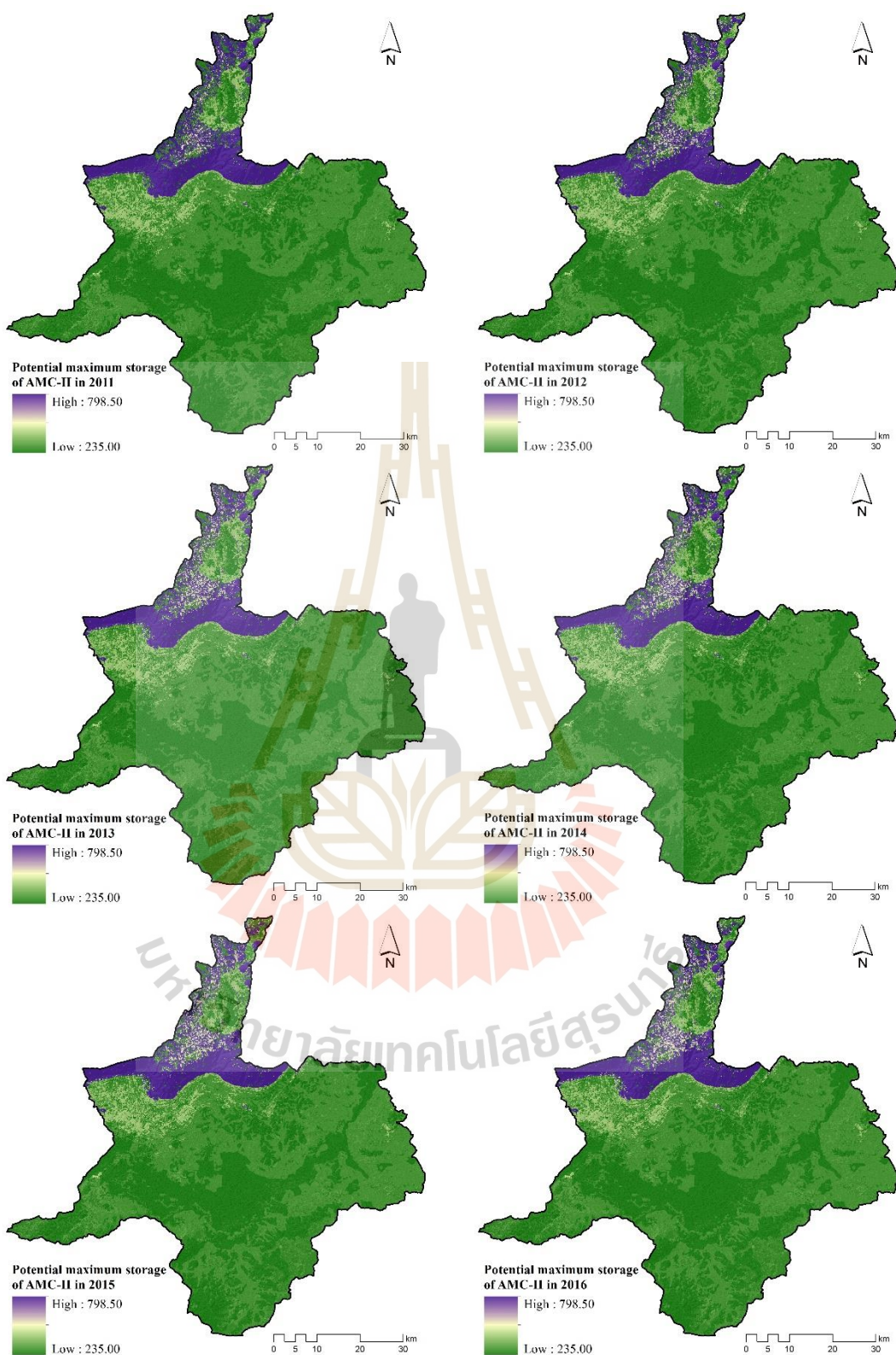
Figure 6.28 Spatial distribution of potential maximum storage (S) with AMC-II between 2011 and 2019.
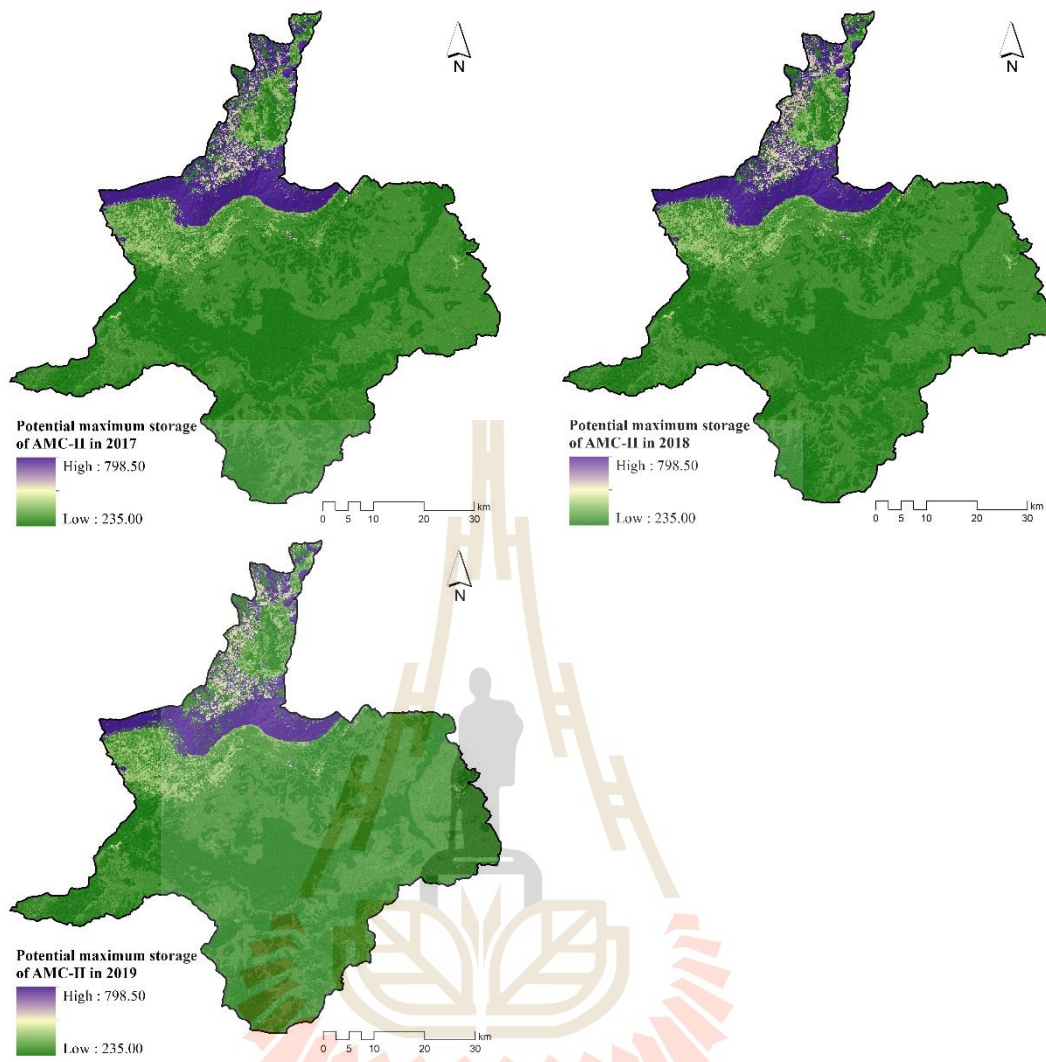
Figure 6.28 (Continued).

Besides, surface runoff estimation with AMC-II between 2011 and 2019 was estimated based on annual rainfall and potential maximum storage using the surface runoff depth equation (Equation 3.4). After that, the estimated surface runoff depth with AMC-II between 2011 and 2019 was converted into surface runoff volume using Equation 3.5. As a result, the spatial distribution of surface runoff with AMC-II between 2011 and 2019 is illustrated in Figure 6.29. Meanwhile, the summary of accumulated surface runoff volume and rainfall between 2001 and 2010 was presented in Table 6.11.
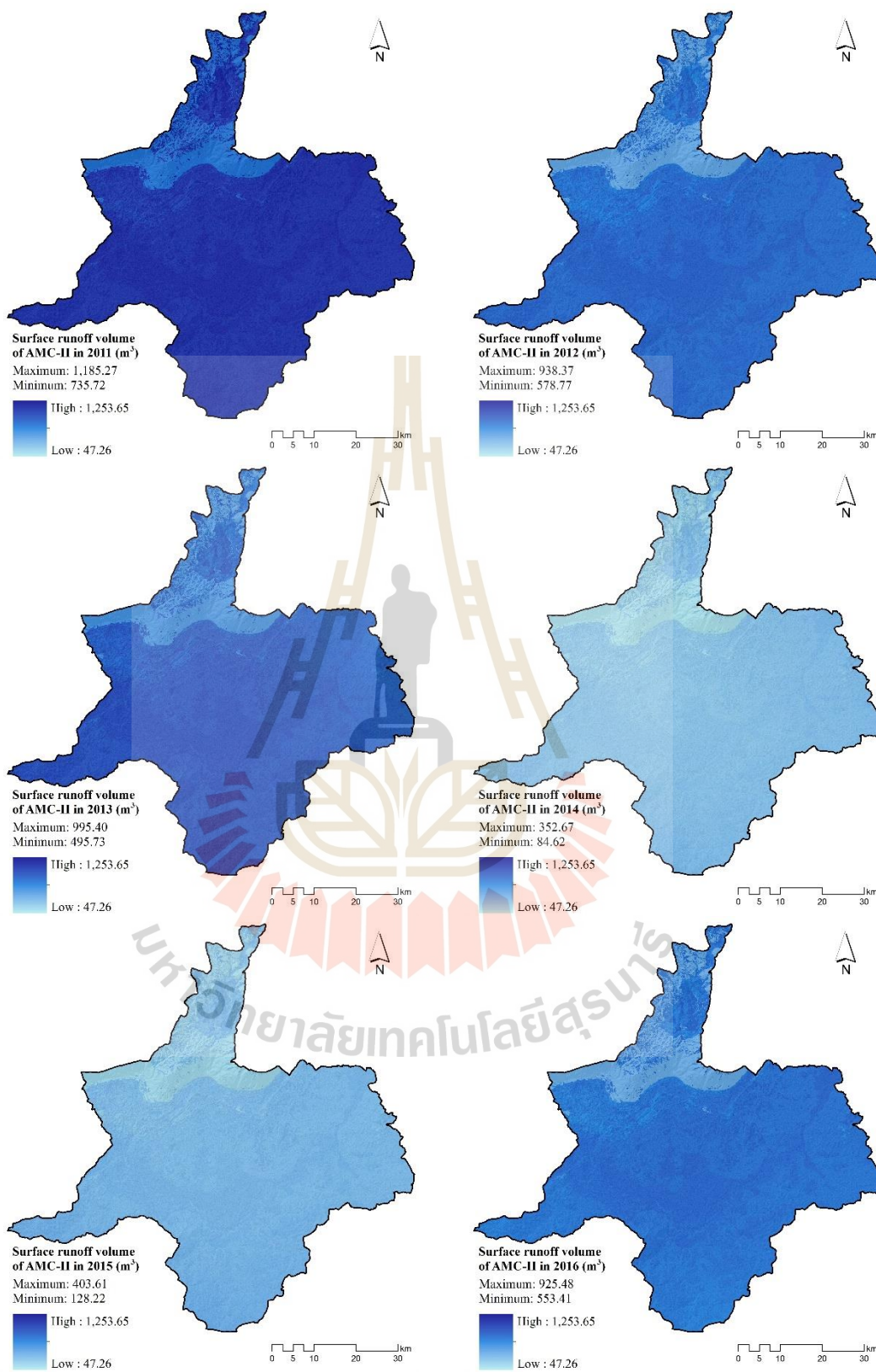
Figure 6.29 Spatial distribution of surface runoff volume between 2011 and 2019.
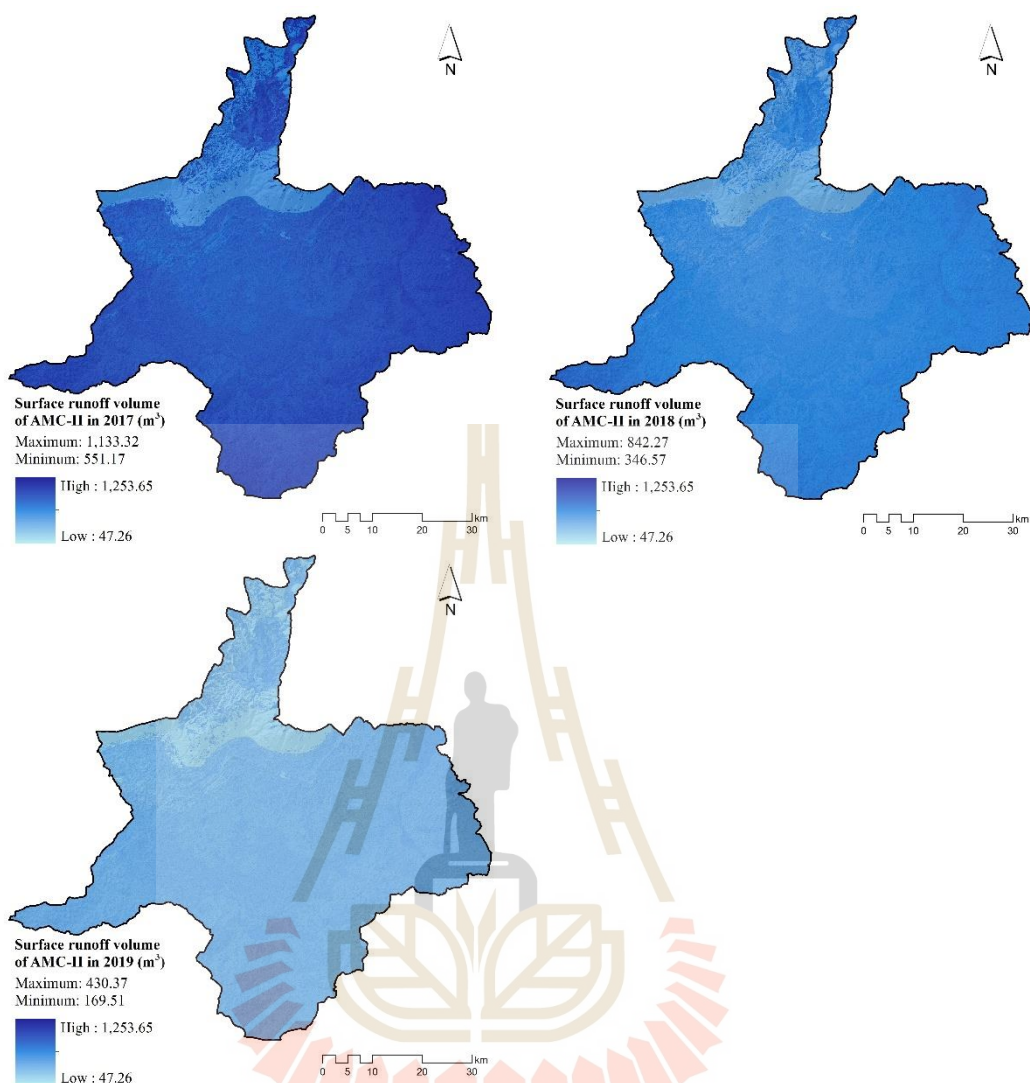
Figure 6.29 (Continued).

Table 6.11 Accumulated surface runoff volume and rainfall between 2011 and 2019.

Year	Annual rainfall (mm)	Surface runoff volume (million m^3)
2011	1,428.30	6,142.43
2012	1,087.20	3,583.03
2013	1,333.30	4,200.48
2014	793.50	1,003.60
2015	919.30	1,233.80
2016	1,044.20	3,475.16
2017	1,281.80	5,433.33
2018	809.00	2,588.57
2019	752.60	1,445.54

As a result, it was found that the accumulated surface runoff volume ranged from 1,003.60 million m^3 in 2014 to 6,142.43 million m^3 in 2011. Figure 6.30 shows the temporal change of the estimated surface runoff volume and annual rainfall data between 2010 and 2019 of the Chaiyaphum Meteorological station, located at the center of the study area. It reveals that the pattern of surface runoff volume and annual rainfall between 2011 and 2019 is similar. The higher the annual rainfall, the higher the surface runoff. This finding was confirmed by simple linear regression analysis, as a result in Figure 6.31. The surface runoff correlates with annual rainfall with the coefficient of determination (R^2) of 0.8511. This coefficient indicates that there is a very good relationship between annual rainfall and surface runoff. The coefficient of determination indicates that the variation in annual rainfall accounts for 85% of the variation in surface runoff.

Additionally, it can be observed that all of them showed positive correlations, showing high correlation coefficient values indicating high variations in the rainfall and the surface runoff. This finding was similar to the previous section of the current study and similar to the results of Canqiang, Wenhua, Biao, and Moucheng (2012). They applied linear regression analysis to identify the relationship between rainfall and runoff in the Xitiaoxi river basin, China.
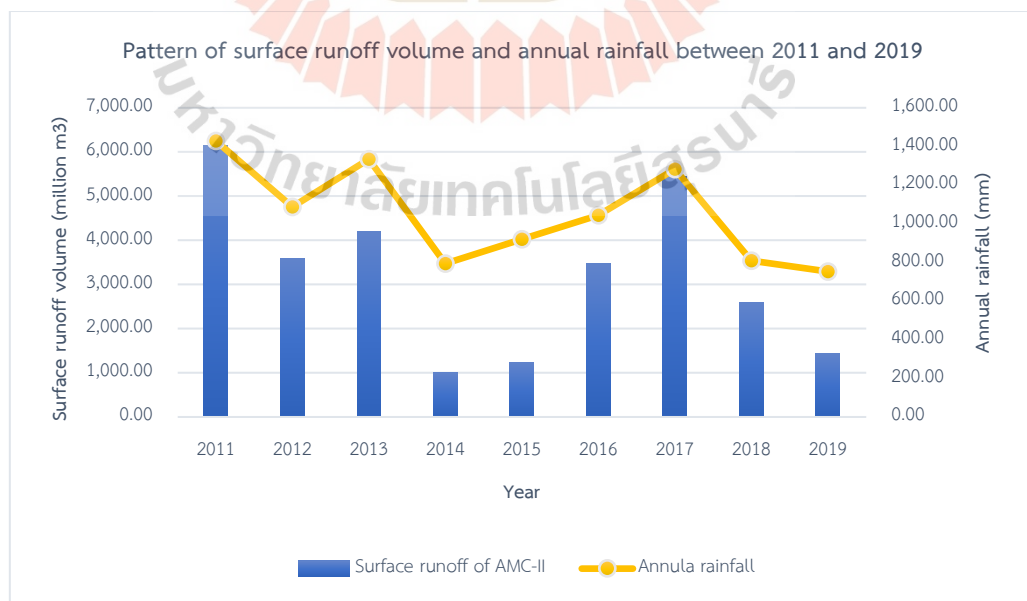
Figure 6.30 Pattern of surface runoff volume and annual rainfall of AMC-II between 2011 and 2019.
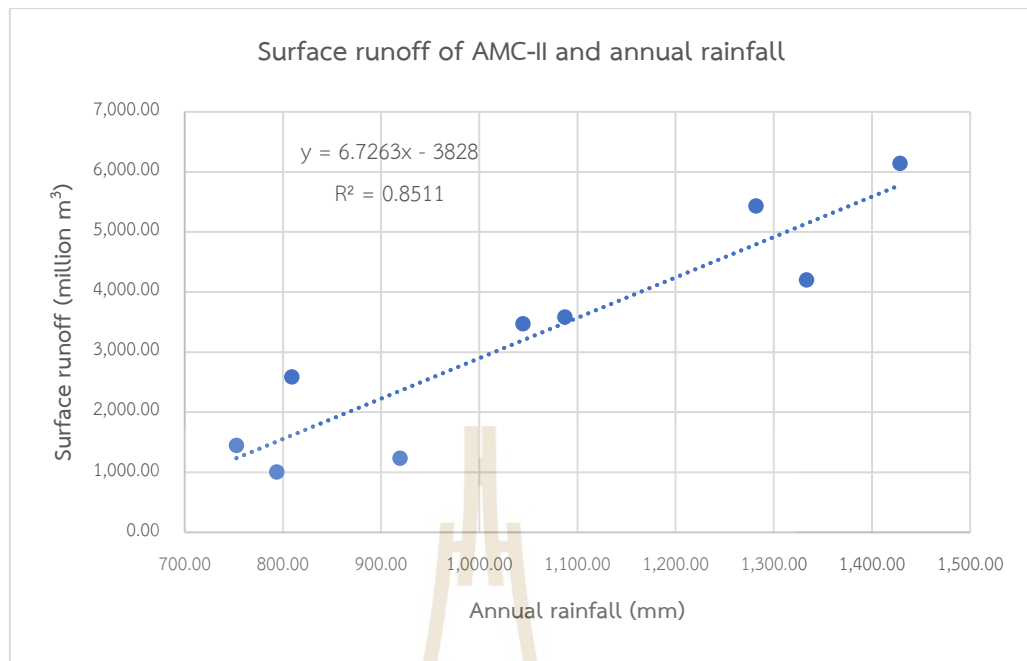
Figure 6.31 Relationship between surface runoff and annual rainfall of AMC-II between 2011 and 2019.

In addition, the estimated surface runoff with AMC-II between 2011 and 2019 from the SCS-CN method was validated based on the observed surface runoff at E.21, E.23, and E6C hydrological station gauges of the Hydrology and Water Center Management for the Upper Northeastern Region using an average NSE, R^2, and PBIAS.

Table 6.12 presented the comparison between observed surface runoff values between 2011 and 2019 from E.21, E23, and E.6C gauge stations and estimated surface runoff with relative error (RE). As a result, the RE ranges from -1,223.63% in 2019 at E.21 hydrological station to 0.82% in 2011 at E.21 hydrological station. A high value of RE indicates a more significant deviation of the computed values from the observed, whereas RE equal to zero shows a perfect fit.

Table 6.12 Compares observed (Q_{obs}) and simulated (Q_{sim}) surface runoff between 2011 and 2019 of three hydrological stations.

Year	E.21 hydrological station			E.23 hydrological station			E.6C hydrological station		
	Q_{obs}	Q_{sim}	RE (%)	Q_{obs}	Q_{sim}	RE (%)	Q_{obs}	Q_{sim}	RE (%)
2011	2,943.40	2,919.23	0.82	2,283.30	1,954.57	14.40	175.78	158.26	9.97
2012	1,989.10	1,694.14	14.83	677.20	882.97	-30.39	112.15	151.54	-35.13
2013	1,884.80	2,058.57	-9.22	1,646.70	1,492.01	9.39	70.59	79.15	-12.12
2014	339.30	600.38	-76.95	330.40	299.17	9.45	19.87	23.05	-15.99
2015	440.80	547.04	-24.10	418.70	272.62	34.89	27.32	53.76	-96.79
2016	1,563.30	1,490.67	4.65	1,058.30	771.66	27.09	87.26	75.27	13.74
2017	2,732.70	2,668.97	2.33	1,823.20	1,563.06	14.27	182.55	166.29	8.91
2018	923.60	1,089.07	-17.92	665.80	573.76	13.82	64.48	78.83	-22.25
2019	60.10	795.50	-1,223.63	84.20	412.55	-389.96	38.25	59.31	-55.07
Avg	1,430.79	1,540.40		998.64	913.60		86.47	93.94	

Note: observed (Q_{obs}) and simulated (Q_{sim}) surface runoff in a million m^3.

Furthermore, the statistical report of model performance for validating surface runoff estimation between 2011 and 2019 is reported in Table 6.13. As a result, the model performance results at the E.21 hydrological station provide NSE and R^2 values of 0.91 and 0.94, respectively. At the same time, PBIAS values range from -5.71% for an overestimation bias in 2019 to 2.29% for an underestimation bias in 2012. These values indicate a perfect fit for surface runoff estimation and a very high correlation between the observed and estimated surface runoff. Meanwhile, the model performance results at the E.23 hydrological station reveal that the NSE and R^2 values are 0.90 and 0.94, which shows a very good fit for surface runoff estimation and a very high correlation between the observed and estimated surface runoff. At the same time, the PBIAS values vary between -3.65% for overestimation bias in 2019 and 3.66% for underestimation bias in 2011. At the same time, the model performance results at the E.6C hydrological station show that the PBIAS values range from -5.06% for overestimation bias in 2012 to 2.25% for underestimation bias in 2011. The NSE and R^2 values are 0.87 and 0.90, which indicate a perfect fit for the surface runoff estimation and a very high correlation between the observed and estimated surface runoff.

Table 6.13 Statistical model performance data for surface runoff estimation between 2011 and 2019 at three hydrological stations.

AMC	Year	E.21 station			E.23 station			E.6C station		
		NSE	R^2	PBIAS	NSE	R^2	PBIAS	NSE	R^2	PBIAS
AMC-II	2011	0.91	0.94	0.19	0.90	0.94	3.66	0.87	0.90	2.25
	2012			2.29			-2.29			-5.06
	2013			-1.35			1.72			-1.10
	2014			-2.03			0.35			-0.41
	2015			-0.83			1.63			-3.40
	2016			0.56			3.19			1.54
	2017			0.49			2.89			2.09
	2018			-1.28			1.02			-1.84
	2019			-5.71			-3.65			-2.71

Furthermore, the scatter plots of the observed and estimated surface runoff between 2011 and 2019 at E.21, E.23, and E.6C hydrological stations, along with the 1:1 line (dash line), are displayed in Figure 6.32. It can be observed that all hydrological station relation lines are almost identical to the 1:1 line. The E.21 and E.6C hydrological station relation lines are slightly above the 1:1 line, indicating that the model is slightly overestimated. In contrast, the E.23 relation line is slightly below the 1:1 line, indicating that the model is slightly underestimated.

According to a statistical report of model performance for surface runoff estimation between 2001 and 2019, the derived NSE and R^2 values are more than 0.65, and the PBIAS value is less than ± 10. These results show a perfect fit for surface runoff estimation with a very high correlation between observed and estimated surface runoff. Thus, it can be concluded that surface runoff estimation using the SCS-CN method in the current study can be validated with acceptable results.

(a) E.21 station

(b) E.23 station

(c) E.6C station
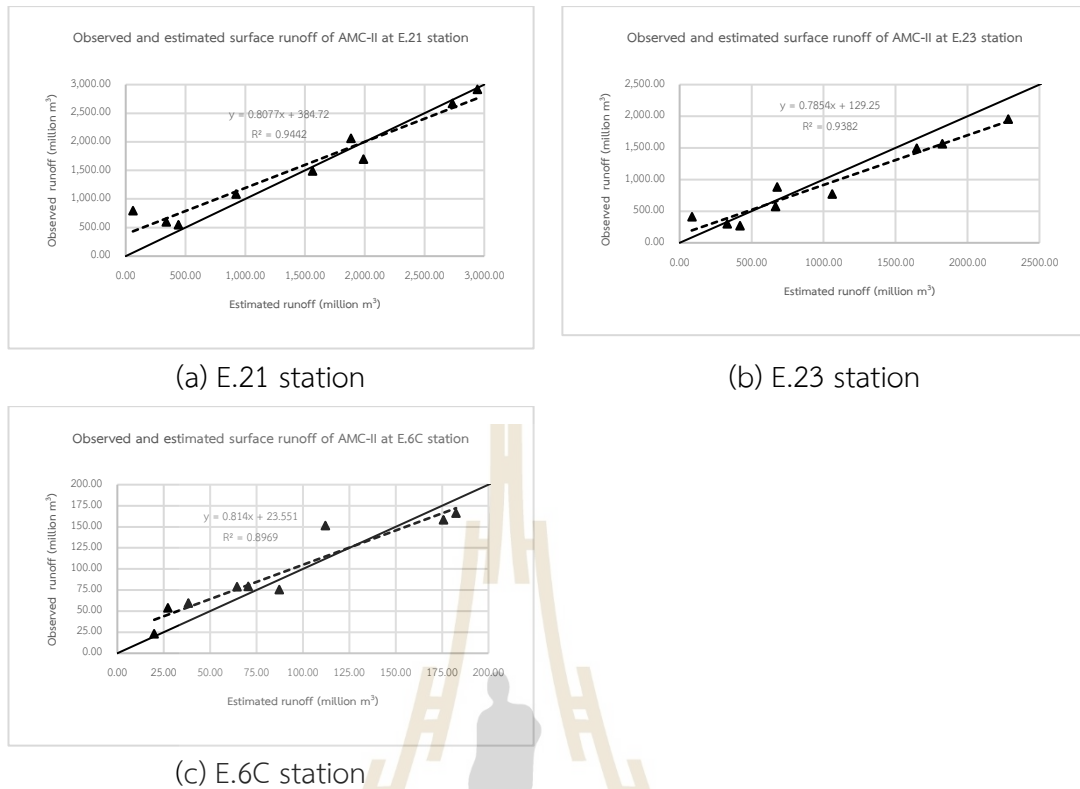
Figure 6.32 Relationship between observed and estimated runoff between 2011 and 2019 at three hydrological stations.

6.4 Contribution of times series LULC data on surface runoff

The time-series estimated surface runoff and LULC data between 2001 and 2019 were used to extract the surface runoff volume of each LULC type using Zonal analysis in the ArcGIS. The surface runoff volume and average surface runoff in each LULC type were presented in Tables 6.14 and 6.15, respectively. In addition, temporal average surface runoff volume by each LULC type was shown in Figure 6.33.

Table 6.14 Characteristics of temporal surface runoff volume by each LULC type between 2001 and 2019.

Item	Year	UR	PA	SU	CA	FC	PR	PO	FO	WA	RA	MA	UL
Surface runoff in million m^3	2001	19.89	948.37	21.72	206.44	0.84	5.72	19.16	163.65	16.33	9.66	5.14	12.84
	2002	58.51	2,931.20	78.69	637.26	2.54	14.74	50.79	572.53	44.98	35.94	18.72	37.71
	2003	24.02	1,120.41	28.52	260.35	1.04	8.89	24.63	191.65	21.16	14.20	9.27	15.32
	2004	22.08	1,011.19	37.31	253.92	1.29	8.70	22.28	181.86	21.68	16.74	10.54	14.78
	2005	28.77	1,295.13	49.84	322.28	1.63	12.68	28.58	238.74	27.28	21.13	13.77	18.06
	2006	64.82	2,795.87	131.60	757.11	3.99	28.46	62.90	634.10	65.27	54.36	33.15	41.10
	2007	53.31	2,195.41	101.77	552.54	3.52	25.30	51.20	474.22	53.98	58.47	31.27	35.14
	2008	90.51	3,753.83	218.18	974.64	7.35	45.48	85.01	893.75	95.31	88.58	55.16	58.99
	2009	68.59	2,704.53	173.42	719.88	5.27	35.16	61.29	621.00	75.53	75.06	45.33	44.83
	2010	94.53	3,521.63	256.02	1,062.73	8.38	45.11	83.01	840.91	99.75	120.34	58.73	58.18
	2011	92.28	3,432.00	249.99	1,066.22	8.32	55.65	81.33	825.69	98.39	118.36	55.75	58.45
	2012	58.21	2,014.75	175.45	603.86	4.87	37.33	47.52	432.15	58.89	69.27	35.47	45.27
	2013	68.08	2,356.67	218.44	678.11	5.64	50.11	58.11	511.41	68.22	80.20	45.00	60.48
	2014	17.41	577.90	52.41	177.70	1.40	13.78	14.36	84.07	18.29	20.12	11.24	14.92
	2015	21.62	698.75	74.42	208.59	1.67	18.86	20.01	105.28	21.91	25.57	12.63	24.48
	2016	59.67	1,955.92	211.29	514.54	5.55	55.98	54.40	381.68	57.12	70.39	35.86	72.78
	2017	89.81	2,987.11	341.87	813.31	8.34	103.60	100.93	631.07	87.87	106.24	47.92	115.26
	2018	44.36	1,425.02	187.82	381.26	3.56	50.55	48.89	261.88	43.86	51.19	28.05	62.14
	2019	28.94	812.89	118.35	199.66	2.45	29.95	32.81	116.98	23.49	28.43	12.55	39.04
	AVG	52.92	2,028.35	143.53	546.86	4.09	34.00	49.85	429.61	52.60	56.01	29.77	43.67

Table 6.15 Characteristics of average surface runoff volume by each LULC type between 2001 and 2019.

Item		LULC type											
	Year	UR	PA	SU	CA	FC	PR	PO	FO	WA	RA	MA	UL
Average surface runoff in million m³ per km²	2001	0.43	0.40	0.35	0.39	0.40	0.35	0.34	0.26	0.44	0.37	0.44	0.45
	2002	1.25	1.27	1.10	1.17	1.04	0.82	0.92	0.91	1.15	1.15	1.33	1.29
	2003	0.50	0.49	0.35	0.47	0.37	0.45	0.45	0.31	0.51	0.39	0.56	0.51
	2004	0.46	0.45	0.41	0.45	0.41	0.41	0.41	0.29	0.50	0.40	0.56	0.48
	2005	0.58	0.58	0.49	0.56	0.47	0.56	0.54	0.39	0.59	0.45	0.65	0.58
	2006	1.30	1.28	1.17	1.29	1.04	1.18	1.19	1.03	1.35	1.05	1.39	1.29
	2007	1.05	1.02	0.83	0.93	0.84	0.99	0.98	0.77	1.07	1.03	1.20	1.08
	2008	1.75	1.76	1.64	1.60	1.63	1.68	1.65	1.46	1.80	1.43	1.93	1.79
	2009	1.31	1.29	1.21	1.16	1.08	1.23	1.21	1.02	1.37	1.12	1.46	1.33
	2010	1.78	1.70	1.67	1.69	1.61	1.50	1.65	1.39	1.74	1.67	1.76	1.69
	2011	1.69	1.66	1.47	1.74	1.56	1.48	1.49	1.40	1.73	1.64	1.70	1.43
	2012	1.04	0.98	0.94	1.01	0.90	0.83	0.81	0.75	1.04	0.96	1.10	0.95
	2013	1.18	1.15	1.07	1.16	1.02	0.96	0.92	0.91	1.22	1.11	1.43	1.12
	2014	0.30	0.28	0.24	0.31	0.25	0.23	0.21	0.15	0.33	0.28	0.36	0.25
	2015	0.36	0.34	0.31	0.38	0.29	0.28	0.28	0.20	0.40	0.36	0.42	0.36
	2016	0.97	0.96	0.83	0.96	0.95	0.75	0.72	0.73	1.04	0.98	1.21	0.99
	2017	1.42	1.48	1.25	1.56	1.40	1.26	1.26	1.24	1.62	1.48	1.66	1.44
	2018	0.69	0.71	0.65	0.75	0.59	0.56	0.58	0.53	0.82	0.71	0.99	0.72
	2019	0.44	0.40	0.39	0.41	0.40	0.31	0.37	0.24	0.44	0.40	0.45	0.42
	AVG	0.97	0.96	0.86	0.95	0.86	0.83	0.84	0.74	1.01	0.89	1.08	0.96
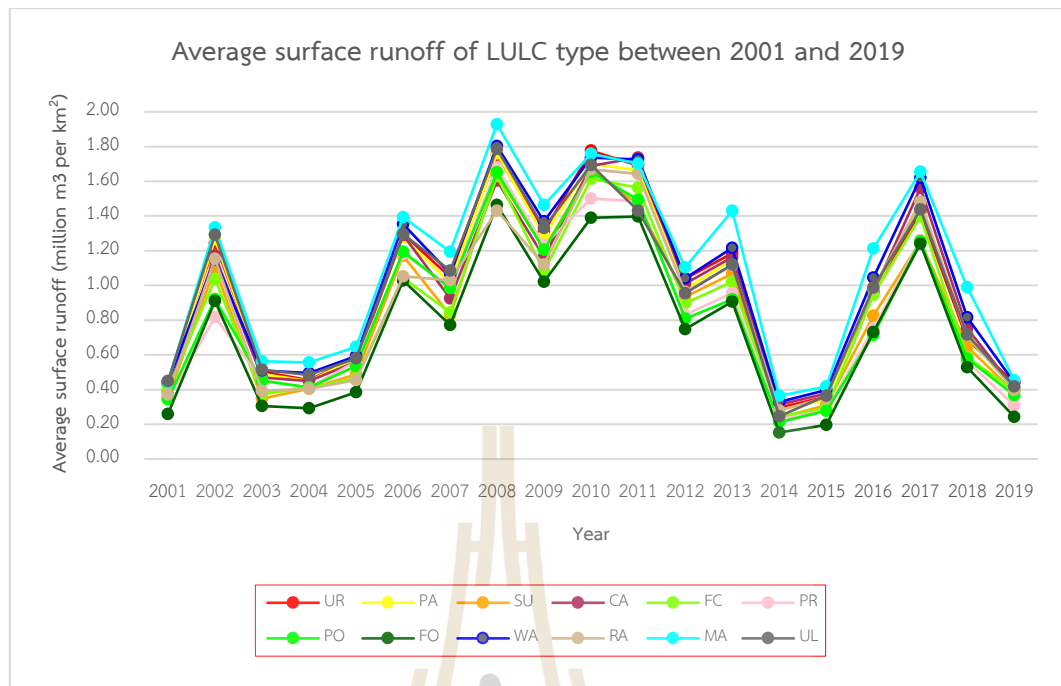
Figure 6.33 Average surface runoff volume of LULC type during 2001 to 2019.

As a result, the top three most dominant LULC types on surface runoff are paddy field, cassava, and forest land, which provide surface runoff of 2,028.35, 546.86, and 429.61 million m^3, respectively. On the other hand, the top three least dominant LULC types on surface runoff are other field crops, marsh and swamp, and unused land, which provides a surface runoff of 4.09, 29.77, and 43.67 million m^3, respectively.

In addition, it can be observed that marsh and swamp provide the highest average surface runoff every year, while forest land provides the lowest surface runoff every year. In the meantime, the average surface runoff of para rubber, orchard and perennial trees, and field crops (sugarcane, cassava, and other field crops) are similar. This character corresponds to the CN values; marsh and swamp provide the highest CN value while forest land provides the lowest CN value. These findings indicate the influence of LULC type on surface runoff.

CHAPTER VII

OPTIMIZATION AND MAPPING OF LAND USE AND LAND COVER

ALLOCATION FOR FLOOD MITIGATION

This chapter presents the fourth and fifth objectives regarding optimization and mapping of LULC allocation for flood mitigation in the Second Part of the Lam Nam Chi watershed. Briefly, the fourth objective focuses on optimizing LULC allocation to minimize surface runoff for flood mitigation using Goal programming. Meanwhile, the fifth objective focuses on mapping LULC allocation for flooding mitigation using the CLUE-S model. The significant results in this chapter consist of (1) SPI calculation for rainfall condition identification, (2) optimization of LULC allocation for flood mitigation, and (3) mapping of LULC allocation for flood mitigation are here described and discussed in detail.

7.1   SPI calculation for rainfall condition identification

The historical rainfall data records from 33 years (between 1987 and 2019) of the Chaiyaphum meteorological station (Figure 7.1) were applied to identify rainfall conditions in the study area using SPI. In this study, 12-month SPI was first calculated for a given month using monthly precipitation data in the current and previous months. After that, the derived cumulative probability of SPI values was further classified into seven drought types (Table 2.3), as suggested by Liu et al. (2014), and they reclassify into three rainfall conditions: drought, normal, and wet year, as mentioned in CHAPTER III: RESEARCH PROCEDURES.

The 12-month SPI distribution between 1987 and 2019 is presented in Figure 7.2 and Table 7.1. As a result, it reveals that the SPI values in the study period range from -1.70 to 2.14. The SPI with values less than or equal to -0.50 are found in 2001, 2003, 2004, 2014, 2015, 2018, and 2019 and these years are categorized as drought year conditions. Meanwhile, the SPI with values between -0.49 and 0.49 are found in 2002, 2005, 2006, 2012, and 2016 and these years are categorized as normal year

conditions. In the meantime, the SPI with values more than or equal to 0.50 are found in 2007, 2008, 2009, 2010, 2011, 2013, and 2017, and they are grouped as wet year conditions. So, the derived surface runoff in drought, normal, and wet year conditions were further applied to calculate the average surface runoff coefficient of each LULC type under three different rainfall conditions (drought, normal, and wet year).

Table 7.1 SPI values, drought categories, and rainfall conditions based on rainfall at Chaiyaphum meteorological station between 1987 and 2019.

Year	SPI	Drought classification[1]	Rainfall condition
1987	0.77	Mild wet	Wet year
1988	-0.21	Near normal	Normal year
1989	-0.58	Mild drought	Drought year
1990	-0.02	Near normal	Normal year
1991	-0.35	Near normal	Normal year
1992	-0.57	Mild drought	Drought year
1993	-0.88	Mild drought	Drought year
1994	-0.12	Near normal	Normal year
1995	1.09	Moderate wet	Wet year
1996	0.36	Mild wet	Wet year
1997	-1.65	Severe drought	Drought year
1998	-0.19	Near normal	Normal year
1999	-0.14	Near normal	Normal year
2000	2.14	Extreme wet	Wet year
2001	-0.76	Mild drought	Drought year
2002	0.31	Near normal	Normal year
2003	-0.95	Mild drought	Drought year
2004	-0.88	Mild drought	Drought year
2005	-0.32	Near normal	Normal year
2006	0.32	Near normal	Normal year
2007	0.87	Mild wet	Wet year
2008	2.06	Extreme wet	Wet year

Table 7.1 (Continued).

Year	SPI	Drought classification[1]	Rainfall condition
2009	1.43	Moderate wet	Wet year
2010	1.45	Moderate wet	Wet year
2011	1.18	Moderate wet	Wet year
2012	-0.12	Near normal	Normal year
2013	0.84	Mild wet	Wet year
2014	-1.48	Moderate drought	Drought year
2015	-0.86	Mild drought	Drought year
2016	-0.30	Near normal	Normal year
2017	0.65	Mild wet	Wet year
2018	-1.40	Moderate drought	Drought year
2019	-1.70	Severe drought	Drought year

Note [1] SPI drought classification by Liu et al. (2014).
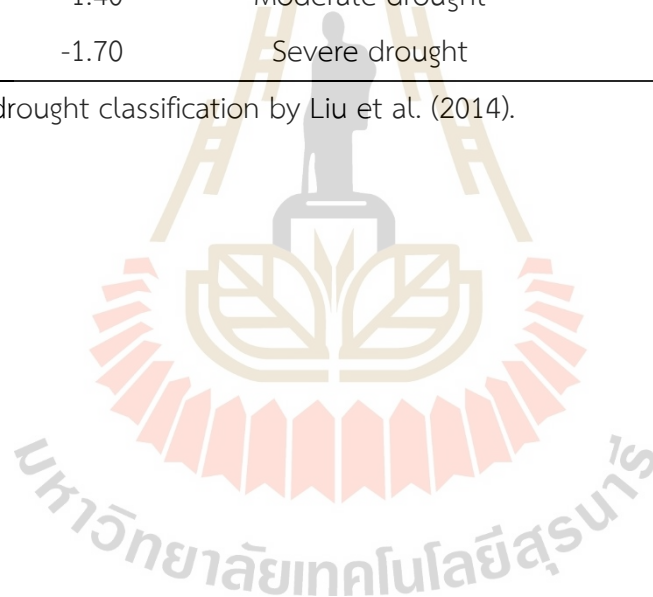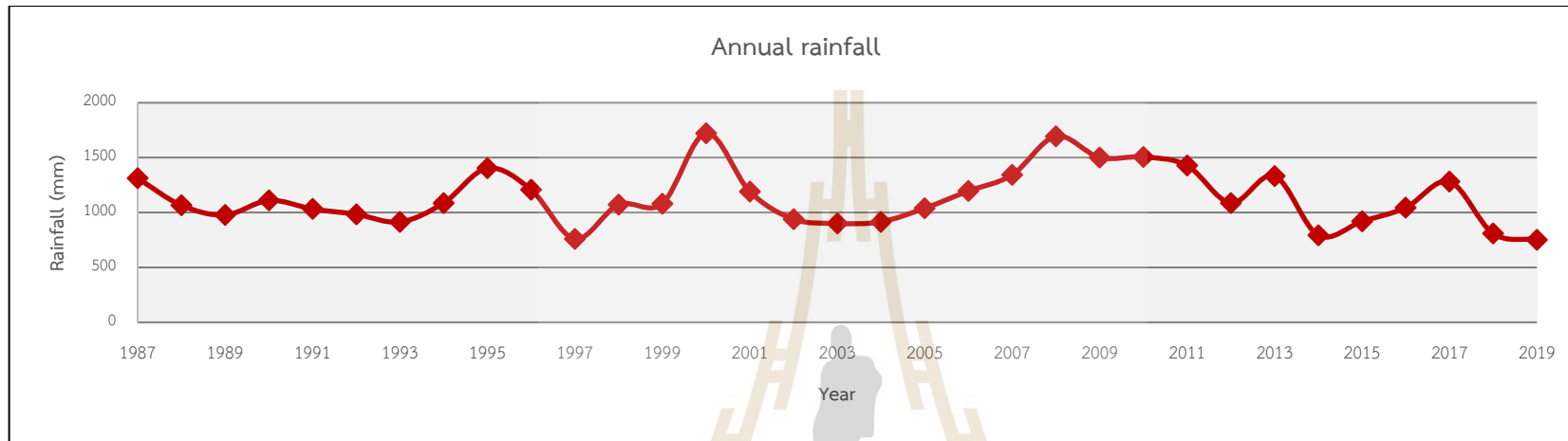
Figure 7.1 Annual rainfall of Chaiyaphum meteorological station between 1987 and 2019.
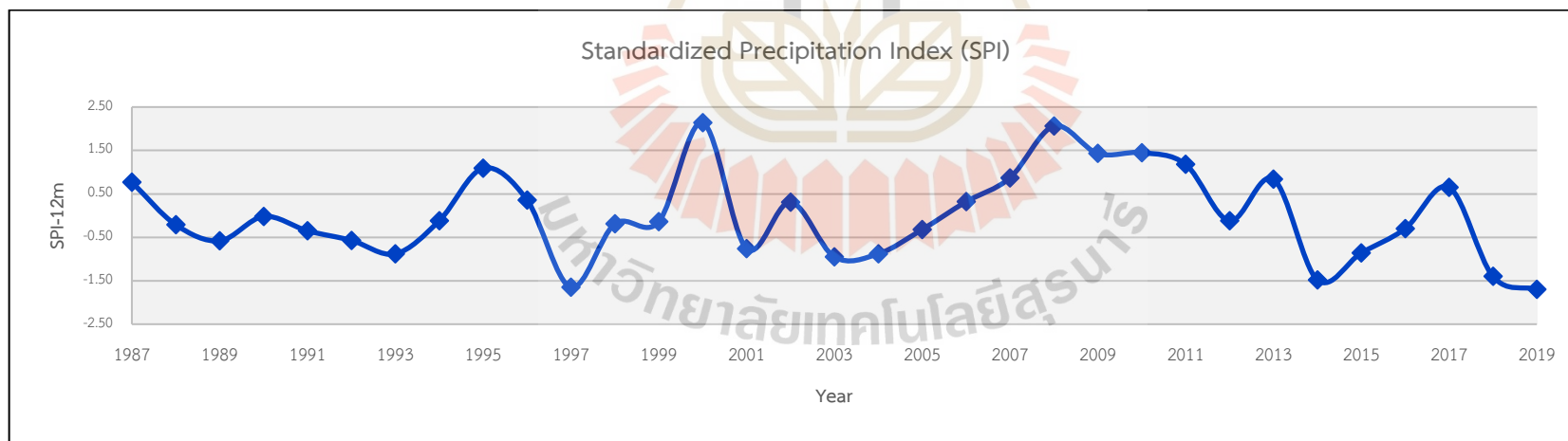
Figure 7.2 SPI values of Chaiyaphum meteorological station between 1987 and 2019.

7.2   Optimization of LULC allocation for flood mitigation

In this study, the Goal programming of multi-objective decision analysis (MODA) was applied to allocate optimum LULC to minimize surface runoff for flood mitigation based on the average surface runoff coefficient from LULC in drought years (2001, 2003, 2004, 2014, 2015, 2018, and 2019), normal years (2002, 2005, 2006, 2012, and 2016), and wet years (2007, 2008, 2009, 2010, 2011, 2013, and 2017). Here, "What's Best!" as an extension program under Microsoft Excel software was used to allocate an area of LULC based on the surface runoff volume in three different rainfall conditions (drought, normal, and wet years) with the simplex method.

In practice, the average annual surface runoff of each LULC type in drought, normal, and wet year conditions were separately calculated and applied as a surface runoff coefficient for optimizing LULC allocation of three different rainfall conditions using the Goal programming. As a result, an average surface runoff coefficient of each LULC type under three different rainfall conditions is separately displayed in Tables 7.2 to 7.4.

At the same time, the constraints of the Goal programming are subjected to the change of LULC area in the study area. The constraints for optimizing LULC allocation for flood mitigation were assigned based on the historical LULC development between 2010 and 2019 using the Markov Chain model. In this study, ten years period was chosen to predict LULC data in 2029, 2039, and 2049 based on a period of input data (2010-2019) for transitional area prediction by the Markov Chain model.

Additionally, the changing area of each LULC type was categorized into two groups: decreased area (paddy field, cassava, forest land, waterbody, rangeland, and marsh and swamp) and increased area (urban and built-up area, sugarcane, other field crops, para rubber, perennial trees and orchard, and unused land) according to the derived transitional change area from Markov Chain model. Details of LULC change to minimize surface runoff in 2029, 2039, and 2049 as constraints of Goal programming are summarized in Tables 7.5 to 7.7.

Table 7.2 Surface runoff coefficient and its average in the drought year condition.

No.	LULC type	Runoff coefficient (million m³/km²)							Average runoff coefficient (million m³/km²)
		2001	2003	2004	2014	2015	2018	2019	
1	Urban and built-up area	0.43	0.50	0.46	0.30	0.36	0.69	0.44	**0.45**
2	Paddy field	0.40	0.49	0.45	0.28	0.34	0.71	0.40	**0.44**
3	Sugarcane	0.35	0.35	0.41	0.24	0.31	0.65	0.39	**0.38**
4	Cassava	0.39	0.47	0.45	0.31	0.38	0.75	0.41	**0.45**
5	Other field crops	0.40	0.37	0.41	0.25	0.29	0.59	0.40	**0.39**
6	Para rubber	0.35	0.45	0.41	0.23	0.28	0.56	0.31	**0.37**
7	Perennial trees and orchard	0.34	0.45	0.41	0.21	0.28	0.58	0.37	**0.38**
8	Forest land	0.26	0.31	0.29	0.15	0.20	0.53	0.24	**0.28**
9	Water body	0.44	0.51	0.50	0.33	0.40	0.82	0.44	**0.49**
10	Rangeland	0.37	0.39	0.40	0.28	0.36	0.71	0.40	**0.42**
11	Marsh and swamp	0.44	0.56	0.56	0.36	0.42	0.99	0.45	**0.54**
12	Unused land	0.45	0.51	0.48	0.25	0.36	0.72	0.42	**0.46**

Table 7.3 Surface runoff coefficient and its average in the normal year condition.

No.	LULC type	Runoff coefficient (million m^3/km^2)					Average runoff coefficient (million m^3/km^2)
		2002	2005	2006	2012	2016	
1	Urban and built-up area	1.25	0.58	1.30	1.04	0.97	**1.03**
2	Paddy field	1.27	0.58	1.28	0.98	0.96	**1.01**
3	Sugarcane	1.10	0.49	1.17	0.94	0.83	**0.90**
4	Cassava	1.17	0.56	1.29	1.01	0.96	**1.00**
5	Other field crops	1.04	0.47	1.04	0.90	0.95	**0.88**
6	Para rubber	0.82	0.56	1.18	0.83	0.75	**0.83**
7	Perennial trees and orchard	0.92	0.54	1.19	0.81	0.72	**0.84**
8	Forest land	0.91	0.39	1.03	0.75	0.73	**0.76**
9	Water body	1.15	0.59	1.35	1.04	1.04	**1.04**
10	Rangeland	1.15	0.45	1.05	0.96	0.98	**0.92**
11	Marsh and swamp	1.33	0.65	1.39	1.10	1.21	**1.14**
12	Unused land	1.29	0.58	1.29	0.95	0.99	**1.02**

Table 7.4 Surface runoff coefficient and its average in the wet year condition.

No.	LULC type	Runoff coefficient (million m³/km²)							Average runoff coefficient (million m³/km²)
		2007	2008	2009	2010	2011	2013	2017	
1	Urban and built-up area	1.05	1.75	1.31	1.78	1.69	1.18	1.42	**1.46**
2	Paddy field	1.02	1.76	1.29	1.70	1.66	1.15	1.48	**1.44**
3	Sugarcane	0.83	1.64	1.21	1.67	1.47	1.07	1.25	**1.30**
4	Cassava	0.93	1.60	1.16	1.69	1.74	1.16	1.56	**1.41**
5	Other field crops	0.84	1.63	1.08	1.61	1.56	1.02	1.40	**1.31**
6	Para rubber	0.99	1.68	1.23	1.50	1.48	0.96	1.26	**1.30**
7	Perennial trees and orchard	0.98	1.65	1.21	1.65	1.49	0.92	1.26	**1.31**
8	Forest land	0.77	1.46	1.02	1.39	1.40	0.91	1.24	**1.17**
9	Water body	1.07	1.80	1.37	1.74	1.73	1.22	1.62	**1.51**
10	Rangeland	1.03	1.43	1.12	1.67	1.64	1.11	1.48	**1.36**
11	Marsh and swamp	1.20	1.93	1.46	1.76	1.70	1.43	1.66	**1.59**
12	Unused land	1.08	1.79	1.33	1.69	1.43	1.12	1.44	**1.41**

Table 7.5 Existing and predicted area of LULC in 2029 for constraint setting.

LULC type	Existing area (km^2)	Predicted area (km^2)	Remark
Urban and built-up area (X_1)	65.84	77.38	Increment by 0.17%
Paddy field (X_2)	2,012.16	1,947.12	Reduction by 0.03%
Sugarcane (X_3)	306.85	424.95	Increment by 0.38%
Cassava (X_4)	489.91	408.26	Reduction by 0.16%
Other field crops (X_5)	6.19	7.72	Increment by 0.27%
Para rubber (X_6)	97.03	134.43	Increment by 0.38%
Perennial trees and orchard (X_7)	88.95	125.36	Increment by 0.40%
Forest land (X_8)	481.30	382.63	Reduction by 0.20%
Waterbody (X_9)	53.30	49.52	Reduction by 0.07%
Rangeland (X_{10})	71.65	70.54	Reduction by 0.01%
Marsh and swamp (X_{11})	27.73	25.13	Reduction by 0.09%
Unused land (X_{12})	93.31	141.20	Increment by 0.51%
SUM	**3,794.22**	**3,794.22**	

Table 7.6 Existing and predicted area of LULC in 2039 for constraint setting.

LULC type	Existing area (km^2)	Predicted area (km^2)	Remark
Urban and built-up area (X_1)	65.84	88.31	Increment by 0.34%
Paddy field (X_2)	2,012.16	1,879.30	Reduction by 0.06%
Sugarcane (X_3)	306.85	520.31	Increment by 0.69%
Cassava (X_4)	489.91	358.65	Reduction by 0.26%
Other field crops (X_5)	6.19	9.4525	Increment by 0.52%
Para rubber (X_6)	97.03	152.02	Increment by 0.56%
Perennial trees and orchard (X_7)	88.95	160.12	Increment by 0.80%
Forest land (X_8)	481.30	304.44	Reduction by 0.36%
Waterbody (X_9)	53.30	47.01	Reduction by 0.13%
Rangeland (X_{10})	71.65	69.91	Reduction by 0.02%
Marsh and swamp (X_{11})	27.73	24.66	Reduction by 0.11%
Unused land (X_{12})	93.31	180.07	Increment by 0.93%
SUM	**3,794.22**	**3,794.22**	

Table 7.7 Existing and predicted area of LULC in 2049 for constraint setting.

LULC type	Existing area (km^2)	Predicted area (km^2)	Remark
Urban and built-up area (X_1)	65.84	99.03	Increment by 0.50%
Paddy field (X_2)	2,012.16	1,812.16	Reduction by 0.09%
Sugarcane (X_3)	306.85	599.36	Increment by 0.95%
Cassava (X_4)	489.91	330.32	Reduction by 0.32%
Other field crops (X_5)	6.19	11.26	Increment by 0.81%
Para rubber (X_6)	97.03	164.41	Increment by 0.69%
Perennial trees and orchard (X_7)	88.95	193.13	Increment by 1.17%
Forest land (X_8)	481.30	242.23	Reduction by 0.49%
Waterbody (X_9)	53.30	42.78	Reduction by 0.19%
Rangeland (X_{10})	71.65	66.05	Reduction by 0.07%
Marsh and swamp (X_{11})	27.73	21.61	Reduction by 0.07%
Unused land (X_{12})	93.31	212.00	Increment by 1.27%
SUM	3,794.22	3,794.22	

Based on the linearity of objective function and constraints, the objective functions of the surface runoff minimization problem for optimizing LULC allocation under drought, normal, and wet year can be formulated as shown in Equations 7.1 to 7.3, respectively:

$$\text{Min}(Z) = 0.45X_1+0.44X_2+0.38X_3+0.45X_4+0.39X_5+0.37X_6+0.38X_7+0.28X_8$$
$$+0.49X_9+0.42X_{10}+0.54X_{11}+0.46X_{12} \tag{7.1}$$

$$\text{Min}(Z) = 1.03X_1+1.01X_2+0.90X_3+1.00X_4+0.88X_5+0.83X_6+0.84X_7+0.76X_8$$
$$+1.04X_9+0.92X_{10}+1.14X_{11}+1.02X_{12} \tag{7.2}$$

$$\text{Min}(Z) = 1.46X_1+1.44X_2+1.30X_3+1.41X_4+1.31X_5+1.30X_6+1.31X_7+1.17X_8$$
$$+1.51X_9+1.36X_{10}+1.59X_{11}+1.41X_{12} \tag{7.3}$$

The above objective functions were then subjected to the constraints to minimize surface runoff in the future for 2029, 2039, and 2049 under three different rainfall conditions.

Details of the objective function constraints to minimize surface runoff for optimized LULC in 2029 under three different rainfall conditions (drought, normal, and wet years) were listed below.

The first constraint is related to the existing area of the urban and built-up area should be more than or equal to 65.84 km^2 as formulated in Equation 7.4.

$$X_1 \geq 65.84 \tag{7.4}$$

The second constraint relates to the existing urban and built-up area is 65.84 km^2, but it can be expandable up to 77.38 km^2 as formulated in Equation 7.5.

$$X_1 \leq 77.38 \tag{7.5}$$

The third constraint is related to the maximum area of the paddy field should be less than or equal to 2,012.16 km^2 as formulated in Equation 7.6.

$$X_2 \leq 2,012.16 \tag{7.6}$$

The fourth constraint relates to the paddy field's existing area is 2,012.16 km^2, but it can be decreased to 1,947.12 km^2 as formulated in Equation 7.7.

$$X_2 \geq 1,947.12 \tag{7.7}$$

The fifth constraint is related to the existing area of sugarcane should be more than or equal to 306.85 km^2 as formulated in Equation 7.8.

$$X_3 \geq 306.85 \tag{7.8}$$

The sixth constraint relates to the maximum sugarcane area is 306.85 km^2, but it can be increased to 424.95 km^2 as formulated in Equation 7.9.

$$X_3 \leq 424.95 \tag{7.9}$$

The seventh constraint is related to the existing area of cassava should be less than or equal to 489.91 km^2 as formulated in Equation 7.10.

$$X_4 \leq 489.91 \tag{7.10}$$

The eighth constraint relates to the maximum area of cassava is 489.91 km^2, but it can be reduced to 408.26 km^2 as formulated in Equation 7.11.

$$X_4 \geq 408.26 \tag{7.11}$$

The ninth constraint is related to the existing area of other field crops should be more than or equal to 6.19 km^2 as formulated in Equation 7.12.

$$X_5 \geq 6.19 \tag{7.12}$$

The tenth constraint is related to the maximum area of other field crops, which is 5.19 km^2 but can be increased to 7.72 km^2 as formulated in Equation 7.13.

$$X_5 \leq 7.72 \tag{7.13}$$

The eleventh constraint is related to the area of para rubber that should be more than or equal to 97.03 km^2 as formulated in Equation 7.14.

$$X_6 \geq 97.03 \tag{7.14}$$

The twelfth constraint is related to the maximum area of para rubber is 97.03 km^2, but it can exceed up to 134.43 km^2 as formulated in Equation 7.15.

$$X_6 \leq 134.43 \tag{7.15}$$

The thirteenth constraint is related to the existing area of the perennial trees and orchards should be more than or equal to 88.95 km^2 as formulated in Equation 7.16.

$$X_7 \geq 88.95 \tag{7.16}$$

The fourteenth constraint relates to the maximum area of perennial trees and orchards is 88.95 km^2, but it can be increased to 125.36 km^2 as formulated in Equation 7.17.

$$X_7 \leq 125.36 \tag{7.17}$$

The fifteenth constraint is related to the existing area of forest land should be less than or equal to 481.30 km^2 as formulated in Equation 7.18.

$$X_8 \leq 481.30 \tag{7.18}$$

The sixteenth constraint relates to the maximum forest land area is 481.30 km^2, but it can be decreased to 382.63 km^2 as formulated in Equation 7.19.

$$X_8 \geq 382.63 \tag{7.19}$$

The seventeenth constraint is related to the existing area of the waterbody should be less than or equal to 53.30 km^2 as formulated in Equation 7.20.

$$X_9 \leq 53.30 \tag{7.20}$$

The eighteenth constraint relates to the maximum area of the waterbody is 53.30 km^2, but it can be reduced to 49.52 km^2 as formulated in Equation 7.21.

$$X_9 \geq 49.52 \tag{7.21}$$

The nineteenth constraint is related to the existing rangeland area should be less than or equal to 71.65 km^2 as formulated in Equation 7.22.

$$X_{10} \leq 71.65 \tag{7.22}$$

The twentieth constraint is related to the maximum rangeland area of 71.65 km^2, but it can be decreased to 70.54 km^2 as formulated in Equation 7.23.

$$X_{10} \geq 70.54 \tag{7.23}$$

The twenty-first constraint is related to marsh and swamp area should be less than or equal to 27.73 km^2 as formulated in Equation 7.24.

$$X_{11} \leq 27.73 \tag{7.24}$$

The twenty-second constraint relates to the maximum area of marsh and swamp is 27.73 km^2, but it can be decreased to 25.13 km^2 as formulated in Equation 7.25.

$$X_{11} \geq 25.13 \tag{7.25}$$

The twenty-third constraint is related to the existing area of unused land should be more than or equal to 93.31 km^2 as formulated in Equation 7.26.

$$X_{12} \geq 93.31 \tag{7.26}$$

The twenty-fourth constraint relates to the maximum area of unused land is 93.31 km^2, but it can be increased to 141.20 km^2 as formulated in Equation 7.27.

$$X_{12} \leq 141.20 \tag{7.27}$$

The twenty-fifth constraint is related to the area of all land use classes must be equal to the allowable area of 3,794.22 km^2 as formulated in Equation 7.28.

$$X_1+X_2+X_3+X_4+X_5+X_6+X_7+X_8+X_9+X_{10}+X_{11}+X_{12} = 3,794.22 \tag{7.28}$$

The last constraint is the non-negative variable, the area of each land use class should be more than or equal to 0 km^2 as formulated in Equation 7.29.

$$X_1, X_2, X_3, X_4, X_5, X_6, X_7, X_8, X_9, X_{10}, X_{11}, X_{12} \geq 0 \tag{7.29}$$

The constraints setting of each LULC type to minimize surface runoff in 2029 under three different rainfall conditions is summarized in Table 7.8.

Table 7.8 Summary of constraints setting for optimizing LULC in 2029.

LULC type	Constraint setting
Urban and built-up area (X_1)	$65.84 \leq X_1 \leq 77.38$
Paddy field (X_2)	$2{,}012.16 \geq X_2 \geq 1{,}947.12$
Sugarcane (X_3)	$306.85 \leq X_3 \leq 424.95$
Cassava (X_4)	$489.91 \geq X_4 \geq 408.26$
Other field crops (X_5)	$6.19 \leq X_5 \leq 7.72$
Para rubber (X_6)	$97.03 \leq X_6 \leq 134.43$
Perennial trees and orchard (X_7)	$88.95 \leq X_7 \leq 125.36$
Forest land (X_8)	$481.30 \geq X_8 \geq 382.63$
Waterbody (X_9)	$53.30 \geq X_9 \geq 49.52$
Rangeland (X_{10})	$71.65 \geq X_{10} \geq 70.54$
Marsh and swamp (X_{11})	$27.73 \geq X_{11} \geq 25.13$
Unused land (X_{12})	$93.31 \leq X_{12} \leq 141.20$

Likewise, details of constraints of the objective function to minimize surface runoff for optimized LULC in 2039 under three different rainfall conditions (drought, normal, and wet years) were listed as the following.

The first constraint is related to the existing area of the urban and built-up area should be more than or equal to 65.84 km^2 as formulated in Equation 7.30.

$$X_1 \geq 65.84 \tag{7.30}$$

The second constraint relates to the existing urban and built-up area is 65.84 km^2, but it can be expandable up to 88.31 km^2 as formulated in Equation 7.31.

$$X_1 \leq 88.31 \tag{7.31}$$

The third constraint is related to the maximum area of the paddy field should be less than or equal to 2,012.16 km^2 as formulated in Equation 7.32.

$$X_2 \leq 2{,}012.16 \tag{7.32}$$

The fourth constraint relates to the paddy field's existing area is 2,012.16 km^2, but it can be decreased to 1,879.30 km^2 as formulated in Equation 7.33.

$$X_2 \geq 1{,}879.30 \tag{7.33}$$

The fifth constraint is related to the existing area of sugarcane should be more than or equal to 306.85 km^2 as formulated in Equation 7.34.

$$X_3 \geq 306.85 \tag{7.34}$$

The sixth constraint relates to the maximum sugarcane area is 306.85 km^2, but it can be increased to 520.31 km^2 as formulated in Equation 7.35.

$$X_3 \leq 520.31 \tag{7.35}$$

The seventh constraint is related to the existing area of cassava should be less than or equal to 489.91 km^2 as formulated in Equation 7.36.

$$X_4 \geq 489.91 \tag{7.36}$$

The eighth constraint relates to the maximum area of cassava is 489.91 km^2, but it can be reduced to 358.65 km^2 as formulated in Equation 7.37.

$$X_4 \geq 358.65 \tag{7.37}$$

The ninth constraint is related to the existing area of other field crops should be more than or equal to 6.19 km^2 as formulated in Equation 7.38.

$$X_5 \geq 6.19 \tag{7.38}$$

The tenth constraint relates to the maximum area of other field crops, which is 5.19 km^2 but can be increased to 9.45 km^2 as formulated in Equation 7.39.

$$X_5 \leq 9.45 \tag{7.39}$$

The eleventh constraint is related to the existing area of para rubber that should be more than or equal to 97.03 km^2 as formulated in Equation 7.40.

$$X_6 \geq 97.03 \tag{7.40}$$

The twelfth constraint is related to the maximum area of para rubber being 97.03 km2, but it can exceed 152.02 km^2 as formulated in Equation 7.41.

$$X_6 \leq 152.02 \tag{7.41}$$

The thirteenth constraint is related to the existing area of the perennial trees and orchards should be more than or equal to 88.95 km^2 as formulated in Equation 7.42.

$$X_7 \geq 88.95 \tag{7.42}$$

The fourteenth constraint is related to the maximum area of perennial trees and orchards is 88.95 km^2, but it can be increased to 160.12 km^2 as formulated in Equation 7.43.

$$X_7 \leq 160.12 \tag{7.43}$$

The fifteenth constraint is related to the existing area of forest land should be less than or equal to 481.30 km^2 as formulated in Equation 7.44.

$$X_8 \leq 481.30 \tag{7.44}$$

The sixteenth constraint is related to the maximum area of forest land is 481.30 km^2, but it can be decreased to 304.44 km^2 as formulated in Equation 7.45.

$$X_8 \geq 304.44 \tag{7.45}$$

The seventeenth constraint is related to the existing area of the waterbody should be less than or equal to 53.30 km^2 as formulated in Equation 7.46.

$$X_9 \leq 53.30 \tag{7.46}$$

The eighteenth constraint is related to the maximum area of the waterbody is 53.30 km^2, but it can be reduced to 47.01 km^2 as formulated in Equation 7.47.

$$X_9 \geq 47.01 \tag{7.47}$$

The nineteenth constraint is related to the existing rangeland area should be less than or equal to 71.65 km^2 as formulated in Equation 7.48.

$$X_{10} \leq 71.65 \tag{7.48}$$

The twentieth constraint is related to the maximum rangeland area of 71.65 km^2, but it can be decreased to 69.91 km^2 as formulated in Equation 7.49.

$$X_{10} \geq 69.91 \tag{7.49}$$

The twenty-first constraint is related to marsh and swamp area should be less than or equal 27.73 km^2 as formulated in Equation 7.50.

$$X_{11} \leq 27.73 \tag{7.50}$$

The twenty-second constraint is related to the maximum area of marsh and swamp is 27.73 km^2, but it can be decreased to 24.66 km^2 as formulated in Equation 7.51.

$$X_{11} \geq 24.66 \tag{7.51}$$

The twenty-third constraint is related to the existing area of unused land should be more than or equal to 93.31 km² as formulated in Equation 7.52.

$$X_{12} \geq 93.31 \tag{7.52}$$

The twenty-fourth constraint is related to the maximum area of unused land is 93.31 km², but it can be increased to 180.07 km² as formulated in Equation 7.53.

$$X_{12} \leq 180.07 \tag{7.53}$$

The twenty-fifth constraint is related to the area of all land use classes must be equal to the allowable area of 3,794.22 km² as formulated in Equation 7.54.

$$X_1 + X_2 + X_3 + X_4 + X_5 + X_6 + X_7 + X_8 + X_9 + X_{10} + X_{11} + X_{12} = 3,794.22 \tag{7.54}$$

The last constraint is the non-negative variable, the area of each land use class should be more than or equal to 0 km² as formulated in Equation 7.55.

$$X_1, X_2, X_3, X_4, X_5, X_6, X_7, X_8, X_9, X_{10}, X_{11}, X_{12} \geq 0 \tag{7.55}$$

The constraints setting of each LULC type to minimize surface runoff in 2039 under three different rainfall conditions is summarized in Table 7.9

Table 7.9 Summary of constraints setting for optimizing LULC in 2039.

LULC type	Constraint setting
Urban and built-up area (X_1)	$65.84 \leq X_1 \leq 88.31$
Paddy field (X_2)	$2,012.16 \geq X_2 \geq 1,879.30$
Sugarcane (X_3)	$306.85 \leq X_3 \leq 520.31$
Cassava (X_4)	$489.91 \geq X_4 \geq 358.65$
Other field crops (X_5)	$6.19 \leq X_5 \leq 9.45$
Para rubber (X_6)	$97.03 \leq X_6 \leq 152.02$
Perennial trees and orchard (X_7)	$88.95 \leq X_7 \leq 160.12$
Forest land (X_8)	$481.30 \geq X_8 \geq 304.44$
Waterbody (X_9)	$53.30 \geq X_9 \geq 47.01$
Rangeland (X_{10})	$71.65 \geq X_{10} \geq 69.91$
Marsh and swamp (X_{11})	$27.73 \geq X_{11} \geq 24.66$
Unused land (X_{12})	$93.31 \leq X_{12} \leq 180.07$

Similarly, details of constraints of the objective function to minimize surface runoff for optimized LULC in 2049 under three different rainfall conditions (drought, normal, and wet years) were listed as the following.

The first constraint is related to the existing area of the urban and built-up area should be more than or equal to 65.84 km^2 as formulated in Equation 7.56.

$$X_1 \geq 65.84 \tag{7.56}$$

The second constraint is related to the existing urban and built-up area is 65.84 km^2, but it can be expandable up to 99.03 km^2 as formulated in Equation 7.57.

$$X_1 \leq 99.03 \tag{7.57}$$

The third constraint is related to the maximum area of the paddy field should be less than or equal to 2,012.16 km^2 as formulated in Equation 7.58.

$$X_2 \leq 2,012.16 \tag{7.58}$$

The fourth constraint is related to the existing area of the paddy field is 2,012.16 km^2, but it can be decreased to 1,812.16 km^2 as formulated in Equation 7.59.

$$X_2 \geq 1,812.16 \tag{7.59}$$

The fifth constraint is related to the existing area of sugarcane should be more than or equal to 306.85 km^2 as formulated in Equation 7.60.

$$X_3 \geq 306.85 \tag{7.60}$$

The sixth constraint related to the maximum sugarcane area is 306.85 km^2, but it can be increased to 599.36 km^2 as formulated in Equation 7.61.

$$X_3 \leq 599.36 \tag{7.61}$$

The seventh constraint is related to the existing area of cassava should be less than or equal to 489.91 km^2 as formulated in Equation 7.62.

$$X_4 \geq 489.91 \tag{7.62}$$

The eighth constraint is related to the maximum area of cassava is 489.91 km^2, but it can be reduced to 330.32 km^2 as formulated in Equation 7.63.

$$X_4 \geq 330.32 \tag{7.63}$$

The ninth constraint is related to the existing area of other field crops should be more than or equal to 6.19 km^2 as formulated in Equation 7.64.

$$X_5 \geq 6.19 \tag{7.64}$$

The tenth constraint related to the maximum area of other field crops is 5.19 km^2, but it can be increased to 11.26 km^2 as formulated in Equation 7.65.

$$X_5 \leq 11.26 \tag{7.65}$$

The eleventh constraint is related to the area of para rubber that should be more than or equal to 97.03 km^2 as formulated in Equation 7.66.

$$X_6 \geq 97.03 \tag{7.66}$$

The twelfth constraint related to the maximum area of para rubber is 97.03 km^2, but it can exceed up to 164.41 km^2 as formulated in Equation 7.67.

$$X_6 \leq 164.41 \tag{7.67}$$

The thirteenth constraint is related to the existing area of the perennial trees and orchards should be more than or equal to 88.95 km^2 as formulated in Equation 7.68.

$$X_7 \geq 88.95 \tag{7.68}$$

The fourteenth constraint is related to the maximum area of perennial trees and orchards is 88.95 km^2, but it can be increased to 193.13 km^2 as formulated in Equation 7.69.

$$X_7 \leq 193.13 \tag{7.69}$$

The fifteenth constraint is related to the existing area of forest land should be less than or equal to 481.30 km^2 as formulated in Equation 7.70.

$$X_8 \leq 481.30 \tag{7.70}$$

The sixteenth constraint is related to the maximum area of forest land is 481.30 km^2, but it can be decreased to 242.23 km^2 as formulated in Equation 7.71.

$$X_8 \geq 242.23 \tag{7.71}$$

The seventeenth constraint is related to the existing area of the waterbody should be less than or equal to 53.30 km^2 as formulated in Equation 7.72.

$$X_9 \leq 53.30 \tag{7.72}$$

The eighteenth constraint is related to the maximum area of the waterbody is 53.30 km^2, but it can be reduced to 42.78 km^2 as formulated in Equation 7.73.

$$X_9 \geq 42.78 \tag{7.73}$$

The nineteenth constraint is related to the existing rangeland area should be less than or equal to 71.65 km² as formulated in Equation 7.74.

$$X_{10} \leq 71.65 \qquad (7.74)$$

The twentieth constraint is related to the maximum rangeland area of 71.65 km², but it can be decreased to 66.05 km² as formulated in Equation 7.75.

$$X_{10} \geq 66.05 \qquad (7.75)$$

The twenty-first constraint is related to marsh and swamp area should be less than or equal to 27.73 km² as formulated in Equation 7.76.

$$X_{11} \leq 27.73 \qquad (7.76)$$

The twenty-second constraint is related to the maximum area of marsh and swamp is 27.73 km², but it can be decreased to 21.61 km² as formulated in Equation 7.77.

$$X_{11} \geq 21.61 \qquad (7.77)$$

The twenty-third constraint is related to the existing area of unused land should be more than or equal to 93.31 km² as formulated in Equation 7.78.

$$X_{12} \geq 93.31 \qquad (7.78)$$

The twenty-fourth constraint is related to the maximum area of unused land is 93.31 km², but it can be increased to 211.89 km² as formulated in Equation 7.79.

$$X_{12} \leq 211.89 \qquad (7.79)$$

The twenty-fifth constraint is related to the area of all land use classes must be equal to the allowable area of 3,794.22 km² as formulated in Equation 7.80.

$$X_1+X_2+X_3+X_4+X_5+X_6+X_7+X_8+X_9+X_{10}+X_{11}+X_{12} = 3,794.22 \qquad (7.80)$$

The last constraint is the non-negative variable, the area of each land use class should be more than or equal to 0 km² as formulated in Equation 7.81.

$$X_1, X_2, X_3, X_4, X_5, X_6, X_7, X_8, X_9, X_{10}, X_{11}, X_{12} \geq 0 \qquad (7.81)$$

The constraints setting of each LULC type to minimize surface runoff in 2039 under three different rainfall conditions is summarized in Table 7.10.

Table 7.10 Summary of constraints setting for optimizing LULC in 2049.

LULC type	Constraint setting
Urban and built-up area (X_1)	$65.84 \leq X_1 \leq 99.03$
Paddy field (X_2)	$2{,}012.16 \geq X_2 \geq 1{,}812.16$
Sugarcane (X_3)	$306.85 \leq X_3 \leq 599.36$
Cassava (X_4)	$489.91 \geq X_4 \geq 330.32$
Other field crops (X_5)	$6.19 \leq X_5 \leq 11.26$
Para rubber (X_6)	$97.03 \leq X_6 \leq 164.41$
Perennial trees and orchard (X_7)	$88.95 \leq X_7 \leq 193.13$
Forest land (X_8)	$481.30 \geq X_8 \geq 242.23$
Waterbody (X_9)	$53.30 \geq X_9 \geq 42.78$
Rangeland (X_{10})	$71.65 \geq X_{10} \geq 66.05$
Marsh and swamp (X_{11})	$27.73 \geq X_{11} \geq 21.61$
Unused land (X_{12})	$93.31 \leq X_{12} \leq 211.89$

The objective functions for drought, normal, wet years (Equations 7.1, 7.2, and 7.3) were then transformed into a Goal programming form as follow:

$$f_k(x)+d_k^- - d_k^+ = a_k \tag{7.30}$$

Results of optimized LULC allocation to minimize surface runoff for flood mitigation in 2029, 2039, and 2049 under three different rainfall conditions (drought, normal, and wet years) are presented in Tables 7.11 to 7.13.

As a result, under drought year conditions, there is no change in the urban and built-up area, other field crops, forest land, and unused land after optimization of LULC allocation. In the meantime, sugarcane, para rubber, and perennial trees and orchard are increased while paddy filed, cassava, waterbody, rangeland, and marsh and swamp are decreased. The significance of increasing LULC type in 2029, 2039, and 2049 is sugarcane, which is increased by about 80.39, 148.09, and 210.28 km^2, respectively. In contrast, cassava decreases LULC type in the same years, which is decreased by 81.65, 132.86, and 200.01 km^2, respectively.

Under normal year conditions, there is no change in the urban and built-up area, forest land, and unused land after optimization of LULC allocation. Meanwhile, sugarcane, other field crops, para rubber, and perennial trees and orchard are increased while paddy filed, cassava, waterbody, rangeland, and marsh and swamp are decreased. So, sugarcane is the most increase LULC area in 2029, 2039, and 2049, which is increased by 78.86, 144.82, and 205.21 km^2, respectively. On the other hand, the significance of decreasing LULC type in the same years are paddy field and sugarcane, which are increased by 65.04, 132.86, 200.01 km^2, and 81.65, 130.27, and 159.59 km^2, respectively.

Under wet year conditions, there is no change in the urban and built-up area, other field crops, perennial trees and orchards, forest land, and unused land after optimization of LULC allocation. At the same time, sugarcane and para rubber are increased while paddy field, cassava, waterbody, rangeland, and marsh and swamp are decreased. The most increasing LULC type in 2029, 2039, and 2049 is sugarcane, increased by 115.29, 213.46, and 292.51 km^2, respectively. Conversely, the most decreasing LULC type in the same years is paddy field and cassava; they decrease by 65.04, 132.86, 200.01 km^2, and 81.65, 131.27, and 159.59 km^2, respectively.

Comparison of allocated LULC type area by the Goal programming for flood mitigation among different rainfall conditions in 2029, 2039, and 2049 are displayed in Figures 7.3 to 7.5. As a result, there are different LULC areas among three different rainfall conditions in a specific year. For instance, sugarcane areas in 2029, 2039, and 2049 under wet year conditions are higher than other conditions, while perennial trees and orchards under this condition in three years are lower than other conditions.

Table 7.11 Optimization of LULC allocation to minimize surface runoff under drought year conditions.

LULC type	2019		2029		2039		2049	
	Area of LULC (km²)	Surface runoff (million m³)	Allocated LULC (km²)	Surface runoff (million m³)	Allocated LULC (km²)	Surface runoff (million m³)	Allocated LULC (km²)	Surface runoff (million m³)
Urban and built-up area	65.84	29.84	65.84	29.84	65.84	29.84	65.84	29.84
Paddy field	2,012.16	942.32	1,947.12	856.54	1,879.30	826.71	1,812.16	797.17
Sugarcane	306.85	70.96	387.24	148.87	454.94	174.90	517.13	198.81
Cassava	489.91	242.89	408.26	184.27	359.65	162.33	330.32	149.09
Other field crops	6.19	1.75	6.19	2.39	6.19	2.39	6.19	2.39
Para rubber	97.03	19.65	134.43	49.86	152.02	56.39	164.41	60.99
Perennial trees and orchard	88.95	25.76	125.36	47.40	160.12	60.54	193.13	73.02
Forest land	481.30	159.21	481.30	136.03	481.30	136.03	481.30	136.03
Waterbody	53.30	23.81	49.52	24.29	47.01	23.06	42.78	20.99
Rangeland	71.65	23.23	70.54	29.36	69.91	29.10	66.05	27.49
Marsh and swamp	27.73	12.69	25.13	13.59	24.66	13.34	21.61	11.69
Unused land	93.31	25.85	93.31	42.57	93.31	42.57	93.31	42.57
SUM	3,794.22	1,577.96	3,794.22	1,565.01	3,794.22	1,557.18	3,794.22	1,550.07

Table 7.12 Optimization of LULC allocation to minimize surface runoff under normal year conditions.

LULC type	2019		2029		2039		2049	
	Area of LULC (km^2)	Surface runoff (million m^3)	Allocated LULC (km^2)	Surface runoff (million m^3)	Allocated LULC (km^2)	Surface runoff (million m^3)	Allocated LULC (km^2)	Surface runoff (million m^3)
Urban and built-up area	65.84	67.58	65.84	67.58	65.84	67.58	65.84	67.58
Paddy field	2,012.16	2,038.95	1,947.12	1,973.05	1,879.30	1,904.33	1,812.16	1,836.29
Sugarcane	306.85	277.30	385.71	348.56	451.67	408.18	512.06	462.76
Cassava	489.91	489.07	408.26	407.56	359.65	359.03	330.32	329.75
Other field crops	6.19	5.43	7.72	6.78	9.45	8.30	11.26	9.88
Para rubber	97.03	80.36	134.43	111.33	152.02	125.89	164.41	136.16
Perennial trees and orchard	88.95	74.28	125.36	104.68	160.12	133.70	193.13	161.27
Forest land	481.30	366.03	481.30	366.03	481.30	366.03	481.30	366.03
Waterbody	53.30	55.23	49.52	51.30	47.01	48.70	42.78	44.33
Rangeland	71.65	65.95	70.54	64.93	69.91	64.35	66.05	60.80
Marsh and swamp	27.73	31.56	25.13	28.60	24.66	28.06	21.61	24.59
Unused land	93.31	95.33	93.31	95.33	93.31	95.33	93.31	95.33
SUM	3,794.22	3,647.07	3,794.22	3,625.72	3,794.22	3,609.48	3,794.22	3,594.76

Table 7.13 Optimization of LULC allocation to minimize surface runoff under wet year conditions.

LULC type	2019 Area of LULC (km²)	2019 Surface runoff (million m³)	2029 Allocated LULC (km²)	2029 Surface runoff (million m³)	2039 Allocated LULC (km²)	2039 Surface runoff (million m³)	2049 Allocated LULC (km²)	2049 Surface runoff (million m³)
Urban and built-up area	65.84	95.82	65.84	95.82	65.84	95.82	65.84	95.82
Paddy field	2,012.16	2,889.20	1,947.12	2,795.81	1,879.30	2,698.43	1,812.16	2,602.02
Sugarcane	306.85	400.38	422.14	552.77	520.31	678.91	599.36	782.05
Cassava	489.91	688.86	408.26	574.05	358.65	505.70	330.32	464.46
Other field crops	6.19	8.09	6.19	8.09	9.45	12.36	11.26	14.71
Para rubber	97.03	126.18	134.43	174.82	152.02	197.69	164.41	213.81
Perennial trees and orchard	88.95	116.42	88.95	116.42	90.48	119.73	103.83	138.51
Forest land	481.30	563.35	481.30	563.35	481.30	563.35	481.30	563.35
Waterbody	53.30	80.24	50.02	74.55	48.01	70.77	43.78	64.41
Rangeland	71.65	97.12	70.54	95.60	69.91	94.76	66.05	89.52
Marsh and swamp	27.73	44.10	26.13	39.97	25.66	39.21	22.61	34.37
Unused land	93.31	131.74	93.31	131.74	93.31	131.74	93.31	131.74
SUM	3,794.22	5,241.52	3,794.22	5,223.01	3,794.22	5,208.46	3,794.22	5,194.79
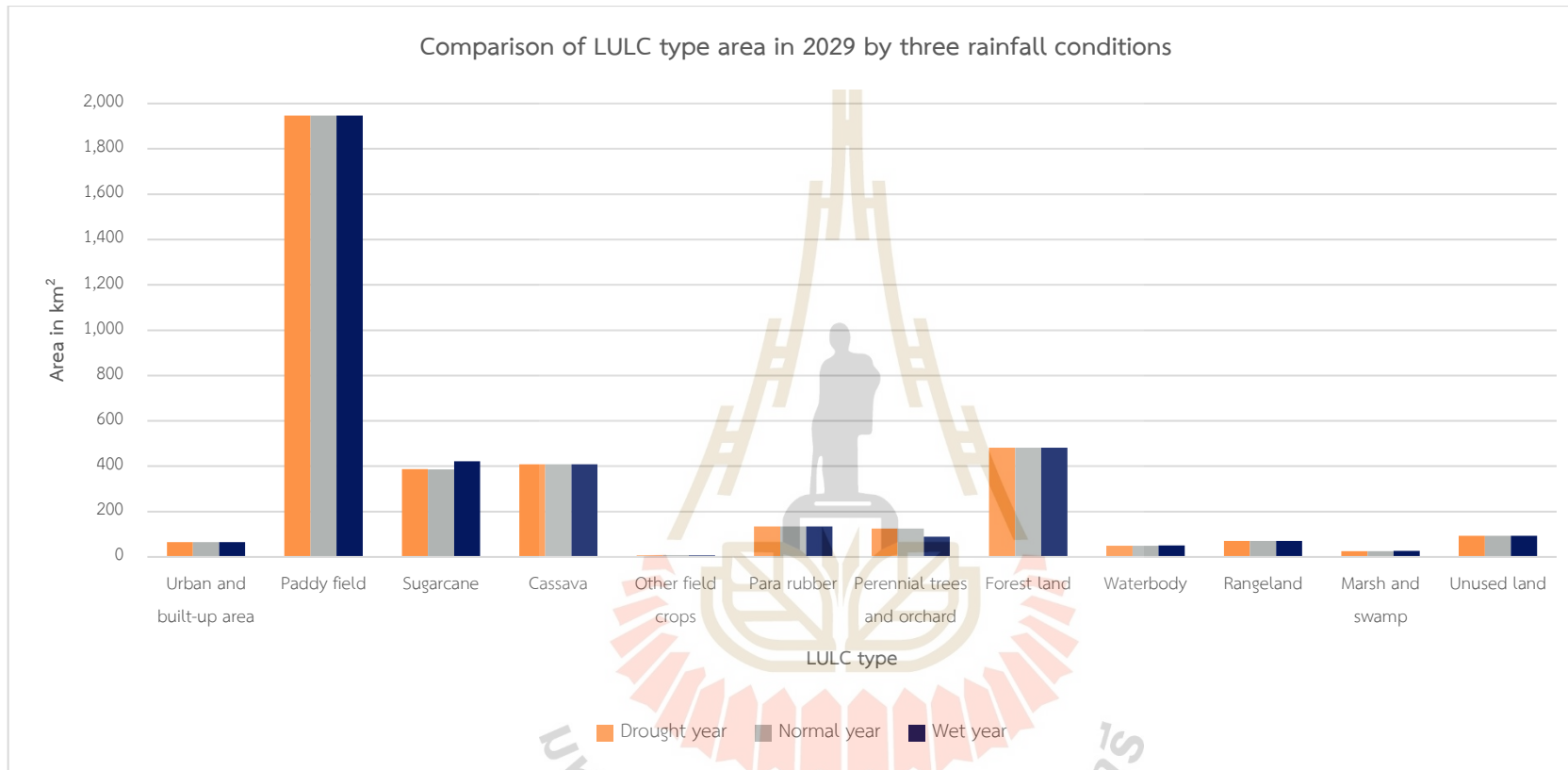
Figure 7.3 Comparison of LULC type area by CLUE-S model prediction for flood mitigation among three rainfall conditions in 2029.
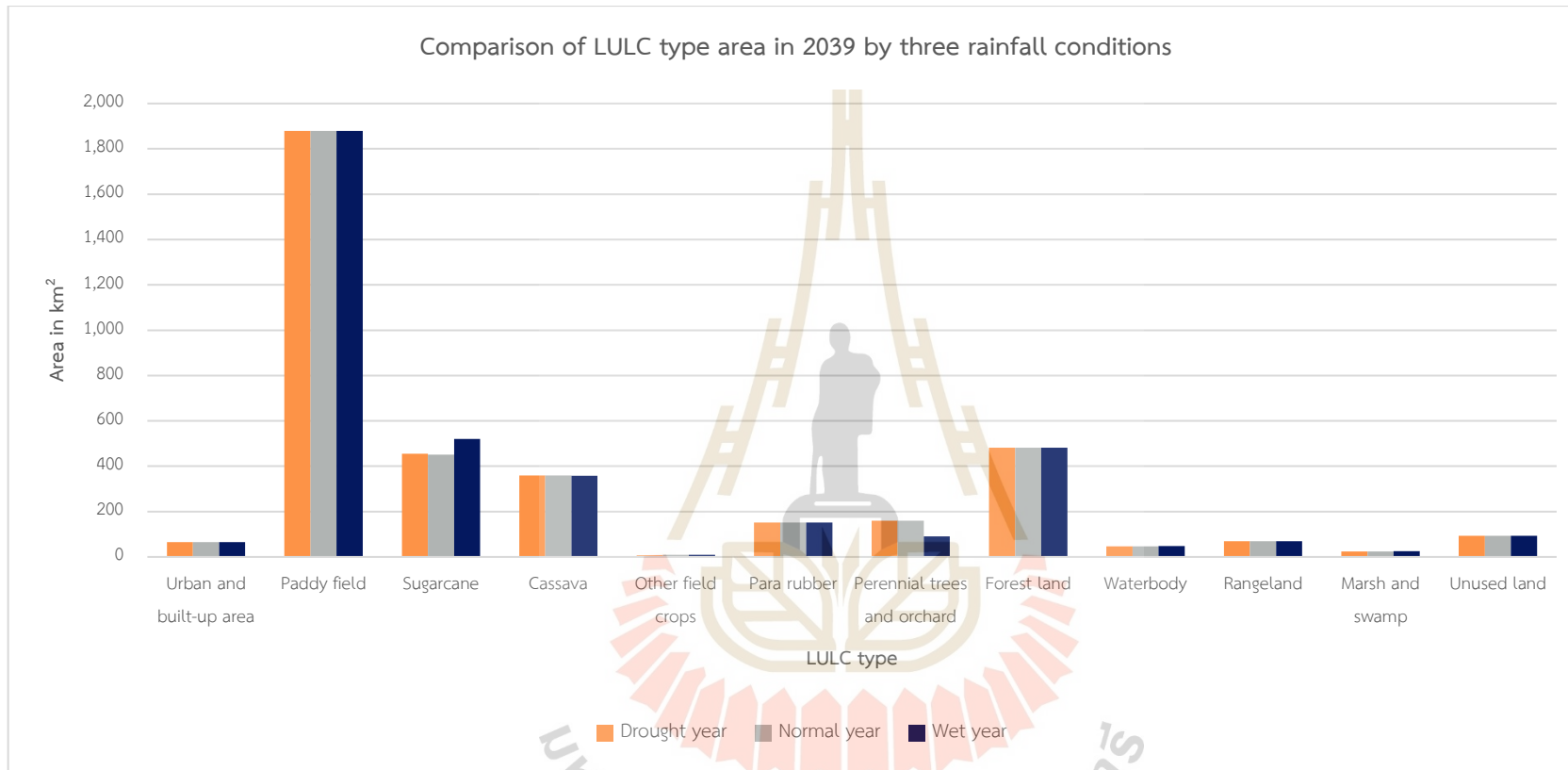
Figure 7.4 Comparison of LULC type area by CLUE-S model prediction for flood mitigation among three rainfall conditions in 2039.
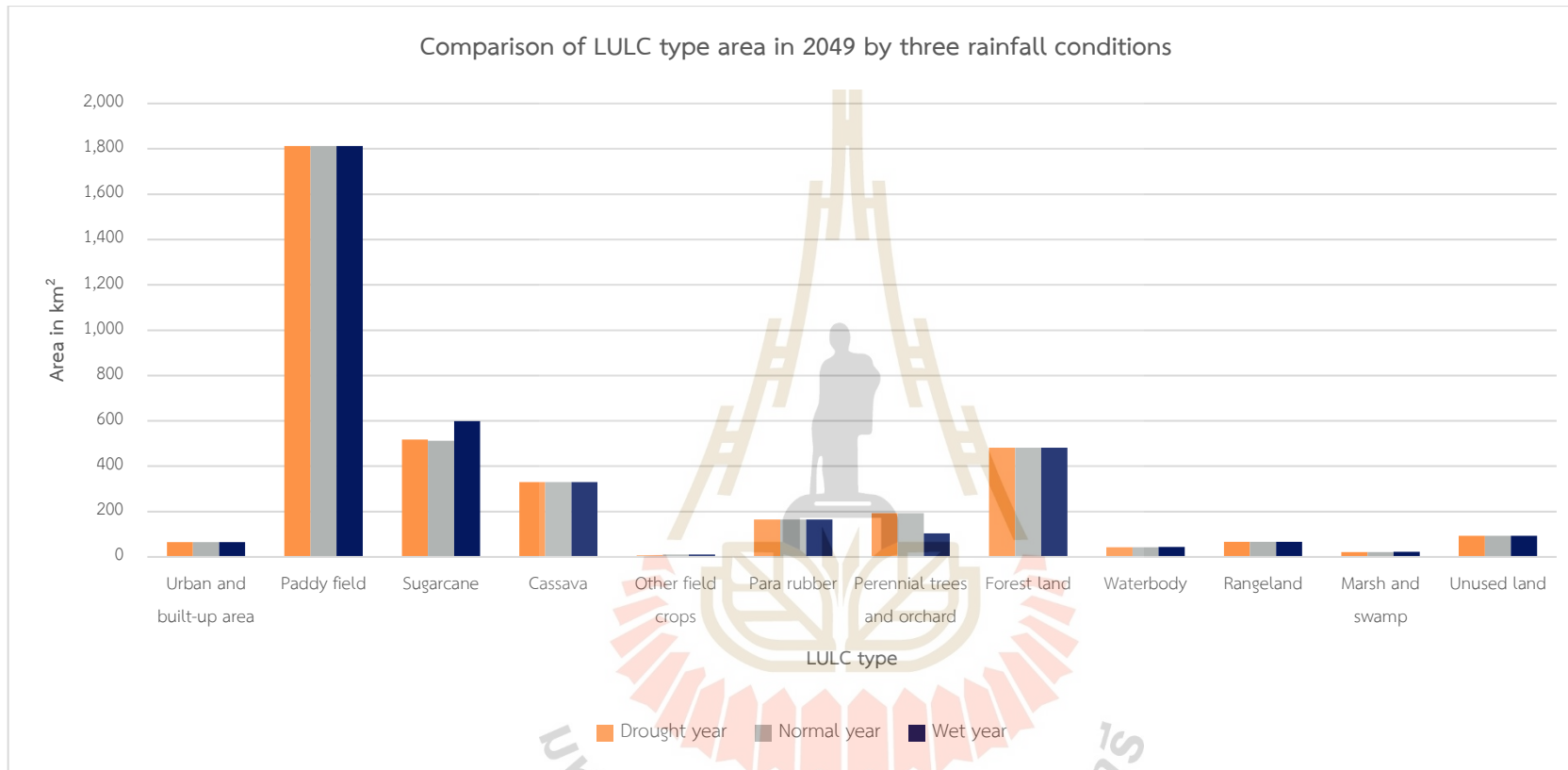
Figure 7.5 Comparison of LULC type area by CLUE-S model prediction for flood mitigation among three rainfall conditions in 2049.

Besides, the results also indicate that after applying LULC optimization, annual surface runoff has decreased in all three different rainfall conditions. Under drought year conditions in 2029, 2039, and 2049, annual surface runoff decreases by 12.95, 20.78, and 27.89 million m^3, or about 0.82, 1.32, and 1.77% from total estimated surface runoff in 2019, respectively. Likewise, the annual surface runoff estimation under normal year conditions in 2029, 2039, and 2049 decreases by 21.34, 37.59, and 52.31 million m^3, or 0.59, 1.03 1.43% of total estimated surface runoff in 2019, respectively. Similarly, annual surface runoff estimation under wet year conditions in 2029, 2039, and 2049 decreases by 18.52, 33.06, and 46.73 million m^3, or about 0.35, 0.63, and 0.89% of the total estimated surface runoff in 2019, respectively.

From these results, it can be concluded that the optimized LULC allocation data in 2049 under three rainfall conditions (drought, normal and wet year) are the most suitable for flood mitigation in the future. The surface runoff in 2049 under drought, normal and wet years will be reduced by about 27.89, 52.31, and 46.73 million m^3. Figure 7.6 compares surface runoff reduction in 2029, 2039, 2049 under drought, normal, and wet year condition.
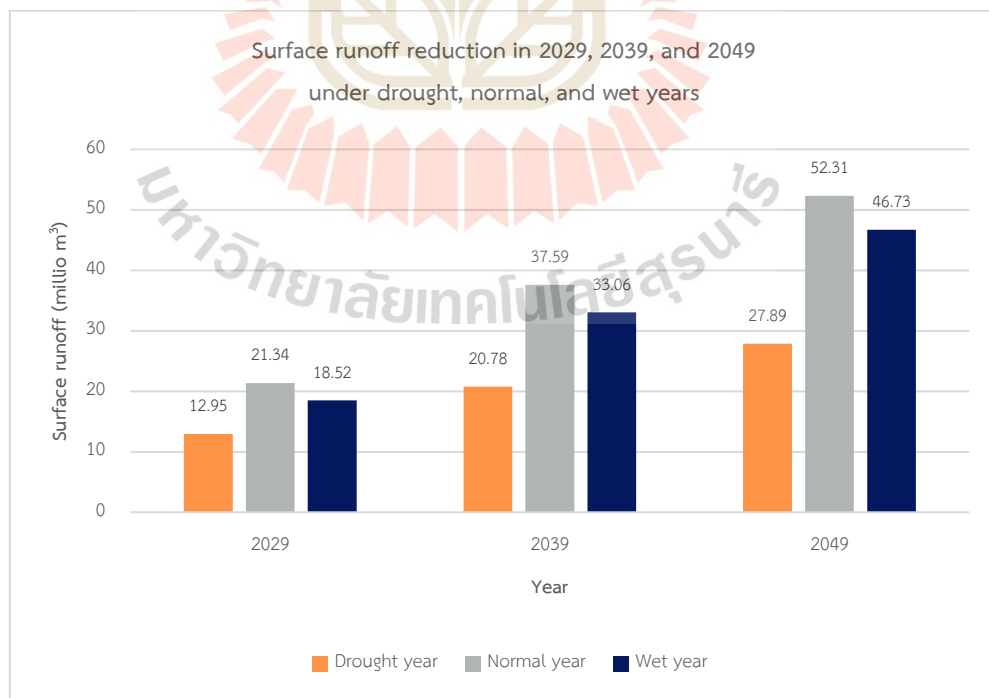
Figure 7.6 Comparison of surface runoff reduction in 2029, 2039, and 2049 under drought, normal, and wet years.

Furthermore, the contribution of surface runoff by each LULC type under three different rainfall conditions in 2029, 2039, and 2049 are displayed in Figures 7.7 to 7.9. As a result, each LULC type's contribution is dictated by the average runoff coefficient under different rainfall conditions. For example, allocated paddy field areas under drought, normal and wet in 2029 are the same, with 1,947.12 km^2 (See Tables 7.11 to 7.13 or Figure 7.3). Still, the average surface runoff coefficient of paddy fields under drought, normal and wet years are different, with a value of 0.44, 1.01, and 1.44 million cubic meters per km^2 (See Tables 7.2 to 7.4).

The deviation of annual surface runoff after minimization from Goal programming is presented in Table 7.14. The optimization of LULC allocation in 2029, 2039, and 2049 under drought, normal, and wet year conditions to minimize surface runoff in the Second Part of the Lam Nam Chi watershed is presented in detail in Appendices A to C.

The notable reduction of annual surface runoff in three different rainfall conditions is allocating paddy field and cassava to sugarcane, para rubber, and perennial trees and orchard after optimization, which changes the hydrological properties. Due to paddy field and cassava fields provides higher runoff coefficients than sugarcane, rubber, and perennial trees and orchard (See Tables 7.2 to 7.4).
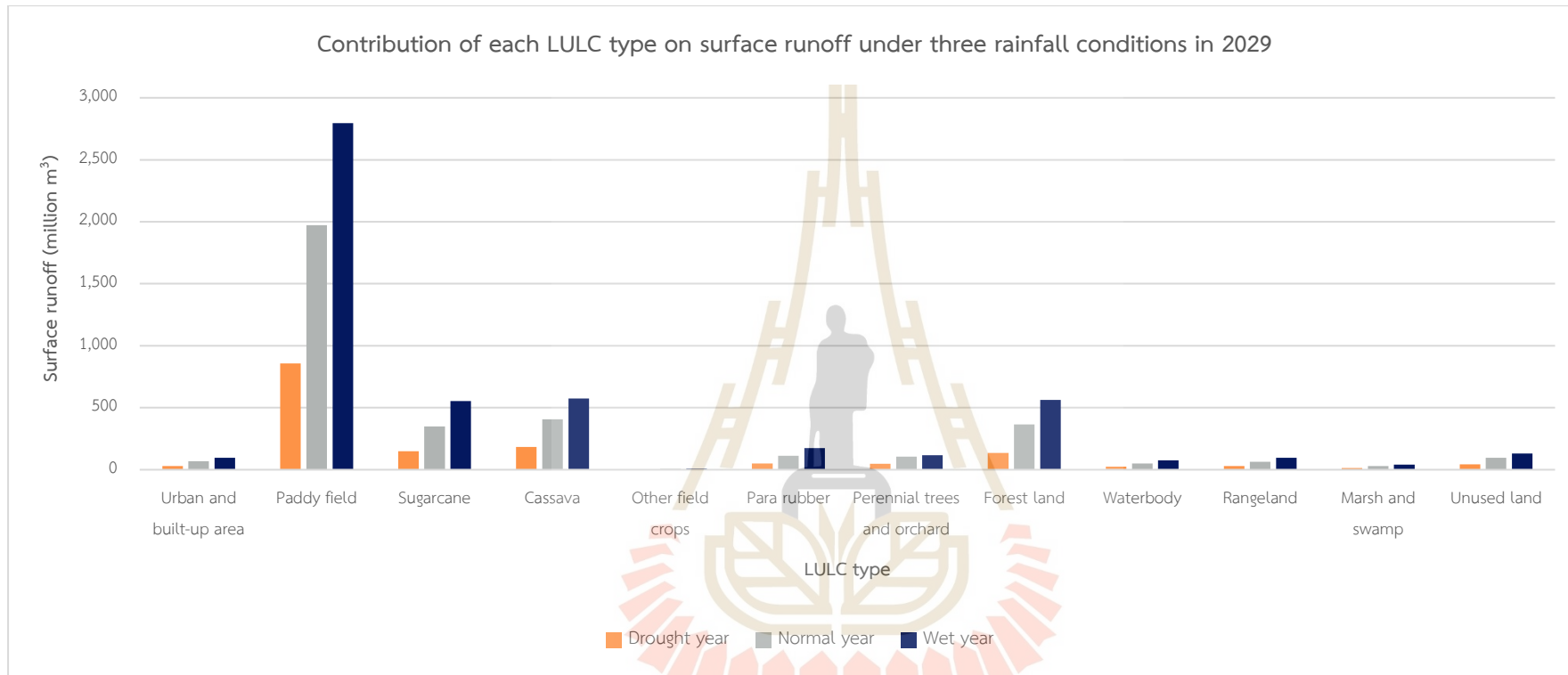
Figure 7.7 Contribution of each LULC type on surface runoff under drought, normal, and wet years in 2029.
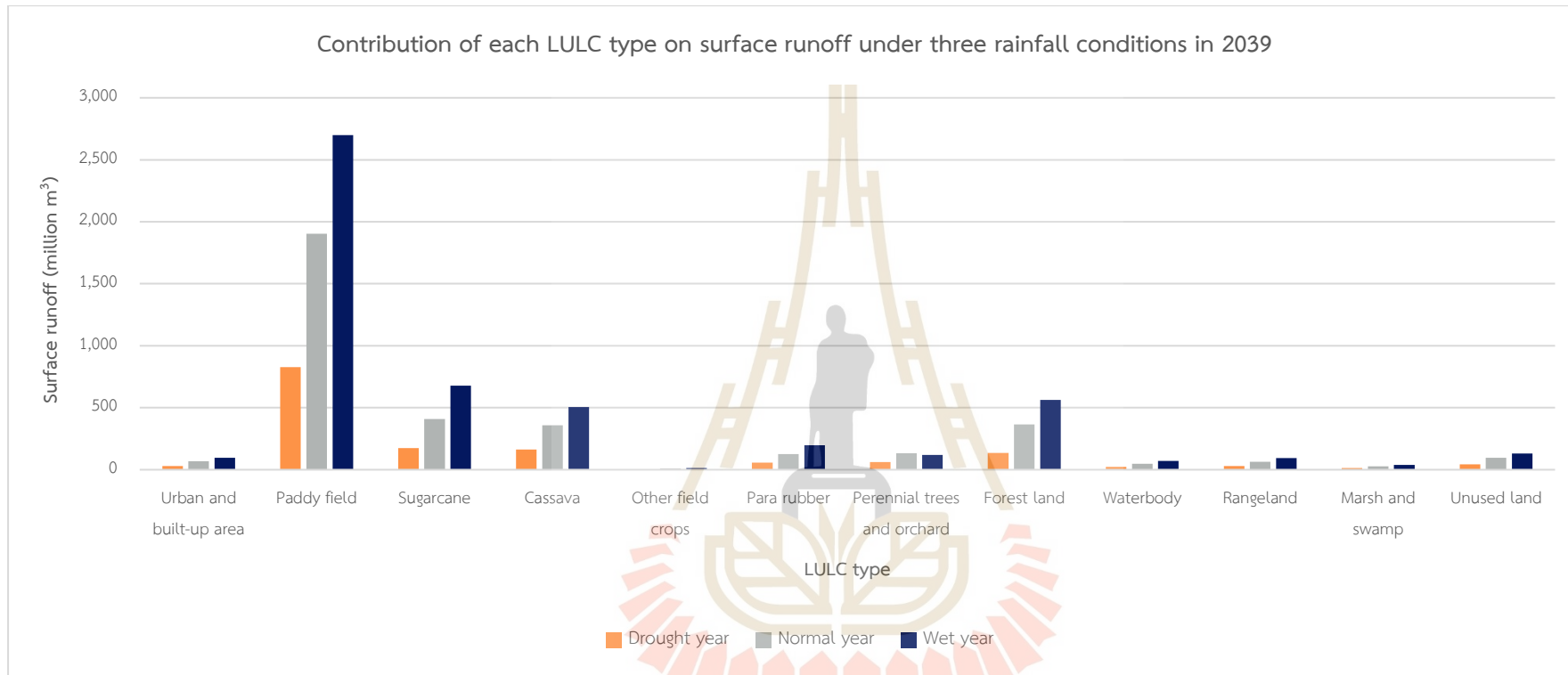
Figure 7.8 Contribution of each LULC type on surface runoff under drought, normal, and wet years in 2039.
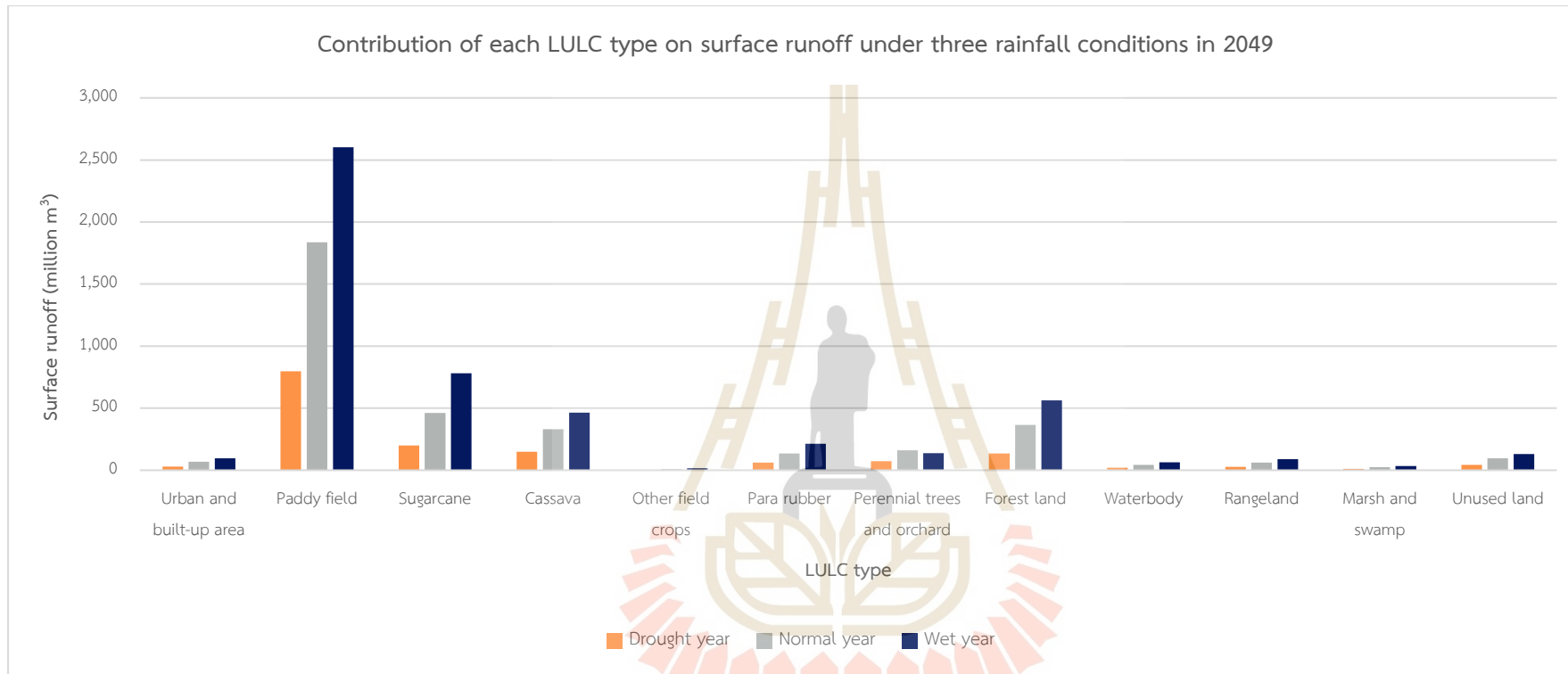
Figure 7.9 Contribution of each LULC type on surface runoff under drought, normal, and wet years in 2049.

Table 7.14 Deviation of annual surface runoff after minimization from Goal programming.

| Items | Surface runoff minimization (million m³) | | | | | | | | |
| | Drought years | | | Normal years | | | Wet years | | |
	2029	2039	2049	2029	2039	2049	2029	2039	2049
Goal of annual surface runoff (million m³)	1,577.96	1,577.96	1,577.96	3,647.07	3,647.07	3,647.07	5,241.52	5,241.52	5,241.52
Annual surface runoff after optimization (million m³)	1,565.01	1,557.18	1,550.07	3,625.72	3,609.48	3,594.76	5,223.01	5,208.46	5,194.79
Deviation from goal (million m³)	-12.95	-20.78	-27.89	-21.34	-37.59	-52.31	-18.52	-33.06	-46.73
Deviation from goal (%)	-0.82	-1.32	-1.77	-0.59	-1.03	-1.43	-0.35	-0.63	-0.89

Besides, the actual surface runoff between 2001 and 2019 was used to compare total surface runoff from optimized LULC allocation for flood mitigation in 2029, 2039, and 2049. The comparison of total surface runoff volume between actual LULC data and optimized LULC allocation was presented in Table 7.15. As a result, it was found that optimized LULC allocation in 2029, 2039, and 2049 for flood mitigation can reduce total surface runoff volume between 2001 and 2019.

In summary, it can be noted that the achievement goal for surface runoff reduction depends on constraint setting (by decreasing and increasing LULC areas) according to the historical trend of LULC change based on LULC data in 2010 and 2019 by Markov Chain model and the average runoff coefficient of each LULC type. Additionally, Goal programming based on Linear programming can be efficiently operated using add-in software under the MS Excel environment, e.g., MS Solver and What's Best of Lindo Systems Inc. On the contrary, the constraint setting should be carefully assigned based on the historical LULC development in the study area, e.g., the annual decreasing or increasing rate of each LULC type. Nevertheless, this finding indicates that if areas of LULC type are optimal allocated, flooding in the study area shall be mitigated since surface runoff is reduced. This finding is similar to the previous study of Owji, Nikkami, Mahdian, and Mahmoudi (2012), who found that the Simplex method's optimal area of land uses can reduce surface runoff. Likewise, the applicability of linear programming in solving optimization problems was proved in minimizing runoff, as mentioned by Yeo, Gordon, and Guldmann (2004) and Hargreaves and Hobbs (2009).

Table 7.15 Comparison of total surface runoff volume between actual LULC data and optimized LULC allocation.

Year	Current runoff volume	Rainfall condition	Runoff volume of optimized LULC in 2029 (million m³)		Runoff volume of optimized LULC in 2039 (million m³)		Runoff volume of optimized LULC in 2049 (million m³)	
			Runoff volume	Different from current	Runoff volume	Different from current	Runoff volume	Different from current
2001	1,429.77	Drought year	1,420.14	-9.63	1,414.18	-15.59	1,408.58	-21.19
2002	4,483.62	Normal year	4,420.53	-63.10	4,394.04	-89.58	4,369.94	-113.68
2003	1,719.46	Drought year	1,697.25	-22.21	1,686.64	-32.82	1,676.78	-42.68
2004	1,602.36	Drought year	1,609.44	7.08	1,604.50	2.14	1,599.83	-2.53
2005	2,057.88	Normal year	2,050.87	-7.01	2,043.99	-13.89	2,037.62	-20.26
2006	4,672.73	Normal year	4,663.63	-9.10	4,650.51	-22.22	4,639.17	-33.56
2007	3,636.14	Wet year	3,639.62	3.48	3,624.07	-12.07	3,609.56	-26.58
2008	6,366.80	Wet year	6,381.44	14.64	6,375.66	8.86	6,368.58	1.78
2009	4,629.86	Wet year	4,662.78	32.92	4,659.39	29.53	4,654.35	24.49
2010	6,249.33	Wet year	6,258.14	8.81	6,251.73	2.40	6,246.08	-3.25
2011	6,142.43	Wet year	6,069.45	-72.98	6,042.95	-99.48	6,020.62	-121.81
2012	3,583.03	Normal year	3,568.11	-14.92	3,555.13	-27.90	3,543.67	-39.36
2013	4,200.48	Wet year	4,178.53	-21.95	4,165.83	-34.65	4,152.55	-47.93
2014	1,003.60	Drought year	983.90	-19.70	976.26	-27.34	969.50	-34.10
2015	1,233.80	Drought year	1,221.05	-12.75	1,213.74	-20.06	1,207.39	-26.41
2016	3,475.16	Normal year	3,438.35	-36.81	3,417.39	-57.77	3,397.81	-77.35
2017	5,433.33	Wet year	5,389.90	-43.43	5,358.54	-74.79	5,331.12	-102.21
2018	2,588.57	Drought year	2,575.27	-13.30	2,561.70	-26.87	2,549.32	-39.25
2019	1,445.54	Drought year	1,432.78	-12.76	1,428.87	-16.67	1,425.52	-20.02

7.3 Mapping of LULC allocation for flood mitigation

Under this section, LULC data in 2019 and the derived optimum local parameter of the CLUE-S model from Section 5.2 of Chapter V SIMULATION OF TIME-SERIES OF LAND USE AND LAND COVER DATA BY CLUE-S MODEL were applied to map LULC data in 2029, 2039, and 2049 for drought, normal, and wet years. Simultaneously, the conversion matrix for each LULC type possibly change in 2029, 2039, and 2049 are set up based on transitional LULC change between 2010 and 2019 as the summary in Table 7.16. So, it can be observed that urban and built-up areas in 2019 do not allow to change to any LULC types in 2029, 2039, and 2049.

Table 7.16 Conversion matrix of the possible change in 2029, 2039, and 2049.

LULC types	LULC type possible change in 2029, 2039, and 2049											
	UR	PA	SU	CA	FC	PR	PO	FO	WA	RA	MA	UL
Urban and built-up area (UR)	1	0	0	0	0	0	0	0	0	0	0	0
Paddy field (PA)	0	1	1	1	0	0	0	0	0	1	1	0
Sugarcane (SU)	1	0	1	1	0	1	1	0	0	0	0	0
Cassava (CA)	1	1	1	1	0	1	1	0	0	1	0	1
Other field crops (FC)	0	0	0	0	1	0	0	0	0	0	0	0
Para rubber (PR)	0	0	1	1	1	1	0	0	0	0	0	1
Perennial trees and orchard (PO)	0	0	1	1	0	0	1	0	0	0	0	0
Forest land (FO)	0	0	0	0	0	1	1	1	0	1	0	1
Waterbody (WA)	0	0	0	0	0	0	0	0	1	0	1	0
Rangeland (RA)	0	1	0	1	0	0	1	0	0	1	0	0
Marsh and swamp (MA)	0	1	1	0	0	0	0	1	0	0	1	0
Unused land (UL)	1	0	0	0	0	0	0	0	0	0	0	1

Remark: 0 is not allowed and 1 is allowed.

The transition probability matrix of LULC change of three periods (2019-2029, 2019-2039, and 2019-2049) from the Markov Chain model are displayed in Tables 7.17 to 7.19. As a result, the elasticity values or land use type resistance can be assigned according to the probability values of the transition probability matrix of LULC change in a specific period, as suggested by Ongsomwang and Iamchuen (2015).

For LULC prediction in 2029, the elasticity value of the urban and built-up area, paddy field, sugarcane, cassava, other field crops, para rubber, perennial trees and orchard, forest land, waterbody, rangeland, marsh and swamp, and unused land are 1.00, 0.93, 0.93, 0.65, 0.99, 0.80, 0.99, 0.80, 0.91, 0.89, 0.56 and 0.96, respectively. (See Table 7.17)

Likewise. the elasticity value of the urban and built-up area, paddy field, sugarcane, cassava, other field crops, para rubber, perennial trees and orchard, forest land, waterbody, rangeland, marsh and swamp, and unused land for LULC prediction in 2039 are 1.00, 0.88, 0.87, 0.43, 0.98, 0.64, 0.97, 0.73, 0.84, 0.80, 0.73 and 0.91, respectively. (See Table 7.18)

Similarly, the elasticity value of the urban and built-up area, paddy field, sugarcane, cassava, other field crops, para rubber, perennial trees and orchard, forest land, waterbody, rangeland, marsh and swamp, and unused land for LULC prediction in 2049 are 1.00, 0.83, 0.83, 0.31, 0.97, 0.52, 0.96, 0.70, 0.76, 0.71, 0.76 and 0.87, respectively. (See Table 7.19)

Table 7.17 Elasticity of LULC change for LULC prediction between 2019 and 2029.

LULC types	LULC type possible change in 2029											
	UR	PA	SU	CA	FC	PR	PO	FO	WA	RA	MA	UL
Urban and built-up area (UR)	1.00	-	-	-	-	-	-	-	-	-	-	-
Paddy field (PA)	-	0.93	0.03	0.02	-	-	0.01	-	-	-	0.01	-
Sugarcane (SU)	0.01	0.01	0.93	0.05	-	-	0.01	-	-	-	-	-
Cassava (CA)	0.01	0.06	0.16	0.65	-	0.07	0.01	-	-	-	-	0.04
Other field crops (FC)	-	-	-	-	0.99	-	0.01	-	-	-	-	-
Para rubber (PR)	-	-	-	0.11	0.01	0.80	0.03	-	-	-	-	0.05
Perennial trees and orchard (PO)	-	-	0.01	0.01	-	-	0.99	-	-	-	-	-
Forest land (FO)	-	0.02	-	0.05	-	0.05	0.01	0.80	-	-	-	0.06
Waterbody (WA)	-	0.04	0.02	0.01	-	-	-	-	0.91	-	0.01	-
Rangeland (RA)	-	0.08	-	0.02	-	-	0.01	-	-	0.89	-	-
Marsh and swamp (MA)	0.01	0.39	0.03	-	-	-	0.02	-	-	-	0.56	-
Unused land (UL)	0.01	0.03	-	-	-	-	-	-	-	-	-	0.96

Table 7.18 Elasticity of LULC change for LULC prediction between 2019 and 2039.

LULC types	LULC type possible change in 2039											
	UR	PA	SU	CA	FC	PR	PO	FO	WA	RA	MA	UL
Urban and built-up area (UR)	1.00	-	-	-	-	-	-	-	-	-	-	-
Paddy field (PA)	-	0.88	0.06	0.03	-	-	0.02	-	-	-	0.01	-
Sugarcane (SU)	0.01	0.02	0.87	0.08	-	-	0.01	-	-	-	-	-
Cassava (CA)	0.02	0.10	0.25	0.43	-	0.10	0.02	-	-	0.01	-	0.06
Other field crops (FC)	-	-	-	-	0.98	-	0.01	-	-	-	-	-
Para rubber (PR)	-	0.01	0.03	0.16	0.02	0.64	0.05	-	-	-	-	0.10
Perennial trees and orchard (PO)	-	-	0.01	0.01	-	-	0.97	-	-	-	-	-
Forest land (FO)	0.01	0.04	0.01	0.08	-	0.08	0.03	0.73	-	-	-	0.01
Waterbody (WA)	0.01	0.07	0.05	0.02	-	-	-	-	0.84	-	0.01	-
Rangeland (RA)	-	0.15	0.01	0.03	-	-	0.01	-	-	0.80	-	-
Marsh and swamp (MA)	0.01	0.15	0.05	0.01	-	-	0.04	-	-	-	0.73	-
Unused land (UL)	0.01	0.06	-	0.01	-	-	-	-	-	-	-	0.91

LULC in 2019

Table 7.19 Elasticity of LULC change for LULC prediction between 2019 and 2049.

LULC types	LULC type possible change in 2049											
	UR	PA	SU	CA	FC	PR	PO	FO	WA	RA	MA	UL
Urban and built-up area (UR)	1.00	-	-	-	-	-	-	-	-	-	-	-
Paddy field (PA)	-	0.83	0.08	0.04	-	-	0.03	-	-	-	0.01	-
Sugarcane (SU)	0.02	0.03	0.83	0.09	-	0.01	0.02	-	-	-	-	0.01
Cassava (CA)	0.03	0.12	0.31	0.31	-	0.11	0.03	-	-	0.01	-	0.08
Other field crops (FC)	-	-	-	-	0.97	-	0.02	-	-	-	-	-
Para rubber (PR)	0.01	0.02	0.05	0.18	0.02	0.52	0.07	-	-	-	-	0.13
Perennial trees and orchard (PO)	-	0.01	0.02	0.01	-	-	0.96	-	-	-	-	-
Forest land (FO)	0.01	0.01	0.03	0.04	-	0.10	0.04	0.70	-	0.01	-	0.04
Waterbody (WA)	0.01	0.10	0.07	0.03	-	-	0.01	-	0.76	-	0.01	-
Rangeland (RA)	-	0.21	0.02	0.03	-	-	0.02	-	-	0.71	-	-
Marsh and swamp (MA)	0.01	0.06	0.08	0.03	-	-	0.05	-	-	-	0.77	-
Unused land (UL)	0.02	0.08	0.01	0.01	-	-	0.01	-	-	-	-	0.87

LULC in 2019

In addition, the area of optimized LULC allocation in drought, normal, and wet years from the previous section was applied as the land requirement to predict LULC maps for flood mitigation by the CLUE-S model. The annual land requirement of each land use type for LULC prediction in drought, normal, and wet years in 2029, 2039, and 2049 are presented in Table 7.20.

Table 7.20 Annual land requirement of each land use type for LULC prediction in 2029, 2039, and 2049 under drought, normal, and wet years.

LULC type	Allocated area of drought years (km^2)			Allocated area of normal years (km^2)			Allocated area of wet years (km^2)		
	2029	2039	2049	2029	2039	2049	2029	2039	2049
Urban and built-up area	65.84	65.84	65.84	65.84	65.84	65.84	65.84	65.84	65.84
Paddy field	1,947.12	1,879.30	1,812.16	1,947.12	1,879.30	1,812.16	1,947.12	1,879.30	1,812.16
Sugarcane	387.24	454.94	517.13	385.71	451.67	512.06	422.14	520.31	599.36
Cassava	408.26	359.65	330.32	408.26	359.65	330.32	408.26	358.65	330.32
Other field crops	6.19	6.19	6.19	7.72	9.45	11.26	6.19	9.45	11.26
Para rubber	134.43	152.02	164.41	134.43	152.02	164.41	134.43	152.02	164.41
Perennial trees and orchard	125.36	160.12	193.13	125.36	160.12	193.13	88.95	90.48	103.83
Forest land	481.30	481.30	481.30	481.30	481.30	481.30	481.30	481.30	481.30
Waterbody	49.52	47.01	42.78	49.52	47.01	42.78	50.02	48.01	43.78
Rangeland	70.54	69.91	66.05	70.54	69.91	66.05	70.54	69.91	66.05
Marsh and swamp	25.13	24.66	21.61	25.13	24.66	21.61	26.13	25.66	22.61
Unused land	93.31	93.31	93.31	93.31	93.31	93.31	93.31	93.31	93.31
SUM	3,794.22	3,794.22	3,794.22	3,794.22	3,794.22	3,794.22	3,794.22	3,794.22	3,794.22

The spatial distribution of the LULC allocation maps in 2029, 2039, and 2049 for drought, normal, and wet years are displayed in Figures 7.10 to 7.12, respectively. Meanwhile, the area and percentage of LULC type in 2029, 2039, and 2049 for drought, normal, and wet years are summarized in Tables 7.21 and 7.22.

As a result, there are unchanged areas in the urban and built-up area, other field crops, forest land, and unused land under drought year conditions. Meanwhile, sugarcane, para rubber, and perennial trees and orchards are increasing LULC types by about 6.49, 1.50, and 3.39 km^2 per year, respectively. In contrast, paddy field, cassava, waterbody, rangeland, and marsh and swamp are decreasing LULC types by about 6.75, 3.90, 0.34, 0.23, and 0.18 km^2 per year, respectively.

Under normal year conditions, there are unchanged areas in the urban and built-up area, forest land, and unused land. In the meantime, sugarcane, para rubber, and perennial trees and orchards are increasing LULC types by about 6.32, 1.50, and 3.39 km^2 per year, respectively. On the other hand, paddy field, cassava, other field crops, waterbody, rangeland, and marsh and swamp are decreasing LULC types by about 6.75, 3.90, 0.18, 0.34, 0.22, and 0.18 km^2 per year, respectively.

Likewise, there are unchanged areas in the urban and built-up area, forest land, and unused land under wet year conditions. Meanwhile, sugarcane, para rubber, perennial trees and orchards are increasing LULC types by about 8.86, 1.50, and 0.75 km^2 per year, respectively. Conversely, paddy field, cassava, other field crops, waterbody, rangeland, and marsh and swamp are decreasing LULC types by about 6.75, 3.90, 0.25, 0.31, 0.22, and 0.18 km^2 per year, respectively.

Predicted LULC in 2029

Predicted LULC in 2039

Predicted LULC in 2049
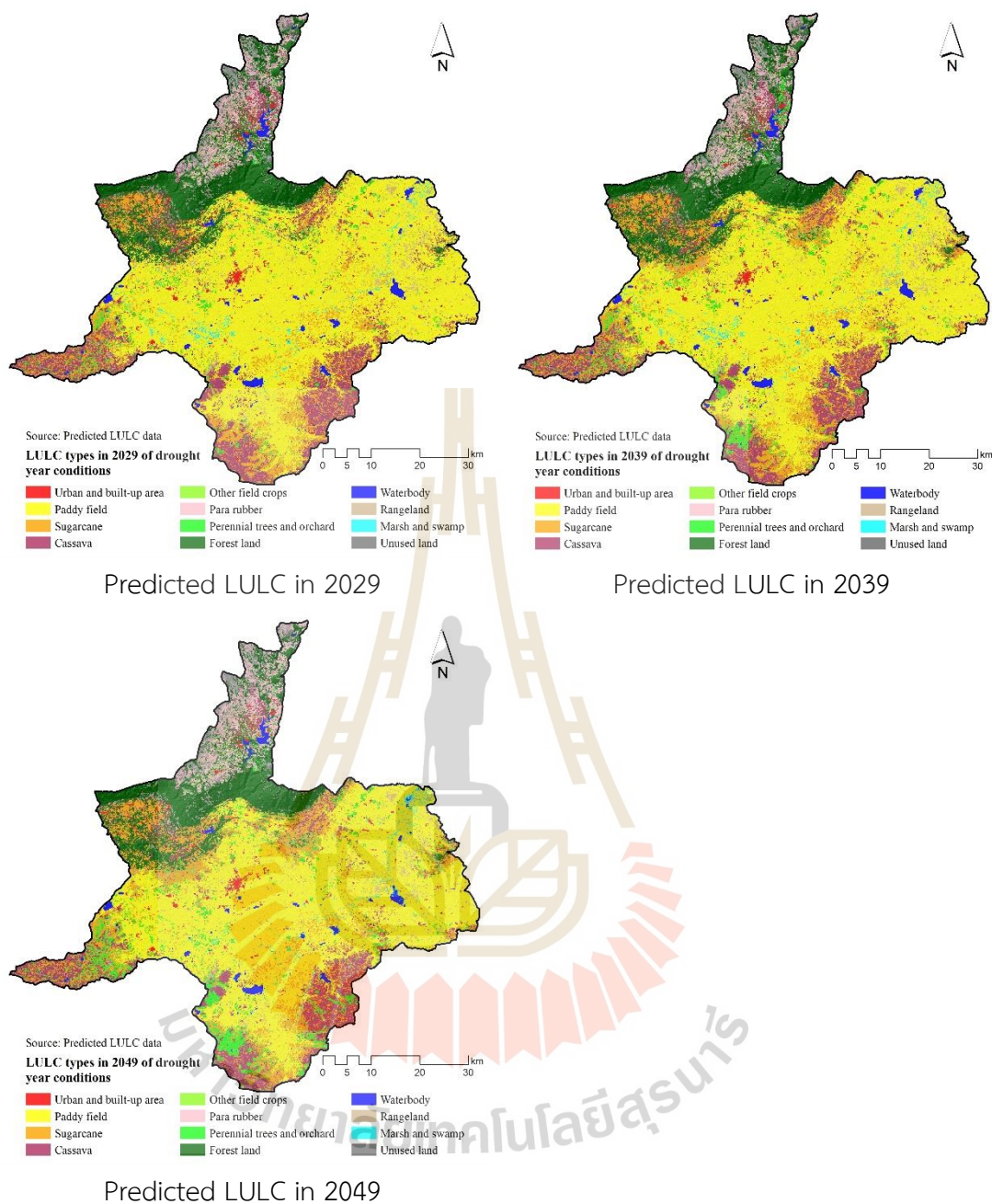
Figure 7.10 Spatial distribution of predicted LULC data in 2029, 2039, and 2049 under drought year conditions.

Predicted LULC in 2029

Predicted LULC in 2039

Predicted LULC in 2049
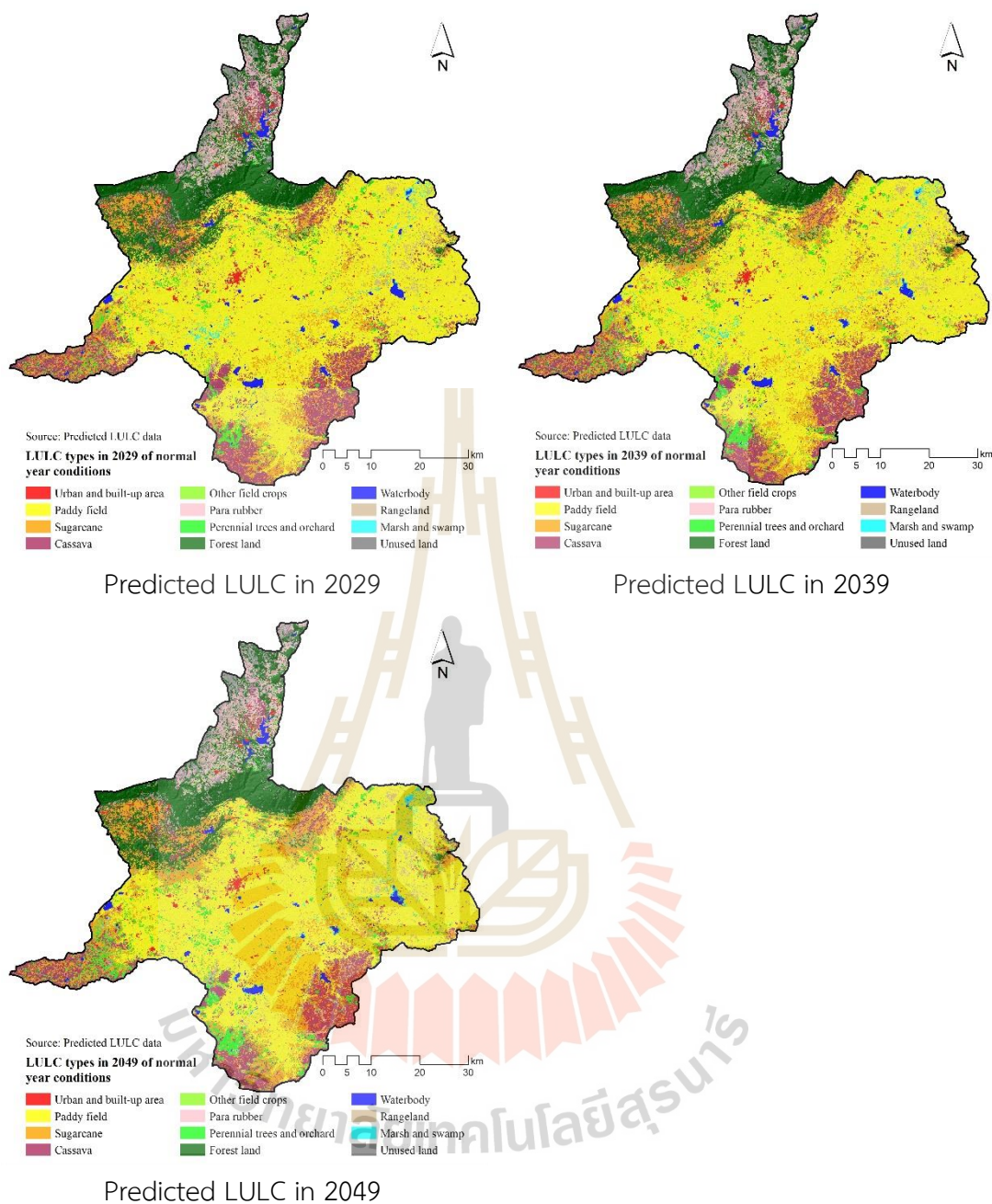
Figure 7.11 Spatial distribution of predicted LULC data in 2029, 2039, and 2049 under normal year conditions.

Predicted LULC in 2029

Predicted LULC in 2039

Simulated LULC in 2049
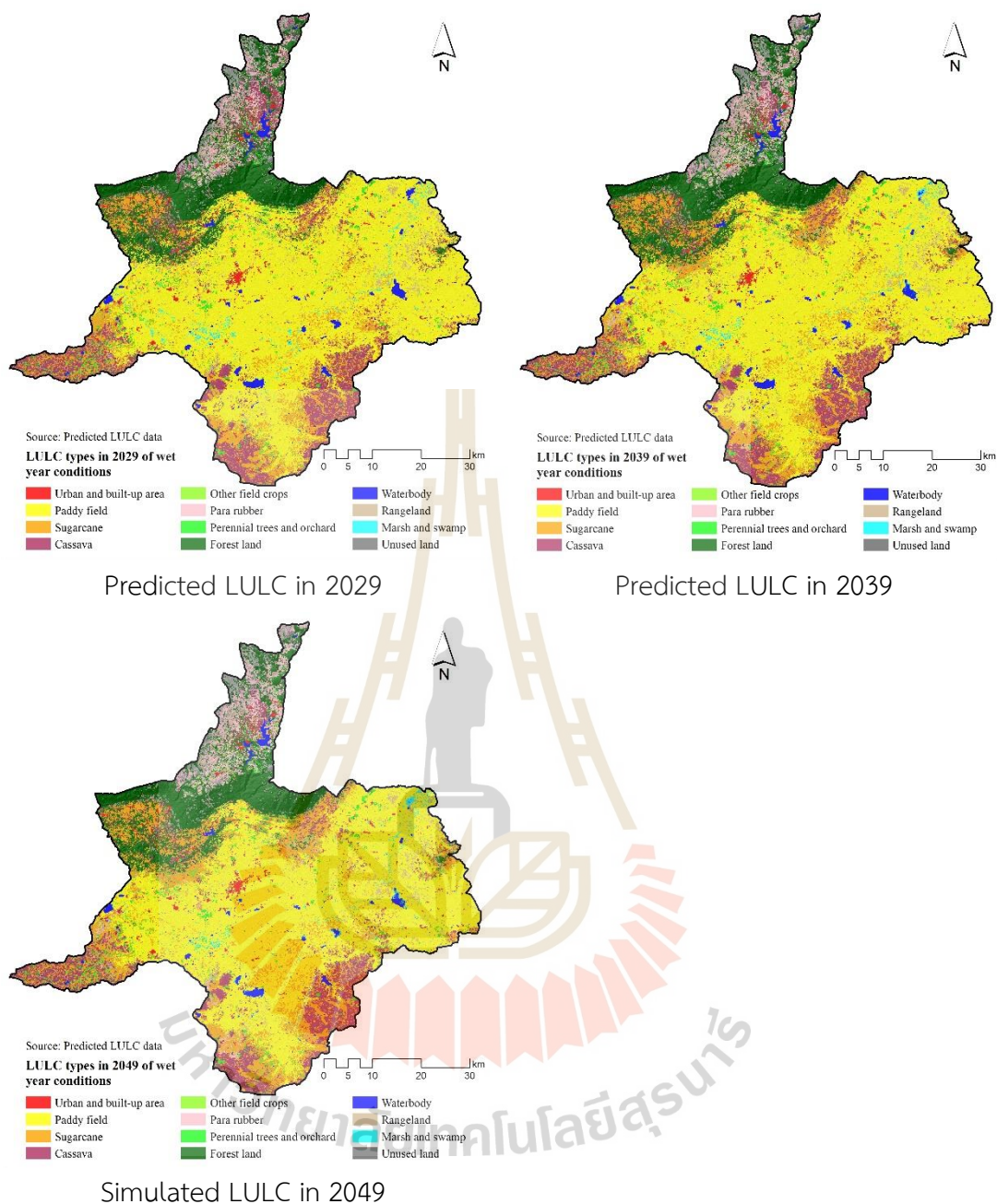
Figure 7.12 Spatial distribution of predicted LULC data in 2029, 2039, and 2049 under wet year conditions.

Table 7.21 Area of predicted LULC type in 2029, 2039, and 2049 in drought, normal, and wet years.

LULC type	LULC area in drought years in km^2				LULC area in normal years in km^2				LULC area in wet years in km^2			
	2029	2039	2049	Annual rate	2029	2039	2049	Annual rate	2029	2039	2049	Annual rate
Urban and built-up area	65.81	65.82	65.88	0.00	65.83	65.89	65.86	0.00	65.87	65.82	65.89	0.00
Paddy field	1,947.07	1,879.28	1,812.14	-6.75	1,947.13	1,879.32	1,812.13	-6.75	1,947.10	1,879.33	1,812.18	-6.75
Sugarcane	387.25	454.96	517.12	6.49	385.69	451.65	512.07	6.32	422.16	520.32	599.34	8.86
Cassava	408.28	359.66	330.33	-3.90	408.29	359.67	330.33	-3.90	408.27	358.67	330.34	-3.90
Other field crops	6.20	6.20	6.19	0.00	7.73	9.44	11.27	-0.18	6.19	9.45	11.25	-0.25
Para rubber	134.45	152.02	164.42	1.50	134.44	152.02	164.41	1.50	134.42	152.02	164.41	1.50
Perennial trees and orchard	125.33	160.10	193.17	3.39	125.35	160.17	193.15	3.39	88.98	90.46	103.88	0.75
Forest land	481.33	481.32	481.26	0.00	481.31	481.30	481.30	0.00	481.32	481.31	481.30	0.00
Waterbody	49.53	47.02	42.77	-0.34	49.52	47.01	42.80	-0.34	50.05	48.01	43.78	-0.31
Rangeland	70.57	69.93	66.07	-0.23	70.49	69.87	66.04	-0.22	70.50	69.91	66.01	-0.22
Marsh and swamp	25.11	24.62	21.57	-0.18	25.16	24.62	21.58	-0.18	26.09	25.63	22.56	-0.18
Unused land	93.29	93.29	93.30	0.00	93.28	93.26	93.28	0.00	93.27	93.30	93.28	0.00
SUM	3,794.22	3,794.22	3,794.22		3,794.22	3,794.22	3,794.22		3,794.22	3,794.22	3,794.22	

Table 7.22 Percentage of simulated LULC type in 2029, 2039, and 2049 in drought, normal, and wet years.

LULC type	LULC area in drought years in percent			LULC area in normal years in percent			LULC area in wet years in percent		
	2029	2039	2049	2029	2039	2049	2029	2039	2049
Urban and built-up area	1.73	1.73	1.74	1.74	1.74	1.74	1.74	1.73	1.74
Paddy field	51.32	49.53	47.76	51.32	49.53	47.76	51.32	49.53	47.76
Sugarcane	10.21	11.99	13.63	10.17	11.90	13.50	11.13	13.71	15.80
Cassava	10.76	9.48	8.71	10.76	9.48	8.71	10.76	9.45	8.71
Other field crops	0.16	0.16	0.16	0.20	0.25	0.30	0.16	0.25	0.30
Para rubber	3.54	4.01	4.33	3.54	4.01	4.33	3.54	4.01	4.33
Perennial trees and orchard	3.30	4.22	5.09	3.30	4.22	5.09	2.35	2.38	2.74
Forest land	12.69	12.69	12.68	12.69	12.69	12.69	12.69	12.69	12.69
Waterbody	1.31	1.24	1.13	1.31	1.24	1.13	1.32	1.27	1.15
Rangeland	1.86	1.84	1.74	1.86	1.84	1.74	1.86	1.84	1.74
Marsh and swamp	0.66	0.65	0.57	0.66	0.65	0.57	0.69	0.68	0.59
Unused land	2.46	2.46	2.46	2.46	2.46	2.46	2.46	2.46	2.46
SUM	100.00	100.00	100.00	100.00	100.00	100.00	100.00	100.00	100.00

The actual LULC data in 2019 and derived suitable LULC data in 2049 for flood mitigation using the Goal Programming under three different rainfall conditions (drought, normal, and wet years) will be further applied to evaluate economic and ecosystem service values using the PV model and simple benefit transfer method of ecosystem service value and to detect value change in terms of gain and loss for project implementation using the image algebra change detection algorithm.

CHAPTER VIII
ECONOMIC AND ECOSYSTEM SERVICE VALUES EVALUATION
AND CHANGE

This chapter presents the sixth objective results focusing on economic and ecosystem service evaluation and change in terms of gain and loss for project implementation. The significant results in this chapter consist of (1) economic value evaluation, (2) assessment of economic value change, (3) ecosystem service value evaluation, and (4) assessment of ecosystem service value change are here described and discussed in detail.

8.1   Economic value evaluation

The future economic value of actual LULC data in 2019 and suitable LULC allocation data in 2049 for flood mitigation under three different rainfall conditions (drought, normal, and wet years) were first estimated based on the present value of the selected LULC type using the PV equation (see Equation 3.14 of Chapter III). Figure 8.1 presents the spatial distribution of actual LULC data in 2019, which was classified using RF classifier, and suitable LULC allocation data in 2049, which were optimized LULC allocation for flood mitigation using Goal programming and were predicted using the CLUE-S model. Areas of actual LULC in 2019 and suitable LULC allocation for flood mitigation in 2049 under drought, normal, and wet years are summarized in Table 8.1.
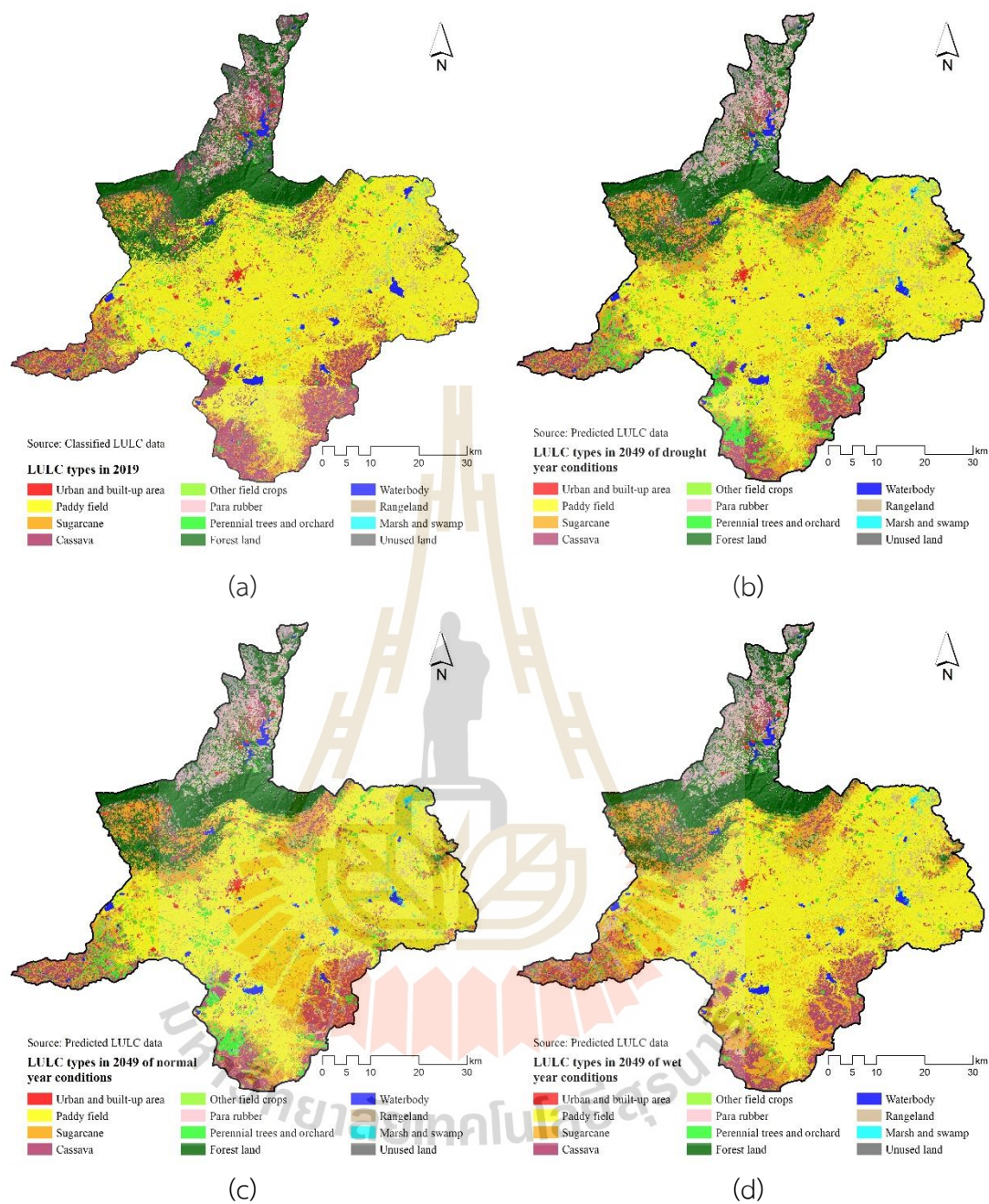
Figure 8.1 Spatial distribution map: (a) actual LULC in 2019, (b) suitable LULC allocation in 2049 under drought year, (c) suitable LULC allocation in 2049 under normal year, and (d) suitable LULC allocation in 2049 under wet year.

Table 8.1 Areas of actual LULC in 2019 and suitable LULC allocation for flood mitigation in 2019 under drought, normal, and wet years.

No.	LULC type	Actual LULC 2019	Suitable LULC allocation in 2049		
			Drought year	Normal year	Wet year
1	Urban and built-up area	65.84	65.84	65.84	65.84
2	Paddy field	2,012.16	1,812.14	1,812.13	1,812.18
3	Sugarcane	306.85	517.12	512.07	599.34
4	Cassava	489.91	330.33	330.33	330.34
5	Other field crops	6.19	6.19	11.27	11.25
6	Para rubber	97.03	164.42	164.41	164.41
7	Perennial trees and orchard	88.95	193.17	193.15	103.88
8	Forest land	481.30	481.26	481.30	481.30
9	Water body	53.30	42.77	42.80	43.78
10	Rangeland	71.65	66.07	66.04	66.01
11	Marsh and swamp	27.73	21.57	21.58	22.56
12	Unused land	93.32	93.30	93.28	93.28
	Total	3,794.22	3,794.22	3,794.22	3,794.22

As a result in Table 8.1, the top three dominant LULC types of actual LULC data in 2019 are paddy field, cassava, and forest land, while the top three dominant LULC types of suitable LULC allocation data in 2049 for flood mitigation under drought, normal, and wet years are paddy field, sugarcane, and forest land.

The future values of LULC types in agricultural and forest land, including paddy fields, sugarcane, cassava, other field crops, para rubber, perennial trees and orchard, and forest land, were applied to calculate the future economic value in 2049 of actual LULC data in 2019 and suitable LULC allocation data in 2049 for flood mitigation under three rainfall conditions. The present economic values (revenue) of each selected LULC type (Baht per km^2), which were derived from the government agency reports, are presented in Table 8.2. Meanwhile, the future economic values of these LULC types (Baht per km^2) are presented in Table 8.3. As a result, the top three highest present economic values of future economic value in 2049 are forest land, perennial trees and orchards, and para rubber.

The future economic value in 2049 of actual LULC data and suitable LULC allocation for flood mitigation from drought, normal, and wet years are presented in Table 8.4 and shown in Figures 8.2 to 8.5.

Table 8.2 Present economic value of the agricultural and forest land in 2019.

LULC type	Price (Baht/ton)	Yield (ton/km[2])	Revenue (Baht/ km[2])
Paddy field[1]	13,287.75	218.75	2,906,695.31
Sugarcane[2]	900.00	4,468.75	4,021,875.00
Cassava[1]	1,430.00	2,240.63	3,204,093.75
Other field crops[1]	8,092.50	415.63	3,363,445.31
Para rubber[3]	43,685.83	131.25	5,733,765.63
Perennial trees and orchard[4]	25,600.00	247.24	6,329,440.00
Forest land[5]	-	-	25,000,000.00

Source: [1]Office of Agricultural Economics: OAE (2019), [2]Office of the cane and sugar board: OCSB (2019), [3]Rubber Authority of Thailand: RAOT (2019), [4]Chaiyaphum Provincial Statistical Office (2019), and [5]Wittawatchutikul and Jirasuktaveekul (2005).

Table 8.3 Future economic value of the agricultural and forest land in 2049.

LULC type	Present value (Baht/km[2])	Discount rate in %*	Period from Present (year)	Future value in 2049 (Baht/km[2])
Paddy field	2,906,695.31	6.50	30	19,225,947.12
Sugarcane	4,021,875.00	6.50	30	26,602,153.91
Cassava	3,204,093.75	6.50	30	21,193,049.28
Other field crops	3,363,445.31	6.50	30	22,247,058.87
Para rubber	5,733,765.63	6.50	30	37,925,225.34
Perennial trees and orchard	6,329,440.00	6.50	30	41,865,233.77
Forest land	25,000,000.00	6.50	30	165,359,154.08

* Discount rate was based on the minimum retail rate of Bank for Agriculture and Agricultural Cooperatives (2019).

Table 8.4 Economic value by LULC types of actual LULC 2019 and suitable LULC allocation for flood mitigation in 2049.

LULC type	Actual LULC in 2019	Economic value in 2049 (Baht)		
		Suitable LULC allocation for flood mitigation in 2049		
		Drought year	Normal year	Wet year
Paddy field	38,654,201,193.72	34,629,199,176.42	34,822,304,589.30	34,826,094,023.48
Sugarcane	8,147,417,736.68	13,678,867,444.77	13,614,032,675.26	15,920,814,509.80
Cassava	10,347,296,501.34	6,783,214,778.67	6,979,083,059.45	6,968,649,721.29
Other field crops	137,813,855.56	136,472,357.91	200,363,686.27	200,684,043.91
Para rubber	3,675,102,243.52	6,145,559,007.00	6,235,430,413.48	6,222,152,792.09
Perennial trees and orchard	3,717,456,924.53	9,041,534,060.10	8,055,821,317.58	4,404,829,638.18
Forest land	79,388,714,905.00	78,164,792,590.19	79,303,885,658.96	79,315,047,401.86
Total in Baht	**144,068,003,360.34**	**148,579,639,415.06**	**149,210,921,400.29**	**147,858,272,130.61**
Total in million Baht	**144,068.00**	**148,579.64**	**149,210.92**	**147,858.27**
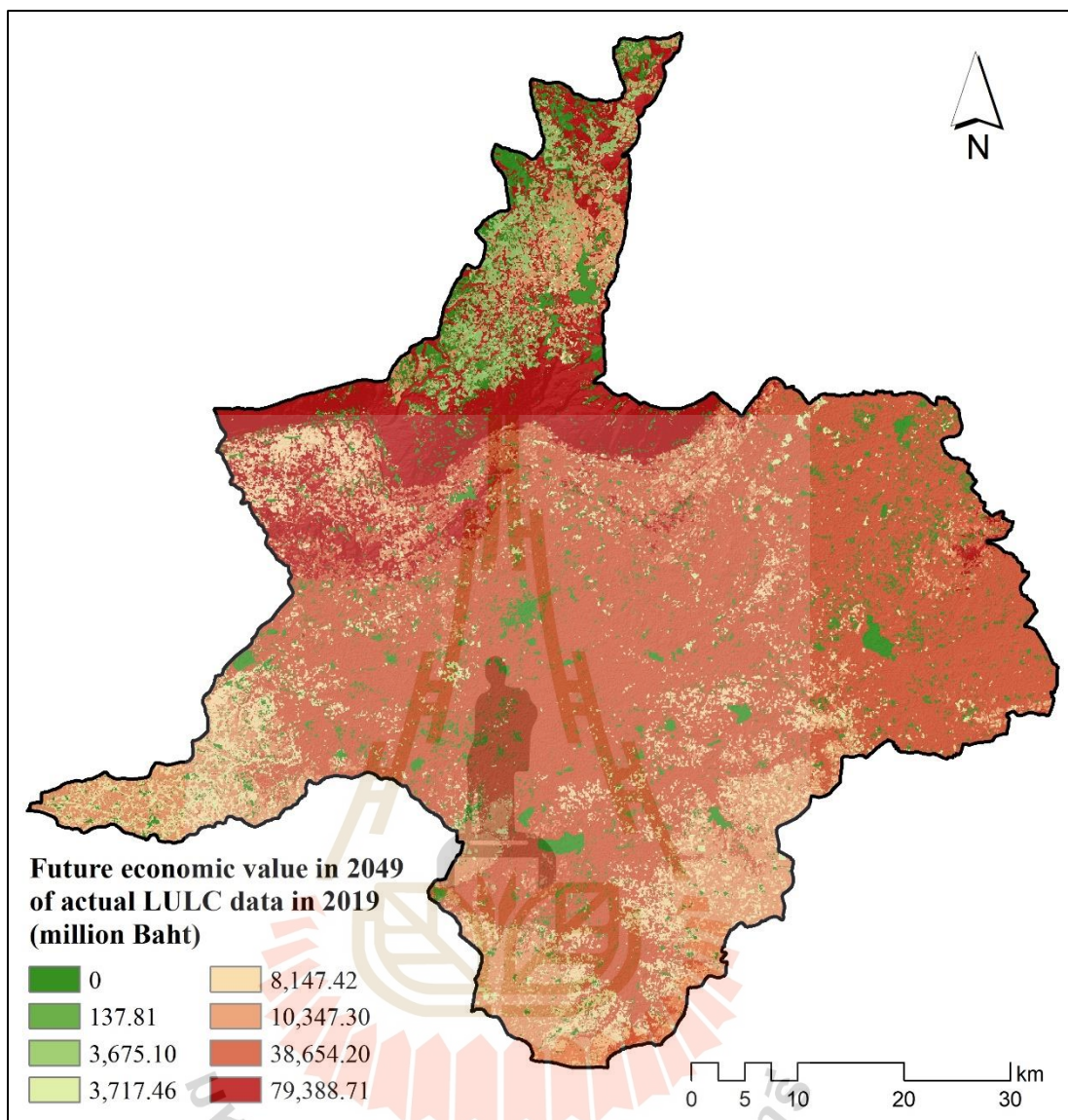
Figure 8.2 Spatial distribution of economic value in 2049 of actual LULC 2019.
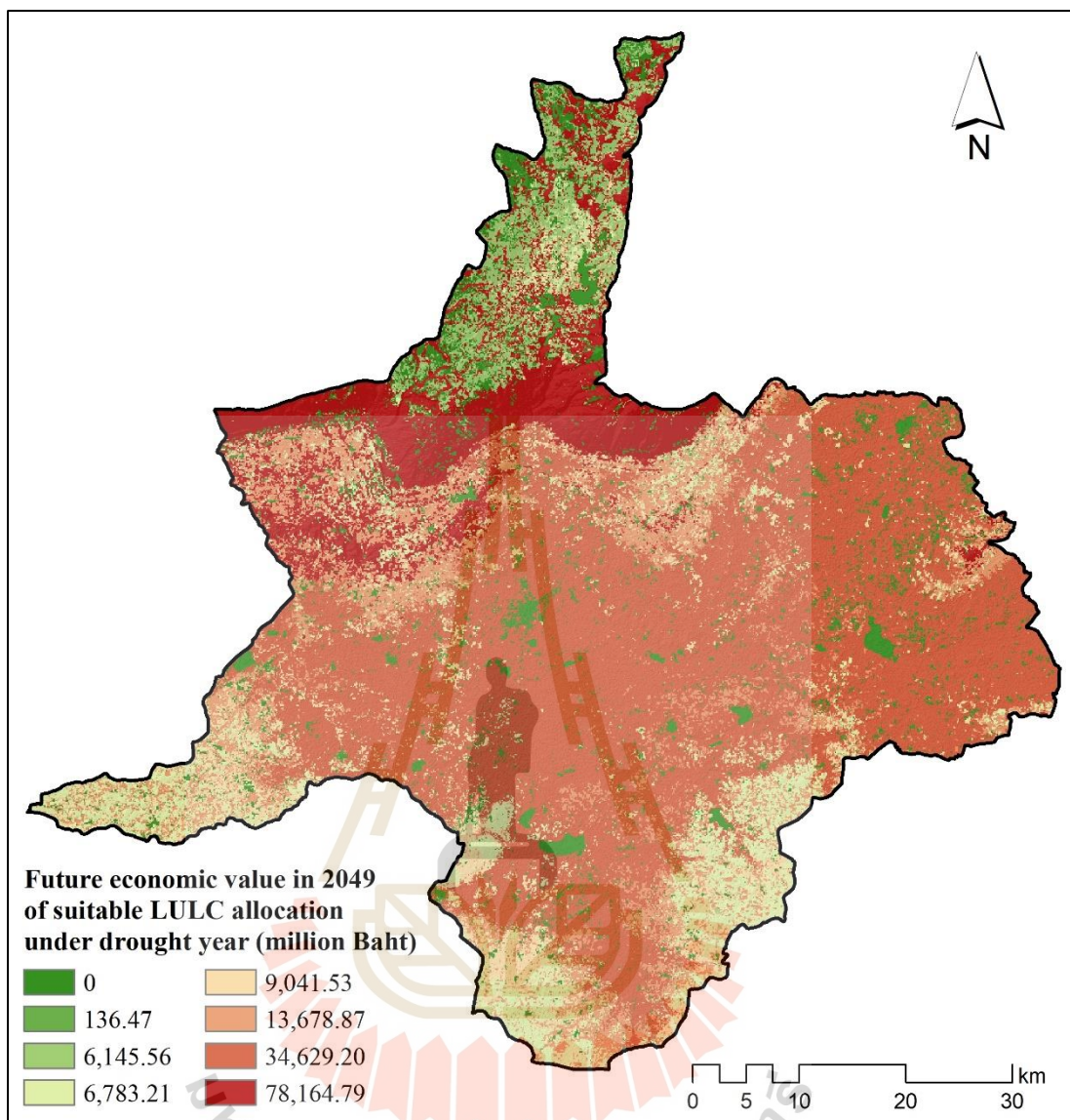
Figure 8.3 Spatial distribution of economic value in 2049 of suitable LULC allocation for flood mitigation under drought year.
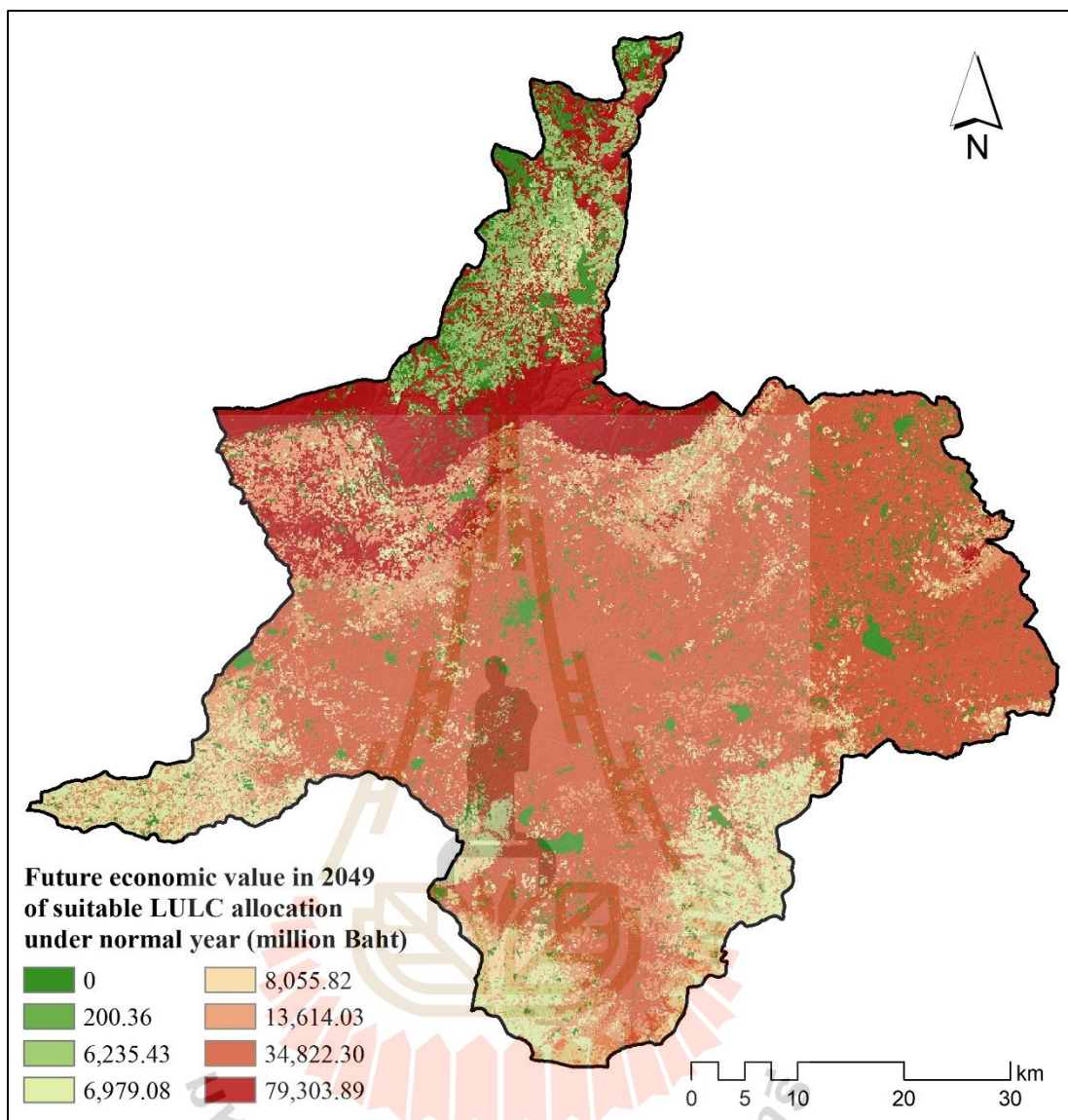
Figure 8.4 Spatial distribution of future economic value in 2049 of suitable LULC allocation for flood mitigation under normal year.
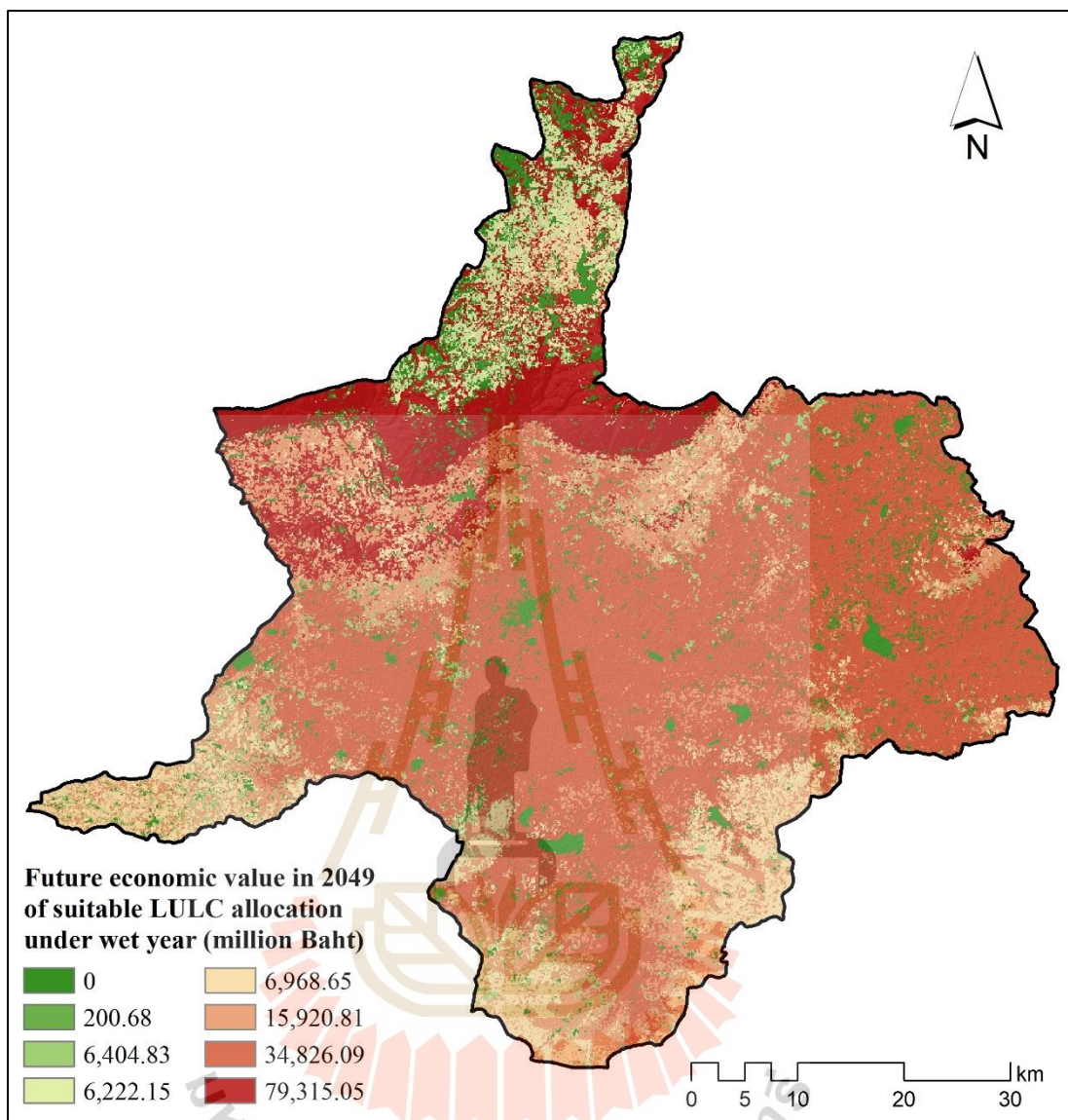
Figure 8.5 Spatial distribution of economic value in 2049 of suitable LULC allocation for flood mitigation under wet year.

As a result, in Table 8.4, the economic value of actual LULC and suitable LULC allocation data for flood mitigation from three rainfall conditions (drought, normal and wet years) are relatively different. The suitable LULC allocation data for flood mitigation under normal year provides the highest economic value, about 149,211 million Baht, while actual LULC allocation in 2019 provides the lowest economic value, about 144,068 million Baht. The comparison of future economic value among actual LULC and suitable LULC allocation data for flood mitigation from three different rainfall conditions is displayed in Figure 8.6. Meanwhile, the contribution of the economic value by LULC type from actual LULC and suitable LULC allocation data for flood mitigation from three different rainfall conditions are compared in Figure 8.7.
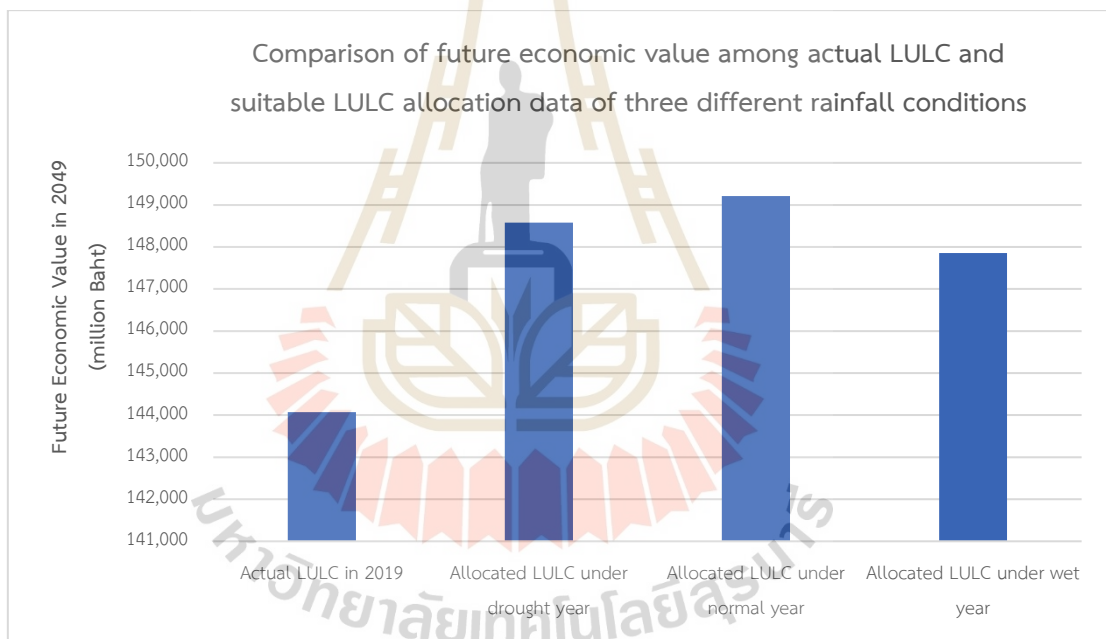
Figure 8.6 Comparing future economic value among actual LULC and suitable LULC allocation data for flood mitigation from three different rainfall conditions.
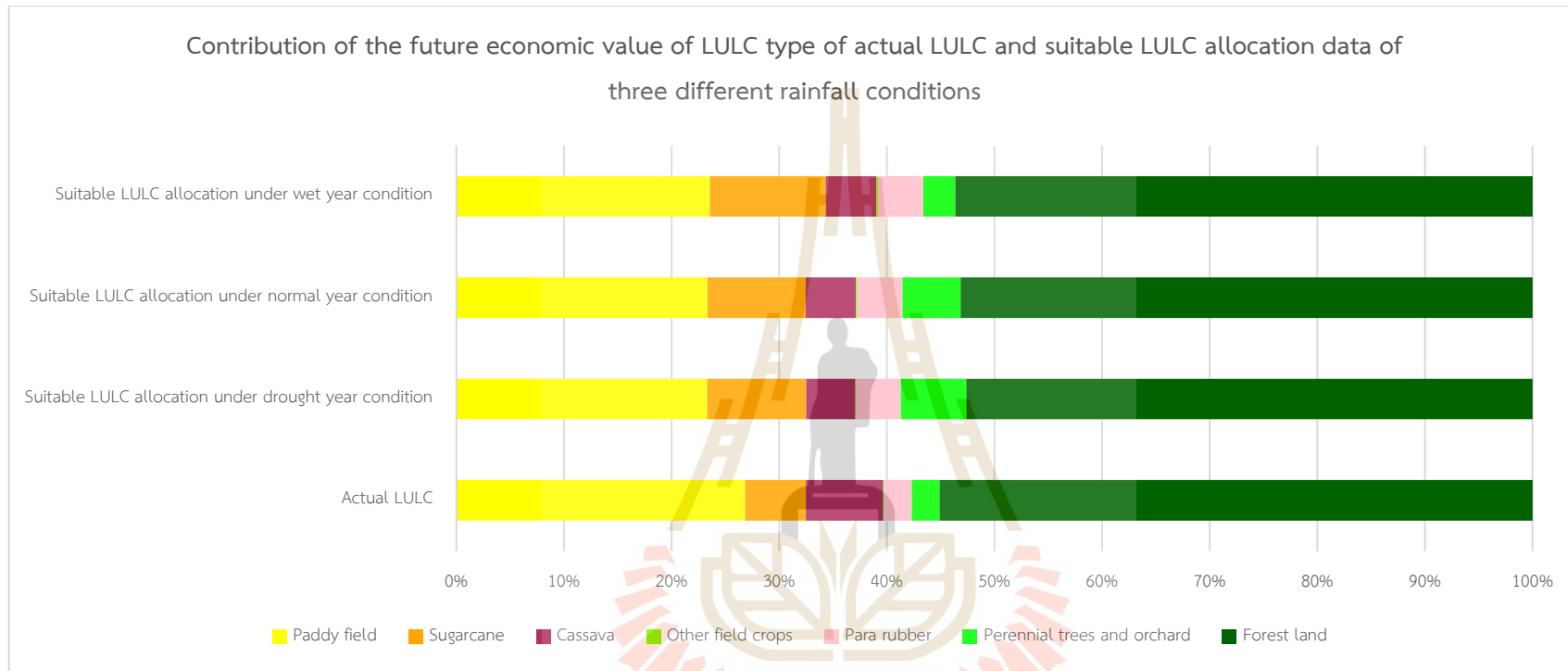
Figure 8.7 Contribution of the future economic value of LULC type of actual LULC and suitable LULC allocation for flood mitigation under drought, normal, and wet years.

According to data in Figure 8.7, the future economic value of forest land from actual LULC and suitable LULC allocation data for flood mitigation under drought, normal and wet years contributes the highest values than other LULC types because the present economic value, about 25,000,000 Baht per km^2 or future economic of forest land, about 165,359,154 Baht per km^2 is exceptionally high when they are compared with other LULC types (See Tables 8.2 or 8.3).

Furthermore, the top three dominant LULC types of actual LULC in 2019, including paddy fields, cassava, and forest land, will provide future economic value in 2049, about 89% of the total value. Meanwhile, the top three dominant LULC types of suitable LULC allocation for flood mitigation under drought, normal, and wet years, including paddy fields, sugarcane, and forest land, deliver future economic value in 2049 about 85%, 86%, and 88% of the total value, respectively.

8.2 Assessment of economic value change

Future economic value maps of actual LULC data and suitable LULC allocation for flood mitigation in 2049 under drought, normal, and wet years were detected future economic value change in terms of gain and loss using the image algebra change detection algorithm.

Results of future economic value change between suitable LULC allocation for flood mitigation in 2049 from drought, normal, and wet years and actual LULC data in 2019 with gain (+sign) and loss (-sign) are reported in Tables 8.5 to 8.7. Meanwhile, the spatial distribution of economic value change in terms of gain and loss of suitable LULC allocation for flood mitigation in 2049 under three different rainfall conditions are displayed in Figures 8.8 to 8.10, respectively.

Table 8.5 Economic value change between suitable LULC allocation in 2049 under drought year and actual LULC in 2019.

ECV in Baht

LULC type		Suitable LULC allocation in 2049 of drought year							SUM
		PA	SU	CA	FC	PR	PO	FO	
Actual LULC in 2019	Paddy field (PA)	0.00	1,507,297,615.23	28,212,966.05	19,033.00	18,108,381.02	602,051,077.63	1,656,229,927.66	3,811,919,000.60
	Sugarcane (SU)	-188,270,302.13	0.00	-105,109,180.24	-987,735.56	14,053,063.95	173,000,904.92	789,999,104.73	682,685,855.69
	Cassava (CA)	-28,205,884.48	207,959,518.38	0.00	279,839.54	813,499,994.33	1,983,531,243.93	1,249,228,131.25	4,226,292,842.96
	Other field crops (FC)	-10,876.00	909,343.85	-110,038.60	0.00	12,191,342.25	423,752.58	104,328,717.41	117,732,241.48
	Para rubber (PR)	0.00	-2,680,171.01	-25,434,580.82	-8,988,292.84	0.00	2,446,745.24	1,167,205,583.50	1,132,549,284.07
	Perennial trees and orchard (PO)	-193,525,150.11	-123,836,998.40	-86,029,362.95	-353,127.15	-5,095,612.90	0.00	237,515,856.93	-171,324,394.58
	Forest land (FO)	-131,256,846.49	-2,240,870,049.85	-630,193,293.88	-95,312,655.41	-2,467,681,569.68	-305,091,730.12	0.00	-5,870,406,145.43
	SUM	-541,269,059.20	-651,220,741.80	-818,663,490.44	-105,342,938.40	-1,614,924,401.03	2,456,361,994.17	5,204,507,321.49	3,929,448,684.79

Table 8.6 Economic value change between suitable LULC allocation in 2049 under normal year and actual LULC in 2019.

ECV in Baht

LULC type		Suitable LULC allocation in 2049 of normal year							SUM
		PA	SU	CA	FC	PR	PO	FO	
Actual LULC in 2019	Paddy field (PA)	0.00	1,453,478,597.63	28,896,337.34	19,033.00	38,034,331.89	563,562,026.40	1,656,229,927.66	3,740,220,253.92
	Sugarcane (SU)	-190,746,494.75	0.00	-108,030,096.74	-1,058,288.10	21,533,084.93	151,873,749.79	789,999,104.73	663,571,059.87
	Cassava (CA)	-29,133,569.86	224,389,673.69	0.00	587,188.74	975,323,561.82	1,546,537,801.69	1,252,861,117.09	3,970,565,773.17
	Other field crops (FC)	-10,876.00	944,620.12	-110,038.60	0.00	12,050,238.75	406,096.22	104,457,518.29	117,737,558.78
	Para rubber (PR)	0.00	-2,690,361.77	-26,548,943.74	-41,851,297.58	0.00	2,446,745.24	1,206,429,746.77	1,137,785,888.91
	Perennial trees and orchard (PO)	-196,662,955.23	-123,246,317.21	-88,764,292.95	-635,628.87	-6,049,488.94	0.00	237,738,145.99	-177,620,537.23
	Forest land (FO)	-152,563,068.06	-2,237,123,610.84	-645,503,734.21	-142,196,177.80	-1,666,338,795.59	-286,864,027.49	0.00	-5,130,589,413.99
	SUM	-569,116,963.90	-684,247,398.40	-840,060,768.91	-185,135,170.60	-625,447,067.15	1,977,962,391.85	5,247,715,560.54	4,321,670,583.44

Table 8.7 Economic value change between suitable LULC allocation in 2049 under wet year and actual LULC in 2019.

<div align="right">ECV in Baht</div>

LULC type		Suitable LULC allocation in 2049 of wet year							SUM
		PA	SU	CA	FC	PR	PO	FO	
Actual LULC in 2019	Paddy field (PA)	0.00	1,525,952,042.21	27,552,609.85	19,033.00	58,566,139.37	323,418,057.23	1,656,229,927.66	**3,591,737,809.33**
	Sugarcane (SU)	-190,819,519.19	0.00	-105,430,481.05	-1,058,288.10	19,270,735.26	97,943,183.43	789,999,104.73	**609,904,735.08**
	Cassava (CA)	-29,160,125.74	565,985,990.11	0.00	587,188.74	971,754,588.66	245,808,811.26	1,252,861,117.09	**3,007,837,570.13**
	Other field crops (FC)	-10,876.00	948,539.70	-120,473.30	0.00	11,923,245.60	353,127.15	104,457,518.29	**117,551,081.45**
	Para rubber (PR)	0.00	-2,690,361.77	-31,352,751.49	-41,893,628.63	0.00	2,446,745.24	1,206,888,508.91	**1,133,398,512.26**
	Perennial trees and orchard (PO)	-196,683,330.59	-141,722,275.38	-90,289,900.17	-635,628.87	-6,212,605.29	0.00	237,738,145.99	**-197,805,594.31**
	Forest land (FO)	-152,826,107.83	-2,360,506,335.39	-653,548,202.86	-143,612,987.54	-1,569,081,221.17	-259,189,039.94	0.00	**-5,138,763,894.74**
	SUM	**-569,499,959.36**	**-412,032,400.52**	**-853,189,199.01**	**-186,594,311.39**	**-513,779,117.57**	**410,780,884.36**	**5,248,174,322.68**	**3,123,860,219.20**
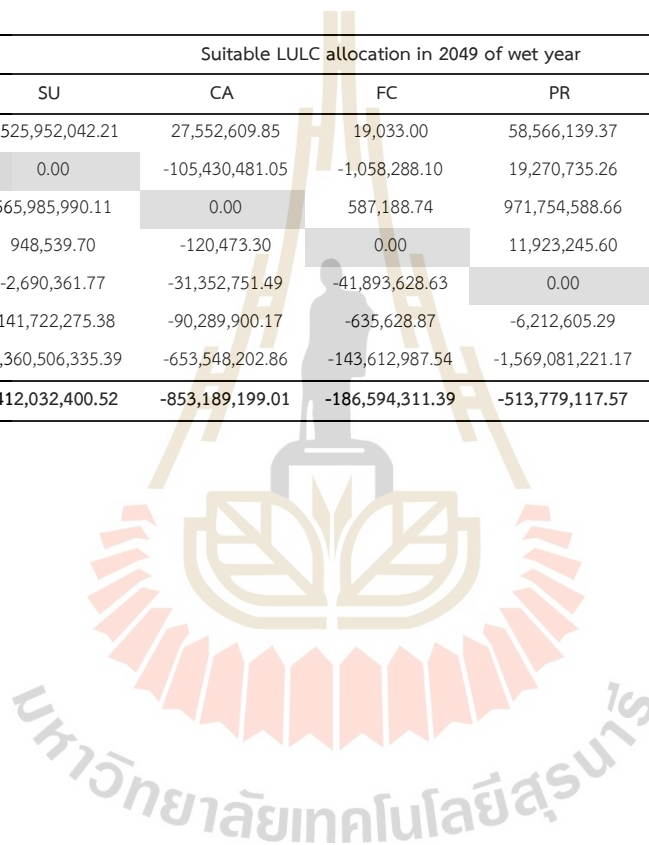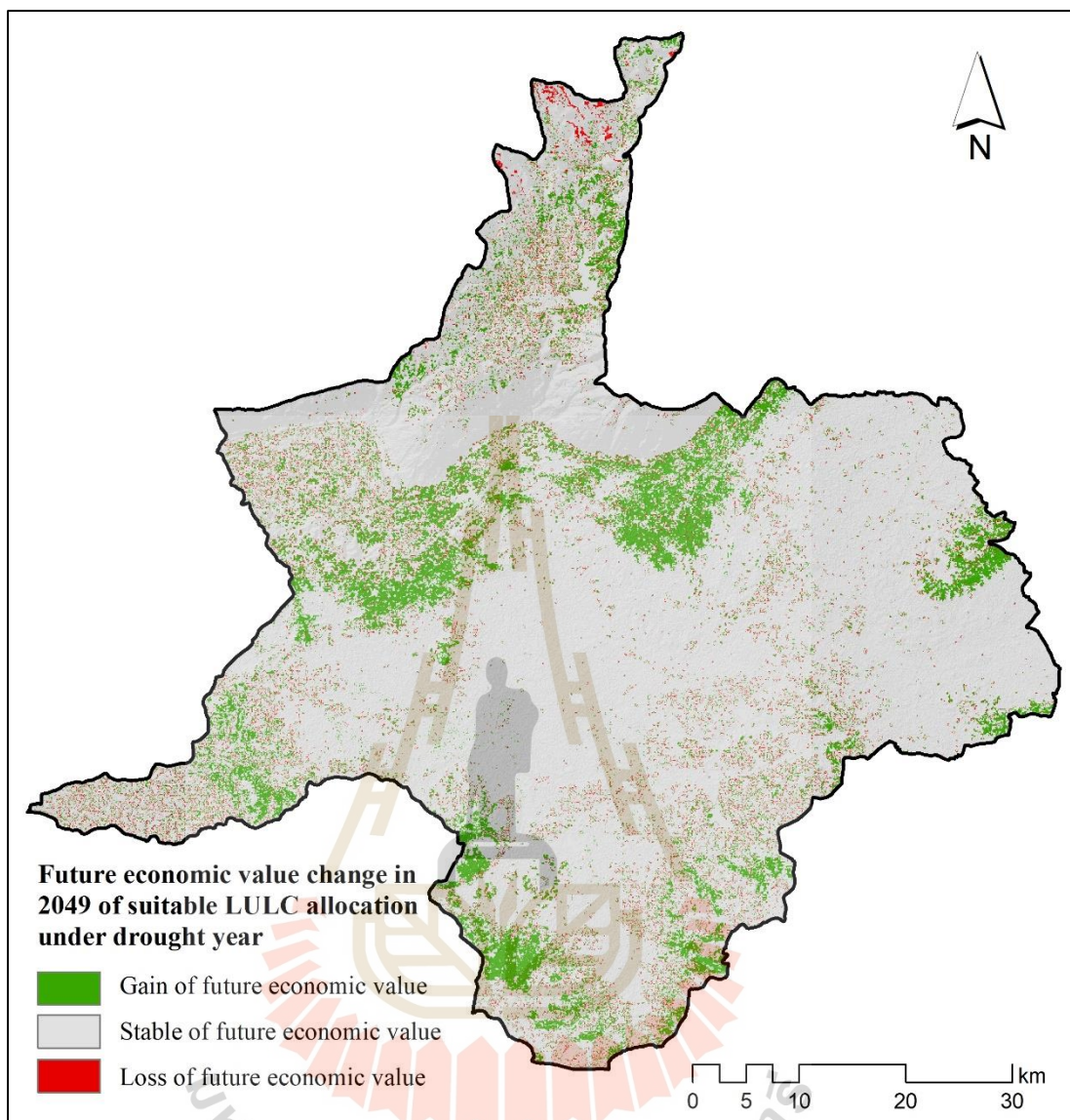
Figure 8.8 Gain and loss of future economic value of suitable LULC allocation for flood mitigation in 2049 under drought year.
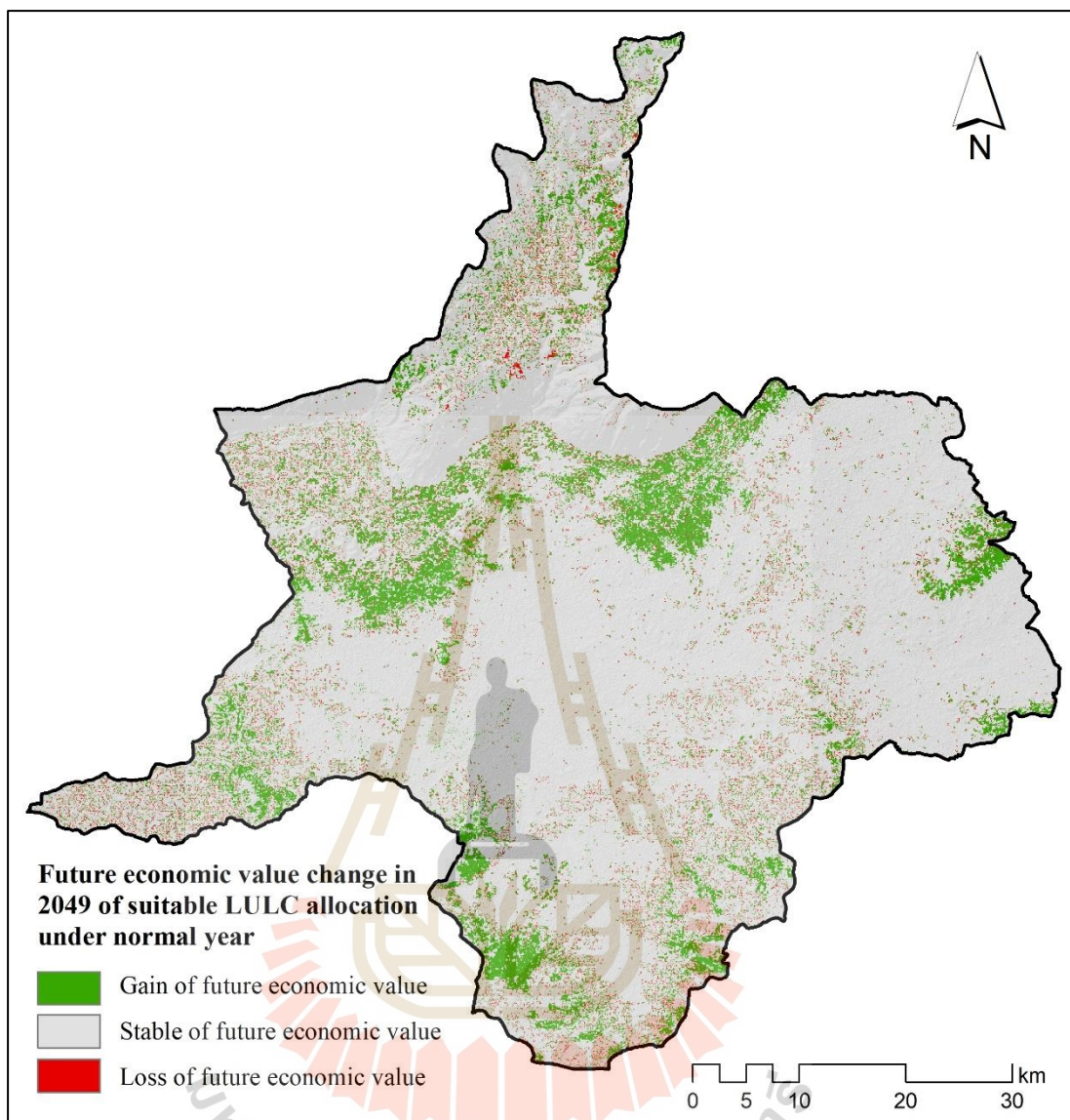
Figure 8.9 Gain and loss of future economic value of suitable LULC allocation for flood mitigation in 2049 under normal year.
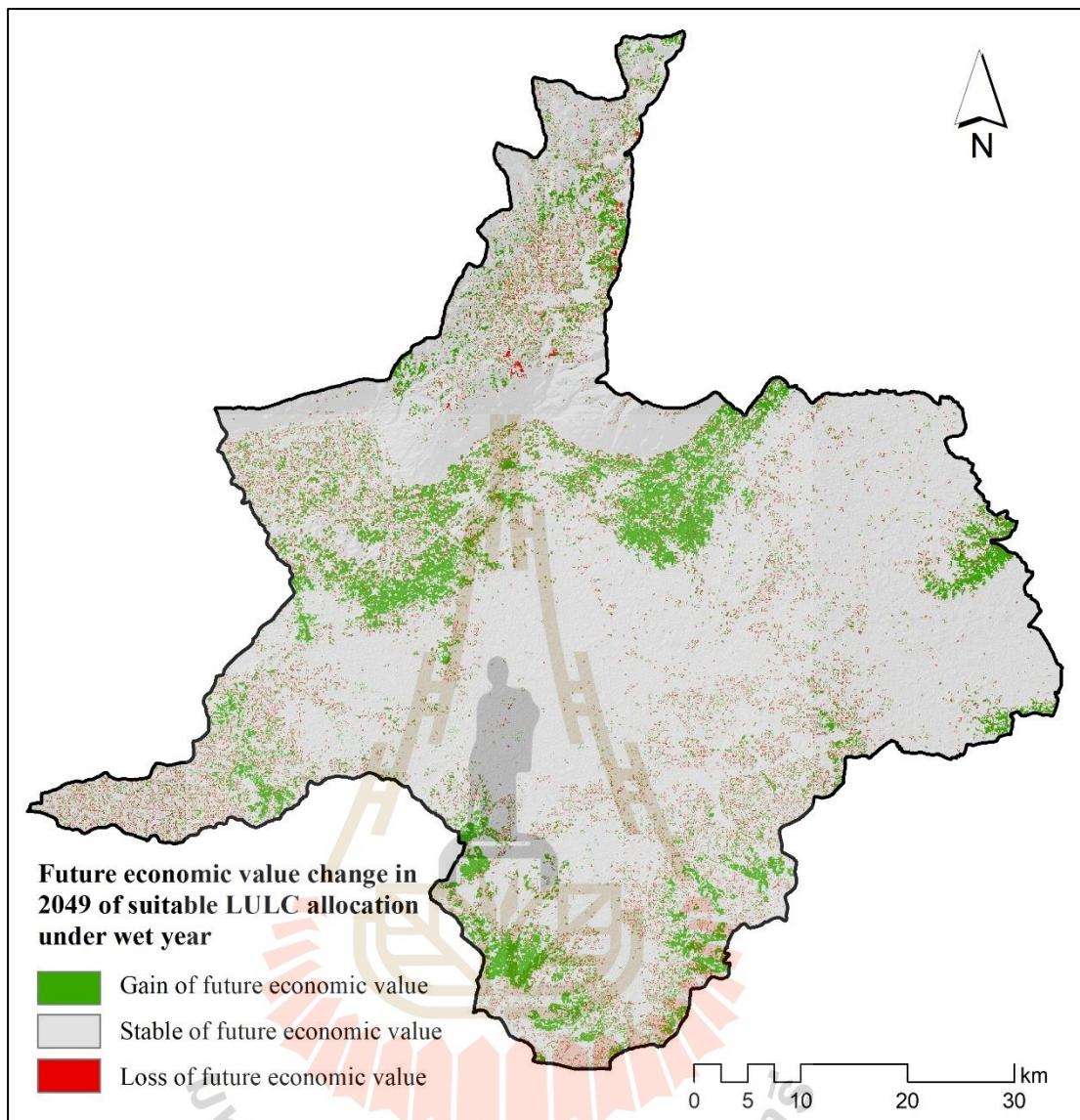
Figure 8.10 Gain and loss of future economic value of suitable LULC allocation for flood mitigation in 2049 under wet year.

According to change detection in Table 8.5, suitable LULC allocation for flood mitigation in 2049 under drought years gains the future economic value of about 3,929 million Baht. Meanwhile, suitable LULC allocation for flood mitigation in 2049 under normal year gains the future economic value of about 4,322 million (Table 8.6). Likewise, suitable LULC allocation for flood mitigation in 2049 under wet year gains about 3,124 million Baht (Table 8.7). These results showed the consequence of LULC allocation for flood mitigation in 2049 using Goal Programming on future economic

value because the future economic value depends on areas of LULC type and their values.

8.3 Ecosystem service values evaluation

The ecosystem service value (ESV) of actual LULC data in 2019 and suitable LULC allocation data in 2049 for flood mitigation under drought, normal, and wet years were first calculated using a simple benefit transfer method (Costanza et al., 1997) (See Eq. 3.15 of Chapter III). Figure 8.11 displays the spatial distribution of LULC type for ESV evaluation of actual LULC data in 2019 and suitable LULC allocation data for flood mitigation in 2049 under drought, normal, and wet years. They include urban and built-up area, paddy field, field crop, forest land, water body, rangeland, marsh and swamp, and unused land. The area of each LULC type for ESV evaluation of actual LULC data and suitable LULC allocation data for flood mitigation under drought, normal and wet years is summarized in Table 8.8. In this table, field crops consist of sugarcane, cassava, and other field crops, while para rubber, perennial trees and orchard are grouped in forest land. The top three dominant LULC types for ESV evaluation of actual LULC data in 2019 and suitable LULC allocation data in 2049 for flood mitigation under drought, normal, and wet years are paddy field, field crop, and forest land.

In the meantime, the detail of the coefficient value of different LULC types for ESV evaluation was presented in Table 3.19. The table shows that the top three highest coefficient values of LULC type for ESV evaluation are marsh and swamp, water body, and forest land.

The result of ESV evaluation of actual LULC data in 2019 and suitable LULC allocation data for flood mitigation in 2049 under drought, normal, and wet years are reported in Table 8.9. Meanwhile, the spatial distribution of ESV of actual LULC in 2019 and suitable LULC allocation for flood mitigation in 2049 under drought, normal, wet years are displayed in Figures 8.12 to 8.15.

Table 8.8 Area of each LULC type for ESV evaluation of actual LULC and suitable LULC allocation for flood mitigation under drought, normal and wet years.

No.	ESV-LULC type	Actual LULC 2019	Suitable LULC allocation in 2049		
			Drought year	normal year	wet year
1	Urban and built-up area	65.84	65.84	65.84	65.84
2	Paddy field	2,012.16	1,812.16	1,812.16	1,812.16
3	Field crop	802.95	853.64	853.64	940.94
4	Forest land	667.28	838.84	838.84	749.54
5	Water body	53.3	42.78	42.78	43.78
6	Rangeland	71.65	66.05	66.05	66.05
7	Marsh and swamp	27.73	21.61	21.61	22.61
8	Unused land	93.32	93.31	93.31	93.31
	Total	3,794.22	3,794.22	3,794.22	3,794.22
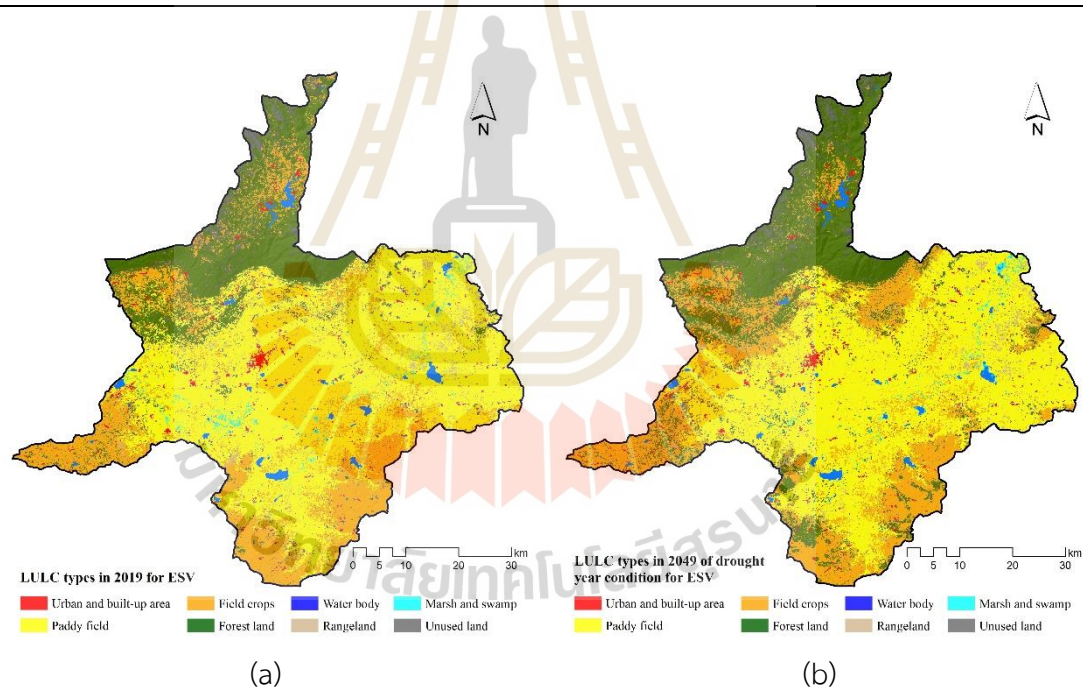
Figure 8.11 Spatial distribution of LULC type for ecosystem service evaluation: (a) actual LULC data in 2019 (b) suitable LULC allocation under drought year condition, (c) suitable LULC allocation under normal year condition, and (d) suitable LULC allocation under wet year condition.

LULC types in 2049 of normal year condition for ESV

■ Urban and built-up area	■ Field crops	■ Water body	■ Marsh and swamp
■ Paddy field	■ Forest land	■ Rangeland	■ Unused land

(c)

LULC types in 2049 of wet year condition for ESV

■ Urban and built-up area	■ Field crops	■ Water body	■ Marsh and swamp
■ Paddy field	■ Forest land	■ Rangeland	■ Unused land

(d)
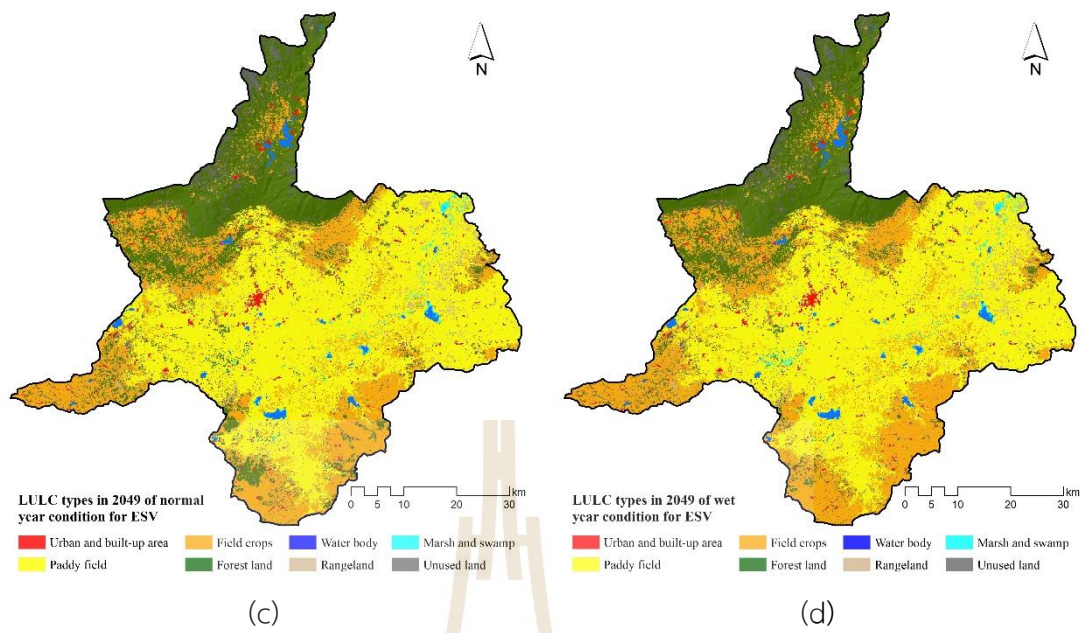
Figure 8.11 (Continued).

Table 8.9 Ecosystem service value by ESV-LULC types of actual LULC 2019 and suitable LULC allocation for flood mitigation in 2049.

ESV-LULC type	Ecosystem service value (Baht)			
	Actual LULC in 2019	Suitable LULC allocation for flood mitigation in 2049		
		Drought year condition	Normal year condition	Wet year condition
Urban and built-up area (UR)	2,601,477.96	2,619,496.20	2,619,496.20	2,619,496.20
Paddy field (PA)	6,478,728,717.87	5,804,108,745.04	5,836,474,634.01	5,837,109,771.08
Field crops (FC)	2,580,196,487.94	2,708,125,854.28	2,739,308,474.19	3,017,196,892.58
Forest land (FO)	4,050,694,542.52	5,175,683,049.75	5,088,763,867.23	4,556,472,852.29
Water body (WA)	1,143,065,207.46	1,019,068,354.90	923,227,149.59	951,981,442.29
Rangeland (RA)	180,645,657.62	176,458,912.81	167,474,335.65	163,551,108.15
Marsh and swamp (MA)	810,570,999.17	566,999,625.41	642,803,121.89	679,994,212.35
Unused land (UL)	27,921,866.31	27,938,099.16	27,938,099.16	27,938,099.16
Total in Baht	15,274,424,956.85	15,481,002,137.55	15,428,609,177.92	15,236,863,874.10
Total in million Baht	15,274.42	15,481.00	15,428.61	15,236.86

Ecosystem service value of actual LULC data in 2019 (million Baht)

■ 2.60		□ 1,143.07	
■ 27.92		■ 2,580.20	
■ 180.65		■ 4,050.69	
□ 810.57		■ 6,478.73	
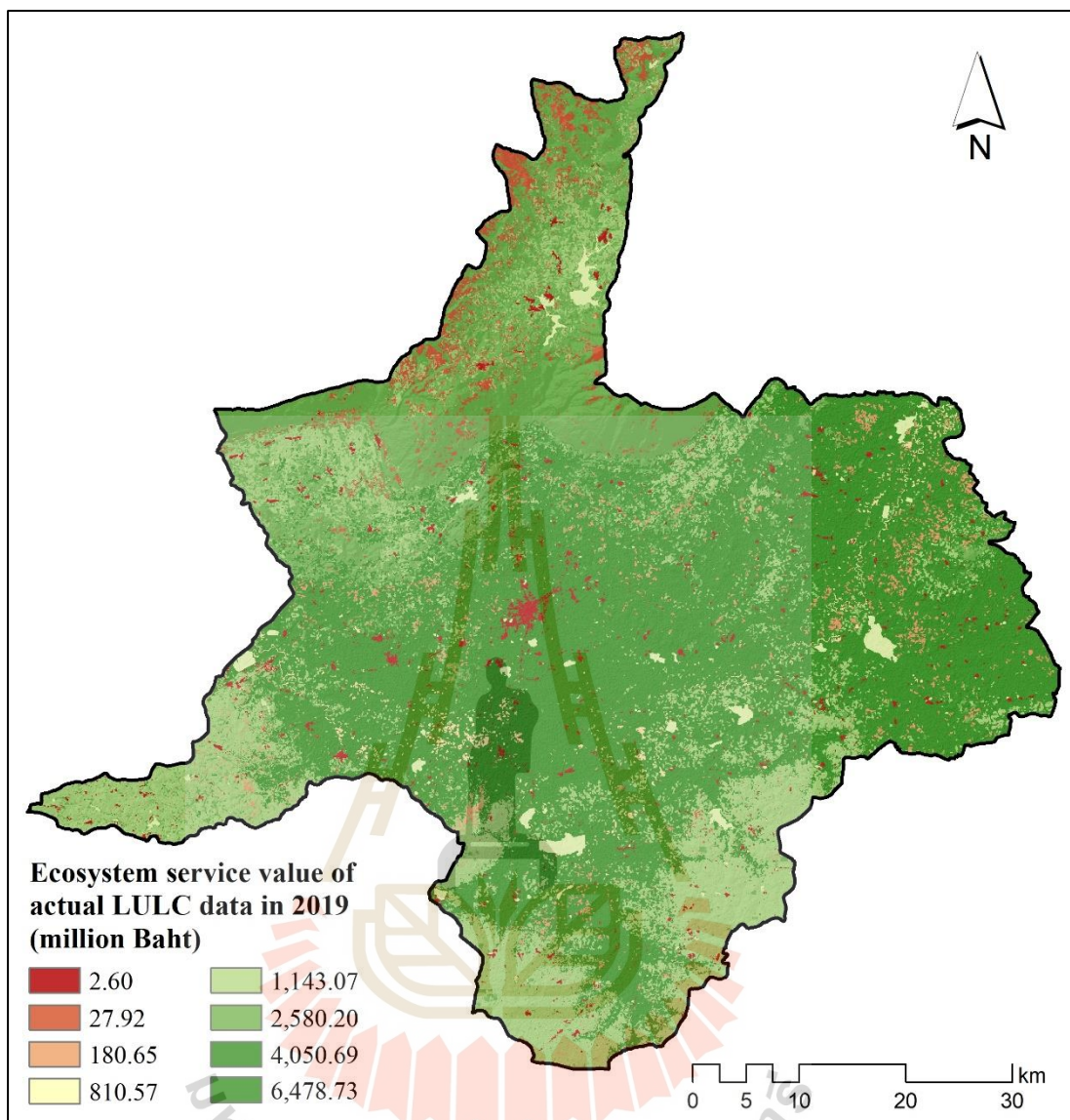
Figure 8.12 Spatial distribution of ecosystem service value of actual LULC in 2019.
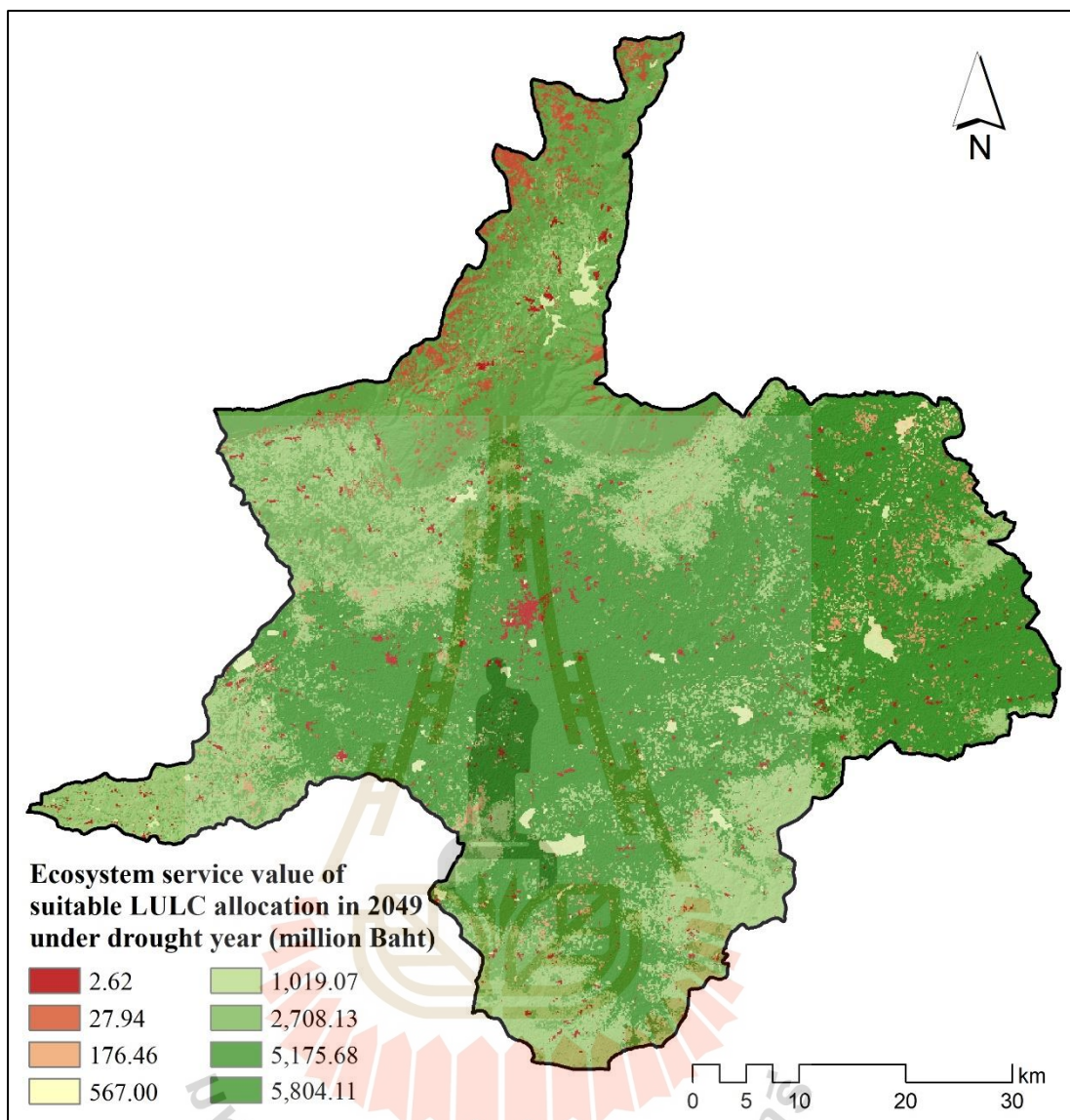
Figure 8.13 Spatial distribution of ecosystem service value of suitable LULC allocation for flood mitigation in 2049 under drought year condition.
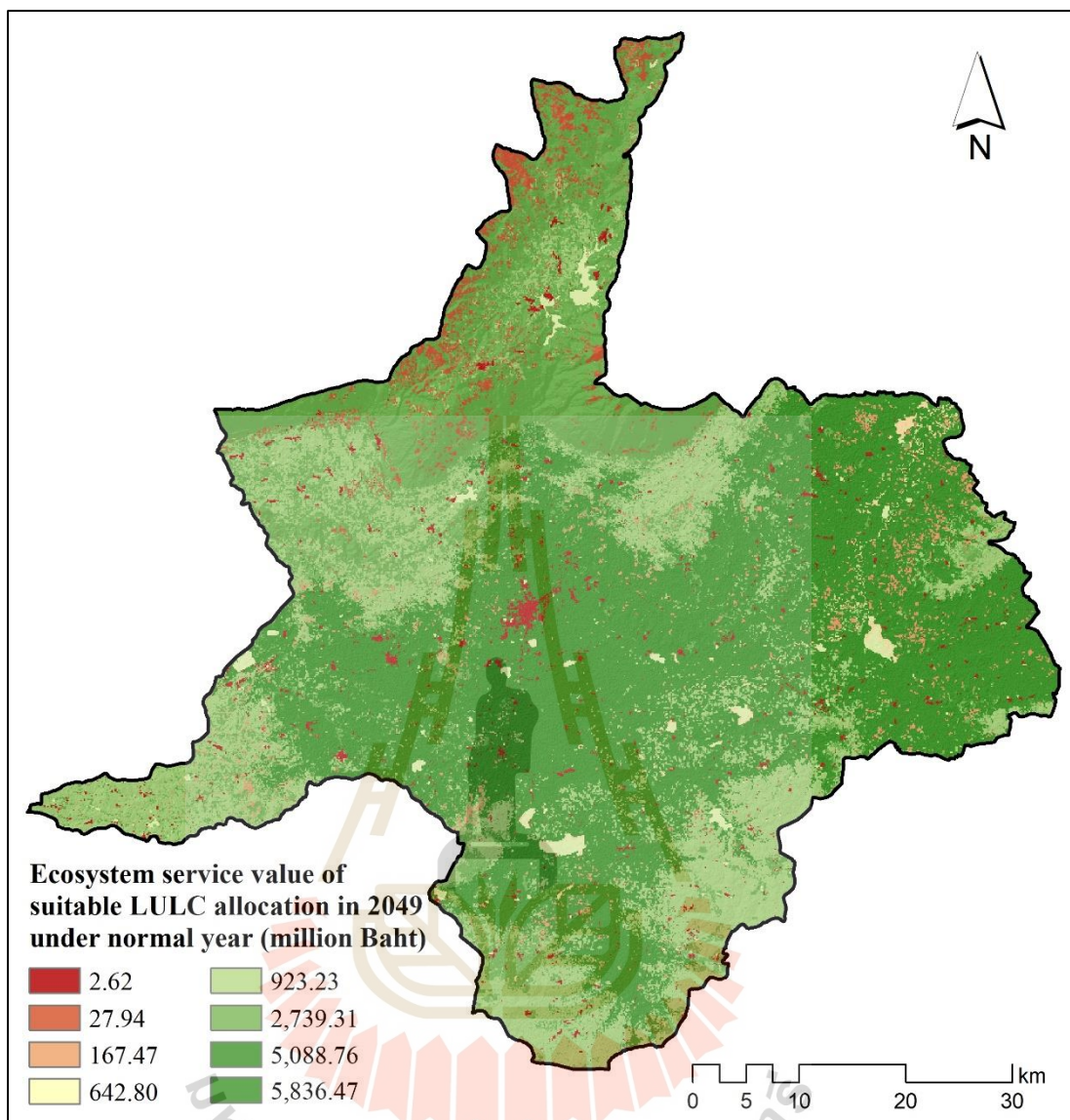
Figure 8.14 Spatial distribution of ecosystem service value of suitable LULC allocation for flood mitigation in 2049 under normal year condition.
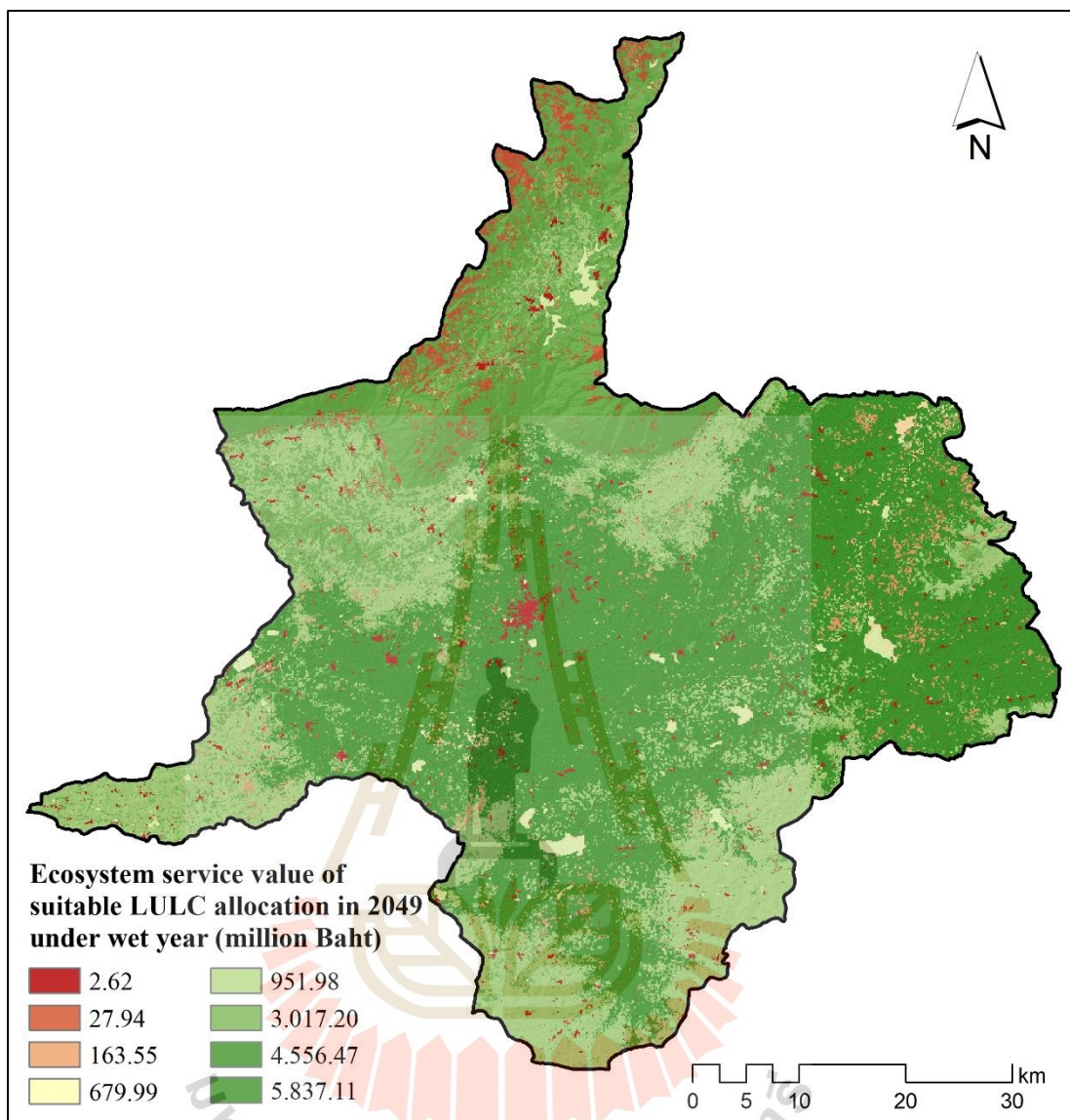
Figure 8.15 Spatial distribution of ecosystem service value of suitable LULC allocation for flood mitigation in 2049 under wet year condition.

As a result, the ESV of actual LULC in 2019 and suitable LULC allocation for flood mitigation in 2049 under drought, normal and wet year conditions are slightly different. The suitable LULC allocation for flood mitigation in 2049 under drought year condition provides the highest ESV, about 15,481 million Baht, while the suitable LULC allocation for flood mitigation in 2049 under wet year condition delivers the lowest ESV, about 15,237 million Baht. The comparison of ESV among actual LULC and suitable LULC allocation data for flood mitigation from three rainfall conditions is displayed in Figure 8.16. The contribution of ESV of each LULC type from actual LULC in 2019 and suitable LULC allocation for flood mitigation in 2049 under three rainfall conditions are compared in Figure 8.17.
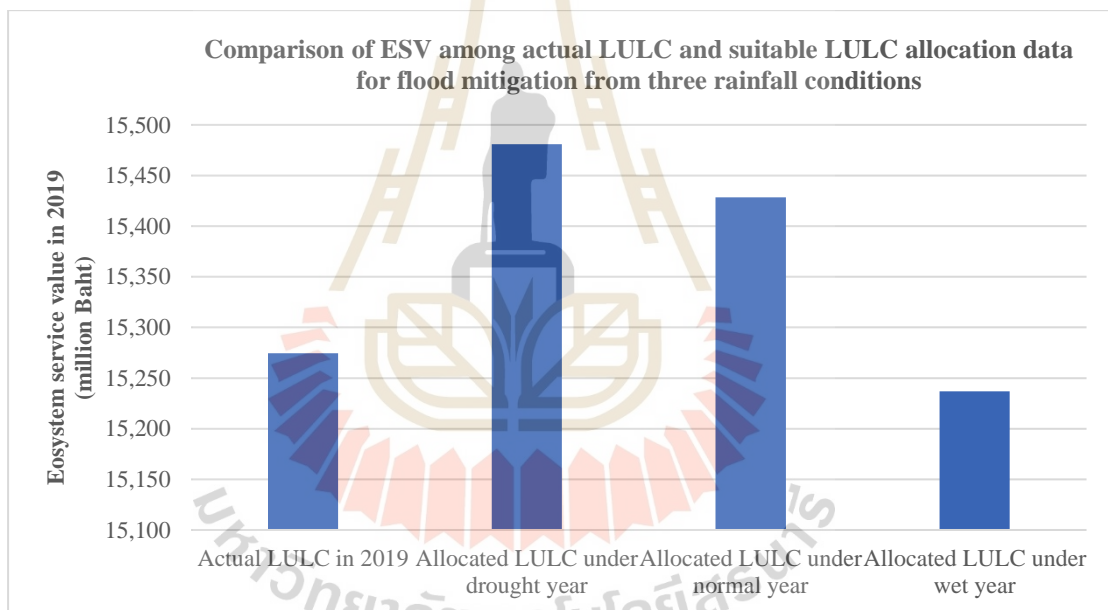
Figure 8.16 The comparison of ESV among actual LULC and suitable LULC allocation data for flood mitigation from three different rainfall conditions.
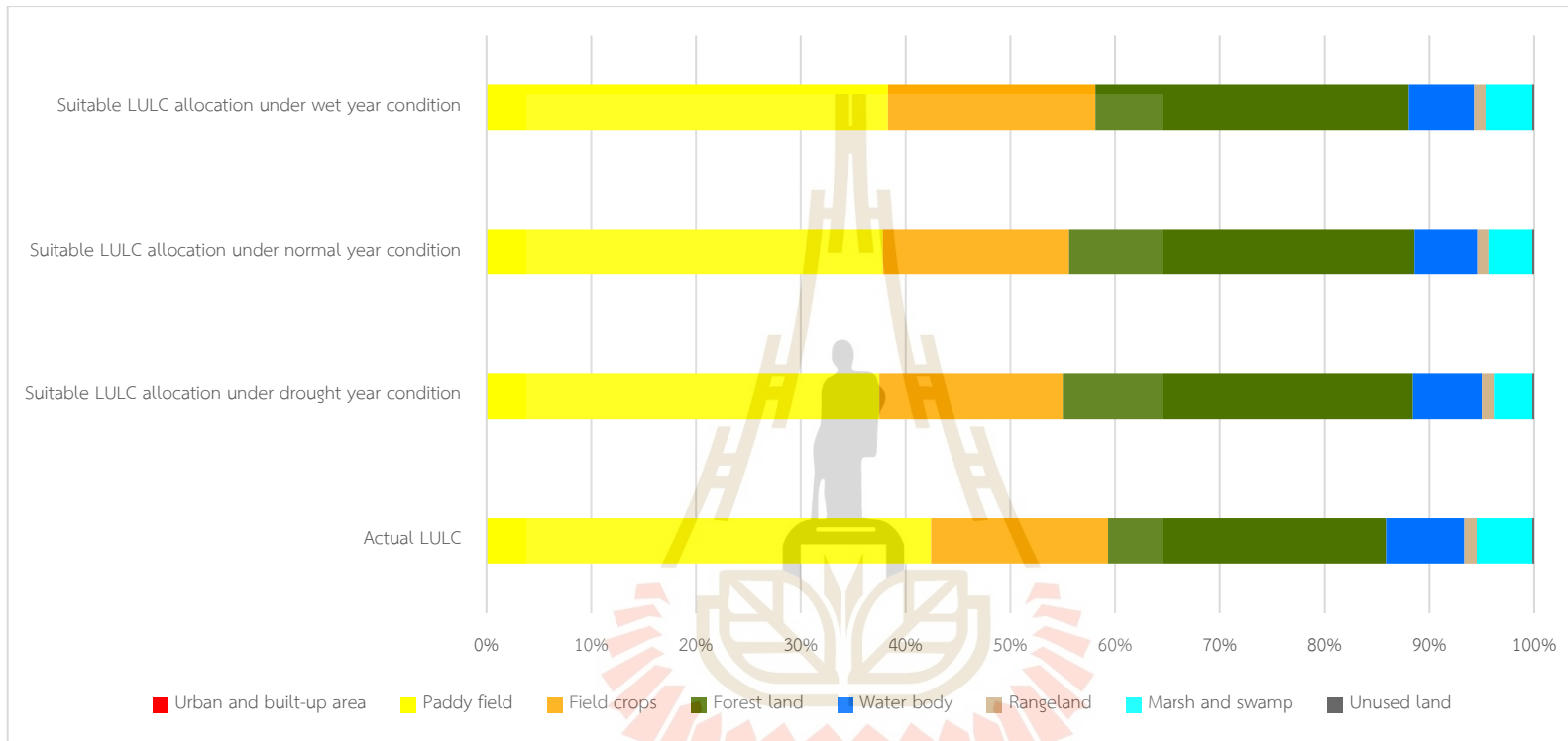
Figure 8.17 Contribution of ecosystem service value of LULC type of actual LULC in 2019 and suitable LULC allocation in 2049 for flood mitigation under drought, normal, and wet year conditions.

As shown in Figure 8.17, paddy fields provide the highest ESV value from actual LULC and suitable LULC allocation data for flood mitigation in 2049 under drought, normal and wet years because the area of paddy fields in actual LULC data in 2019 is about 53%, while paddy fields cover an area of about 48% in suitable LULC allocation data for flood mitigation in 2049 under drought, normal and wet years.

Moreover, the top three dominate LULC type for ESV evaluation, including paddy field, field crop, and forest land of actual LULC and suitable LULC allocation data for flood mitigation in 2049 under drought, normal, and wet years deliver ESV about 86%, 88%, 89%, and 88%, respectively.

8.4   Assessment of ecosystem service value change

Ecosystem service value maps of actual LULC in 2019 and suitable LULC allocation for flood mitigation in 2049 under drought, normal, and wet year were detected ESV change in terms of gain and loss using the image algebra change detection algorithm.

Results of ESV change between suitable LULC allocation for flood mitigation in 2049 from drought, normal, and wet year and actual LULC data in 2019 with gain (+sign) and loss (-sign) are informed in Tables 8.10 to 8.12. In the meantime, the spatial distribution of ecosystem service value change in terms of gain and loss between suitable LULC allocation for flood mitigation in 2049 under drought, normal, and wet years and actual LULC in 2019 are displayed in Figures 8.18 to 8.20, respectively.

Table 8.10 Ecosystem service value change between actual LULC in 2019 and suitable LULC allocation in 2049 under drought year.

ESV in Baht

	LULC type	Suitable LULC allocation in 2049 of drought year								
		UR	PA	FC	FO	WA	RA	MA	UL	SUM
Actual LULC in 2019	Urban and built-up area (UR)	0.00	33,070,532.05	14,033,134.39	14,056,674.00	4,876,692.35	169,937.61	2,050,228.35	82,438.64	68,339,637.39
	Paddy field (PA)	-36,361,830.56	0.00	0.00	111,301,051.04	40,042,777.20	-10,787,659.00	119,186,869.73	-1,864,401.75	221,516,806.65
	Field crops (FC)	-14,694,831.48	0.00	0.00	495,143,780.72	16,804,837.64	-3,059,383.86	5,105,666.65	-18,864,905.72	480,435,163.96
	Forest land (FO)	-9,595,964.76	-27,031,395.79	-102,472,580.69	0.00	13,129,960.21	-3,091,732.70	646,197.77	-91,863,422.71	-220,278,938.67
	Water body (WA)	-4,934,518.74	-46,672,810.80	-15,459,137.75	-20,490,485.85	0.00	-136,315.54	39,863,111.67	-818,745.62	-48,648,902.64
	Rangeland (RA)	-158,757.51	8,882,771.47	4,299,980.36	12,485,473.94	187,433.87	0.00	745,517.68	-22,012.69	26,420,407.13
	Marsh and swamp (MA)	-1,971,373.41	-184,811,080.57	-6,065,906.71	-249,411,495.71	-911,236.95	-1,635,329.12	0.00	0.00	-444,806,422.47
	Unused land (UL)	-70,695.24	1,283,255.37	8,822,380.64	112,928,144.32	628,339.67	8,004.61	0.00	0.00	123,599,429.36
	SUM	-67,787,971.70	-215,278,728.27	-96,842,129.77	476,013,142.46	74,758,803.99	-18,532,478.00	167,597,591.86	-113,351,049.85	206,577,180.71

Table 8.11 Ecosystem service value change between actual LULC in 2019 and suitable LULC allocation in 2049 under normal year.

ESV in Baht

	LULC type	Suitable LULC allocation in 2049 of normal year								
		UR	PA	FC	FO	WA	RA	MA	UL	SUM
Actual LULC in 2019	Urban and built-up area (UR)	0.00	33,213,756.53	14,245,106.62	13,469,165.95	4,683,937.71	145,341.38	2,181,653.24	82,438.64	68,021,400.07
	Paddy field (PA)	-36,361,830.56	0.00	0.00	109,485,394.21	31,328,549.86	-10,297,453.70	119,538,177.07	-1,864,401.75	211,828,435.14
	Field crops (FC)	-14,694,831.48	0.00	0.00	460,303,772.89	16,739,193.75	-2,723,781.77	4,871,461.76	-18,864,905.72	445,630,909.43
	Forest land (FO)	-9,595,964.76	-27,845,222.11	-110,136,970.35	0.00	13,129,960.21	-2,745,714.95	646,197.77	-91,863,422.71	-228,411,136.89
	Water body (WA)	-4,934,518.74	-46,672,810.80	-16,378,152.31	-19,964,734.02	0.00	-136,315.54	70,466,654.06	-818,745.62	-18,438,622.98
	Rangeland (RA)	-158,757.51	8,984,583.34	4,272,327.75	20,190,776.69	153,354.98	0.00	769,566.64	-22,012.69	34,189,839.22
	Marsh and swamp (MA)	-1,971,373.41	-184,811,080.57	-54,007,648.18	-238,613,739.35	-686,932.47	-1,635,329.12	0.00	0.00	-481,726,103.10
	Unused land (UL)	-70,695.24	1,317,440.45	9,308,860.64	111,897,550.09	628,339.67	8,004.61	0.00	0.00	123,089,500.21
	SUM	-67,787,971.70	-215,813,333.16	-152,696,475.83	456,768,186.46	65,976,403.71	-17,385,249.08	198,473,710.54	-113,351,049.85	154,184,221.08

Table 8.12 Ecosystem service value change between actual LULC in 2019 and suitable LULC allocation in 2049 under wet year.

ESV in Baht

	LULC type	Suitable LULC allocation in 2049 of wet year								
		UR	PA	FC	FO	WA	RA	MA	UL	SUM
Actual LULC in 2019	Urban and built-up area (UR)	0.00	33,219,485.51	15,585,687.73	10,912,417.97	4,761,039.57	143,105.36	2,102,798.30	82,438.64	66,806,973.08
	Paddy field (PA)	-36,361,830.56	0.00	0.00	82,273,720.44	34,282,525.23	-10,040,410.15	130,264,761.14	-1,864,401.75	198,554,364.35
	Field crops (FC)	-14,694,831.48	0.00	0.00	268,925,817.40	16,788,426.67	-2,639,567.01	3,653,596.32	-18,864,905.72	253,168,536.17
	Forest land (FO)	-9,595,964.76	-27,852,948.31	-117,373,843.65	0.00	13,129,960.21	-2,623,967.96	854,648.67	-91,863,422.71	-235,325,538.51
	Water body (WA)	-4,934,518.74	-46,672,810.80	-19,200,839.89	-17,571,179.63	0.00	-136,315.54	61,417,370.22	-818,745.62	-27,917,040.00
	Rangeland (RA)	-158,757.51	8,989,611.09	4,675,804.43	21,783,099.13	153,354.98	0.00	721,468.73	-22,012.69	36,142,568.16
	Marsh and swamp (MA)	-1,971,373.41	-184,811,080.57	-214,156,953.59	-48,068,776.36	-757,027.62	-1,635,329.12	0.00	0.00	-451,400,540.66
	Unused land (UL)	-70,695.24	1,320,070.07	10,000,451.14	110,523,424.44	628,339.67	8,004.61	0.00	0.00	122,409,594.68
	SUM	-67,787,971.70	-215,807,673.01	-320,469,693.83	428,778,523.39	68,986,618.71	-16,924,479.81	199,014,643.38	-113,351,049.85	-37,561,082.72
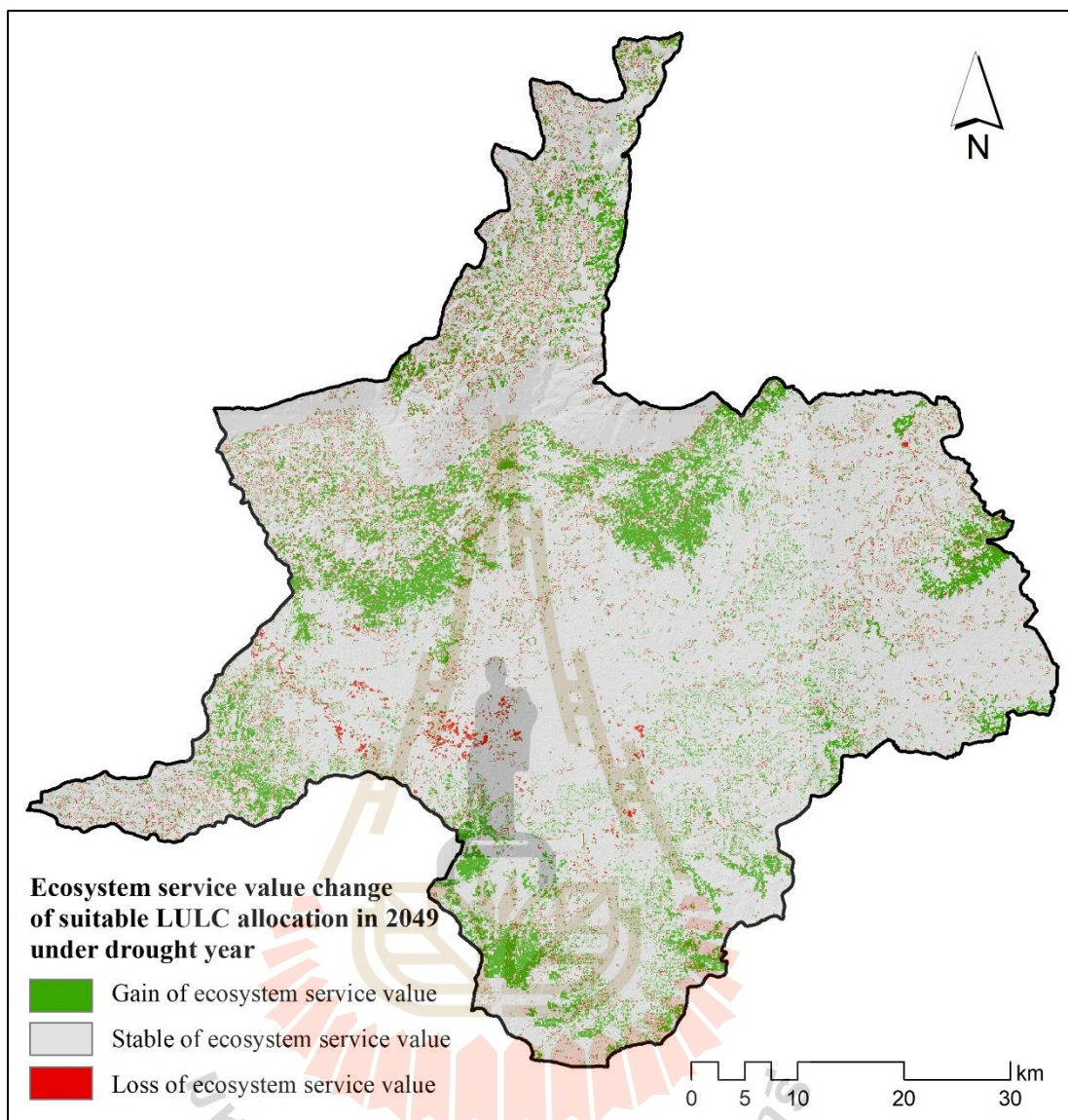
Figure 8.18 Gain and loss of ESV of suitable LULC allocation for flood mitigation in 2049 under drought year.
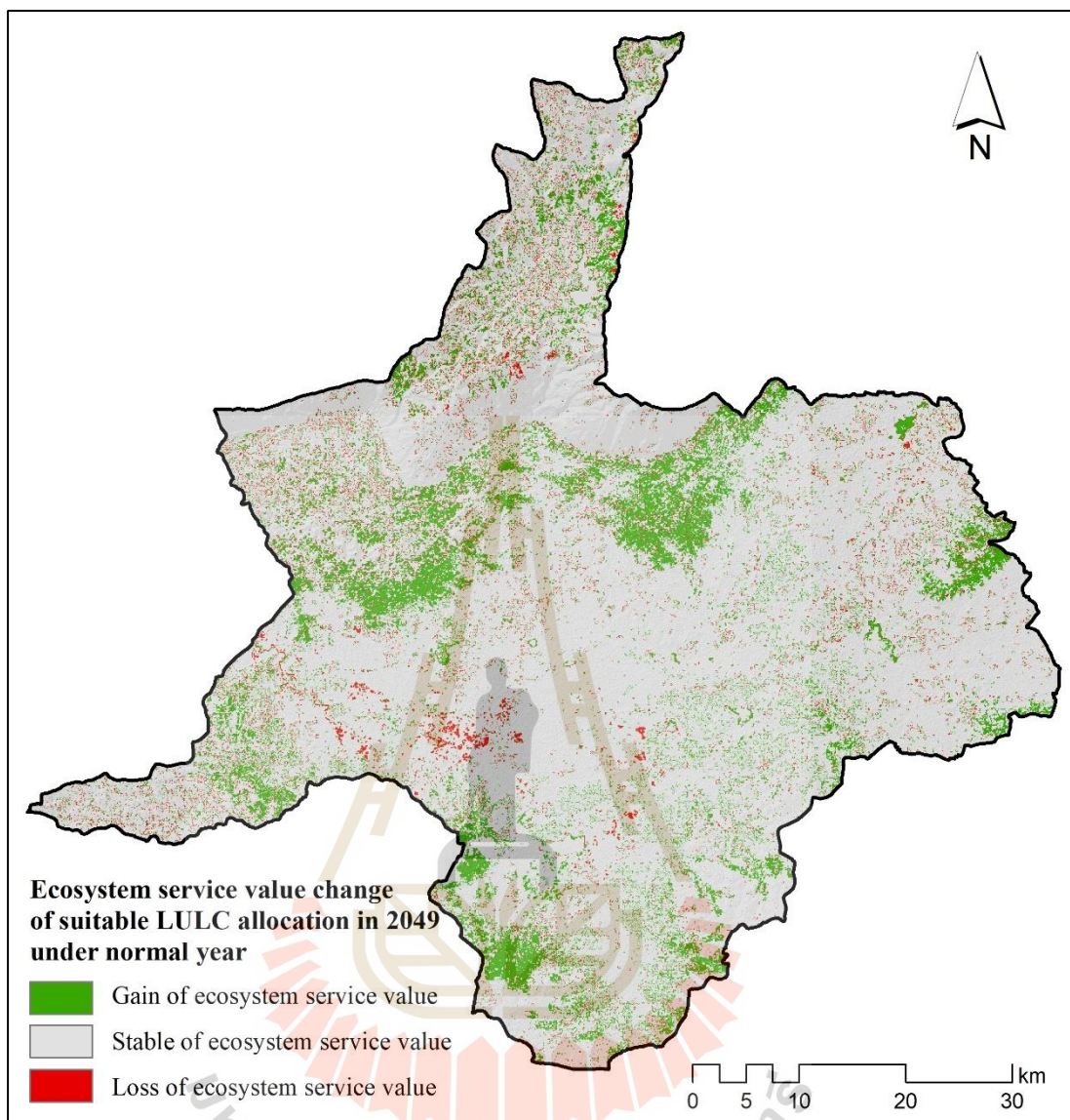
Figure 8.19 Gain and loss of ESV of suitable LULC allocation for flood mitigation in 2049 under normal year.
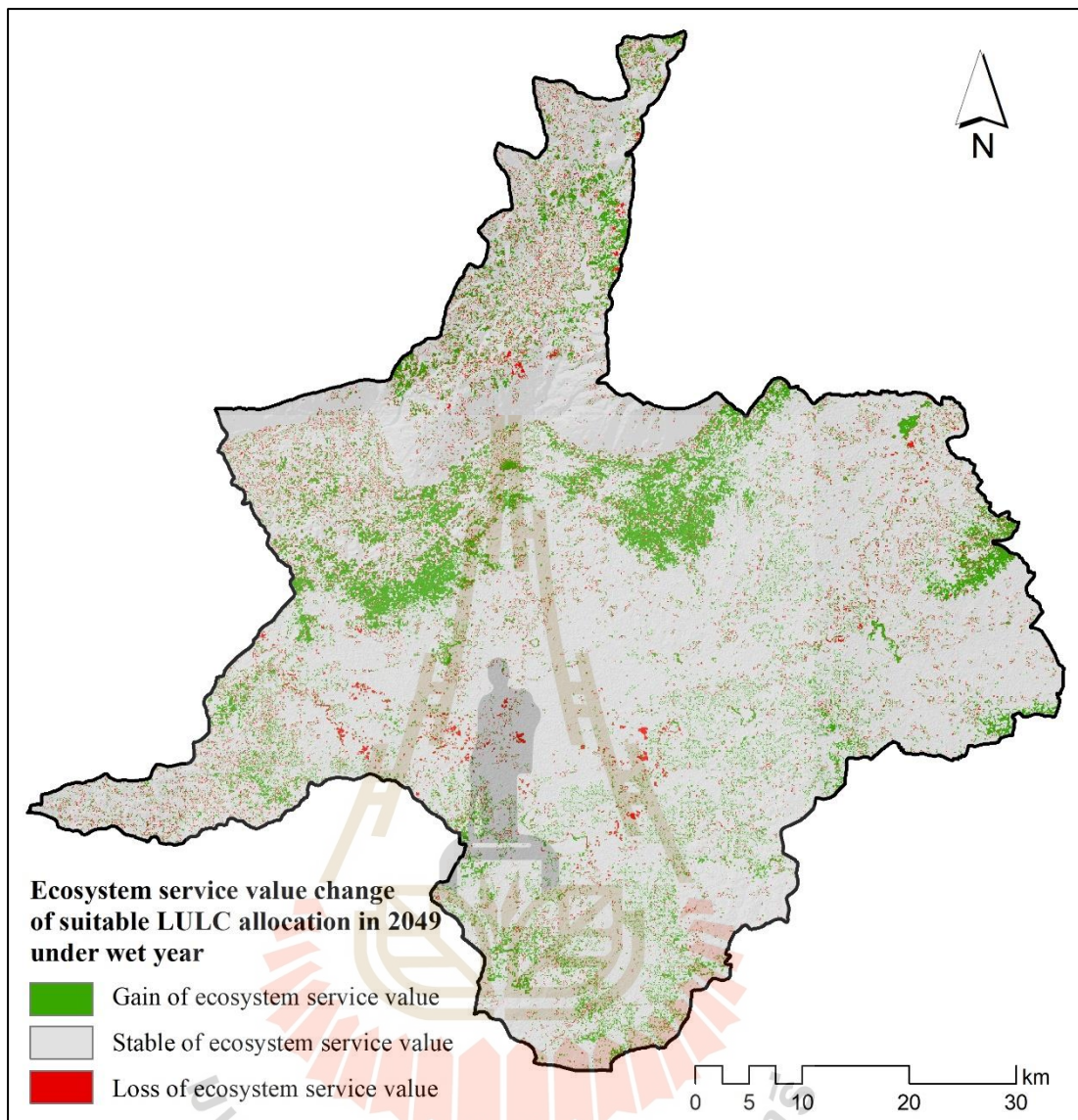
Figure 8.20 Gain and loss of ESV of suitable LULC allocation for flood mitigation in 2049 under wet year.

As a result, in Table 8.10, suitable LULC allocation for flood mitigation in 2049 under drought year gains the ESV of about 207 million Baht. Meanwhile, suitable LULC allocation for flood mitigation in 2049 under normal year gains the ESV of about 154 million (Table 8.11). On the contrary, suitable LULC allocation for flood mitigation in 2049 under wet year losses the ESV about 38 million Baht (Table 8.12). This finding indicates that the ESV of suitable LULC allocation for flood mitigation in 2049 under wet year is lower than actual LULC in 2019 (See Table 8.9). Herein, actual LULC in 2019

provides the ESV about 15,274 million Baht but suitable LULC allocation for flood mitigation in 2049 under wet year deliver the ESV about 15,237 million Baht. Similar to the change of future economic value, these results show the consequence of LULC allocation for flood mitigation in 2049 using Goal Programming on ESV because the ESV depends on areas of LULC type and their coefficient values.

Besides, it can be observed that forest land, water body, and marsh and swamp provide a gain of ESV (+sign) while urban and built-up area, paddy field, field crops, rangeland, and unused land give a loss of ESV (-sign) for all three different rainfall conditions. These findings indicate that the ecosystem service value was dictated by the coefficient value of each LULC type.

In summary, the suitable LULC allocation for flood mitigation in 2049 under normal year provides the highest value for future economic value evaluation, about 149,210 million Baht. On the contrary, the suitable LULC allocation for flood mitigation in 2049 under wet year provides the lowest value, 147,858 million Baht. Meanwhile, the assessment of gain and loss of future economic value by comparing with the future economic value of LULC in 2019 shows that the suitable LULC allocation for flood mitigation in 2049 under the normal year provides the highest gain value. In contrast, the suitable LULC allocation for flood mitigation in 2049 under wet year provides the lowest gain value for this assessment.

In the meantime, the suitable LULC allocation for flood mitigation in 2049 under dry year provides the highest value for ecosystem service evaluation, about 15,481 million Baht. On the contrary, the suitable LULC allocation for flood mitigation in 2049 under wet year provides the lowest value, about 15,237 million Baht. Meanwhile, the assessment of gain and loss of the ESV by comparing with the value of LULC data in 2019, the suitable LULC allocation for flood mitigation in 2049 under drought year gains the ESV about 207 million Baht. In contrast, the suitable LULC allocation for flood mitigation in 2049 under wet year losses the ESV about 38 million Baht for this assessment.

In addition, the estimation of surface runoff and its reduction by comparing with the value of LULC data in 2019, the suitable LULC allocation for flood mitigation in 2049 under wet year delivers the highest surface runoff 5,195 million m^3. On the

contrary, the suitable LULC allocation for flood mitigation in 2049 under drought year provides the lowest value, about 1,550 million m^3. Meanwhile, the runoff reduction by comparing with the value of LULC data in 2019, the suitable LULC allocation for flood mitigation in 2049 under normal year can reduce surface runoff by about 52 million m^3. In contrast, the suitable LULC allocation for flood mitigation in 2049 under drought year can reduce surface runoff by about 28 million m^3. (See more detail in CHAPTER VII). The future economic value evaluation and change, ecosystem service values evaluation and change, and surface runoff by comparing with the baseline information of LULC data in 2019 are summarized in Table 8.13.

Table 8.13 Comparison of the future economic value evaluation and change, ecosystem service values evaluation and change, and surface runoff by comparing with the baseline information of LULC data in 2019.

Item	Suitable LULC allocation for flood mitigation in 2049		
	Drought year	Normal year	Wet year
Future economic value (million Baht)	148,579.64	149,210.92	147,858.27
Gain or Loss by economic value (million Baht)	3,929.45	4,321.67	3,123.86
Ecosystem service value (million Baht)	15,481.00	15,428.61	15,236.86
Gain or Loss by ESV (million Baht)	206.58	154.18	-37.56
Surface runoff (million m^3)	1,550.07	3,594.76	5,194.79
Runoff reduction (million m^3)	27.89	52.31	46.73

Consequently, it can be concluded that the most suitable LULC allocation for flood mitigation in 2049 in Chaiyaphum district, Chaiyaphum province under the Second Part of the Lam Nam Chi watershed based on future economic value and ecosystem service value evaluation should be suitable LULC allocation for flood mitigation in 2049 under normal year scenario. This information can be used as primary data for supporting project implementation.

The limitation of flood mitigation in the future is LULC allocation which was estimated by Goal Programming and mapped by CLUE-S model in the whole study area, the Second Part of the Lam Nam Chi watershed.

CHAPTER IX
CONCLUSION AND RECOMMENDATION

Land use optimization is a practical approach for soil and water conservation and management at the watershed level to help decision-makers determine the best scenario of various land use alternatives without sacrificing economic and ecosystem service values obtained from the available land use. This study aimed to optimize LULC allocation for flood mitigation at Mueang Chaiyaphum district, Chaiyaphum province, Thailand, by integrating advanced LULC classification method, land use change modeling, distributed hydrological model, and Goal programming.

Six main objectives included (1) to classify LULC data in 2001, 2010, and 2019 using Random Forests classifier, (2) to predict LULC change in two periods (2002-2009 and 2011-2018) based on historical LULC in 2001, 2010, and 2019 using CLUE-S model, (3) to estimate surface runoff from 2001 to 2019 using SCS-CN method, (4) to optimize LULC allocation for flood mitigation based on average runoff coefficient of LULC type between 2001 and 2019 under three different rainfall conditions using Goal programming, (5) to map an optimizing LULC allocation under three different rainfall conditions for flood mitigation of Mueang Chaiyaphum district, Chaiyaphum province using CLUE-S model, and (6) to examine economic and ecosystem service evaluation and change of suitable LULC allocation under three different rainfall conditions using the PV model and simple benefit transfer method in terms of gain and loss, were successfully implemented in this study. Thus, the conclusion by research objective with brief methodology and significant results were first concluded, and some recommendations were then suggested in this chapter.

9.1 Conclusions

9.1.1 Land use and land cover classification and change detection

Random Forests (RF) classifier has been proposed in recent years for classifying multi-sources of remote sensing and geographic data. This method has been

proven to improve classification accuracy considerably. In this study, LULC data in 2001, 2010, and 2019 were successfully classified based on Landsat 5-TM and Landsat 8-OLI with supplementary data, including NDVI, MNDWI, NDBI, and DEM, using the RF classifier under EnMap BOX software. The classified LULC data consisted of urban and built-up area, paddy field, sugarcane, cassava, other field crops, para rubber, perennial trees and orchard, forest land, water body, rangeland, marsh and swamp, and unused land. By considering the performance of the RF classifier for LULC classification, the derived thematic accuracy of LULC maps showed the overall accuracy and Kappa hat coefficient of agreement between classified LULC maps and ground reference data in 2001, 2010, and 2019 were 89.88% and 84.88%, 90.71% and 87.03%, and 91.37% and 88.26%, respectively. Besides, LULC change detection between 2001 and 2019 revealed that urban and built-up areas, sugarcane, para rubber, other field crops, and unused land significantly increased LULC types, while paddy fields and forest land significantly decreased LULC types. Meanwhile, cassava, perennial trees and orchards, waterbody, and marsh and swamps are unstable and unpredictable LULC types.

In conclusion, the RF classifier can be used as an efficient tool to classify the LULC from remotely sensed data since it can provide high classification accuracy. Furthermore, the post-classification comparison change detection algorithm can provide detailed from-to-change class information in two different study periods.

9.1.2 Prediction of time-series of land use and land cover by CLUE-S model

LULC change models are essential for analyzing LULC change and predicting land use requirements and are valuable for guiding proper land use planning and management. Predicting LULC change can indicate anthropogenic impact, identify land use problems, such as degradation and deforestation, and land use planning. This study successfully predicted the time-series LULC data using the CLUE-S model. Eight driving forces for LULC change included elevation, slope, annual rainfall, average income per capita at the sub-district level, population density at the sub-district level, distance to the road network, distance to stream, and distance to the existing urban area were applied to analyze for specific LULC type allocation using binomial logistic

regression analysis, which provided the AUC values from 0.61857 (poor fit) to 0.98239 (excellent fit) for specific LULC type allocation.

LULC prediction between 2002 and 2009 was dictated by the historical LULC development between 2001 and 2010. The result indicated that the most increasing LULC types were cassava and sugarcane, with an increasing annual change rate of 10.71 and 10.24 km^2 per year, while the paddy field was the most decreasing LULC type with decreasing annual change rate of 30.42 km^2 per year. In the meantime, LULC prediction between 2011 and 2018 was enforced by the historical LULC development between 2010 and 2019. Again, the result revealed that sugarcane was the most increasing LULC type, with an increasing annual rate of 17.04 km^2 per year, while cassava and forest land were the most decreasing LULC types, with decreasing annual change rates of 15.49 and 13.71 km^2 per year.

To sum up, it can be concluded that the predicted LULC map in the study period by the CLUE-S model can provide realistic results as expected. The deviation values between the land use requirement and the predicted area of each LULC type varies from -0.0005% to 0.0005% or -0.05 km^2 (underestimation) to 0.05 km^2 (overestimation).

9.1.3 Time-series surface runoff estimation using SCS-CN method

This study successfully implemented time-series surface runoff estimation using the SCS-CN method under a GIS raster-based environment. The process worked on spatial variation of land use, hydrologic soil group, and rainfall data. In practice, a suitable AMC condition was first examined and validated for time-series surface runoff estimation between 2001 and 2010. Then a suitable AMC condition is further chosen to estimate time-series surface runoff between 2011 and 2019.

For surface runoff estimation between 2001 and 2010 with three AMC conditions, the accumulated surface runoff volume ranged from 1,178.41 million m^3 to 6,558.70 million m^3. In the meantime, the observed runoff data from the hydrological station gauge at E.21, E.23, and E6C of the RID were used to measure model performance using NSE, R^2, and PBIAS for model validation. The derived NSE and R^2 values were more than 0.65, and the PBIAS value was less than ± 10. Thus, surface runoff estimation using the SCS-CN method in the current study can be

accepted. Besides, NSE, R^2, and PBIAS of all AMCs were compared to identify the suitable AMC for surface runoff estimation between 2011 and 2019. As a result, AMC-II can provide all average statistics measurements better than other AMCs. Consequently, the AMC-II condition was chosen as the suitable AMC for time-series surface runoff between 2011 and 2019.

For surface runoff estimation between 2011 and 2019 based on the suitable AMC (AMC-II), the accumulated surface runoff volume ranged from 1,003.60 million m^3 to 6,142.43 million m^3. Furthermore, the validation result of surface runoff estimation with observed data from the hydrological station of RID at E.21, E.23, and E6C could provide a very good fit for surface estimation with NSE ranging from 0.87 to 0.91 and a very high correlation between the observed and estimated surface runoff with R^2 varied from 0.90 to 0.94. Meanwhile, the PBIAS values ranged between -5.71% for overestimation bias and 3.66% for underestimation bias.

As the result of the case study at the Second Part of the Lam Nam Chi watershed, it can be concluded that distributed surface runoff modeling using the SCS-CN method is applicable to estimate surface runoff effectively.

9.1.4 Optimization and mapping of land use and land cover allocation for flood mitigation

Optimized LULC allocation for flood mitigation at Mueang Chaiyaphum district, Chaiyaphum province, was successfully implemented using Goal programming based on the average surface runoff coefficient from LULC in three different rainfall conditions (drought, normal, and wet years). Herein, "What's Best!" as an extension program under Microsoft Excel software was used to allocate an area of LULC with the simplex method. The average annual surface runoff volume of each LULC type under three different rainfall conditions was separately calculated and applied as a surface runoff coefficient. At the same time, the constraints for optimizing LULC allocation for flood mitigation were assigned based on the historical LULC development between 2010 and 2019 using the Markov Chain model.

As a result, surface runoff has decreased in all three different rainfall conditions. Under a drought year, annual surface runoff in 2029, 2039, and 2049 decreases by 12.95, 20.78, and 27.89 million m^3 from the total estimated surface runoff

in 2019, respectively. Similarly, under a normal year, the annual surface runoff estimation in the same years decreases by 21.34, 37.59, and 52.31 million m^3 of total estimated surface runoff in 2019. Likewise, annual surface runoff estimation under a wet year in the same years decreases by 18.52, 33.06, and 46.73 million m^3 of the total estimated surface runoff in 2019. Additionally, suitable LULC allocation for flood mitigation under three different rainfall conditions was in 2049.

These results indicate that Goal programming can be efficiently operated using add-in software under the MS Excel environment to minimize surface runoff in the watershed area.

Furthermore, the derived optimum local parameters of the CLUE-S model were applied to map optimizing LULC allocation data in 2029, 2039, and 2049 of three different rainfall conditions using the CLUE-S model. As a result, it revealed that urban and built-up areas, other field crops, forest land, and unused land are unchanged. Meanwhile, sugarcane, para rubber, and perennial trees and orchards increase LULC types by about 7.22, 1.50, and 2.51 km^2 per year, respectively. In contrast, paddy field, cassava, waterbody, rangeland, and marsh and swamp are decreasing LULC types by about 6.75, 3.90, 0.33, 0.22, and 0.18 km^2 per year, respectively for all three different rainfall conditions.

9.1.5 Economic and ecosystem service values evaluation and change

The economic and ecosystem service values of actual LULC data in 2019 and suitable LULC allocation data in 2049 for flood mitigation under three different rainfall conditions were first estimated using the PV model and a simple benefit method. Then they were applied to detect its value change in terms of gain and loss using the image algebra change detection algorithm.

As a result, the suitable LULC allocation for flood mitigation in 2049 under normal year could provide the highest value for future economic value, about 149,210 million Baht, and the highest economic value gain compared with actual LULC in 2019. In the meantime, the suitable LULC allocation for flood mitigation in 2049 under dry year could provide the highest ecosystem service value, about 15,481 million Baht, and the highest ecosystem service value gain, about 207 million Baht. However, the suitable LULC allocation for flood mitigation in 2049 under a normal year

could reduce the highest surface runoff by about 52 million m^3 compared with the actual value of LULC data in 2019. Consequently, it can be concluded that the most suitable LULC allocation for flood mitigation in 2049 in Chaiyaphum district, Chaiyaphum province under the Second Part of the Lam Nam Chi watershed based on future economic value and ecosystem service value evaluation and reduction of surface runoff should be suitable LULC allocation for flood mitigation in 2049 under normal year scenario.

In conclusion, the derived results of this study can be used as primary information for flood mitigation project implementation. Additionally, the presented conceptual framework and research workflows can be used as a guideline for government agencies to investigate in more detail flood mitigation at Mueang Chaiyaphum district, Chaiyaphum province.

9.2   Recommendations

Many objectives were here investigated includes LULC assessment and its change, prediction of time-series of LULC, surface runoff estimation, optimization of LULC allocation for flood mitigation and mapping, evaluation of economic and ecosystem service values in Mueang Chaiyaphum district, Chaiyaphum province, Thailand. The possible expected recommendations and implications could be made for further studies as follows:

(1) The classified LULC data are fundamental input data for time-series LULC prediction under the CLUE-S model and time-series surface runoff estimation using the SCS-CN method, the accessible data from very high spatial resolution imageries, such as Sentinel-2, should be applied to classify multi-level of LULC types using the RF classifier.

(2) According to the driving force on LULC change, more significant factors at a local scale (social factor and culture) should be considered since the driving factor plays an essential role for land allocation under the CLUE-S model based on binary logistic regression analysis.

(3) The study results show that Goal programming based on Linear programming provides better total surface runoff in the optimized LULC allocation for flood

mitigation. However, this study deals only with a single objective function. For future studies, multi-objective functions are recommended to maximize more meaning value, for example, economic value and ecosystem service value.
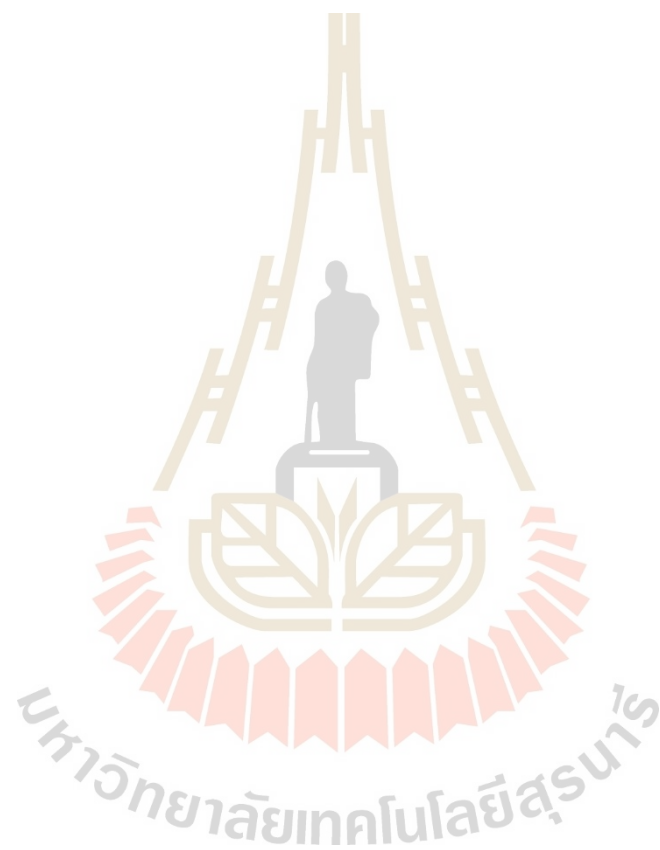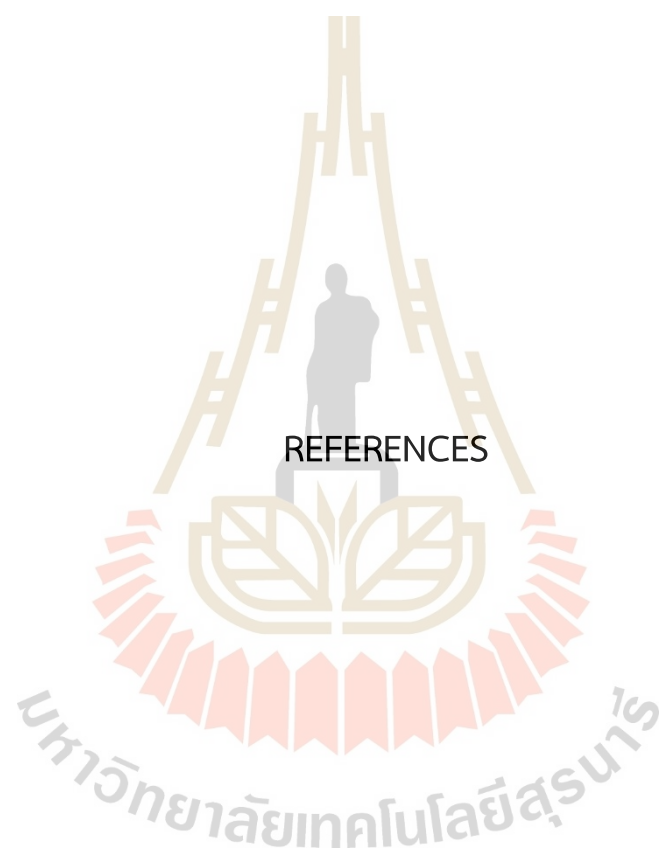
REFERENCES

REFERENCES

Ahmad, I., Ahmad, I., & Verma, M. K. (2015). *Application of Curve Number Method for Estimation of Runoff Potential in GIS Environment*. Paper presented at The 2nd International Conference on Geological and Civil Engineering, 10-11 January 2015.

Al-Zahrani, M., Musa, A., & Chowdhury, S. (2016). Multi-objective optimization model for water resource management: a case study for Riyadh, Saudi Arabia. *Environment, Development and Sustainability, 18*, 777-798.

Anderson, J. R., Hardy, E. E., Roach, J. T., & Witmer, R. E. (1976). *A land use and land cover classification system for use with remote sensor data*.

Arowolo, A. O., & Deng, X. (2018). Land use/land cover change and statistical modelling of cultivated land change drivers in Nigeria. *Regional Environmental Change, 18*(1), 247-259.

Banba, M. (2016). *Influences of Regional Development on Land Use of Nagara Basin and Flood Risk Control*. Paper presented at The 3rd European Conference on Flood Risk Management.

Bazaraa, M. S., Jarvis, J. J., & Sherali, H. D. (2009). *Linear Programming and Network Flows* (4th ed.). New Jersey: John Wiley & Sons, Inc.

Beckers, J., Smerdon, B., Redding, T., Anderson, A., Pike, R., & Werner, A. (2009). Hydrologic Models for Forest Management Applications: Part 1: Model Selection. *Streamline Watershed Management Bulletin, 13*(1), 35-44.

Breiman, L. (2001). Random Forests. *Machine Learning, 45*(1), 5-32.

Breiman, L., Friedman, J., Olshen, R. A., & Stone, C. J. (1984). *Classification and regression trees: The Wadsworth statistics/probability*. United Kingdom: Chapman & Hall.

Calow, P., & Petts, G. E. (1994). *The Rivers Handbook: Hydrological and Ecological Principles, Volume 2*. Oxford, United Kingdom: Wiley-Blackwell.

Canqiang, Z., Wenhua, L., Biao, Z., & Moucheng, L. (2012). Water Yield of Xitiaoxi River Basin Based on InVEST Modeling. *Journal of Resources and Ecology, 3*(1), 50-54.

Chow, V. T., Maidment, D. R., & Mays, L. W. (1988). *Applied hydrology*. New York: McGraw-Hill.

Congalton, R. G., & Green, K. (2019). *Assessing the Accuracy of Remotely Sensed Data: Principles and Practices* (2nd ed.). Boca Raton, Florida: CRC Press.

Costanza, R., d'Arge, R., de Groot, R., Farber, S., Grasso, M., Hannon, B., Limburg, K., Naeem, S., O'Neill, R. V., Paruelo, J., Raskin, R. G., Sutton, P., & van den Belt, M. (1997). The value of the world's ecosystem services and natural capital. *Nature, 387*(6630), 253-260.

Danumah, J. H. (2016). *Assessing Urban Flood Risks under Changing Climate and Land Use in Abidjan District, South Cote d'Ivoire.* (Ph.D. Thesis). Department of Civil Engineering, Kwame Nkrumah University of Science and Technology,

de Koning, G. H. J., Verburg, P. H., Veldkamp, A., & Fresco, L. O. (1999). Multi-scale modelling of land use change dynamics in Ecuador. *Agricultural Systems, 61*(2), 77-93.

Department of Disaster Prevention and Mitigation. (2019). *Report of damage from a flooding situation*: Department of Disaster Prevention and Mitigation, Ministry of Interior.

Du, J., Fang, J., Xu, W., & Shi, P. (2013). Analysis of dry/wet conditions using the standardized precipitation index and its potential usefulness for drought/flood monitoring in Hunan Province, China. *Stochastic Environmental Research and Risk Assessment, 27*(2), 377-387.

Eisavi, V., Homayouni, S., Yazdi, A. M., & Alimohammadi, A. (2015). Land cover mapping based on random forest classification of multitemporal spectral and thermal images. *Environmental Monitoring and Assessment, 187*(5), 291.

Evelyn, O. B. (2009). Utilizing geographic information system (GIS) to determine optimum forest cover for minimizing runoff in a degraded watershed in Jamaica. *International Forestry Review 11*(3), 375-393.

Fitzpatrick-Lins, K. (1981). Comparison of Sampling Procedures and Data Analysis for a Land-use and Land-cover Map. *Photogrammetric Engineering and Remote Sensing, 47*(3), 343-351.

Gao, C., Zhou, P., Jia, P., Liu, Z., Wei, L., & Tian, H. (2016). Spatial driving forces of dominant land use/land cover transformations in the Dongjiang River watershed, Southern China. *Environmental Monitoring and Assessment, 188*(2), 84.

Gartzia, M., Alados, C. L., Pe´rez-Cabello, F., & Bueno, C. G. (2013). Improving the Accuracy of Vegetation Classifications in Mountainous Areas: A Case Study in the Spanish Central Pyrenees. *Mountain Research and Development, 33*(1), 63-74.

Geo-Informatics and Space Technology Development Agency. (2019). Thailand Flood Monitoring System. Retrieved from http://flood.gistda.or.th/.

Gislason, P. O., Benediktsson, J. A., & Sveinsson, J. R. (2006). Random Forests for land cover classification. *Pattern Recognition Letters, 27*(4), 294-300.

Gonfa, Z. B., & Kumar, D. (2015). Optimal Land Use Planning in Mojo Watershed with Multi-Objective Linear Programming. *American International Journal of Research in Humanities, Arts and Social Sciences, 13*(1), 10-17.

Grunwald, S., & Norton, L. D. (2000). Calibration and validation of a non-point source pollution model. *Agricultural Water Management, 45*(1), 17-39.

Han, H., Yang, C., & Song, J. (2015). Scenario Simulation and the Prediction of Land Use and Land Cover Change in Beijing, China. *Sustainability, 7*(4), 4260-4279.

Hargreaves, J. J., & Hobbs, B. F. (2009). Optimal Selection of Priority Development Areas Considering Tradeoffs Between Hydrology and Development Configuration. *Environmental Modeling & Assessment, 14*(3), 289-302.

Harris, J. R., & Grunsky, E. C. (2015). Predictive lithological mapping of Canada's North using Random Forest classification applied to geophysical and geochemical data. *Computers & Geosciences, 80*, 9-25.

Hawkins Richard, H., Hjelmfelt Allen, T., & Zevenbergen Adrian, W. (1985). Runoff Probability, Storm Depth, and Curve Numbers. *Journal of Irrigation and Drainage Engineering, 111*(4), 330-340.

Huang, T.-W., Kuo, H.-F., & Tsou, K.-W. (2013). A Multi-objective spatial optimization method for land use allocation in high flood risk areas. *International Journal of Bioscience, Biochemistry and Bioinformatics, 3*(3), 201-205.

Jensen, J. R. (2005). *Introductory Digital Image Processing: A Remote Sensing Perspective* (3rd ed.). New Jersey: Prentice-Hall.

Jhonnerie, R., Siregar, V. P., Nababan, B., Prasetyo, L. B., & Wouthuyzen, S. (2015). Random Forest Classification for Mangrove Land Cover Mapping Using Landsat 5 TM and Alos Palsar Imageries. *Procedia Environmental Sciences, 24*, 215-221.

Jones, D., & Tamiz, M. (2010). *Practical goal programming*. Berlin: Springer.

Jothityangkoon, C., Maskong, H., Sangthong, P., & Kosa, P. (2015). Development processes of a master plan for flood protection and mitigation in a community area: A case study of Roi Et province. *KKU Engineering Journal, 42*(4), 287-291.

Karavitis, C. A., Alexandris, S., Tsesmelis, D. E., & Athanasopoulos, G. (2011). Application of the Standardized Precipitation Index (SPI) in Greece. *Water, 3*(3).

Kasei, R. A., Ampadu, B., & Sapanbil, G. S. (2013). Relationship between Rainfall-Runoff on the White Volta River at Pwalugu of the Volta Basin in Ghana. *Journal of Environment and Earth Science, 3*(11), 92-99.

Kok, K., & Winograd, M. (2002). Modelling land-use change for Central America, with special reference to the impact of hurricane Mitch. *Ecological Modelling, 149*(1), 53-69.

Kucsicsa, G., Popovici, E.-A., Bălteanu, D., Grigorescu, I., Dumitraşcu, M., & Mitrică, B. (2019). Future land use/cover changes in Romania: regional simulations based on CLUE-S model and CORINE land cover database. *Landscape and Ecological Engineering, 15*(1), 75-90.

Kulkarni, A., & Lowe, B. (2016). Random Forest Algorithm for Land Cover Classification. *International Journal on Recent and Innovation Trends in Computing and Communication, 4*(3), 58-63.

Kuntiyawichai, K. (2012). *Interactions between Land Use and Flood Management in the Chi River Basin.* (Ph.D. Thesis). UNESCO-IHE Institute for Water Education, Wageningen University.

Lal, M., Mishra, S. K., Pandey, A., Pandey, R. P., Meena, P. K., Chaudhary, A., Jha, R. K., Shreevastava, A. K., & Kumar, Y. (2017). Evaluation of the Soil Conservation Service curve number methodology using data from agricultural plots. *Hydrogeology Journal, 25*(1), 151-167.

Li, F., Chen, J., Liu, Y., Xu, P., Sun, H., Engel, A. B., & Wang, S. (2019). Assessment of the Impacts of Land Use/Cover Change and Rainfall Change on Surface Runoff in China. *Sustainability, 11*(13).

Li, X., Wang, Y., Li, J., & Lei, B. (2016). Physical and Socioeconomic Driving Forces of Land-Use and Land-Cover Changes: A Case Study of Wuhan City, China. *Discrete Dynamics in Nature and Society, 2016*, 1-11.

Liang, X., Liu, X., Chen, G., Leng, J., Wen, Y., & Chen, G. (2020). Coupling fuzzy clustering and cellular automata based on local maxima of development potential to model urban emergence and expansion in economic development zones. *International Journal of Geographical Information Science, 34*(10), 1930-1952.

Liu, M., Wang, Y., Li, D., & Xia, B. (2013). *Dyna-CLUE Model Improvement Based on Exponential Smoothing Method and Land Use Dynamic Simulation*. Paper presented at the Geo-Informatics in Resource Management and Sustainable Ecosystem, Berlin, Heidelberg.

Liu, W., & Liu, L. (2019). Analysis of Dry/Wet Variations in the Poyang Lake Basin Using Standardized Precipitation Evapotranspiration Index Based on Two Potential Evapotranspiration Algorithms. *Water, 11*(7), 1380.

Liu, Y., Gong, W., Hu, X., & Gong, J. (2018). Forest Type Identification with Random Forest Using Sentinel-1A, Sentinel-2A, Multi-Temporal Landsat-8 and DEM Data. *Remote Sensing, 10*(6), 946.

Liu, Y., Zhou, Y., Ju, W., Wang, S., Wu, X., He, M., & Zhu, G. (2014). Impacts of droughts on carbon sequestration by China's terrestrial ecosystems from 2000 to 2011. *Biogeosciences, 11*(10), 2583-2599.

Malczewski, J. (1999). *GIS and multicriteria decision analysis*. New York: John Wiley & Sons.

Malczewski, J., & Rinner, C. (2015). *Multicriteria Decision Analysis in Geographic Information Science*. New York: Springer.

Mamat, A., Halik, Ü., & Rouzi, A. (2018). Variations of Ecosystem Service Value in Response to Land-Use Change in the Kashgar Region, Northwest China. *Sustainability, 10*(1), 200.

Mbow, C., Diop, A., Diaw, A. T., & Niang, C. I. (2008). Urban sprawl development and flooding at Yeumbeul suburb (Dakar-Senegal). *African Journal of Environmental Science and Technology, 2*(4), 75-88.

McDill, M. E. (1999). *Forest Resource Management*. State College, PA: Pennsylvania State University.

McKee, T. B., Doesken, N. J., & Kleist, J. (1993). *The relationship of drought frequency and duration to time scales*. Paper presented at the Eighth Conference on Applied Climatology, 17-22 January 1993.

Me, W., Abell, J. M., & Hamilton, D. P. (2015). Effects of hydrologic conditions on SWAT model performance and parameter sensitivity for a small, mixed land use catchment in New Zealand. *Hydrology and Earth System Sciences, 19*(10), 4127-4147.

Midekisa, A., Holl, F., Savory, D. J., Andrade-Pacheco, R., Gething, P. W., Bennett, A., & Sturrock, H. J. W. (2017). Mapping land cover change over continental Africa using Landsat and Google Earth Engine cloud computing. *PLOS ONE, 12*(9), e0184926.

Millennium Ecosystem Assessment. (2005). *Ecosystems and Human Well-being: Synthesis*. Washington, D.C.: Island Press.

Mishra, A. K., Singh, V. P., & Desai, V. R. (2009). Drought characterization: a probabilistic approach. *Stochastic Environmental Research and Risk Assessment, 23*(1), 41-55.

Mishra, S. K., Jain, M. K., Suresh Babu, P., Venugopal, K., & Kaliappan, S. (2008). Comparison of AMC-dependent CN-conversion Formulae. *Water Resources Management, 22*(10), 1409-1420.

Mishra, S. K., & Singh, V. P. (2003). *Soil Conservation Service Curve Number (SCS-CN) methodology*. Dordrecht, The Netherlands.: Kluwer Academic Publishers.

Mohammady, M., Moradi, H. R., Zeinivand, H., Temme, A. J. A. M., Yazdani, M. R., & Pourghasemi, H. R. (2018). Modeling and assessing the effects of land use

changes on runoff generation with the CLUE-s and WetSpa models. *Theoretical and Applied Climatology, 133*(1), 459-471.

Mohammed, H., Yohannes, F., & Zeleke, G. (2004). Validation of agricultural non-point source (AGNPS) pollution model in Kori watershed, South Wollo, Ethiopia. *International Journal of Applied Earth Observation and Geoinformation, 6*(2), 97-109.

Na, X., Zhang, S., Li, X., Yu, H., & Liu, C. (2010). Improved Land Cover Mapping using Random Forests Combined with Landsat Thematic Mapper Imagery and Ancillary Geographic Data. *Photogrammetric Engineering & Remote Sensing, 76*(7), 833-840.

National Resources Conservation Service. (2004). *National Engineering Handbook, title 210–VI–NEH. Part 630, Chapter 10 Estimation of Direct Runoff from Storm Rainfall*. Washington, D.C.: United States Department of Agriculture.

National Resources Conservation Service. (2009). *National Engineering Handbook, title 210–VI–NEH. Part 630, Chapter 7 Hydrologic Soil Groups*. Washington, D.C.: United States Department of Agriculture.

Neitsch, S. L., Arnold, J. G., Kiniry, J. R., Williams, J. R., & King, K. W. (2002). *Soil and water assessment tool (SWAT): theoretical documentation, version 2000*: Texas Water Resources Institute, College Station, TX, TWRI Report TR-191.

Nikkami, D., Elektorowicz, M., & Mehuys, G. R. (2002). Optimizing the Management of Soil Erosion. *Water Quality Research Journal of Canada, 37*(3), 577-586.

Ongsomwang, S., & Boonchoo, K. (2016). Integration of geospatial models for the allocation of deforestation hotspots and forest protection units. *Suranaree Journal of Science and Technology, 23*(3), 283-307.

Ongsomwang, S., & Iamchuen, N. (2015a). Integration of geospatial models for optimum land use allocation in three different scenarios. *Suranaree Journal of Science and Technology 22*(4), 377-396.

Ongsomwang, S., & Iamchuen, N. (2015b). Integration of geospatial models for optimum land use allocation in three different scenarios. *Suranaree Journal of Science and Technology, 22*(4), 377-396.

Ongsomwang, S., Pattanakiat, S., & Srisuwan, A. (2019). Impact of Land Use and Land Cover Change on Ecosystem Service Values: A Case Study of Khon Kaen City, Thailand. *Environment and Natural Resources Journal, 17*(4), 43-58.

Ongsomwang, S., & Pimjai, M. (2014). Land use and land cover prediction and its impact on surface runoff. *Suranaree Journal of Science and Technology, 22*(2), 205-223.

Owji, M. R., Nikkami, D., Mahdian, M. H., & Mahmoudi, S. (2012). Minimizing Surface Runoff by Optimizing Land Use Management. *World Applied Sciences Journal, 20*(1), 170-176.

Palchowdhuri, Y., & Roy, P. S. (2018). Driver based statistical model for simulating land use/land cover change in Indus river basin, India. *Remote Sensing of Land, 2*(1), 15-30.

Pareeth, S., Karimi, P., Shafiei, M., & De Fraiture, C. (2019). Mapping Agricultural Landuse Patterns from Time Series of Landsat 8 Using Random Forest Based Hierarchical Approach. *Remote Sensing, 11*(5), 601-616.

Phetprayoon, T. (2010). *Potential Assessment of Nonpoint Source Pollution on Surface Water Quality in Upper Lam Phra Phloeng Watershed using Geospatial Models.* (Ph. D. Thesis). Suranaree University of Technology,

Phetprayoon, T., Sarapirome, S., Navanugraha, C., & Wonprasaid, S. (2012). Runoff and sediment yield estimation using distributed geospatial models for agricultural watershed in Thailand. *Suranaree Journal of Science and Technology, 19*(3), 295-308.

Phompila, C., Lewis, M., Ostendorf, B., & Clarke, K. (2017). Forest Cover Changes in Lao Tropical Forests: Physical and Socio-Economic Factors are the Most Important Drivers. *Land, 6*(2), 23.

Polikar, R. (2006). Ensemble based systems in decision making. *IEEE Circuits and Systems Magazine, 6*(3), 21-45.

Pontius, R. G., & Schneider, L. C. (2001). Land-cover change model validation by an ROC method for the Ipswich watershed, Massachusetts, USA. *Agriculture, Ecosystems & Environment, 85*(1), 239-248.

Rahmat, S. N., Jayasuriya, N., & Bhuiyan, M. (2015). Assessing droughts using meteorological drought indices in Victoria, Australia. *Hydrology Research, 46*(3), 463-476.

Rawat, K. S., & Singh, S. K. (2017). Estimation of Surface Runoff from Semi-arid Ungauged Agricultural Watershed Using SCS-CN Method and Earth Observation Data Sets. *Water Conservation Science and Engineering, 1*(4), 233-247.

Riedel, C. (2003). Optimizing land use planning for mountainous regions using LP and GIS towards sustainability. *Indian Journal of Soil Conservation, 34*(1), 121-124.

Rizeei, H. M., Pradhan, B., & Saharkhiz, M. A. (2018). Surface runoff prediction regarding LULC and climate dynamics using coupled LTM, optimized ARIMA, and GIS-based SCS-CN models in tropical region. *Arabian Journal of Geosciences, 11*(3), 53.

Rodriguez-Galiano, V. F., Ghimire, B., Rogan, J., Chica-Olmo, M., & Rigol-Sanchez, J. P. (2012). An assessment of the effectiveness of a random forest classifier for land-cover classification. *ISPRS Journal of Photogrammetry and Remote Sensing, 67*, 93-104.

Rossiter, D. G. (1994). Lecture Notes: "Land Evaluation," Part 4: Economic Land Evaluation: College of Agriculture & Life Sciences, Department of Soil, Crop, & Atmospheric Sciences: Cornell University.

Rouse, J., Haas, R. H., Schell, J. A., & Deering, D. (1973). *Monitoring vegetation systems in the great plains with ERTS*. Paper presented at the Third Earth Resources Technology Satellite-1 Symposium- Volume I: Technical Presentations. NASA SP-351.

Sadeghi, S. H. R., Jalili, K., & Nikkami, D. (2009). Land use optimization in watershed scale. *Land Use Policy, 26*, 186-193.

Sayari, N., Bannayan, M., Alizadeh, A., & Farid, A. (2013). Using drought indices to assess climate change impacts on drought conditions in the northeast of Iran (case study: Kashafrood basin). *Meteorological Applications, 20*(1), 115-127.

Seiler, R. A., Hayes, M., & Bressan, L. (2002). Using the standardized precipitation index for flood risk monitoring. *International Journal of Climatology, 22*(11), 1365-1376.

Shrestha, P. P., & Shrestha, K. J. (2017). Factors associated with crash severities in built-up areas along rural highways of Nevada: A case study of 11 towns. *Journal of Traffic and Transportation Engineering (English Edition), 4*(1), 96-102.

Sobhani, G. (1975). *A review of selected small watershed design methods for possible adoption to Iranian conditions.* (M.S. Thesis). Utah State University, Logan, UT,

Sokouti, R., & Nikkami, D. (2017). Optimizing land use pattern to reduce soil erosion. *Eurasian Journal of Soil Science, 6*(1), 75-83.

Srichaichana, J., Trisurat, Y., & Ongsomwang, S. (2019). Land Use and Land Cover Scenarios for Optimum Water Yield and Sediment Retention Ecosystem Services in Klong U-Tapao Watershed, Songkhla, Thailand. *Sustainability, 11*(10), 2895-2916.

Sriwongsitanon, N. (2010). Flood Forecasting System Development for the Upper Ping River Basin. *Kasetsart Journal (Natural Science), 44*, 717-731.

Sunandar, A. D., Suhendang, E., Hendrayanto, Jaya, I. N. S., & Marimin. (2014). Land Use Optimization in Asahan Watershed with Linear Programming and SWAT Model. *International Journal of Sciences: Basic and Applied Research, 18*(1), 63-78.

Tajbakhsh, S. M., Memarian, H., & Kheyrkhah, A. (2018). A GIS-based integrative approach for land use optimization in a semi-arid watershed. *Global Journal of Environmental Science and Management, 4*(1), 31-46.

Tan, C., Yang, J., & Li, M. (2015). Temporal-Spatial Variation of Drought Indicated by SPI and SPEI in Ningxia Hui Autonomous Region, China. *Atmosphere, 6*(10), 1399-1421.

Tatsumi, K., Yamashiki, Y., Canales Torres, M. A., & Taipe, C. L. R. (2015). Crop classification of upland fields using Random forest of time-series Landsat 7 ETM+ data. *Computers and Electronics in Agriculture, 115*, 171-179.

TEEB. (2010). *The Economics of Ecosystems and Biodiversity Ecological and Economic Foundations. Edited by Pushpam Kumar.* London and Washington: Earthscan Publications.

Tingsanchali, T., & Karim, F. (2010). Flood-hazard assessment and risk-based zoning of a tropical flood plain: case study of the Yom River, Thailand. *Hydrological Sciences Journal, 55*(2), 145-161. doi:10.1080/02626660903545987

Trisurat, Y., Alkemade, R., & Verburg, P. H. (2010). Projecting Land-Use Change and Its Consequences for Biodiversity in Northern Thailand. *Environmental Management, 45*(3), 626-639.

United States Department of Agriculture. (1986). *Urban Hydrology for Small Watersheds, title 210-VI-TR-55.* (2nd ed.). Washington, D.C.: Conservation Engineering Division, National Resources Conservation Service, United States Department of Agriculture.

van Asselen, S., & Verburg, P. H. (2013). Land cover change or land-use intensification: simulating land system change with a global-scale land change model. *Global Change Biology, 19*(12), 3648-3667.

Veldkamp, A., & Fresco, L. O. (1996). CLUE-CR: An integrated multi-scale model to simulate land use change scenarios in Costa Rica. *Ecological Modelling, 91*(1), 231-248.

Verburg, P. H. (2010). *The CLUE model Hands-on exercises*: Amsterdam: Institute for Environmental Studies, University Amsterdam.

Verburg, P. H., Chen, Y., & Veldkamp, T. (2000). Spatial explorations of land use change and grain production in China. *Agriculture, Ecosystems & Environment, 82*(1), 333-354.

Verburg, P. H., Koning, G. H. J. d., Koning, G. H. J. d., Veldkamp, A., & Bouma, J. (1999). A spatial explicit allocation procedure for modelling the pattern of land use change based upon actual land use. *Ecological Modelling, 116*, 45-61.

Verburg, P. H., & Lesschen, J.-P. (2014). *Practical: Explorative modeling of future land use for the Randstad region of the Netherlands*: Wageningen University, Netherlands.

Verburg, P. H., Soepboer, W., Veldkamp, A., Limpiada, R., Espaldon, V., & Mastura, S. S. A. (2002). Modeling the Spatial Dynamics of Regional Land Use: The CLUE-S Model. *Environmental Management, 30*(3), 391-405. doi:10.1007/s00267-002-2630-x

Verburg, P. H., Veldkamp, T., & Bouma, J. (1999). Land use change under conditions of high population pressure: the case of Java. *Global Environmental Change, 9*(4), 303-312.

Vilar del Hoyo, L., Martín Isabel, M. P., & Martínez Vega, F. J. (2011). Logistic regression models for human-caused wildfire risk estimation: analysing the effect of the spatial accuracy in fire occurrence data. *European Journal of Forest Research, 130*(6), 983-996.

Weng, Q. (2010). *Remote Sensing and GIS Integration Theories, Methods, and Applications*. New York: McGraw-Hill.

Xu, H. (2008). A new index for delineating built‑up land features in satellite imagery. *International Journal of Remote Sensing, 29*(14), 4269-4276.

Xu, L., Li, Z., Song, H., & Yin, H. (2013). Land-Use Planning for Urban Sprawl Based on the CLUE-S Model: A Case Study of Guangzhou, China. *Entropy, 15*, 3490-3506.

Xu, X., Du, Z., & Zhang, H. (2016). Integrating the system dynamic and cellular automata models to predict land use and land cover change. *International Journal of Applied Earth Observation and Geoinformation, 52*, 568-579.

Yeo, I.-Y., Gordon, S. I., & Guldmann, J.-M. (2004). Optimizing Patterns of Land Use to Reduce Peak Runoff Flow and Nonpoint Source Pollution with an Integrated Hydrological and Land Use Model. *Earth Interactions, 8*, 1-20.

Yu, D., Xie, P., Dong, X., Hu, B., Ji, L., Li, Y., Peng, T., Ma, H., Wang, K., & Xu, S. (2018). Improvement of the SWAT model for event-based flood simulation on a sub-daily timescale. *Hydrology and Earth System Sciences, 22*, 5001-5019.

Zare, M., Nazari Samani, A. A., Mohammady, M., Salmani, H., & Bazrafshan, J. (2017). Investigating effects of land use change scenarios on soil erosion using CLUE-s and RUSLE models. *International Journal of Environmental Science and Technology, 14*(9), 1905-1918. doi:10.1007/s13762-017-1288-0

Zha, Y., Gao, J., & Ni, S. (2003). Use of normalized difference built-up index in automatically mapping urban areas from TM imagery. *International Journal of Remote Sensing, 24*(3), 583-594.

Zhang, A., & Jia, G. (2013). Monitoring meteorological drought in semiarid regions using multi-sensor microwave remote sensing data. *Remote Sensing of Environment, 134*, 12-23.

Zhang, Q., Xu, C.-Y., & Zhang, Z. (2009). Observed changes of drought/wetness episodes in the Pearl River basin, China, using the standardized precipitation index and aridity index. *Theoretical and Applied Climatology, 98*(1), 89-99.

Zheng, H. W., Shen, G. Q., Wang, H., & Hong, J. (2015). Simulating land use change in urban renewal areas: A case study in Hong Kong. *Habitat International, 46*, 23-34.

Zhou, R., Zhang, H., Ye, X. Y., Wang, X. J., & Su, H. L. (2016). The Delimitation of Urban Growth Boundaries Using the CLUE-S Land-Use Change Model: Study on Xinzhuang Town, Changshu City, China. *Sustainability, 8*(11).

APPENDICES
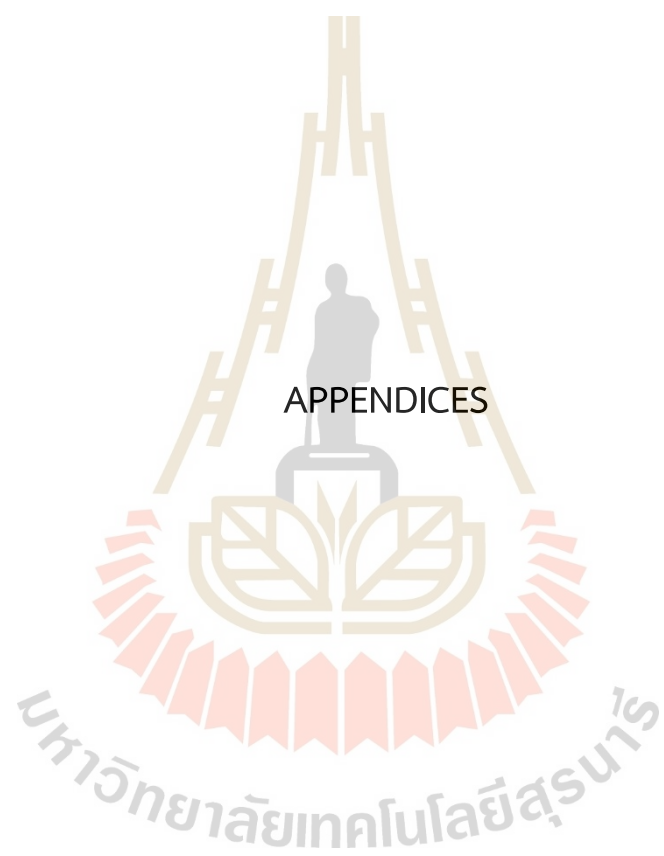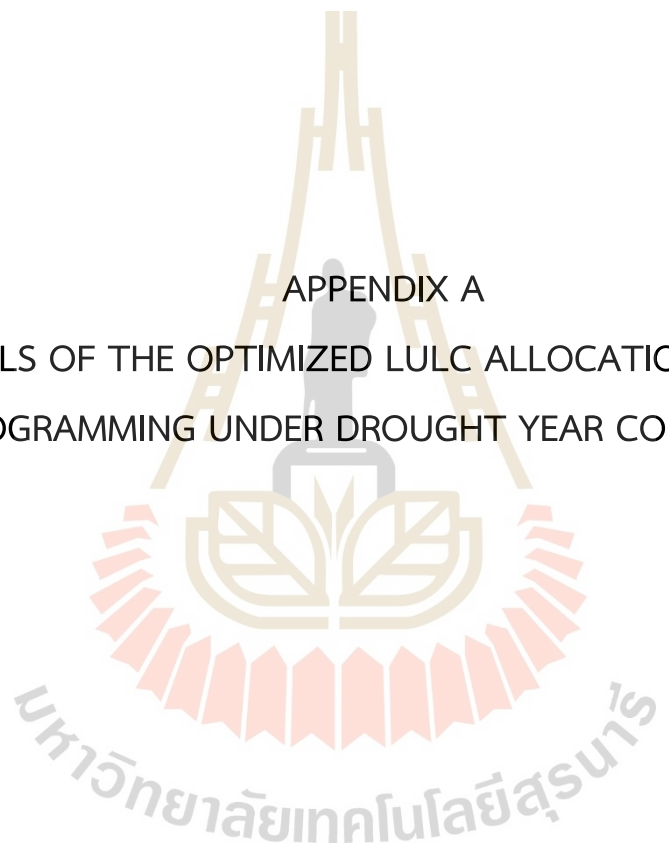
APPENDIX A

DETAILS OF THE OPTIMIZED LULC ALLOCATION BY GOAL

PROGRAMMING UNDER DROUGHT YEAR CONDITIONS

Table A1 Details of the optimized LULC allocation in 2029 under drought year conditions using Goal programming.

LULC type	X_1	X_2	X_3	X_4	X_5	X_6	X_7	X_8	X_9	X_{10}	X_{11}	X_{12}	Objective function	Minimized surface runoff (million m³)
Allocated area	65.84	1947.12	387.24	408.26	6.19	134.43	125.36	481.30	49.52	70.54	25.13	93.31		
Runoff coefficient	0.45	0.44	0.38	0.45	0.39	0.37	0.38	0.28	0.49	0.42	0.54	0.46	Best cell	1,565.01
Constraints	X_1	X_2	X_3	X_4	X_5	X_6	X_7	X_8	X_9	X_{10}	X_{11}	X_{12}	Total	Operator	Right hand side (Bi)
Constraint 1	1	0	0	0	0	0	0	0	0	0	0	0	65.84	=>=	65.84
Constraint 2	1	0	0	0	0	0	0	0	0	0	0	0	65.84	<=	77.38
Constraint 3	0	1	0	0	0	0	0	0	0	0	0	0	1,947.12	<=	2,012.16
Constraint 4	0	1	0	0	0	0	0	0	0	0	0	0	1,947.12	=>=	1,947.12
Constraint 5	0	0	1	0	0	0	0	0	0	0	0	0	387.24	>=	306.85
Constraint 6	0	0	1	0	0	0	0	0	0	0	0	0	387.24	<=	424.95
Constraint 7	0	0	0	1	0	0	0	0	0	0	0	0	408.26	<=	489.91
Constraint 8	0	0	0	1	0	0	0	0	0	0	0	0	408.26	=>=	408.26
Constraint 9	0	0	0	0	1	0	0	0	0	0	0	0	6.19	=>=	6.19
Constraint 10	0	0	0	0	1	0	0	0	0	0	0	0	6.19	<=	7.72
Constraint 11	0	0	0	0	0	1	0	0	0	0	0	0	134.43	>=	97.03
Constraint 12	0	0	0	0	0	1	0	0	0	0	0	0	134.43	=<=	134.43
Constraint 13	0	0	0	0	0	0	1	0	0	0	0	0	125.36	>=	88.95
Constraint 14	0	0	0	0	0	0	1	0	0	0	0	0	125.36	=<=	125.36
Constraint 15	0	0	0	0	0	0	0	1	0	0	0	0	481.30	=<=	481.30
Constraint 16	0	0	0	0	0	0	0	1	0	0	0	0	481.30	>=	382.63
Constraint 17	0	0	0	0	0	0	0	0	1	0	0	0	49.52	<=	53.30
Constraint 18	0	0	0	0	0	0	0	0	1	0	0	0	49.52	=>=	49.52
Constraint 19	0	0	0	0	0	0	0	0	0	1	0	0	70.54	<=	71.65
Constraint 20	0	0	0	0	0	0	0	0	0	1	0	0	70.54	=>=	70.54
Constraint 21	0	0	0	0	0	0	0	0	0	0	1	0	25.13	<=	27.73
Constraint 22	0	0	0	0	0	0	0	0	0	0	1	0	25.13	=>=	25.13
Constraint 23	0	0	0	0	0	0	0	0	0	0	0	1	93.31	=>=	93.31
Constraint 24	0	0	0	0	0	0	0	0	0	0	0	1	93.31	<=	141.20
Constraint 25	1	1	1	1	1	1	1	1	1	1	1	1	3,794.22	=	3,794.22
Runoff (million m³)	29.84	856.54	148.87	184.27	2.39	49.86	47.40	136.03	24.29	29.36	13.59	42.57		

Goal programming: minimized surface runoff	d1-	d1+	Best cell	Operator	Goal
	12.95	0	1,565.01	=	1,577.96

Note: X_1 is urban and built-up area, X_2 is paddy field, X_3 is sugarcane, X_4 is cassava, X_5 is other field crops, X_6 is para rubber, X_7 is perennial trees and orchards, X_8 is forest land, X_9 is waterbody, X_{10} is rangeland, X_{11} is marsh and swamp, and X_{12} is unused land.

```
What's Best! 16.0.2.0 (Nov 27, 2018) - Lib.:12.0.3977.115 - 64-bit - Status
Report -
DATE GENERATED:            Jun 23, 2021                        09:25 PM
MODEL INFORMATION:
CLASSIFICATION DATA        Current   Capacity Limits
---------------------------------------------------------
Total Cells                442
Numerics                   416
Adjustables                 14          300
Continuous                  14
Free                         0
Integers/Binaries          0/0          30
Constants                  375
Formulas                    27
Strings                      0
Constraints                 26          150
Nonlinears                   0          30
Coefficients               130

Minimum coefficient value:       1 on GoalProgramming!O4
Minimum coefficient in formula:   GoalProgramming!O4
Maximum coefficient value:       1.5779605409352e+009 on <RHS>
Maximum coefficient in formula:   GoalProgramming!G39

MODEL TYPE:                Linear (Linear Program)
SOLUTION STATUS:           GLOBALLY OPTIMAL
OBJECTIVE VALUE:           1,565,011,489.186
BEST OBJECTIVE BOUND:      . . .
INFEASIBILITY:             0.0
DIRECTION:                 Minimize
SOLVER TYPE:               . . .
ITERATIONS:                1.0
STEPS:                     . . .
ACTIVE:                    . . .
SOLUTION TIME:             0 Hours 0 Minutes 2 Seconds
End of Report
```

Table A2 Details of the optimized LULC allocation in 2039 under drought year conditions using Goal programming.

LULC type	X_1	X_2	X_3	X_4	X_5	X_6	X_7	X_8	X_9	X_{10}	X_{11}	X_{12}	Objective function		Minimized surface runoff (million m³)
Allocated area	65.84	1,879.30	454.94	359.65	6.19	152.02	160.12	481.30	47.01	69.91	24.66	93.31			
Runoff coefficient	0.45	0.44	0.38	0.45	0.39	0.37	0.38	0.28	0.49	0.42	0.54	0.46	Best cell		1,557.18
Constraints	X_1	X_2	X_3	X_4	X_5	X_6	X_7	X_8	X_9	X_{10}	X_{11}	X_{12}	Total	Operator	Right hand side (Bi)
Constraint 1	1	0	0	0	0	0	0	0	0	0	0	0	65.84	=>=	65.84
Constraint 2	1	0	0	0	0	0	0	0	0	0	0	0	65.84	<=	88.31
Constraint 3	0	1	0	0	0	0	0	0	0	0	0	0	1,879.30	<=	2,012.16
Constraint 4	0	1	0	0	0	0	0	0	0	0	0	0	1,879.30	=>=	1,879.30
Constraint 5	0	0	1	0	0	0	0	0	0	0	0	0	454.94	>=	306.85
Constraint 6	0	0	1	0	0	0	0	0	0	0	0	0	454.94	<=	520.31
Constraint 7	0	0	0	1	0	0	0	0	0	0	0	0	359.65	<=	489.91
Constraint 8	0	0	0	1	0	0	0	0	0	0	0	0	359.65	=>=	359.65
Constraint 9	0	0	0	0	1	0	0	0	0	0	0	0	6.19	=>=	6.19
Constraint 10	0	0	0	0	1	0	0	0	0	0	0	0	6.19	<=	9.45
Constraint 11	0	0	0	0	0	1	0	0	0	0	0	0	152.02	>=	97.03
Constraint 12	0	0	0	0	0	1	0	0	0	0	0	0	152.02	=<=	152.02
Constraint 13	0	0	0	0	0	0	1	0	0	0	0	0	160.12	>=	88.95
Constraint 14	0	0	0	0	0	0	1	0	0	0	0	0	160.12	=<=	160.12
Constraint 15	0	0	0	0	0	0	0	1	0	0	0	0	481.30	=<=	481.30
Constraint 16	0	0	0	0	0	0	0	1	0	0	0	0	481.30	>=	304.44
Constraint 17	0	0	0	0	0	0	0	0	1	0	0	0	47.01	<=	53.30
Constraint 18	0	0	0	0	0	0	0	0	1	0	0	0	47.01	=>=	47.01
Constraint 19	0	0	0	0	0	0	0	0	0	1	0	0	69.91	<=	71.65
Constraint 20	0	0	0	0	0	0	0	0	0	1	0	0	69.91	=>=	69.91
Constraint 21	0	0	0	0	0	0	0	0	0	0	1	0	24.66	<=	27.73
Constraint 22	0	0	0	0	0	0	0	0	0	0	1	0	24.66	=>=	24.66
Constraint 23	0	0	0	0	0	0	0	0	0	0	0	1	93.31	=>=	93.31
Constraint 24	0	0	0	0	0	0	0	0	0	0	0	1	93.31	<=	180.07
Constraint 25	1	1	1	1	1	1	1	1	1	1	1	1	3,794.22	=	3,794.22
Runoff (million m³)	29.84	826.71	174.90	162.33	2.39	56.39	60.54	136.03	23.06	29.10	13.34	42.57			

Goal programming: minimized surface runoff		d1-	d1+	Best cell	Operator	Goal
		20.78	0	1,557.18	=	1,577.96

Note: X_1 is urban and built-up area, X_2 is paddy field, X_3 is sugarcane, X_4 is cassava, X_5 is other field crops, X_6 is para rubber, X_7 is perennial trees and orchards, X_8 is forest land, X_9 is waterbody, X_{10} is rangeland, X_{11} is marsh and swamp, and X_{12} is unused land.

```
What's Best! 16.0.2.0 (Nov 27, 2018) - Lib.:12.0.3977.115 - 64-bit - Status
Report -
DATE GENERATED:            Jun 23, 2021                    09:39 PM
MODEL INFORMATION:
CLASSIFICATION DATA        Current   Capacity Limits
--------------------------------------------------------
Total Cells                442
Numerics                   416
Adjustables                 14         300
Continuous                  14
Free                         0
Integers/Binaries          0/0         30
Constants                  375
Formulas                    27
Strings                      0
Constraints                 26         150
Nonlinears                   0          30
Coefficients               130


Minimum coefficient value:        1 on GoalProgramming!O4
Minimum coefficient in formula:   GoalProgramming!O4
Maximum coefficient value:        1.5779605409352e+009 on <RHS>
Maximum coefficient in formula:   GoalProgramming!G39


MODEL TYPE:                Linear (Linear Program)
SOLUTION STATUS:           GLOBALLY OPTIMAL
OBJECTIVE VALUE:           1,557,179,342.789
BEST OBJECTIVE BOUND:      . . .
INFEASIBILITY:             0.0
DIRECTION:                 Minimize
SOLVER TYPE:               . . .
ITERATIONS:                1.0
STEPS:                     . . .
ACTIVE:                    . . .
SOLUTION TIME:             0 Hours 0 Minutes 2 Seconds
End of Report
```

Table A3 Details of the optimized LULC allocation in 2049 under drought year conditions using Goal programming.

LULC type	X_1	X_2	X_3	X_4	X_5	X_6	X_7	X_8	X_9	X_{10}	X_{11}	X_{12}	Objective function	Minimized surface runoff (million m^3)	
Allocated area	65.84	1,812.16	517.13	330.32	6.19	164.41	193.13	481.30	42.78	66.05	21.61	93.31	Objective function	Minimized surface runoff (million m^3)	
Runoff coefficient	0.45	0.44	0.38	0.45	0.39	0.37	0.38	0.28	0.49	0.42	0.54	0.46	Best cell	1,550.07	
Constraints	X_1	X_2	X_3	X_4	X_5	X_6	X_7	X_8	X_9	X_{10}	X_{11}	X_{12}	Total	Operator	Right hand side (Bi)
Constraint 1	1	0	0	0	0	0	0	0	0	0	0	0	65.84	=>=	65.84
Constraint 2	1	0	0	0	0	0	0	0	0	0	0	0	65.84	<=	99.03
Constraint 3	0	1	0	0	0	0	0	0	0	0	0	0	1,812.16	<=	2,012.16
Constraint 4	0	1	0	0	0	0	0	0	0	0	0	0	1,812.16	=>=	1,812.16
Constraint 5	0	0	1	0	0	0	0	0	0	0	0	0	517.13	>=	306.85
Constraint 6	0	0	1	0	0	0	0	0	0	0	0	0	517.13	<=	599.36
Constraint 7	0	0	0	1	0	0	0	0	0	0	0	0	330.32	<=	489.91
Constraint 8	0	0	0	1	0	0	0	0	0	0	0	0	330.32	=>=	330.32
Constraint 9	0	0	0	0	1	0	0	0	0	0	0	0	6.19	=>=	6.19
Constraint 10	0	0	0	0	1	0	0	0	0	0	0	0	6.19	<=	11.26
Constraint 11	0	0	0	0	0	1	0	0	0	0	0	0	164.41	>=	97.03
Constraint 12	0	0	0	0	0	1	0	0	0	0	0	0	164.41	=<=	164.41
Constraint 13	0	0	0	0	0	0	1	0	0	0	0	0	193.13	>=	88.95
Constraint 14	0	0	0	0	0	0	1	0	0	0	0	0	193.13	=<=	193.13
Constraint 15	0	0	0	0	0	0	0	1	0	0	0	0	481.30	=<=	481.30
Constraint 16	0	0	0	0	0	0	0	1	0	0	0	0	481.30	>=	242.23
Constraint 17	0	0	0	0	0	0	0	0	1	0	0	0	42.78	<=	53.30
Constraint 18	0	0	0	0	0	0	0	0	1	0	0	0	42.78	=>=	42.78
Constraint 19	0	0	0	0	0	0	0	0	0	1	0	0	66.05	<=	71.65
Constraint 20	0	0	0	0	0	0	0	0	0	1	0	0	66.05	=>=	66.05
Constraint 21	0	0	0	0	0	0	0	0	0	0	1	0	21.61	<=	27.73
Constraint 22	0	0	0	0	0	0	0	0	0	0	1	0	21.61	=>=	21.61
Constraint 23	0	0	0	0	0	0	0	0	0	0	0	1	93.31	=>=	93.31
Constraint 24	0	0	0	0	0	0	0	0	0	0	0	1	93.31	<=	211.89
Constraint 25	1	1	1	1	1	1	1	1	1	1	1	1	3,794.22	=	3,794.22
Runoff (million m^3)	29.84	797.17	198.81	149.09	2.39	60.99	73.02	136.03	20.99	27.49	11.69	42.57			

Goal programming: minimized surface runoff			d1-		d1+		Best cell		Operator		Goal	
			27.89		0		1,550.07		=		1,577.96	

Note: X_1 is urban and built-up area, X_2 is paddy field, X_3 is sugarcane, X_4 is cassava, X_5 is other field crops, X_6 is para rubber, X_7 is perennial trees and orchards, X_8 is forest land, X_9 is waterbody, X_{10} is rangeland, X_{11} is marsh and swamp, and X_{12} is unused land.

```
What's Best! 16.0.2.0 (Nov 27, 2018) - Lib.:12.0.3977.115 - 64-bit - Status
Report -
DATE GENERATED:              Jun 23, 2021                        10:09 PM
MODEL INFORMATION:
CLASSIFICATION DATA          Current   Capacity Limits
---------------------------------------------------------
Total Cells                  442
Numerics                     416
Adjustables                   14          300
Continuous                    14
Free                           0
Integers/Binaries            0/0          30
Constants                    375
Formulas                      27
Strings                        0
Constraints                   26          150
Nonlinears                     0      b   30
Coefficients                 130


Minimum coefficient value:       1 on GoalProgramming!O4
Minimum coefficient in formula:   GoalProgramming!O4
Maximum coefficient value:       1.5779605409352e+009 on <RHS>
Maximum coefficient in formula:   GoalProgramming!G39


MODEL TYPE:             Linear (Linear Program)
SOLUTION STATUS:        GLOBALLY OPTIMAL
OBJECTIVE VALUE:        1,550,070,101.8611
BEST OBJECTIVE BOUND:   . . .
INFEASIBILITY:          0.0
DIRECTION:              Minimize
SOLVER TYPE:            . . .
ITERATIONS:            1.0
STEPS:                  . . .
ACTIVE:                 . . .
SOLUTION TIME:          0 Hours 0 Minutes 2 Seconds
End of Report
```

APPENDIX B

DETAILS OF THE OPTIMIZED LULC ALLOCATION BY GOAL

PROGRAMMING UNDER NORMAL YEAR CONDITIONS

Table B1 Details of the optimized LULC allocation in 2029 under normal year conditions using Goal programming.

LULC type	X₁	X₂	X₃	X₄	X₅	X₆	X₇	X₈	X₉	X₁₀	X₁₁	X₁₂	Objective function	Minimized surface runoff (million m³)
Allocated area	65.84	1,947.12	385.71	408.26	7.72	134.43	125.36	481.30	49.52	70.54	25.13	93.31		
Runoff coefficient	1.03	1.03	1.03	1.03	1.03	1.03	1.03	1.03	1.03	1.03	1.03	1.03	Best cell	3,625.72
Constraints	X₁	X₂	X₃	X₄	X₅	X₆	X₇	X₈	X₉	X₁₀	X₁₁	X₁₂	Total	Operator	Right hand side (Bi)
Constraint 1	1	0	0	0	0	0	0	0	0	0	0	0	65.84	=>=	65.84
Constraint 2	1	0	0	0	0	0	0	0	0	0	0	0	65.84	<=	77.38
Constraint 3	0	1	0	0	0	0	0	0	0	0	0	0	1,947.12	<=	2,012.16
Constraint 4	0	1	0	0	0	0	0	0	0	0	0	0	1,947.12	=>=	1,947.12
Constraint 5	0	0	1	0	0	0	0	0	0	0	0	0	385.71	>=	306.85
Constraint 6	0	0	1	0	0	0	0	0	0	0	0	0	385.71	<=	424.95
Constraint 7	0	0	0	1	0	0	0	0	0	0	0	0	408.26	<=	489.91
Constraint 8	0	0	0	1	0	0	0	0	0	0	0	0	408.26	=>=	408.26
Constraint 9	0	0	0	0	1	0	0	0	0	0	0	0	7.72	>=	6.19
Constraint 10	0	0	0	0	1	0	0	0	0	0	0	0	7.72	=<=	7.72
Constraint 11	0	0	0	0	0	1	0	0	0	0	0	0	134.43	>=	97.03
Constraint 12	0	0	0	0	0	1	0	0	0	0	0	0	134.43	=<=	134.43
Constraint 13	0	0	0	0	0	0	1	0	0	0	0	0	125.36	>=	88.95
Constraint 14	0	0	0	0	0	0	1	0	0	0	0	0	125.36	=<=	125.36
Constraint 15	0	0	0	0	0	0	0	1	0	0	0	0	481.30	=<=	481.30
Constraint 16	0	0	0	0	0	0	0	1	0	0	0	0	481.30	>=	382.63
Constraint 17	0	0	0	0	0	0	0	0	1	0	0	0	49.52	<=	53.30
Constraint 18	0	0	0	0	0	0	0	0	1	0	0	0	49.52	=>=	49.52
Constraint 19	0	0	0	0	0	0	0	0	0	1	0	0	70.54	<=	71.65
Constraint 20	0	0	0	0	0	0	0	0	0	1	0	0	70.54	=>=	70.54
Constraint 21	0	0	0	0	0	0	0	0	0	0	1	0	25.13	<=	27.73
Constraint 22	0	0	0	0	0	0	0	0	0	0	1	0	25.13	=>=	25.13
Constraint 23	0	0	0	0	0	0	0	0	0	0	0	1	93.31	=>=	93.31
Constraint 24	0	0	0	0	0	0	0	0	0	0	0	1	93.31	<=	141.20
Constraint 25	1	1	1	1	1	1	1	1	1	1	1	1	3,794.22	=	3,794.22
Runoff (million m³)	67.58	1,973.05	348.56	407.56	6.78	111.33	104.68	366.03	51.30	64.93	28.60	95.33			

Goal programming: minimized surface runoff			d1-		d1+		Best cell		Operator	Goal	
			21.34		0		3,625.72		=	3,647.07	

Note: X₁ is urban and built-up area, X₂ is paddy field, X₃ is sugarcane, X₄ is cassava, X₅ is other field crops, X₆ is para rubber, X₇ is perennial trees and orchards, X₈ is forest land, X₉ is waterbody, X₁₀ is rangeland, X₁₁ is marsh and swamp, and X₁₂ is unused land.

```
What's Best! 16.0.2.0 (Nov 27, 2018) - Lib.:12.0.3977.115 - 64-bit - Status
Report -
DATE GENERATED:              Jun 23, 2021                        09:31 PM
MODEL INFORMATION:
CLASSIFICATION DATA         Current   Capacity Limits
------------------------------------------------------------
Total Cells                 442
Numerics                    416
Adjustables                  14          300
Continuous                   14
Free                          0
Integers/Binaries           0/0          30
Constants                   375
Formulas                     27
Strings                       0
Constraints                  26         150
Nonlinears                    0          30
Coefficients                130


Minimum coefficient value:      1 on GoalProgramming!O4
Minimum coefficient in formula:   GoalProgramming!O4
Maximum coefficient value:      3.6524257537736e+009 on <RHS>
Maximum coefficient in formula:   GoalProgramming!G39


MODEL TYPE:              Linear (Linear Program)
SOLUTION STATUS:        GLOBALLY OPTIMAL
OBJECTIVE VALUE:        3,625,723,294.9744
BEST OBJECTIVE BOUND:   . . .
INFEASIBILITY:          0.0
DIRECTION:              Minimize
SOLVER TYPE:            . . .
ITERATIONS:             1.0
STEPS:                  . . .
ACTIVE:                 . . .
SOLUTION TIME:          0 Hours 0 Minutes 2 Seconds
End of Report
```

Table B2 Details of the optimized LULC allocation in 2039 under normal year conditions using Goal programming.

LULC type	X_1	X_2	X_3	X_4	X_5	X_6	X_7	X_8	X_9	X_{10}	X_{11}	X_{12}	Objective function	Minimized surface runoff (million m³)	
Allocated area	65.84	1,879.30	451.67	359.65	9.45	152.02	160.12	481.30	47.01	69.91	24.66	93.31			
Runoff coefficient	1.03	1.03	1.03	1.03	1.03	1.03	1.03	1.03	1.03	1.03	1.03	1.03	Best cell	3,609.48	
Constraints	X_1	X_2	X_3	X_4	X_5	X_6	X_7	X_8	X_9	X_{10}	X_{11}	X_{12}	Total	Operator	Right hand side (Bi)
Constraint 1	1	0	0	0	0	0	0	0	0	0	0	0	65.84	=>=	65.84
Constraint 2	1	0	0	0	0	0	0	0	0	0	0	0	65.84	<=	88.31
Constraint 3	0	1	0	0	0	0	0	0	0	0	0	0	1,879.30	<=	2,012.16
Constraint 4	0	1	0	0	0	0	0	0	0	0	0	0	1,879.30	=>=	1,879.30
Constraint 5	0	0	1	0	0	0	0	0	0	0	0	0	451.67	>=	306.85
Constraint 6	0	0	1	0	0	0	0	0	0	0	0	0	451.67	<=	520.31
Constraint 7	0	0	0	1	0	0	0	0	0	0	0	0	359.65	<=	489.91
Constraint 8	0	0	0	1	0	0	0	0	0	0	0	0	359.65	=>=	359.65
Constraint 9	0	0	0	0	1	0	0	0	0	0	0	0	9.45	>=	6.19
Constraint 10	0	0	0	0	1	0	0	0	0	0	0	0	9.45	=<=	9.45
Constraint 11	0	0	0	0	0	1	0	0	0	0	0	0	152.02	>=	97.03
Constraint 12	0	0	0	0	0	1	0	0	0	0	0	0	152.02	=<=	152.02
Constraint 13	0	0	0	0	0	0	1	0	0	0	0	0	160.12	>=	88.95
Constraint 14	0	0	0	0	0	0	1	0	0	0	0	0	160.12	=<=	160.12
Constraint 15	0	0	0	0	0	0	0	1	0	0	0	0	481.30	=<=	481.30
Constraint 16	0	0	0	0	0	0	0	1	0	0	0	0	481.30	>=	304.44
Constraint 17	0	0	0	0	0	0	0	0	1	0	0	0	47.01	<=	53.30
Constraint 18	0	0	0	0	0	0	0	0	1	0	0	0	47.01	=>=	47.01
Constraint 19	0	0	0	0	0	0	0	0	0	1	0	0	69.91	<=	71.65
Constraint 20	0	0	0	0	0	0	0	0	0	1	0	0	69.91	=>=	69.91
Constraint 21	0	0	0	0	0	0	0	0	0	0	1	0	24.66	<=	27.73
Constraint 22	0	0	0	0	0	0	0	0	0	0	1	0	24.66	=>=	24.66
Constraint 23	0	0	0	0	0	0	0	0	0	0	0	1	93.31	=>=	93.31
Constraint 24	0	0	0	0	0	0	0	0	0	0	0	1	93.31	<=	180.07
Constraint 25	1	1	1	1	1	1	1	1	1	1	1	1	3,794.22	=	3,794.22
Runoff (million m³)	67.58	1,904.33	408.18	359.03	8.30	125.89	133.70	366.03	48.70	64.35	28.06	95.33			

Goal programming: minimized surface runoff	d1-		d1+		Best cell		Operator	Goal	
	37.59		0		3,609.48		=	3,647.07	

Note: X_1 is urban and built-up area, X_2 is paddy field, X_3 is sugarcane, X_4 is cassava, X_5 is other field crops, X_6 is para rubber, X_7 is perennial trees and orchards, X_8 is forest land, X_9 is waterbody, X_{10} is rangeland, X_{11} is marsh and swamp, and X_{12} is unused land.

```
What's Best! 16.0.2.0 (Nov 27, 2018) - Lib.:12.0.3977.115 - 64-bit - Status
Report -
DATE GENERATED:            Jun 23, 2021                        09:42 PM
MODEL INFORMATION:
CLASSIFICATION DATA         Current   Capacity Limits
---------------------------------------------------------
Total Cells                 442
Numerics                    416
Adjustables                  14          300
Continuous                   14
Free                          0
Integers/Binaries           0/0          30
Constants                   375
Formulas                     27
Strings                       0
Constraints                  26          150
Nonlinears                    0           30
Coefficients                130


Minimum coefficient value:      1 on GoalProgramming!O4
Minimum coefficient in formula:   GoalProgramming!O4
Maximum coefficient value:      3.6524257537736e+009 on <RHS>
Maximum coefficient in formula:   GoalProgramming!G39


MODEL TYPE:            Linear (Linear Program)
SOLUTION STATUS:      GLOBALLY OPTIMAL
OBJECTIVE VALUE:      3,609,477,587.1418
BEST OBJECTIVE BOUND:   . . .
INFEASIBILITY:        0.0
DIRECTION:            Minimize
SOLVER TYPE:           . . .
ITERATIONS:           1.0
STEPS:                 . . .
ACTIVE:                . . .
SOLUTION TIME:        0 Hours 0 Minutes 2 Seconds
End of Report
```

Table B3 Details of the optimized LULC allocation in 2049 under normal year conditions using Goal programming.

LULC type	X₁	X₂	X₃	X₄	X₅	X₆	X₇	X₈	X₉	X₁₀	X₁₁	X₁₂	Objective function	Minimized surface runoff (million m³)	
Allocated area	65.84	1,812.16	512.06	330.32	11.26	164.41	193.13	481.30	42.78	66.05	21.61	93.31	Objective function		
Runoff coefficient	1.03	1.03	1.03	1.03	1.03	1.03	1.03	1.03	1.03	1.03	1.03	1.03	Best cell	3,594.76	
Constraints	X₁	X₂	X₃	X₄	X₅	X₆	X₇	X₈	X₉	X₁₀	X₁₁	X₁₂	Total	Operator	Right hand side (Bi)
Constraint 1	1	0	0	0	0	0	0	0	0	0	0	0	65.84	=>=	65.84
Constraint 2	1	0	0	0	0	0	0	0	0	0	0	0	65.84	<=	99.03
Constraint 3	0	1	0	0	0	0	0	0	0	0	0	0	1,812.16	<=	2,012.16
Constraint 4	0	1	0	0	0	0	0	0	0	0	0	0	1,812.16	=>=	1,812.16
Constraint 5	0	0	1	0	0	0	0	0	0	0	0	0	512.06	>=	306.85
Constraint 6	0	0	1	0	0	0	0	0	0	0	0	0	512.06	<=	599.36
Constraint 7	0	0	0	1	0	0	0	0	0	0	0	0	330.32	<=	489.91
Constraint 8	0	0	0	1	0	0	0	0	0	0	0	0	330.32	=>=	330.32
Constraint 9	0	0	0	0	1	0	0	0	0	0	0	0	11.26	>=	6.19
Constraint 10	0	0	0	0	1	0	0	0	0	0	0	0	11.26	=<=	11.26
Constraint 11	0	0	0	0	0	1	0	0	0	0	0	0	164.41	>=	97.03
Constraint 12	0	0	0	0	0	1	0	0	0	0	0	0	164.41	=<=	164.41
Constraint 13	0	0	0	0	0	0	1	0	0	0	0	0	193.13	>=	88.95
Constraint 14	0	0	0	0	0	0	1	0	0	0	0	0	193.13	=<=	193.13
Constraint 15	0	0	0	0	0	0	0	1	0	0	0	0	481.30	=<=	481.30
Constraint 16	0	0	0	0	0	0	0	1	0	0	0	0	481.30	>=	242.23
Constraint 17	0	0	0	0	0	0	0	0	1	0	0	0	42.78	<=	53.30
Constraint 18	0	0	0	0	0	0	0	0	1	0	0	0	42.78	=>=	42.78
Constraint 19	0	0	0	0	0	0	0	0	0	1	0	0	66.05	<=	71.65
Constraint 20	0	0	0	0	0	0	0	0	0	1	0	0	66.05	=>=	66.05
Constraint 21	0	0	0	0	0	0	0	0	0	0	1	0	21.61	<=	27.73
Constraint 22	0	0	0	0	0	0	0	0	0	0	1	0	21.61	=>=	21.61
Constraint 23	0	0	0	0	0	0	0	0	0	0	0	1	93.31	=>=	93.31
Constraint 24	0	0	0	0	0	0	0	0	0	0	0	1	93.31	<=	211.89
Constraint 25	1	1	1	1	1	1	1	1	1	1	1	1	3,794.22	=	3,794.22
Runoff (million m³)	67.58	1,836.29	462.76	329.75	9.88	136.16	161.27	366.03	44.33	60.80	24.59	95.33			

Goal programming: minimized surface runoff	d1-	d1+	Best cell	Operator	Goal
	52.31	0	3,594.76	=	3,647.07

Note: X₁ is urban and built-up area, X₂ is paddy field, X₃ is sugarcane, X₄ is cassava, X₅ is other field crops, X₆ is para rubber, X₇ is perennial trees and orchards, X₈ is forest land, X₉ is waterbody, X₁₀ is rangeland, X₁₁ is marsh and swamp, and X₁₂ is unused land.

```
What's Best! 16.0.2.0 (Nov 27, 2018) - Lib.:12.0.3977.115 - 64-bit - Status
Report -
DATE GENERATED:            Jun 23, 2021                          10:13 PM
MODEL INFORMATION:
CLASSIFICATION DATA        Current   Capacity Limits
-------------------------------------------------------
Total Cells                442
Numerics                   416
Adjustables                 14          300
Continuous                  14
Free                         0
Integers/Binaries          0/0          30
Constants                  375
Formulas                    27
Strings                      0
Constraints                 26         150
Nonlinears                   0          30
Coefficients               130

Minimum coefficient value:       1 on GoalProgramming!O4
Minimum coefficient in formula:  GoalProgramming!O4
Maximum coefficient value:       3.6524257537736e+009 on <RHS>
Maximum coefficient in formula:  GoalProgramming!G39

MODEL TYPE:               Linear (Linear Program)
SOLUTION STATUS:          GLOBALLY OPTIMAL
OBJECTIVE VALUE:          3,594,757,921.784
BEST OBJECTIVE BOUND:     . . .
INFEASIBILITY:            0.0
DIRECTION:                Minimize
SOLVER TYPE:              . . .
ITERATIONS:               1.0
STEPS:                    . . .
ACTIVE:                   . . .
SOLUTION TIME:            0 Hours 0 Minutes 2 Seconds
End of Report
```

APPENDIX C

DETAILS OF THE OPTIMIZED LULC ALLOCATION BY GOAL

PROGRAMMING UNDER WET YEAR CONDITIONS
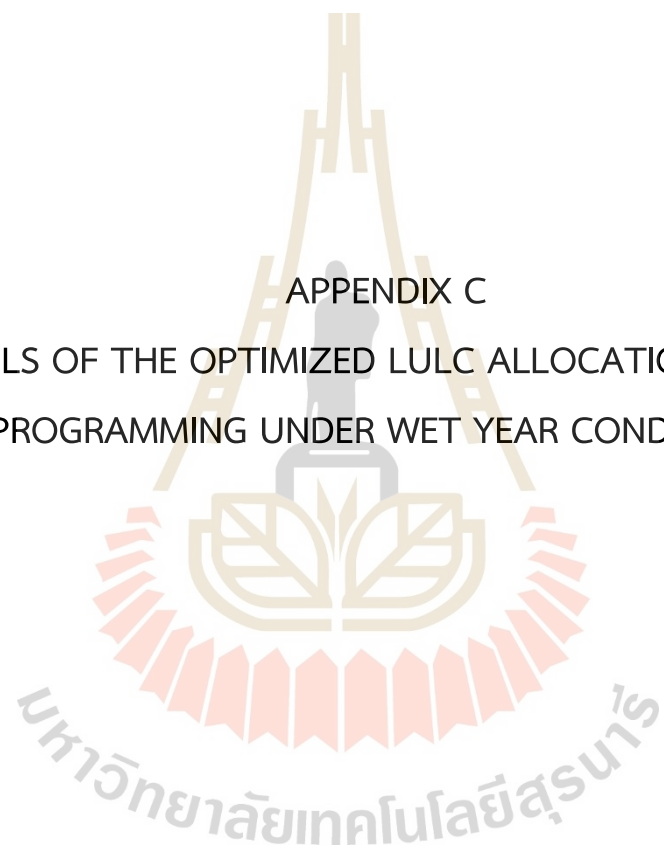
Table C1 Details of the optimized LULC allocation in 2029 under wet year conditions using Goal programming.

LULC type	X_1	X_2	X_3	X_4	X_5	X_6	X_7	X_8	X_9	X_{10}	X_{11}	X_{12}	Objective function	Minimized surface runoff (million m³)
Allocated area	65.84	1,947.12	423.64	408.26	6.19	134.43	88.95	481.30	49.52	70.54	25.13	93.31		
Runoff coefficient	0.45	0.44	0.38	0.45	0.39	0.37	0.38	0.28	0.49	0.42	0.54	0.46	Best cell	5,223.01
Constraints	X_1	X_2	X_3	X_4	X_5	X_6	X_7	X_8	X_9	X_{10}	X_{11}	X_{12}	Total	Operator	Right hand side (Bi)
Constraint 1	1	0	0	0	0	0	0	0	0	0	0	0	65.84	=>=	65.84
Constraint 2	1	0	0	0	0	0	0	0	0	0	0	0	65.84	<=	77.38
Constraint 3	0	1	0	0	0	0	0	0	0	0	0	0	1,947.12	<=	2,012.16
Constraint 4	0	1	0	0	0	0	0	0	0	0	0	0	1,947.12	=>=	1,947.12
Constraint 5	0	0	1	0	0	0	0	0	0	0	0	0	423.64	>=	306.85
Constraint 6	0	0	1	0	0	0	0	0	0	0	0	0	423.64	<=	424.95
Constraint 7	0	0	0	1	0	0	0	0	0	0	0	0	408.26	<=	489.91
Constraint 8	0	0	0	1	0	0	0	0	0	0	0	0	408.26	=>=	408.26
Constraint 9	0	0	0	0	1	0	0	0	0	0	0	0	6.19	=>=	6.19
Constraint 10	0	0	0	0	1	0	0	0	0	0	0	0	6.19	<=	7.72
Constraint 11	0	0	0	0	0	1	0	0	0	0	0	0	134.43	>=	97.03
Constraint 12	0	0	0	0	0	1	0	0	0	0	0	0	134.43	=<=	134.43
Constraint 13	0	0	0	0	0	0	1	0	0	0	0	0	88.95	=>=	88.95
Constraint 14	0	0	0	0	0	0	1	0	0	0	0	0	88.95	<=	125.36
Constraint 15	0	0	0	0	0	0	0	1	0	0	0	0	481.30	=<=	481.30
Constraint 16	0	0	0	0	0	0	0	1	0	0	0	0	481.30	>=	382.63
Constraint 17	0	0	0	0	0	0	0	0	1	0	0	0	49.52	<=	53.30
Constraint 18	0	0	0	0	0	0	0	0	1	0	0	0	49.52	=>=	49.52
Constraint 19	0	0	0	0	0	0	0	0	0	1	0	0	70.54	<=	71.65
Constraint 20	0	0	0	0	0	0	0	0	0	1	0	0	70.54	=>=	70.54
Constraint 21	0	0	0	0	0	0	0	0	0	0	1	0	25.13	<=	27.73
Constraint 22	0	0	0	0	0	0	0	0	0	0	1	0	25.13	=>=	25.13
Constraint 23	0	0	0	0	0	0	0	0	0	0	0	1	93.31	=>=	93.31
Constraint 24	0	0	0	0	0	0	0	0	0	0	0	1	93.31	<=	141.20
Constraint 25	1	1	1	1	1	1	1	1	1	1	1	1	3,794.22	=	3,794.22
Runoff (million m³)	95.82	2,795.81	552.77	574.05	8.09	174.82	116.42	563.35	74.55	95.60	39.97	131.74			

Goal programming: minimized surface runoff	d1-	d1+	Best cell	Operator	Goal
	18.52	0	5,223.01	=	5,241.52

Note: X_1 is urban and built-up area, X_2 is paddy field, X_3 is sugarcane, X_4 is cassava, X_5 is other field crops, X_6 is para rubber, X_7 is perennial trees and orchards, X_8 is forest land, X_9 is waterbody, X_{10} is rangeland, X_{11} is marsh and swamp, and X_{12} is unused land.

```
What's Best! 16.0.2.0 (Nov 27, 2018) - Lib.:12.0.3977.115 - 64-bit - Status
Report -
DATE GENERATED:             Jun 23, 2021                    09:35 PM
MODEL INFORMATION:
CLASSIFICATION DATA         Current    Capacity Limits
---------------------------------------------------------
Total Cells                 442
Numerics                    416
Adjustables                  14            300
Continuous                   14
Free                          0
Integers/Binaries           0/0            30
Constants                   375
Formulas                     27
Strings                       0
Constraints                  26            150
Nonlinears                    0             30
Coefficients                130


Minimum coefficient value:       1 on GoalProgramming!O4
Minimum coefficient in formula:   GoalProgramming!O4
Maximum coefficient value:       5.2540864516891e+009 on <RHS>
Maximum coefficient in formula:   GoalProgramming!G39


MODEL TYPE:             Linear (Linear Program)
SOLUTION STATUS:       GLOBALLY OPTIMAL
OBJECTIVE VALUE:       5,223,005,584.5182
BEST OBJECTIVE BOUND:  . . .
INFEASIBILITY:         0.0
DIRECTION:             Minimize
SOLVER TYPE:           . . .
ITERATIONS:            1.0
STEPS:                 . . .
ACTIVE:                . . .
SOLUTION TIME:         0 Hours 0 Minutes 2 Seconds
End of Report
```

Table C2 Details of the optimized LULC allocation in 2039 under wet year conditions using Goal programming.

LULC type	X_1	X_2	X_3	X_4	X_5	X_6	X_7	X_8	X_9	X_{10}	X_{11}	X_{12}	Objective function	Minimized surface runoff (million m³)
Allocated area	65.84	1,879.30	520.31	359.65	9.45	152.02	91.48	481.30	47.01	69.91	24.66	93.31		
Runoff coefficient	0.45	0.44	0.38	0.45	0.39	0.37	0.38	0.28	0.49	0.42	0.54	0.46	Best cell	5,208.46
Constraints	X_1	X_2	X_3	X_4	X_5	X_6	X_7	X_8	X_9	X_{10}	X_{11}	X_{12}	Total	Operator	Right hand side (Bi)
Constraint 1	1	0	0	0	0	0	0	0	0	0	0	0	65.84	=>=	65.84
Constraint 2	1	0	0	0	0	0	0	0	0	0	0	0	65.84	<=	88.31
Constraint 3	0	1	0	0	0	0	0	0	0	0	0	0	1,879.30	<=	2,012.16
Constraint 4	0	1	0	0	0	0	0	0	0	0	0	0	1,879.30	=>=	1,879.30
Constraint 5	0	0	1	0	0	0	0	0	0	0	0	0	520.31	>=	306.85
Constraint 6	0	0	1	0	0	0	0	0	0	0	0	0	520.31	=<=	520.31
Constraint 7	0	0	0	1	0	0	0	0	0	0	0	0	359.65	<=	489.91
Constraint 8	0	0	0	1	0	0	0	0	0	0	0	0	359.65	=>=	359.65
Constraint 9	0	0	0	0	1	0	0	0	0	0	0	0	9.45	>=	6.19
Constraint 10	0	0	0	0	1	0	0	0	0	0	0	0	9.45	=<=	9.45
Constraint 11	0	0	0	0	0	1	0	0	0	0	0	0	152.02	>=	97.03
Constraint 12	0	0	0	0	0	1	0	0	0	0	0	0	152.02	=<=	152.02
Constraint 13	0	0	0	0	0	0	1	0	0	0	0	0	91.48	>=	88.95
Constraint 14	0	0	0	0	0	0	1	0	0	0	0	0	91.48	<=	160.12
Constraint 15	0	0	0	0	0	0	0	1	0	0	0	0	481.30	=<=	481.30
Constraint 16	0	0	0	0	0	0	0	1	0	0	0	0	481.30	>=	304.44
Constraint 17	0	0	0	0	0	0	0	0	1	0	0	0	47.01	<=	53.30
Constraint 18	0	0	0	0	0	0	0	0	1	0	0	0	47.01	=>=	47.01
Constraint 19	0	0	0	0	0	0	0	0	0	1	0	0	69.91	<=	71.65
Constraint 20	0	0	0	0	0	0	0	0	0	1	0	0	69.91	=>=	69.91
Constraint 21	0	0	0	0	0	0	0	0	0	0	1	0	24.66	<=	27.73
Constraint 22	0	0	0	0	0	0	0	0	0	0	1	0	24.66	=>=	24.66
Constraint 23	0	0	0	0	0	0	0	0	0	0	0	1	93.31	=>=	93.31
Constraint 24	0	0	0	0	0	0	0	0	0	0	0	1	93.31	<=	180.07
Constraint 25	1	1	1	1	1	1	1	1	1	1	1	1	3,794.22	=	3,794.22
Runoff (million m³)	95.82	2,698.43	678.91	505.70	12.36	197.69	119.73	563.35	70.77	94.76	39.21	131.74		

Goal programming: minimized surface runoff	d1-	d1+	Best cell	Operator	Goal
	33.06	0	5,208.46	=	5,241.52

Note: X_1 is urban and built-up area, X_2 is paddy field, X_3 is sugarcane, X_4 is cassava, X_5 is other field crops, X_6 is para rubber, X_7 is perennial trees and orchards, X_8 is forest land, X_9 is waterbody, X_{10} is rangeland, X_{11} is marsh and swamp, and X_{12} is unused land.

```
What's Best! 16.0.2.0 (Nov 27, 2018) - Lib.:12.0.3977.115 - 64-bit - Status
Report -
DATE GENERATED:            Jun 23, 2021                        10:01 PM
MODEL INFORMATION:
CLASSIFICATION DATA        Current   Capacity Limits
-------------------------------------------------------
Total Cells                442
Numerics                   416
Adjustables                 14          300
Continuous                  14
Free                         0
Integers/Binaries          0/0          30
Constants                  375
Formulas                    27
Strings                      0
Constraints                 26          150
Nonlinears                   0          30
Coefficients               130


Minimum coefficient value:       1 on GoalProgramming!O4
Minimum coefficient in formula:   GoalProgramming!O4
Maximum coefficient value:       5.2540864516891e+009 on <RHS>
Maximum coefficient in formula:   GoalProgramming!G39


MODEL TYPE:                Linear (Linear Program)
SOLUTION STATUS:           GLOBALLY OPTIMAL
OBJECTIVE VALUE:           5,208,463,112.9479
BEST OBJECTIVE BOUND:      . . .
INFEASIBILITY:             0.0
DIRECTION:                 Minimize
SOLVER TYPE:               . . .
ITERATIONS:                1.0
STEPS:                     . . .
ACTIVE:                    . . .
SOLUTION TIME:             0 Hours 0 Minutes 2 Seconds
End of Report
```

Table C3 Details of the optimized LULC allocation in 2049 under wet year conditions using Goal programming.

LULC type	X_1	X_2	X_3	X_4	X_5	X_6	X_7	X_8	X_9	X_{10}	X_{11}	X_{12}	Objective function		Minimized surface runoff (million m³)
Allocated area	65.84	1812.16	599.36	330.32	11.26	164.41	105.83	481.30	42.78	66.05	21.61	93.31			
Runoff coefficient	0.45	0.44	0.38	0.45	0.39	0.37	0.38	0.28	0.49	0.42	0.54	0.46	Best cell		5,194.79
Constraints	X_1	X_2	X_3	X_4	X_5	X_6	X_7	X_8	X_9	X_{10}	X_{11}	X_{12}	Total	Operator	Right hand side (Bi)
Constraint 1	1	0	0	0	0	0	0	0	0	0	0	0	65.84	=>=	65.84
Constraint 2	1	0	0	0	0	0	0	0	0	0	0	0	65.84	<=	99.03
Constraint 3	0	1	0	0	0	0	0	0	0	0	0	0	1,812.16	<=	2,012.16
Constraint 4	0	1	0	0	0	0	0	0	0	0	0	0	1,812.16	=>=	1,812.16
Constraint 5	0	0	1	0	0	0	0	0	0	0	0	0	599.36	>=	306.85
Constraint 6	0	0	1	0	0	0	0	0	0	0	0	0	599.36	=<=	599.36
Constraint 7	0	0	0	1	0	0	0	0	0	0	0	0	330.32	<=	489.91
Constraint 8	0	0	0	1	0	0	0	0	0	0	0	0	330.32	=>=	330.32
Constraint 9	0	0	0	0	1	0	0	0	0	0	0	0	11.26	>=	6.19
Constraint 10	0	0	0	0	1	0	0	0	0	0	0	0	11.26	=<=	11.26
Constraint 11	0	0	0	0	0	1	0	0	0	0	0	0	164.41	>=	97.03
Constraint 12	0	0	0	0	0	1	0	0	0	0	0	0	164.41	=<=	164.41
Constraint 13	0	0	0	0	0	0	1	0	0	0	0	0	105.83	>=	88.95
Constraint 14	0	0	0	0	0	0	1	0	0	0	0	0	105.83	<=	193.13
Constraint 15	0	0	0	0	0	0	0	1	0	0	0	0	481.30	=<=	481.30
Constraint 16	0	0	0	0	0	0	0	1	0	0	0	0	481.30	>=	242.23
Constraint 17	0	0	0	0	0	0	0	0	1	0	0	0	42.78	<=	53.30
Constraint 18	0	0	0	0	0	0	0	0	1	0	0	0	42.78	=>=	42.78
Constraint 19	0	0	0	0	0	0	0	0	0	1	0	0	66.05	<=	71.65
Constraint 20	0	0	0	0	0	0	0	0	0	1	0	0	66.05	=>=	66.05
Constraint 21	0	0	0	0	0	0	0	0	0	0	1	0	21.61	<=	27.73
Constraint 22	0	0	0	0	0	0	0	0	0	0	1	0	21.61	=>=	21.61
Constraint 23	0	0	0	0	0	0	0	0	0	0	0	1	93.31	=>=	93.31
Constraint 24	0	0	0	0	0	0	0	0	0	0	0	1	93.31	<=	211.89
Constraint 25	1	1	1	1	1	1	1	1	1	1	1	1	3,794.22	=	3,794.22
Runoff (million m³)	95.82	2,602.02	782.05	464.46	14.71	213.81	138.51	563.35	64.41	89.52	34.37	131.74			

Goal programming: minimized surface runoff	d1-	d1+	Best cell	Operator	Goal
	46.73	0	5,194.79	=	5,241.52

Note: X_1 is urban and built-up area, X_2 is paddy field, X_3 is sugarcane, X_4 is cassava, X_5 is other field crops, X_6 is para rubber, X_7 is perennial trees and orchards, X_8 is forest land, X_9 is waterbody, X_{10} is rangeland, X_{11} is marsh and swamp, and X_{12} is unused land.

```
What's Best! 16.0.2.0 (Nov 27, 2018) - Lib.:12.0.3977.115 - 64-bit - Status
Report -
DATE GENERATED:              Jun 23, 2021                    10:15 PM
MODEL INFORMATION:
CLASSIFICATION DATA         Current   Capacity Limits
-------------------------------------------------------
Total Cells                 442
Numerics                    416
Adjustables                  14          300
Continuous                   14
Free                          0
Integers/Binaries           0/0          30
Constants                   375
Formulas                     27
Strings                       0
Constraints                  26          150
Nonlinears                    0          30
Coefficients                130

Minimum coefficient value:       1 on GoalProgramming!O4
Minimum coefficient in formula:   GoalProgramming!O4
Maximum coefficient value:        5.2540864516891e+009 on <RHS>
Maximum coefficient in formula:   GoalProgramming!G39

MODEL TYPE:              Linear (Linear Program)
SOLUTION STATUS:        GLOBALLY OPTIMAL
OBJECTIVE VALUE:        5,194,788,823.2877
BEST OBJECTIVE BOUND:   . . .
INFEASIBILITY:          0.0
DIRECTION:              Minimize
SOLVER TYPE:            . . .
ITERATIONS:             1.0
STEPS:                  . . .
ACTIVE:                 . . .
SOLUTION TIME:          0 Hours 0 Minutes 2 Seconds
End of Report
```

CURRICULUM VITAE

Name   Mr. Athiwat Phinyoyang

Date of Birth   April 19, 1992

Place of Birth Chaiyaphum Province, Thailand

Education   2013   Bachelor of Science in Geoinformatics (Second Class Honor), Program of Geoinformatics, Faculty of Science and Technology, Nakhon Ratchasima Rajabhat University.

2016   Master of Science in Geoinformatics, School of Geoinformatics, Institute of Science, Suranaree University of Technology.

Grant and Fellowships   SUT kittibandit scholarship, Suranaree University of Technology.